Differential Pathogenic Mechanisms Driving Stromal Cell Inflammatory Pathways in RA and PsA

Órla Rachel Tynan, B.Sc.(Hons)

February 2025

Thesis submitted to Trinity College Dublin in fulfilment of the requirement for the degree of Doctor in Philosophy (PhD) in Clinical Medicine

Under the supervision of Prof. Ursula Fearon

Department of Molecular Rheumatology

Trinity Biomedical Science Institute

School of Medicine, Trinity College Dublin

Head of School: Professor Colin Doherty

Declaration of Authorship

I, Órla Tynan, declare that this thesis has not been submitted as an exercise for a degree at this or any other university and it is entirely my own work.

I agree to deposit this thesis in the University's open access institutional repository or allow the library to do so on my behalf, subject to Irish Copyright Legislation and Trinity College Library conditions of use and acknowledgement. I consent to the examiner retaining a copy of the thesis beyond the examining period, should they so wish (EU GDPR May 2018).

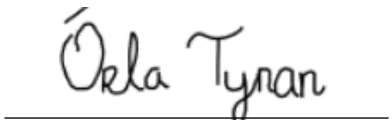

Signed: Órla Tynan **2025**

Acknowledgements

After writing a thesis you would think this would be the easiest part but getting across how much I genuinely appreciate the people who made this thesis possible has proven far more challenging than I expected! In brief, the word 'rollercoaster' really encapsulates my PhD journey. The past few years have undoubtedly been some of the most difficult yet rewarding times of my life, and I would like to acknowledge that I wouldn't have gotten through it without the support and friendships I made along the way. Whilst there were moments of frustration and exhaustion, hand-on-heart, the sheer sense of exhilaration when an experiment finally worked, the sense of achievement after giving a presentation, or the moments of laughter we shared in the reading room, made all the challenges worth it in my eyes. I have gained so much knowledge and many skills (especially perseverance and determination) and have genuinely grown so much in confidence in myself and my abilities since I first arrived in the lab.

First and foremost, I want to express my deepest gratitude to my supervisor, Prof. Ursula Fearon. Thank you for seeing something in me and giving me the opportunity to join your lab over three and a half years ago, I can honestly say it has been one of the best decisions of my life. Your wisdom, enthusiasm, and passion are infectious and have inspired me in so many ways that I can't even begin to explain. Thank you from the bottom of my heart for your unwavering guidance and advice, always having an open door, your hugs at just the right moment, and your understanding – you genuinely are the best mentor I could ever have asked for.

To the clinical team over in St. Vincent's Hospital, particularly Prof. Veale and Dr Carl Orr, for their steadfast efforts in providing us with the samples needed to conduct this research. Additionally, to the funding support and importantly the patients that made all of this work possible – I am deeply grateful.

To all Fearon lab members that have come and gone throughout my PhD journey, all the current members, and everyone in the reading room. Thank you for the countless things you've all done to help me along this journey ranging from baking treats to tech support to seemingly endless proofreading (special thank you to Siobhán) and putting up with my constant sighs and random moments of talking aloud! You have all made me feel truly myself and I can with all sincerity say it's been an absolute pleasure working alongside you. A special mention to Conor, the 'RNAseq guru', I want to say thank you for not only all your RNA-seq work but also your constant 'character-building' teasing and of course those moments where your kindness shone through (although you like to hide that side). To Vivi, your advice on flow and 'compensation' has been invaluable, as have your random chats during the day when you need a break from your office. To Mary, thank

you for your constant advice, thoughtfulness, and picking me up when I was at my lowest, I will be eternally grateful. To Alyssa, your guidance in so many experimental techniques has been indispensable – I have gained so much scientific knowledge from you. Throughout this PhD I have had the privilege of being surrounded by such incredible female scientists that have taught me one of the most important things - there are no limits. I really hope to get to work alongside all of you in the future if I'm lucky enough.

To the LGALS, thank you each individually for the constant support, laughs, dinner trips, afterwork runs, and of course daily coffee breaks – especially coming towards the end, those coffee trips to Honey Truffle were genuinely the highlight of my day! To Aoife, fellow running buddy, and Hannah for your constant willingness to help. A special thank you to Aenea for providing me with constant high-fives and cat memes, always giving me much needed laughter at the perfect time, and Niamh, for always noticing the small things and lending a hand, no matter how big or small the task. Thank you both so much for your friendship and kindness in some of the most challenging times over the past few months (and of course all the proofreading) – I hope I can repay it and more when it is your time! And finally to Brianne, my 'twin' – what can I say? Words cannot fully capture how much I value our friendship. From the moment we both met during my Undergraduate project and your Masters project, we just clicked, and I genuinely could not have made it through these last few years without you. From my personal hairdresser to my therapist, you've seen me at my highest and my lowest, lifted me up when I couldn't lift myself, been my sounding-board and life-coach in so many respects, and embraced my silly self. I honestly have made a best friend for life, and I can't thank you enough for everything.

To the self-designated 'anatomy squad' – Catherine, Volga, and Hannah, thank you for being my constant cheerleaders and motivators over our 3-hour zoom chats. I couldn't ask for a better group of friends, thank you for loving me just as I am.

To Aaron, my rock, I want to express my heartfelt gratitude to you for putting up with me, especially over the last few months though the rollercoaster of emotions of my PhD and perfectly understanding that at times all I really needed was a hug. Your unwavering belief in my abilities has meant the world to me and kept me going through everything. I am so lucky to have you in my life.

Finally, to my family, this accomplishment is as much mine as it is yours. From providing me with my first human body book for Christmas when I was little, to asking me how my 'cell-babies' are getting on, you have always been my biggest advocates. To Aoife and Eimear, thank you for being my best friends, for all the times you've cheered me up and supported me, gave me 'sisterly'

advice, and listened to me rant. To dad, thank you for all those early morning calls, they always brightened up my day. To mam, thank you for always being at the other end of the phone when I needed you most. Both of you have shaped me into the person I am today, giving me constant love and support and believing in me against all the odds. You are all my driving force, and I will be forever grateful.

Without doubt, this PhD has shaped me, not only as a researcher, but in a personal respect, pushing me to grow in ways I never anticipated. Words cannot capture how much I will cherish my PhD memories forever.

Table of Contents

List of Figures

List of Tables

Author Publications

Loss of Synovial Tissue Macrophage Homeostasis Precedes Rheumatoid Arthritis Clinical Onset.
Hanlon MM, Smith CM, Canavan M, Neto N, Song Q, Lewis MJ, **Tynan Ó,** Barker BE, Gallagher P, Mullan R, Hurson C, Moran B, Monaghan MG, Pitzalis C, Fletcher JM, Nagpal S, Veale DJ, Fearon U. *Science Advances*, 2024 Sep 27;10(39):eadj1252. doi: 10.1126/sciadv.adj1252. Epub 2024 Sep 25.

Distinct Stromal and Immune Cell Interactions Shape the Pathogenesis of Rheumatoid and Psoriatic Arthritis.
Floudas A, Smith CM, **Tynan Ó**, Neto N, Krishna V, Wade SM, Hanlon MM, Cunningham C, Marzaioli V, Canavan M, Fletcher JM, Mullan MH, Cole S, Hao LY, Monaghan MG, Nagpal S, Veale DJ, Fearon U. *Annals of Rheumatic Disease*, 2022 Aug 11;81(9):1224-1242. doi: 10.1136/annrheumdis-2021-221761.

Serum microRNA Signatures as Diagnostic Tools that Distinguish Rheumatoid and Psoriatic Arthritis.
Fearon U, **Tynan Ó**. *Hospital Professional News (HPN).* May 2022:42-42.

To be Submitted/Manuscripts in Preparation

Immune Cell-Derived Cytokines Synergistically Interact to Drive Synovial Fibroblast Invasive Function and Metabolic Capacity.
Tynan Ó, Floudas A, Gilmore A, Brugman A, Neto N, Monaghan M, Marzaioli V, Wade S, Anton D, Orr C, Veale DJ, Fearon U.
To be submitted to JCI Insights

RA and PsA Synovial Tissue Single-Cell Analysis Demonstrates Differential Fibroblast Populations with Distinct Phenotype and Functional Capacity.
Tynan Ó, Brugman A, Smith C, Floudas A, Canavan M, O'Rourke A, Anton D, Wade S, Orr C, Veale DJ, Fearon U.
To be submitted to Cell Reports

Biomarker Potential of a Circulatory microRNA Signature Distinguishing Rheumatoid Arthritis and Psoriatic Arthritis.
Tynan Ó, Hanlon MM, Floudas A, Wade S, Veale DJ, Fearon U.
To be submitted to Rheumatology

Published Abstracts

Distinct FLS Populations and Immune-Stromal Cell Receptor-Ligand-Interactions Define Rheumatoid and Psoriatic Arthritis Pathotypes.
Tynan Ó, Smith C, Floudas A, Canavan M, Neto N, O'Rourke A, Anton D, Wade S, Orr C, Veale DJ, Fearon U. *Irish Society for Rheumatology (ISR), Kildare, Ireland (September 2024)* ***(Poster Presentation).***

Differential FLS Populations Define Rheumatoid and Psoriatic Arthritis Pathotypes via their Functional Response to Distinct Immune Regulators.
Tynan Ó, Smith C, Floudas A, Canavan M, Neto N, O'Rourke A, Anton D, Wade S, Orr C, Veale DJ, Fearon U. *European Congress of Immunology (ECI), Dublin, Ireland (September 2024)* ***(Poster Presentation).***

Distinct FLS Populations with Unique Functional Properties and Regulators Define Rheumatoid and Psoriatic Arthritis Pathotypes.
Tynan Ó, Smith C, Floudas A, Canavan M, Neto N, O'Rourke A, Anton D, Wade S, Orr C, Veale DJ, Fearon U. *European Workshop for Rheumatology Research (EWRR), Genoa, Italy (May 2024)* ***(Poster Presentation).***

Circulatory miRNA Signature Distinguishes Rheumatoid Arthritis and Psoriatic Arthritis.
Tynan Ó, Hanlon MM, Floudas A, Wade S, Veale DJ, Fearon U. *European Workshop for Rheumatology Research (EWRR), Genoa, Italy (May 2024)* ***(Poster Presentation).***

***Synovial Tissue Single-Cell Analysis Demonstrates Differential Fibroblast Populations between RA and PsA which Display Distinct Function.**
Tynan Ó, Smith C, Floudas A, Canavan M, O'Rourke A, Anton D, Orr C, Veale DJ, Fearon U. *American College of Rheumatology (ACR), San Diego, USA (November 2023)* ***(Oral Presentation).***

Immune Cell-Derived Cytokines Synergistically Interact to Drive Synovial Fibroblast Invasive Function and Metabolic Capacity.
Tynan Ó, Floudas A, Neto N, Monaghan M, Wade S, Orr C, Veale DJ, Fearon U. *American College of Rheumatology (ACR), San Diego, USA (November 2023)* ***(Poster Tour).***

***RA and PsA Synovial Tissue Single-Cell Analysis Demonstrates Differential Fibroblast Populations with Distinct Phenotype and Functional Capacity.**
Tynan Ó, Floudas A, Smith C, Canavan M, O'Rourke A, Anton D, Orr C, Veale DJ, Fearon U. *Irish Society for Rheumatology (ISR), Dublin, Ireland (September 2023)* ***(Oral Presentation).***

Invasive Synovial Fibroblast Populations Differ between RA and PsA, Functional Capacity of which are Driven by Immune Cell-Derived Cytokines.
Tynan Ó, Floudas A, Neto N, Wade S, Orr C, Veale DJ, Fearon U. *European Workshop for Rheumatology Research (EWRR), Dublin, Ireland (March 2023)* ***(Poster Presentation).***

Distinct Trajectories of RA and PsA Synovial Fibroblasts give rise to Proinflammatory Fibroblast Cell Subsets.
Tynan Ó, Floudas A, Smith C, Canavan M, O'Rourke A, Anton D, Orr C, Veale DJ, Fearon U. *European Workshop for Rheumatology Research (EWRR), Dublin, Ireland (March 2023)* ***(Poster Presentation).***

***Synovial Fibroblast Populations Associated with Invasive Function Differ between RA and PsA, Functional Capacity of which are Driven by Immune Cell-Derived Cytokines.**
Tynan Ó, Floudas A, Neto N, Wade S, Orr C, Veale DJ, Fearon U. *Irish Society for Rheumatology* (ISR*), Belfast, Ireland (September 2022)* ***(Oral Presentation).***

Differential miRNA Expression and Endothelial Cell Activity in Rheumatoid Arthritis and Psoriatic Arthritis.
Tynan Ó, Hanlon MM, Floudas A, Wade S, Veale DJ, Fearon U. *European Alliance of Associations for Rheumatology (EULAR), Copenhagen, Denmark (June 2022)* ***(Poster Presentation).***

***Comparison between miRNA Biomarker Expression and Endothelial Cell Pathogenicity in Rheumatoid Arthritis and Psoriatic Arthritis.**
Tynan Ó, Hanlon MM, Floudas A, Wade S, Veale DJ, Fearon U. *European Workshop for Rheumatology Research (EWRR), Vienna, Austria (May 2021)* ***(Oral Presentation).***

***Comparison of the Differential Pathogenic Mechanisms Driving Rheumatoid Arthritis and Psoriatic Arthritis.**
Tynan Ó, Hanlon MM, Floudas A, Wade S, Veale DJ, Fearon U. *Irish Society for Rheumatology Autumn Conference (ISR), Ireland (October 2021)* ***(Oral Presentation).***

****Oral Presentation***

Awards Received

Emerging Investigator Excellence Award for:

Immune Cell-Derived Cytokines Synergistically Interact to Drive Synovial Fibroblast Invasive Function and Metabolic Capacity.
Tynan Ó, Floudas A, Neto N, Monaghan M, Wade S, Orr C, Veale DJ, Fearon U. *American College of Rheumatology (ACR), San Diego, USA (November 2023)* ***(Poster Tour).***

Best Scientific Oral Presentation (1st) for:

RA and PsA Synovial Tissue Single-Cell Analysis Demonstrates Differential Fibroblast Populations with Distinct Phenotype and Functional Capacity.
Tynan Ó, Floudas A, Smith C, Canavan M, O'Rourke A, Anton D, Orr C, Veale DJ, Fearon U. *Irish Society for Rheumatology (ISR), Dublin, Ireland (September 2023)* ***(Oral Presentation).***

EWRR Travel Bursary for:

Invasive Synovial Fibroblast Populations Differ between RA and PsA, Functional Capacity of which are Driven by Immune Cell-Derived Cytokines.
Tynan Ó, Floudas A, Neto N, Wade S, Orr C, Veale DJ, Fearon U. *European Workshop for Rheumatology Research (EWRR), Dublin, Ireland (March 2023)* ***(Poster Presentation).***

EWRR Travel Bursary for:

Distinct Trajectories of RA and PsA Synovial Fibroblasts Give Rise to Proinflammatory Fibroblast Cell Subsets.
Tynan Ó, Floudas A, Smith C, Canavan M, O'Rourke A, Anton D, Orr C, Veale DJ, Fearon U. *European Workshop for Rheumatology Research (EWRR), Dublin, Ireland (March 2023)* ***(Poster Presentation).***

EULAR Travel Bursary for:

Differential miRNA Expression and Endothelial Cell Activity in Rheumatoid Arthritis and Psoriatic Arthritis.
Tynan Ó, Hanlon MM, Floudas A, Wade S, Veale DJ, Fearon U. *European Alliance of Associations for Rheumatology (EULAR), Copenhagen, Denmark (June 2022)* ***(Poster Presentation).***

Abbreviations

2-DG	2-Deoxy-d-glucose
3PO	(3-(3-pyridinyl)-1-(4-pyridinyl)-2-propen-1-one)
ACPA	Anti-citrullinated Protein
ACR	American College of Rheumatology
AGO	Argonaute
Ang	Angiopoietin
ATP	Adenosine Triphosphate
AUC	Area Under the Curve
bDMARd	Biological Disease Modifying Anti-Rheumatic Drug
BMI	Body Mass Index
BMP	Bone Morphogenetic Factor
BSA	Bovine Serum Albumin
Cad11	Cadherin-11
CASPAR	Classification Criteria for Psoriatic Arthritis
cDNA	Complementary Deoxyribonucleic acid
CI	Confidence Interval
CIA	Collagen Induced Arthritis
CM	Conditioned Media
CRP	C reactive Protein
csDMARD	Conventional Synthetic Disease Modifying Anti-Rheumatic Drug
Ct	Comparative Threshold
CTAP	Cell Type Abundance Phenotype
CVD	Cardiovascular Disease
DAS28	Disease Activity Score in 28 Joints
DC	Dendritic Cell
DEG	Differentially expressed gene
DGCR8	DiGeorge Syndrome Critical Region 8
DIANA	DNA Intelligent Analysis
DLL4	Delta-like Ligand 4
DM	Diabetes Mellitus
DMARD	Disease-Modifying Anti-Rheumatic Drug
DMSO	Dimethyl Sulfoxide
DNA	Deoxyribonucleic Acid
EBV	Epstein Barr Virus
EC	Endothelial Cells
ECAR	Extracellular Acidification Rate
ECM	Extracellular Matrix
ELISA	Enzyme-linked Immunosorbent Assay
EMT	Epithelial-Mesenchymal Transition
ER	Endoplasmic Reticulum
ESR	Erythrocyte Sedimentation Rate
EULAR	European League Against Rheumatism
FACS	Fluorescence-Activated Cell Sorting
FADH	Flavin Adenine Dinucleotide

FBS	Fetal Bovine Serum
FCCP	Trifluorocarbonylcyanide Phenylhydrazone
FGF	Fibroblast Growth Factor
FLS	Fibroblast-like synoviocytes
FMO	Fluorescent Minus One
GAPDH	Glyceraldehyde-3-phosphate dehydrogenase
GDF-5	Growth Differentiation Factor 5
GLUT-1	Glucose Transporter 1
GM-CSF	Granulocyte-Macrophage Colony-Stimulating Factor
GRAPPA	Group for Research and Assessment of Psoriasis and Psoriatic Arthritis
H&E	Haematoxylin and Eosin
HC	Healthy Control
HIF	Hypoxia Inducible Factor
HIV	Human Immunodeficiency Virus
HK2	Hexokinase 2
HLA-DR	Human Leukocyte Antigen – DR isotype
HUVEC	Human Umbilical Vein Endothelial Cell
IA	Inflammatory Arthritis
IAR	Individuals at Risk
IBD	Inflammatory Bowel Disease
ICAM-1	Intracellular Adhesion Molecule 1
IL	Interleukin
JAG	Jagged Canonical Notch Ligand
JAK	Janus Kinase
KEGG	Kyoto Encyclopaedia of Genes and Genomes
LDH(A)	Lactate Dehydrogenase (A)
LPS	Lipopolysaccharide
MCP	Monocyte Chemoattractant Protein
M-CSF	Macrophage Colony Stimulating Factor
MERTK	Macrophage Type I Tyrosine Kinase Receptor
MFI	Median Fluorescent Intensity
MHC	Major Histocompatibility Complex
MI	Myocardial Infarction
miRISC	microRNA-Induced Silencing Complex
miRNA	microRNA
MMP	Matrix Metalloproteinase
MO-DC	Monocyte-derived DC
MRE	miRNA Recognition Element
MS	Multiple Sclerosis
MSD	Mesoscale Discovery
mTOR	Mammalian Target of Rapamycin
MTX	Methotrexate
NADH	Nicotinamide Adenine Dinucleotide
NF-κB	Nuclear Factor kappa B
NSAID	Non-Steroidal Anti-Inflammatory Drug
NSCLC	Non-Small Cell Lung Cancer

OA	Osteoarthritis
OCR	Oxygen Consumption Rate
OSM	Oncostatin M
P0/1/2	Passage 0/1/2
PBS	Phosphate Buffered Saline
PCA	Principle Component Analysis
PDE4	Phosphodiesterase-4
PDGFR	Platelet Derived Growth Factor Receptor
PDGF	Platelet Derived Growth Factor
PDI	Protein Disulphide Isomerase
PDPN	Podoplanin
PER	Proton Efflux Rate
PFA	Paraformaldehyde
PFKFB3	6-phosphofructo-2-kinase/fructose-2,6-biphosphatase 3 enzyme
PKM2	Pyruvate Kinase M2
pO_2	Partial Pressure of Oxygen
PRG4	Proteoglycan-4
PsA	Psoriatic Arthritis
RA	Rheumatoid Arthritis
RANKL	Receptor Activator of Nuclear Factor kappa-B Ligand
RCT	Randomised Control Trial
RF	Rheumatoid Factor
RISC	RNA-Induced Silencing Complex
RNA	Ribonuclease Acid
ROC	Receiver Operating Characteristics
ROS	Reactive Oxygen Species
RT	Room Temperature
RT-PCR	Real-time Polymerase Chain Reaction
scRNA-seq	Single-cell RNA-sequencing
SE	Shared Epitope
SEM	Standard Error of the Mean
SF	Synovial Fluid
SJC	Swollen Joint Count
SNP	Single Nucleotide Polymorphisms
SpA	Spondylarthritis
SPICE	Simplified Presentation of Incredibly Complex Evaluations
STAT	Signal Transducers and Activators of Transcription
STM	Synovial Tissue Macrophage
TAK1	Transforming Growth Factor Beta-Activated Kinase
TCA	Tricarboxylic Acid Cycle
TGF-β	Transforming Growth Factor Beta
Tie2	Receptor Tyrosine Kinase 2
TIMP	Tissue Inhibitor of Metalloprotease
TJC	Tender Joint Count
TLR	Toll-Like Receptor
TMRM	Tetramethylrhodamine-Methyl-Ester

TNF	Tumour Necrosis Factor
TNFi	Tumour Necrosis Factor Inhibitor
tsDMARD	Targeted Synthetic Disease Modifying Anti-Rheumatic Drug
UMAP	Uniform Manifold Approximation and Projection
UPR	Unfolded Protein Response
UTR	Untranslated Region
VAS	Visual Analogue Scale
VCAM-1	Vascular Cell Adhesion Molecule 1
VEGF	Vascular Endothelial Growth Factor
VEGFR2	Vascular Endothelial Growth Factor Receptor 2

Chapter 3 Cluster Marker Gene Abbreviations

APOE	Apolipoprotein E
CCL2	Chemokine (CC-motif) Ligand 2
CHI3L2	Chitinase 3-Like 2
CLIC5	Chloride Intracellular Channel 5
CSN1S1	Casein Alpha S1
CXCL12	C-X-C Motif Chemokine Ligand 12
CXCL8	Chemokine (C-X-C motif) Ligand 8
IER2	Immediate Early Response Gene 2 Protein
INHBA	Inhibin Subunit Beta A
INT	Intermediate
LL	Lining Layer
POSTN	Periostin
SL	Sub-lining
TM4SF1	Trans membrane 4 L six family member 1
VCAN	Versican

Abstract

Rheumatoid arthritis (RA) and Psoriatic arthritis (PsA) encompass two of the most prevalent forms of inflammatory arthritis (IA), an umbrella term for the vast range of autoimmune driven arthropathies characterised by highly dysregulated and destructive immune and stromal activity within the joint, resulting in debilitating effects on patient quality of life. Several features are common to both pathologies including the extensive synovial inflammation which precedes bone and cartilage erosion in addition to the widespread systemic manifestations observed. However, although not fully understood currently, it is becoming increasingly recognised that there are a number of distinguishing characteristics in relation to circulating biomarkers in addition to disease pathogenesis at the clinical, immunological, cellular, and molecular levels. At the cellular level, a critical perpetuator of disease in both arthropathies is the fibroblast-like synoviocyte (FLS), a key stromal cell that assumes a central role in maintaining the integrity of the joint under homeostasis. However, as of yet, differences in their transcriptional profile and regulation in RA vs PsA remain unexplored. Therefore, the aims of this thesis are to identify phenotypic and functional characteristics that define distinct FLS populations and regulators in RA vs PsA, in addition to identifying circulatory miRNA as cellular biomarkers that can distinguish RA from PsA and to evaluate the potential implications for disease pathogenesis.

In Chapter 2, following global scRNA-seq analysis of all cells within the synovium and through receptor-ligand interactions analysis, the existence of a population of THY1+FAP+ FLS enriched in RA specifically was identified, whose pathogenic activity was being driven by the combined effects of IL-1β and TGF-β, derived from macrophages and T cells respectively, within the inflamed joint microenvironment. It was demonstrated that IL-1β and TGF-β synergistically/additively interact to promote the expression of several proinflammatory cytokines and chemokines, adhesive and angiogenic molecules, and matrix degrading MMPs, whilst altering the cellular bioenergetics in favour of glycolysis. Moreover, this was paralleled by changes in endoplasmic reticulum stress and mitochondrial fission/fusion properties, further supporting mitochondrial dysfunction and invasive capacity in RA FLS. Finally, it was demonstrated that addition of Takinib, the TAK1 inhibitor, could suppress some of these synergy-induced effects both in RA FLS and RA *ex vivo* synovial explants, highlighting the central role of this downstream molecule in coordinating the synergistic interactions of IL-1β and TGF-β in RA FLS. Cumulatively, the data suggests that the pathogenic nature of specific populations of FLS enriched in RA is in part driven by synergistic interactions between T cell and macrophage-derived cytokines, thus, blocking specific immune-stromal cell interactions may offer new avenues of therapeutic intervention in RA and PsA.

Whilst emphasis has been placed on stratifying phenotypically and functionally distinct subsets of FLS in RA, analysis of FLS subsets in PsA exclusively, in addition to direct comparisons of FLS populations in RA vs PsA remain largely uninvestigated. Therefore, expanding on Chapter 3, for the first time, an enrichment of THY1+ sub-lining FLS in RA and conversely, an enrichment of THY1- lining FLS in PsA was identified. Moreover, following cell sorting, it was revealed that THY1+ FLS are functionally distinct from THY1- FLS with heightened angiogenic and chemokine markers observed in the THY1+ population, and greater MMPs in the THY1- FLS. This correlated with the histological analysis demonstrating significantly elevated immune cell infiltration and lymphoid aggregate presence in RA whilst lining layer thickness was increased in PsA. Further flow cytometry stratification of FLS subsets identified six distinct FLS populations in RA and PsA based on surface marker expression of THY1, in addition to CD34, CD55, and FAP, with two of these populations enriched in RA: THY1+CD34+CD55-FAP+ and THY1+CD34-CD55-FAP+ and conversely, two others enriched in PsA: THY1-CD34-CD55+FAP+ and THY1+CD34-CD55+FAP+. In parallel, reanalysis of scRNA-seq data on FLS exclusively revealed sixteen distinct FLS clusters, with enrichment of three sub-lining clusters in RA

compared to PsA: THY1+POSTN+, CXCL12+CHI3L2+, and CXCL12+APOE+. scRNA-seq analysis focused only on synovial FLS and *ex vivo* experiments highlighted differences in their functional properties with immune/inflammatory responses associated with RA dominant populations in contrast to high matrix degradative gene expression in PsA dominant populations. Finally, whilst passage 0 RA and PsA FLS maintained similar profiles to *ex vivo* FLS, once expanded to passage 3, the FLS started to lose specific phenotypic characteristics, suggesting that once removed from the joint microenvironment FLS subset stability appears transient with convergence towards common phenotypes.

Lastly, it has been widely accepted that the earlier the diagnosis the superior the outcomes in rheumatic disease, thus identifying biomarkers that can provide a reliable and non-invasive method of achieving this are important. In this thesis, seven miRNAs were successfully identified that were significantly increased in RA serum compared to PsA and importantly also healthy controls (HC). Further sub analysis revealed that these miRNAs were not affected by the ACPA status of the patient while the differences between RA and PsA were not affected by differences in disease activity measures. Moreover, further PCA and biplot analysis determined that three miRNAs in particular were more skewed towards RA in contrast to PsA, specifically miR-22-3p, miR-223-3p, and miR-29b-3p. Downstream analysis using DIANA and STRING software identified several pathways of interest as being primary targets of these three specific miRNA all of which assume important roles in driving aspects of RA pathogenesis such as angiogenesis, cell death, and bone metabolism. These included the FoxO signalling pathway, the Hippo signalling pathway, and importantly the P13K-AKT pathway which had the greatest number of target genes at 87. Thus this data highlights the valuable nature of using circulating miRNA not only as diagnostic biomarkers that can distinguish RA from PsA, but additionally to deepen understanding of their differential pathogenesis.

Cumulatively, the data collated in this thesis suggests there is considerable heterogeneity between RA and PsA, not only at the cellular but additionally the biomarker level. It provides a deeper insight into the roles of FLS subsets with unique functions in driving differential pathogenic mechanisms in RA and PsA, whilst highlighting the impact of immune-stromal communication in augmenting this activity. Moreover, the data indicates that serum miRNA may indeed provide a method of distinguishing RA from PsA patients. Taken together, this knowledge can facilitate earlier and more rapid diagnosis whilst additionally, improving understanding of disease pathogenesis and consequently, the implementation of more targeted therapeutic approaches in RA and PsA.

CHAPTER ONE:

General Introduction

1.1 Inflammatory Arthritis

Inflammatory arthritis (IA), of which Rheumatoid arthritis (RA) and Psoriatic arthritis (PsA) are two of the most prevalent types, is defined by a range of autoimmune conditions in which the body's own immune system inflicts potentially irreversible damage on organs and tissues in an uncontrolled manner (Veale and Fearon, 2015; Merola, Espinoza and Fleischmann, 2018; Smolen *et al.*, 2018; Veale and Fearon, 2018; Alivernini, Firestein and McInnes, 2022). In the instance of RA and PsA, a critical pathogenic component centres around the synovial joint in which features including soft tissue swelling and significant joint inflammation precede debilitating cartilage destruction and bone erosion (Veale and Fearon, 2015; Veale and Fearon, 2018; Gravallese and Firestein, 2023). Whilst both arthropathies share this common inflammatory microenvironment, widespread systemic manifestations, and a complex and heterogenous synovial aetiology, distinct differences exist not only in the clinical aspects, but additionally across the molecular, cellular, and genetic levels.

Some of the most prominent differences that assist in distinguishing these two pathologies include the striking absence of RA associated autoantibodies, anti-citrullinated protein antibody (ACPA) and rheumatoid factor (RF) in the majority of patients with PsA, with studies also detecting lower level of the classic inflammatory markers such as C reactive protein (CRP) and erythrocyte sedimentation rate (ESR) in PsA patient cohorts compared to their RA counterparts, demonstrating clear differences in the autoimmune aspect of these two arthropathies (Cunnane *et al.*, 2000; Inanc *et al.*, 2007; Veale and Fearon, 2015; Merola, Espinoza and Fleischmann, 2018). Moreover, different clinical and anatomical features are also important in distinguishing RA from PsA leading to the classification of PsA as a form of spondyloarthropathy first described by Moll and Wright (Wright, 1956; Moll and Wright, 1973b). Whilst radiographic imaging has distinguished that joint involvement and bony lesions in RA are predominantly symmetric with defined demarcations and are accompanied by an absence of new bone growth and cervical spine involvement, PsA contrasts directly with asymmetric and axial bone involvement observed, and a characteristic poorly demarcated lesion (Moll and Wright, 1973a; Veale and Fearon, 2015; Merola, Espinoza and Fleischmann, 2018). Additionally, certain clinical features are hallmarks of PsA specifically including nail dystrophy, dactylitis, the concept of inflammation at the site where tendons/ligaments insert into bone termed enthesitis, and the accompanying psoriatic rash as shown in Figure 1.1 below (McGonagle, Conaghan and Emery, 1999; McGonagle *et al.*, 2019; Veale and Fearon, 2015; Merola, Espinoza and Fleischmann, 2018; Watad *et al.*, 2018).

Furthermore, one of the most striking differences between RA and PsA is the pattern of de novo blood vessels that form within the inflamed synovium. Early investigations identified elongated, tortuous vessels in PsA compared to straight vessels with regular branching in RA (Reece *et al.*, 1999). Detailed microscopic investigations have expanded on this with a higher abundance of new blood vessels in conjunction with a notably reduced expansion of the synovial lining layer in PsA compared to RA, in addition to differences in angiogenic and growth factor expression levels (Veale *et al.*, 1993; Fraser *et al.*, 2001; Fearon *et al.*, 2003). Studies have demonstrated a mixture of mature and immature blood vessels in both the RA and PsA synovium, with immature blood vessels demonstrating a lack of surrounding pericytes more associated with PsA pathophysiology (Kennedy *et al.*, 2010). The immune cell infiltrates and inflammatory milieu also demonstrate notable differences. Whilst both RA and PsA are mediated by the upregulation of a vast number of proinflammatory cytokines and chemokines that act concurrently to drive chronic inflammation, differences in the importance of certain cytokines have been identified with interleukin (IL) -6 assuming a more central role in RA compared to the IL-17/IL-23 pathway in PsA, evidence supported by the success/failure of therapeutic interventions (Schett *et al.*, 2013; Veale and Fearon, 2015; Schinnerling *et al.*, 2017; Merola, Espinoza and Fleischmann, 2018; Schett, McInnes and Neurath, 2021; Schett *et al.*, 2022). Additionally, whilst the frequency of lymphocyte infiltration is highly comparable between both disease states, the mixed B and T cell presence in RA contrasts with the T cell predominance observed in PsA (Veale and Fearon, 2018). Synovial analysis of infiltrating T cells demonstrated CD4+ T cells are enriched in the RA synovium, whilst conversely, PsA synovial fluid (SF) displayed a marked enrichment of the CD8+ T cell population (Costello *et al.*, 1999; Menon *et al.*, 2014; Zhang *et al.*, 2019b; Povoleri *et al.*, 2023). Indeed, specifically elevated levels of cytotoxic IL-17 expressing CD8+ T cells have been identified in the joints of PsA patients but not RA highlighting the distinction in T cell subtypes that are associated with both diseases (Menon *et al.*, 2014; Veale and Fearon, 2015; Povoleri *et al.*, 2023).

However, more in-depth studies focused on these differences are critical in gaining a better understanding of the differential therapeutic responses observed in RA vs PsA which impacts directly on disease prognosis and overall patient quality of life.

RA  **PsA**

Figure 1.1. Representative images of the hands of RA and PsA patients. Images courtesy of Prof. Veale, Rheumatology Dept., St. Vincent's University Hospital.

1.2 Rheumatoid Arthritis

1.2.1 History

The field of rheumatology first came into existence as a consequence of Guillaume de Baillou, who is renowned as the 'Father of Rheumatology' (Kaiser and Keitel, 2006). Building off of his posthumous description of rheumatism being a disease that afflicted multiple joints throughout the body, the first modern medical acknowledgement of RA can be attributed to the dissertation describing the unexplained joint pain and stiffness of patients written by Augustin Jacob Landré-Beauvais in the year 1800 (Entezami *et al.*, 2011; Pineda and Sandoval, 2023). Indeed, although his interpretation of the disease as being a form of gout was inaccurate, it encouraged further research of this disease. In 1859, it was the work of an English physician, Alfred Garrod, that definitively classified RA as being a separate entity from gout with distinct etiology (Entezami *et al.*, 2011; Pineda and Sandoval, 2023). Furthermore, his son is the individual accredited with coining the term widely accepted today as 'Rheumatoid Arthritis' in 1890, derived from the Greek words meaning 'flow' and 'joint' (Garrod, 1890).

Although not medically investigated before this time, historical evidence of rheumatic diseases were identified in the skeletons of individuals unearthed in several locations, including Pompei and ancient Egypt (Entezami *et al.*, 2011). Indeed, the Greek Philosopher Hippocrates described what we now understand as arthritis in 400 BC in which he termed it 'a disease with fever, severe joint pain, fixing itself in one joint now, then in another, of short duration, acute, not leading to death, more apt to attack the young than the old' (Parish, 1963). Moreover, several ancient art pieces depict deformities in the limbs of subjects that perfectly mirrors the disfigurement observed in RA patients such as the Renaissance painting 'The Temptation of St. Anthony' dating from the 15th century and Peter Paul Rubens 'The Three Graces (1638)', all evidence which highlights the presence of RA long before being definitively classified (Entezami *et al.*, 2011).

1.2.2 Classification

The main purpose of disease classification is to primarily ensure patients are diagnosed at an early stage before significant clinical manifestations emerge. Therefore, the American College of Rheumatology (ACR) established the criteria to diagnose RA in patients in 1988 (Arnett *et al.*, 1988). However, the low sensitivity and specificity of these criteria were widely criticised in later years due to their inability to successfully achieve the aim of diagnosing patients at the critical earlier stages of disease pathogenesis (van der Linden *et al.*, 2011). Whilst detectable levels of

autoantibodies and raised CRP levels have been measured in the serum of individuals in the years preceding RA development, these measurements were not sufficient alone to utilise as a diagnostic tool (Nielen *et al.*, 2004a; Nielen *et al.*, 2004b). Thus, in order to overcome these previous inadequacies, and to attempt to diagnose patients before they reach a chronically erosive disease level, the revised current guidelines for the classification of RA were jointly established by the ACR and the European League Against Rheumatism (EULAR) in 2010 (Aletaha *et al.*, 2010). Although patients typically present with highly heterogenous clinical manifestations of RA, these guidelines assist in providing a standardised, multidisciplinary approach for diagnosing patients presenting in a clinical setting, considering CRP and autoantibody levels in addition to several other factors. To meet the criteria, patients must present with at least one swollen joint for which no alternative diagnosis is available whilst additionally achieving a combined score of ≥ 6 from the individual scores in four domains defined below in *Table 1.1.*

Classification Criteria	
1. Joint involvement	1 large joint >1-10 large, asymmetric >1-10 large, symmetric 1-3 small joints 4-10 small joints >10 joints (1 must be small)
2. Serology	RF (-) and ACPA (-) RF (low +) or ACPA (low +) RF (high +) or ACPA (high +)
3. Acute-phase reactants	Normal CRP and normal ESR Abnormal CRP or abnormal ESR
4. Duration of symptoms	<6 weeks ≥6 weeks

Table 1.1. **Classification criteria for RA.** Adapted from the ACR/EULAR classification criteria 2010 (Aletaha *et al.*, 2010).

1.2.3 Epidemiology

RA is a worldwide, immune-mediated, systemic disease that can develop at any age but typically peaks in incidence in the third to fifth decades of life (Nagaratnam, Nagaratnam and Cheuk, 2017; McInnes and Schett, 2017; Gravallese and Firestein, 2023). With an unusually consistent global prevalence of 0.5-1%, this disease typically initiates years before the clinical symptoms manifest and a definitive classification of RA can be provided. Interestingly, the consistent global prevalence is not equally distributed as there appears to be a strong association between higher incidence rates and developed countries, with studies conducted in Northern European and American

territories reporting an RA incidence rate of 0.5-1.1% in contrast to the lower rates of 0.1-0.5% detected in underdeveloped regions (McInnes and Schett, 2017; Gravallese and Firestein, 2023). However, whilst genetics may assume a role in these prevalence differences, it is likely that socioeconomic factors in addition to insufficient access to healthcare and diagnostic facilities may be attributed to the stark differences observed (Yang *et al.*, 2018). Furthermore, individual studies have highlighted geographical variations in prevalence with some of the highest rates of RA detected in North America's Indigenous population, with the Blackfeet Indians and Chippewa Indians displaying prevalence rates that were approximately five times greater than those in white Northern American and Western European populations (Peschken and Esdaile, 1999). Moreover, the influence of gender on RA development cannot be underestimated, with studies reporting a 2-3 times higher incidence in members of the female sex, which may in part be linked to the stimulating effects of oestrogen on both innate and adaptive components of the immune system, with androgens and testosterone having a significantly more immune-suppressive impact (Nagaratnam, Nagaratnam and Cheuk, 2017; McInnes and Schett, 2017; Cutolo and Straub, 2020).

1.2.4 Genetic Risk Factors

As an extraordinarily complex disease, the development of RA cannot be attributed to a single causal agent but rather it arises due to the complex interactions between individual genetics and environmental influences, highlighting its multifactorial nature.

The notion that RA could be associated with genetics is not a new concept, but one initially proposed by William Heberden in 1806 in which he wrote 'Is [rheumatism] not in some degree hereditary?' (Copeman, 2012). Although familial recurrence risk for RA is significantly lower in comparison to other autoimmune diseases, there is a genetic link, with first-degree relatives of an individual with RA having a 2-5 factor increase in disease risk (Gravallese and Firestein, 2023). Indeed, the human leukocyte antigen – DR isotype (HLA-DR) locus on chromosome 6 and the 'shared epitope' (SE) hypothesis is of particular relevance, with specific sequences within the hypervariable region of the HLA-DRβ chain strongly correlated with a heightened risk of developing RA (Holoshitz, 2010; Padyukov, 2022). The presence of the HLA DRB1*0404 allele specifically has been identified as the strongest susceptibility factor in worldwide populations, accounting for 1/3 of the genetic risk, particularly in ACPA positive patient cohorts (Gregersen, Silver and Winchester, 1987; Raychaudhuri *et al.*, 2012; Smolen *et al.*, 2018). As HLA-DR itself normally functions in the process of T cell directed antigen presentation and activation, RA associated HLA-DR genes can predispose T cell receptors to recognise a more autoimmune

repertoire thus triggering an autoimmune disease such as RA (Ishigaki *et al.*, 2022). Moreover, several other associations outside the HLA-DR locus have also been identified, with many of these genes directly associated with immune system responses. To date, over 150 genetic loci are associated with RA including *STAT4, PRKCQ, TRAF1, IFNγ, IL-10, IL-2, IL-5R, DAP, WISP1, PRKCB,* and *SMC1B,* in addition to recently identified candidate genes at novel loci directly implicated in the immune system, *TNIP1* and *TNFRSF11* (Gregersen, Silver and Winchester, 1987; Nepom, Hansen and Nepom, 1987; Ollier and Thomson, 1992; Begovich *et al.*, 2004; Hinks *et al.*, 2007; Plenge *et al.*, 2007; Remmers *et al.*, 2007; Thomson *et al.*, 2007; Barton *et al.*, 2008; Ha, Bae and Kim, 2021; Ishigaki *et al.*, 2021). Additionally, a gain-of-function mutation in the tyrosine-phosphatase gene *PTPN22* situated on chromosome 1 has also been reported as a key RA susceptibility factor due to its effects on self-reactive T cell deletion (Lee *et al.*, 2005).

Furthermore, the potential role epigenetics, defined by changes to the existing genetic material, may play in linking non-genetic risk factors to the emergence of symptoms is becomingly an increasingly more recognised field of study. Research conducted on RA patients has identified post-translational alterations to the genetic material including deoxyribonucleic acid (DNA) methylation in addition to histone modifications and abnormal expression of non-coding ribonucleic acids (RNA), reversible changes that predispose the individual to greater joint inflammation and destruction associated with RA (Nemtsova *et al.*, 2019; Ospelt and Gay, 2022). Recent work has successfully identified five central hub genes in an epigenetic regulatory network; *CHD3*, *SETD1B*, *FBXL19*, *SMARCA4*, and *SETD1A*, all of which assume key roles in immune-mediated and inflammatory responses, key features involved in disease development and progression, thus highlighting the importance of recognising epigenetic modulation in RA pathogenesis (Chen *et al.*, 2022).

1.2.5 Environmental Risk Factors

It is strongly hypothesised that environmental and lifestyle factors can have a significant role in RA development, with this being of particular significance for those already genetically predisposed (Klareskog *et al.*, 2006; Jiang and Alfredsson, 2020).

Of all the lifestyle choices, smoking has been implicated as one of the most significant risk factors for the development of ACPA positive RA due to its direct association with the major immune related HLA-DR SE genes and subsequent immune reactions to citrullinated proteins (Vessey, Villard-Mackintosh and Yeates, 1987; Silman, Newman and MacGregor, 1996; Klareskog *et al.*, 2006; Stolt *et al.*, 2010; Källberg *et al.*, 2011). It has been hypothesised that the introduction

of cigarette smoke to the body can result in the post-translational modification of peptides in which arginine is converted to citrulline in a process referred to as 'citrullination', either through direct activation of the citrullination enzymes peptidyl arginine deiminases (PADs) or indirectly through the enhanced formation of antigen presentation zones (Catrina *et al.*, 2016). In genetically susceptible individuals in possession of major histocompatibility complex (MHC) class II molecules with the SE, this citrullination of peptides increases their affinity for the MHC molecules, thus leading to heightened activation of autoreactive CD4+ T cells and the initiation of a highly dysregulated, autoimmune response (Hill *et al.*, 2003; Klareskog *et al.*, 2006; Källberg *et al.*, 2011). Indeed, research has demonstrated that the combined effect of smoking and possessing double copies of the HLA-DR SE genes can lead to a 21-fold increase in RA risk compared to non-smokers lacking these genes reinforcing the notion that RA development can result from a complex etiology of a specific genotype and the introduction of an environmental stimulus such as smoking (Klareskog *et al.*, 2006). Furthermore, other inhaled substances have also shown strong associations with a significant increase in RA risk including silica/dust, airborne pathogens, and air pollutants, although the evidence for this is mixed due to a multitude of confounding factors (Stolt *et al.*, 2010; Mohamed *et al.*, 2012).

In stark contrast to cigarette smoke, recent evidence indicates that alcohol may exert the opposite effect on RA development (Jiang and Alfredsson, 2020). Whilst the Vasterbotten Intervention Program Cohort demonstrated an absence of a correlation between alcohol intake and RA development, observational studies have actually suggested a possible protective effect of alcohol due to the antioxidant and immunosuppressive nature of its composition (Källberg *et al.*, 2009; Sundström, Johansson and Rantapää-Dahlqvist, 2015). However, whilst multiple epidemiologic studies regarding the modest consumption of alcohol have exhibited a slightly protective effect this was contradicted by a British study conducted solely on ACPA positive RA individuals which failed to detect this protective role (Rakieh *et al.*, 2015; Deane *et al.*, 2017). This conflicting evidence highlights the need for further alcohol related RA studies to understand the true association.

However, smoking and alcohol are not the only lifestyle choices that have been attributed to affecting the risk of RA development. Obesity, and specifically adipose tissue itself, has an extremely immunomodulatory role and is frequently associated with increased inflammation due to the plethora of cytokines, chemokines, and metabolically active hormones it secretes. Long established evidence indicates that obesity may be an important risk factor for RA development and progression, with several studies detecting a marked elevation in the circulating levels of key adipokines including leptin, adiponectin, visfatin, resistin, chemerin, and SERPIN in both the serum

and SF of RA patients compared to their healthy counterparts (Symmons, 2005; Feng *et al.*, 2016; Skoczyńska and Świerkot, 2018; Bilski *et al.*, 2023). Recent evidence has highlighted the role dietary choices and obesity can have on RA risk, with higher body mass index (BMI) at middle age and at 18 years, in addition to a greater waist circumference, associated with increased RA risk and elevated levels of macroscopic synovitis and vascularity (Low *et al.*, 2018; Bae and Lee, 2019; Ohno, Aune and Heath, 2020). Studies have also demonstrated reduced responsiveness to biological therapies in patient with RA who are classified as obese, with a 2013 study demonstrating poor remission rates with anti-tumour necrosis factor (TNF)-α in individuals with a BMI of >30kg/m^2 (Gremese *et al.*, 2013). Interestingly, a systematic review identified a much stronger correlation between BMI and RA in the female population compared to their male counterparts, whilst additionally the ACPA negative group demonstrated a higher risk (Feng *et al.*, 2016). Diet itself is also significant in relation to RA with several studies highlighting that diets containing a greater proportion of vegetables and whole grains and minimal quantities of animal fats and sugar, are associated with decreased disease risk (He *et al.*, 2016; Hu *et al.*, 2017b; Skoczyńska and Świerkot, 2018). Indeed, research has shown that high fat diets result in increased systemic inflammation mediated through Th1 and Th17 cells and M1 macrophages, all of which contributes to a more severe arthritis phenotype (Na *et al.*, 2017). Conversely, supplementation with omega-3 reduced RA development in individuals at risk of developing RA, whilst daily consumption of orange juice containing a natural carotenoid, beta-cryptoxanthin, displayed an inverse correlation with RA development also (Pattison *et al.*, 2005; Navarini *et al.*, 2017).

Furthermore, due to the strong association between diet and RA development, the role of microbiota and the gut mucosa is becomingly increasingly more recognised. Studies have highlighted the common disease mechanisms shared between RA and celiac disease, both of which are driven by a strong autoimmunologic component (Lerner and Matthias, 2015). Alterations to the microbes residing within the mucosal surfaces of the gut can have major implications for homeostatic maintenance and immunologic changes related to initiation of such diseases. Several studies have detected alterations in the bacterial diversity detected in fecal samples of untreated recent-onset RA patients compared to controls, with research into specific patient populations identifying reduced levels of bacteroides and concurrently, heightened levels of the gram-negative bacterium *P. copri,* a species recently associated with inflammatory bowel disease (IBD) and atherosclerosis, in the gut microenvironment (Vaahtovuo *et al.*, 2008; Scher *et al.*, 2013; Koeth *et al.*, 2013; Maeda *et al.*, 2016; Catrina *et al.*, 2016).

Aside from the intestinal mucosa, alterations to the oral mucosa have also been highlighted as a potential site for preclinical RA pathology induction. A significant overlap in terms

of an association with increased presence of citrullinated proteins and HLA-DR SE alleles, in addition to smoking, has been shown between RA and periodontitis, a condition characterised by chronic inflammation of the gingival tissues of the mouth (Catrina *et al.*, 2016). This connection is further supported by the high prevalence of periodontal dysbiosis detected in patients presenting with new-onset RA (Scher *et al.*, 2012). Interestingly, elevated levels of the bacteria '*Porphyromonas gingivalis* (*P ging)* responsible for activating the enzymes that drive citrullination, have been demonstrated in periodontal inflammation, suggesting this bacteria may assume a central role in the early breaks in immune tolerance in RA development (Wegner *et al.*, 2010; Laugisch *et al.*, 2016). Furthermore, mass spectrometric analysis of the gingival crevicular fluid collected from patients with periodontitis identified hypercitrullination of peptides, reflecting the autoantigens detected in RA joints, induced by the abundant presence of the specific bacteria *Aggregatibacter actinomycetemcomitans (Aa) (Konig et al., 2016)*. Indeed, on this basis it has been hypothesised that *Aa* may encompass a novel primary microbe present in the oral cavity that can trigger RA autoimmunity.

Moreover, bacteria are not the only microbes that demonstrate a role in perpetuating RA development. Multiple lines of evidence highlight the key involvement of viruses, hypothesised to be functioning as adjuvants in the development of autoimmune diseases such as polyarthritis including rubella, human T cell leukaemia virus-1, parvovirus B19, and hepatitis B and C (Naides, 1998; Masuko-Hongo, Kato and Nishioka, 2003). In particular, the Epstein Barr virus (EBV), a virus associated with multiple malignancies and exhibiting significant immunomodulatory effects in both latent and replicating forms through its ability to non-specifically stimulate innate immune responses, has been identified as an environmental trigger in RA (Costenbader and Karlson, 2006). Alspaugh and Tan were the first to implicate EBV in RA pathogenesis following identification of a nuclear antigen in EBV-transformed lymphocytes that RA patients were reactive towards (Alspaugh *et al.*, 1978). Continuing on from these early studies, it has been determined that the levels of EBV DNA and mRNA are significantly higher in RA patients compared to both osteoarthritis (OA) patients and healthy controls (HC) whilst elevated anti-EBV antibody levels and clonal expansion of CD8+ EBV-specific T cells have been observed in patients with RA compared to their healthy counterparts (Takeda *et al.*, 2000; Blaschke *et al.*, 2000; Klatt *et al.*, 2005).

1.2.6 Co-morbidities and Malignancy

Due to the systemic inflammatory and autoimmune nature of RA, a myriad of co-morbidities are frequently detected in patients upon assessment and are associated with an increased risk of

morbidity and mortality (Taylor *et al.*, 2021). The range of co-morbidities extends from physical to psychological, with the international COMOrbidities in Rheumatoid Arthritis (COMORA) study identifying the following diseases as the most commonly observed co-morbidities – asthma (7%), chronic obstructive pulmonary disease (4%), depression (15%), solid organ malignancies (5%), and cardiovascular disease events (CVD) (6%) (Dougados *et al.*, 2014). CVD is a significant and critical co-morbidity attributing to half of the deaths in RA patients, with a 2020 study demonstrating a 33% higher risk of CVD events including myocardial infarction (MI), stroke, or heart failure, in those with early RA compared to matched healthy comparators (Nikiphorou *et al.*, 2020; Figus *et al.*, 2021). These observations were further supported by the CARdiovascular research and RhEumatoid arthritis (CARRÉ) prospective cohort study which determined RA individuals possessed a two-fold increased risk of multiple CV events compared to the general population, evidence which may be explained by the significantly higher prevalence of calcium deposits in the major coronary arteries of RA patients as demonstrated by imaging studies (Khalid *et al.*, 2020; Tinggaard *et al.*, 2020). In addition, this study revealed that the risk of developing CVD was further heightened in patients exhibiting symptoms of both RA and diabetes mellitus (DM). Indeed, estimates show approximately 20% of RA patients have DM as a co-morbidity with several inflammatory mediators demonstrating central roles in perpetuating both pathologies, evidence which suggests a potential inflammation-related association between RA and DM (Cacciapaglia *et al.*, 2023). Moreover, as mentioned in the COMORA study, when compared to the general population, the frequency of malignancy is significantly higher in RA, with a recent observational study detecting an all-cancer relative excess risk of 20% in these individuals, a risk higher in males compared to females at 34% and 8%, respectively (Dougados *et al.*, 2014; Beydon *et al.*, 2023). Interestingly, the evidence indicates the existence of a site-specific increased cancer risk with a high prevalence of particular cancers including lung, ovarian, bladder, kidney and upper urinary tract, melanoma, cervix, and prostate, in addition to haematological cancers including Hodgkin's lymphoma, diffuse large B cell lymphoma, and multiple myeloma, in RA. Moreover, the data collected infers an effect of RA treatment on heightening cancer incidence, with the commonly utilised drugs abatacept and rituximab resulting in greater risk of lung cancer and multiple myeloma in individuals receiving them, compared to the general population (Beydon *et al.*, 2023).

1.3 Psoriatic Arthritis

1.3.1 History

In an equivalent manner to RA, the evolution of PsA dates back before medical records to the 13th century, when the very first reports were made regarding a Saxon skeleton identified with distinct abnormalities we now commonly associate with PsA (Rogers, Watt and Dieppe, 1981). Over the following years, numerous inferences were made about PsA being a distinct disease with Fray Felipe Colombo in 1674 providing written texts and the French physician Baron Jean Louis Alibert making the initial connection between joint related symptoms and psoriasis (Castillo-Ojugas and Hernández, 1989; Moll and Wright, 1973b). Building on this connection, Ernest Bazin coined the term 'psoriasis arthritique' in 1860, suggesting a shared pathogenic pathway for skin and joint involvement, whilst in 1888, Charles Bourdillon provided a concise written description of PsA (Bazin and Sergent, 1860; Espinoza, 2018). However, it was the work of Verna Wright in the 1950s that successfully characterised the range of disorders referred to as seronegative spondylarthritis (SpA), a category under which PsA falls, thus reinforcing its distinction from other rheumatic diseases such as RA (Wright, 1956).

Despite these advances, PsA as a distinct disease was still not acknowledged by the ACR, a point reinforced by the proposal put forward by the New York Rheumatism Association in 1941 in which PsA was included and classified as a subset of RA (Hench, Bauer and et al., 1948). However, from the 1940s there was a gradual shift in opinions partially influenced by the work of Hench and others which demonstrated comprehensive links between psoriasis and articular involvement (Hench, 1927). Finally in 1964, following advancements regarding the discovery of RF and well-documented IA cases in which RF was absent, the American Rheumatism Association (ARA) officially chose to classify PsA as a distinct entity, a classification that would open an entire field of future study (Waaler, 1940; Blumberg *et al.*, 1964).

1.3.2 Classification

In a similar manner to RA, the classification criteria for PsA have evolved significantly overtime. Whilst historical diagnosis was based on the descriptive definition provided by Moll and Wright which stated that 'PsA is an inflammatory arthritis in the presence of psoriasis and usually the absence of rheumatoid factor', more definitive and universally agreed upon guidelines were proposed in 2006 with the objective of providing a more specific and data-supported method of diagnosing PsA (Moll and Wright, 1973b; Taylor *et al.*, 2006). Utilising a combination of clinical, dermatological, and radiographic features, the Classification Criteria for Psoriatic Arthritis

(CASPAR) group was established to identify a sufficient level of homogeneity in the signs/symptoms patients were presenting with that could be defined universally as a PsA diagnosis.

Using this standardised approach, a definitive diagnosis of PsA can be provided to individuals presenting with an inflammatory articular disease in addition to a combined score of ≥ 3 across the five domains, as defined below in *Table 1.2* (Taylor *et al.*, 2006). Whilst there have been some concerns raised about the validity of these criteria in relation to attempting to discern IA pains from normal, non-specific aches in tendons/joints, the CASPAR criteria still remains the cornerstone for PsA diagnosis in clinical settings (Leung *et al.*, 2018). However, it was updated in 2015 by the global association of multidisciplinary experts in the field called the 'Group for Research and Assessment of Psoriasis and Psoriatic Arthritis (GRAPPA)' due to the need to concurrently address co-morbidities and remains an ever-evolving area as the understanding of PsA is deepened (Coates *et al.*, 2016).

CASPAR Classification Criteria		Score
1. Psoriasis	Current psoriasis OR	2
	Personal history of psoriasis OR	1
	Family history of psoriasis	1
2. Psoriatic nail dystrophy	Onycholysis, pitting, or hyperkeratosis	1
3. RF	Negative RF test result	1
4. Dactylitis	Current dactylitis OR	1
	History of dactylitis recorded by rheumatologist	1
5. Radiological evidence of juxta-articular new bone formation	Ill-defined ossification near joint margins on hand/foot plain radiographs	1

***Table 1.2.* Classification criteria for PsA.** Adapted from the classification criteria defined in CASPAR guidelines (Taylor *et al.*, 2006).

1.3.3 Epidemiology

Affecting 0.1-1% of the general population, PsA can be defined as a chronically progressive, musculoskeletal disease of a systemic nature, driven predominantly by dysregulation of the immune system. Whilst higher prevalence rates of ~20% have been reported in individuals with the existing inflammatory skin disease, psoriasis, the emergence of the arthritic component can develop before the appearance of skin involvement, a situation which occurs in 10%-15% of

patients (LEUNG and LIM, 2007; Coates and Helliwell, 2017). While the evidence indicates there is no association between the level of skin involvement and the severity of arthritis, studies have shown that patients presenting with nail dystrophy and severe psoriatic plaques/lesions have a significantly greater risk of developing concomitant joint inflammation (Gelfand *et al.*, 2005; Langenbruch *et al.*, 2014). However, the majority of patients with PsA demonstrate mild-moderate skin disease on clinical presentation (Gelfand *et al.*, 2005; Wilson *et al.*, 2009). In 2018, a thorough systematic review identified levels of PsA to be 133 per 100,000 people in the general population, although the validity of these statistics was limited by the considerable heterogeneity between disease classification in the included studies (Scotti *et al.*, 2018). Moreover, geographical location has proven to have a significant effect on PsA prevalence, with dramatic differences not solely identified between different continents but between neighbouring countries. For example, regions such as Norway exhibited significantly higher incidence rates compared to their neighbouring country Sweden – 20 and 670 per 100,000, respectively (Karmacharya, Chakradhar and Ogdie, 2021). Moreover, South American in addition to Asian countries have reported significantly lower incidence rates, with levels of 0.1, 2, and 4 per 100,000 reported in Japan, China, and Taiwan, respectively, figures that may in part be influenced by a failure to diagnose efficiently in addition to substantial differences in genetic composition and lifestyle habits (Kerschbaumer *et al.*, 2016; Karmacharya, Chakradhar and Ogdie, 2021).

Furthermore, there is a similar level of variability in the reported studies related to PsA prevalence in those with pre-existing psoriasis. A meta-analysis reported a pooled PsA prevalence of 19.7% in psoriasis patients, although the levels of PsA were significantly higher in adult patient cohorts in comparison to children/adolescents at 21.6% and 3.3%, respectively (Alinaghi *et al.*, 2019). Moreover, this study further highlighted the diversity in levels of PsA in psoriasis patients across different continents with the greatest difference observed between Asia at 14% and Europe at 22.7%. Interestingly, this research also demonstrated a strong association between the severity of the psoriasis affecting the skin and the development of PsA, with higher PsA incidence rates being reported by those with moderate to severe psoriasis compared to those presenting with mild cases, a dose-response effect that suggests the existence of a specific threshold trigger point for PsA development (Alinaghi *et al.*, 2019).

1.3.4 Genetic Risk Factors

Several complex genetic risk factors have been implicated in PsA although the significant level of clinical heterogeneity has made the identification of specific genes challenging. The existence of

a strong genetic component was reinforced in data obtained from previous family pedigree studies in which estimates for the heritability of PsA were far higher than for psoriasis alone, at 30.4 and 7.6 respectively, although evidence supporting this is conflicting with more comparable heritability being identified in newer studies (Moll and Wright, 1973b; Chandran *et al.*, 2009; Li *et al.*, 2020; Soomro *et al.*, 2022). However, despite these inconsistencies, the evidence does suggest that whilst many major susceptibility loci may be shared between the two phenotypes of disease indicating that the genetic risks for psoriasis and PsA are strongly associated, PsA specific risk-loci do exist, a hypothesis that has been supported by recent emerging data. The role of MHC variants cannot be underestimated in this regard with common variation in the HLA class 1 region and particularly with the alleles HLA-B*27, HLA-B*08, and HLA-C*38 conferring the strongest predisposition to PsA, whilst HLA-C*06 demonstrates susceptibility to psoriasis solely and is potentially protective in or for PsA (Winchester *et al.*, 2012; Okada *et al.*, 2014; Bowes *et al.*, 2015; Bowes *et al.*, 2017). Interestingly, a 2016 study provided evidence to explain the association between genetic variation of MHC alleles and the clinical heterogeneity observed in PsA. This study suggested that HLA susceptibility genes culminate in differential phenotypic presentations of PsA, with the HLA-B*27:05:02 haplotype positively associated with enthesitis and symmetric sacroiliitis compared to the HLA-B*08:01:01–HLA-C*07:01:01 haplotypes which were related to the presentation of joint fusion and asymmetric sacroiliitis (Haroon *et al.*, 2016). Moreover, outside of the MHC complex, several additional risk variants at different loci have been shown with a genotyping study conducted in 2015 identifying eight significant loci including the IL23R gene located at chromosome 5q31 which conferred risk for PsA solely (Bowes *et al.*, 2015; Budu-Aggrey *et al.*, 2016). A specific PsA single nucleotide polymorphism (SNP) at this locus appeared to co-localise with epigenetic markers of open chromatin in the cytotoxic CD8+ memory T cell subset, reinforcing the key role this cell type and this specific SNP assume in the development of PsA (Costello *et al.*, 1999; Bowes *et al.*, 2015).

Widescale analysis of SNPs have also proven beneficial in this regard with recent work by Soomro *et al*. (2022) identifying 17 genome wide associations, with the aforementioned IL23R associated SNP of particular significance. Whilst individual SNPs did demonstrate considerable overlap between psoriasis and PsA such as rs5754467 which is in close proximity to the genes *UBE2L3, YDJC*, and *CCDC116,* on chromosome 22q11, multiple PsA specific SNPs were determined. Interestingly, these PsA specific SNPs were related to important inflammatory and bone forming pathways including nuclear factor kappa B (NF-κB) signalling and Wnt signalling, providing insight into disease mechanisms that may be specific to PsA pathogenesis (Soomro *et al.*, 2022). Furthermore, several other genetic risk factors related to important immune related and cytokine

pathways have been discovered. These include *IL-4, IL-5, IL-13, IL-12B, B3GNT2*, the Th17 cell promoting transcription factor *RUNX1,* IL-1 family related gene *REL* and *TRAF3IP2* which has demonstrated significant roles in driving adaptive Th17 and B cell-mediated cellular immune responses, in addition to susceptibility loci directly associated with key signalling pathways implicated in the pathogenic progression of both psoriasis and PsA including TNF, IL-23, and IL-17 (Alenius *et al.*, 2004; Hüffmeier *et al.*, 2010; Ellinghaus *et al.*, 2012; Tsoi *et al.*, 2012; Bowes *et al.*, 2015; Veale and Fearon, 2018; Soomro *et al.*, 2022).

1.3.5 Environmental Risk Factors

A combination of genetic predisposition and the appropriate environmental stimuli can precipitate and drive the onset of disease in PsA. A number of environmental factors are also known to contribute to PsA risk including infection, injury/bone trauma, obesity, severe psoriasis, smoking, rubella vaccination, and hypercholesteremia, thus further emphasising the highly complex nature of this pathology (Pattison *et al.*, 2008; Eder *et al.*, 2012; Veale and Fearon, 2018).

As an autoimmune disease, PsA itself is mediated predominantly by significant dysregulation of both the innate and adaptive arms of the immune defence system, an effect which can be exacerbated by the introduction of a stimulus in the form of an infection. Indeed, studies have previously confirmed a relationship between PsA and the human immunodeficiency virus (HIV), with research suggesting that the HIV-induced immune dysregulation can contribute to PsA development (Njobvu and McGill, 2000). Additionally, previous research has identified a strong association between streptococcal infection and PsA/psoriasis exacerbation, with the presence of RNA of three different streptococcal bacterial species in the peripheral blood in addition to the SF of PsA patients (Telfer *et al.*, 1992; Wang *et al.*, 1999; Thorleifsdottir *et al.*, 2016; Dagan *et al.*, 2019). Recent evidence suggests that the location of the infection may constitute a more important trigger than the infecting pathogen itself with a significant site-specific correlation detected between bacterial cultures from the pharynx and a heightened PsA risk (Thrastardottir *et al.*, 2023).

Interestingly, perturbations to the normal microflora residing at the barriers of the body have also been identified as prominent risk factors for PsA development (Azuaga, Ramírez and Cañete, 2023). A recent study identified alterations to the microbiome of the skin of PsA patients, with reduced diversity in the bacteria present but a heightened presence specifically of the *Corynebacterium*, whilst fecal analysis of PsA patients identified significant reductions in several species including *Akkermansia, Ruminococcus*, and *Pseudobutyrivibrio* (Scher, Littman and

Abramson, 2016; Boix-Amorós *et al.*, 2023). Moreover, a study conducted on patients with SpA demonstrated that a damaged intestinal mucosal barrier and significant dysbiosis are characteristic features that result in enhanced intestinal permeability and monocyte recruitment (Ciccia *et al.*, 2017).

In relation to modifiable risk factors, obesity plays a significant role. Due to the highly active inflammatory nature of adipose tissue and the plethora of proinflammatory cytokines and adipokines it releases, an excess of adipose tissue also comprises a risk factor for PsA induction (Azuaga, Ramírez and Cañete, 2023). Obesity and a higher BMI have been shown to be associated with an increased PsA risk, with similar pathogenic mechanisms observed in both conditions hypothesised to be regulated in part by the adipokine, leptin (Bhole *et al.*, 2012; Russolillo *et al.*, 2013). Interestingly, higher levels of circulating cholesterol, an effect that commonly arises as a direct consequence of a high fat diet and obesity, can itself result in elevated probability of developing both psoriasis alone and psoriasis with concurrent PsA (Wu *et al.*, 2014). Moreover, obesity can also contribute to biomechanical stress, an additional risk factor for PsA as a consequence of the immune-mediated repair response it initiates (Azuaga, Ramírez and Cañete, 2023). Whilst normal, physiological levels of mechanical loading are required for healthy maintenance of tendons and ligaments within the joint, pathological levels of force upon the enthesis, such as occupations requiring the lifting of heavy weights, are established risk factors for chronic IA (Eder *et al.*, 2011; Thorarensen *et al.*, 2017; Cambré *et al.*, 2018; Veale and Fearon, 2018). Evidence indicates that PsA is particularly susceptible to developing at sites of previous trauma that were sufficiently severe to warrant medical intervention, referred to as the 'Koebner Phenomenon' (Pattison *et al.*, 2008; Veale and Fearon, 2018). The individual and combined effect of these factors including obesity and physical trauma to the bones/joints can result in significant mechanical stress and microdamage, thus focusing the activity of the systemic immune response specifically on the joint itself. Through the release of an abundance of cytokines and growth factors such as TNF and transforming growth factor beta (TGF-β), secondary synovitis at this site is induced, a defining characteristic of spondyloarthropathies such as PsA (Pattison *et al.*, 2008; Thorarensen *et al.*, 2017; Veale and Fearon, 2018; Gracey *et al.*, 2020).

Conversely, smoking demonstrates a paradoxical relationship in terms of PsA development leading to the term the so-called 'smoking paradox', an effect similarly seen in ulcerative colitis, a disease that shares many clinical and genetic similarities to PsA (Eder *et al.*, 2011; Azuaga, Ramírez and Cañete, 2023). Research has shown that whilst cigarette smoke is associated with an increased risk of developing PsA in HC, in individuals with already pre-existing psoriasis this risk is absent, whilst a lower prevalence of peripheral arthritis was also observed in

PsA patients defined as regular smokers (Duffin *et al.*, 2009; Ladehesa-Pineda *et al.*, 2023). This protective role has been attributed potentially to polymorphisms in the IL-13 gene, an example that clearly highlights the genetic-environmental link in triggering autoimmune arthropathies such as PsA (Nguyen *et al.*, 2018).

1.3.6 PsA Co-morbidities and Malignancy

In recent years, research has focused on recognising the spectrum of clinical conditions that frequently manifest in individuals living with PsA, conditions that have been termed 'psoriatic disease' as a consequence of their characteristic occurrence in this patient population. Indeed, the evidence suggests PsA patients are subjected to premature multimorbidity, of which the most common co-occurring diseases include CVD, metabolic disorders, disturbances related to the gastrointestinal tract such as IBD, and mental health disorders, with depression incidence three- to five-fold greater in PsA patients compared to RA (Fragoulis *et al.*, 2020; Sun, Li and Zhang, 2022; Panagiotopoulos and Fragoulis, 2023). Conversely, such differences are not observed in the context of CVD, a significant co-morbidity in both RA and PsA alike, with its PsA association in part attributed to several factors including the heightened levels of vascular endothelial growth factor (VEGF), increased oxidative stress, greater arterial stiffness, and chronic inflammatory conditions, all of which are characteristic of PsA (Fragoulis *et al.*, 2020; Panagiotopoulos and Fragoulis, 2023). It has been shown that successful blockade of certain inflammatory pathways central to driving PsA pathogenesis including IL-17 can result in improved vascular and myocardial function compared to other treatments, suggesting a protective effect in relation to CVD development (Makavos *et al.*, 2020). Moreover, studies have reported that PsA patients frequently demonstrate the classic risk factors for CVD including hypertension, fatty liver disease, and metabolic disorders including DM and obesity, increasing their CV event potential substantially (Tobin *et al.*, 2010; Ishchenko *et al.*, 2024). Research has demonstrated that the prevalence of type 2 DM in PsA cohorts can range from 6.1-20.2%, figures that are substantially higher than those observed in the general population or in sufferers of psoriasis alone (Charlton *et al.*, 2019; Dal Bello *et al.*, 2020). Although a definitive reason for this strong association had not yet been elucidated, several hypotheses have been proposed. These include the presence of reduced levels of insulin sensitising factors including adiponectin detected in PsA patient serum, the potential disrupting effect of conventional PsA treatments on glucose homeostasis, and additionally, elevated levels of mediators such as TNF-α or endothelial cell (EC) dysfunction, both of which mechanistically result in promotion of insulin resistance (Hotamisligil *et al.*, 1996; Shibata *et al.*, 2009; Petersons *et al.*,

2013; Chen *et al.*, 2017a; Dal Bello *et al.*, 2020; Babalic *et al.*, 2022). Indeed, this connection between insulin resistance, a defining hallmark of metabolic syndrome, and PsA was reinforced by recent work which revealed a significant positive association between disease activity measured using the Disease Activity in Psoriatic Arthritis Score (DAPSA) and insulin resistance levels (Yuliasih *et al.*, 2023).

Moreover, in contrast to RA, the vast majority of available evidence is limited and inconclusive in relation to PsA and the development of malignancies. Whilst an abundance of literature suggests a lack of an association between PsA and increased risk of multiple different cancer types, a significant association was detected between PsA and breast cancer (Wilton, Crowson and Matteson, 2016; Vaengebjerg *et al.*, 2020). Additionally, recent work has demonstrated a moderately increased underlying risk of 35% in the development of haematological malignancies of both lymphoid and myeloid subtypes compared to the general population (Dommasch *et al.*, 2011; Cordtz *et al.*, 2022). Furthermore, in support of previous research, this study suggested treatment with tumour necrosis factor inhibitor (TNFi) has no effect on malignancy incidence, thus reinforcing the safety of these mainstream interventions in the context of cancer promotion (Dommasch *et al.*, 2011; Cordtz *et al.*, 2022).

1.4 The Normal Synovial Joint

The normal, healthy synovial joint, termed a 'diarthrosis', is a functionally and architecturally specialised structure that has been well defined previously in the literature (Veale and Fearon, 2015). Beneath the outer fibrous layer of the capsule surrounding the internal joint resides the synovium, which is composed of a continuous, smooth layer of cells termed the intima (lining layer) and the underlying tissue termed the subintima (sub-lining layer). Between this space, hyaluronan-rich fluid responsible for ensuring the viscosity and elasticity of the articular cartilage is maintained in addition to providing joint lubrication, thus facilitating smooth, frictionless movement (Smith, 2011; Kemble and Croft, 2021). Whilst relatively acellular, the subintima is composed of loose connective tissue containing dispersed nerve fibres and an embedded microvascular network that is not only needed to provide essential nourishment to the highly active synovium itself but additionally to enable joint access to the infiltrating peripheral immune cells in pathogenesis. In a healthy synovial joint, these blood vessels are mature and stable, thus capable of maintaining appropriate oxygenation of the joint at approx. 7% (Ng *et al.*, 2010). In contrast, the intima, a thin structure comprised of 1-3 layers, is primarily composed of two cell types derived from a macrophage (type A synoviocytes) and fibroblast-like synoviocytes (FLS)

(type B synoviocytes) cell lineage, with the quantity of Type B FLS dominating at 80%. Both of these resident cells have important roles in maintaining a homeostatic environment within the joint through phagocytic functions and SF production and volume maintenance, respectively (Smith, 2011; Orr *et al.*, 2017; Ospelt, 2017; Kemble and Croft, 2021). In the normal joint, these cells work cooperatively to create a protective shield for the joint against potential insults, with studies showing that the formation of tight junctions between the lining layer FLS and the distinct population of CX_3CR1+ tissue resident macrophages is a key factor for restricting the inflammatory reaction and maintaining a sterile joint environment (Culemann *et al.*, 2019; Hanlon *et al.*, 2024). Moreover, the FLS in the synovial sub-lining layer also assume a major role in homeostatic maintenance through the production of several essential components of the extracellular matrix (ECM) including fibronectin, laminin, proteoglycans, and collagens, thus facilitating physiological remodelling roles in addition to playing a role in the innate immune system through the sensing of joint invading pathogens (Ospelt, 2017). Due to the constant weight-bearing stresses and minor locomotive traumas the joint is subjected to, these dynamic processes including the synthesising and bone/cartilage remodelling capabilities of the FLS, in addition to the ability of the macrophages to sequester any potentially disrupting cellular debris in the intra-articular space, are particularly important in ensuring synovial integrity is maintained. Thus, it is this synovium that has been implicated as the central area of pathology in IA (Smith, 2011; Veale and Fearon, 2015; Orr *et al.*, 2017; Ospelt, 2017; Kemble and Croft, 2021).

1.5 The Inflamed Joint

It is these synovial layers that have been identified as the primary area of pathology in arthropathies of an inflammatory nature such as RA and PsA, as shown in Figure 1.2 below, with the synovium becoming progressively compromised as a consequence of unresolved inflammation (Smith, 2011; Veale and Fearon, 2015; Orr *et al.*, 2017; Veale and Fearon, 2018; Gravallese and Firestein, 2023). Whist the exact initiating trigger has yet to be elucidated, neovascularisation defined as the formation of new blood vessels, is an important early instigating factor in IA due to its governance over several key aspects of the inflammatory sequence of events. Indeed, a central pathogenic event facilitated by the expanded vascular network is the significant influx of immune cells including monocytes, T cells, B cells, and dendritic cells (DCs), from the periphery through a coordinated series of interactions with the activated endothelium. This 'leukocyte extravasation cascade' involves upregulation of several EC adhesion molecules such as E/P-Selectin, $\alpha_L\beta_2$-integrins, intracellular adhesion molecule 1 (ICAM-1), and vascular adhesion

molecule 1 (VCAM-1), in addition to the creation of a chemotactic gradient which precedes the stepwise cell tethering, rolling, activation, crawling, and finally trans-endothelial entry of the immune cells to the synovium (Zhang *et al.*, 2011; Tas *et al.*, 2016; Firestein *et al.*, 2020; Manning *et al.*, 2021).

Unfortunately, the dysfunctional nature of the newly formed blood vessels creates an imbalance between energy supply and demand, thus disrupting the immunomodulatory pathways and nurturing the creation of a highly hypoxic microenvironment within the synovium, all occurrences that are remarkably similar to observations in the cancer related tumour microenvironment (Skuli *et al.*, 2009). Consequently, these events evoke a metabolic switch of the endogenous stromal cells and infiltrating leukocytes towards a far more glycolytic and aggressive energy profile characterised by the release of a plethora of highly proinflammatory mediators including cytokines, chemokines, and matrix degrading enzymes such as matrix metalloproteinases (MMPs), along with the activation of key inflammatory related transcription factors (Fearon *et al.*, 2016; Biniecka *et al.*, 2016; Bustamante *et al.*, 2017; Fearon *et al.*, 2019; Kim *et al.*, 2020). In concert, these factors further exacerbate the inflammatory surroundings in a positive feedback loop, culminating in extensive proliferation of the synovial tissue resident FLS and macrophages, thus inducing significant thickening and hyperplasia particularly of the lining layer of the synovium (Fearon *et al.*, 2016; Biniecka *et al.*, 2016; Croft *et al.*, 2016; Ospelt, 2017; Orr *et al.*, 2017; McGarry *et al.*, 2018a; Fearon *et al.*, 2019). Indeed, in 1994, it was suggested that it was not just infiltrating immune cells but in fact the expansion of the resident stromal FLS themselves that was contributing to the heightened cell numbers in the synovial lining layer in RA (Qu *et al.*, 1994).

Due to the persistent, unresolving nature of this inflammation, which has been in part attributed to an 'imprinted aggressor' state adopted by the lining layer macrophages and FLS that renders them resistant to apoptosis, a destructive tumour-like pannus structure forms overtime which invades into the surrounding structures (Firestein, Yeo and Zvaifler, 1995; Bottini and Firestein, 2013; Ospelt, 2017; Firestein *et al.*, 2020; Kemble and Croft, 2021). This is further aggravated by the transformation of monocyte progenitors not only into proinflammatory macrophages and DCs but additionally into bone-resorbing osteoclasts, a bone erosive cell whose activity has been shown to be induced in a receptor activator of nuclear factor kappa-B ligand (RANKL) dependent manner by the combination of proinflammatory molecules present in this persistent inflammatory milieu, an event which correlates with further damage to adjacent cartilage, subchondral bone, and joint soft tissue (Sudoł-Szopińska *et al.*, 2012; Shang *et al.*, 2016; O'Brien *et al.*, 2016; Xue *et al.*, 2020; Marzaioli *et al.*, 2020).

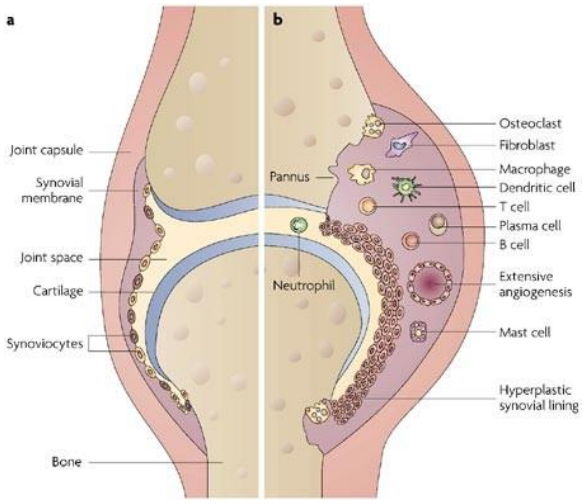

Figure 1.2. The healthy joint versus the inflamed synovial joint. (A) The healthy joint comprises a 1-3 cell thick lining layer that encapsulates the SF containing joint space, with a relatively acellular sub-lining layer. **(B)** The inflamed joint is characterised by synovial membrane hyperplasia, dysregulated neoangiogeneis, and extensive infiltration of immune cells, culminating in pannus development and destruction of adjacent cartilage/bone. Adapted from (Strand, Kimberly and Isaacs, 2007).

In recent years, the use of newer approaches including single-cell analysis and advanced RNA-seq have demonstrated the significant diversity of cells within the inflamed synovium and the considerable heterogeneity in phenotype and function of immune and stromal cell subpopulations including macrophages, T cells, and FLS (Culemann *et al.*, 2019; Alivernini *et al.*, 2020; Kemble and Croft, 2021; Hanlon *et al.*, 2023). A recent study stratified RA synovial tissues into six distinct groups based on the cell types enriched within the tissue. Moreover, an association was identified between these cell type abundance phenotypes (CTAPs) and several clinically relevant parameters/outcomes including treatment responses, thus reinforcing the importance of delineating the cellular composition of the inflamed synovium to gain novel insights into the pathogenesis of IA (Zhang *et al.*, 2023a).

1.6 Innate and Adaptive Immune Cells

As mentioned, whilst the synovium itself is the main area of pathology, the role both innate and adaptive immune cells derived from the periphery assume in perpetuating IA pathogenesis cannot be underestimated. The first responders including the neutrophil, histamine producing mast cells,

in addition to monocytes, are key innate immune cells with established roles in IA development and progression.

1.6.1 Monocyte Subsets

Monocytes represent a phenotypically heterogeneous population of immune cells derived from the bone marrow with the capability to contribute significantly to the inflammatory microenvironment through the release of a plethora of proinflammatory cytokines and the upregulation of several immune-stimulating cell-surface markers including B1/B2 integrins, HLA-DR, and Toll-like receptors (TLRs) (Rana *et al.*, 2018). One of their most defining characteristics is their highly plastic nature which under the guidance of specific environmental cues, enables them to differentiate into bone-destroying osteoclasts, in addition to macrophages and DCs (Sudoł-Szopińska *et al.*, 2012; Marzaioli *et al.*, 2020; Xue *et al.*, 2020). Studies have shown that RA CD14+ monocytes are metabolically rewired for sustained induction of proinflammatory responses that are enhanced in the circulation of RA patients compared to HC, a phenotype that was shown to precede clinical disease onset, thus introducing the hypothesis that circulatory monocytes are primed for inflammation (McGarry *et al.*, 2021). Furthermore, monocyte-derived macrophages retain this proinflammatory metabolically active phenotype when expanded *ex vivo*, an effect that is mediated through signal transducer and activator of transcription 3 (STAT3) signalling (Hanlon *et al.*, 2023). In recent years, extensive emphasis has been placed on characterising these monocyte subsets with transcriptionally distinct subsets identified based on combinations of the expression of two surface markers – CD14 and CD16 (Ziegler-Heitbrock *et al.*, 2010; Rana *et al.*, 2018). Currently, monocytes can be categorised into three subsets – classical monocytes (CD14++ CD16-), intermediate monocytes (CD14++ CD16++), and non-classical monocytes (CD14+ CD16++), with the intermediate subset demonstrating a higher prevalence in the blood and synovium of RA patients (Ziegler-Heitbrock *et al.*, 2010; Rossol *et al.*, 2012; Boyette *et al.*, 2017). Moreover, the functions implemented by these subsets are distinct with each subset assuming a different role in IA progression. Interestingly, evidence indicates classical monocytes behave as phagocytic scavenger cells in the circulation but additionally, have the potential to differentiate into both antigen presenting DCs and bone-resorbing osteoclasts under the influence of RANKL in the joint (Yang *et al.*, 2014; Boyette *et al.*, 2017; Marzaioli *et al.*, 2020). Research has shown that RA monocytes in the blood are primed to develop into monocyte-derived DCs (Mo-DCs) as evidenced by the rate of their differentiation compared to PsA monocytes, a process that can be successfully blocked in both disease states through Janus kinase (JAK)/STAT inhibition with

Tofacitinib (Marzaioli *et al.*, 2020; Marzaioli *et al.*, 2021). The literature also suggests that whilst present in both RA and PsA, these Mo-DCs exhibit phenotypic differences with RA Mo-DCs associated with an altered morphology, early dendrite formation, and significant increases in CD40 expression, all indicative of a more mature state, in addition to different migratory characteristics, distinctions which may assist in understanding the difference in RA and PsA pathogenesis (Marzaioli *et al.*, 2020; Marzaioli *et al.*, 2021). Furthermore, the intermediate subset which has been shown to correlate directly with disease activity in RA, expresses elevated levels of the proinflammatory cytokines TNF-α, IL-1β, and IL-6, and is defined as a precursor to the inflammation related M1 macrophage (Amoruso *et al.*, 2016; Boyette *et al.*, 2017; Tsukamoto *et al.*, 2017). In contrast, whilst the non-classical monocytes have been shown to be patrollers involved in the immediate inflammatory response due to their high propensity to extravasate from the vascular endothelium in instances of tissue injury, they also form the precursor for the tissue resident, inflammation-resolving, M2 macrophage (Misharin *et al.*, 2014; Thomas *et al.*, 2015; Boyette *et al.*, 2017).

1.6.2 Macrophage Subsets

Tissue resident macrophages themselves are central to the architecture of the synovial lining layer where upon appropriate stimulation, they assist in articular destruction and pannus formation through the release of an abundance of cytokines including TNF-α, IL-1β, oncostatin M (OSM), and IL-6, in addition to ECM degrading MMPs (Orr *et al.*, 2017; Firestein and McInnes, 2017). Similarly to monocytes, their highly heterogenous nature is becomingly increasingly more recognised with different subsets identified based on their polarisation status, a concept involving IL-4 that was first established in the 1900s (Stein *et al.*, 1992). Classically defined as major phagocytic cells of the joint, the literature indicates that macrophage phenotypes exist across a continuous spectrum with the two most opposing phenotypes being the 'classically activated' M1 and 'alternatively activated' M2 macrophage. Whilst the M1 macrophage is typically associated with a highly proinflammatory nature and release of vast quantities of TNF-α, IL-1, IL-6, IL-12, IL-23, and reactive oxygen species (ROS), all of which contribute to synovial inflammation, the M2 macrophage assumes a role in resolution of inflammation and wound healing through expression of IL-10, IL-1Ra, decoy IL-1RII, and TGF-β (Rana *et al.*, 2018).

Moreover, historical identification of macrophage phenotype was typically based on CD68 and CD163 expression, with the levels of CD68+ macrophages directly correlated with the degree of disease activity and inversely correlated with the synovial pO2 levels *in vivo* (Bresnihan *et al.*,

2009; Ng *et al.*, 2010; Li, Hsu and Mountz, 2012). Studies have shown that sub-lining CD68+ macrophages are the only cell type in the synovial microenvironment to significantly correlate with response to therapy indicated through reduction in disease activity score (DAS28), independent of the therapeutic intervention employed (Haringman *et al.*, 2005). However, the importance of examining novel surface markers such macrophage type I tyrosine kinase receptor (MERTK), involved in efferocytosis, are being recognised in their capacity to define functionally and transcriptionally distinct macrophage populations. MERTK has been shown by many studies to distinguish between synovial macrophage subsets and their contribution to the resolution of joint inflammation (Lu and Lemke, 2001; Waterborg *et al.*, 2018; Kemble and Croft, 2021). The evidence indicates that CCR2+ monocyte-derived MERTK macrophages are expanded during active inflammatory processes whilst in contrast, tissue resident immune regulatory MERTK+ macrophages have demonstrated enrichment in healthy synovial tissue and those in clinical remission (Waterborg *et al.*, 2018; Culemann *et al.*, 2019; Zhang *et al.*, 2019b). Indeed, the introduction of single-cell RNA sequencing (scRNA-seq)/single-cell transcriptomics in recent years has revolutionised our understanding of macrophage phenotype in disease and importantly remission. Utilising this technique, the characterisation of four discrete synovial tissue macrophages (STMs) with extremely diverse homeostatic and inflammatory related functions based on the expression of MERTK and their specific lining/sub-lining location has been performed. Amongst the typical proinflammatory subsets, this work highlighted the existence of two specific macrophage populations, defined as MerTK^{pos}TREM2^{high} and MerTK^{pos}LYVE1^{pos} respectively, which may be important in RA remission due to their potent release of anti-inflammatory lipid mediators and induction of a growth arrest specific-6 (GAS-6) repair phenotype in the aggressive FLS, thus possibly contributing to resolution of the existing synovitis (Alivernini *et al.*, 2020).

1.6.3 Dendritic Cell Subsets

Furthermore, the DC, a major antigen-presenting cell, also demonstrates a highly heterogenous nature within the joint. Whilst recognised for their important role at the interface of innate and adaptive immune responses, the literature indicates they may be critical in perpetuating IA associated inflammation through adoption of an exceedingly more pathogenic profile when exposed to the joint microenvironment. An eloquent study previously demonstrated a significant glycolytic shift in metabolism paralleled by increases in the expression of proinflammatory cytokines, chemokines, and adhesion molecules in Mo-DCs exposed to RA explant-conditioned

media (CM), thus effectively highlighting the ability of the synovial microenvironment to influence the DC phenotype (Canavan *et al.*, 2020). Whilst broad classification into conventional myeloid and plasmacytoid DCs has been well-established, recent evidence has provided more detailed categorisation based on surface marker expression and corresponding functional behaviour. The existence of functionally mature CD1c+ DCs with unique transcriptional profiles that accumulate in the inflamed IA synovium have been described, in addition to a CD141+ subset that demonstrate a superior ability to cross-present exogenous antigens and are significantly more transcriptionally active than the same population in the periphery, reinforcing the effect of anatomical location on cell behaviour (Segura *et al.*, 2013; Canavan *et al.*, 2018; Canavan *et al.*, 2021; Suwa *et al.*, 2023). In addition to conventional subsets, as previously mentioned, Mo-DCs in the context of IA are also becomingly increasingly recognised. Research has clearly outlined the leading role monocyte-derived CD209/CD14+ DCs assume in RA and PsA pathogenesis, with significant enrichment of this subset in the circulation of individuals with IA compared to HC. Moreover, this study highlighted that these circulatory CD209/CD14+ DCs are not only different in number in disease compared to healthy comparators but additionally in function, with disease associated CD209/CD14+ DCs possessing a unique chemokine receptor profile, higher cytokine producing capabilities, and a propensity to accumulate at the site of inflammation where further maturation occurs, all characteristics notably diminished in HC (Marzaioli *et al.*, 2020).

1.6.4 T and B Cell Subsets

Whilst the innate immune system is important, the adaptive arm of the immune system – namely B and T cells, are also central instigators of synovial inflammation, working cooperatively with the innate cells to drive the disease. Both T and B cells demonstrate the capability to reside in the inflamed synovium where they contribute exponentially to the inflammatory microenvironment, but additionally can circulate in the periphery perpetuating the systemic nature of inflammatory arthropathies such as RA and PsA (Veale and Fearon, 2015; Kondo *et al.*, 2018; Yap *et al.*, 2018; Tu *et al.*, 2021). Several T cell subsets have been identified and established in many autoimmune diseases, they can be broadly classified into CD4+ helper T cells and CD8+ cytotoxic T cells (Kondo *et al.*, 2018; Yap *et al.*, 2018). Whilst it was previously hypothesised that RA was predominantly a Th1-mediated disease and Th17 activity was more exclusively associated with PsA pathogenesis, it is now understood that Th17 cells play a major function in both arthropathies in early and established disease (Leipe *et al.*, 2010; Alunno *et al.*, 2015). Activated in part through their interactions with antigens presented by the autoreactive B cells, their predominant function is to

stimulate the resident stromal cells and macrophages transforming them into proinflammatory, tissue destructive cells (Yap *et al.*, 2018; Tu *et al.*, 2021). Furthermore, B cells of an autoreactive nature dominate in forms of IA where they secrete biologically significant autoantibodies including RF and ACPA, two key diagnostic markers utilised to identify RA exclusively in a clinical setting (Veale and Fearon, 2015; Yap *et al.*, 2018). Whilst B cells are not present in the same frequency in the circulation of PsA patients, it has been suggested that they still maintain a key role in cooperatively driving autoreactive T cell activation (Veale and Fearon, 2015).

The research indicates lymphoid aggregates of B and T cells are a hallmark of PsA synovium and can provide useful information regarding disease pathogenesis, with increased aggregate size linked to heightened disease activity and conversely, the disappearance of these aggregates providing a reliable marker of disease remission (Baeten *et al.*, 2005; Cañete *et al.*, 2007; Veale and Fearon, 2018). T cell subpopulations including Th1, Th2, Th17, Th9, Th22, and Tregs, constitute a vast proportion of the inflammatory infiltrate in these lymphoid aggregates in PsA where they produce an array of specific proinflammatory cytokines such as interferon-γ, IL-2, IL-4, TNF-α, and IL-17A, responsible for activating the resident cells (van Kuijk *et al.*, 2006; Veale and Fearon, 2018). Moreover, therapies targeting both CD4+ and CD8+ T cell populations have demonstrated high efficacy in PsA, highlighting the prominent role of these cells in driving this disease (Veale and Fearon, 2018).

However, recently, more emphasis has been placed on defining T cell subsets driving disease in IA beyond the classic CD4+ vs CD8+ phenotype. In this regard, using global transcriptomic analysis, we identified five synovial T cell clusters, with a significant enrichment of the CD8+ cluster in RA compared to PsA (Floudas *et al.*, 2022b). Additional groups also successfully identified a population of ex-Th17 cells, also referred to as non-classical Th1 cells, which accumulate in RA joints and demonstrate a distinct phenotype and function compared to traditional Th1 and Th17 cells (Basdeo *et al.*, 2017). Moreover, a novel subtype of CD69 and/or CD103 expressing T cells, termed tissue resident memory T cells (T_{RM}) due to their tissue-specific immune surveillance function, are a current area of intense research focus (Masopust and Soerens, 2019). Whilst an abundance of evidence indicates these T_{RM} play an essential role in driving inflammation and disease flare in both RA and PsA, the eloquent work of Povoleri *et al*. (2023) was the first to demonstrate differences in the phenotype of these cells between RA and PsA. This group showed enrichment specifically of type 17-like CD8+ CD103+ T_{RM} in addition to CD8+ non-tissue resident T cells in PsA compared to RA, further supporting the differential immunopathogenesis of these two diseases (Povoleri *et al.*, 2023).

1.7 Synovial Fibroblasts

1.7.1 Phenotype and Function

FLS are key mesenchymal/stromal cells that constitute an integral part of the healthy joint where they reside in the intima and are important producers of hyaluronan and lubrican, both essential components of SF needed for protective joint lubrication, in addition to providing support to the abundant immune cell populations (Ospelt, 2017; Koliaraki *et al.*, 2020).

Initially observed in the mid-1800s by Virchow and Duvall, and subsequently identified by Barland in 1962 as being distinct from the macrophage lineage cells located within the synovial intimal layer, Ghadially was the first to coin the term 'Type B synoviocytes' to definitively classify them within the RA synovium (Barland, Novikoff and Hamerman, 1962; Hollywell *et al.*, 1983; Molenaar, 2003; Muhl *et al.*, 2020; Li *et al.*, 2019). Further research identified their distinct morphological appearance and lineage specific markers including vimentin, collagens, platelet-derived growth factor receptor alpha/beta (PDGFRα/β) and Podoplanin (PDPN), abundance of rough endoplasmic reticulum (ER), and high propensity to synthesis hyaluronic acid and fibrous collagen, an early indicator of their normal function within a homeostatic joint (Bottini and Firestein, 2013; Li *et al.*, 2019).

However, whilst essential for joint maintenance, several studies have highlighted the critical role of chronically activated FLS in inflammatory joint pathology where they are central drivers of the formation of the thickened, invasive pannus, as first suggested by Fassbender in 1983, and irreversible destruction of synovial cartilage (Fassbender and Simmling-Annefeld, 1983; Bottini and Firestein, 2013; Bustamante *et al.*, 2017; Koliaraki *et al.*, 2020). The invasive capacity of FLS has been well defined with studies in severe combined immunodeficiency disease (SCID) mice demonstrating the ability of RA FLS to migrate to naïve cartilage, thus proposing a mechanism in which FLS may mediate the spread of destructive arthritis from affected joints to unaffected regions (Lefèvre *et al.*, 2009). A further hypothesis to explain this phenomenon was recently proposed in which researchers identified the existence of pre-inflammatory mesenchymal cells (PRIME cells) that are detectable in the blood prior to RA flares and may migrate to non-inflamed tissues, transitioning into proinflammatory FLS on arrival (Orange *et al.*, 2020). Furthermore, numerous studies have highlighted the role FLS-derived MMP-1 and MMP-3 have in matrix degradation, with RA FLS demonstrating the capability to invade through Matrigel further than OA FLS, a behaviour that correlated directly with MMP-1 and MMP- 3 expression levels (Pap *et al.*, 2000; Tolboom *et al.*, 2002; Bottini and Firestein, 2013).

Moreover, through the production and release of a plethora of proinflammatory cytokines and immune-cell recruiting chemokines including IL-6, IL-18, granulocyte-macrophage colony-

stimulating factor (GM-CSF), CCL2, in addition to growth factors such as VEGF-A and mediators of osteoclastogenesis, FLS are central in driving the destructive chain of inflammatory events (Takayanagi *et al.*, 2000; Bottini and Firestein, 2013; Zhang *et al.*, 2019b; Kondo, Kuroda and Kobayashi, 2021). Indeed, research shows that accumulation of IL-6 from FLS has the ability to drive CD4+ T cell proliferation and differentiation of Th17 cells, highlighting the immense effect of one FLS-derived cytokine alone in perpetuating RA pathogenesis (Ogura *et al.*, 2008). Much of this inflammatory behaviour is supported by the metabolic swich of FLS towards a glycolytic profile characterised by increased glucose uptake, a metabolic change driven in part by the hypoxic conditions that ensures the correct amounts of metabolic intermediates are present to facilitate anabolic processes (Biniecka *et al.*, 2016; Bustamante *et al.*, 2017; Fearon *et al.*, 2019). Stimulation with TNF or platelet-derived growth factor (PDGF), two cytokines present in abundance in the inflamed joint microenvironment, demonstrated the capacity to increase glucose metabolism and the expression of glucose transporter 1 (GLUT-1) in RA FLS, with glycolytic inhibition using 2-Deoxy-d-glucose (2-DG) or bromopyruvate (BrPa) having a significant dampening effect on FLS proinflammatory, proliferative, and invasive behaviour (Garcia-Carbonell *et al.*, 2016). Moreover, several of the metabolic intermediates generated as a consequence of the aforementioned FLS metabolic adaptations have a direct effect on their function. Lactate has been shown to promote the level of FLS invasiveness, and interestingly results in acidification of the ECM and subsequent resistance to apoptosis, another hallmark of FLS in RA (Hu *et al.*, 2012; Lee *et al.*, 2013b; Biniecka *et al.*, 2016). Conversely, succinate, a metabolite abundant in the SF of RA patients, demonstrates the ability to induce alterations to their epigenome through inhibition of histone and DNA demethylases (Xiao *et al.*, 2012; Littlewood-Evans *et al.*, 2016). Recent evidence has suggested that RA FLS may undergo epigenetic modifications that makes them more predisposed to adopt this aggressive phenotype to their surrounding inflammatory milieu, with a recent study highlighting dramatic changes to FLS DNA methylation status from the preclinical stage to established disease (Parsonage *et al.*, 2005; Bottini and Firestein, 2013; Karouzakis *et al.*, 2018). However, to date, much of the research into FLS pathogenesis has been focused on RA FLS thus currently, there is a lack of knowledge regarding FLS contribution to joint destruction in PsA.

1.7.2 Synovial Fibroblast Heterogeneity

Whilst FLS are located in different organs, studies have highlighted the distinct differences in FLS phenotype and function depending on the anatomical location in which they reside and thus stimuli and molecular cues they are exposed to, highlighting their intrinsic plastic nature (Muhl *et al.*, 2020; Kemble and Croft, 2021). For example, stark differences in the nature of the response elicited and mediators such as MMPs produced by dermal fibroblasts versus FLS upon interactions

with nearby immune cells, and their control over EC recruitment of peripheral leukocytes, have been demonstrated (Ospelt *et al.*, 2008; McGettrick *et al.*, 2009; Koliaraki *et al.*, 2020). Interestingly, it has also been established that FLS from different joints may have differential phenotypes influenced by epigenetic imprinting and particularly the expression of homeobox genes (Frank-Bertoncelj *et al.*, 2017). Moreover, although it was previously assumed that FLS located within the same tissue or joint behaved in the same manner, this has been disproved in recent years, with an explosion of research focusing on identifying and stratifying different subsets of FLS within the synovium of the same joint. Using differences in surface expression of key markers and epigenetic patterns, several distinct subsets of FLS with non-overlapping functions have been identified within the RA synovium, as shown in Figure 1.3 below (Croft *et al.*, 2016; Stephenson *et al.*, 2018; Mizoguchi *et al.*, 2018; Croft *et al.*, 2019; Muhl *et al.*, 2020; Buechler *et al.*, 2021; Micheroli *et al.*, 2022; Floudas *et al.*, 2022b; Zhang *et al.*, 2023a; McHugh, 2024). It is well-established that lining layer FLS can be characterised by high expression of typical markers such as the complement protein CD55, the proteoglycan-4 (PRG4), and the adhesion molecule VCAM-1, in addition to high expression of osteoclast associated RANKL and ECM degradative MMPs including MMP-1 and MMP-3, thus suggesting a role for them in joint lubrication, in addition to bone and cartilage destruction. In comparison, the sub-lining FLS are typically well defined by the presence of THY1 and a more inflammatory gene expression profile, with an eloquent study showing their propensity to heighten the expression of chemokines and cytokines, alongside the promotion of cellular invasion (Croft *et al.*, 2019). The different functions of FLS based on the presence/absence of THY1 and thus their categorisation as lining versus sub-lining demonstrates the integral role positional identity has on determining whether the FLS display a tendency towards a more invasive versus immune-related phenotype (Croft *et al.*, 2016; Stephenson *et al.*, 2018; Mizoguchi *et al.*, 2018; Croft *et al.*, 2019; Kemble and Croft, 2021; Buechler *et al.*, 2021; Micheroli *et al.*, 2022; Floudas *et al.*, 2022b; Rauber *et al.*, 2024). However, recent work has demonstrated that these subsets may not be completely distinct with markers not exclusively expressed on one specific FLS subtype, thus introducing the concept that FLS phenotypes exist across a continuous and dynamic spectrum (Kemble and Croft, 2021). Previous trajectory analysis revealed a gradual change in the FLS surface expression levels of THY1 and PRG4 which directly correlated with their proximity to the EC-derived instructional cues, highlighting the existence of intermediate FLS subsets and thus the challenges of definitively stratifying FLS into discrete populations (Wei *et al.*, 2020).

Moreover, although the inflammatory role of FLS has been well-established in inflammatory arthropathies, significant changes to the transcriptomic phenotype and function of

FLS once removed from the joint and by consequence the direct stimulating influence of the surrounding inflammatory mediators, have been identified, reinforcing the significance of surroundings on the pathogenicity of FLS behaviour (Zimmermann *et al.*, 2001; Neumann *et al.*, 2010; Mizoguchi *et al.*, 2018). It has been shown that repeated *in vitro* culturing has direct impacts on FLS proliferation rates in addition to alterations in various phenotypic features such as the percentage of MHC-II+ cells, whilst expanding on these findings, analysis has demonstrated significant changes in mRNA expression across later passages (Zimmermann *et al.*, 2001; Neumann *et al.*, 2010). Similarly, Wei *et al.* (2020) demonstrated a stark loss of the distinct FLS transcriptional signatures once removed from the influence of the EC-mediated delta like canonical Notch ligand 4/jagged canonical Notch ligand 1: Notch receptor 3 (DLL4/JAG1:NOTCH3) signalling interaction in the joint. However, following *ex vivo* expansion, the extent to which the FLS alter their transcriptomic profiles, the degree of homogeneity that develops, and the timescale at which this occurs in RA and PsA remains to be elucidated.

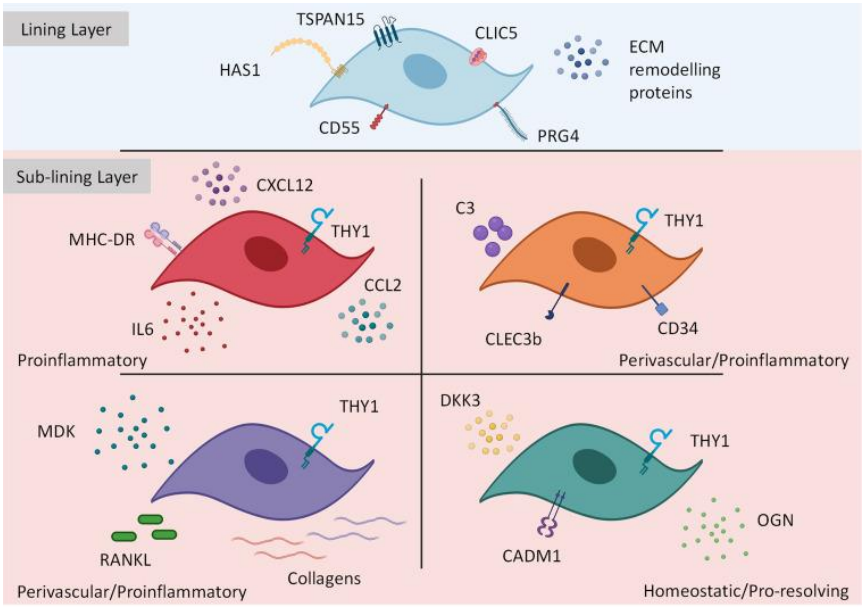

Figure 1.3. RA FLS subsets and their distinct transcriptomic and phenotypic profiles. RA FLS exist as distinct populations within the inflamed RA joint. Lining layer FLS are characterised by low THY1 and high CD55 and PRG4, with functions related to bone and cartilage degradation. In contrast, sub-lining FLS exhibit high THY1+ expression, with four differentially activated subsets previously identified based on their anatomical location within the synovial joint. This figure is based on both human and mouse model analysis. Adapted from (Kemble and Croft, 2021).

1.8 Summary

In summary, whilst categorised under the umbrella of IA, as mentioned above, there are a considerable number of defining features between RA and PsA. In particular, there are distinct morphological and quantitative features of the synovial vascularity formed through neoangiogeneis, with a higher vessel density in addition to an elongated, tortuous shape associated with PsA compared to the straight, regular branching of the RA blood vessels (Reece *et al.*, 1999; Fearon *et al.*, 2003; Veale and Fearon, 2015; Merola, Espinoza and Fleischmann, 2018). Furthermore, whilst RA is associated with a greater level of synovial lining layer hyperplasia and macrophage cell infiltration, features including lymphoid aggregate formation within the sub-lining layer is comparable between both diseases (Veale *et al.*, 1993; Veale and Fearon, 2015; Merola, Espinoza and Fleischmann, 2018; Smolen *et al.*, 2018; Veale and Fearon, 2018). Indeed, both T cells and B cells comprise an important part of this extensive inflammatory infiltrate characteristic to both arthropathies. However, the evidence shows that PsA demonstrates a T-lymphocyte predominance with markedly higher levels of Th17 associated CD8+ T cells and newly recognised type 17-like CD8+ CD103+ T_{RM} (Povoleri *et al.*, 2023). In contrast, B cells assume a more significant role in RA compared to PsA, producing the RA correlated circulating autoantibodies – ACPA and RF (Veale and Fearon, 2015; Merola, Espinoza and Fleischmann, 2018; Smolen *et al.*, 2018; Veale and Fearon, 2018).

Summary of key differences in PsA and RA

	Psoriatic arthritis	Rheumatoid arthritis
Clinical/anatomical	▸ DIP joint and axial arthritis ▸ Often asymmetrical ▸ Enthesitis common	▸ MCP and wrist joints ▸ Predominantly symmetrical
Genetic	▸ HLA Cw6 and B27 ▸ IL23 receptor	▸ HLA DRB1
Pathogenesis	▸ Absence of circulating autoantibodies ▸ Distinct vascular pathology ▸ T-lymphocyte predominance ▸ Early expression of vascular growth factors	▸ Circulating autoantibodies RF/ACPA ▸ T-lymphocyte and B-lymphocyte infiltrate ▸ Late expression of vascular growth factors
Response to therapy	▸ DMARDs, eg, methotrexate ▸ TNF inhibitors ▸ Abatacept ▸ Ustekinumab ▸ Secukinumab	▸ DMARDs, eg, methotrexate ▸ TNF inhibitors ▸ Abatacept ▸ Rituximab ▸ Tocilizumab

***Table 1.3*. Summary of the differences between RA and PsA.** Table summarising the key differences at a clinical, genetic, mechanistic, and therapeutic level between RA and PsA disease states (Veale and Fearon, 2015).

1.9 Cytokines

1.9.1 Cytokines in the Synovial Joint

Cytokines are small, membrane-bound, or soluble proteins, secreted by a vast repertoire of the immune and stromal cells in the body, that through their capacity to function as transient molecular messengers are highly involved in the coordinated regulation of immune responses of the innate and adaptive systems. Due to their pleiotropic nature, they can have a variety of inflammatory or anti-inflammatory effects that are highly context dependent and can be determined by the target cell (Kany, Vollrath and Relja, 2019). Interestingly, they can not only act locally, but additionally as autocrine, paracrine, or juxtracrine messengers, thus leading to widescale effects that are induced upon initiation of a signal transduction cascade when bound to the correct receptor on the target cell (Miyajima *et al.*, 1992). However, their function is not solely limited to inflammation regulation but additionally several other important normal, physiological phenomena including tissue growth and repair, cellular migration, differentiation, control of cell replication and cell death, in addition to both beneficial and harmful processes such as organogenesis and oncogenesis (Foster, 2001).

Many cytokines have been well-established as major orchestrators of the inflammatory environment created within IA (Kany, Vollrath and Relja, 2019). From the initial discovery of IL-1 as the first cytokine in 1974 and the subsequent identification of IL-1 in the SF of RA patients in 1982, this interleukin has been studied extensively in the years since revealing there are eleven family members, with IL-1β in particular demonstrating a significant involvement in joint inflammation in RA through the activation/proliferation of stomal and immune cells, in addition to chondrocytes (Dinarello, Goldin and Wolff, 1974; Fontana *et al.*, 1982; Dinarello, 2019; Kondo, Kuroda and Kobayashi, 2021). Furthermore, TNF, defined as a 'master regulator' of RA pathogenesis also has several significant roles in coordinating dysregulation within the inflamed synovium including the activation of both types of stromal cells, ECs and FLS, alongside immune cell activation, antibody production, osteoclast differentiation, and the stimulation of the expression of additional proinflammatory cytokines (Smolen, Aletaha and McInnes, 2016; Kany, Vollrath and Relja, 2019; Kondo, Kuroda and Kobayashi, 2021). Interestingly, TNF-stimulated production of IL-6 from FLS is a major characteristic of RA and together they assume a key role in regulating the process of bone absorption and erosion through osteoclastogenesis (Lee *et al.*, 2013a; Kany, Vollrath and Relja, 2019). Indeed, IL-6, one of the most prototypical cytokines studied, demonstrates dysregulated and continuous production in IA and has been implicated in driving inflammation and angiogenesis in the RA synovium along with several other cytokines including the hemopoietic growth factor GM-CSF, IL-18 which correlates with acute phase

response in RA tissue, interferons whose gene signature is present in multiple autoimmune diseases including RA, the chemoattracts IL-8, IL-33, IL-37, IL-17, and IL-2, amongst others (Joosten *et al.*, 2003; Tanaka and Kishimoto, 2014; Alunno *et al.*, 2017; Okamoto and Takayanagi, 2019; Kany, Vollrath and Relja, 2019; Kondo, Kuroda and Kobayashi, 2021; Cooles *et al.*, 2022). Multiple cytokines are also crucial in driving the mechanisms of disease in PsA, particular emphasis has been placed on the role of TNF-α, IL-17, and IL-23 for their downstream inflammation-associated bone erosive and tissue destructive effects observed in PsA patients (Lee and Moon, 2023). Whilst IL-23 has been identified as key to the initial development of the disease, IL-17 and TNF-α are implicated in driving the disease progression (Sherlock *et al.*, 2012; Cuthbert *et al.*, 2019; Bridgewood *et al.*, 2019; Schett, McInnes and Neurath, 2021; Lee and Moon, 2023).

Conversely, the existence of several anti-inflammatory/immunoregulatory cytokines have also been identified within the synovial environment, with two of the most well-established being IL-10 and TGF-β (Finnegan *et al.*, 2003; Sanjabi *et al.*, 2009; Kany, Vollrath and Relja, 2019). Through multiple studies conducted in collagen-induced arthritis (CIA) mouse models, the exact mechanism by which IL-10 exerts its anti-inflammatory effects are becomingly increasingly more understood and involve regulation of IFN-γ responses, suppression of M1 macrophage development, and increased differentiation and functioning of Treg populations (Finnegan *et al.*, 2003; Tao *et al.*, 2011; Carter, Rosser and Mauri, 2012; Ye *et al.*, 2014). In contrast, the defined role of TGF-β is more challenging to characterise due to its ability to function in both a proinflammatory and anti-inflammatory capacity. Whilst it plays a major role in the process of regulating peripheral tolerance and T cell suppression, paradoxically it can assume a key role in angiogenesis and can promote increased FLS MMP expression and chemotactic migration (Bira *et al.*, 2005; Pohlers *et al.*, 2007; Sanjabi *et al.*, 2009).

Therefore, as a consequence of the significant role cytokines play in perpetuating many of the processes culminating in joint damage, cytokines have been exploited as targets for developing biologics and therapeutic interventions in both RA and PsA. Unfortunately, despite their significant involvement in disease pathophysiology in RA, targets of both IL-1 and IL-17 have failed to be successful in treating patients (Kondo, Kuroda and Kobayashi, 2021). However, IL-17 inhibition has demonstrated higher levels of success in PsA treatment highlighting its more prominent role in this disease (Veale and Fearon, 2015; Merola, Espinoza and Fleischmann, 2018; Nash *et al.*, 2018). Indeed, the evidence suggests IL-17A may be critical for enhancing the disease process in PsA through its targeted effects on FLS, osteoclasts, and chondrocytes (Merola, Espinoza and Fleischmann, 2018). Similarly, IL-23 is a well characterised cytokine produced by DCs and macrophages in PsA and is implicated in the process of disease initiation due to its integral

mediatory role in the induction of inflammation in the skin and gut, with the targeting of this cytokine proving highly efficacious in relation to ameliorating clinical manifestations of PsA (Veale and Fearon, 2015; Merola, Espinoza and Fleischmann, 2018; Fragoulis and Siebert, 2022). Moreover, although TNF-α inhibitors have achieved a significantly higher level of efficacy in both diseases and are used mainstream in clinical practice, their propensity to block the activity of suppressor cells poses an additional concern. Thus blocking central components within the signalling pathways of these cytokines such as Transforming growth factor-β-activated kinase 1 (TAK1) mediator or alternatively the JAK/STAT pathway which has been very successful in RA and PsA treatment recently, may be safer long-term (Kondo, Kuroda and Kobayashi, 2021; Lee and Moon, 2023).

1.9.2 TAK1 Signalling and Blockade

TAK1 is a prominent member of the MAPKK family, with roles in the modulation of several different biological phenomena related to health and disease. Through association with various binding partners, TAK1 transduces the signals from multiple cytokines found abundantly in the inflamed joint including IL-1β, TNF-α, and IL-17, in addition to TLR ligands, resulting in the activation of two key proinflammatory signalling pathways – NF-κB and MAPKs (Takaesu *et al.*, 2001; Totzke *et al.*, 2017; Xu and Lei, 2020). Interestingly, the ability of pleiotropic cytokines including TGF-β to activate TAK1 activity have also been previously recognised, with research suggesting the interactions of TGF-β with TAK1 are specifically associated with the non-canonical, SMAD-independent signalling pathway (Yamaguchi *et al.*, 1995; Kim and Choi, 2012; Xu and Lei, 2020). The pathways used by various cytokines and proinflammatory mediators to activate TAK1 are highlighted in Figure 1.4 below.

Due to the prominent role TAK1 assume in propagating inflammatory pathways, several TAK1 inhibitors are currently being investigated in preclinical trials to combat this inflammation, with Takinib of particular interest due to its propensity to serve as a highly specific blocker of TAK1 activity (Totzke *et al.*, 2017; Panipinto *et al.*, 2021). Indeed, multiple studies have demonstrated its ability to induce a stark reduction in the expression of many proinflammatory mediators, although the exact mechanisms through which it achieves these effects remain unknown (Totzke *et al.*, 2017; Scarneo *et al.*, 2019; Panipinto *et al.*, 2021). The potential utility of Takinib induced TAK1 inhibition in malignant disease has been shown, with a recent study conducted highlighting the ability of TAK1 inhibition to trigger apoptosis of cancerous cells (Totzke *et al.*, 2017; Damhofer *et al.*, 2024). In the context of arthritis specifically, intervention with Takinib in a CIA mouse model

resulted in the alleviation of clinical manifestations including pannus formation and associated bone and cartilage resorption (Scarneo *et al.*, 2019). Moreover, in one of the primary studies to examine Takinib effects in human RA FLS, treatment with Takinib significantly reduced the expression of several IL-1β/TNF-α induced proinflammatory cytokines and chemokines including IL-6, IL-8, and MCP-1, thus diminishing the inflammatory signature greatly (Panipinto *et al.*, 2021). Cumulatively, the evidence indicates inhibition of TAK1 with Takinib may be an effective therapeutic strategy in inflammatory disease to reduce disease burden.

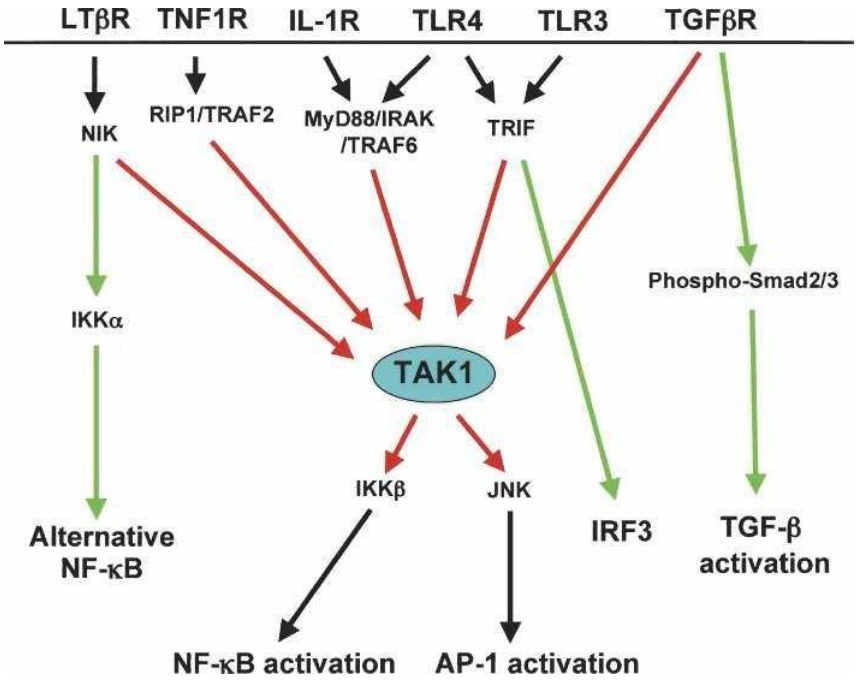

Figure 1.4. Representative image showing the role of the signalling molecule TAK1 in several inflammatory signalling pathways. Red lines show TAK1 dependent signalling pathways whilst green lines indicate pathways that are independent of TAK1. Adapted from (Shim *et al*., 2005).

1.10 Endothelial Cells and Angiogenesis

Angiogenesis, which involves the sprouting of new capillaries from vessels that already exist under the governance of pro- and anti-angiogenic stimuli, is a normal physiological phenomenon that becomes significantly dysregulated in IA, resulting in a highly dysfunctional vascular network that is unable to meet the heightened metabolic requirements of the expanding synovium and abundance of infiltrating immune cells (Kennedy *et al.*, 2010; Balogh *et al.*, 2019). In this regard, ECs, another key stromal cell that lines the internal surface of the vascular network throughout

the body, are critical, with early studies demonstrating that synovial ECs exist in a pre-primed state and are imprinted with a disease-specific tissue memory (Abbot *et al.*, 1999). The endothelium is officially classified as an endocrine organ that through specific signalling pathways, assumes responsibility for maintaining homeostatic conditions, with particular importance in wound healing. Although recent advances have uncovered significant phenotypic heterogeneity in ECs depending on the location of the vascular network, their prominent role in diseases of an inflammatory nature is apparent due to control over immune-cell infiltration into the joint (Fearon *et al.*, 2019; Lee, Shin and Simons, 2022; Urbanczyk, Zbinden and Schenke-Layland, 2022). Therefore, endothelial dysfunction is a major contributing factor to several pathologies such as DM, cardiovascular issues and importantly, autoimmune diseases including RA and PsA (Bernatova *et al.*, 2014).

Upon appropriate signalling, which relies on the correct balance of growth factors and angiogenic mediators, the ECs lose their quiescent state and become activated resulting in degradation of the ECM through catabolic enzyme release to facilitate their migration (Elshabrawy *et al.*, 2015). Concurrently, the ECs are designated transient roles – specific ECs adopt a 'tip cell' phenotype characterised by expression of an abundance of vascular endothelial growth factor receptor 2 (VEGFR2), the notch ligand DLL4, and dynamic filopodia, all of which enable the cells to respond to angiogenic cues and guide the new sprout (Gerhardt *et al.*, 2003; Blanco and Gerhardt, 2013; Balogh *et al.*, 2019; Firestein *et al.*, 2020; Lee, Shin and Simons, 2022). The remaining ECs either develop a stalk cell phenotype, which is highly proliferative and assists in forming the nascent vascular lumen that ensures the *de novo* vessels remain attached to the pre-existing capillary bed, or a quiescent phalanx cell state. Finally, following stabilisation through basement membrane synthesis and the recruitment of contractile cells important for regulating blood flow, the pericyte, new yet paradoxically highly dysfunctional blood vessel formation is completed (Blanco and Gerhardt, 2013; Elshabrawy *et al.*, 2015; Attwell *et al.*, 2016; Balogh *et al.*, 2019; Firestein *et al.*, 2020).

Although this constitutes a shared characteristic process in the early stages of both RA and PsA that facilitates peripheral immune cell influx, differences in the structure of these vascular abnormalities is a key distinguishing feature easily identifiable at the macroscopic level, with previous studies demonstrating straight, regular branching vessels in RA compared to dilated, tortuous vessels associated with the PsA joint (Reece *et al.*, 1999; Fiocco *et al.*, 2001; Fearon *et al.*, 2003). Additionally, at the microscopic level, the quantity of new blood vessels differs notably with an increased number of blood vessels observed in the PsA synovium compared to RA joints

(Ceponis *et al.*, 1998; Fearon *et al.*, 2003). These macroscopic/microscopic differences in vascularity are shown in Figure 1.5 below.

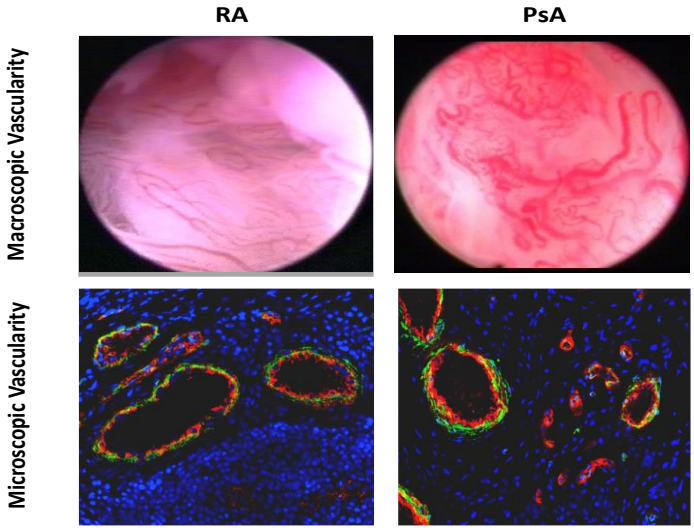

Figure 1.5. Macroscopic and microscopic images of blood vessels in RA and PsA synovial tissue. Representative macroscopic and immunofluorescent microscopic images demonstrating straight regular branching vessels in RA vs tortuous vessels in PsA, in addition to increased immature blood vessels in the PsA synovium. Images taken with permission from Prof Fearon's Lab, Molecular Rheumatology, TCD.

Studies suggest that the differential blood vessel pattern observed in RA vs PsA may be attributed to the balance of pro-angiogenic versus anti-angiogenic mediators in the synovium. Indeed, differences in the expression of growth factors have been observed, of which VEGF and angiopoietins are of particular significance (Fearon *et al.*, 1999; Reece *et al.*, 1999; Fearon *et al.*, 2003). Both VEGF and Angiopoietin-2 (Ang2) demonstrate a significant surge in expression in early PsA compared to RA and are thought to possibly dictate the distinct vascular morphology observed between the two diseases (Fearon *et al.*, 1999; Reece *et al.*, 1999; Veale and Fearon, 2018). VEGF itself is critical due to its ability to stimulate EC differentiation, proliferation, and migration, three of the central processes in angiogenesis, thus leading to it being defined in the literature as the main angiogenic 'on switch' (Blanco and Gerhardt, 2013; Claesson-Welsh, 2016). It mediates its effects through interactions with two potential receptors, Flt-1 and Flk-1, with differential effects resulting depending on the receptor bound. Interestingly, research shows that Flt-1 may be involved in EC differentiation, whilst Flk-1 assumes a role in the later stages of vascular growth (Fearon *et al.*, 2003). In addition, the presence of a high level of VEGF is critical in ensuring angiogenesis is controlled to a certain extent. Upon exposure to VEGF, DLL4 signalling

and downstream target genes are upregulated culminating in a subsequent reduction in the number of ECs adopting a tip cell phenotype, thus ultimately inducing vascular quiescence and a reduction in the number of new sprouts (Blanco and Gerhardt, 2013; Lee, Shin and Simons, 2022).

The angiopoietins Ang1 and Ang2 act through a distinct tyrosine kinase receptor – endothelial-specific receptor tyrosine kinase 2 (Tie2), which is almost exclusively located on the membranes of vascular ECs. Studies have shown that the interaction of VEGF and Ang2 destabilises blood vessels, promoting vessel sprouting and thus the formation of the immature vessels (Fearon *et al.*, 2003; Kennedy *et al.*, 2010; Gao *et al.*, 2013; Gao *et al.*, 2015). In contrast, as the blood vessel matures, its reliance on VEGF and Ang2 are reduced significantly and additional maturation factors come to the forefront, one of which is Ang1, which promotes the recruitment of pericytes and thus stabilisation of the newly synthesised blood vessel (Firestein *et al.*, 2020). However, although the complementary involvement of angiopoietins and VEGF is integral, neoangiogenesis is a coordinated process requiring numerous other mediators that have been implicated both directly and indirectly at different stages including TGF-β, neural cell adhesion molecule (NCAM), fibroblast growth factor-1/2 (FGF-1/2), PDGF, and proteases, along with several cytokines such as TNF-α, OSM, IL-8, and IL-17A, in addition to the adhesion molecules endothelial-leukocyte adhesion molecule-1 (ELAM-1), VCAM-1, and ICAM-1 (Fearon *et al.*, 2003; Balogh *et al.*, 2019; Fromm *et al.*, 2019; Firestein *et al.*, 2020). Additionally, the chemokines CCL2 and CX3CL1 have also been shown to be involved through their chemotactic recruitment of immune cells which further exacerbate the inflammatory angiogenesis, highlighting an indirect mechanism by which angiogenesis can be affected (Tas *et al.*, 2016).

1.11 Fibroblasts, Endothelial Cells, and Angiogenesis

Interestingly, within the inflamed synovial microenvironment of both RA and PsA joints, FLS have been identified as having a pivotal role in the angiogenic process through their secretion of necessary angiogenic growth factors needed to interact with the ECs, highlighting the significance of stromal-stromal cell interactions in exacerbating both forms of IA. Many of the pathways associated with the transformed FLS, including several proinflammatory cytokines such as TNF, IL-6, IL-8, and IL-17, JAK/STAT activation, and hypoxia related hypoxia inducible factor (HIF), have all been shown to contribute to the promotion of VEGF synthesis and release (Elshabrawy *et al.*, 2015; Lu *et al.*, 2017; He *et al.*, 2020). Whilst Matrigel implants exhibit higher levels of vascularisation in mouse models containing RA FLS CM compared to OA and HC, direct comparisons of RA and PsA FLS CM indicate the induction of a more robust angiogenic phenotype

upon exposure of ECs to PsA FLS CM (del Rey *et al.*, 2009; Fromm *et al.*, 2019). Within the PsA joint microenvironment, higher levels of FLS secreted VEGF-A, thymic stromal lymphopoietin, Flt-1, Tie2, matrix degrading MMP-1, MMP-3, and MMP-9, in addition to 6-phosphofructo-2-kinase/fructose-2,6-biphosphatase 3 enzyme (PFKFB3), which has been implicated in angiogenesis though its stimulation of glycolysis, have been detected, the combination of which result in significantly elevated levels of EC tube formation, migration, and invasion (Fromm *et al.*, 2019). Thus, this study introduces the concept that the inflammatory microenvironment of the joint can induce differential EC function, with soluble mediators present in the PsA joint prompting the development of a more pathogenic, pro-angiogenic EC phenotype than that observed in the RA joint, an observation which may in-part contribute to the distinct vascular morphology observed in both disease joints.

1.12 Cellular Metabolism

Cellular metabolism encompasses a multitude of biochemical processes that coordinate to ensure the balance between energy production and energy expenditure is maintained at appropriate levels to facilitate normal cellular function and maintenance of a homeostatic state. Through finely tuned signalling networks, eukaryotic cells can adapt rapidly to alterations in the environment to switch from anabolic states to catabolic states, a conversion that is bidirectional depending on the available metabolites and specific job required (Gomes and Blenis, 2015). However, due to the heavy reliance on tightly regulated metabolism for normal cellular functioning, the connection between metabolic perturbations and different disease phenotypes is becomingly increasingly more recognised, particularly in the context of diseases of an inflammatory nature, including RA and PsA (Fearon *et al.*, 2019; Wang *et al.*, 2020c; Tandon *et al.*, 2021; Wang, Jiao and Zhang, 2021; Fearon *et al.*, 2022; Meyer *et al.*, 2024).

Whilst several overlapping metabolic pathways can be utilised by cells to generate the variety of substrates they require to perform their range of catabolic and anabolic activities, including the pentose phosphate pathway, fatty acid metabolism, and importantly amino acid metabolism, the two most prominent metabolic pathways involved in generating the required cellular energy are oxidative phosphorylation and glycolysis. Whilst both pathways generate energy in the form of adenosine triphosphate (ATP), oxidative phosphorylation is far more efficient, creating approx. thirty-six molecules of ATP using the electrochemical gradient created by the electron transport chain in the inner mitochondrial membrane (Fearon *et al.*, 2019; Fearon *et al.*, 2022). Under normal homeostatic conditions, glucose entering into the cells is converted

into pyruvate, a molecule whose fate relies predominantly on the presence or absence of oxygen within the cellular environment. In suitable aerobic conditions, decarboxylated pyruvate feeds into the tricarboxylic acid (TCA) cycle, generating the necessary electron carriers required for oxidative phosphorylation to occur - nicotinamide adenine dinucleotide (NADH) and flavin adenine dinucleotide-2 (FADH2). In contrast, under anaerobic conditions, the glycolytic pathway is instigated with activation of several key enzymes including lactate dehydrogenase A (LDHA), pyruvate kinase M2 (PKM2), glyceraldehyde-3-phosphate dehydrogenase (GAPDH), and hexokinase 2 (HK2), resulting in the conversion of glucose into two individual pyruvate molecules. In the absence of oxygen, this pyruvate is unable to enter the TCA cycle so instead undergoes conversion within the cytosol to lactate by lactate dehydrogenase (LDH), a process which culminates in the generation of two ATP molecules (Fearon *et al.*, 2022). Interestingly, many immune cells such as natural killer cells, monocytes, and macrophages switch towards a glycolytic profile under inflammatory influences, with this alteration driving their pathogenic activity (Pålsson-McDermott and O'Neill, 2020; Wang *et al.*, 2020c; Hanlon *et al.*, 2022). Although inefficient in comparison to oxidative phosphorylation, due to the rapid nature at which energy can be produced, the evidence indicates this glycolytic pathway is favourably adopted by cells under conditions of chronic inflammation, high stress, or importantly low oxygen, all events directly associated with the environment observed within the inflamed joint (Senyilmaz and Teleman, 2015; Bustamante *et al.*, 2017; McGarry *et al.*, 2017; Wang *et al.*, 2020c; Fearon *et al.*, 2022). A summary of the metabolic pathways utilised by the activated cells to generate energy within the inflamed synovial joint are highlighted in Figure 1.6 below.

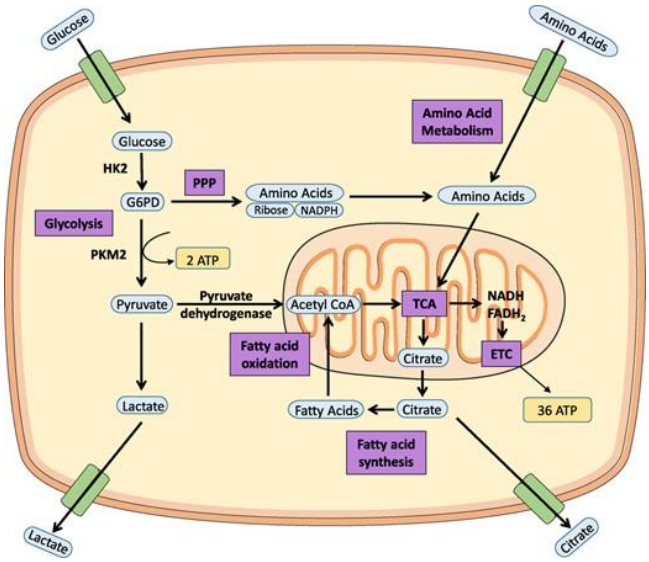

Figure 1.6. Schematic of the key metabolic pathways in the inflamed synovium. GLUT-1 transporter facilitates the entry of glucose into the cell where it enters the glycolytic cycle. Through glycolytic enzymes such as HK2 and PKM2, pyruvate is generated which is either secreted from the cell or enters the TCA cycle. The TCA cycle generates NADH and FADH which feed into the electron transport chain, resulting in the production of 36 molecules of ATP. Other metabolic pathways and intermediates including fatty acid oxidation, amino acid metabolism, and the pentose phosphate pathway, can contribute to further energy production. Adapted from (Fearon *et al.*, 2019).

1.13 Metabolism and Hypoxia

The original suggestion that the inflamed joint microenvironment is profoundly lacking in adequate oxygen levels or 'hypoxic,' was first proposed in the 1970s by Lund-Olesen whom demonstrated significantly reduced levels of oxygen partial pressure (pO_2) in the SF of RA compared to OA individuals (Lund-Olesen, 1970). Expanding on this, a direct correlation has been shown between tpO_2 levels and the level of joint inflammation, specifically immune cell infiltrates and proinflammatory cytokine production (Ng *et al.*, 2010). Subsequent studies additionally showed that joint hypoxia inversely correlates with an abundance of other disease related factors including blood vessel maturity, synovitis, mitochondrial DNA damage, and the extent of oxidative stress (Kennedy *et al.*, 2010; Biniecka *et al.*, 2011; Harty *et al.*, 2012). Moreover, research has shown an association between hypoxia induced glycolysis and increased cellular invasion and pannus formation, highlighting the clear link between hypoxia, metabolism, and overall pathogenic cell behaviour, thus providing insights into the complex pathogenesis of IA (Biniecka *et al.*, 2016).

As the established powerhouse of the cell, mitochondrial dysfunction has been implicated as a direct contributor to the dysregulated bioenergetics observed in the inflamed joint (Biniecka 2011). A plethora of studies have shown correlations between synovial inflammation, in part mediated by NLRP3 inflammasome activation, and heightened levels of mitochondrial DNA mutations, respiratory chain defects, and increased apoptosis (Zhou *et al.*, 2011; Biniecka *et al.*, 2011; Harty *et al.*, 2012; McGarry *et al.*, 2017). Upon encountering these energy defects, evolutionarily conserved responses are engaged with the primary transcriptional responses mediated by HIF-1α, the master regulator of oxygen homeostasis which has been shown by several studies to be elevated significantly in the joint (Giatromanolaki *et al.*, 2003; Biniecka *et al.*, 2016; Guo and Chen, 2020; Fearon *et al.*, 2022). Through the elevated expression of glucose transporters and glycolytic enzymes such as GLUT-1, LDHA, GAPDH, and PKM2, HIF-1α can further drive the metabolism of cells towards a glycolytic phenotype, thus worsening the levels of hypoxia and ultimately creating a positive feedback loop (Majmundar, Wong and Simon, 2010; Biniecka *et al.*, 2016). Moreover, through its interactions with several additional proinflammatory and metabolic related signalling molecules in the joint including STAT3, PI3K-AKT, NF-κB, and NOTCH-1, HIF-1α stimulates a vast range of pathways involved in cellular inflammation, angiogenesis, and invasion (Ahn *et al.*, 2008; Taylor, 2008; Oliver *et al.*, 2009; Gao *et al.*, 2013; Gao *et al.*, 2015; McGarry *et al.*, 2017; McGarry *et al.*, 2018a; Fearon *et al.*, 2019; Fearon *et al.*, 2022). Interestingly, a predominant characteristic of the invasive, inflammatory phenotype of RA FLS that discriminates them from OA FLS, is alterations in key metabolic pathways related to glucose metabolism including glycolysis and oxidative phosphorylation, in addition to amino acid metabolism, the balance of which are highly dependent on influences in the surrounding microenvironment (Ahn *et al.*, 2016; Garcia-Carbonell *et al.*, 2016; Bustamante *et al.*, 2017; Bustamante *et al.*, 2018; Petrasca *et al.*, 2020; Gallagher *et al.*, 2020). For example, under hypoxic conditions, RA FLS demonstrate increased expression of invasion promoting MMPs, chemokines, and proinflammatory cytokines including MMP-1, MMP-3, IL-8, TNF-α converting enzyme, and stromal cell-derived factor-1 expression, whilst protein levels of tissue inhibitor of metalloproteinase 1 (TIMP-1) are reduced (Hitchon *et al.*, 2002; Charbonneau *et al.*, 2007; Cha *et al.*, 2003; Ahn *et al.*, 2008; Petrasca *et al.*, 2020). In addition to HIF-1α, several metabolic intermediates generated as a consequence of the heightened cellular glycolysis within the inflamed joint including lactate, glutamine, and succinate, have also been shown to directly activate both immune and stromal cells, further perpetuating the inflammatory response, with some even assuming the role of secondary autoantigens (Haas *et al.*, 2015; Michopoulos *et al.*, 2016; Biniecka *et al.*, 2016; Pucino *et al.*, 2017; Li *et al.*, 2018b; Fearon *et al.*, 2019; Fearon *et al.*, 2022; Hanlon *et al.*, 2022). Succinate

has a direct effect on inflammatory macrophages by promoting HIF-1α-induced IL-1β production and ROS generation, an effect also regulated in part by itaconate (Mills *et al.*, 2016; Lampropoulou *et al.*, 2016). Similarly, glutamine metabolism has been shown to be central to the inflammatory response by driving the balance of T cells towards the Th17 subset, with blockade of this glutamine pathway exhibiting anti-proliferative and invasive effects on RA FLS in both human and murine models (Garcia-Carbonell *et al.*, 2016; Takahashi *et al.*, 2017; Johnson *et al.*, 2018).

Specifically in relation to FLS, a hallmark characteristic of FLS in the inflamed joint is their invasive phenotype characterised by a highly active metabolic state driven by the hypoxic conditions (Fearon *et al.*, 2019; Pucino *et al.*, 2020; Fearon *et al.*, 2022; Hanlon *et al.*, 2022). Alongside their previously mentioned glycolytic transformation, this heightened metabolism in activated FLS has been effectively demonstrated by several metabolic profiling studies revealing increases in other forms of metabolism including sugar metabolism, amino acid metabolism, lipid metabolism, and glutamine metabolism (Guma *et al.*, 2015; Ahn *et al.*, 2016; Takahashi *et al.*, 2017; Fearon *et al.*, 2019; Pucino *et al.*, 2020; Fearon *et al.*, 2022; Hanlon *et al.*, 2022). In addition to the aforementioned HIF-1α, the metabolic sensor mammalian target of rapamycin (mTOR) has proven instrumental in driving RA FLS invasive and proliferative behaviour through enhanced glycolysis, a metabolic effect that can be abrogated upon the addition of the mTOR inhibitor; rapamycin (Laragione and Gulko, 2010; Barker *et al.*, 2023). Moreover, FLS metabolic capacity can be highly influenced by interactions with immune cells in the inflamed joint with studies demonstrating a rapid shift towards aerobic glycolysis in FLS and subsequent heightened invasive capacity upon exposure to CD4+ T cell CM, an effect that can be reversed through glycolytic inhibition with 2-DG (Petrasca *et al.*, 2020).

In summary, this highly hypoxic milieu within the joint and heightened metabolic demands results in the forced adaption of infiltrating and resident cells, including FLS, to a hypermetabolic state which drives their function, a newly emerging and exciting concept referred to as ‘metabolic reprogramming' (Aghakhani, Soliman and Niarakis, 2022).

1.14 Metabolism and Angiogenesis

In recent years, immense emphasis has been placed on the crucial role metabolic shifts assume in providing the biosynthetic requirements needed for the angiogenic process within the inflamed joint. Despite the superior levels of ATP produced through oxidative phosphorylation, it has been shown that the primary energy pathway utilised within the joint by ECs of the tip and to a lesser

extent the stalk cell phenotype, is glycolysis (Firestein *et al.*, 2020). The conversion of glucose into lactate generates 85% of their total ATP requirements associated with phenotypic differentiation into tip and stalk cell phenotypes, a process which is inhibited with toxic effects upon suppression of glycolysis with the potent glycolytic inhibitor 2-DG (Wang *et al.*, 2011; Firestein *et al.*, 2020). The exact reason for the preference for EC glycolytic metabolism in tip cells specifically is unknown but may be based on a combination of the following lines of evidence, all related to the easier facilitation of angiogenesis (Eelen *et al.*, 2018). Firstly, glycolysis is a direct producer of the aforementioned lactate, a by-product which can double as a pro-angiogenic signalling molecule whilst additionally evoking glycosylation, a process that potentiates VEGFR-2 and NOTCH signalling (Végran *et al.*, 2011; Ruan and Kazlauskas, 2013; Croci *et al.*, 2014). Moreover, a reliance on glycolysis ensures that oxidative stress inducing ROS levels are kept low whilst O_2 levels remain adequate for surrounding tissue perfusion. Additionally, as external glucose is non-limiting, glycolysis is capable of producing ATP at a significantly faster rate than oxidative phosphorylation (Parra-Bonilla *et al.*, 2010; Locasale and Cantley, 2011). Finally, by already using an anaerobic form of energy, the ECs are capable of migrating towards hypoxic regions when forming blood vessels without having to alter their metabolism any further, a method used by tumour cells also to support invasion (Gatenby and Gillies, 2004).

Angiogenesis itself is a major contributor to the generation of the hypoxic microenvironment within the inflamed joint. Despite the increased vascular networks observed in both RA and PsA, the *de novo* blood vessels are highly dysfunctional, failing to supply adequate nutrients to the rapidly expanding synovium, thus producing a microenvironment severely deficient in oxygen. Interestingly, the work of J. Folkman first introduced the concept of hypoxia being a significant driving factor for angiogenesis itself, a hypothesis that has now been well-established in forms of IA with existing research showing that synovial blood vessel instability is associated with oxidative damage and with low levels of synovial pO_2 (Folkman, 1971; Biniecka *et al.*, 2016). When working alone and in combination, both hypoxia and oxidative stress are pivotal in inducing EC tube formation, migration, and proinflammatory mediators, in addition to VEGF and activation of intracellular Notch-1IC and its ligand DLL-4 which has been implicated as central to the process of tip cell selection and activation (Fearon *et al.*, 2003; Kennedy *et al.*, 2010; Gao *et al.*, 2013; Weyand and Goronzy, 2017). Indeed, an eloquent study demonstrated that through inhibition of a key hypoxia-induced enzyme enriched on the synovial ECs in RA, glucose 6-phosphate isomerase (G6PI), release of FLS VEGF was reduced, resulting in blockade of hypoxia driven angiogenesis (Lu *et al.*, 2017). Moreover, in animal models of arthritis, the activity of the metabolic intermediate succinate has demonstrated strong pro-angiogenic effects through its

governance over VEGF production. Studies have identified succinate and its cognate receptor G protein-coupled receptor-91 (GPR91) as potent mediators of vascularisation in the context of the retina, with additional research illustrating the significance of succinate in VEGF-dependent HIF-1α pathways in the induction of synovial angiogenesis itself (Sapieha *et al.*, 2008; Li *et al.*, 2018b). The key angiogenic mediator VEGF has itself proven to further enhance EC glycolytic flux and promote the expression of several enzymes and transporters in the glycolytic pathway including GLUT-1, LDHA, and PFKFB3 (Peters *et al.*, 2009; Parra-Bonilla *et al.*, 2010; De Bock *et al.*, 2013). Thus, the continual cycle of hypoxia and angiogenesis only serves to drive synovial expansion and dysregulation in a self-perpetuating manner.

Moreover, countless studies have reinforced the bidirectional connection between EC glycolysis and synovial angiogenesis by demonstrating how blockade of glycolytic mediators and metabolites can supress the levels of angiogenesis. In the tumour microenvironment, blocking the influx of lactate through the monocarboxylate transporter 1 attenuates the activation of HIF-1α and subsequently reduces the levels of tumour angiogenesis (Sonveaux *et al.*, 2012). Furthermore, substantial evidence exhibits impairment in *in vitro* EC vessel sprouting, branching, and outgrowth following blockade of the glycolytic regulator PFKFB3 with the small molecule inhibitor (3-(3-pyridinyl)-1-(4-pyridinyl)-2-propen-1-one) (3PO), whilst additionally, PFKFB3-silenced human umbilical vein endothelial cells (HUVECs) demonstrate a significant loss in the ability to acquire a tip cell phenotype (De Bock *et al.*, 2013; Schoors *et al.*, 2014). Interestingly, Biniecka *et al.* (2016) highlighted its propensity to not solely affect ECs but additionally FLS, with the results indicating that 3PO administration significantly reduced activation of HIF-1α, pSTAT3, and Notch-1IC, in addition to angiogenic tube formation (Biniecka *et al.*, 2016). The use of 3PO has demonstrated preliminary success in attenuating pathogenic angiogenesis in several models of inflammation including IBD and importantly, skin psoriasis, highlighting the potential of targeting glycolysis as an anti-angiogenic therapy (Schoors *et al.*, 2014).

In conclusion, more extensive knowledge of metabolic disturbances in pathological conditions such as RA and PsA and their constant crosstalk with immune and stromal cells might offer novel therapeutic opportunities, particularly in early disease.

1.15 MicroRNA

1.15.1 MicroRNA Background

Endogenous microRNAs (miRNAs) constitute a unique class of dynamic RNAs of a non-coding nature that assume a major role in normal post-transcriptional processes, namely gene silencing,

within the cellular environment (O'Brien *et al.*, 2018). The field of molecular biology was revolutionised following the discovery of the miRNA lin-4 in 1993 by the Ambros and Ruvkun groups in *Caenorhabditis elegans*. Whilst continuously increasing in number, a recent validation study extrapolated 2300 true human mature miRNA, thus reinforcing the understanding that the majority of gene transcripts contained within the genome are not directly translated into protein themselves but instead are processed into small, non-coding RNA of which miRNA are one of the most important (Alles *et al.*, 2019). Comprising 21-25 nucleotides in length, miRNA are ubiquitously expressed in eukaryotic cells and demonstrate a remarkable level of evolutionary conservation thus supporting their central role in gene regulation (Ha and Kim, 2014; O'Brien *et al.*, 2018). Whilst critical for normal physiological phenomena including cell proliferation, cell differentiation, immune functioning, migration, and reproduction, their aberrant expression is becomingly increasingly recognised in the context of multiple human diseases including cancer and importantly, inflammatory driven autoimmune related arthropathies such as RA (Liu *et al.*, 2020; Smolarz *et al.*, 2022; Das and Rao, 2022; Nag *et al.*, 2023).

1.15.2 MicroRNA Biogenesis

miRNA biogenesis is a multi-step process involving sequential activity of a number of different enzymes that occurs through canonical and non-canonical pathways. Whilst miRNA biogenesis predominantly occurs via the canonical pathway, non-canonical synthesis is also possible and is achieved through the activity of various combinations of the key proteins involved in the canonical pathway (Ha and Kim, 2014; O'Brien *et al.*, 2018).

In relation to the dominant canonical pathway, the process is initiated following the generation of a primary miRNA transcript which is transcribed typically through the activity of RNA polymerase II, although the literature reports similar effects with RNA polymerase III (Borchert, Lanier and Davidson, 2006). Within the nucleus, this pri-miRNA is subsequently cleaved by the heterodimeric initiator complex consisting of the enzyme Drosha and DiGeorge syndrome critical region 8 (DGCR8) to generate precursor miRNA (pre-miRNA) (Denli *et al.*, 2004; Ha and Kim, 2014; Ipsaro and Joshua-Tor, 2015; O'Brien *et al.*, 2018). By recognising a specific N6-methyladenylated GGAC, DGCR8 acts as a guide for appropriate positioning of DROSHA, thus facilitating the generation of 70nt pre-miRNA though enzymatic cleavage (Alarcón *et al.*, 2015). The current available database of miRNAs has identified the existence of 1881 human pre-miRNAs, with origins of both intragenic and intergenic nature (Kozomara and Griffiths-Jones, 2014). The evidence indicates that approximately 54% are produced from the intergenic non-coding pri-miRNA

transcripts and thus are regulated by their own promoters, with the remaining 46% originating from the excision of introns of protein-coding genes (de Rie *et al.*, 2017).

Through the activity of nuclear exportin 5 and ran-guanosine triphosphate, this precursor miRNA undergoes exportation to the cytoplasmic region where its characteristic hairpin secondary structure consisting of a double stranded stem approximately 33 base-pairs long and a terminal loop, enables it to be recognised and further processed by the endoRNase Dicer to release the mature miRNA Duplex competent for RNA-induced silencing complex (RISC) loading (Ha and Kim, 2014; Ipsaro and Joshua-Tor, 2015; O'Brien *et al.*, 2018). Subsequently, this RNA duplex is unwound, generating the 'guide' and 'passenger' strands, a designation that is based primarily on their thermodynamic stability with a preference for the strand with the least stable 5' hydrogen bonds of the mature form to assume the role as 'guide' (Kwak and Tomari, 2012; Ha and Kim, 2014; O'Brien *et al.*, 2018). To achieve this, the strands are loaded into the Argonaute (AGO) family of proteins (AGO2 specifically in humans), in an ATP-dependent fashion, culminating in the formation of the microRNA-induced silencing complex (miRISC), a complex also ultimately generated as an end-product of the non-canonical pathway (Yoda *et al.*, 2010; Ha and Kim, 2014; Ipsaro and Joshua-Tor, 2015; O'Brien *et al.*, 2018; Sadakierska-Chudy, 2020). This complex is essential for the translational interference of miRNAs as the 'guide' strand effectively directs the miRISC to the 3' untranslated region (UTR) of the intended target mRNA where through imperfect base-pairing, it enables appropriate action to occur (Ha and Kim, 2014; Ipsaro and Joshua-Tor, 2015; O'Brien *et al.*, 2018). A diagrammatic representation of the sequential steps of miRNA biogenesis are demonstrated in Figure 1.7 below.

1.15.3 MicroRNA Mechanism of Action

miRNA localization within the cell enables this interaction with the target mRNAs where they induce mRNA post-transcriptional regulation either directly or indirectly through 3 primary mechanisms – the induction of mRNA cleavage or decay or alternatively, evoking translational repression directly, all of which culminate in a negative impact on gene expression (Ipsaro and Joshua-Tor, 2015; O'Brien *et al.*, 2018).The interaction between the miRISC and its target is mediated by the 'guide' strand itself which contains a specific region named the 'seed sequence,' comprising highly conserved nucleotides between 2 and 8 from the 5' UTR end. This 'seed sequence' base-pairs with the miRNA recognition elements (MREs) situated on the mRNA targets at the 3'UTR, with the level of complementarity i.e. perfect/partial between these two regions, determining the functional outcome mediated by the miRNA (Ipsaro and Joshua-Tor, 2015;

O'Brien *et al.*, 2018; Sadakierska-Chudy, 2020). For successful cleavage to be induced, there must be full complementarity between the 'seed sequence' and the MRE, thus activating the endonuclease activity of AGO2 (Jo *et al.*, 2015; O'Brien *et al.*, 2018; Kilikevicius, Meister and Corey, 2021). However, incomplete base-pairing is more prevalent in animal models and primarily results in either mRNA decay or direct translational inhibition (Bartel, 2009; O'Brien *et al.*, 2018; Kilikevicius, Meister and Corey, 2021). Indeed, incomplete base-pairing inhibits the activity of AGO2 and instead facilitates the recruitment of GW182 protein family, a protein capable of promoting mRNA deadenylation thus rendering it susceptible to exoribonuclease 1 degradation (Behm-Ansmant *et al.*, 2006; Braun *et al.*, 2012; O'Brien *et al.*, 2018). A previously conducted study highlighted the vital role this pathway assumes in the gene repression mediated by miRNA with 66-90% of the translational repression arising from mRNA decay (Eichhorn *et al.*, 2014). Furthermore, gene translation inhibition can occur in a more direct manner as a consequence of the failure of different rate-limiting steps essential for efficient translation including interference with the initiation factors 4A, elongation, or early termination, all of which can simply occur as a consequence of a bulge induced by a single nucleotide mismatch between the miRNA and the mRNA target (Mathonnet *et al.*, 2007; Carthew and Sontheimer, 2009; Fukao *et al.*, 2014; Oliveto *et al.*, 2017). Interestingly, whilst gene suppression is more commonly associated with the function of miRNA, several studies have also demonstrated potential evidence for the role of miRNA in gene upregulation for example during cell cycle arrest, in quiescent cells such as oocytes, during instances of amino acid starvation, or following binding of the miRNA to the 5'UTR region/promoter of the target gene, thus suggesting that miRNA-mediated upregulation of gene expression can occur but is highly contextually specific (Vasudevan and Steitz, 2007; Ørom, Nielsen and Lund, 2008; Shimakami *et al.*, 2012; Vasudevan, 2012; Dharap *et al.*, 2013; Bukhari *et al.*, 2016). Furthermore, the complexity of elucidating miRNA gene control is enhanced by the fact that not only can a single mature miRNA bind many different target mRNAs, with each miRNA estimated to be capable of recognising approximately 100-200 target sites of the human transcriptome, but additionally, a single mRNA transcript can be bound and regulated by multiple miRNA (Sadakierska-Chudy, 2020; Kilikevicius, Meister and Corey, 2021). Thus, it is apparent that miRNA-mediated gene regulation is highly dynamic and is a fine-tuned balance between maintenance of normal physiological states and the development of pathological states. A brief summary of the mechanism by which miRNA control gene expression is shown in Figure 1.7 below.

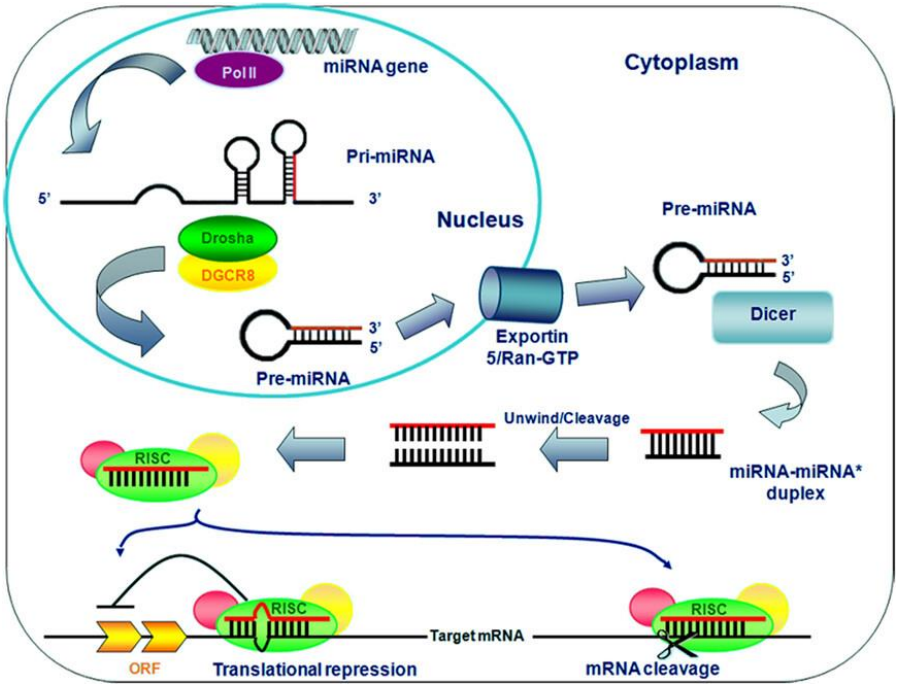

Figure 1.7. Schematic summary of miRNA biogenesis and mechanisms of action. In the biogenesis process, Pol. II transcribes miRNA into pri-miRNA. The pri-miRNA is then cleaved into pre-miRNA by the Drosha/DGCR8 microprocessor complex, before entering the cytoplasm where the Dicer enzyme generates the mature miRNA duplex. This RNA duplex is then unwound, generating a 'guide' and a 'passenger' strand, forming the functional miRISC complex. Mechanism of action of miRNAs: The miRISC complex bind the 3'UTR region of a target gene through base pairing, resulting in either translational repression or mRNA degradation. Adapted from (Rani and Sengar, 2022).

1.15.4 MicroRNA in Disease

Although well-established in relation to their gene regulatory functions and maintenance of homeostatic conditions, extensive research has implicated aberrant and dysregulated expression of these cellular and extracellular miRNAs in the pathogenesis of many human diseases. To date, a robust body of research has demonstrated the involvement of miRNAs in cancer, and particularly their role in mediating the cellular processes of migration and invasion involved in tumorigenesis though regulation of pathways including epithelial-mesenchymal transition (EMT), Wnt/Hippo signalling, TGF-β, PI3K/AKT/mTOR, FoxO, JAK/STAT, PD-1/PD-L1, and HIF-1 (Tang *et al.*, 2017a; Liu *et al.*, 2018; Contreras-Rodríguez *et al.*, 2023; Zhu *et al.*, 2023; Chakrabortty *et al.*, 2023). Interestingly, certain miRNA expression profiles have also proven to be valuable biomarkers in cancer diagnosis as a consequence of their ability to classify cancer groups and subsets (Lu *et al.*, 2005; Garzon, Calin and Croce, 2009a; Kim and Croce, 2023; Chakrabortty *et al.*, 2023). In this regard, a large number of clinical trials are currently ongoing investigating the diagnostic potential

of various miRNAs in relation to several forms of cancer including miR-155 to diagnose non-muscle-invasive bladder cancer, let-7a and miR-124 to diagnose non-Hodgkin's lymphoma and acute leukaemia, and the ability of 10 miRNAs to define undetermined types of thyroid cancer (Kim and Croce, 2023).

Moreover, recently, miRNAs as potential biomarkers are becoming increasingly more understood in the context of autoimmune diseases due to their central involvement in the maintenance of immunological tolerance in both peripheral and central lymphoid organs, in addition to their governance over a myriad of inflammatory processes and signalling pathways (Simpson and Ansel, 2015; Das and Rao, 2022). Several studies have demonstrated a strong association between autoimmune diseases including systemic lupus, type-1 DM, multiple sclerosis (MS), and IBD, where their presence and abnormal behaviour is associated with characteristic patterns of disease pathogenesis (Nag *et al.*, 2023). Importantly, miRNA dysregulation has also been acknowledged in the context of RA and PsA, where it is currently being intensely investigated for diagnostic, prognostic, and therapeutic purposes (Shaikh *et al.*, 2023; Nag *et al.*, 2023).

An abundance of studies exist demonstrating the importance of miRNA activity in driving RA pathogenicity specifically, with a recent analysis highlighting the following miRNA as the most frequently published miRNA in this field; miR-146, miR-155, miR-223, miR-21, miR-125, miR-124, and miR-26 (Shaikh *et al.*, 2023). Indeed, miR-155 and miR-146 constitute two of the most well reported miRNA in the context of rheumatic disease, with several studies highlighting their increase in the synovial tissues, lymphocytes, and whole blood obtained from RA patients compared to HC and/or OA comparators (Stanczyk *et al.*, 2008; Feng *et al.*, 2011; Liu *et al.*, 2022). Dysregulation of these miRNA have been shown to exert differential effects on different cell types depending on the context and miRNA of interest. A more down-regulatory role of miR-146a has been demonstrated in RA driven inflammatory processes through mechanisms such as suppression of RA FLS proliferative and inflammatory functions, whilst additionally pushing macrophages polarisation towards the M2 phenotype (Huang *et al.*, 2016; Liu *et al.*, 2018). Interestingly, whilst miR-155 has been shown to affect the behaviour of macrophages also, the effect induced is not anti-inflammatory but rather proinflammatory, resulting in a defective M2 polarisation and instead a preferential shift towards inflammation-instigating M1 macrophages (Paoletti *et al.*, 2019). Moreover, the evidence indicates that the effects of these miRNA in RA can be induced as a consequence of their over-expression or in some instances under-expression. Although pathogenicity is frequently associated with miRNA over-expression as seen in the miR-21 study in which SF memory Treg cells exhibited heightened expression of this miRNA, contributing to their enhanced proliferative and anti-apoptotic capabilities, a reduction in certain

miRNAs can also prove detrimental (van der Geest *et al.*, 2014). This was depicted eloquently in previous work highlighting a downregulation of miR-124 in RA synovial tissue compared to healthy tissue, a decrease which was inversely correlated with histone deacetylase 1 (HDAC1), a central effector of synovial hyperplasia (Meng, Pan and Sheng, 2021). The combination of the sheer number of cell targets and differential up/down regulation of miRNAs contributes significantly to the complexity of understanding the role of miRNA in rheumatic disease.

1.15.5 Serum MicroRNA as Biomarkers

Whilst initial analysis was focused on intracellular miRNAs, recent literature has highlighted the role of circulating miRNAs and their potential to serve as reliable biomarkers of disease development and prognosis (Iftikhar and Carney, 2016; Zhang *et al.*, 2023d). Following their initial detection in maternal plasma in 2008, circulating miRNA have since been identified in several biological fluids including blood (serum and plasma), cerebrospinal fluid, urine, saliva, lacrimal and seminal fluids, and the bronchial lavage (Chim *et al.*, 2008; Gilad *et al.*, 2008; Weber *et al.*, 2010; Fujimoto *et al.*, 2019). Interestingly, in comparison to cellular RNA, the stability of endogenous miRNAs is high with studies highlighting their ability to resist degradation by the abundant endogenous ribonucleases in addition to extreme temperature and pH fluctuations and cycles of freeze-thawing vs boiling, a property that reinforces their strong biomarker potential (Mitchell *et al.*, 2008; O'Brien *et al.*, 2018). Secreted from both circulating blood cells and other tissues directly impacted by disease, these circulating miRNA are released and exist via two possible mechanisms – firstly, vesicle-free miRNA that from protein complexes with AGO2 or nucleophosmin 1, and secondly, miRNAs that are secreted into the extracellular space in vesicular transport of which there are three main types - exosomes, micro vesicles, and apoptotic bodies (Gallo *et al.*, 2012; Iftikhar and Carney, 2016; O'Brien *et al.*, 2018). Exosomes are widely considered the primary mode of release of extracellular miRNAs but to date what controls their release is still unclear, with studies demonstrating a role for both passive and active processes (O'Brien *et al.*, 2018). Furthermore, the reason for extracellular miRNA release is an area under investigation with an abundance of studies suggesting it may facilitate intercellular communication and signalling thus affecting several biological responses (O'Brien *et al.*, 2018). Whilst studies have highlighted a beneficial role of exosomal miRNAs in multiple autoimmune diseases with specific miRNA in exosomes demonstrating the ability to suppress angiogenesis in atopic dermatitis and additionally assist in soft tissue wound healing in mouse models of cutaneous injury, their involvement in disease pathogenesis has also been detected (Hu *et al.*, 2018; Shi *et al.*, 2023; Zhang *et al.*, 2023d).

Extracellular miRNA have been shown to influence immune responses through interactions with several TLRs such as human TLR8 (Fabbri *et al.*, 2012; Fabbri, 2018). Furthermore, in 2021, a novel study demonstrated that miRNA containing exosomes were capable of promoting Th1 and Th17 polarisation and proinflammatory cytokine upregulation in psoriasis highlighting their disease-promoting role (Jiang *et al.*, 2021).

Moreover, the high propensity of extracellular miRNA to serve as biomarkers is a current field of focus due to a number of intrinsic properties:

1. They are highly stable following secretion into extracellular fluid (Mitchell *et al.*, 2008; O'Brien *et al.*, 2018).
2. miRNA have a tissue specific expression profile (Keller *et al.*, 2022).
3. Aberrant expression has been associated with a number of diseases (Wu *et al.*, 2021b; Chakrabortty *et al.*, 2023).
4. miRNA expression profiles can assist in identifying 'individuals at risk' (IAR) of disease development and for diagnostic purposes (Zhang *et al.*, 2020b; Wade *et al.*, 2020; Cunningham *et al.*, 2021).
5. Can indicate disease progression and severity (Giannoudis *et al.*, 2019; Saadawy, El-Ghareeb and Talaat, 2024).
6. Expression profiles alter if therapeutic intervention is effective (Singh, Patro and Aggarwal, 2019; Cunningham *et al.*, 2021).
7. Expression profiles can give an indication of disease recurrence risk (Zellinger *et al.*, 2022).
8. Can predict responders versus non-responders at baseline (Wade *et al.*, 2020).

Tangible proof of the biomarker potential of circulating miRNA in RA and PsA has been demonstrated by several studies, thus opening an ongoing avenue of intense research focus. Whilst serum miR-22 has been identified as a significant predictor of both the onset and further development of RA due to its heightened presence from IAR to established RA, miR-103a-3p has also been shown to be a reliable indicator of those at risk of imminent RA progression, with serum levels approximately 7.6-fold higher than in HC (Ouboussad *et al.*, 2017; Anaparti *et al.*, 2017). Recent work in our own group has successfully reinforced the value of miRNA as biomarkers in RA and PsA, with analysis focusing on panels of miRNA exhibiting a high sensitivity and specificity for the individual diseases compared to healthy comparators, with both studies additionally showing a correlation between the circulating miRNA present and the effectiveness of therapeutic intervention (Wade *et al.*, 2020; Cunningham *et al.*, 2021). This concept of using miRNA as biomarkers to predict the efficacy of therapies may be crucial in the advancements towards more personalised medicine. In this regard, circulating levels of miR-19b exhibit high proficiency as not

only a biomarker of RA disease progression but additionally can provide a valuable indication of the efficacy of baricitinib treatment through profiling the miRNA of monocytes (Ciechomska *et al.*, 2023). Moreover, in the context of PsA, previous research identified a set of seven specific miRNAs (miR-155-5p, miR-140-3p, miR-432-5p, miR-382-5p, miR-532-5p, miR-139-3p, and miR-379-5p) capable of functioning as biomarkers for the effectiveness of methotrexate (MTX) treatment, particularly in relation to cutaneous responses (Cruz Correa *et al.*, 2023).

1.16 RA and PsA Therapeutic Interventions

Achieving and maintaining a sustained level of disease remission within patients is the long-term goal within both RA and PsA, a goal primarily achieved through the use of targeted biologic and pharmacological interventions. Whilst initial treatment strategies involve administration of non-steroidal anti-inflammatory drugs (NSAIDs) such as aspirin that solely focused on symptomatic relief, current day interventions assume a more preventative role and are primarily focused on ensuring prevention of radiographic damage and concurrent disability (Hyndman, 2017). In recent years, improved understanding of the inflammatory mediators and reciprocal communication between tissue resident and invading immune cells that are synergistically driving the destruction of the synovial joint has facilitated the development of a vast repertoire of therapeutic interventions (Smolen, Aletaha and McInnes, 2016; Shams *et al.*, 2021; Schett, McInnes and Neurath, 2021; Azuaga, Ramírez and Cañete, 2023; Lee and Moon, 2023; Ding *et al.*, 2023). However, despite these advancements, due to the highly heterogenous manifestations of inflammatory arthropathies such as RA and PsA, a considerable proportion of patients still fail to achieve remission or suffer with intolerable side effects that are severe enough to warrant discontinuation (Veale and Fearon, 2018; Wang, Zhou and Liu, 2018). Moreover, as a consequence of the chronic and progressive nature of both RA and PsA, the timing of diagnosis is also of critical importance in maintaining patient quality of life. Indeed, studies have highlighted the significance of prompt assessment and intervention in both RA and PsA, with studies showing significantly negative impacts on the severity of joint damage, physical mobility, and ability to achieve disease-modifying anti-rheumatic drugs (DMARD)-free remission following 3-, 6-, and 12-month delays in diagnosis (van der Linden *et al.*, 2010; Tillett *et al.*, 2013). Furthermore, delays in diagnosis can heighten the financial burden dramatically, with several studies demonstrating the significant monetary effects of RA arising from musculoskeletal disability and consequential reduced socioeconomic participation. A recent survey conducted on an RA patient cohort in the USA estimated that the average accumulated cost per annum for an individual RA patient is between

$12,509 and $36,053 depending on the treatments used, with the negative effects of such costs affecting patient adherence (Hresko, Lin and Solomon, 2018). Additional burdens identified include a shortening of lifespan, and significant CVD-related co-morbidity, with direct correlations between the severity of RA-associated pain and early retirement, all of which can have devastating impacts for affected patients and highlights the importance of ensuring early diagnosis before a significant amount of irreversible joint and extra-articular damage is induced (Gelfand *et al.*, 2006; Widdifield *et al.*, 2018; Galloway *et al.*, 2020).

1.16.1 Disease-Modifying Anti-Rheumatic Drugs

DMARDs are a specific class of drugs with potent immunosuppressive and immunomodulatory properties that makes them suitable for use in diseases driven by a strong inflammatory component such as RA and PsA. Classified into two broad categories; conventional and biologic, these drugs have unique mechanisms of action but generally target specific aspects of the immune cascade including reduction of IL-6, IL-1, and IL-8, suppression of neutrophil adhesion, and stimulation of FLS adenosine release (Benjamin, Goyal and Lappin, 2024). Current EULAR and GRAPPA guidelines for RA and PsA advise clinicians to prescribe conventional synthetic disease-modifying anti-rheumatic drugs (csDMARDs) initially, with subsequent options if adequate responses are not obtained including the incorporation of biological disease modifying anti-rheumatic drugs (bDMARDs) or targeted synthetic DMARDs (tsDMARDs) (Coates *et al.*, 2022; Smolen *et al.*, 2023).

1.16.2 Conventional Synthetic Disease-Modifying Anti-rheumatic Drugs

First-line treatment strategies that target mediators relatively high up in the inflammatory cascade are commonly shared between RA and PsA and involve the use of csDMARDs including MTX, hydroxychloroquine, leflunomide, and sulfadiazine. According to the EULAR guidelines, they constitute the staple recommended treatment in clinical practice globally and are frequently utilised as a monotherapy initially or subsequently in combination with additional interventions such as a bDMARD or tsDMARD if inadequate responses are observed (Gossec *et al.*, 2020; Smolen *et al.*, 2023). A recent study highlighted that the combined usage of csDMARDs and bDMARDs at seven years was more strongly associated with remission in patients than csDMARDs alone (Larid *et al.*, 2022). MTX itself is defined as a folic acid antagonist originally utilised as a chemotherapeutic agent, which affects adenosine and guanine metabolism resulting in

suppressive impacts on T cell and B cell proliferation and diminishing effects on proinflammatory cytokine production (Genestier *et al.*, 1998; Hobl *et al.*, 2011). Moreover, the evidence highlights its direct influence on the pathogenic phenotype of FLS through the suppression of MMP-1, MMP-13, IL-6, IL-17, and osteoclast related RANKL, and induction of the correct balance of autophagy-apoptosis in the activated cells (Lee *et al.*, 2004; Shervington *et al.*, 2018; Misra *et al.*, 2021). Several placebo-controlled trials and studies have highlighted the success of MTX in treating RA, with new research suggesting the effectiveness may be associated with the microbiome composition of the gastrointestinal tract (Williams *et al.*, 1985; Weinblatt *et al.*, 1998; Artacho *et al.*, 2021). Due to this success of MTX in RA, it was introduced as first-line therapy for PsA also, although the limited trials conducted in PsA patient cohorts have demonstrated insufficient evidence to support its efficacy. A recently conducted Cochrane review concluded that based on the evidence from eight clinical trials, administration of <15 mg MTX for six months may only be slightly more effective than placebo, evidence which indicates if MTX is prescribed, higher doses may be required to obtain any beneficial effects (Wilsdon *et al.*, 2019). However, despite its use as a first-line treatment, more than one third of patients are intolerant to MTX, thus leading to the development of multiple additional therapies which can be used in combination or as a monotherapy to achieve optimal patient outcomes (Nikiphorou *et al.*, 2014).

1.16.3 Biological DMARDs

1.16.3.1 TNF Inhibitors

Better understanding of the integral role of proinflammatory cytokines including TNF and IL-6 have in driving the pathogenic mechanisms of both RA and PsA, led to the revolutionary introduction of bDMARDs. With five TNFi currently licensed by the FDA (etanercept, infliximab, adalimumab, certolizumab pegol, and golimumab) and in widespread clinical use as second line treatments if patients fail to respond to csDMARDs, they have exhibited positive effects in RA with significant reduction in structural damage, potentially mediated through the downregulation of MMPs and overall disease activity (Catrina *et al.*, 2002; Weinblatt *et al.*, 2003; Keystone *et al.*, 2009). Similarly, TNFi have demonstrated superior efficacy in treating PsA patients compared to their synthetic counterparts, with beneficial effects on spinal symptoms, dactylitis, and even more importantly, the level of bone erosion observed radiographically (Glintborg *et al.*, 2011; Mease *et al.*, 2014). Interestingly, a comparative study that included both RA and PsA patients matched for disease activity, suggested TNFi may exert better effects on remission rates in PsA compared to RA, with rates of 60% and 44%, respectively (Glintborg *et al.*, 2011). This evidence supported a

previous study showing that even at the 1-year follow-up time period, higher remission was detected in PsA (58%) compared to RA (44%) individuals receiving TNFi therapy (Saber *et al.*, 2010). Furthermore, a prospective study that followed RA and PsA patients receiving biologic therapy for a time period of 12 years demonstrated that at this timepoint, the PsA cohort still exhibited superior biologic responses, thus not only reinforcing the previous studies but also importantly implying that the superior effects are not transitionary but sustained, information which highlights the value of biologics in long term PsA disease management (Murray *et al.*, 2021). At the cellular level, studies have shown that TNFi can impact the destructive behaviour of the FLS directly, with decreased production of CCL20 and the proinflammatory transcription factor ID-1 and heightened induction of apoptosis, particularly with the use of etanercept (Kawashiri *et al.*, 2009; Pattacini *et al.*, 2010; Ohara *et al.*, 2019). Unfortunately, even if well tolerated, TNFi are associated with an increased risk of infection, drug-induced sarcoidosis disease, latent tuberculosis, and increased incidence of neoplasms, thus ongoing and careful monitoring and screening by a healthcare professional is warranted (Kourbeti, Ziakas and Mylonakis, 2014; Yun *et al.*, 2015; Theunssens *et al.*, 2022).

1.16.3.2 IL-6 Inhibitors

The differential response to certain therapies is further observed with the IL-6 inhibitors such as tocilizumab, sarilumab, and sirukumab, all of which exert their effects through interactions with IL-6 directly or indirectly through the IL-6 receptor (IL-6R). Whilst the synovial levels of IL-6 have been shown to be elevated in both active RA and PsA, the results from use of the IL-6 targeting drug clazakizumab in a placebo-controlled Phase II randomised controlled trial (RCT) involving a PsA patient cohort demonstrated minimal effects (Mease *et al.*, 2016). In contrast, multiple studies support the highly beneficial use of drugs supressing IL-6 activity in RA patients, with reductions in disease activity after one year and minimal side effects observed with sarilumab (Tony *et al.*, 2022; Park *et al.*, 2022). Similarly, tocilizumab, an inhibitor of the IL-6R, has improved RA clinical signs and symptoms, laboratory parameters, and patient recorded quality of life outcomes, thus currently making it the most widely used humanised monoclonal antibody against the IL-6R in RA (Smolen *et al.*, 2008; Takeuchi *et al.*, 2011; Strand *et al.*, 2017; Prasad *et al.*, 2023). Interestingly, a double-blind RCT identified that when utilised as a monotherapy, tocilizumab demonstrates superior efficacy in reducing DAS28 from baseline compared to the TNFi adalimumab (Gabay *et al.*, 2013).

1.16.3.3 IL-17/IL-23 Inhibitors

However, while IL-6 based therapeutic interventions are more associated with RA, further understanding of the key cytokines driving the pathway of inflammation specifically in PsA, have led to the development of monoclonal antibodies targeting the IL-17/IL-23 pathways. Several clinical trials have highlighted the efficacy of secukinumab, the first fully human monoclonal antibody approved for active PsA treatment in 2015, in diminishing clinical and radiographic scores of PsA by selectively binding to IL-17A (Kavanaugh *et al.*, 2017; Mease *et al.*, 2018). Moreover, another IL-17 monoclonal antibody ixekizumab and IL-17A receptor binding drug brodalumab, were subsequently FDA approved for PsA treatment, with ixekizumab also effective in patients who were either naïve or had failed TNFi based interventions (Nash *et al.*, 2017; Mease *et al.*, 2021). As a consequence of the success of these therapies in PsA, a number of potential IL-17 inhibitors including bimekizumab are in the pipeline and recently have shown promising effects in improving PsA-mediated joint, skin, and radiographic damage in Phase III trials (McInnes *et al.*, 2023). Furthermore, in addition to IL-17, IL-23 is a signature cytokine responsible for PsA pathogenesis. The fully human anti-IL-12/IL-23 mAb, ustekinumab, blocks the differentiation of Th1 and Th17 cells and has been shown by several large, Phase III randomised clinical trials to be safe and effective in PsA, leading to its introduction as the first IL-23 inhibitor on the market (McInnes *et al.*, 2013; Ritchlin *et al.*, 2014). Recently, two more IL-23 inhibitors have gained FDA approval for PsA, guselkumab and risankizumab, with IL-17 type effector cytokines reaching similar levels to HC following 24 weeks of treatment with guselkumab (Sweet *et al.*, 2021; Östör *et al.*, 2022). Due to the complexity of the proinflammatory environment, there has been a recent shift towards dual therapies capable of blocking multiple cytokines over monotherapies. Investigations showing blockade of both TNF and IL-17 co-currently have demonstrated early success in a mouse model of SpA with significant reductions in inflammation and structural alterations, thus highlighting the potential of this dual-blockade avenue from a clinical perspective (Hammoura *et al.*, 2022).

1.16.3.4 B and T cell Targeting Therapies

Additionally, bDMARDs targeting the immune cells generating the proinflammatory environment are also commonly used in RA and PsA therapy. The B cell depleting monoclonal antibody 'rituximab' specifically targeting the CD20 molecules located on B cells, has demonstrated high efficacy in RA but not PsA patients, which could in part be attributed to the more central role of B cells and their autoantibodies in RA pathogenesis (Veale and Fearon, 2015; Alivernini, Firestein and McInnes, 2022). Whilst meta-analysis have shown good efficacy when rituximab is utilised in

combination with MTX, one study observed that 50% of RA patients have low/absent B cells within the synovium. Thus, when compared in a Phase 4 RCT, tocilizumab treatment was more effective in this patient cohort, highlighting the need for patient stratification (Wang, Bao and Ji, 2020; Humby *et al.*, 2021). Moreover, the concept of more personalised medicine is further supported by an accumulating body of evidence indicating differential responses in RA patients based on their underlying serology and ACPA status (Huizinga *et al.*, 2015; Harrold *et al.*, 2018; Courvoisier *et al.*, 2021; Harrold *et al.*, 2022). An eloquent study effectively demonstrated that ACPA+ patients receiving rituximab or abatacept exhibited a significantly greater clinical response by the 6-month follow-up compared to their ACPA- counterparts (Harrold *et al.*, 2022). In relation to 'abatacept,' it is a specific fusion protein targeting the co-stimulatory molecules on antigen presenting cells that has demonstrated success in both RA and PsA through its suppressive effect on T cell activation and cytokine release. Studies have highlighted its efficacy in reducing disease activity in RA patients who have inadequate responses to MTX or TNFi, whilst similarly a 2017 Phase III study highlighted the ability of abatacept to resolve several PsA associated symptoms including enthesitis and dactylitis in PsA patients that had failed TNFi treatment, with these improvements sustained throughout the follow-up period (Kremer *et al.*, 2006; Genovese *et al.*, 2008; Mease *et al.*, 2017). A revolutionary study was recently published highlighting the ability of intervention with abatacept for a 12-month period in IAR exhibiting ACPA positivity to successfully attenuate their progression to RA. Despite the fact these effects were not sustained at 24 months suggesting that the pathogenic immune responses modulated by the drug are not permanent, the clinical signs and symptoms were reduced substantially during this 'at-risk' period. Importantly, this study not only provided unambiguous evidence of the critical role of the adaptive immune system in driving RA development but additionally, demonstrated that RA interception trials are highly feasible and could open a pathway in personalised medicine towards treating with the intent to prevent disease onset in suitable individuals (Cope *et al.*, 2024).

1.16.4 Targeted Synthetic DMARDs

In an analogous manner to biologics, tsDMARDs directly target components of the immune system but more specifically the complex interactions of the signalling pathways driving the plethora of immune cell activity. Indeed, the JAK/STAT pathway is critically important in this regard, with direct involvement in inflammatory pathways driving the activity of T helper cells and expression of IL-17/IL-23 receptors in the joints. Tofacitinib, a small molecule inhibitor that specifically blocks the activity of JAK1 and JAK3, has demonstrated high efficacy in PsA by reducing peripheral

arthritis, dactylitis, enthesitis, and psoriasis, in addition to attenuating radiographic progression (Nash *et al.*, 2020). Similarly, it is approved for clinical use in RA patients with inadequate responses or intolerance to MTX since 2016 and has been shown by several studies to reduce active disease, structural deterioration, and health-related quality of life (Lee *et al.*, 2014; Wallenstein *et al.*, 2016; Strand *et al.*, 2016). Interestingly, a large body of recent research has highlighted the mechanisms by which tofacitinib may be exerting its beneficial effects at the cellular level. Studies have shown tofacitinib induced a reduction in synovial inflammation, cellular invasion, and proinflammatory metabolic pathways in RA and PsA FLS and explants and additionally decreased the pathogenic, proinflammatory state of RA and PsA CD209+/CD14+ DC (Gao *et al.*, 2016; McGarry *et al.*, 2018b; Diller *et al.*, 2019; Marzaioli *et al.*, 2021). Indeed, tofacitinib's ability to block multiple characteristic features of RA has further been highlighted through its blockade of the differentiation of blood-derived monocytes to antigen presenting DCs along with its attenuation of effective TNF-induced, IFN-β-mediated chemokine synthesis in RA FLS (Rosengren *et al.*, 2012; Marzaioli *et al.*, 2020). Furthermore, peficitinib, another inhibitor of JAK activity, has shown success in significantly supressing the production of FLS invasive and chemotactic mediators including MMP-3, CXCL8, and CXCL1 in *ex vivo* experiments (Diller *et al.*, 2019). The JAK inhibitor, upadacitinib, which specifically targets JAK1, has also received approval for PsA treatment with Phase III clinical trials demonstrating significantly greater ACR20 responses compared to placebo, especially in those patients non-responsive or intolerant to TNFi (Mease *et al.*, 2023). Similarly to tofacitinib, scientific studies have highlighted its ability to supress OSM induced IL-6, monocyte chemoattractant protein 1 (MCP-1), and MMP expression in FLS, whilst additionally preventing IFN-ɣ induced transformation of FLS to an inflammatory phenotype characterised by HLA-DR (O'Brien *et al.*, 2021; Zhao *et al.*, 2022).

Moreover, another signalling pathway that can be targeted is phosphodiesterase-4 (PDE4), an enzyme that regulates the levels of second messengers cAMP and cGMP, thus exerting widespread effects through the upregulation of inflammatory responses. Apremilast, an oral small molecule inhibitor of PDE4 that received FDA approval for PsA treatment in 2014, demonstrated efficacy in the PALACE 4 clinical trial by improving clinical signs and symptoms with minimal adverse effects (Wells *et al.*, 2018). However, a Phase II clinical trial failed to show beneficial effects of apremilast compared to placebo in active RA patients with inadequate response to MTX, suggesting it may be more PsA specific (Genovese *et al.*, 2015). Ultimately, a more comprehensive understanding of RA and PsA at the molecular and cellular levels will facilitate the novel targeting of specific molecules/pathways. These approaches may revolutionise future therapeutic interventions by attenuating the effects of multiple proinflammatory cytokine hubs

simultaneously, thus exerting widespread suppressive effects on RA and PsA synovial and systemic inflammation.

1.16.5 MicroRNA as Therapeutic Targets

As evidenced by the existing literature, miRNA assume a significant role in contributing to the development and progression of a number of pathologies including joint damage through their governance over inflammatory pathways, and thus provide a desirable target for therapeutic intervention/modulation. However, the feasibility and success of such therapies is complicated by various limitations, one being the ability of miRNA to regulate multiple different mRNA gene targets in multiple different cell types thus heightening the risk substantially for adverse and systemic side effects (Diener, Keller and Meese, 2022). Indeed, several miRNA therapeutics that initially demonstrated success in Phase II clinical trials have since been terminated as a consequence of the severe adverse effects including miravirsen, the pioneering miRNA therapeutic to enter clinical trials capable of targeting chronic hepatitis C infection (Gebert *et al.*, 2014; Iacomino, 2023). Nonetheless, despite its failure, the early success of the miravirsen clinical trials in human subjects opened the gateway for numerous currently ongoing human trials investigating the effects of a number of different miRNA related therapies. For example, promising preliminary results were observed in the first human clinical trial targeting miR-92a with a synthetic inhibitor MRG-110 which resulted in accelerated angiogenesis and wound healing in diabetic wounds (Abplanalp *et al.*, 2020). The results from a first-in-human Phase 1b randomised, double-blind trial targeting cardiac miRNA-132-3p, a miRNA significantly increased in heart failure with cardiac remodelling effects, were equally promising. Interestingly, when targeted with the inhibitor CDR132L, patients demonstrated significantly improved cardiac function and heart failure attenuation, with minimal side effects (Täubel *et al.*, 2021). However, it is clear that further advances in understanding the roles of individual and combinations of miRNAs in driving pathophysiology, in addition to optimising the efficacy and safety of anti-miRNA-based strategies, is essential before widespread clinical use.

1.17 Primary Objectives of this Thesis:

1. To explore the heterogeneity of FLS in RA and PsA synovial tissue and to identify unique mediators that drive differential pathogenic activity.

2. To delineate differences in the transcriptomic profiles and corresponding function of FLS subsets in RA vs PsA pathotypes.
3. To identity biomarkers that can provide a minimally invasive and reliable method of distinguishing RA from PsA disease.

CHAPTER TWO:

Immune Cell-Derived Cytokines Synergistically Interact to Drive Synovial Fibroblast Pathogenic Function and Metabolic Capacity

2.1 Introduction

FLS are stromal cells, integral to the maintenance of the homeostatic joint through their continuous production of lubricants and SF, and regulation of the structure of the supporting ECM (Ospelt, 2017; Nygaard and Firestein, 2020). However, in RA, FLS undergo a distinctive pathogenic transformation, displaying strong proliferative, anti-apoptotic, and invasive characteristics, mediated through their abundant production of ECM-degrading MMPS including MMP-1 and MMP-3, angiogenic promoting mediators such as VEGF, immune homing chemokines including CXCR3, CXCR4, CXCR5, and CCR6, and proinflammatory cytokines such as IL-6, MCP-1, and IL-8, all of which is paralleled by shifts in their metabolism to a predominantly glycolytic phenotype (Tang *et al.*, 2017b; Fearon *et al.*, 2019; Nygaard and Firestein, 2020; Kondo, Kuroda and Kobayashi, 2021; Fearon *et al.*, 2022). Moreover, studies have highlighted a role for mitochondrial dysfunction and alterations to the fission/fusion behaviour of these mitochondria, in addition to ER stress triggered autophagy in driving the destructive behaviour of RA FLS (Biniecka *et al.*, 2016; Wang *et al.*, 2020a; Wang *et al.*, 2022). Interestingly, the evidence indicates that whilst FLS are not mere 'passive responders' to the inflammatory milieu but epigenetically imprinted with an 'aggressor phenotype', this predisposition only serves to make them more responsive to the influences and stimuli in the surrounding microenvironment (Bottini and Firestein, 2013; Frank-Bertoncelj *et al.*, 2017; Nygaard and Firestein, 2020; Elhai *et al.*, 2023). The complexity of FLS is compounded by the fact that this aggressive FLS transcriptomic signature demonstrates stark differences not solely between two disease states such as RA and OA, but additionally across different disease pathotypes and anatomical joints in the same patient thus, highlighting the effects of both pathotype and site specificity in dictating FLS behaviour/phenotype and function (Ai *et al.*, 2016; Frank-Bertoncelj *et al.*, 2017; Micheroli *et al.*, 2022; Elhai *et al.*, 2023; Choi *et al.*, 2024). There have been revolutionary discoveries in recent years highlighting the vast variation in FLS phenotypes and the association between this phenotype and their characteristic function (Croft *et al.*, 2019; Rauber *et al.*, 2024). The eloquent delineation of FLS based on THY1 expression into immune regulatory sub-lining versus bone and cartilage degradative lining, with the former highly influenced once again by their anatomical proximity to EC-derived NOTCH signalling has driven this field of study, with recent research identifying several additional subsets including a novel inflammation resolving FLS subset, further emphasising the scope of FLS heterogeneity (Croft *et al.*, 2019; Wei *et al.*, 2020; Rauber *et al.*, 2024).

The direct interaction between cells, of both stromal and immune origin, and its central role in exacerbating IA pathology, is a growing field of interest as the chronically inflamed synovium is a highly complex microenvironment containing an abundance of cell types, each

releasing different/overlapping mediators. Recently conducted scRNA-seq examining the cellular composition of the inflamed synovium, demonstrated a multitude of both resident and non-resident innate and adaptive immune cells of haematopoietic origin, myeloid-derived, and stromal cells, with a higher predominance of activated FLS states in synovial regions in close proximity to higher frequencies of infiltrating $CD45^+$ leukocytes, supporting the hypothesis that such interactions can influence FLS behaviour (Carmona-Rivera *et al.*, 2017; Zhang *et al.*, 2023a; Smith *et al.*, 2023). Indeed, due to the high influx of peripheral immune cells to the synovial joint, investigating their impact on the endogenous stromal cells is of critical importance in understanding the mechanisms of inflammatory pathogenesis (Smith *et al.*, 2023). Whilst Petrasca *et al*. (2020) demonstrated direct cell-to-cell contact with the FLS is required for T cell activation, multiple studies have also highlighted the fact that communication is not limited to direct contact but can additionally be mediated through the plethora of proinflammatory cytokines and chemokines that are expressed constitutively by the extensive cellular network (Petrasca *et al.*, 2020; Kang *et al.*, 2022; Smith *et al.*, 2023; Matsuda, Shiba and Hiraoka, 2023). Smith *et al.* (2023) effectively reported an impact on FLS morphology and gene expression of markers including MMP-3 and CXCL1 following stimulation with a combination of myeloid and T cell-derived cytokines including TNF, IFN-γ, and IL-1β. Similarly, the effect of such cytokines including TNF-α and IL-1 on the induction of RANKL on 'tissue destructive FLS' and the subsequent rapid increase in osteoclastogenesis and bone resorption, a defining RA characteristic, has also been eloquently shown in the literature, an effect that could be attenuated in mouse models through blockade of the specific RANKL enhancer E3 (Matsuda, Shiba and Hiraoka, 2023). Moreover, it is becomingly increasingly recognised that many cytokines do not act alone but act in coordination with other prevalent cytokines to potentiate the proinflammatory response thus, introducing the concept of cytokine synergy. An abundance of literature exists demonstrating the ability of several key cytokines including TNF, OSM, IL-1, and IL-17A, to synergise and potentiate the proinflammatory response within the synovial joint microenvironment (Barksby *et al.*, 2006; Fearon *et al.*, 2006; Zrioual *et al.*, 2009; Moran *et al.*, 2009; van Hamburg *et al.*, 2011; Griffin *et al.*, 2012; Le Goff *et al.*, 2014; Hanlon *et al.*, 2019; Slowikowski *et al.*, 2020).

Furthermore, a recent study highlighted that soluble mediators released by the FLS, such as the chemokine CXCL12, can influence the accumulation of T cells in particular regions of the inflamed RA synovium (Bradfield *et al.*, 2003). This is a bi-directional network supported by research identifying the ability of T helper-derived soluble mediators themselves to drive a significantly more proinflammatory and glycolytic FLS phenotype, a phenotype that can be supressed through the introduction of JAK inhibitors (Bradfield *et al.*, 2003; Kvacskay *et al.*, 2021).

However, T cells are not the only immune cells in constant communication with FLS, with research depicting reciprocal contact between macrophage populations and FLS in the RA synovium and the induction of a pro-resolving, remission phenotype in both cell types. Whilst this work identified a reduction in the expression of CXCL8, CXCL1, MMP-1, and MMP-3, and heightened expression of tissue repair genes in FLS in the vicinity of remission associated lining layer $MerTK^{neg}CD206^{neg}$ STMs, the significant influence of GAS6 released by the FLS themselves in regulating the remission phenotype of these $MerTK^{neg}CD206^{neg}$ STMs was also highlighted (Alivernini *et al.*, 2020). Furthermore, additional analysis demonstrated that soluble mediators secreted from synovial sorted $CD206^{+}CD163^{+}$ macrophages induces a pathogenic phenotype in HC FLS (Hanlon *et al.*, 2024). However, these effects are not solely limited to immune cells but also stromal cells within the synovial joint, with research showing constant communication between FLS and the blood vessel associated ECs. Indeed, as previously mentioned, whilst Wei *et al.* (2020) illustrated the impact of EC-derived NOTCH signals on FLS phenotype, Fromm *et al*. (2019) highlighted the ability of RA and PsA FLS to regulate EC function through soluble mediators, with PsA FLS inducing a potent pro-angiogenic EC response.

A key method of communication between these cell types responsible for perpetuating inflammation within the synovium is the release of the cellular signalling cytokines, of which IL-1β is of particular importance. In 1982, Fontana *et al.* demonstrated the presence of high levels of IL-1β in the SF of RA patients, a discovery that has been reinforced by multiple other studies that have provided clearer insights into its proinflammatory, pathogenic function in IA (Fontana *et al.*, 1982; Eastgate *et al.*, 1988; Hofbauer *et al.*, 1999; Yang *et al.*, 2019; Levescot *et al.*, 2021). The mean plasma levels of IL-1β in RA patients have been shown to correlate positively with several clinical parameters and inflammatory markers including the pain score and the ESR, whilst correlating negatively with haemoglobin concentration (Eastgate *et al.*, 1988). Moreover, the effect of IL-1β stimulation appears to exert different pathogenic effects on differential cell types with a comparative study highlighting its propensity to drive osteoclastogenesis through induction of osteoprotegerin ligand gene expression in human osteoblastic cells, whilst additional research detected a significant increase in the release of inflammatory factors by human FLS (Hofbauer *et al.*, 1999; Yang *et al.*, 2019). Similarly, its ability to drive Tregs towards a highly bone erosive phenotype has also been shown, with early administration of IL-1 blockade significantly attenuating the swelling and bone erosion that developed (Levescot *et al.*, 2021). IL-1β exerts its effects by predominantly signalling through the NF-κB pathway, a pathway that has been shown to be constitutively activated in chronic inflammatory conditions including RA, contributing to the abundant production of proinflammatory cytokines, MMPs, and adhesion molecules (Bondeson

et al., 1999). Interestingly, studies specifically targeting IL-1β have demonstrated efficacy in ameliorating the aggressive symptoms of RA by primarily inhibiting correct functioning of the NF-κB signalling pathway (Li *et al.*, 2018a; Yang *et al.*, 2019).

Ubiquitously expressed throughout the body, unlike IL-1β, TGF-β is a highly pleotropic cytokine with various functions in normal homeostatic mechanisms including tissue repair but additionally can be involved in a plethora of diseases, predominantly as a consequence of its central role in balancing multiple signalling networks. Its multifaceted nature is reinforced in the context of tumorigenesis where at early stages it serves the role as a tumour suppressor through governance over cell proliferation and apoptosis (Jang *et al.*, 2002; Baba *et al.*, 2022; Hanusek *et al.*, 2022). However, as malignancy progresses, research has highlighted its ability to transform the FLS within the tumour stroma into cancer-associated fibroblasts displaying a characteristic pro-carcinogenic phenotype that promote cell stemness, ECM remodelling and thus, tumour cell invasion (Gaggioli *et al.*, 2007; Baba *et al.*, 2022). In the context of arthritis, studies dating from the 1980s identified an association with RA and OA, with high levels of the active form of TGF-β found in the SF of both RA and OA patients at 10 ng/mL and 4 ng/mL, respectively (Fava *et al.*, 1989). Moreover, recent genetic studies have identified the existence of SNPs in the gene encoding TGF-β as risk variants for both OA and RA, with these variants directly related to disease activity and circulating autoantibodies in the RA cohort (Rice *et al.*, 2021; Iriyoda *et al.*, 2022). Its role in OA has been well-established with research suggesting it assumes a major role in driving chondrocytes preferentially towards a hypertrophic state, with a direct correlation identified between the severity of OA in the human hip joint and the levels of total TGF-β in the subchondral bone (Zgoda *et al.*, 2005; van der Kraan, 2018). Moreover, several mouse models directly blocking TGF-β have shown promising results in attenuating OA pathogenesis by significantly supressing degeneration of articular cartilage, osteophyte formation, and synovial hyperplasia (Scharstuhl *et al.*, 2003; Zhen *et al.*, 2013). Furthermore, in RA specifically, genome-wide gene expression analysis has demonstrated constitutive upregulation of pathways governed by TGF-β1 in RA FLS (Pohlers *et al.*, 2007). Additionally, the central role local TGF-β1 plays in shifting the balance of differentiated T cells in favour of Th17 whilst simultaneously reducing Treg numbers has been established, with a more equal balance restored through TGF-β1 inhibition (Pohlers *et al.*, 2007; Aarts *et al.*, 2022).

As a consequence of the high number of individual pro- and anti-inflammatory cytokines influencing the aggressive phenotype and destructive behaviour of the cells within the synovium, the aforementioned concept of cytokine synergy and its contribution to the progression of inflammatory arthropathies is becoming increasingly recognised, particularly in the context of

their effects on FLS. Indeed, the existence of a synergistic interaction between the growth factors PDGF-β and TGF-β has been shown, an interaction that was capable of potentiating the synthesis of inflammatory mediators including IL-6, IL-8, MCP-1, and MMP-3 by RA FLS (Rosengren, Corr and Boyle, 2010). Moreover, the synergistic inflammatory response mediated by TNF-α and IL-17A has been extensively studied in recent years due to the central involvement of both cytokines in synovial damage. Whilst their synergy has been reported to induce FLS production of IL-6 in addition to shifting the ratio of MMPs versus TIMPS in favour of cartilage destruction, a previous study successfully identified 26 genes that were only induced in RA FLS upon co-stimulation with TNF-α and IL-17A, an effect mediated through the typical inhibitor of kappa B factor IκBζ in a dose dependent manner (Zrioual *et al.*, 2009; Moran *et al.*, 2009; Koenders *et al.*, 2011; Slowikowski *et al.*, 2020). Interestingly, the clinical relevance of their synergy has been reinforced by analysis of RA synovial tissue identifying that the levels of TNF-α and IL-17A mRNA is predictive of future bone erosion, with therapeutic blockade of both of these cytokines proving more effective in alleviating inflammatory mediator expression compared to blockade of each cytokine alone (Kirkham *et al.*, 2006; van Hamburg *et al.*, 2011). Moreover, their synergistic effects are not solely limited to FLS, with studies demonstrating their ability to significantly enhance the expression of adhesion molecules P-selectin and E-selectin on endothelium, alongside increased release of the chemokines CXCL1, CXCL2, and CXCL5, culminating in a sustained level of neutrophil recruitment (Griffin *et al.*, 2012). Whilst the combined effects of TNF-α and IL-17A have been well-established, synergism existing between several other IA associated cytokines has also been identified. IL-2 and the alarmin IL-33 synergistically augment the expression of FLS-derived GM-CSF and expansion of synovial-resident innate lymphoid cells, potent drivers of autoimmune arthritis (Hirota *et al.*, 2018). Similarly, the synergistic combination of TNF-α and OSM have been shown to exert powerful effects on both FLS and ECs in RA (Hanlon *et al.*, 2019). Whilst similar synergistic upregulation of IL-6, MCP-1, ICAM-1, and VEGF was observed in both cell types, differential regulation of VCAM-1 and metabolic activity was detected, with the synergy producing a heightened glycolytic capacity and simultaneous reduction in mitochondrial respiration in the RA FLS in addition to STAT3 upregulation, all outcomes not induced in the ECs, thus introducing the concept of cell specific effects of cytokine synergy (Hanlon *et al.*, 2019).

IL-1β and TGF-β themselves have demonstrated the capability to synergise with additional factors to drive specific responses in different cell types and disease states. IL-1β has been shown to synergise with OSM and induce a variety of effects ranging from markedly enhanced expression of proinflammatory IL-6 from FLS *in vitro*, to regulating genes such as RANKL directly implicated in the balance of cartilage destruction and repair in chondrocytes and RA FLS (Richards and Agro,

1994; Barksby *et al.*, 2006; Fearon *et al.*, 2006; Le Goff *et al.*, 2014). Moreover, the synergistic effect of TGF-β3 and growth differentiation factor 5 (GDF-5) has been shown to augment chondrogenesis whilst TGF-β and Th2-derived cytokines synergistically drive FLS residing in the human airway to elevate the levels of Eotaxin produced (Wenzel *et al.*, 2002). Additionally, whilst synergistic effects have been observed on the production of IL-6 and IL-8 mRNA in retinal epithelial cells, preliminary studies conducted specifically on human synovial FLS examining IL-1β and TGF-β in combination suggested their effects were additive on the induction of VEGF expression (Kuppner, McKillop-Smith and Forrester, 1995; Berse *et al.*, 1999).

To date, the specific effects of immune cell-derived cytokines on driving the differential FLS populations and function in RA vs PsA has yet to be investigated. Therefore, in this study, the relationship between the major proinflammatory cytokine IL-1β and the pleiotropic cytokine TGF-β, both highly abundant cytokines in the inflamed synovial joint, in driving proinflammatory, invasive, angiogenic, and bioenergetic mechanisms in RA FLS were examined.

2.2 Specific Aims of this Chapter

- To conduct in-depth global synovial transcriptomic analysis of the ligand-receptor interactions driving the distinct phenotype and function of FLS subsets that differ between RA and PsA.

- To assess the synergistic effects of macrophage-derived IL-1β and T cell-derived TGF-β on mitochondrial dynamics and the metabolic profile of RA FLS.

- To determine the synergistic effects of IL-1β and TGF-β on the ER stress response.

- To determine the synergistic effect of IL-1β and TGF-β treatment on the expression of proinflammatory cytokines, chemokines, adhesion molecules, and angiogenic growth factors in RA FLS.

- To establish the effect of cytokine synergy on the invasive and migratory behaviour of the RA FLS.

- To determine the effect of TAK1 inhibition on IL-1β/TGF-β induced pathogenic responses in RA FLS.

- To assess the effects of TAK1 inhibition on the spontaneous release of proinflammatory, invasive, and angiogenic mediators from RA synovial explants.

- To assess the effect of TAK1 inhibition on RA synovial explants size over a 21-day time course.

2.3 Materials & Methods

2.3.1 Patient Recruitment and Arthroscopy

Patients with RA or PsA, all of which fulfilled the criteria established by the ACR and CASPAR respectively, were previously recruited from the outpatient clinic at the Department of Rheumatology, St Vincent's University Hospital and Tallaght University Hospital, TCD (Taylor *et al.*, 2006; Aletaha *et al.*, 2010). Using Wolf 2.7 mm needle arthroscopy or ultrasound guided biopsy, synovial tissue samples from the knee were obtained from actively inflamed RA and PsA patients as previously described (Ng *et al.*, 2010). Macroscopic synovitis (synovial thickness and villi formation) and vascularity (vessel number, vascular pattern) scores were also graded at the time of arthroscopy (Reece *et al.*, 1999). In addition to personal patient information, clinical assessment included tender joint count (TJC), swollen joint count (SJC), ESR, CRP, DAS28, and the global health visual analogue scale (VAS). Before commencing the research, all patients were fully informed of the nature of their involvement and subsequently provided written consent to partake and provide their biological samples and corresponding medical information. Ethical approval was granted by St. Vincent's University Hospital Medical Research and Ethics Committee and all research was performed in accordance with the Declaration of Helsinki.

2.3.2 Bioinformatic Analysis

2.3.2.1 Synovial Tissue Sample Preparation

Synovial tissue single-cell suspensions were generated following enzymatic and mechanical digestion of the synovial biopsies. Briefly, approximately 15 synovial biopsies per patient were digested using the GentleMacs Tumour Dissociation Kit, human (Miltenyi Biotech) as per manufacturers' instructions. Immediately after isolation, biopsies are washed with RPMI (Merck) before being placed in 4.7 mL RPMI-1640 supplemented with 200 µl of enzyme H (protease), 100 µl enzyme R (protease) and 25 µl enzyme A (nuclease) in a GentleMacs C Tube followed by initial mechanical disruption of the tissue using programme h_tumor_01 on a GentleMacs Dissociator. Samples were enzymatically digested for a total of 1 h at 37°C under continuous rotation using the MACSmix Tube Rotator with further applications of the GentleMacs Dissociator at the halfway point and at the end of the 1 h incubation. The cell suspension was then passed through a 70 µM cell strainer. Viability of the cells was assessed with trypan blue exclusion staining and immediately cryopreserved in sterile filtered 10% dimethyl sulfoxide (DMSO)/fetal bovine serum (FBS) at a concentration of 1×10^6cells per mL. Frozen synovial biopsy cell suspensions were thawed quickly in a 37°C water bath and transferred to sterile tubes with warm RPMI-1640 media (10% FBS). After

washing and counting, a dead cell removal kit (Miltenyi cat#130-090-101) was implemented to increase viability. Using the Chromium Next GEM Single Cell 3' Reagent Kits V.3.1 (10X Genomics), cells were loaded onto the GEM Chips. The 10X Genomics Chromium Next GEM Single Cell 3' user manual was followed for all steps to generate complementary DNA (cDNA) libraries for each sample. cDNA quantifications and quality control were determined using the Agilent TapeStation. Final libraries were normalised, quantified (Illumina/ROX low, Kappa Biosystems), pooled based on 40 k reads/sample. Pooled libraries were sequenced on the Illumina NovaSeq using and S2 NovaSeq 6000 Reagents V.1 kit and a 100-cycle sequencing run.

2.3.2.2 ScRNA-seq Data Analysis

Cell ranger V.3.1 (10X Genomics, California, USA), was used to process the synovial tissue single-cell suspensions and generate gene expression raw sequencing data, with the 10X human transcriptome GRCh38.3.0.0 serving as a reference. Following this, the R package Seurat (V.4.0.3) in R (V.4.1) was utilised to convert the single-cell reads for each sample to a Seurat object. Data containing genes being expressed in less than 3 cells, empty droplets (removed with function EmptyDrops), cell doublets (removed by DoubletFinder), and apoptotic cells (removed by eliminating cells with a mitochondrion associated gene expression of over 25%) were excluded from any further downstream analysis. A high number of apoptotic cells in one RA donor led to its exclusion resulting in a total of four RA synovial tissue samples and five PsA synovial tissue samples being used for further analysis. Scaling and normalisation of the data were performed with the newly described Sctransform. (V.0.3.2) package and integration of the Seurat objects representing synovial tissue samples from the nine patients was performed using Harmony (V.0.1.0). Global synovial scRNA-seq analysis was performed by bioinformatic post-doc, Dr Achilleas Floudas.

2.3.2.3 Population Clustering

Downstream cell clustering was subsequently implemented with clusters being identified by the FindCluster function of Seurat and visualised on a Uniform Manifold Approximation and Projection (UMAP) plot. To assess clustering efficiency, the observed to expected edge weight ratios for all pairs of clusters was examined. To annotate the clusters identified, differential gene expression profiles derived from using the FindMarkers function of Seurat with Wilcoxon test and p values adjusted by Bonferroni correction, were used.

2.3.2.4 Cell-Cell Interaction Analysis

Nichenetr (V.1.0) package was used to identify cell-cell interactions. 'Receiver cell' was assigned to one cell cluster with its expression data intersected with known receptors and the role of 'sender' cells was given to all other cell types with their expression data intersected with known ligands. Receptors, downstream target genes of interest, and ligands were based on differentially expressed genes (DEGs) between a defined condition of interest and a reference condition. Furthermore, a multi-ligand random forest model was utilised to determine the extent by which IL-1β and TGF-β modulate the F11 FLS in RA compared to PsA. The % of RA-specific or PsA-specific genes which belong to the 5% most strongly predicted targets were determined and a one-sided Fisher's exact test was used to test the significance of the association between the RA-specific and PsA-specific genes and whether they are part of the 5% most strongly predicted targets.

2.3.2.5 Pathway Analysis

PathfindR (V.1.6.2) active subnetwork analysis was utilised for pathway enrichment analysis. FindMarkers identified DEGs were filtered according to their log2 fold change and adjusted p value followed by run_pathfinR based on the Kyoto Encyclopaedia of Genes and Genomes (KEGG) database.

2.3.2.6 Transcription Factor Usage Analysis

Transcription factor usage was estimated with package dorothea (V.1.4.1) with human regulons A, B, C. Calculation of viper score differences between RA and PsA cell clusters was performed to assist with data visualisation.

2.3.3 Bulk RNA Sequencing Analysis

Transcriptomic analysis was performed on our previously published synovial tissue RNA-seq dataset (Guo *et al.*, 2017). An Agilent bioanalyzer evaluated the quality of the RNA before RNA sequencing was performed by Q2 Solutions (Morrisville, NC, USA). The Illumina Ribo- Zero protocol on TruSeq stranded total RNA was used to create sequencing libraries which were pooled and sequenced on an Illumina HiSeq 2000. Raw reads were assessed for quality using FastQC and trimmed based on sequence quality and adaptors. Reads were then aligned to the human reference genome b37.3 using STAR v2.4 (30). RSEM v1.2.14 with the University of California Santa Cruz (UCSC) transcriptome model was utilised to quantify the aligned reads before undergoing further quality evaluation based on numerous metrics including coverage, mapping

rate, and deviation from PCA. Conversion of counts to log2 counts per million, precision weighting, and quantile normalisation was performed. The human donors included in this bulk RNA-seq that were analysed included healthy (n=28), early RA (n=57), and established RA (n=95), with detailed patient demographics previously outlined (Guo *et al.*, 2017). Briefly, healthy donors were defined as individuals with an absence of historic arthritis in addition to no evidence of arthritis when clinically evaluated. Early RA patients were individuals who had received an official diagnosis within the last 12 months and whom were treatment naïve prior to this. Established RA patients had an average disease duration of 68 months and fulfilled two other criteria; all were diagnosed > 1 year before the sample collection and additionally, all patients had received therapeutic intervention of either disease modifying anti-rheumatic drugs or anti–TNF-α.

2.3.4 Synovial Biopsy Digestion & Culture of FLS

Fresh synovial biopsies were digested with 1 mg/ml collagenase type II (Worthington Biochemical, Freehold, NJ, USA) in RPMI-1640 (Gibco-BRL, Paisley, UK) for 4 h at 37°C in humidified air with 5% CO_2, with gentle agitation every hour. Following digestion, dissociated cells were seeded into T25 cell culture flasks and grown to confluence in the RPMI-1640, supplemented with 10% FBS (Gibco-BRL), 10 ml of 1 mmol/l HEPES (Gibco-BRL), penicillin (100 units/ml; Bioscience, UK), streptomycin (100 units/ml; Bioscience, UK) and fungizone (0.2 µg/ml; Bioscience, UK) before passaging with trypsin. Cells were used between passages 3-8 for the various experiments. For functional experiments, FLS were treated with either IL-1β (1 ng/ml), TGF-β (10 ng/ml), or a combination of IL-1β (1 ng/ml) and TGF-β (10 ng/ml). The concentrations of cytokines selected were based on optimisation experiments in which 0.1 ng/ml, 1 ng/ml, 10 ng/ml IL-1β and 1 ng/ml, 10 ng/ml, and 100 ng/ml TGF-β were tested. Unstimulated FLS were used as the basal control. For the Takinib inhibitor experiments in which TAK1 activation is supressed, the FLS were pre-treated with Takinib (20 µM) (Bio-Techne Ireland Limited) or the control DMSO (20 µM) for 2 h prior to treatment with IL-1β (1 ng/ml), TGF-β (10 ng/ml), or a combination of both.

2.3.5 Cellular Bioenergetic Functional Analysis

The analysis of the oxidative and glycolytic metabolic profiles of the RA FLS was performed using the Seahorse-XFe96 analyser (Seahorse Biosciences, Agilent Technologies, USA). RA FLS were seeded at a density of 15,000 cells per well in a 96-well cell culture XFe microplate (Seahorse Biosciences) and allowed to adhere overnight. Following this, cells were then treated with either

IL-1β (1 ng/ml), TGF-β (10 ng/ml) or a combination of both for a further 24 h. For the Takinib experiments, cells were incubated with Takinib (20 μM) (Bio-Techne Ireland Limited) or control DMSO (20 μM) for 2 h before IL-1β (1 ng/ml) and TGF-β (10 ng/ml) addition. The calibrator plate was incubated overnight at 37°C in a non-CO_2 incubator with XF Calibrant, pH 7.4 (Agilent Technologies, USA). On the day of the experiment, cells were then washed with assay medium (unbuffered DMEM (pH 7.4) supplemented with 10 mM glucose; Sigma UK, 1 mM Sodium Pyruvate; Gibco, and L-Glutamine 2 mM; Biosciences) before incubation with assay medium for 1 h at 37°C in a non-CO_2 incubator.

Using the Mitochondrial Stress Test, basal oxidative phosphorylation/glycolysis of the stimulated RA FLS versus baseline was calculated by the average of three baseline oxygen consumption rate (OCR)/extracellular acidification rate (ECAR) measurements respectively, obtained before injection of specific metabolic inhibitors; oligomycin (ATP-synthase-inhibitor), (2 μg/ml; Seahorse Biosciences, UK), trifluorocarbonylcyanide phenylhydrazone (FCCP) (mitochondrial uncoupler) (5 μM; Seahorse Biosciences) and Antimycin A (complex-III inhibitor) (2 μM; Seahorse Biosciences) and Rotenone (2 μM; Seahorse Biosciences). Additional calculations included: the ECAR:OCR ratio, the level of ATP synthesis which was calculated by subtracting the OCR following oligomycin addition from the baseline OCR, the spare respiratory capacity calculated by subtracting the baseline OCR from the maximal respiratory capacity OCR, and the maximum respiratory capacity calculated by subtracting the average of the three OCR readings following FCCP addition from the baseline OCR. The extent of proton leakage was determined by subtraction of the non-mitochondrial respiration from the minimum rate measurement following oligomycin addition. The above calculations are all shown visually in Figure 2.1.1A below.

For the Glycolytic Rate Assay Stress Test, the assay was performed as per the manufacturer's recommendations (Agilent Technologies, USA). Following ECAR measurement at baseline, basal glycolysis, basal proton efflux rate, % proton efflux rate (PER) from glycolysis, the Mito OCR/Glyco PER, compensatory glycolysis, and post 2-DG acidification, were measured following injection of metabolic inhibitors Antimycin A (complex-III inhibitor) (2 μM; Seahorse Biosciences) and Rotenone (2 μM; Seahorse Biosciences), and 2-DG (250 Mm) (Sigma). Quantification of the parameters were determined as outlined in Figure 2.1.1B and *Table 2.1* below.

(A)

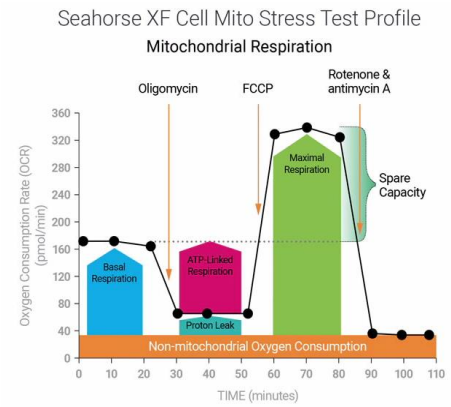

(B)

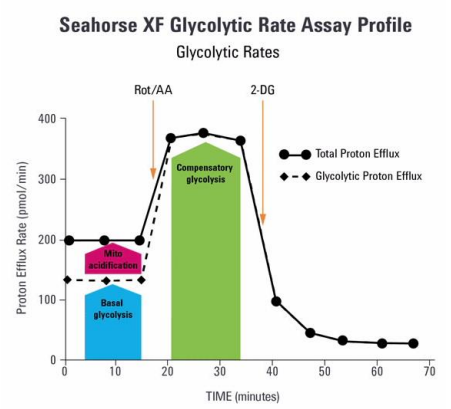

Figure 2.1.1. Seahorse metabolic assay measurable parameters. (A) Representative Seahorse Mitochondrial Stress Test and **(B)** Representative Seahorse Glycolytic Rate Assay depicting measurable parameters.

PARAMETER	EQUATION
Basal Glycolysis	The last glycoPER measurement before first injection of Rotenone and Antimycin
Basal Proton Efflux Rate	The last PER measurement before the first injection of Rotenone and Antimycin
% PER from Glycolysis	Basal Glycolysis/(Basal PER) X 100%
Mito OCR/Glyco PER	(Last OCR measurement before the first injection) – (Minimum OCR after Rot/AA injection)/(Basal Glycolysis)
Compensatory Glycolysis	Maximum glycoPER measurement after the Rot/AA injection
Post 2-DG Acidification	The minimum glycoPER measurement after the 2-DG injection

Table 2.1. **Parameters measured by the Glycolytic Rate Assay.** Equations used to determine the parameters in the Agilent Seahorse XF Glycolytic Rate Assay.

2.3.6 Tetramethylrhodamine-Methyl-Ester Mitochondrial Staining

To determine the effect of cytokine stimulation on mitochondrial activity and morphology in the RA FLS, mitochondrial tetramethylrhodamine-methyl-ester (TMRM) staining was performed using a custom upright (Olympus BX61WI) laser multiphoton microscopy system. FLS at a density of $8x10^4$ were seeded in 35 mm petri-dishes and allowed to adhere overnight in a 37°C incubator with 5% CO_2. Subsequently, FLS were incubated in 1% RPMI-1640 for 24 h before being stimulated with IL-1β (1 ng/ml), TGF-β (10 ng/ml), or a mixture of both for a further 24 h. The RA FLS were then stained with 250 nM of TMRM at 37°C for 30 min before being washed with sterile phosphate

buffered saline (PBS). Two-photon excitation was performed at 850 nm, and fluorescence emission was collected at 580–638 nm. Fluorescence images were acquired and quantified for their intensity and mitochondria morphology using CellProfiler.

2.3.7 Measurement of Mitochondrial Mass

To assess mitochondrial mass, $5x10^4$ RA FLS were seeded into a ViewPlate-96 black (PerkinElmer) and allowed to adhere overnight in a 37°C incubator with 5% CO_2. Cells were then washed with sterile PBS before being centrifuged for 3 min at 1400 rpm. Following this, cells were resuspended in pre-warmed RPMI-1640, and room temperature (RT) thawed MitoTracker green FM (Thermofisher) (diluted to the working concentration of 1 μM in DMSO) to form the staining solution at 50 nM and incubated in the 37°C incubator with 5% CO_2 for 25 min. Cells were then washed with pre-warmed Hanks' Balanced Salt Solution before undergoing centrifugation at 1400 rpm for 3 min. Following this, RA FLS were resuspended in Hanks' Balanced Salt Solution containing the appropriate dilution of the stimulations; IL-1β (1 ng/ml), TGF-β (10 ng/ml), or a combination of both. A positive and negative control containing FCCP (5 μM) and DMSO (50 nM) respectively were also included. The fluorescent emission from the MitoTracker dye was then read immediately on kinetic mode at time intervals of 15 min for 24 h on the Spectra Max Gemini System, with excitation and emission wavelengths of 490 nm and 516 nm respectively.

2.3.8 Measurement of ER Size

To assess the effect of stimulation with IL-1β (1 ng/ml), TGF-β (10 ng/ml), or a combination of both on RA FLS ER size/stress, ER staining was performed. RA FLS were seeded at a density of $1x10^5$ RA FLS into a 12-well plate and allow to adhere overnight in a 37°C incubator with 5% CO_2. Following 6 h or 24 h stimulation with IL-1β (1 ng/ml), TGF-β (10 ng/ml), or a combination of both, ER tracker green (Invitrogen, Fisher Scientific, UK) was used to stain the ER-localized ATP-sensitive K^+ channels of the RA FLS following the manufacturer's instructions. Flow cytometry was performed to detect ER tracker signal on the Canto Flow Cytometer (BD Biosciences). All analysis was performed using FlowJo (v10) software (FlowJo LCC, Oregon, USA). Cells without ER Tracker dye but containing the comparable concentration of DMSO were used as a negative control. Cell debris and doublets were removed from the analysis and the median fluorescent intensity (MFI) of the ER Tracker dye was determined as outlined by the gating strategy shown in Figure 2.13. Intensity of ER tracker staining (MFI) was taken as a correlation of the size of ER membranes.

Fluorescence microscopy was also performed using a custom upright (Olympus BX61WI) laser multiphoton microscopy system. Fluorescent images were acquired, and the volume of the ER compared to the volume of the entire cell was determined using CellProfiler.

2.3.9 Immunofluorescence for Protein Disulphide Isomerase and MitoTracker Red CMXRos

RA FLS were seeded at a density of $1x10^4$ into 18-well chamber slides (Ibidi u-slides) in 100 µL RPMI-1640 and allowed to adhere for 48 h in a 37°C incubator with 5% CO_2. The media was removed and replaced with 100µl fresh pre-warmed RPMI-1640 containing the appropriate concentrations of the stimulations; IL-1β (1 ng/ml), TGF-β (10 ng/ml), or a combination of both. Prior to fixation, cells were stained with MitoTracker Red CMXRos (Life Technologies, M46792) for 20 min at 37°C. All remaining steps were carried out protected from light. RA FLS were then fixed with 4% paraformaldehyde (PFA) for 15 min at RT, permeabilised with ice-cold methanol for 10 min at 4°C and blocked for 1 h at RT on the shaker with 5% donkey serum (in PBS). Blocking solution was then aspirated and 40 µL of the primary antibody Anti-Protein Disulphide Isomerase (PDI) mouse mAb (1:100, Thermo Fisher Scientific, RL90) was added. Overnight incubation with the primary PDI antibody at 4°C in a sealed black box was performed. On day 2, the cells were washed with gentle shaking three times for 10 min in PBS with 0.01% Tween before incubation with 50 µL secondary antibody Alexa Fluor 594 donkey anti-mouse IgG (1:200, Abcam) for 1 h at RT in the dark. Following this, three consecutive 10 min washes in PBS were conducted before mounting and cell nuclei staining was performed with VECTASHIELD[R] Antifade Mounting Medium with DAPI (VectorLabs, H-1200). The chamber slide was then stored protected from the light at 4°C until imaging. Images were taken using the Leica SP8 Scanning Confocal microscope and software.

2.3.10 Enzyme-Linked Immunosorbent Assay (ELISA)

To assess the effects of treatment with IL-1β (1 ng/ml) or TGF-β (10 ng/ml) alone and in combination on the production of proinflammatory mediators and growth factors, RA FLS were seeded in 24 well-plates at a density of $5x10^5$ per well and allowed to attach overnight. Cells were then incubated in 1% RPMI-1640 for 24 h and subsequently stimulated with IL-1β (1 ng/ml), TGF-β (10 ng/ml), or a combination of both for a further 24 h. Supernatants were harvested and levels of IL-6 (IL-6, R&D systems, UK) (min detection range of 9.4 pg/ml and standard range of 9.4-600 pg/ml), IL-8 (IL-8, R&D systems, UK) (min detection range of 31.2 pg/ml and standard range of

31.2-2000 pg/ml), MCP-1 (MCP-1: eBiosciences, USA) (min detection of 7 pg/ml and standard range of 7-1000 pg/ml), VEGF (VEGF, R&D Systems, UK) (min detection of 9 g/ml and standard range of 15.6-1000 pg/ml), and OPG (OPG, R&D Systems, UK) (min detection of 1 g/ml and standard range of 62.5 - 4,000 pg/ml) were determined according to the manufacturer's conditions. For the Takinib experiments, RA FLS were incubated with Takinib (20 µM) or DMSO (20 µM) 2 h prior to stimulation with the cytokines (Bio-Techne Ireland Limited). Supernatants were harvested, and levels of IL-6, IL-8, and MCP-1 were quantified as per the manufacturer's guidelines.

2.3.11 Multiplex ELISA Analysis

Using the cultured supernatants prepared and harvested for the IL-1β/TGF-β and Takinib experiments as described above (Section 2.3.10), protein concentrations of the angiogenic mediators; PIGF, VEGF-A, VEGF-C, VEGF-D, Tie-2, bFGF, and Flt-1, chemokine proteins; MCP-1, MCP-4, IL-8, IP-10, TARC, MDC, Eotaxin, Eotaxin-3, MIP-1β, and MIP-1α, and the MMPs; MMP-1, MMP-3, and MMP-9 were quantified using the V-PLEX Angiogenesis Panel 1 (human) kit (Meso Scale Discovery, USA), the V-PLEX Chemokine Panel 1 (human) kit (Meso Scale Discovery, USA), and the Human MMP 3-Plex Ultra-Sensitive Kit (Meso Scale Discovery, USA), respectively as per the manufacturer's recommendation's. Levels of osteoclastogenic related proteins RANKL, macrophage colony-stimulating factor (M-CSF), and bone morphogenetic protein 2 (BMP2) were also analysed using the U-PLEX RANKL/TNFSF11 (human) kit (Meso Scale Discovery, USA) and the R-PLEX BMP2 (human) kit (Meso Scale Discovery, USA) respectively. Briefly, 50 µl or 25 µl (where appropriate) of supernatants (stored at -20 °C) were added to precoated/coated multiplex wells for 1/2 h at RT under constant shaking. Simultaneously, an eight-point standard curve was added to the plate. The plate was subsequently washed three times using PBS/Tween, after which 2 5µl of Detection antibody was added for 1/2 h at RT under constant shaking. Finally, after washing three times, 150 µl of the appropriate Read buffer was added, and the electrochemiluminescence of the plate was analysed using a Meso Sector S600 Imager. A complete list of the specific Meso Scale Discovery (MSD) assays and the analytes measured are depicted in the table below.

ASSAY	ANALYTES MEASURED
V-PLEX Angiogenesis Panel 1 (human) kit	PIGF, VEGF-A, VEGF-C, VEGF-D, Tie-2, bFGF, Flt-1
V-PLEX Chemokine Panel 1 (human) kit	MCP-1, MCP-4, IL-8, IP-10, TARC, MDC, Eotaxin, Eotaxin-3, MIP-1β, MIP-1α
Human MMP 3-Plex Ultra-Sensitive Kit	MMP-1, MMP-3, MMP-9
U-PLEX RANKL/TNFSF11 (human) kit	RANKL, M-CSF
R-PLEX Human BMP2 (human) kit	BMP2

Table 2.2. List of MSDs performed, and the analytes measured.

2.3.12 mRNA Extraction and cDNA Synthesis

To assess the effects of IL-1β and TGF-β on specific inflammatory and metabolic genes, RA FLS were seeded into 6-well plates at a density of $1x10^6$ and allowed to grow to confluence. Cells were incubated in 1% CRPMI-1640 for 24 h and subsequently stimulated with IL-1β (1 ng/ml), TGF-β (10 ng/ml) alone or a combination. For the Takinib experiments, RA FLS were cultured with Takinib (20 µM) or DMSO control (20 µM) 2 h prior to stimulation with the cytokines. Once confluent, cells were lysed with Qiazol according to the manufacturer's protocol, and total RNA was isolated using the miRNeasy Mini Kit (Qiagen, Germany). The integrity of RNA samples was assessed using a bioanalyzer (Agilent, CA, USA) to ensure high quality including a 260:280 ratio >1.8, and subsequently stored at -80°C until needed. Total RNA (100 ng) was reverse transcribed to complementary cDNA using a high-capacity cDNA reverse transcription kit (Applied Biosystems, Cheshire, UK) containing a mixture of 10x RT Buffer, DNTPs, 10 Random Primers, RNase Inhibitor, Multiscribe Reverse Transcriptase Inhibitor, and RNase-free H_2O, and stored at -20°C until further use. Negative controls consisted of samples lacking multiscribe reverse transcriptase were also prepared alongside.

2.3.13 Gene Expression Analysis

Using the Quant Studio 5 Thermal Cycler (Applied Biosystem, Lewes, UK), gene expression data were quantified by real-time polymerase chain reaction (RT-PCR). Reaction mixtures for amplification contained 1 µl of cDNA, SYBR green PCR mastermix (Applied Biosystems), RNase-free water, and specifically designed target mRNA primer pairs of the following genes (dependent on specific experiments): IL-6, MCP-1, IL-8, CXCL5, CXCL10, VEGF, MMP-1, MMP-3, MFN1, MFN2, OPA1, DRP1, HIF-1α, LDHA, PKM2, GLUT-1, PFKFB3, BIP, XBPI, ATF6, ILβR1, TGFβR1, TGFβR2, PGC-

1α, TFAM, NRF1, and CPT1b. Specific sequences of the primers are outlined in *Table 2.3* below. Negative controls consisted of samples lacking multiscribe reverse transcriptase which enabled the testing of target specific quantification and samples lacking RNA which enabled identification of primer-dimer formation. Using pre-optimised conditions, the comparative threshold cycle (CT) method was used to analyse the data with all thermal cycling conditions performed as recommended by the manufacturer (Applied Biosystems). Using a 96-well plate format, all samples were run in duplicate whilst negative controls were run in singlet alongside. For analysis, all acquired data were normalised to the expression of the housekeeper RPLP0 which acted as an endogenous control and was selected based on optimisation experiments. To represent the relative changes in gene expression of the data, the CT method and specifically the $2^{(-\delta\delta Ct)}$ method was used to graphically represent the results.

Gene Name	Forward Primer	Reverse Primer
RPLP0	5’ GCGTCCTCGTGGAAGTGACAT 3’	5’ TCAGGGATTGCCACGCAGGG 3’
IL-6	5’ CCCTGAGAAAGGAGACATGTAAC 3’	5’ CCTCTTTGCTGCTTTCACACATG 3’
MCP-1	5’ GCTCGCTCAGCCAGATGCAA 3’	5’ TGGTGAAGTTATAACAGCAGGTGA 3’
IL-8	5’ TTGGCAGCCTTCCTGATTTC 3’	5’ TGGCAAAACTGCACCTTCAC 3’
CXCL5	5’ GTCTTCAGCAGAGAAGTTTTCTG 3’	5’ CAGGAAGAAAGCTAACTACTGGA 3’
CXCL10	5’ TTCAAGGAGTACCTCTCTCTAGAA 3’	5’ GGTTGATTACTAATGCTGATGCAG 3’
VEGF	5’ GCAGAATCATCACGAAGTGGTG 3’	5’ TCTCGATTGGATGGCAGTAGCT 3’
MMP-1	5’ GCTAACAAATACTGGAGGTATGAT 3’	5’ ATTTTGGGATAACCTGGATCCATA 3’
MMP-3	5’ CGGTTCCGCCTGTCTCAAG 3’	5’ CGCCAAAAGTGCCTGTCTT 3’
MFN1	5’ GACAGTCCAGGCACAGATGT 3’	5’ GGCTTGGAAAGCCGCTCATT 3’
MFN2	5’ GAAGACACGTACAGGAATGCAG 3’	5’ GTAACCTTTGACGTCCAGAACC 3’
OPA1	5’ CCTGTGAGGTCTGCCAGTCT 3’	5’ CCTTAATTGGGGTCGTTGAAGC 3’
DRP1	5’ CTAAAGGGGTGGAAGCAGAAGA 3’	5’ CCGTGTAAAGCTTATTTTTGGTGTG 3’
HIF-1α	5’ GAAACTTCTGGATGCTGGTGATTT 3’	5’ GCAATTCATCTGTGCTTTCTGTCA 3’
LDHA	5’ ATGGAGATTCCAGTGTGCCTG 3’	5’ CAGAGAGACACCAGCAACATT 3’
PKM2	5’ ATTATTTGAGGAACTCCGCCG 3’	5’ ATTCCGGGTCACAGCAATGAT 3’
GLUT-1	5’ CTTCCAGTATGTGGAGCAACT 3’	5’ GCACAGTGAAGATGATGAAGA 3’
PFKFB3	5’ CCATGAAAGTCCGGAAGCAATG 3’	5’ GCTTTTGACATCTCTCAAGGCAG 3’
BIP	5’ TCCTGCGTCGGCGTGTTCAA 3’	5’TGCCCTGATCGTTGGCGATG 3’
XBPI	5’ GGAGGAAACTGAAAACAGAGTAG 3’	5’ CATTCGAGCCTTCTTTCGATCTC 3’
AFT6	5’ TCAGGTTAAATCATGAACTTCGAGG 3’	5’TGACTTGGTCCTTTCTACTTCATG 3’
ILβR1	5’ GGCCAGTTGAGTGACATTGCT 3’	5’ TGTGATGAGGGTACTCCTTCTTT 3’
TGFβR1	5’ GCTGTATTGCAGACTTAGGACTG 3’	5’ TTTTTGTTCCCACTCTGTGGTT 3’
TGFβR2	5’ AAGATGACCGCTCTGACATCA 3’	5’CTTATAGACCTCAGCAAAGCGAC 3’
CPT1b	5’ CATGTATCGCCGTAAACTGGAC 3’	5’ TGGTAGGAGCACATAGGCACT 3’
PGC-1α	5’ GCTTTCTGGGTGGACTCAAGT 3’	5’ GAGGGCAATCCGTCTTCATCC 3’
NRF1	5’ AGGAACACGGAGTGACCCAA 3’	5’ TATGCTCGGTGTAAGTAGCCA 3’
TFAM	5’ ATGGCGTTTCTCCGAAGCAT 3’	5’ TCCGCCCTATAAGCATCTTGA 3’

Table 2.3. Primer sequences designed and used for RT-PCR analysis.

2.3.14 Flow Cytometry

Multiparameter flow cytometric analysis was used to analyse the expression of surface and intracellular markers in the basal versus stimulated RA FLS. Surface marker expression of RA FLS following stimulation with IL-1β (1 ng/ml), TGF-β (10 ng/ml) alone or in combination was examined. For extracellular staining, cells were seeded at $5x10^5$ cells/well in a 24 well plate, incubated with 1% RPMI-1640 for 24 h when confluent and then stimulated with 1% RPMI-1640 supplemented with the specific cytokines IL-1β (1 ng/ml) or TGF-β (10 ng/ml) for 24 h prior to staining. The following optimised staining protocol was used: Adherent RA FLS were removed from the 24-well plates using RT Accutase cell detachment solution (Sigma-Aldrich, Ireland) to preserve cell viability and cell surface marker expression and transferred to the appropriate wells of a 96-well round-bottomed plate. Following washing in ice-cold PBS, cells were resuspended in LIVE/DEAD fixable NIR (Molecular Probes, Thermofisher Scientific) viability dye diluted in PBS (1:1000) for 30 min at 4°C in the dark in order to eliminate dead cells. Samples were then blocked with a human FcγR-binding inhibitor (TruStain FcX Receptor blocking solution (BioLegend UK)) diluted 1:10 in Fluorescence-Activated Cell Sorting (FACS) buffer ((Dulbecco's PBS without $Mg2^+$ or $Ca2^+$ (Sigma Aldrich), 2% heat-inactivated FBS (Biosciences), 0.05% sodium azide (Sigma-Aldrich), and 0.5 M EDTA pH 8.0 (Ambion)) prior to antibody staining for 10 min to prevent non-specific binding of antibodies. The following extracellular antibodies were then used in combination to investigate surface expression of activation and functional markers by the stimulated RA FLS: PDPN FITC (Clone NC-08) (BioLegend), Human FAP Alexa Fluor 700 (Clone 427819) (RnD), THY1/CD90 Brilliant Violet 421 (Clone 5E10) (BioLegend), CD34 Brilliant Violet 510 (Clone 581) (BioLegend), CD54 Brilliant Violet 605 (Clone HA58) (BD), CD45 Brilliant Violet 650 (Clone HI30) (BioLegend), CD146 Brilliant Violet 711 (Clone P1H12) (BioLegend), HLA-DR Brilliant Violet 785 (Clone L243) (BioLegend), FAS-L PE (Clone NOK-1) (BioLegend), and CD309 PE/Cy7 (Clone 7D4-6) (BioLegend). For the chemokine panel, the following fluorochrome-conjugated antibodies were used – VCAM-1 APC (Clone STA) (BioLegend), CCR6 Brilliant Violet 421 (Clone 11A9) (BD), CXCR3 Brilliant Violet 510 (Clone G025H7) (BioLegend), CXCR4 Pe-CF594 (Clone 12G5) (BD), CXCR5 Brilliant Violet 785 (Clone J252D4) (BioLegend), and PDPN PeCy7 (Clone NC-08) (BioLegend). A full list of the antibodies used is outlined in *Table 2.4* below.

Samples were incubated with the appropriate fluorochrome-conjugated extracellular antibodies and Brilliant Stain Buffer mixture (30 µl Brilliant Stain Buffer + 1 µl/ab per sample) for 30 min at 4°C in the dark. Following fixation with 75 µl 1% PFA for 10 min, consecutive washes with PBS and FACS buffer and centrifugation at 1400 rpm for 3 min following each wash was performed, before the cells were resuspended in 200 µl FACS buffer and transferred from the 96-

well round bottomed plate to labelled flow tubes. Samples were stored at 4°C in the dark until sample acquisition on the LSR Fortessa Flow Cytometer (BD), with single stained beads (BD, UK) used for compensation purposes to adjust for spectral overlap. All analysis was performed using FlowJo (v10) software (FlowJo LCC, Oregon, USA). For gating purposes, fluorescent minus one (FMO) controls were used to determine gate boundaries between markers. Cell debris and doublets were removed from the analysis and marker expression on the FLS was determined as outlined by the gating strategy shown in Figure 2.20 and Figure 2.23, respectively.

Marker	Other Name	Fluorochrome	Clone	Company
FUNCTIONAL PANEL				
CD45		BV650	HI30	BioLegend
THY1	CD90	BV421	5E10	BioLegend
CD34		BV510	581	BioLegend
CD146		BV711	P1H12	BioLegend
FAP		AF700	427819	RnD
ICAM-1	CD54	BV605	HA58	BD
HLA-DR		BV786	L243	BioLegend
VEGFR-2	CD309	PeCy7	7D4-6	BioLegend
FAS-L	CD178	PE	NOK-1	BioLegend
PDPN		FITC	NC-08	BioLegend
CHEMOKINE PANEL				
VCAM-1	CD106	APC	STA	BioLegend
CCR6	BN1	BV421	11A9	BD
CXCR3	CD183	BV510	G025H7	BioLegend
CXCR4	CD184	Pe-CF594	12G5	BD
CXCR5	CD185	BV785	J252D4	BioLegend
PDPN		PeCy7	NC-08	BioLegend

Table 2.4. Extracellular antibodies used for RA FLS flow cytometric staining.

2.3.15 Wound Repair Assay

RA FLS were seeded into 48-well plates at a density of 3 x10^4 cells/well and grown to confluence. Once confluent, a sterile P200 pipette tip was used to induce a single linear scratch wound through

the middle of each well. The media, including dead cells, was then removed and the appropriate concentrations of the stimulants; IL-1β (1 ng/ml), TGF-β (10 ng/ml), or a combination of both, were added in RPMI-1640, before the cells were placed back in the 37°C incubator for a further 24 h. The cells were then washed in PBS, fixed in 4% PFA for 30 min, and then stained with 0.1% crystal violet for a further 30 min. FLS migration was subsequently assessed by taking 3 high-power images of each well using a phase contrast microscope at 10x magnification (Nikon TMS microscope linked to a Canon S70 camera). Semi-quantitative analysis was then performed by counting the number of cells that had repopulated the wound margins as previously described (Barker *et al.*, 2023). This process was repeated for all biological replicates.

2.3.16 Crystal Violet Cell Viability Assay

To assess the effects of Takinib and DMSO addition on FLS viability, all media was removed from the cells and fixation in 4% PFA was performed for 30 min at RT. Subsequently, 0.1% crystal violet was applied to the cells for a further 30 min at RT. The wells were then washed three times in distilled H_2O before being left to dry overnight. The following day, 1% SDS solution in dH_2O was prepared and the cells were incubated for 30 min with approx. 400 µL/well with gentle shaking. A 96-well plate was then prepared with 100 µL in triplicate of each condition added and 1% SDS x3 included for the blank. The absorbance was read on the ELISA plate reader at 530 nm.

2.3.17 RA and PsA *ex vivo* Synovial Explants

Fresh RA and PsA biopsies were obtained from arthroscopy and immediately sectioned into small pieces before being cultured in 96-well plates in full media, creating an environment that closely resembles the *in vivo* joint environment. To assess the effect of TAK1 inhibition on the release of proinflammatory mediators, the biopsies were cultured in the presence of Takinib (20 µM) or DMSO (20 µM) vehicle control for 24 h at 37°C. Following culture, the supernatants were harvested and assayed for the spontaneous release of angiogenic mediators, chemokines, and MMPs by MSD multiplex assay as outlined in Section 2.3.11 above.

To assess the effect of Takinib inhibition on overall biopsy size, an *ex vivo* synovial explant model was utilised (McGarry *et al.*, 2018b). Briefly, 50 µl of Matrigel (Biosciences) was added to a 96 well plate and incubated for 1 h at 37°C, before sections of the synovial tissue were embedded in the Matrigel and cultured in the presence of Takinib (20 µM) or DMSO (20 µM) vehicle control. The supernatants were collected, fresh media and inhibitors were added, and microscopic images

were taken repeatedly at day 0, 4, 8, 12, 16, and 21. Biopsies were imaged by taking a single high-power image of the entire biopsy at 10x magnification in addition to 3 high-power images using a phase contrast microscope at 20x magnification (Nikon TMS microscope linked to a Canon S70 camera).

2.3.18 Statistical Analysis

All statistical analysis was performed using GraphPad Prism 9 software (GraphPad Software Inc., California, USA). Analysis of non-parametric data was performed using either the unpaired T test with the Wilcoxon-Signed Rank Test (#) or the one-way ANOVA with Friedman's Test (*). Statistical significance was defined by *p≤0.05, **p≤0.01, ***p≤0.001, ****p≤0.0001 for Friedman's Test. Statistical significance was defined by $^{\#}$p≤0.05, $^{\#\#}$p≤0.01, $^{\#\#\#}$p≤0.001, $^{\#\#\#\#}$p≤0.0001 for the Wilcoxon-Signed Rank Test. For the bulk RNA-seq data, statistical analysis was performed using the Kruskal-Wallis Test with Dunn's Multiples Comparisons, with *p≤0.05, **p≤0.01, ***p≤0.001, ****p≤0.0001 defined as statistically significant. Outliers were identified and excluded using the ROUT method. All data were represented as Mean +/- Standard Error of the Mean (SEM).

2.4 Results

2.4.1 The distribution of FLS clusters is different between RA and PsA synovial biopsies.

Global scRNA-seq analysis was performed on RA and PsA synovial tissue cell suspensions. Nine mega clusters were identified including FLS, ECs, T cells, B cells, macrophages, DCs, plasma cells, pericytes, natural killer cells and additionally an undefined population. Further analysis of the FLS mega-subset identified eleven distinct clusters in synovial biopsies obtained from RA and PsA patients. Figure 2.1 shows that while both RA and PsA synovial tissue had all eleven clusters, the frequency of the clusters differed between the two pathotypes, with PsA displaying a significant increase in the number of FLS in the F1 cluster (***$p<0.001$), whilst an increase in the number of FLS in the F8, F9, and F11 cluster were observed in RA (**$p=0.006$, ***$p<0.001$, ***$p<0.001$, respectively). Further analysis was performed to identify the expression of the key FLS markers FAP and THY1 across clusters F1-F11. It was identified that FAP and THY1 were enriched in the RA F11 FLS cluster, and to a lesser extent were also enriched in the F9 and F10 clusters. In contrast, the F1 cluster which demonstrates dominance in PsA synovium, had minimal FAP/THY1 expressing cells (Figure 2.1A-B and Figure 2.2A). Next, data imputation was performed to determine the number of cells co-expressing THY1 and FAP that were present in the F1 and F11 clusters. Figure 2.2B shows that while RA F11 FLS cluster demonstrated an enrichment of co-expressing FAP/THY1 cells, the PsA F1 FLS cluster did not. These data demonstrate the significant heterogeneity of FLS across the two disease states, with distinct predominance of differential clusters identified between RA and PsA. Subsequently, this could explain the differential regulation of pathogenic mechanisms within the synovium that defines their disease pathotype, progression, and response to intervention.

2.4.2 Macrophage-derived IL-1β and T cell-derived TGF-β interact to promote the pathogenic phenotype of proinflammatory RA F11 FLS.

As mentioned above in Section 2.3.2.2, scRNA-seq analysis was conducted on the whole synovial cells' suspension, thus enabling the global analysis of potential receptor-ligand interaction networks that may be driving the transcriptomic profile of inflammatory FLS. The role of receiver cells was designated to the F1 cluster enriched in PsA, and the F11 cluster enriched in RA (Figures 3A and 3B) thus, their potential ligands were hypothesised to be derived from all other cell types within the synovium. Figure 3B demonstrates a Circo plot that depicts the top ligand and downstream target interactions that are enriched in the RA F11 cluster. Macrophage-derived IL-1β and T cell-derived TGF-β are the main ligands that potentially may be interacting with receptors

on the THY1+FAP+ F11 FLS, and potentially driving their proinflammatory phenotype within the joint. Direct comparison of RA and PsA indicates that whilst IL-1β alone could significantly predict (*p=0.028) the expression of downstream genes of cluster F11 in PsA synovium, in RA, when analysed alone, neither IL-1β or TGF-β could predict downstream expression of genes (Figure 3C). However, examination of IL-1β or TGF-β together in the context of synergy demonstrated high significance in predicting the downstream expression of differentially expressed genes of F11 FLS in RA (***p<0.001). Cumulatively, these results suggest that the synergistic interactions between the macrophage-derived IL-1β and T cell-derived TGF-β may drive the pathogenic functional activity of the F11 THY1+FAP+ FLS enriched in RA patients specifically.

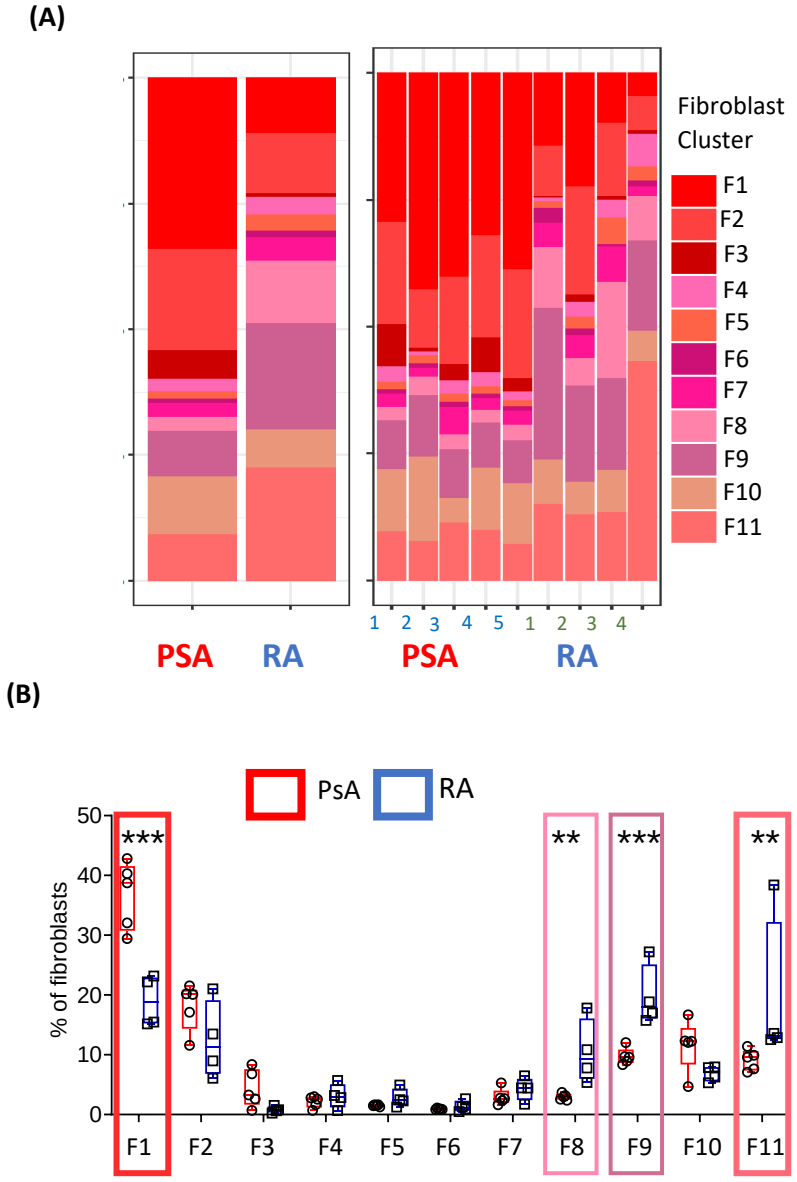

Figure 2.1. Distinct FLS cluster distribution in RA compared to PsA synovial biopsies. High dimensionality scRNA-seq analysis identifies specific cell clusters in the synovial tissue biopsies of patients with RA (n=4) and PsA (n=5). **(A)** Abundance of FLS clusters in RA and PsA patient synovial biopsies. **(B)** Frequency of FLS clusters (calculated as a percentage of all FLS/sample) in PsA (n=5) and RA (n=4) synovial biopsies, data are presented as box and whiskers plots (min to max), symbols represent individual samples, statistical significance was determined by two-way analysis of variance with Sidak's multiple comparisons test (***p<0.001, **p=0.0062). FLS clusters with significantly different abundances between RA and PsA are indicated by blue (higher in RA) and red (higher in PsA) boxes.

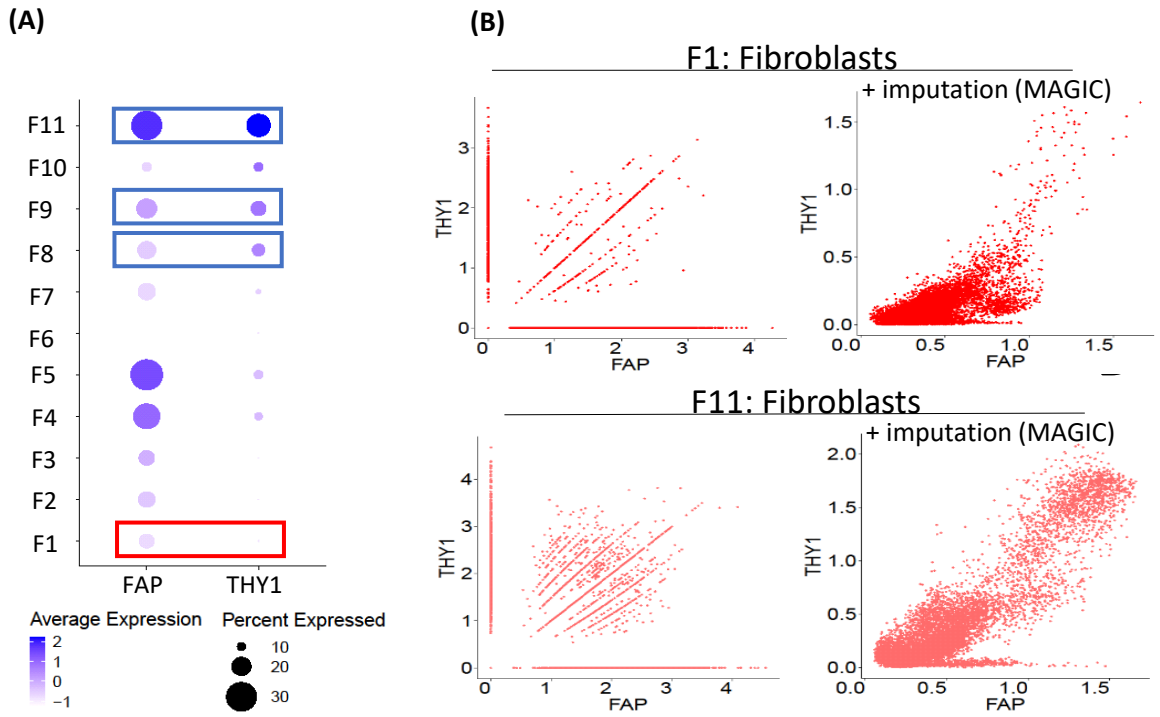

Figure 2.2. Distinct FLS cluster distribution in RA compared to PsA synovial biopsies. (A) Expression and percentage of positive cells per FLS cluster for the markers FAP and THY1. FLS clusters with significantly different abundances between RA and PsA are indicated by blue (higher in RA) and red (higher in PsA) boxes. **(B)** Scatterplots showing the relationship between THY1 and FAP expressing cells before and after data imputation for RA and PsA FLS cluster F1 and FLS cluster F11.

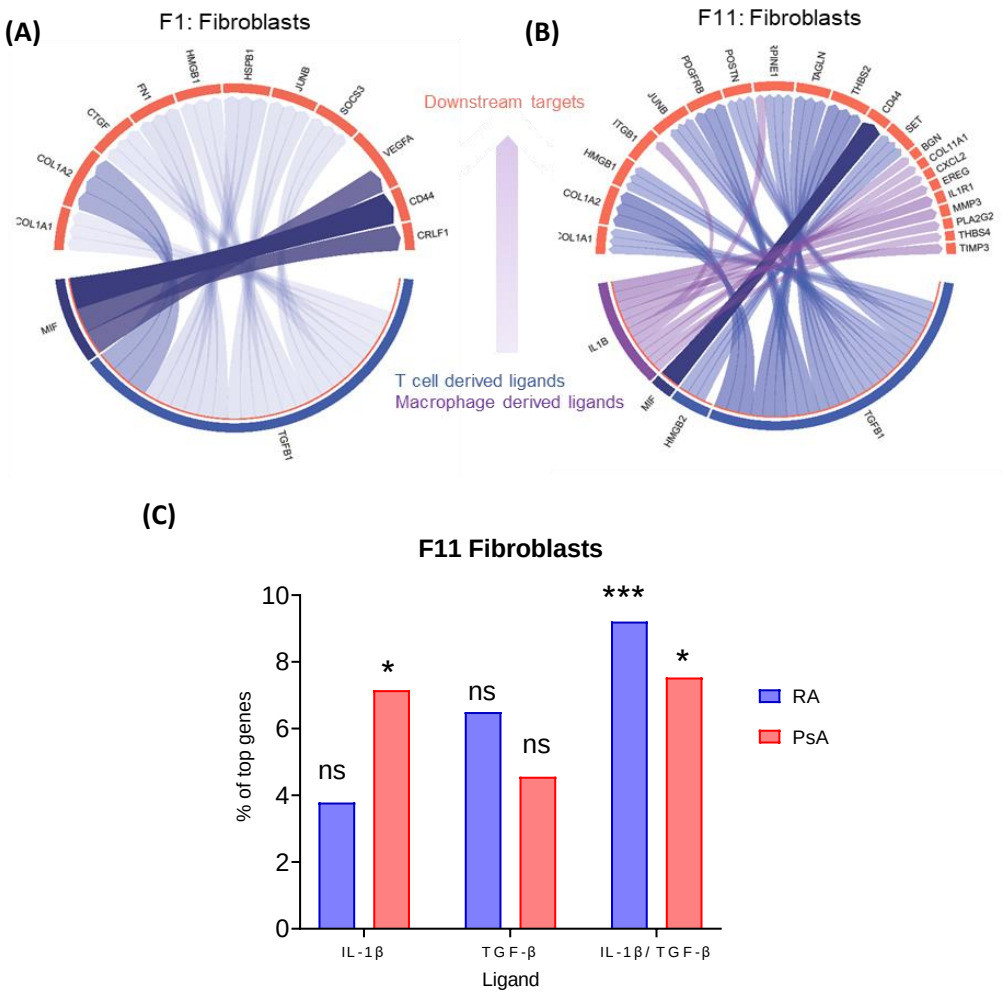

Figure 2.3. Identification of ligand receptor interactions that promote invasive FLS. (A) Circo plot depicting the top ligand and downstream target interaction enriched in PsA FLS cluster F1. **(B)** Circo plot depicting the top ligand and downstream target interaction enriched in RA, invasive FLS cluster F11. **(C)** Percentage of gene targets downstream of IL-1β, TGF-β, or IL-1β/TGF-β, as part of the top targets regulated by F11 FLS cluster receptors. Asterisks indicate significance of ligand-target interactions.

2.4.3 Dysregulated expression of the IL-1β and TGF-β signalling pathways in healthy vs early RA vs established RA synovial tissue.

To investigate the prevalence of mediators related to the IL-1β and TGF-β signalling pathways in HC vs early RA vs established RA, transcriptomic analysis was conducted. Bulk RNA-seq on synovial tissue biopsies obtained from a healthy cohort (n=28), those with early RA (n=57), and those with established RA (n=95) revealed enrichment in several critical ligands, receptors, mediators, and effectors in both the IL-1β and TGF-β signalling pathways. Specifically, a significant increase in the expression of the following genes was detected between HC and early RA/established RA; IL-1A (Figure 2.4A), IL-1β itself (Figure 2.4B), the receptors IL-1R1 (Figure 2.4C), IL-1R2 (Figure 2.4D), and IL-1RAP (Figure 2.4E), the mediators IRAK4 (Figure 2.4J), TAB2 (Figure 2.4L), TAB3 (Figure 2.4M), and the effectors NF-κB1 (Figure 2.4N) and NLRP3 (Figure 2.4O) ($p<0.05$, $p<0.01$, $p<0.001$, $p<0.0001$). Moreover, both TRAF6 (Figure 2.4F) and IRAK3 (Figure 2.4I) exhibited a significant stepwise increase in expression from HC to early RA to established RA. Conversely, IRAK1 (Figure 2.4G), IRK2 (Figure 2.4H), and TAB1 (Figure 2.4K) demonstrated a significant decrease in expression from HC to established RA ($p<0.0001$). Furthermore, in relation to TGF-β signalling, a significant increase in the expression of the following genes was detected between HC and early RA/established RA; the receptors TGF-βR1 (Figure 2.5B) and TGF-βR2 (Figure 2.5C), SMAD2 (Figure 2.5D), SMAD4 (Figure 2.5F), SMURF2 (Figure 2.5H), and the effector PI3K (Figure 2.5I) ($p<0.05$, $p<0.01$, $p<00001$). Interestingly, both TGF-β1 itself (Figure 2.5A) and the SMADs, SMAD3 and SMAD7 (Figures 2.5E and 2.5G), showed a reduction in expression from HC to established RA ($p<0.0001$). Collectively, this identified increase and dysregulation of several key components of the IL-1β and TGF-β signalling pathways in RA synovial tissue compared to healthy comparators suggests a prominent functional role for IL-1β and TGF-β alone and in synergy to drive RA FLS pathogenic phenotype.

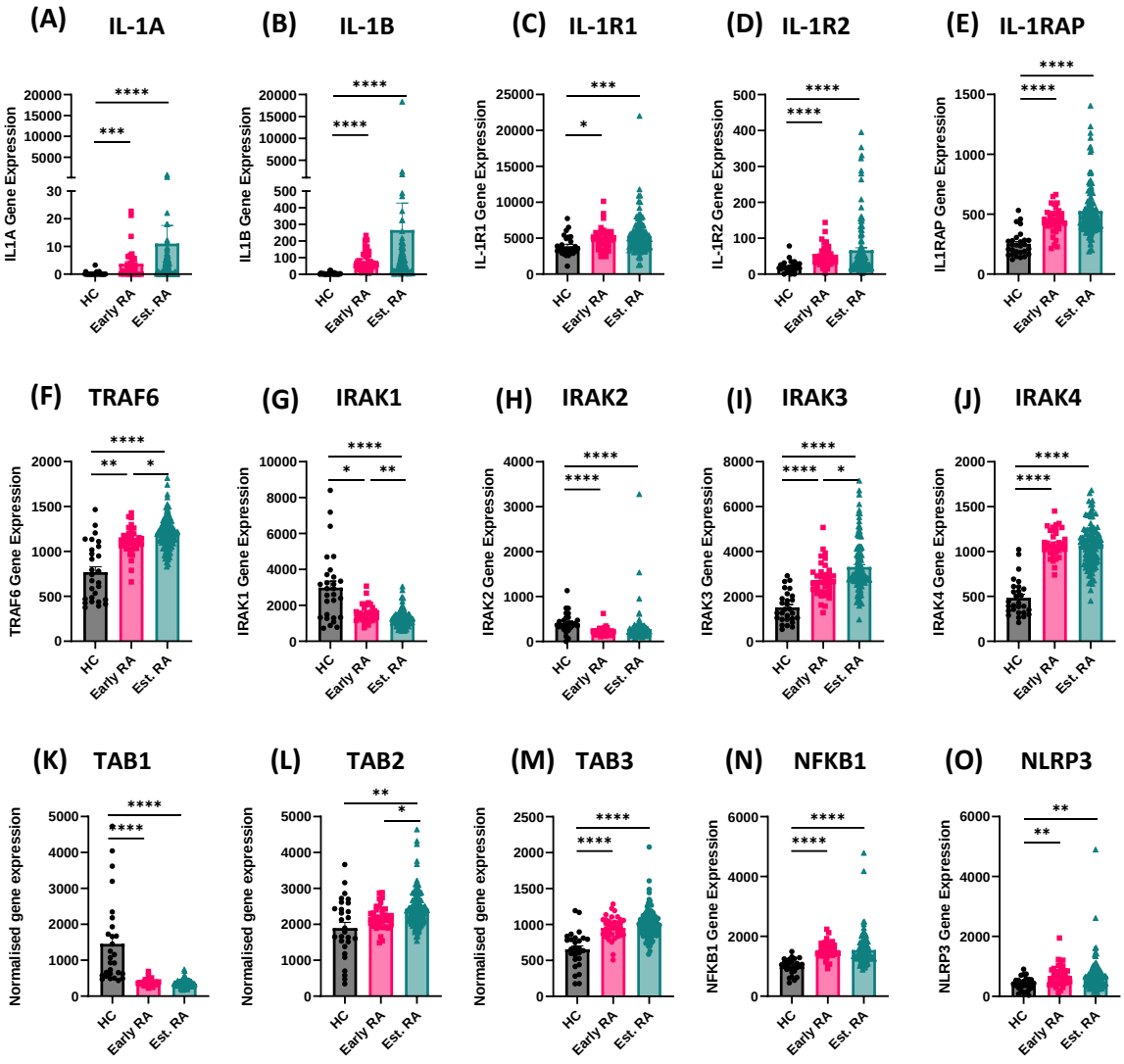

Figure 2.4. Dysregulated expression of the IL-1β signalling pathway in healthy vs early RA vs established RA synovial tissue. (A-O) Bar graphs demonstrating normalised gene expression of key mediators involved in the IL-1β signalling pathway (IL-1A, IL-1β, IL-1R1, IL-1R2, IL-1RAP, TRAF6, IRAK1, IRAK2, IRAK3, IRAK4, TAB1, TAB2, TAB3, NF-κB1, NLRP3) via transcriptomic analysis of bulk RNA-seq on synovial biopsies from HC (n=28), individuals with early RA (n=57), and established RA patients (n=95). All data represented as Mean +/- SEM. Statistical analysis was performed using the Kruskal-Wallis Test with Dunn's Multiples Comparisons, with *p≤0.05, **p≤0.01, ***p≤0.001, ****p≤0.0001 defined as statistically significant.

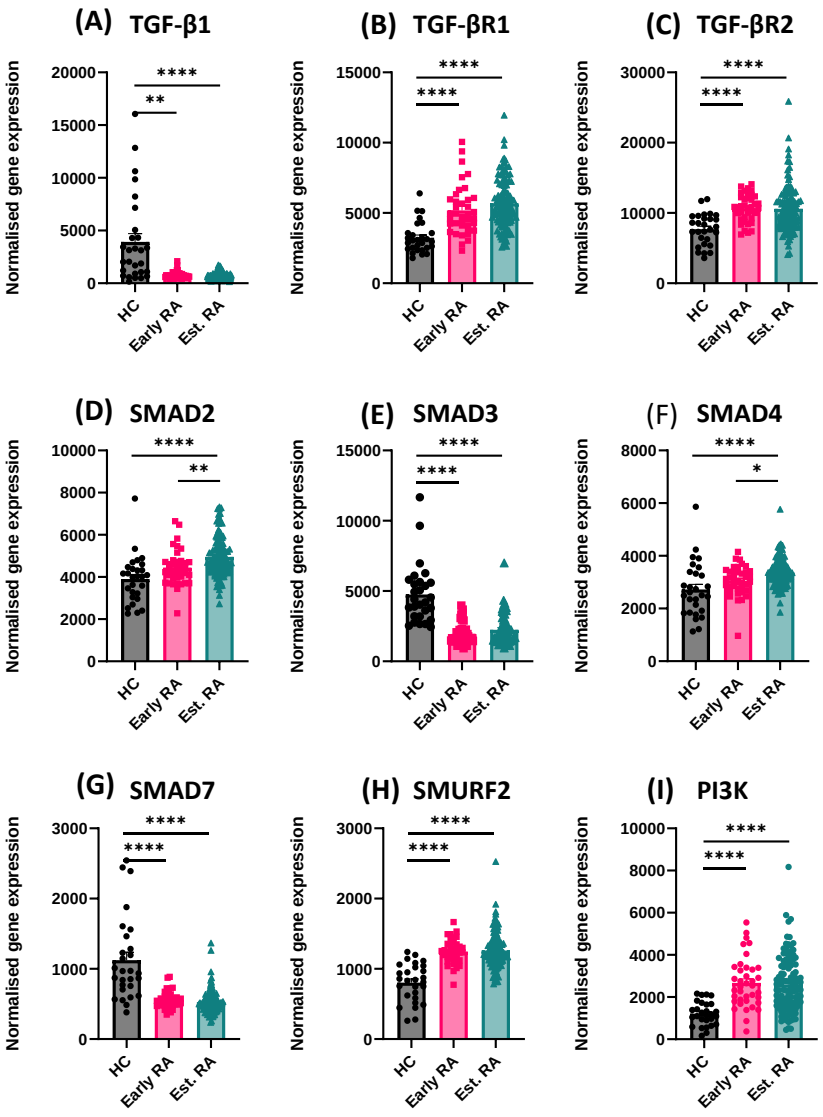

Figure 2.5. Dysregulated expression of the TGF-β signalling pathway in healthy vs early RA vs established RA synovial tissue. (A-I) Bar graphs demonstrating normalised gene expression of key mediators involved in the TGF-β signalling pathway (TGF-β, TGF-βR1, TGF-βR2, SMAD2, SMAD3, SMAD4, SMAD7, SMURF2, PI3K) via transcriptomic analysis of bulk RNA-seq on synovial biopsies from HC (n=28), individuals with early RA (n=57), and established RA patients (n=95). All data represented as Mean +/- SEM. Statistical analysis was performed using the Kruskal-Wallis Test with Dunn's Multiples Comparisons, with *p≤0.05, **p≤0.01, ***p≤0.001, ****p≤0.0001 defined as statistically significant.

2.4.4 The synergistic effect of IL-1β and TGF-β drive the metabolic adaptation of RA FLS.

To understand the functional impacts of IL-1β and TGF-β on RA FLS behaviour, the effect of cytokine synergy on the levels of oxidative phosphorylation and glycolysis, the primary energy pathways employed by the activated FLS, in addition to various other metabolic measures, were examined using the Seahorse XFe-Analyser in real-time.

Figures 2.6A and 2.6B demonstrate the average ECAR and OCR bioenergetic profiles in RA FLS following stimulation with IL-1β and TGF-β alone and in combination. A significant increase in the glycolytic activity (ECAR) of RA FLS was demonstrated in response to IL-1β/TGF-β together compared to stimulation with either cytokine alone (Figures 2.6B and 2.6E) ($p<0.05$). In parallel, the levels of oxidative phosphorylation (Figure 2.6C) and ATP synthesis (Figure 2.6D) were both significantly decreased ($p<0.01$, $p<0.001$) compared to TGF-β treatment only indicating that IL-1β may be having an inhibitory effect. This led to a significant shift in the metabolic profile of the RA FLS resulting in a significant increase in the ECAR:OCR ratio compared to stimulation with either IL-1β or TGF-β alone (Figure 2.6F) ($p<0.05$, $p<0.01$ respectively). The individual breakdown of the levels of ECAR and OCR across the four conditions is summarised visually in Figure 2.6G with a marked dominance of glycolysis under synergy, whilst additionally the metabolic map demonstrates that RA FLS treated with IL-1β and TGF-β shifted from a more quiescent phenotype to a highly energetic energy profile (Figure 2.6H).

Interestingly, no significant changes under synergy conditions were observed for spare respiratory capacity, maximal respiratory capacity, proton leak, or non-mitochondrial respiration (Figures 2.7A-D). Pie charts describe the relative contribution of the OxPhos potential within each condition as a percentage of total OCR output for RA FLS in response to basal, IL-1β, TGF-β, and IL-1β/TGF-β (Figure 2.7E(i-iv)). No changes from basal were observed for ATP synthesis (green) in response to TGF-β (Figure 2.7E(iii)) but it was decreased following treatment with IL-1β (Figure 2.7E(ii)), with the greatest decrease observed in response to IL-1β and TGF-β treatment (Figure 2.7E(iv)). Moreover whilst treatment with IL-1β led to a detectable increase in maximal respiratory capacity (red) compared to basal (Figure 2.7E(ii)), TGF-β demonstrated the opposite effect with a slight decrease demonstrated (Figure 2.7E(iii)). Interestingly, IL-1β/TGF-β conditions resulted in the greatest increase in maximal respiratory capacity compared to either cytokine alone (Figure 2.7E(iv)). No considerable differences for non-mitochondrial respiration (purple) or proton leak (blue) were detected between synergy and the other conditions.

Similarly, the glycolytic rate assay showed that although individually IL-1β and TGF-β both increased ECAR measurements compared to basal, the synergistic effect of these cytokines led to a significant increase in basal glycolysis and basal proton efflux rate (Figure 2.8A-B), with a

significant additive increase in % PER from glycolysis and compensatory glycolysis (Figure 2.8C-D) also observed compared to IL-1β or TGF-β only treated RA FLS ($p<0.05$). However, as shown in Figure 2.8E, Mito OCR/Glyco PER exhibited the opposite effect with a significant decrease observed with the synergy conditions compared to treatment with IL-1β ($p<0.05$) or TGF-β ($p<0.05$) only, reflective of a reduction in oxidative phosphorylation. No significant differences in post 2D-G acidification with IL-1β/TGF-β conditions were detected compared to treatment with either cytokine alone (Figure 2.8F). Pie charts describe the relative contribution of the glycolytic rate assay outputs in RA FLS as a percentage of total glycolytic capacity in response to basal (Figure 2.8G(i)), IL-1β (Figure 2.8G(ii)), TGF-β (Figure 2.8G(iii)), and synergy (Figure 2.8G(iv)) conditions. Basal proton efflux rate (blue) was increased in response to IL-1β (Figure 2.8E(ii)) and TGF-β (Figure 2.8E(iii)) alone compared to basal (Figure 2.8E(i)). However, treatment with IL-1β and TGF-β (Figure 2.8E(iv)) led to a greater increase in basal proton efflux rate than treatment with either cytokine alone. Conversely, % PER from glycolysis demonstrated a decrease following IL-1β (Figure 2.8E(ii)) and TGF-β (Figure 2.8G(iii)) treatment alone in comparison to basal, with the largest decrease observed following the addition of IL-1β and TGF-β in combination (Figure 2.8G(iv)). Moreover, whilst the proportion of compensatory glycolysis (green) was slightly higher under synergy conditions compared to either cytokine alone, no considerable differences were detected amongst any of the four conditions for the percentage contribution of mitoOCR/Glyco PER (purple) or post 2-DG acidification (orange).

The effect of cytokine treatment alone and in synergy on the FLS expression of metabolic genes was next determined. Whilst GLUT-1 gene expression demonstrated an upregulation in response to IL-1β alone ($p<0.05$) compared to basal, treatment with IL-1β and TGF-β resulted in a significant synergistic induction that was greater than either cytokine alone ($p<0.01$ and $p<0.05$ respectively) (Figure 2.9A). In contrast, LDHA expression was upregulated with IL-1β ($p<0.05$) and TGF-β ($p<0.001$) separately compared to basal controls, with IL-1β and TGF-β together resulting in an additive effect on LDHA expression (Figure 2.9B). Similarly, whilst HIF-1α was significantly upregulated in response to IL-1β ($p<0.001$) and TGF-β ($p<0.01$) individually, the addition of both IL-1β and TGF-β did not result in a potentiation/synergy effect but an additive effect (Figure 2.9C). IL-1β and TGF-β induced a significant synergistic increase in the expression of key glycolytic enzymes PKM2 ($p<0.05$) and PFKFB3 ($p<0.01$) compared to either cytokine alone. In summary, these results indicate that the shift in metabolic profile towards glycolysis was also paralleled by a synergetic and additive increase in the gene expression of key glycolytic enzymes, indicative of the RA FLS reliance on glycolytic metabolic processes over oxidative phosphorylation in response to IL-1β and TGF-β treatment.

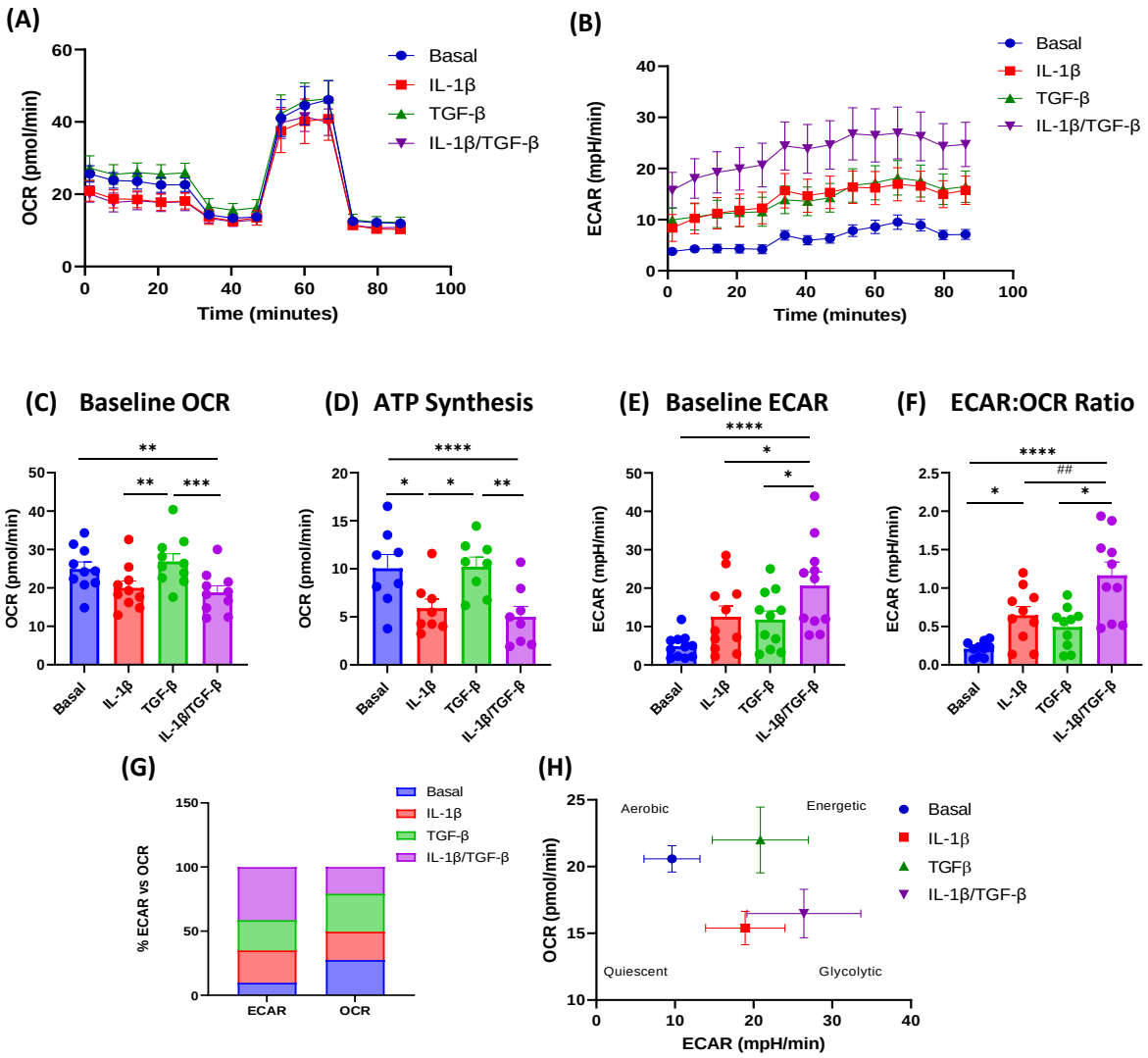

Figure 2.6. IL-1β and TGF-β synergistically drive the metabolic adaptation of RA patient FLS. Average **(A)** OCR and **(B)** ECAR profiles of RA FLS (n=8-11) treated with IL-1β (1 ng/ml), TGF-β (10 ng/ml), or a combination of both for 24 h before and after injections of metabolic inhibitors oligomycin, FCCP, and Rotenone and Antimycin A. **(C-F)** Representative bar graphs demonstrating baseline OCR, ATP synthesis, baseline ECAR, and ECAR/OCR ratio in RA FLS. **(G)** Stacked bar graph and **(H)** representative energy map showing average ECAR and OCR across the four conditions. All data represented as Mean +/- SEM. Statistical analysis was performed using the non-parametric, Wilcoxon Signed-Rank Test (#) or the one-way ANOVA with Friedman's Test (*) where appropriate. Statistical significance was defined by *$^{(\#)}$p≤0.05, **$^{(\#\#)}$p≤0.01, ***$^{(\#\#\#)}$p≤0.001, ****$^{(\#\#\#\#)}$p≤0.0001.

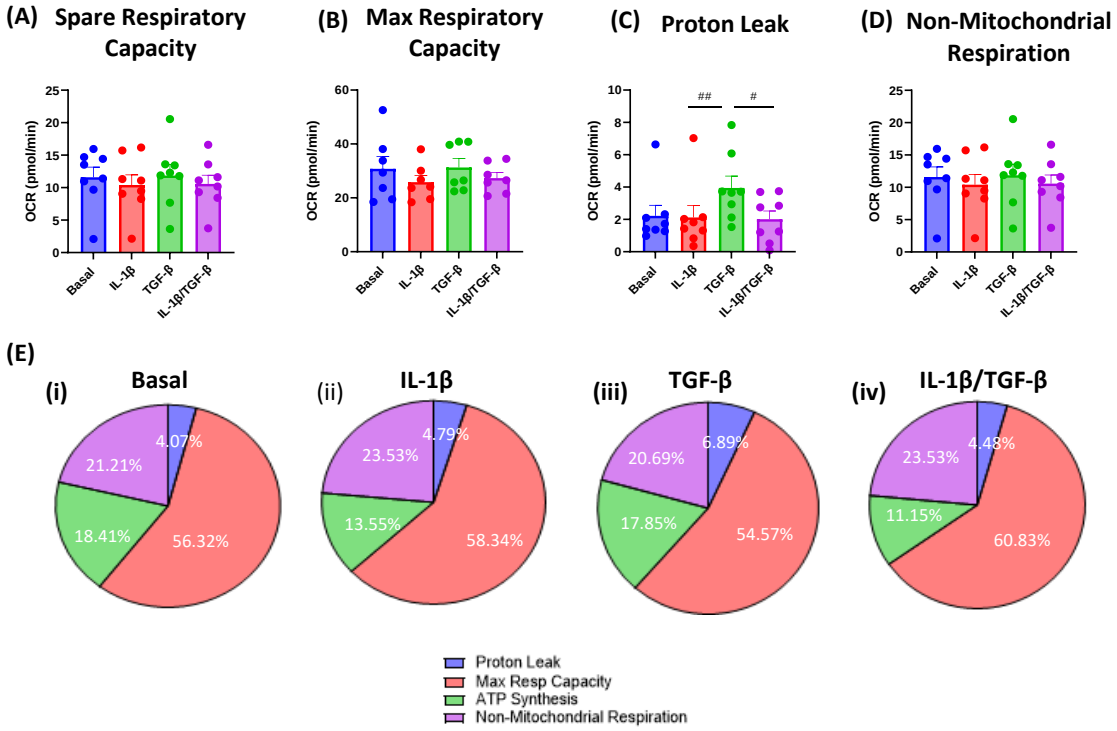

Figure 2.7. IL-1β and TGF-β synergistically drive the metabolic adaptation of RA patient FLS. Bar charts show quantification of **(A)** Spare Respiratory Capacity, **(B)** Max Respiratory Capacity, **(C)** Proton Leak, and **(D)** Non-Mitochondrial Respiration in RA FLS (n=7-8) following 24 h stimulation with IL-1β (1 ng/ml), TGF-β (10 ng/ml), or a combination of both. All data represented as Mean +/- SEM. **(E)** Pie charts reveal the breakdown of OCR outputs within each condition. Statistical analysis was performed using the non-parametric, Wilcoxon Signed-Rank Test (#) with statistical significance defined by $^{\#}p \leq 0.05$ and $^{\#\#}p \leq 0.01$.

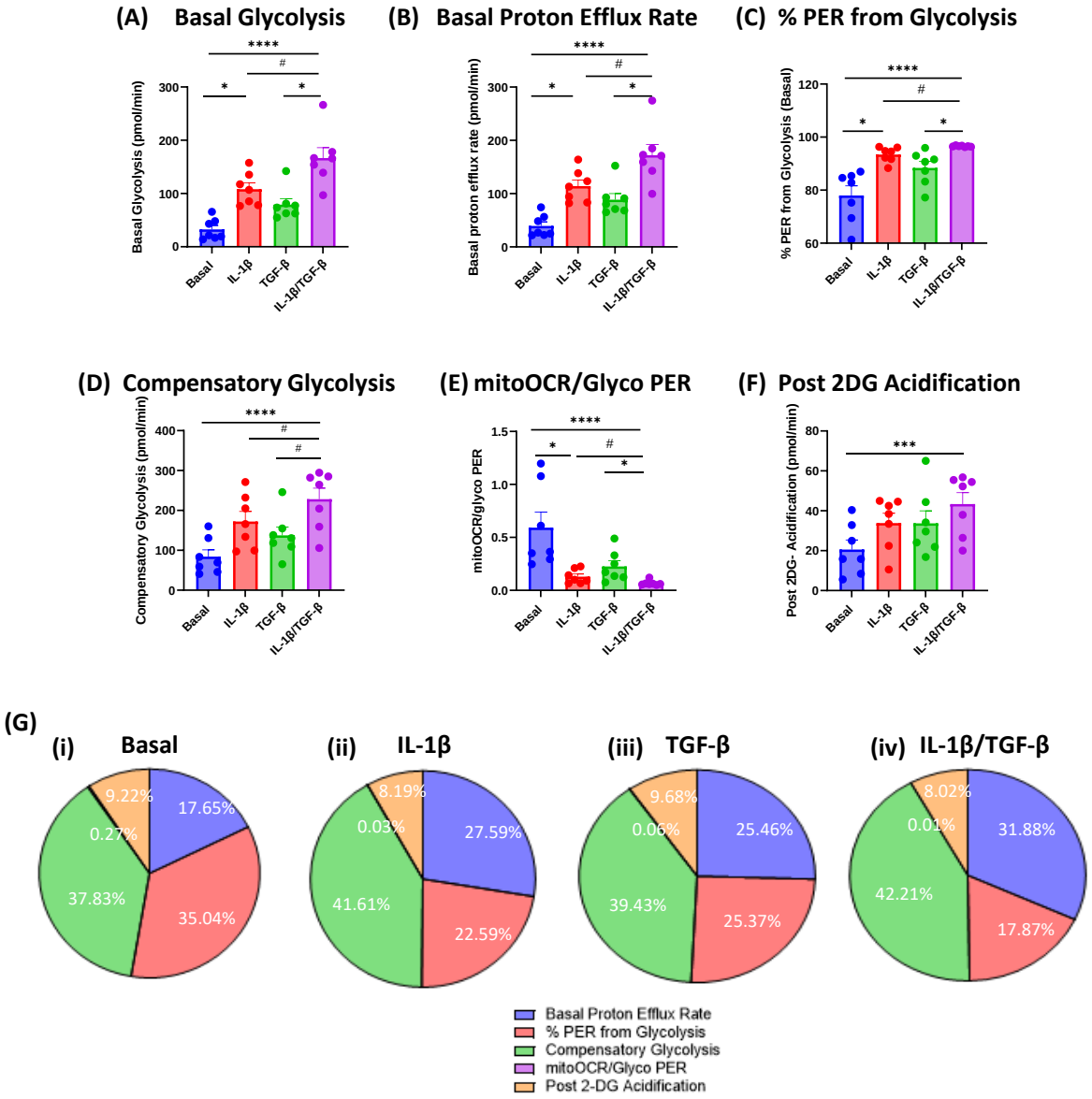

Figure 2.8. IL-1β and TGF-β synergistically drive the metabolic adaptation of RA patient FLS towards a more glycolytic phenotype. Average glycolytic rate assay derived profiles of RA FLS (n=7) stimulated with IL-1β (1 ng/ml), TGF-β (10 ng/ml), or a combination of both, before and after injections of metabolic inhibitors Rotenone, Antimycin A, and 2-DG. **(A-F)** Representative bar graphs demonstrating Basal Glycolysis, Basal Proton Efflux Rate, % PER from Glycolysis, Compensatory Glycolysis, Mito OCR/Glyco PER, and Post 2-DG Acidification. All data represented as Mean +/- SEM. **(G)** Pie charts reveal breakdown of Glycolytic Rate Assay outputs within each condition. Statistical analysis was performed using the non-parametric, Wilcoxon Signed-Rank Test (#) or the one-way ANOVA with Friedman's Test (*) where appropriate, with statistical significance defined by $*^{(\#)}p\leq0.05$, $**^{(\#\#)}p\leq0.01$, $***^{(\#\#\#)}p\leq0.001$, $****^{(\#\#\#\#)}p\leq0.0001$.

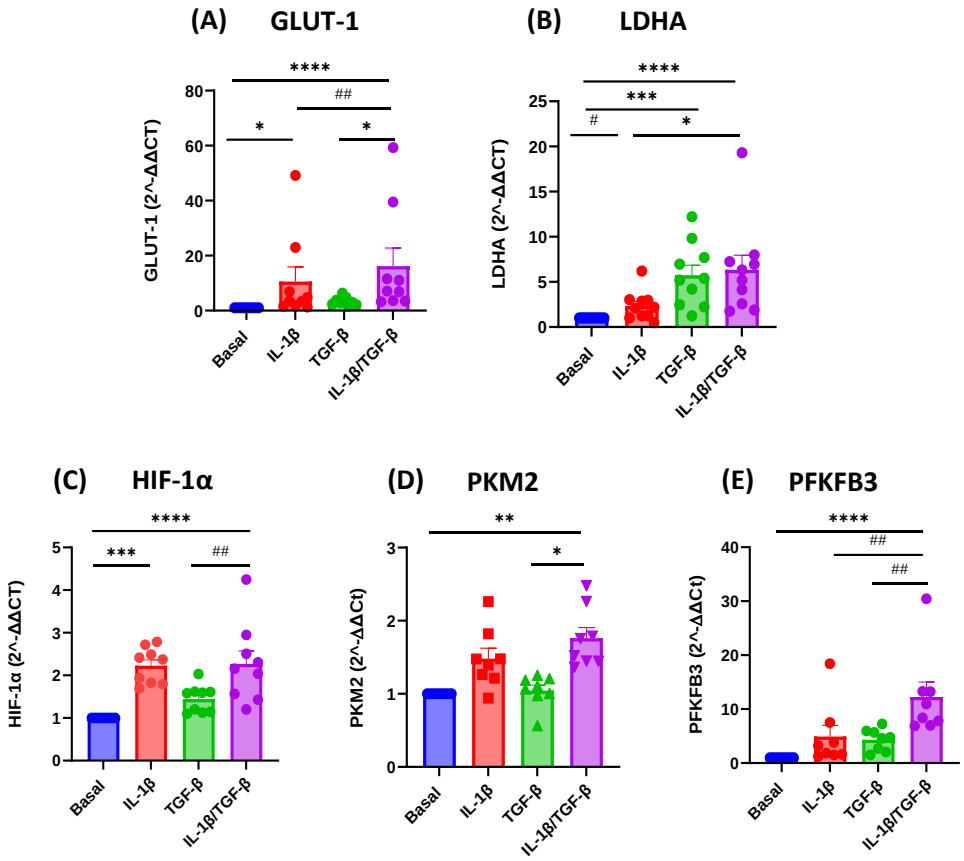

Figure 2.9. IL-1β and TGF-β synergistically drive an increase in the expression levels of glycolytic enzymes. Bar graphs showing quantification of gene mRNA expression of GLUT-1, LDHA, HIF-1α, PKM2, and PFKFB3 in RA FLS (n= 8-10) stimulated with IL-1β (1 ng/ml), TGF-β (10 ng/ml), or a combination of both for **(A-C)** 24 h or **(D-E)** 6 h compared to basal controls. Data is represented as fold expression, normalized to housekeeping control RPLP0. $2^{-\delta\delta ct}$ indicates fold induction. All data represented as Mean +/- SEM. Statistical analysis was performed using the non-parametric, Wilcoxon Signed-Rank Test (#) or the one-way ANOVA with Friedman's Test (*) where appropriate, with statistical significance defined by $*^{(\#)}p\leq0.05$, $**^{(\#\#)}p\leq0.01$, $***^{(\#\#\#)}p\leq0.001$, $****^{(\#\#\#\#)}p\leq0.0001$.

2.4.5 IL-1β and TGF-β synergistically induce alterations in FLS mitochondrial morphology, in addition to fission/fusion activity.

Changes to the metabolic capacity of the RA FLS when stimulated with IL-1β and TGF-β was mirrored in the function and morphology of the mitochondria as shown in the representative images examining their ultrastructure (Figure 2.10A). The synergistic effect of IL-1β and TGF-β led to a significant decrease in the intensity of TMRM expression in RA FLS compared to either cytokine alone ($p<0.01$), suggesting IL-1β/TGF-β are inducing a decrease in mitochondrial membrane potential, which aligns with the observed seahorse data where reduced levels of oxidative phosphorylation and heightened glycolytic activity was demonstrated (Figure 2.10B). Similarly, as shown in Figure 2.10C, compared to IL-1β only stimulated RA FLS, treatment with both IL-1β and TGF-β resulted in a significant decrease in the aspect ratio of the mitochondria ($p<0.05$), indicative of a reduction in size and an overall decrease in the level of mitochondrial fusion occurring.

To further establish if this change in mitochondrial shape was due to alterations in the fission/fusion capacity of RA FLS, the effect of stimulation alone and combination on the expression of key fission/fusion proteins – DRP1, OPA1, MFN1, and MFN2, was investigated. Interestingly, there was a significant synergistic increase in the levels of fission protein DRP1 when stimulated with the combination of IL-1β and TGF-β, compared to IL-1β or TGF-β treatment only (Figure 2.10D) ($p<0.05$). Conversely, there was no significant changes in the levels of fusion proteins OPA1, MFN1, or MFN2 under IL-1β/TGF-β conditions compared to basal or either cytokine alone (Figure 2.10E-G). Moreover, MitoTracker Green staining of the FLS mitochondria was performed following treatment with the various cytokines and the RFU monitored over a 24 h time period to determine changes in mitochondrial mass. As demonstrated in Figure 2.11A, whilst the positive FCP control peaked at 3 h (Figure 2.11B), the RFU of the synergy gradually increased over the time-period compared to all other conditions, with a significant synergistic effect detected by 22 h compared to IL-1β or TGF-β treatment only ($p<0.05$) (Figure 2.11C). This was paralleled by a significant reduction in the mRNA levels of mitochondrial biogenesis proteins including PGC-1α ($p<0.01$) and NRF1 ($p<0.07$) under synergy conditions compared to IL-1β alone (Figure 2.12A-B). However, interestingly, TGF-β treatment alone resulted in an even greater significant decrease in the mRNA of both of these proteins compared to IL-1β ($p<0.01$ and $p<0.05$, respectively), suggesting that IL-1β may be in fact exerting a rescue effect. Although no significant differences were observed for the genes CPT1b or mitochondrial TFAM, they did appear to follow the same trend (Figure 2.12C-D). Overall, these results suggest that when stimulated with IL-1β and TGF-β in combination, RA FLS mitochondria demonstrate disrupted homeostasis and show a preference

towards fission, which is reflected in increased mitochondrial mass and a reduction in the process of biogenesis.

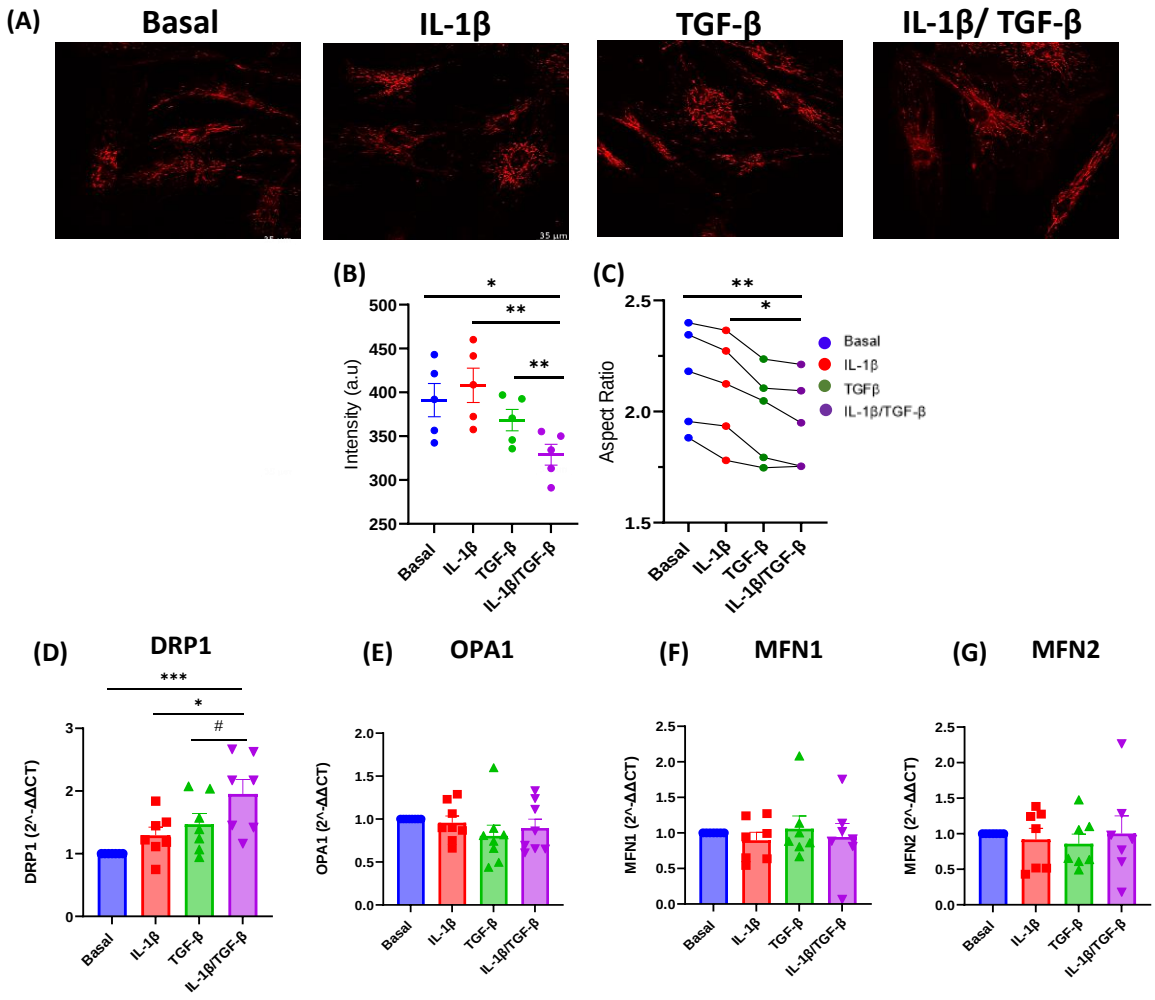

Figure 2.10. IL-1β & TGF-β synergistically induce alterations in FLS mitochondrial morphology, in addition to fission/fusion activity. (A) Representative multiphoton microscope images of TMRM stained FLS mitochondria under the indicated conditions. Scatter plot/ line graphs demonstrating **(B)** fluorescent intensity of TMRM and **(C)** mitochondrial aspect ratio following treatment with IL-1β (1 ng/ml), TGF-β (10 ng/ml), or a combination of both. **(D-G)** Bar graphs showing quantification of gene mRNA expression of the fission protein DRP1 and the fusion proteins OPA1, MFN1, and MFN2 in RA FLS (n=7-8) stimulated with IL-1β (1 ng/ml), TGF-β (10 ng/ml), or a combination of both for 24 h compared to basal controls. Data represented as fold expression, normalized to housekeeping control RPLP0. $2^{-\delta\delta ct}$ indicates fold induction. All data represented as Mean +/- SEM. Statistical analysis was performed using the non-parametric, Wilcoxon Signed-Rank Test (#) or the one-way ANOVA with Friedman's Test (*) where appropriate, with statistical significance defined by *$^{(\#)}$p≤0.05, **$^{(\#\#)}$p≤0.01, ***$^{(\#\#\#)}$p≤0.001.

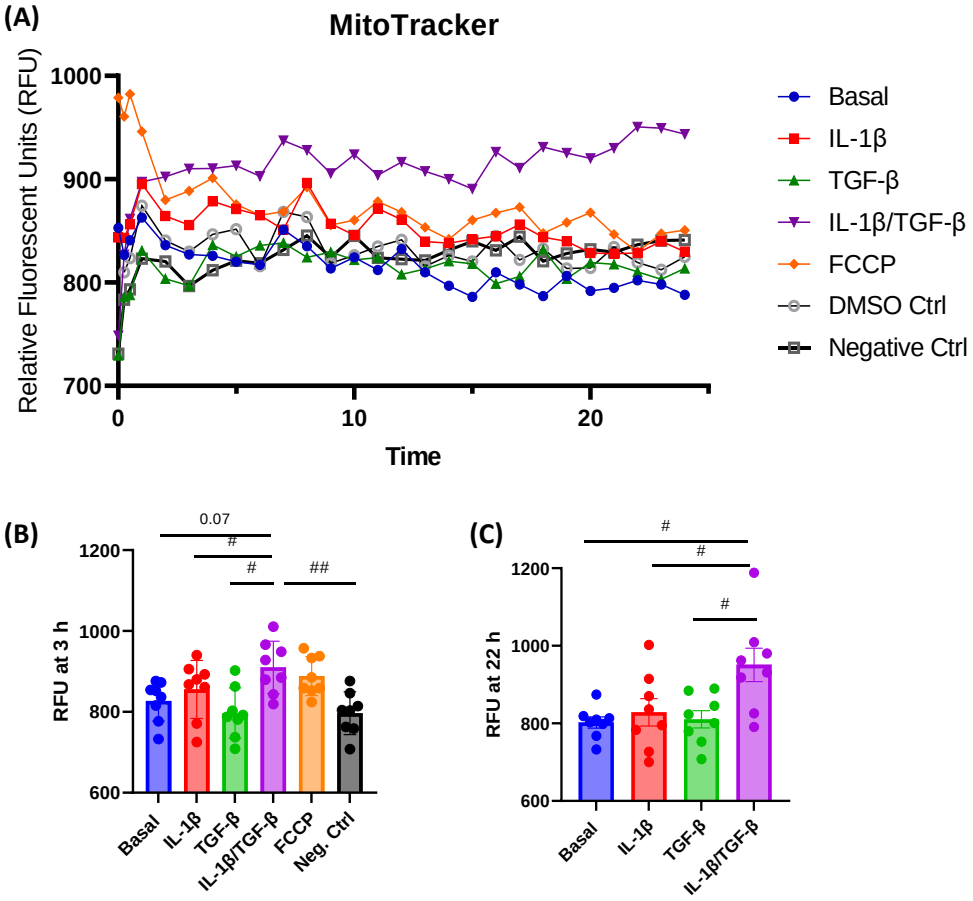

Figure 2.11. IL-1β and TGF-β synergistically alter mitochondrial mass. (A) Representative time plot depicting the mean relative fluorescence intensity (RFU) of RA FLS (n=8) stained with MitoTracker Green dye to assess total mitochondrial content after stimulation with the following conditions: Basal, IL-1β (1 ng/ml), TGF-β (10 ng/ml), or a combination of both over 24 h. A positive FCCP control and a negative DMSO control were included for comparative purposes. MitoTracker emission was read using the kinetic mode of the Spectra Max Gemini System with excitation and emission wavelengths of 490 nm and 516 nm, respectively. Readings were performed every 15 min for a period of 24 h. Representative bar graphs demonstrating the RFU of MitoTracker green at the **(B)** 3 h and **(C)** 22 h timepoint under the various conditions. All data represented as Mean +/- SEM. Statistical analysis was performed using the non-parametric, Wilcoxon Signed-Rank Test with statistical significance defined as $^{\#}p \leq 0.05$, $^{\#\#}p \leq 0.01$.

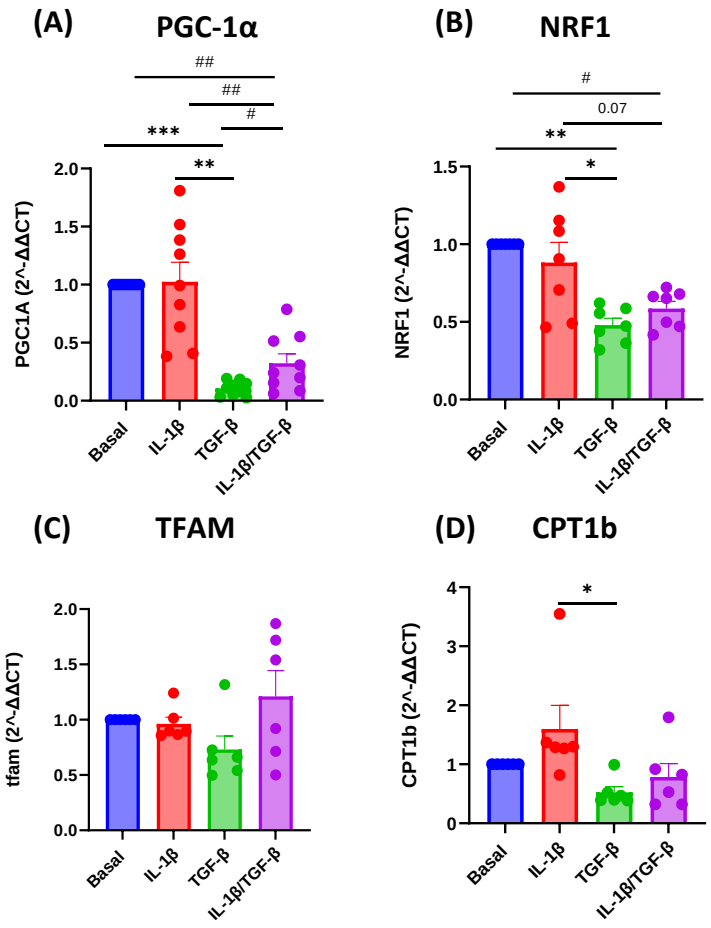

Figure 2.12. IL-1β and TGF-β affect the expression of mitochondrial biogenesis genes. (A-D) Bar graphs showing quantification of gene mRNA expression of PGC-1α, NRF1, TFAM, and CPT1b in RA FLS (n= 6-9) stimulated with IL-1β (1 ng/ml), TGF-β (10 ng/ml), or a combination of both for 24 h compared to basal controls. Data represented as fold expression, normalized to housekeeping control RPLP0. $2^{-\delta\delta ct}$ indicates fold induction. All data represented as Mean +/- SEM. Statistical analysis was performed using the non-parametric, Wilcoxon Signed-Rank Test (#) or the one-way ANOVA with Friedman's Test (*) where appropriate, with statistical significance defined by $*^{(\#)}p\leq0.05$, $**^{(\#\#)}p\leq0.01$, $***^{(\#\#\#)}p\leq0.001$.

2.4.6 IL-1β and TGF-β alter the level of ER stress compared to single cytokine stimulation alone.

To evaluate how alterations in mitochondrial fitness and functioning following stimulation with IL-1β and/or TGF-β impact other cellular organelles, the ER was examined. As the expansion of the ER is partially under the regulation of ER stress signals, whether the ER stress response was altered under synergy conditions in the RA FLS was investigated further (Mateus *et al.*, 2018). Firstly, assessment of the MFI of the ER under the various conditions was performed, with a greater MFI indicative of a larger ER size and heightened ER stress. Representative flow plots of the gating strategy are shown in Figure 2.13. Following the elimination of debris and cell doublets (Figure 2.13A-C), cells positive for ER tracker dye were gated (Figure 2.13D). As indicated quantitatively and in the representative histograms (Figure 2.14A(i-ii)), at the 6 h timepoint, a synergistic increase in ER tracker MFI ($p<0.05$) was detected. However, by the 24 h timepoint, there were no significant differences in the MFI of ER tracker between any of the conditions (Figure 2.14B(i-ii)). The changes in the mean MFI at the 6 h and 24 h timepoint under the four conditions is shown in the representative heatmap (Figure 2.14C), with the reduction in the MFI of the IL-1β/TGF-β treated cells over the time period clearly visible. Representative confocal microscopy images of the cells treated with ER tracker dye under the various conditions are shown in Figure 2.15A.

To examine ER stress mechanisms further, analysis of the effect of cytokine stimulation on the mRNA expression of ER stress related proteins at the 6 h timepoint was conducted. As shown in Figure 2.15B, the combination of IL-1β and TGF-β demonstrated a significant synergistic increase in the expression of BIP that was greater than either cytokine alone ($p<0.05$). Moreover, a significant additive increase in both XBP1 and ATF6 expression with IL-1β/TGF-β compared to TGF-β alone ($p<0.05$, $p<0.05$) was observed (Figure 2.15C-D). Moreover, confocal imaging for the ER-resident protein PDI was performed. Interestingly, as demonstrated in the representative images and quantitatively, at the 6 h timepoint a trending synergistic increase in PDI relative fluorescent expression following addition of IL-1β and TGF-β compared to either cytokine alone was identified (Figure 2.16A-B). Cumulatively, the data suggests that cytokine synergy disrupts ER homeostasis, inducing an early ER associated stress response to mitigate and resolve the effects.

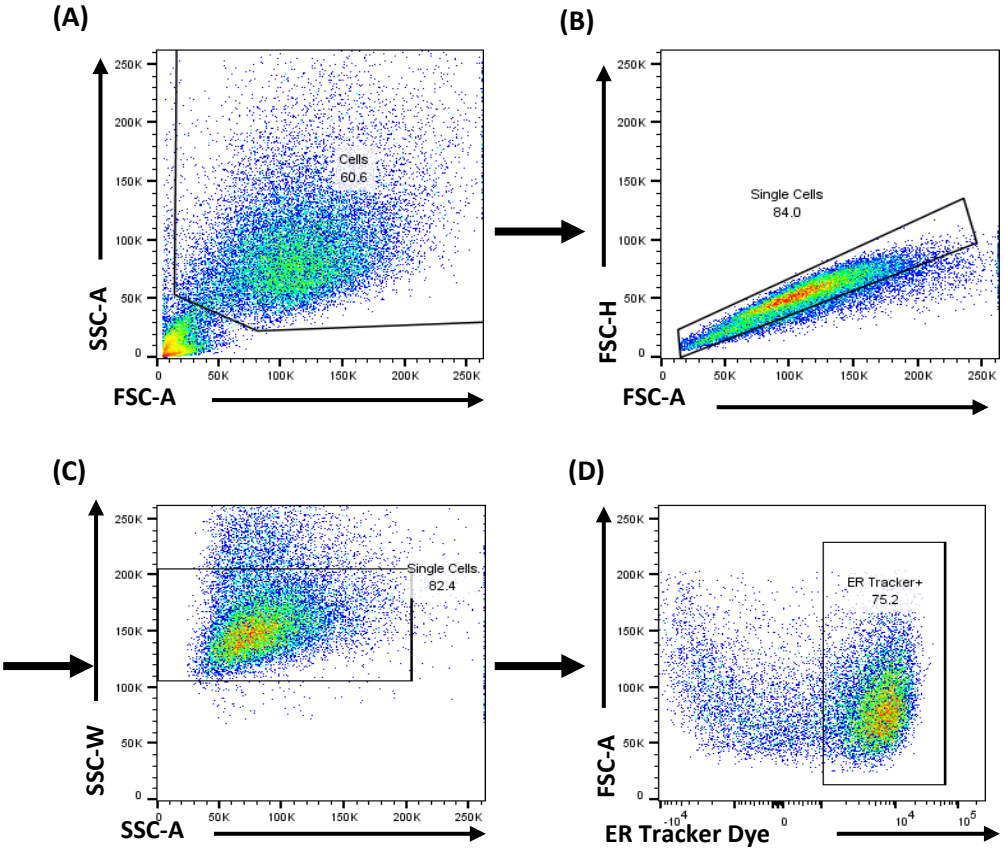

Figure 2.13. Gating strategy to analyse the effects of IL-1β and TGF-β on the size of the ER over time indicative of ER-related stress. RA FLS were incubated with IL-1β (1 ng/ml), TGF-β (10 ng/ml), or a combination of both for 24 h following serum starvation before flow cytometric analysis was performed using MitoTracker Green dye. **(A-D)** Representative dot plots depicting the gating strategy used to detect ER Tracker dye fluorescence. The forward and side scatter parameters of cells were set before doublet exclusion.

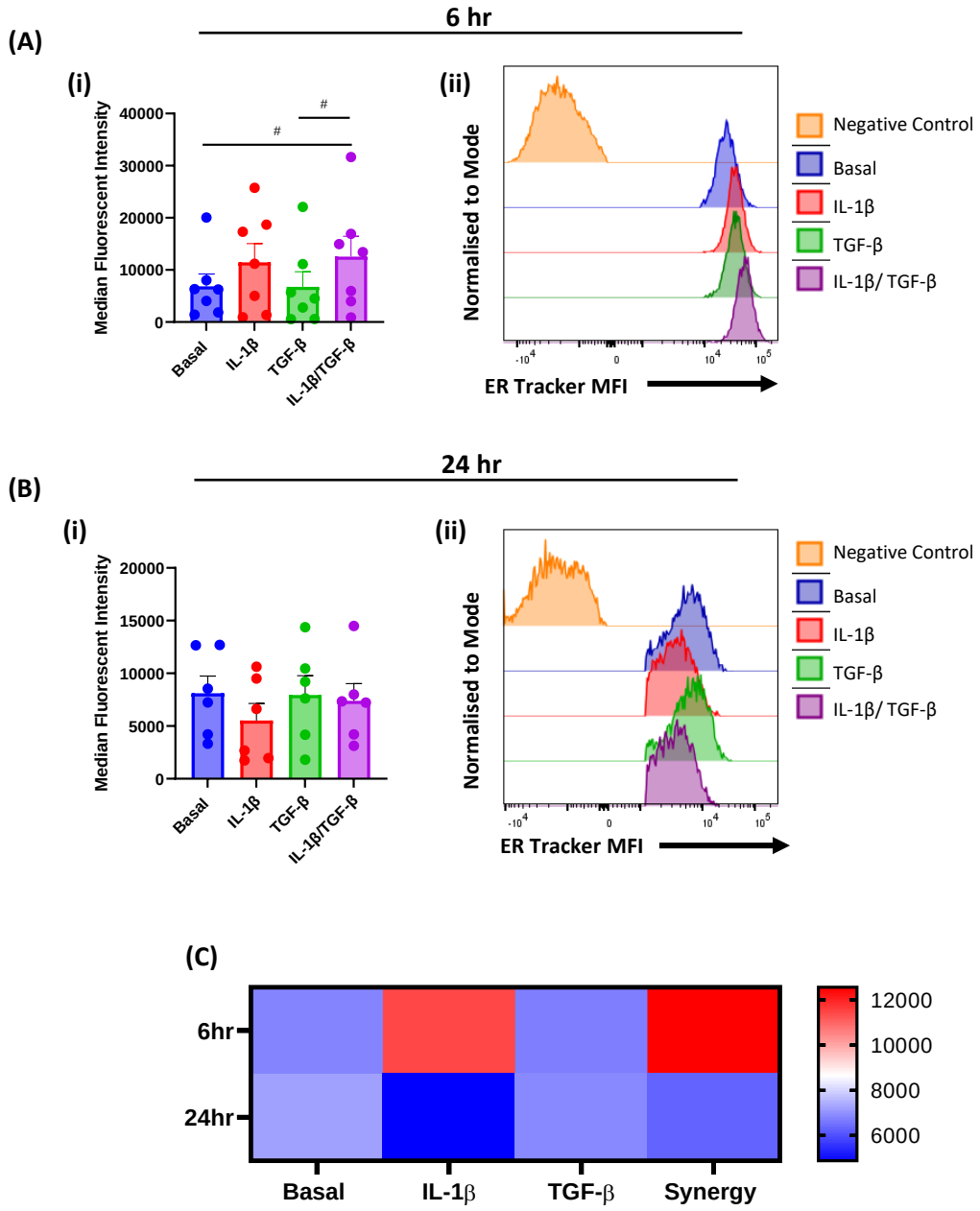

Figure 2.14. IL-1β and TGF-β induce changes to the size of the ER over time indicative of ER-related stress. RA FLS were incubated with IL-1β (1 ng/ml), TGF-β (10 ng/ml), or a combination of both for 24 h following serum starvation before flow cytometric analysis was performed using MitoTracker Green dye. **(A-B)** Flow cytometric quantification of ER size represented by **(i)** bar graphs of ER Green Tracker MFI and **(ii)** accompanying representative histograms showing the MFI shifts in RA FLS (n=7) following stimulation with IL-1β, TGF-β or a combination of both for **(A)** 6 h and **(B)** 24 h, respectively. **(C)** Representative heatmap depicting the mean % ER Tracker MFI at 6 h vs 24 h in RA FLS (n=7) across the four conditions. All data represented as Mean +/- SEM. Statistical analysis was performed using the non-parametric, Wilcoxon Signed-Rank Test with statistical significance defined as $^{\#}p \leq 0.05$.

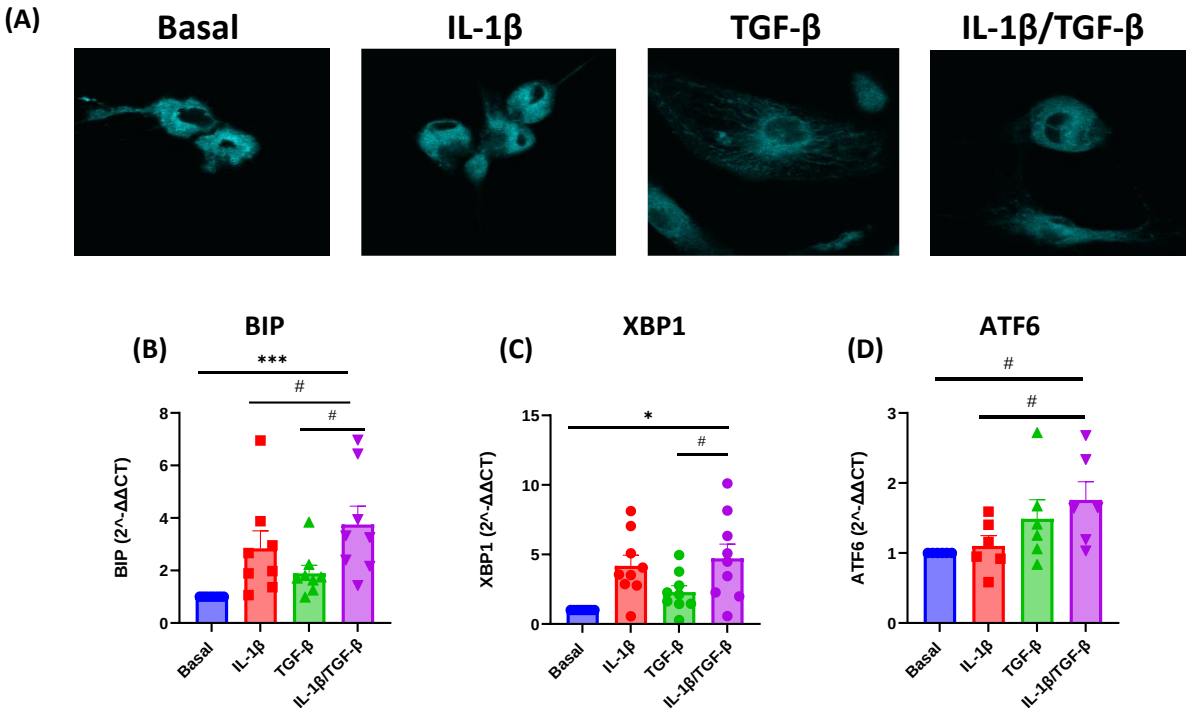

Figure 2.15. IL-1β and TGF-β synergistically impact the ER morphology and the ER stress response. (A) Representative multiphoton microscope images of FLS ER under the indicated conditions, following staining with green ER-Tracker dye. **(B-D)** Bar graphs showing quantification of gene mRNA expression of BIP, XBP1, and ATF6 in RA FLS (n=6-8) stimulated with IL-1β (1 ng/ml), TGF-β (10 ng/ml), or a combination of both for 24 h compared to basal controls. Data represented as fold expression, normalized to housekeeping control RPLP0. $2^{-\delta\delta ct}$ indicates fold induction. All data represented as Mean +/- SEM. Statistical analysis was performed using the non-parametric, Wilcoxon Signed-Rank Test (#) or the one-way ANOVA with Friedman's Test (*) where appropriate, with statistical significance defined by $*^{(\#)}p\leq0.05$, $**^{(\#\#)}p\leq0.01$, $***^{(\#\#\#)}p\leq0.001$.

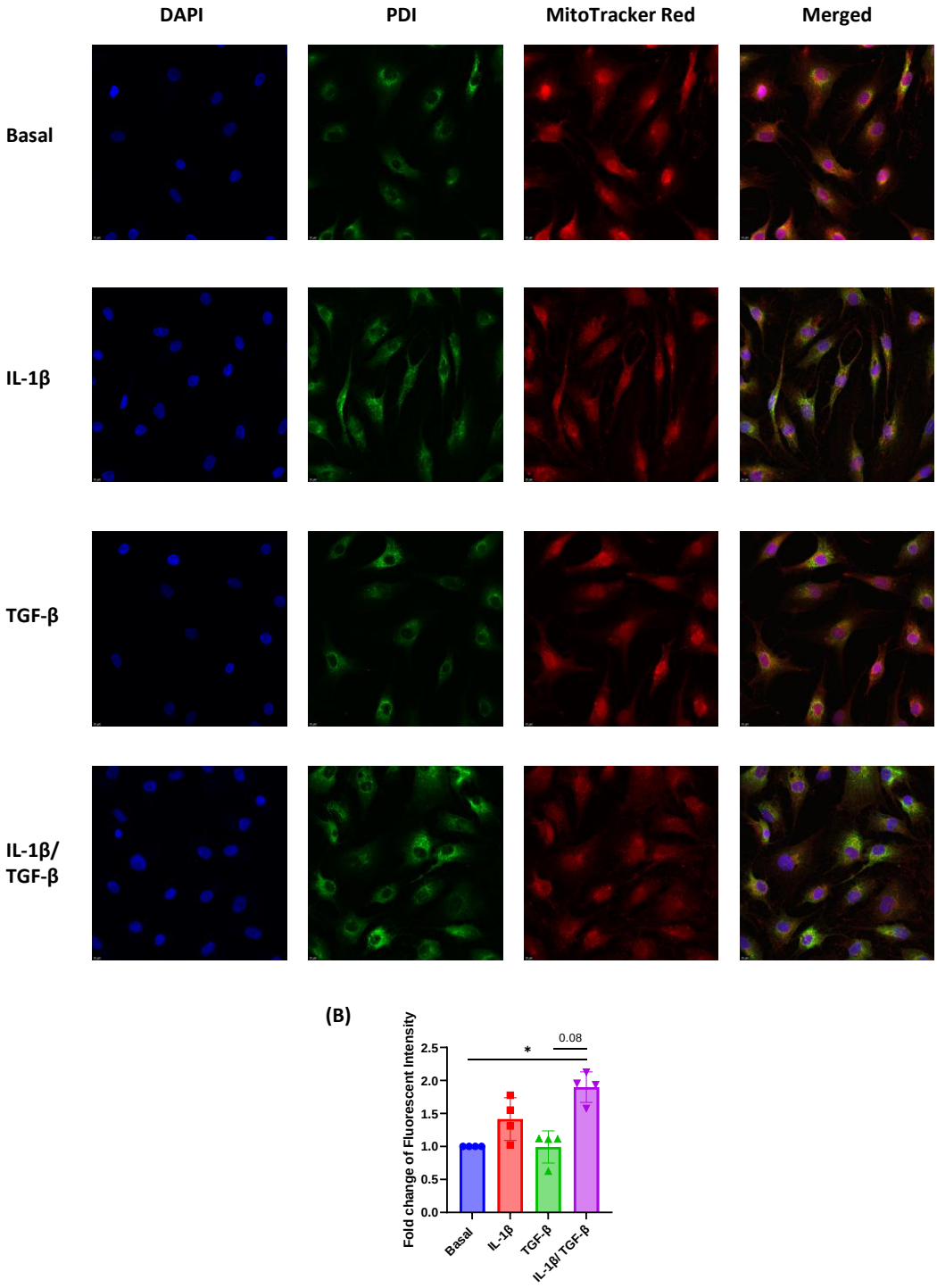

Figure 2.16. IL-1β and TGF-β induce higher expression of the ER stress related chaperone PDI in RA FLS. (A) Representative confocal microscopy imaging of the ER enzyme PDI and mitochondrial tracker (MitoTracker Red) from RA FLS (n=4) following stimulation with IL-1β (1 ng/ml), TGF-β (10 ng/ml), or a combination of both for 6 h. Green indicates a cell with abundant ER, red indicates a cell with high mitochondrial activity. Scale bar, 10 µm. Nuclei were counterstained with DAPI (blue). **(B)** Representative bar graph demonstrating the fold change RFI of PDI in the RA FLS (n=4) following 6 h treatment with IL-1β (1 ng/ml), TGF-β (10 ng/ml), or a combination of both compared to baseline. All data represented as Mean +/- SEM. Statistical analysis was performed using the one-way ANOVA with Friedman's Test (*) with significance defined by *p≤0.05.

2.4.7 IL-1β and TGF-β synergistically drive the expression of RA FLS proinflammatory mediators, angiogenic factors, and specific chemokines, but not the chemokine receptors.

Based on the effect of IL-1β and TGF-β in combination on FLS metabolic profile, the impact of these metabolic adaptations on the promotion of RA FLS proinflammatory function *ex vivo* was investigated. Primary RA FLS were grown to confluence and cultured with 1% CRPM1-1640 for 24 h, followed by stimulation with IL-1β (1n g/ml) and TGF-β (10 ng/ml) alone or in combination. Following the appropriate stimulations, supernatants were harvested and RNA isolated. Figures 2.17A(i-ii) and 2.17B(i-ii) demonstrate that IL-1β and TGF-β synergistically increased the expression of the proinflammatory cytokine IL-6 and the chemoattractant IL-8 at both the gene and protein level compared to treatment with IL-1β or TGF-β alone (all $p<0.05$). Similarly, protein levels of the chemoattractant MCP-1 exhibited a significant increase under synergy conditions compared to either cytokine individually ($p<0.01$) (Figure 2.17C(i)), although at the mRNA level, MCP-1 showed a trend towards a reduction in expression compared to IL-1β alone indicating a slightly suppressive effect of TGF-β on IL-1β's inflammatory abilities (Figure 2.17C(ii)).

A hallmark characteristic of synovial inflammation that further facilitates immune cell entry and exacerbates the hypoxic joint microenvironment is the process of angiogenesis (Balogh *et al.*, 2019). Therefore, the effect of cytokine synergy on the levels of angiogenic mediators at the mRNA and protein level were investigated. As demonstrated by the representative heatmap (Figure 2.18A), MSD assay analysis indicated no significant difference in the expression of several angiogenic mediators including PIGF, bFGF, Flt1, and VEGF-C between the RA FLS treated with IL-1β, TGF-β, or the combination of both. However, the addition of IL-1β appeared to generate a potentiating effect on TGF-β induced VEGF-A production, with a significant increase in the protein levels of the main angiogenic growth factor VEGF-A in response to IL-1β and TGF-β together compared to either cytokine alone (both $p<0.05$) (Figure 2.18B).

Moreover, the ability of stromal cells resident in the joint to attract infiltrating immune cells is a key feature responsible for driving RA pathogenesis, a process achieved through the expression of different chemokine ligands and chemokine receptors (Veale and Fearon, 2015; Tas *et al.*, 2016). Therefore, to expand the understanding of synergy treatment on immune cell recruitment, MSD analysis was performed using a panel that focused on a broader spectrum of chemokines being expressed by the FLS. While no differences in the expression of several chemokines including MCP-4, TARC, MIP1- β, MIP1-α, and Eotaxin-3 under IL-1β/TGF-β conditions compared to either cytokine alone were observed (Figure 2.19A), significant synergistic effects were observed for the chemokines Eotaxin (Figure 2.19B(i)), IP-10 (Figure 2.19B(ii)), and MDC (Figure 2.19B(iii)), ($p<0.05$, $p<0.01$, $p<0.05$ respectively). Moreover, at the mRNA level, significant

synergistic increases in CXCL5 and CXCL10 were detected compared to single cytokine treatment only ($p<0.05$, $p<0.01$) (Figures 2.19C(i) and 2.19C(ii)).

Next, examination of the expression of the chemokine receptors themselves on the cytokine-treated RA FLS using flow cytometry was performed. Representative flow plots of the gating strategy are shown in Figure 2.20. Following the elimination of debris and cell doublets (Figures 2.20A-C), dead cells were gated out (Figure 2.20D) allowing specific chemokine receptors to be analysed on the live cells (Figure 2.20E). Figure 2.21A(i) demonstrates representative dot plots for CXCR3 expression for basal, IL-1β, TGF-β, and IL-1β/TGF-β treated RA FLS. Interestingly, treatment with IL-1β and TGF-β resulted in a significant reduction in CXCR3 expression compared to IL-1β alone ($p<0.09$), whilst conversely, it was significantly higher than TGF-β treatment alone suggesting that TGF-β may potentially be exerting a rescue effect on the pathogenic effects of IL-1β ($p<0.05$) (Figure 2.21A(ii)). This was paralleled by no significant difference from basal (Figure 2.21A(ii)). Similar effects were observed for CXCR4. As highlighted by the representative flow plots (Figure 2.21B(i)) and quantification (Figure 2.21B(ii)), the synergy induced a significant increase in CXCR4 % frequency compared to TGF-β, whilst simultaneously showing a significant reduction compared to IL-1β treatment (both $p<0.05$), once again indicating a potential rescue effect. Furthermore, as depicted in the representative flow plots of the various conditions (Figure 2.22A(i) and 2.22B(i)) and the accompanying bar graphs (Figure 2.22A(ii) and 2.22B(ii)), no differences in the % frequency of CXCR5 or CCR6 were detected following cytokine treatment. Therefore, these results suggest that in the case of CXCR3 and CXCR4 specifically, TGF-β may be mitigating the proinflammatory, chemokine receptor inducing effects of IL-1β, thus returning the cellular state towards baseline. Cumulatively, the data implies that the combination of IL-1β and TGF-β differentially induce the expression of various chemokines and chemokine receptors on RA FLS thus, finely regulating the contribution of circulating leukocytes to the inflammatory joint microenvironment.

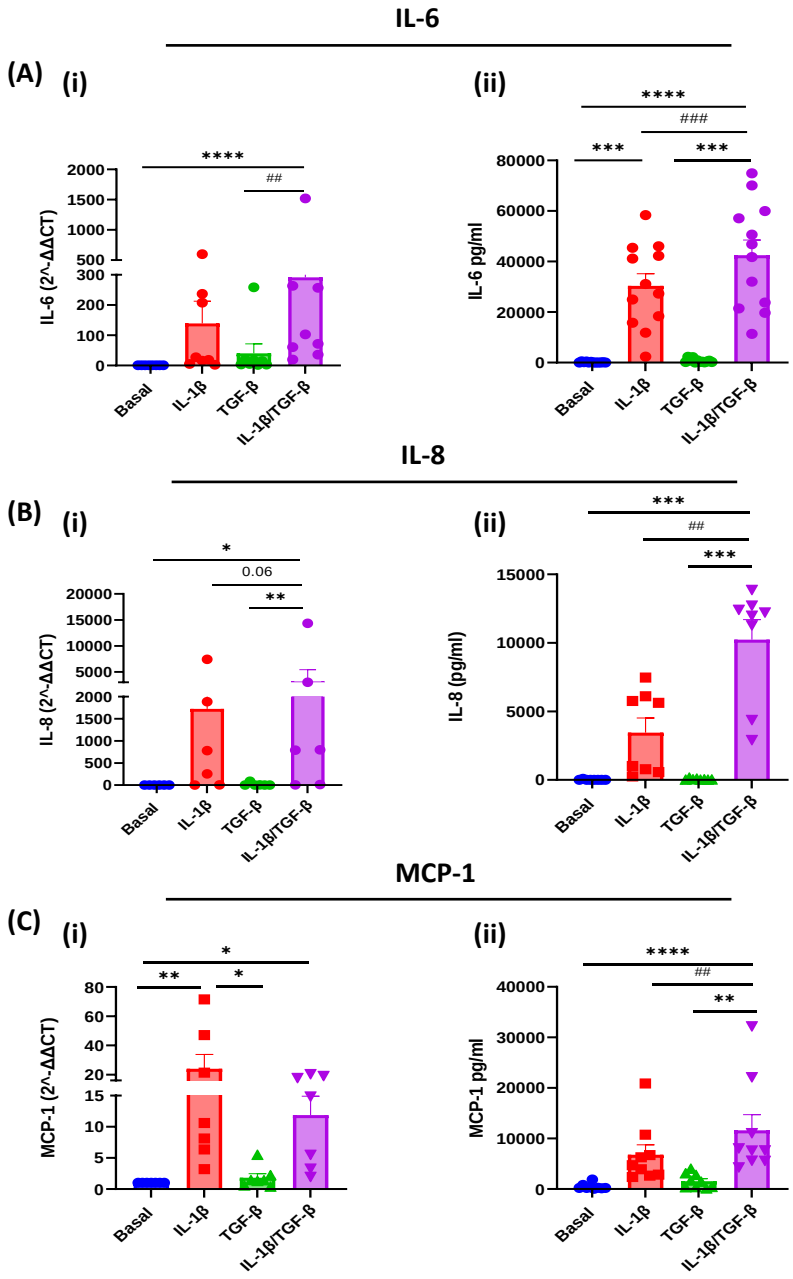

Figure 2.17. IL-1β and TGF-β synergistically drive the expression of RA FLS proinflammatory mediators. RA FLS were incubated with IL-1β (1 ng/ml), TGF-β (10 ng/ml), or a combination of both for 24 h following serum starvation before RNA isolation, cDNA synthesis, and RT-PCR was performed. Matched supernatants were removed and analysed for IL-6, IL-8, and MCP-1 secretion by ELISA. Bar graph showing quantification of gene mRNA expression of **(A(i))** IL-6, **(B(i))** IL-8, and **(C(i))** MCP-1 in RA FLS (n=6-8) in response to cytokine stimulation. Data represented as fold expression, normalized to housekeeping control RPLP0. $2^{-\delta\delta ct}$ indicates fold induction. Bar graph representations of level of secretion of **(A(ii))** IL-6, **(B(ii))** IL-8, and **(C(ii))** MCP-1 in RA FLS (n=8-12). All data represented as Mean +/- SEM. Statistical analysis was performed using the non-parametric, Wilcoxon Signed-Rank Test (#) or the one-way ANOVA with Friedman's Test (*) where appropriate, with statistical significance defined by $*^{(\#)}p\leq0.05$, $**^{(\#\#)}p\leq0.01$, $***^{(\#\#\#)}p\leq0.001$, $****^{(\#\#\#\#)}p\leq0.0001$.

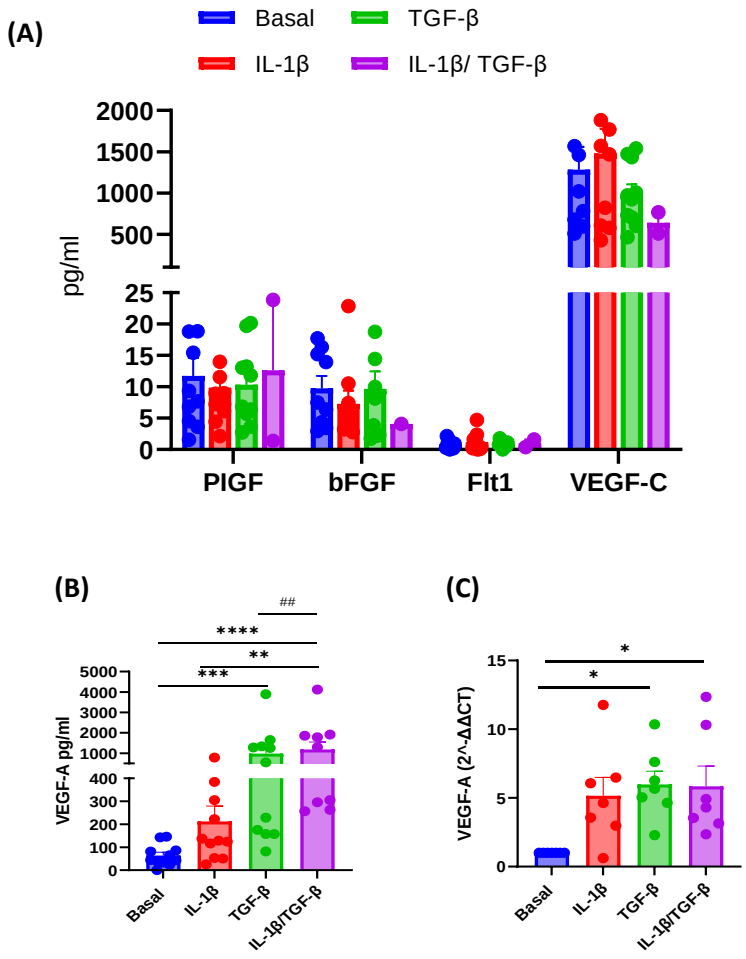

Figure 2.18. IL-1β and TGF-β additively alter the expression of the angiogenic marker VEGF-A by the RA FLS. RA FLS were incubated with IL-1β (1 ng/ml), TGF-β (10 ng/ml), or a combination of both for 24 h following serum starvation before RNA isolation, cDNA synthesis, and RT-PCR was performed and matching supernatants were harvested. **(A)** Bar graph representation of the level of expression of PlGF, bFGF, Flt1, and VEGF-C in RA FLS (n=7-8) following stimulation with the appropriate cytokines as determined by the Angiogenic MSD assay**. (B)** Bar graph representation of the level of secretion of VEGF-A in RA FLS (n=11) as determined by ELISA. **(C)** Bar graph showing quantification of gene mRNA expression of VEGF-A in RA FLS (n=7). Data is represented as fold expression, normalized to housekeeping control RPLP0. All data is represented as Mean +/- SEM. Statistical analysis was performed using the non-parametric, Wilcoxon Signed-Rank Test (#) or the one-way ANOVA with Friedman's Test (*) where appropriate, with statistical significance defined by $*^{(\#)}p\leq0.05$, $**^{(\#\#)}p\leq0.01$, $***^{(\#\#\#)}p\leq0.001$, $****^{(\#\#\#\#)}p\leq0.0001$.

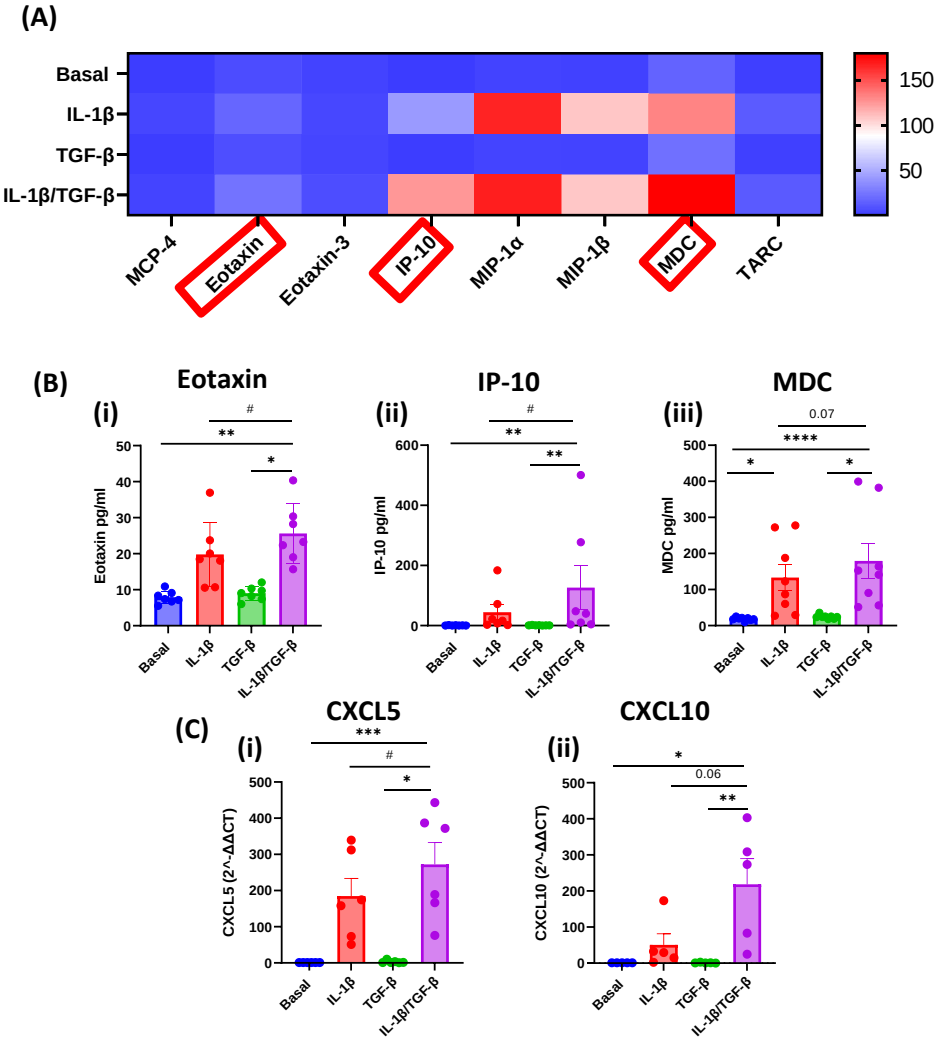

Figure 2.19. IL-1β and TGF-β synergistically alter the expression of RA FLS chemokine ligands. RA FLS were incubated with IL-1β (1 ng/ml), TGF-β (10 ng/ml), or a combination of both for 24 h following serum starvation before supernatants were harvested and chemokines quantified. **(A)** Heatmap representation of the mean level of expression of MCP-4, Eotaxin, Eotaxin-3, IP-10, MIP-1α, MIP-1β, MDC, and TARC in RA FLS (n=7-8) following stimulation with the appropriate cytokines as determined by a Chemokine MSD assay. **(B)** Bar graphs depicting the expression level in pg/ml of **(i)** Eotaxin, **(ii)** IP-10, and **(iii)** MDC in the stimulated RA FLS supernatants as determined by the MSD assay. **(C)** Representative bar graphs of the mRNA levels of **(i)** CXCL5 at 6 h (n=6) and **(ii)** CXCL10 at 24 h (n=5) as determined by RT-PCR analysis. Data represented as fold expression, normalized to housekeeping control RPLP0. $2^{-\delta\delta ct}$ indicates fold induction. All data represented as Mean +/- SEM. Statistical analysis was performed using the non-parametric, Wilcoxon Signed-Rank Test (#) or the one-way ANOVA with Friedman's Test (*) where appropriate, with statistical significance defined by *$^{(\#)}$p≤0.05, **$^{(\#\#)}$p≤0.01, ***$^{(\#\#\#)}$p≤0.001, ****$^{(\#\#\#\#)}$p≤0.0001.

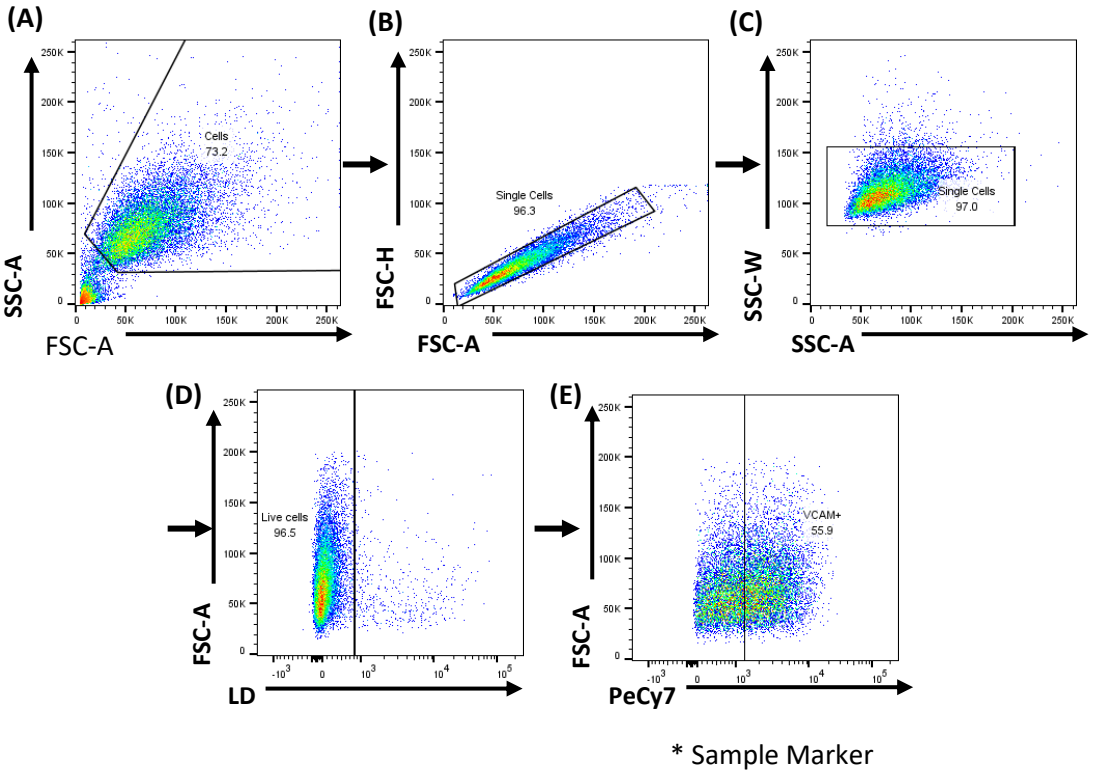

Figure 2.20. FLS chemokine panel gating strategy. RA FLS were incubated with IL-1β (1 ng/ml), TGF-β (10 ng/ml), or a combination of both for 24 h following serum starvation before being stained with a panel of fluorochrome antibodies (CXCR3, CXCR4, CXCR5, CCR6, and VCAM-1). Representative dot plots depicting the gating strategy used to phenotype the FLS under the various conditions. The forward and side scatter parameters of cells were set before doublet exclusion and elimination of dead cells **(A-D). (E)** Representative flow plot shows the gating for an example marker e.g. VCAM-1.

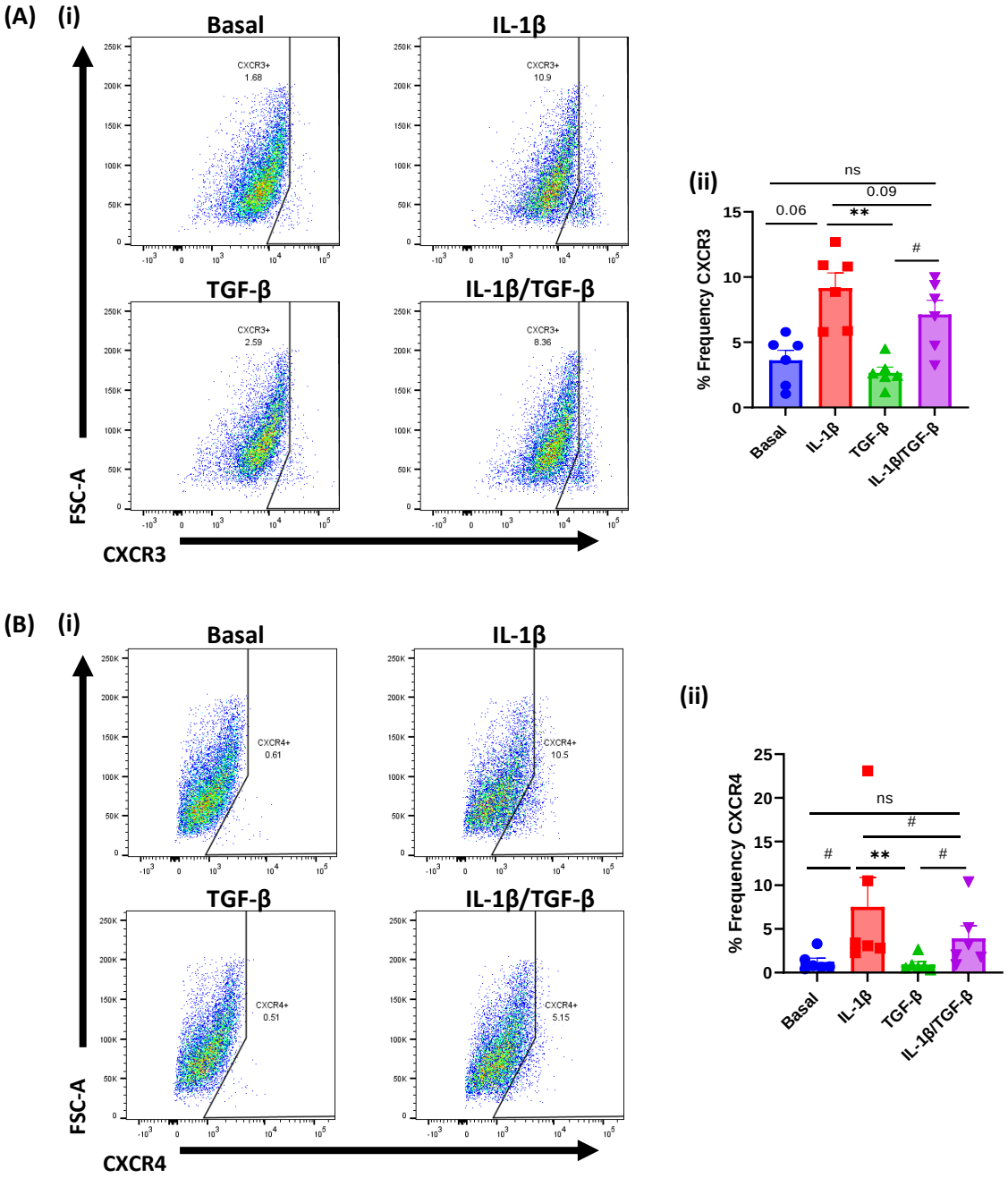

Figure 2.21. The effect of synergy on the expression of chemokine receptors CXCR3 and CXCR4 in RA FLS. RA FLS were incubated with IL-1β (1 ng/ml), TGF-β (10 ng/ml), or a combination of both for 24 h following serum starvation before flow cytometric analysis was performed. Representative flow plots depicting **(A(i))** CXCR3 and **(B(i))** CXCR4 expression in RA FLS under the indicated conditions; basal, IL-1β, TGF-β, and synergy. Bar charts represent the percentage frequency of **(A(ii))** CXCR3 and **(B(ii))** CXCR4 expression in RA FLS (n=6). All data represented as Mean +/- SEM. Statistical analysis was performed using the non-parametric, Wilcoxon Signed-Rank Test (#) or the one-way ANOVA with Friedman's Test (*) where appropriate, with statistical significance defined by $*^{(\#)}p\leq0.05$, $**^{(\#\#)}p\leq0.01$.

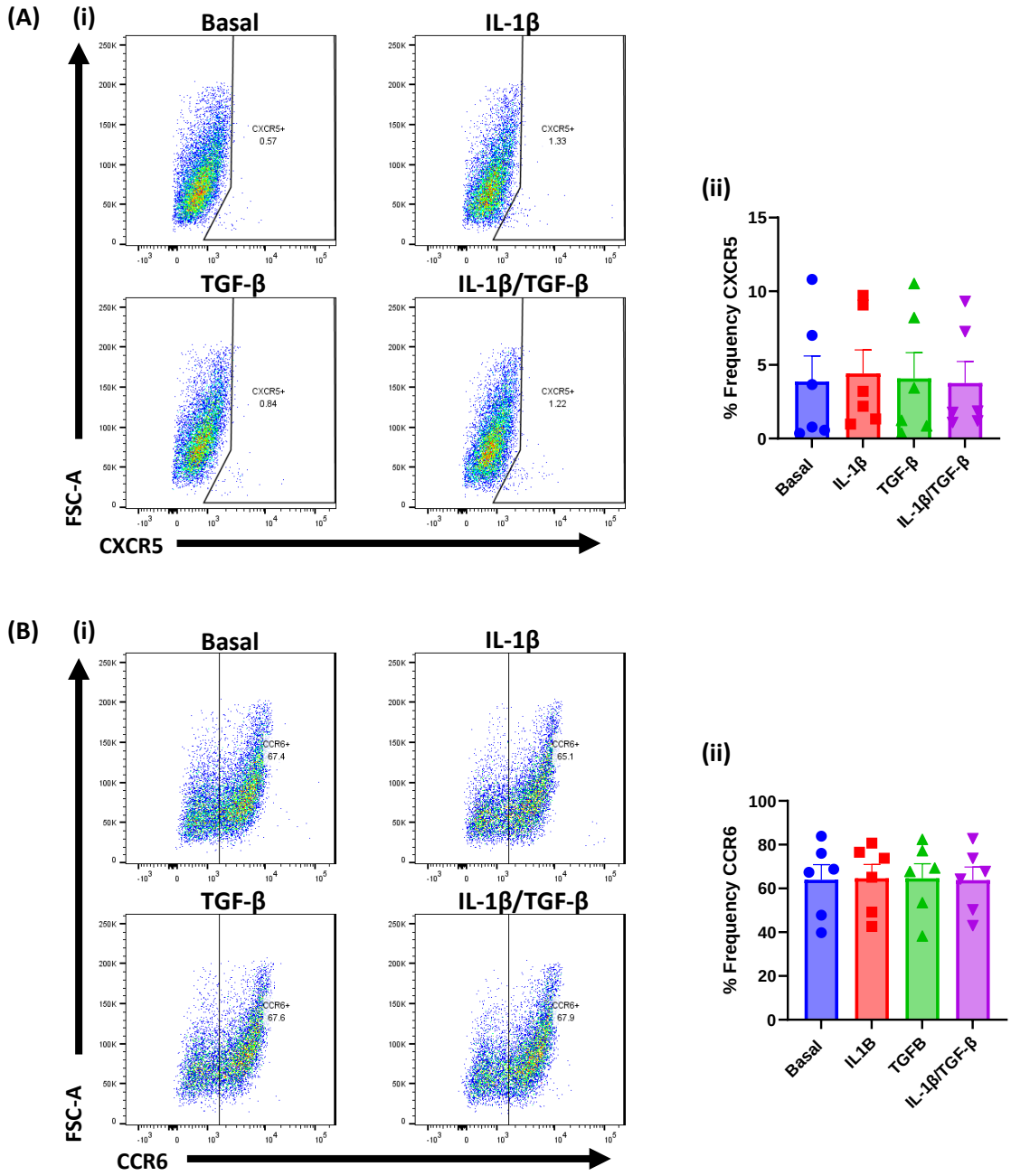

Figure 2.22. The effect of synergy on the expression of chemokine receptors CXCR5 and CCR6 in RA FLS. RA FLS were incubated with IL-1β (1 ng/ml), TGF-β (10 ng/ml), or a combination of both for 24 h following serum starvation before flow cytometric analysis was performed. Representative flow plots depicting **(A(i))** CXCR5 and **(B(i))** CCR6 expression in RA FLS under the indicated conditions; basal, IL-1β, TGF-β, and synergy. Bar charts represent the percentage frequency of **(A(ii))** CXCR5 and **(B(ii))** CCR6 expression in RA FLS (n=6). All data represented as Mean +/- SEM. Statistical analysis was performed using the non-parametric, Wilcoxon Signed-Rank Test (#) or the one-way ANOVA with Friedman's Test (*) where appropriate.

2.4.8 IL-1β and TGF-β synergistically drive the expression of RA FLS adhesion molecule ICAM-1 but not VCAM-1.

Once homing to the joint has been achieved, retaining the immune cells in the vicinity of the inflammatory foci is a critical step in perpetuating joint inflammation (Manning *et al.*, 2021). Therefore, cell surface expression of the adhesion molecules ICAM-1 and VCAM-1 on cultured FLS treated with IL-1β (1 ng/ml) and/or TGF-β (10 ng/ml) for 24 h was investigated by flow cytometric analysis. Representative flow plots outlining the gating strategy used for VCAM-1 and ICAM-1 are shown in Figure 2.23. Following the elimination of debris and cell doublets (Figures 2.23A-C), live cells were gated on (Figure 2.23D) allowing the specific adhesion markers to be analysed on this live population (Figure 2.23E). Figure 24A demonstrates representative dot plots for ICAM-1 expression for the FMO, basal, IL-1β, TGF-β, and IL-1β/TGF-β treated RA FLS. As demonstrated quantitatively (Figure 2.24B(i)) and in the accompanying histogram plot (Figure 2.24B(ii)), there was a synergistic increase in ICAM-1 MFI in response to IL-1β and TGF-β together compared to IL-1β or TGF-β stimulation alone ($p<0.01$, $p<0.001$). Figure 2.25A demonstrates representative dot plots for VCAM-1 expression for the FMO, basal, IL-1β, TGF-β, and IL-1β/TGF-β treated RA FLS. Interestingly, as accentuated by the quantitative graph (Figure 2.25B(i)) and histogram (Figure 2.25B(ii)), the combination of both IL-1β and TGF-β induced a significant increase in VCAM-1 MFI compared to TGF-β alone, whilst simultaneously showing a significant reduction compared to IL-1β treatment alone (both $p<0.05$). However, no effects were observed for VCAM-1 MFI in response to IL-1β and TGF-β compared to the basal comparator, suggesting an attenuating effect of TGF-β on IL-1β's stimulatory ability. Collectively, these results highlight that IL-1β and TGF-β synergy exert different outcomes on different adhesion molecules within the inflamed RA joint.

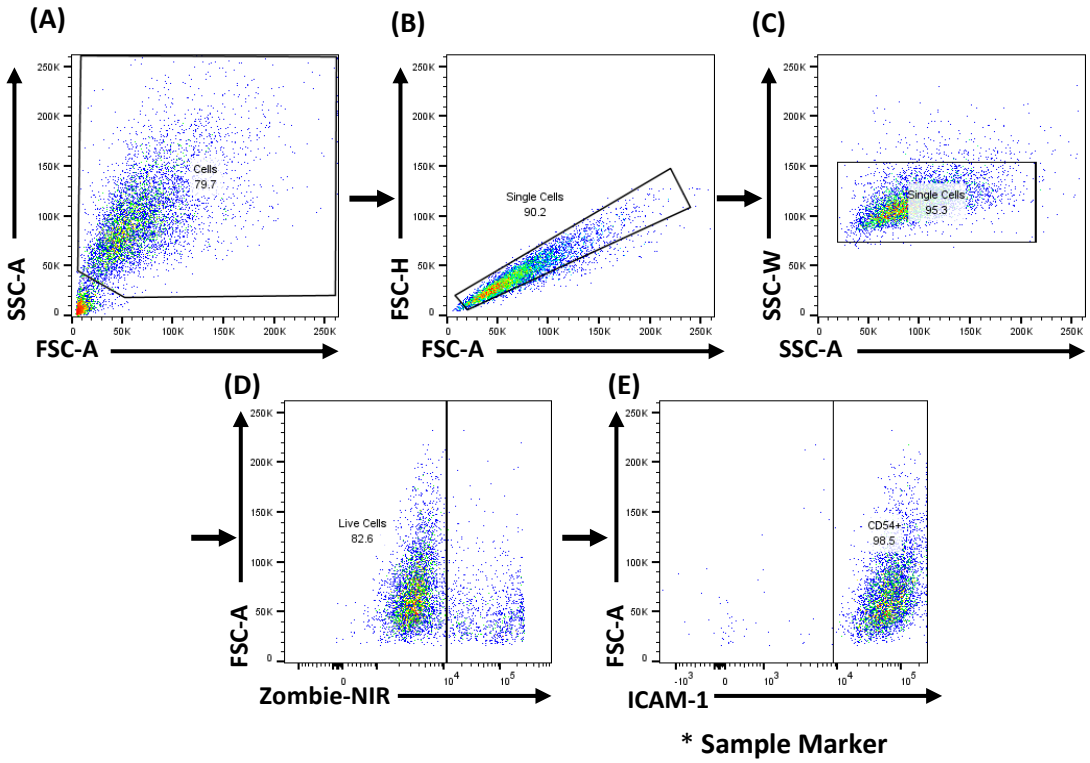

Figure 2.23. FLS functional panel gating strategy. RA FLS were incubated with IL-1β (1 ng/ml), TGF-β (10 ng/ml), or a combination of both for 24 h following serum starvation before being stained with a panel of fluorochrome antibodies (THY1, CD34, CD45, CD146, HLA-DR, ICAM-1, FAP, PDPN, FAS-L, CD309). Representative dot plots depicting the gating strategy used to identify and phenotype the FLS under the various conditions. The forward and side scatter parameters of cells were set before doublet exclusion and elimination of dead cells **(A-D). (E)** Representative flow plot shows the gating for an example marker e.g. ICAM-1 (CD54).

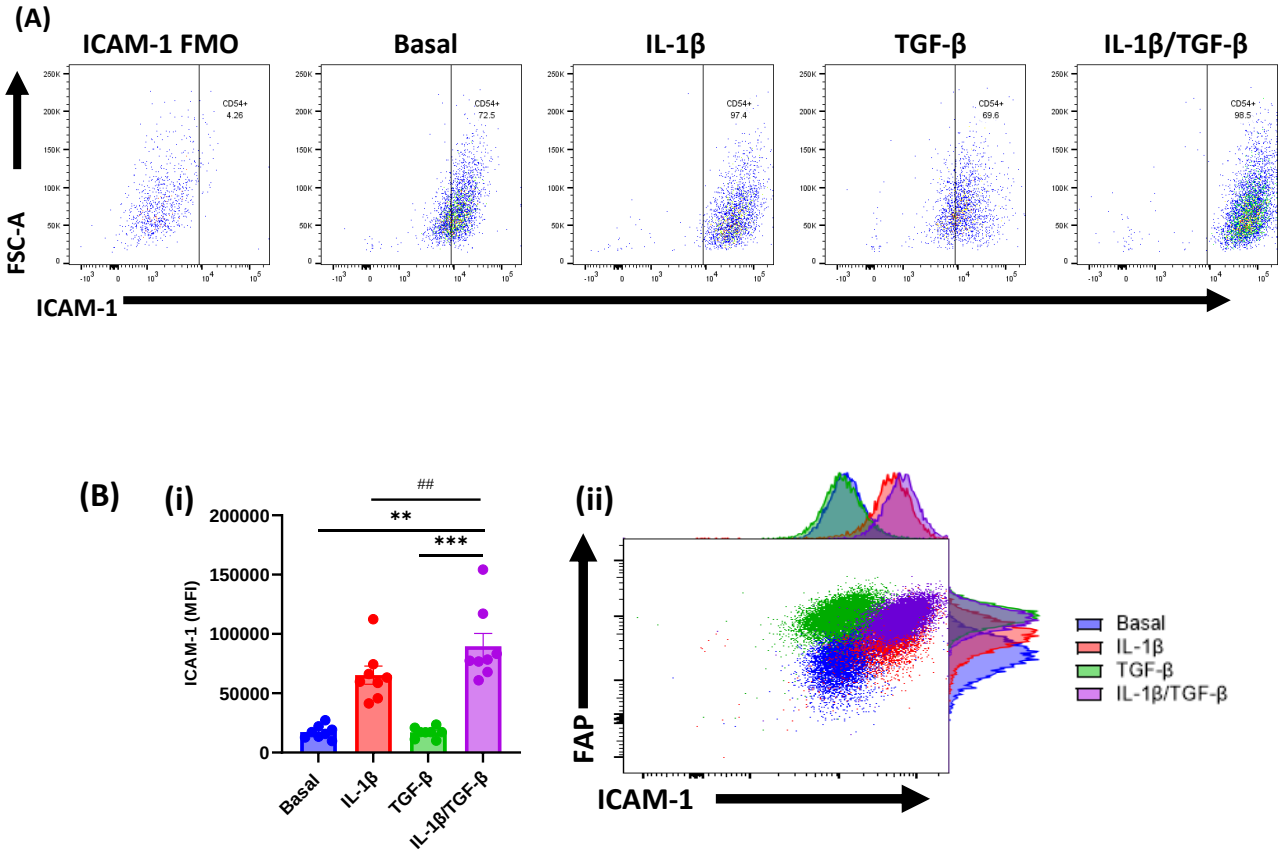

Figure 2.24. IL-1β and TGF-β synergistically drive the expression of ICAM-1 adhesion molecule on RA FLS. RA FLS were incubated with IL-1β (1 ng/ml), TGF-β (10 ng/ml), or a combination of both for 24 h following serum starvation before flow cytometric analysis was performed. **(A(i))** Representative flow dot plots show RA FLS ICAM (CD54) expression under the conditions FMO, basal, IL-1β (1 ng/ml), TGF-β (10 ng/ml), and synergy. **(B(i-ii)** Bar graph and accompanying histogram representation of the MFI of ICAM-1 in the RA FLS (n=8). All data represented as Mean +/- SEM. Statistical analysis was performed using the non-parametric, Wilcoxon Signed-Rank Test (#) or the one-way ANOVA with Friedman's Test (*) where appropriate, with statistical significance defined by $**^{(\#\#)}p\leq0.01$, $***^{(\#\#\#)}p\leq0.001$.

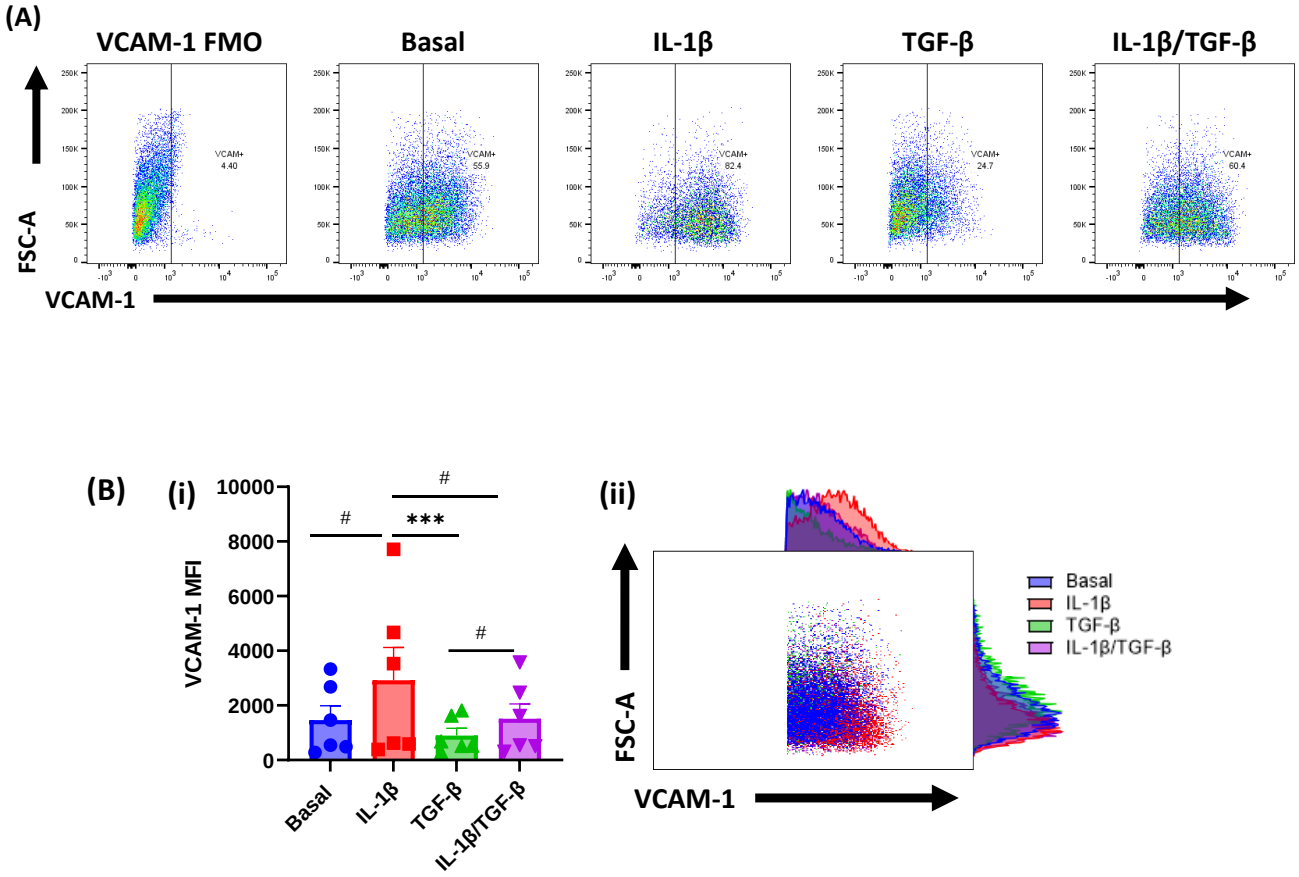

Figure 2.25. The effect of synergy on the expression of the adhesion molecule VCAM-1 on RA FLS. RA FLS were incubated with IL-1β (1 ng/ml), TGF-β (10 ng/ml), or a combination of both for 24 h following serum starvation before flow cytometric analysis was performed. **(A)** Representative flow dot plots show RA FLS VCAM-1 expression under the conditions FMO, basal, IL-1β (1 ng/ml), TGF-β (10 ng/ml), and synergy. **(B(i-ii)** Bar graph and accompanying histogram representation of the MFI of VCAM-1 in the cytokine treated RA FLS (n=6). All data represented as Mean +/- SEM. Statistical analysis was performed using the non-parametric, Wilcoxon Signed-Rank Test (#) or the one-way ANOVA with Friedman's Test (*) where appropriate, with statistical significance defined by $*^{(\#)}p\leq0.05$, $**^{(\#\#)}p\leq0.01$, $***^{(\#\#\#)}p\leq0.001$.

2.4.9 IL-1β and TGF-β synergistically drive the expression of specific RA FLS invasion markers.

Previous research has highlighted that RA FLS demonstrate an aggressive phenotype characterised by the release of cartilage/matrix degrading proteins and an invasive capacity which further perpetuates joint damage (Nygaard and Firestein, 2020). Thus, RA FLS migratory/invasive capacity was assessed in response to cytokine stimulation by analysing the expression of the critical degradative mediators MMP-1 and MMP-3 by RT-PCR and MSD assays.

RA FLS grown to confluence and treated with 1% RPM1-1640 for 24 h, were then treated with IL-1β (1 ng/ml), TGF-β (10 ng/ml) alone or in combination, supernatants were harvested, and RNA isolated from cells. As shown in Figure 2.26A(i) IL-1β and TGF-β together had no potentiation/synergy effect on MMP-1 gene expression compared to IL-1β alone. Similarly, at the protein level a trending increase in MMP-1 was demonstrated in response to IL-1β alone and in combination with TGF-β, however this didn't differ from IL-1β alone (Figure 2.26A(ii)). Conversely, Figures 2.26B(i) and 2.26B(ii) demonstrate a significant increase in MMP-3 expression at both the RNA ($p<0.01$) and protein levels ($p<0.05$) following stimulation with both IL-1β and TGF-β together compared to treatment with TGF-β alone.

To further assess their invasive properties following cytokine stimulation, a wound repair scratch assay was performed where the ability of treated FLS to repopulate the wound margins was quantified. Representative images of FLS wound repair assays in response to 24 h IL-1β and/or TGF-β stimulation are shown in Figure 2.26C where an increase in FLS repopulating the wound margins was exhibited in response to IL-1β and TGF-β compared to basal or either cytokine alone. Quantification demonstrated a stepwise increase on migratory capacity with a significant increase in the % wound closure with IL-1β/TGF-β compared to basal ($p<0.01$) and TGF-β ($p<0.05$) alone (Figure 2.26D). Overall, these results indicate that stimulation with IL-1β and TGF-β induces a significant synergistic effect on the invasive capacity of RA FLS within the joint through the induction of specific joint-destructive MMPs.

2.4.10 IL-1β and TGF-β induce differential effects on bone resorbing/forming protein expression in RA FLS.

The irreversible erosion of bone and cartilage is a characteristic feature of RA driven by an imbalance between bone homeostatic and resorbing proteins including OPG, RANKL, BPM2, and M-CSF (Lories *et al.*, 2003; Tunyogi-Csapo *et al.*, 2008; Yoshitomi, 2019). RA FLS grown to confluence and treated with 1% RPMI-1640 for 24 h, were then treated with IL-1β (1 ng/ml), TGF-β (10 ng/ml) alone or in combination. Supernatants were then harvested and subjected to MSD

analysis for the markers RANKL, M-CSF, and BMP2, whilst OPG levels were quantified using ELISA. Interestingly, RANKL expression from the RA FLS was notably low, with no significant differences in production observed following cytokine stimulation compared to basal (Figure 2.27A). As demonstrated in Figure 2.27B, IL-1β/TGF-β had no additive/synergistic effect on the production of OPG compared to IL-1β alone. Moreover, whilst IL-1β induced a significant increase in the expression of M-CSF compared to basal ($p<0.05$), the combination of IL-1β/TGF-β did not result in any change to the levels indicating TGF-β has no effect on M-CSF production (Figure 2.27C). Conversely, there was a synergistic effect on the release of BMP2 with the combination treatment of IL-1β/TGF-β, with a significantly higher level detected compared to basal or IL-1β alone ($p<0.01$, $p=0.06$) (Figure 2.27D). Cumulatively, these results suggest that IL-1β and TGF-β may be exerting highly specific regulatory effects on certain processes involved in bone formation/resorption.

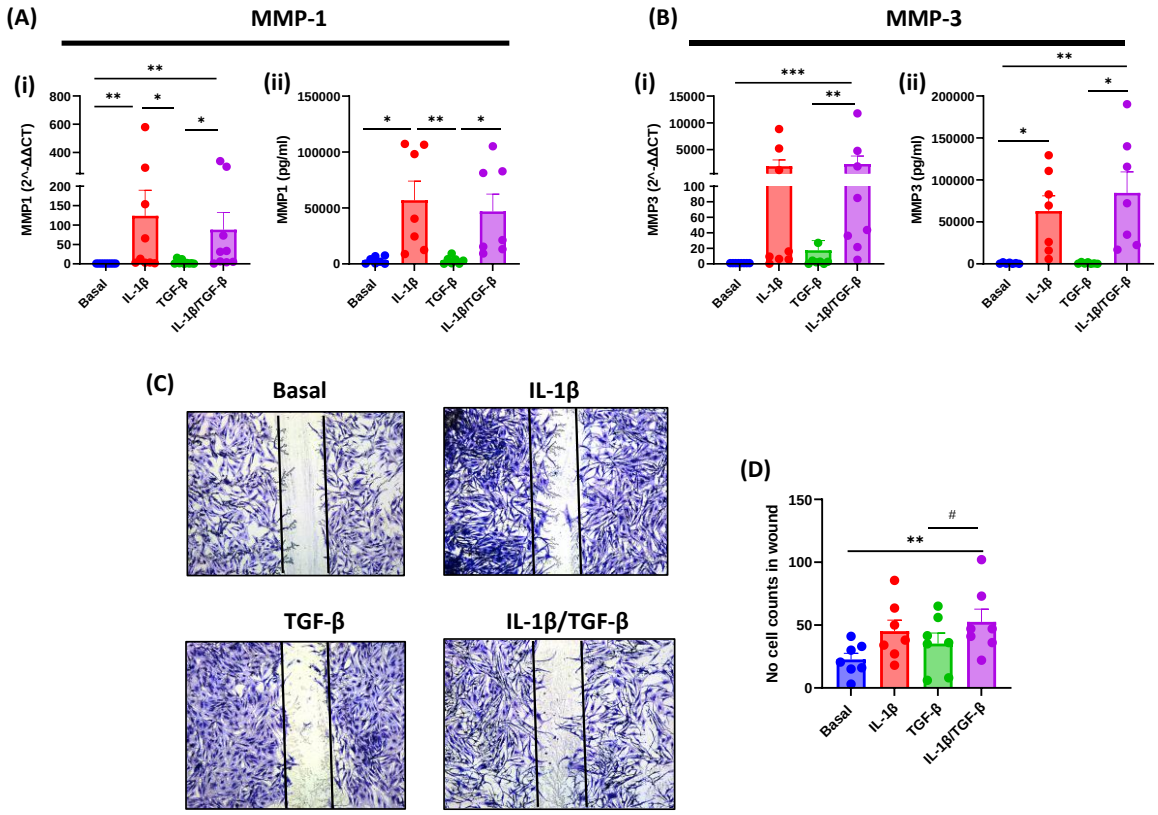

Figure 2.26. IL-1β and TGF-β synergistically drive the expression of RA FLS invasion markers and migratory capacity. RA FLS were incubated with IL-1β (1 ng/ml), TGF-β (10 ng/ml), or a combination of both for 24 h following serum starvation before supernatants were harvested and MMPs quantified. Bar graphs showing quantification of gene mRNA expression of **(A(i))** MMP-1 and **(B(i))** MMP-3 in RA FLS (n=7-8) following treatment. Data represented as fold expression, normalized to housekeeping control RPLP0. $2^{-\delta\delta ct}$ indicates fold induction. Bar graph representations of the level of secretion of **(A(ii))** MMP-1 and **(B(ii))** MMP-3 in RA FLS (n=7) as determined by an MSD. **(C)** Representative photomicrographs and **(D)** accompanying bar graph demonstrating the average number of migrating cells and in response to treatment with the various cytokines (n=7). All data represented as Mean +/- SEM. Statistical analysis was performed using the non-parametric, Wilcoxon Signed-Rank Test (#) or the one-way ANOVA with Friedman's Test (*) where appropriate, with statistical significance defined by $*^{(\#)}p\leq0.05$, $**^{(\#\#)}p\leq0.01$, $***^{(\#\#\#)}p\leq0.001$.

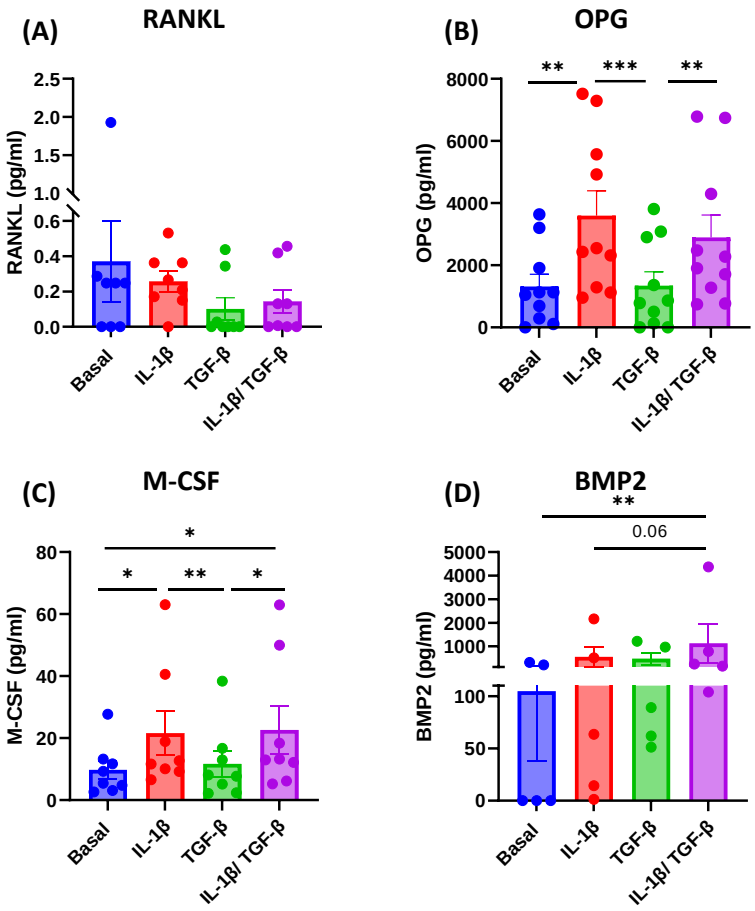

Figure 2.27. Differential effects on osteoclastogenesis related proteins in the presence of IL-1β and TGF-β stimulation. RA FLS were incubated with IL-1β (1 ng/ml), TGF-β (10 ng/ml), or a combination of both for 24 h following serum starvation before supernatants were removed and analysed for OPG, RANKL, M-CSF, and BMP2 using ELISA or MSD assays. Bar graph representations of level of secretion of **(A)** RANKL (n=8), **(B)** OPG (n=10), **(C)** M-CSF (n=8), and **(D)** BMP2 (n=5) in RA FLS. All data represented as Mean +/- SEM. Statistical analysis was performed using the non-parametric, one-way ANOVA with Friedman's Test (*) with statistical significance defined by *p≤0.05, **p≤0.01, ***p≤0.001.

2.4.11 Determination of the effect of different concentrations of Takinib on RA FLS cell viability and proinflammatory cytokine production.

TAK1 has previously been implicated as a central downstream signalling intermediate in both the IL-1β and TGF-β pathways (Xu and Lei, 2020). Therefore, to gain a deeper understanding of the key downstream pathway involved in driving the effects of the synergistic and additive interaction between IL-1β and TGF-β, the role of Takinib, a selective TAK1 inhibitor, was assessed, in mediating the effects induced by the cytokine treatment in RA FLS.

To initially investigate the effect of Takinib on RA FLS viability, confluent RA FLS were pre-treated with increasing concentrations of Takinib (1 μM, 10 μM, and 20 μM respectively) or vehicle control before a crystal violet cell viability assay was performed. Figures 2.28A and 2.28B highlight that there was no difference in the number of viable cells between the three concentrations (1 μM, 10 μM, and 20 μM) themselves or compared to basal/DMSO controls. Furthermore, to determine which concentration of Takinib exerted maximum effects, confluent RA FLS were pre-treated with increasing concentrations of Takinib (1 μM, 10 μM, and 20 μM respectively) or vehicle control prior to stimulation with IL-1β (1 ng/ml) and TGF-β (10 ng/ml) alone or in combination, before secretion of proinflammatory cytokines was assessed by ELISA. As demonstrated in Figure 2.28C and 2.28D, both IL-6 and MCP-1 protein levels were downregulated in a dose dependent manner with the greatest decrease in levels observed compared to the DMSO control for each condition at a concentration of 20 μM Takinib. Cumulatively, these results suggest that a concentration of 20 μM Takinib is not toxic and exerts the maximum inhibitory effects and thus this concentration was chosen for all future experiments.

2.4.12 Takinib has a suppressive effect on the secretion of proinflammatory cytokines, chemokines, and invasion markers from IL-1β and TGF-β treated FLS, in addition to their glycolytic capacity.

Analysis of the mRNA revealed that although IL-6 ($p<0.0001$), IL-8 ($p<0.05$), and MCP-1 ($p<0.05$), were all significantly increased in response to treatment with the combination of IL-1β and TGF-β compared to the basal control, a decrease in the expression of all three mediators was demonstrated under synergy condition in the presence of Takinib ($p<0.0001$) (Figures 2.29A(i-iii)). A similar effect was observed at the protein level, with the stimulatory effects of the cytokine synergy being significantly decreased ($p<0.05$, $p<0.0001$) in the presence of 20 μM Takinib for IL-6 (Figure 2.29B(i)), IL-8 (Figure 2.29B(ii)), and MCP-1 (Figure 2.29B(iii)). Furthermore, as demonstrated by the representative heatmap (Figure 30A), MSD analysis revealed a significant

reduction in the expression of several chemokines following the addition of Takinib compared to the IL-1β and TGF-β only treated control, including Eotaxin (Figure 2.30B(i)), IP-10 (Figure 2.30B(ii)), and MDC (Figure 2.30B(iii)). Interestingly, whilst Takinib did reduce the expression slightly of several angiogenic factors, their initial differences in expression from baseline following the addition of IL-1β and TGF-β was not significant (Figure 2.31A). Conversely, PCR and MSD analysis of MMPs revealed a striking decrease in the expression of mRNA and protein levels of MMP-1 (Figure 2.32A and 2.32B(i)) and MMP-3 (Figure 2.32A and 2.32B(ii)), in addition to protein levels of MMP-9 (Figure 2.32A) in the Takinib + IL-1β/TGF-β treated FLS compared to the IL-1β/TGF-β treated control.

Moreover, to investigate if blocking TAK1 could suppress the glycolytic metabolic shift induced in IL-1β and TGF-β treated RA FLS, a glycolytic rate assay was performed on cultured FLS treated with Takinib for 2 h prior to 24 h cytokine stimulation. Interestingly, the addition of Takinib to the IL-1β/TGF-β treated FLS resulted in a significant reduction in the level of basal glycolysis (Figure 2.33A), basal proton efflux rate (Figure 2.33B), and compensatory glycolysis (Figure 2.33C) compared to the IL-1β/TGF-β DMSO control (all $p<0.05$). Pie charts describe the relative contribution of each of the conditions: basal control, IL-1β/TGF-β control, IL-1β/TGF-β + Takinib, as a percentage of the total glycolytic outputs – basal glycolysis, basal protein efflux rate, and compensatory glycolysis (Figure 2.33D(i-iii)). Interestingly, for all three glycolytic outputs, whilst IL-1β/TGF-β treatment alone (purple) demonstrated the greatest contribution, the addition of Takinib to the IL-1β/TGF-β (grey) resulted in a decrease back towards baseline (blue) indicating that TAK1 may be critical in mediating the synergistic effects of IL-1β and TGF-β on RA FLS glycolytic metabolism.

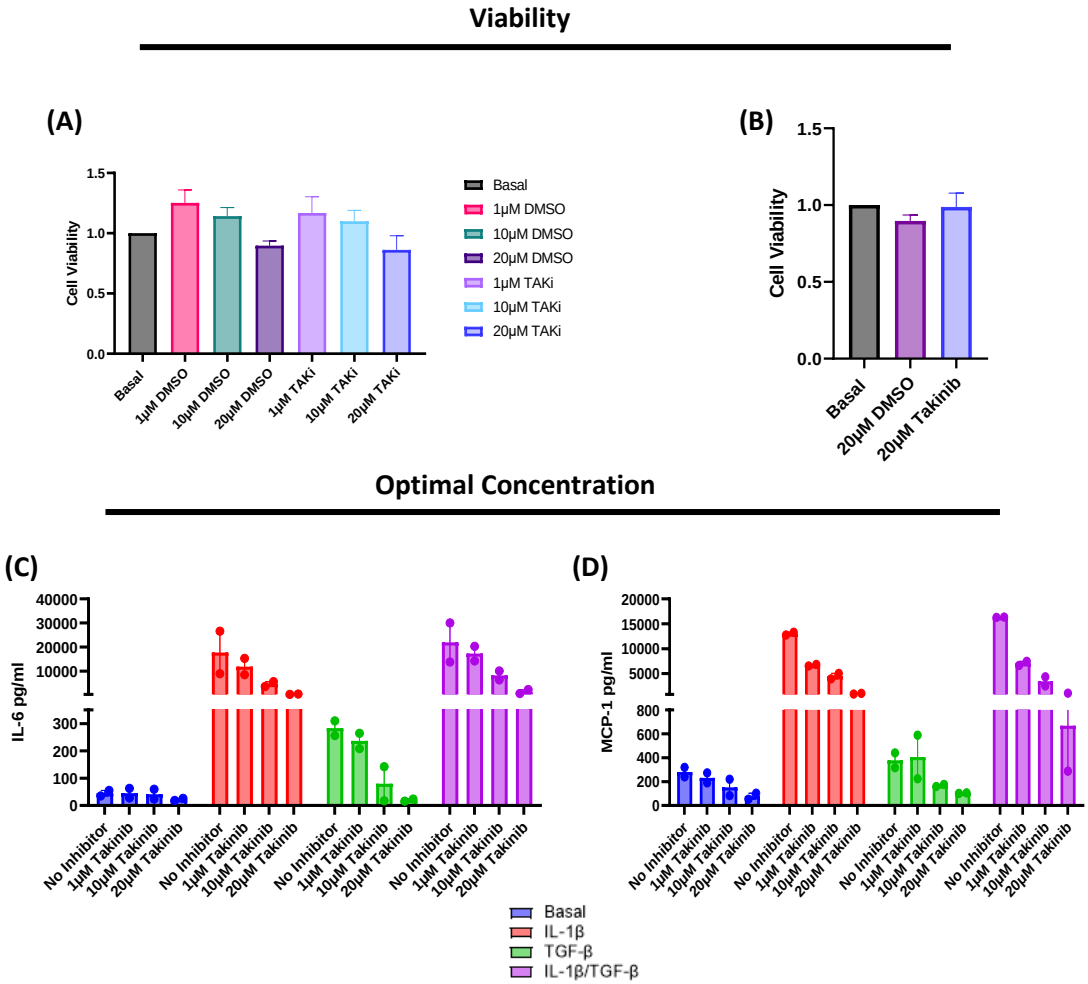

Figure 2.28. Effect of different concentrations of TAK1 inhibitor on RA FLS cell viability and proinflammatory cytokine production. Following 24 h serum starvation, RA FLS were pre-treated with various concentrations of TAK1 inhibitor (Takinib) or DMSO vehicle control – 1 μM, 10 μM, and 20 μM for 2 h prior to incubation with IL-1β (1 ng/ml), TGF-β (10 ng/ml), or a combination of both for a further 24 h. Supernatants were collected and analysed by ELISA and cell viability was assessed using the crystal violet viability assay. **(A)** Bar graph showing cell viability relative to baseline following treatment of basal cells with 1 μM, 10 μM, and 20 μM Takinib or DMSO vehicle. **(B)** Bar graph showing cell viability relative to baseline following treatment of basal cells with 20 μM Takinib or DMSO vehicle control. Bar graph representations of level of secretion of **(C)** IL-6 and **(D)** MCP-1 in RA FLS (n=2) following treatment with increasing concentrations of the inhibitor and the various stimulations. All data represented as Mean +/- SEM.

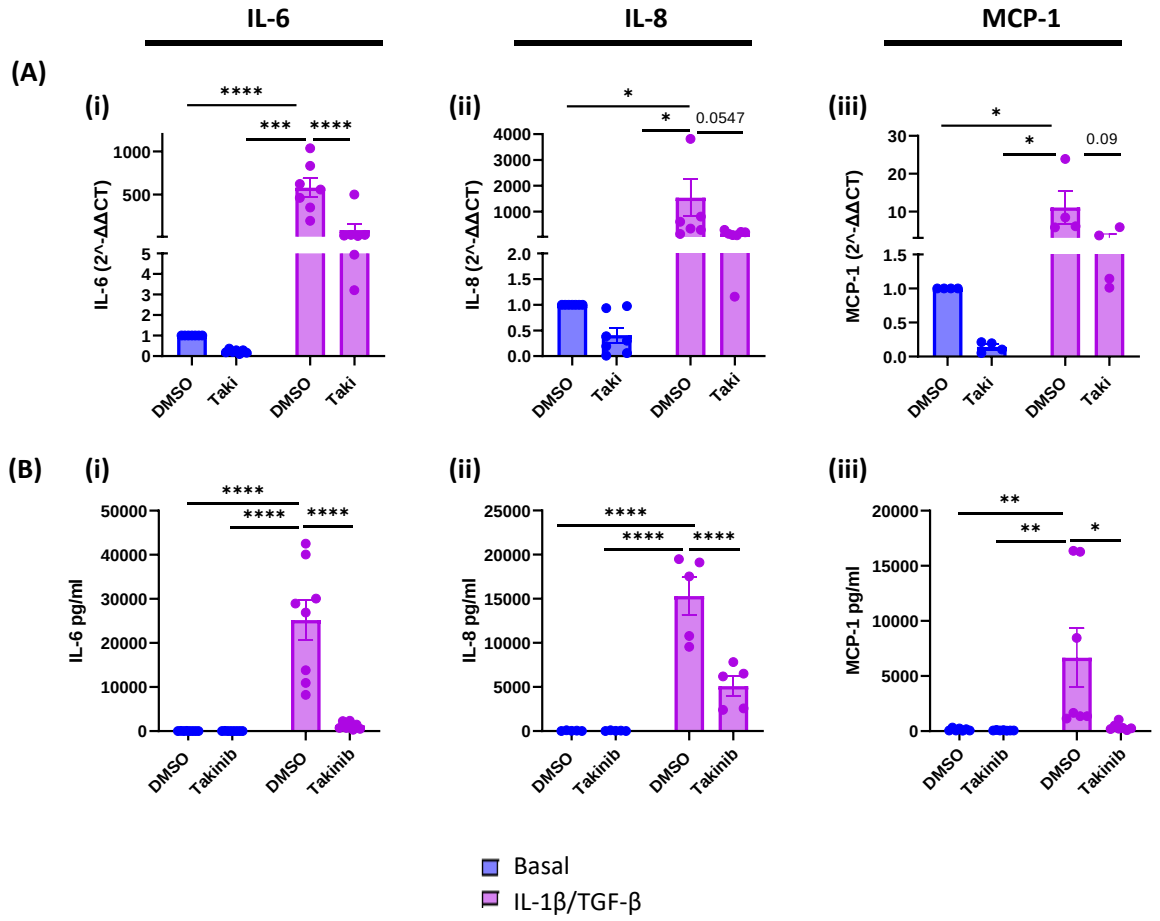

Figure 2.29. TAK1 inhibitor has a suppressive effect on the secretion of proinflammatory mediators from IL-1β and TGF-β treated FLS. Following 24 h serum starvation, RA FLS were pre-treated with 20 µM Takinib or DMSO vehicle control for 2 h prior to incubation with IL-1β (1 ng/ml), TGF-β (10 ng/ml), or a combination of both for a further 24 h. Supernatants were collected and analysed for IL-6, IL-8, and MCP-1 secretion by ELISA and mRNA levels of IL-6, IL-8, and MCP-1 were measured by RT-PCR. **(A(i-iii))** Bar graph showing quantification of gene mRNA expression of IL-6, IL-8, and MCP-1 in RA FLS (n=4-7). Data represented as fold expression, normalized to housekeeping control RPLP0. $2^{-\delta\delta ct}$ indicates fold induction. **(B(i-iii))** Bar graph representations of the level of secretion of IL-6, IL-8, and MCP-1 in the treated RA FLS (n=6-8)**.** All data represented as Mean +/- SEM. Statistical analysis was performed using the two-way ANOVA with Turkey's Multiple Comparisons Test (*) with significance defined by *p≤0.05, **p≤0.01, ***p≤0.001, ****p≤0.0001.

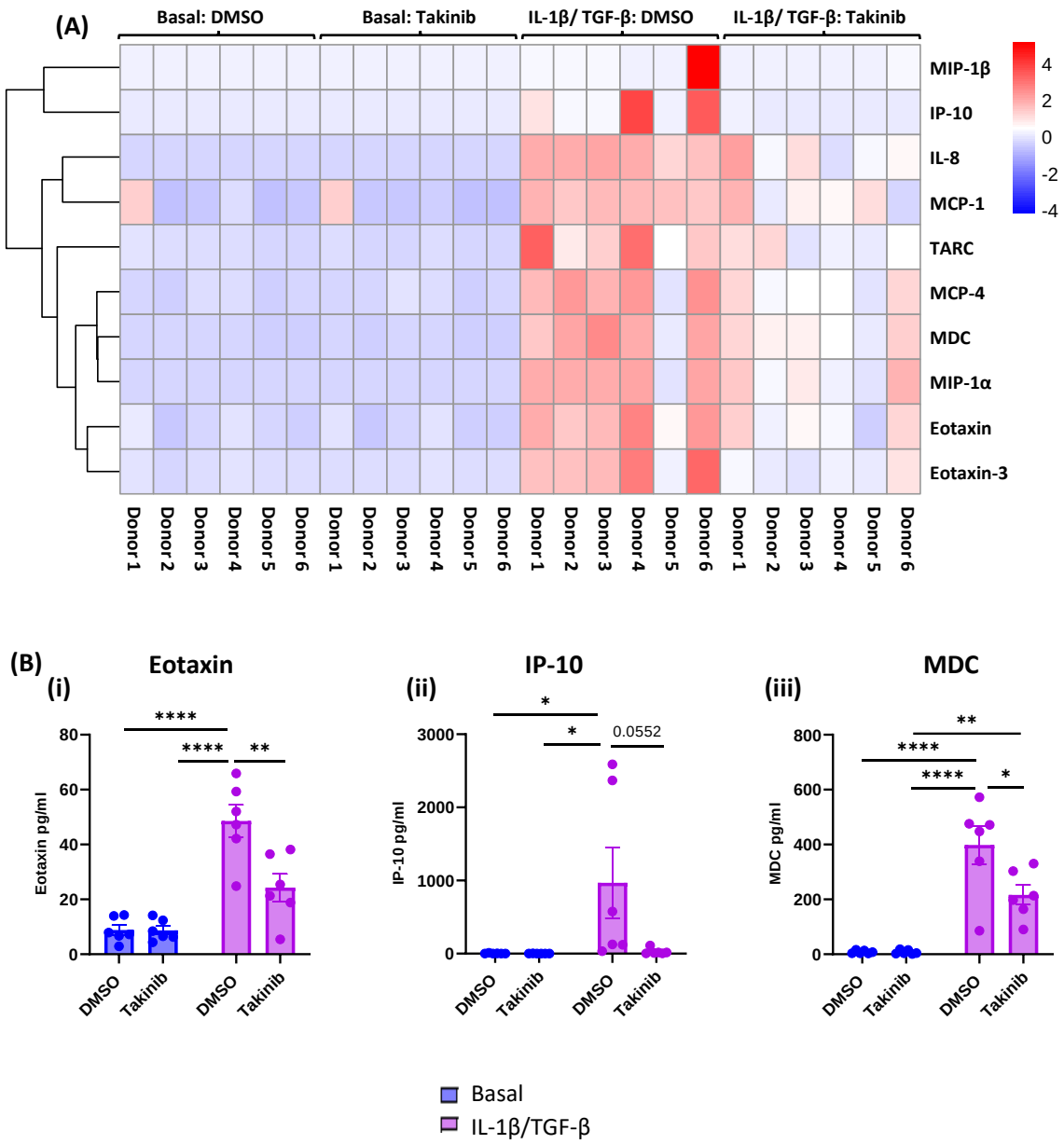

Figure 2.30. TAK1 Inhibitor has a suppressive effect on the secretion of chemokine ligands from IL-1β and TGF-β treated FLS. Following 24 h serum starvation, RA FLS were pre-treated with 20 µM Takinib or DMSO vehicle control for 2 h prior to incubation with IL-1β (1 ng/ml), TGF-β (10 ng/ml), or a combination of both for a further 24 h. Supernatants were collected and analysed for MIP-1β, IP-10, IL-8, MCP-1, TARC, MCP-4, MDC, MIP-1α, Eotaxin, and Eotaxin-3 using the Chemokine MSD assay. **(A)** Clustered heatmap representing the expression of the various chemokines in RA FLS (n=6 separate donors) following stimulation with the appropriate cytokines and inhibition with Takinib. **(B)** Bar graphs depicting the expression level in pg/ml of **(i)** Eotaxin, **(ii)** IP-10, and **(iii)** MDC in the stimulated RA FLS supernatants as determined by the MSD assay. All data represented as Mean +/- SEM. Statistical analysis was performed using the two-way ANOVA with Turkey's Multiple Comparisons Test (*) with significance defined by *p≤0.05, **p≤0.01, ***p≤0.001, ****p≤0.0001.

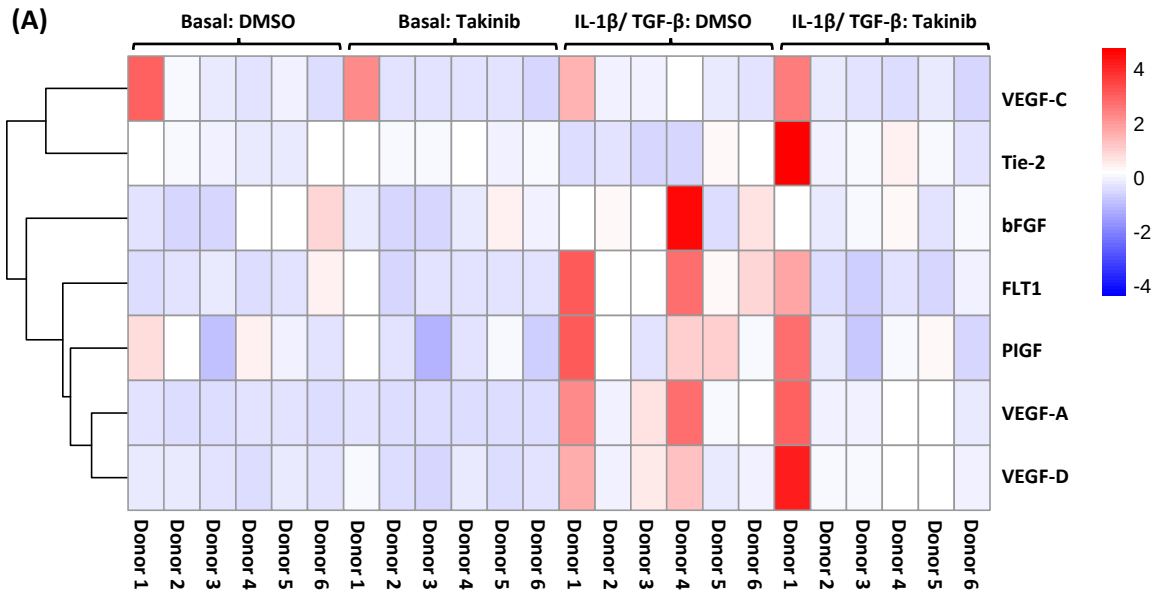

Figure 2.31. TAK1 inhibitor has minimal effects on the secretion of angiogenic factors from IL-1β and TGF-β treated FLS. Following 24 h serum starvation, RA FLS were pre-treated with 20 µM Takinib or DMSO vehicle control for 2 h prior to incubation with IL-1β (1 ng/ml), TGF-β (10 ng/ml), or a combination of both for a further 24 h. Supernatants were collected and analysed for VEGF-C, Tie-2, bFGF, FLT1, PIGF, VEGF-A, and VEGF-D using the Angiogenic MSD assay. **(A)** Clustered heatmap representing the expression of the various angiogenic mediators in RA FLS (n=6) separated out into individual donors following stimulation with the appropriate cytokines and inhibition with Takinib.

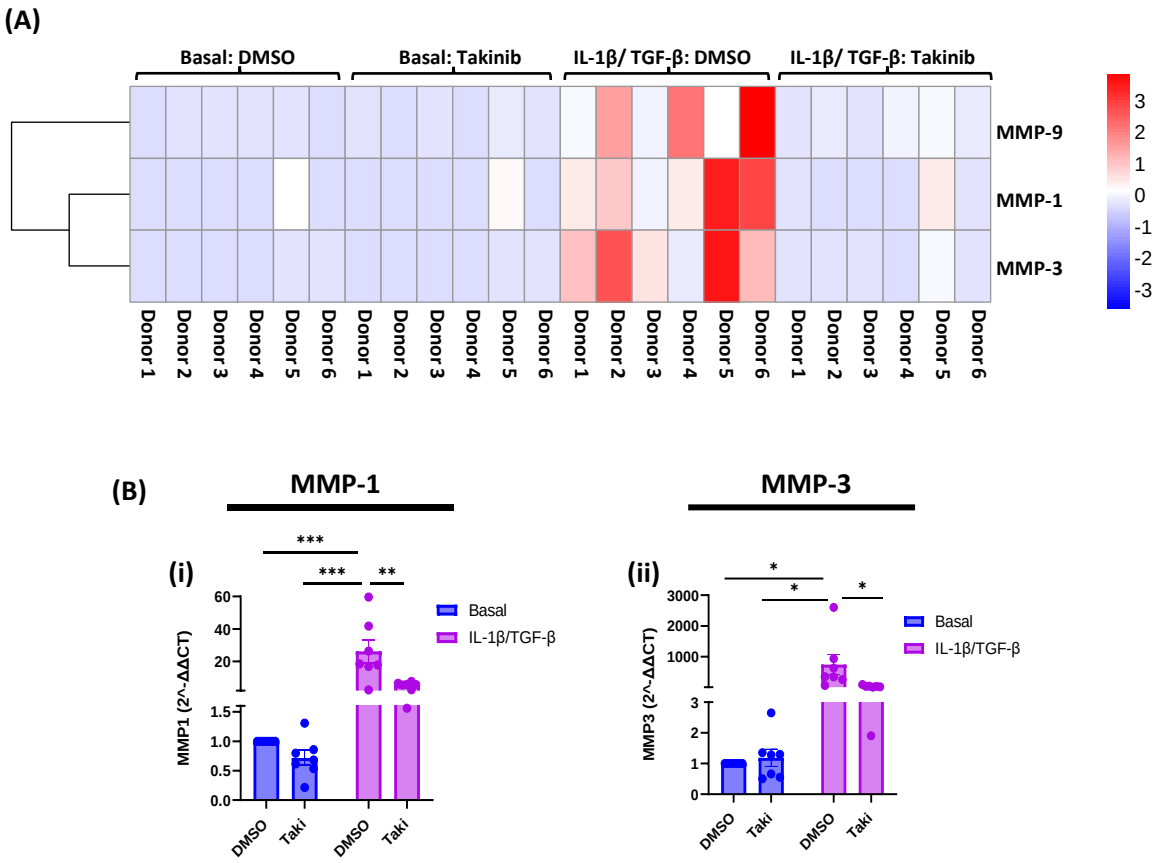

Figure 2.32. TAK1 inhibitor has a suppressive effect on the secretion of MMP-1 and MMP-3 from IL-1β and TGF-β treated FLS. Following 24 h serum starvation, RA FLS were pre-treated with 20 µM Takinib or DMSO vehicle control for 2 h prior to incubation with IL-1β (1 ng/ml), TGF-β (10 ng/ml), or a combination of both for a further 24 h. Supernatants were collected and analysed for MMP-1, MMP-3, and MMP-9 using the MMP MSD assay. **(A)** Clustered heatmap representing the expression of the various MMPs in RA FLS (n=6 individual donors) following stimulation with the appropriate cytokines and inhibition with Takinib. **(B)** Bar graph showing quantification of gene mRNA expression of **(i)** MMP-1 and **(ii)** MMP-3 in RA FLS (n=4-7). Data is represented as fold expression, normalized to housekeeping control RPLP0. $2^{-\delta\delta ct}$ indicates fold induction. All data represented as Mean +/- SEM. Statistical analysis was performed using the two-way ANOVA with Turkey's Multiple Comparisons Test (*) with significance defined by *p≤0.05, **p≤0.01, ***p≤0.001.

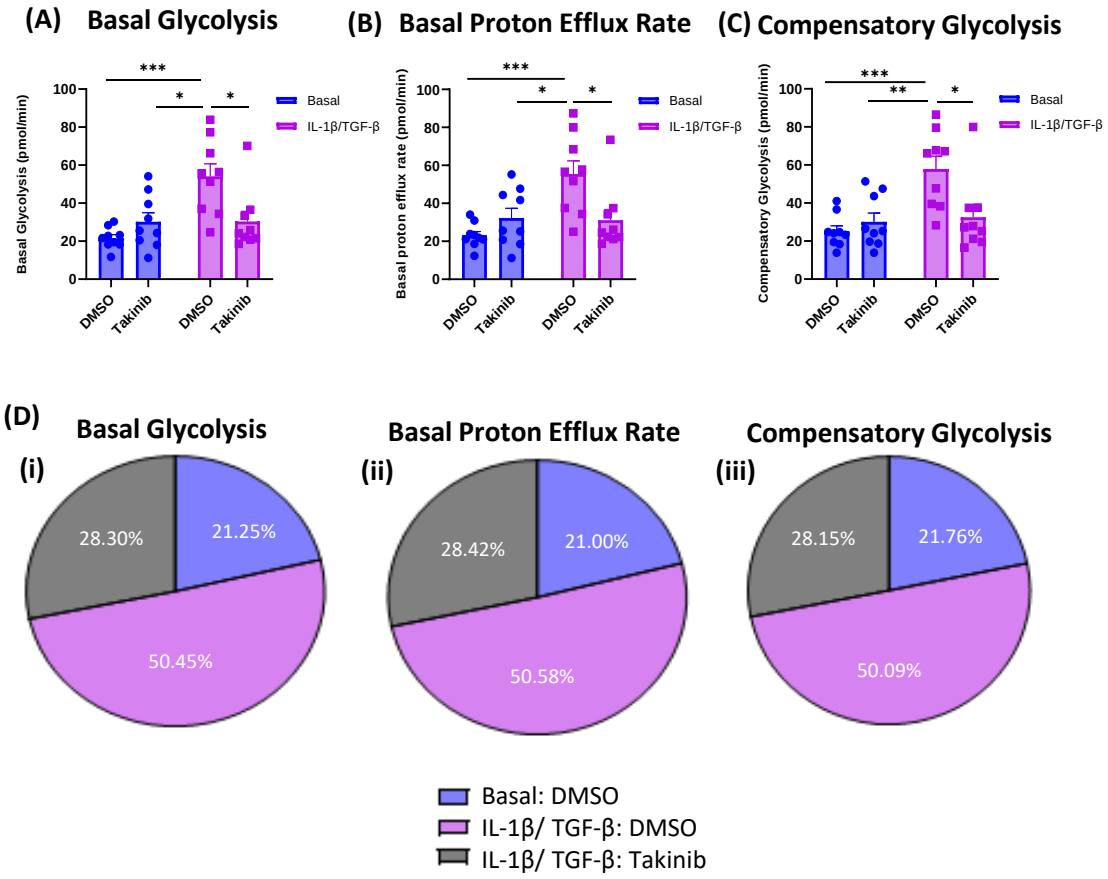

Figure 2.33. TAK1 inhibitor has a suppressive effect on synergy induced glycolysis in RA FLS. Following 24 h serum starvation, RA FLS (n=9) were pre-treated with 20 µM Takinib or DMSO vehicle control for 2 h prior to incubation with IL-1β (1 ng/ml), TGF-β (10 ng/ml), or a combination of both for a further 24 h. **(A-C)** Representative bar graphs demonstrating Basal Glycolysis, Basal Proton Efflux Rate, and Compensatory Glycolysis before and after injections of metabolic inhibitors Rotenone, Antimycin A, and 2-DG. All data represented as Mean +/- SEM. **(D(i-iii))** Pie charts reveal the breakdown of each condition within each Glycolytic Rate Assay output. Statistical analysis was performed using the two-way ANOVA with Turkey's Multiple Comparisons Test (*) with statistical significance defined by *p≤0.05, **p≤0.01, and ***p≤0.001.

2.4.13 TAK1 inhibition induces a compaction phenotype in *ex vivo* RA synovial explants over a time period.

To investigate the effects of TAK1 inhibition on synovial pathogenesis, RA synovial biopsies were sectioned and embedded into Matrigel coated 96-well plates immediately after arthroscopy and subsequently cultured for 21 days in the presence of Takinib (20 µM) or DMSO control (20 µM). Explant media was collected, and the conditions were replaced every 4-5 days. As demonstrated in the representative images in Figure 2.34A and quantitatively in Figure 2.34B, Takinib treated explants exhibit a more stable phenotype with less fluctuation and a gradual decrease in size compared to the DMSO control which consistently remains at a bigger size over the designated time period of 21 days (Figure 2.34A). The change in size over the time period of each individual donor is shown in Figure 2.34C(i-v), reinforcing the heterogeneity of donors in response to treatments. This data suggests that Takinib induces a more compact morphology of the biopsy, ultimately suppressing the expansion associated with increased proinflammatory conditions and maintaining a more homeostatic environment resemblant of a healthy joint.

2.4.14 Takinib inhibits the spontaneous release of proinflammatory chemokines and MMPs and from RA *ex vivo* explants.

To further elucidate the role of TAK1 signalling in driving proinflammatory and invasive aspects of synovial inflammation, an *ex vivo* explant model was utilised (McGarry *et al.*, 2018b). RA synovial explants were placed into a 96-well plate in the presence of Takinib (20 µM) or DMSO control (20 µM) and the supernatants were subsequently collected at 24 h. The spontaneous secretion of proinflammatory chemokines and MMPs into this collected culture media was quantified using MSD assays. Interestingly, Takinib treatment resulted in a suppressive effect on the production and release of chemokine ligands and all three MMPS; MMP-1, MMP-3, and MMP-9 compared to the DMSO control, with similar decreasing trends in chemokines and MMPs observed across the three separate donors (Figure 2.35 and Figure 2.36 respectively), suggesting TAK1 plays a role in both the inflammatory and invasive processes within the synovium.

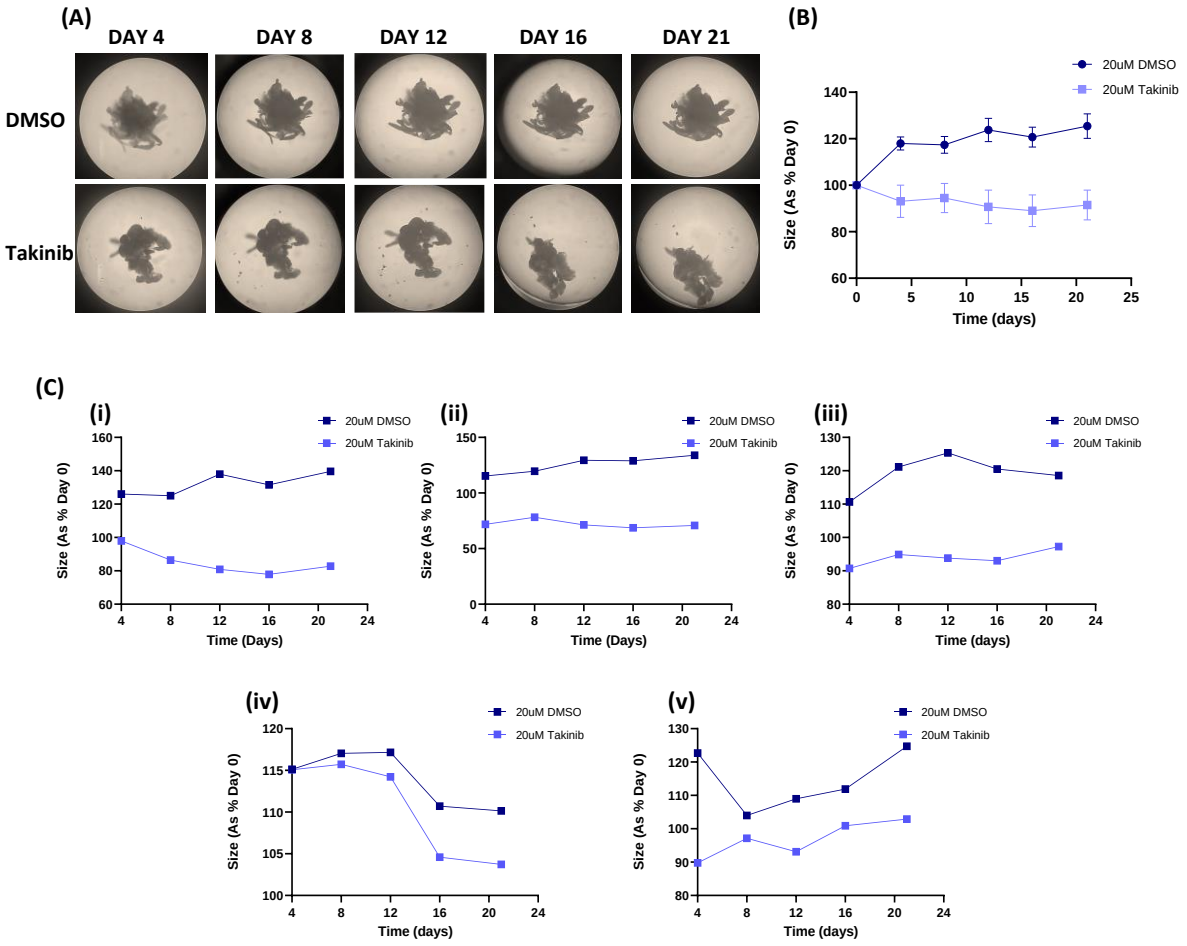

Figure 2.34. TAK1 inhibition maintains a more compact phenotype of ex vivo RA synovial explants compared to DMSO control. (A) Representative photomicrographs showing *ex vivo* RA synovial explant culture in Matrigel in response to TAK1 inhibition using Takinib (20 µM) or DMSO (20 µM) vehicle control over a time-course of 4-21 days. Original magnification 4x. **(B)** Quantitative time plot demonstrating the change in explant size (n=5) as a % of the size on day 0 in response to treatment with DMSO or Takinib. **(C)** Representative time plot for each individual donor (n=5) demonstrating the change in explant size as a % of the size on day 0 in response to treatment with DMSO or Takinib from day 4-21.

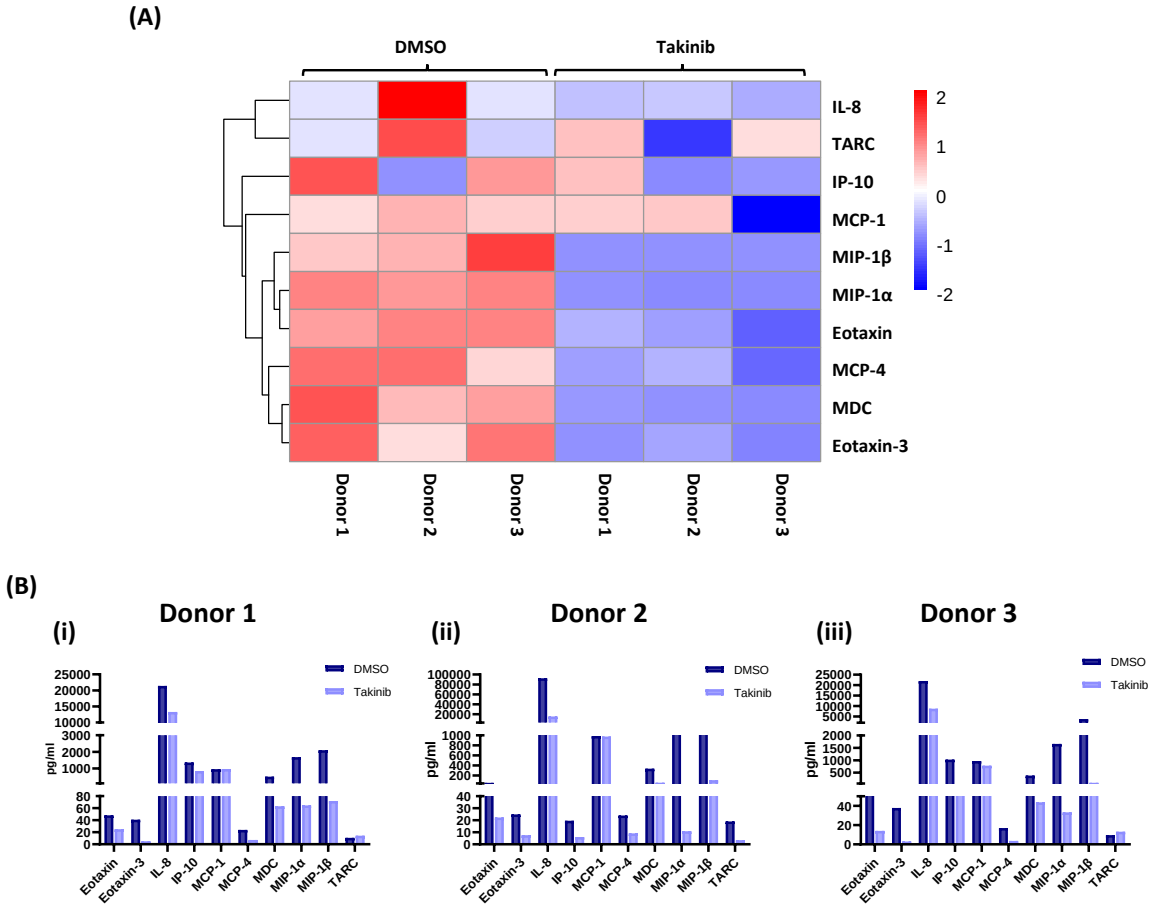

Figure 2.35. TAK1 inhibitor has a differential patient specific effect on the secretion of chemokine ligands from RA synovial explants. (A) Clustered heatmap and **(B(i-iii))** individual patient bar graphs (n=3) representing the expression of the chemokines Eotaxin, Eotaxin-3, IL-8, IP-10, MCP-1, MCP-4, MDC, MIP-1α, MIP-1β, and TARC in RA synovial explants incubated with Takinib (20 µM) or DMSO vehicle control (20 µM) for 24 h.

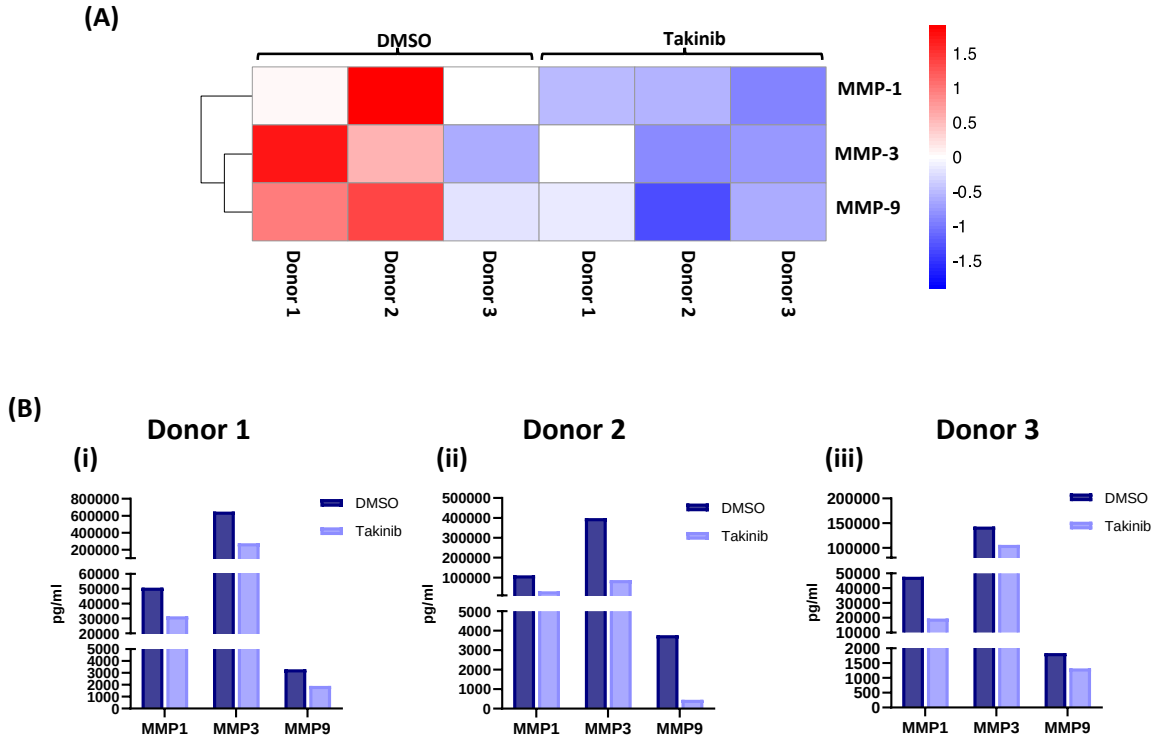

Figure 2.36. TAK1 inhibitor has a suppressive effect on the secretion of the MMPs; MMP-1, MMP-3, and MMP-9 from RA synovial explants. (A) Clustered heatmap and **(B(i-iii))** individual patient bar graphs (n=3) representing the decrease in expression of the MMPs; MMP-1, MMP-3, and MMP-9 from RA synovial explants incubated with Takinib (20 µM) compared to DMSO vehicle control (20 µM) for 24 h.

2.5 Discussion

An abundance of literature has reinforced the central role of FLS in RA and PsA where their destructive and immune cell-like behaviour perpetuates the chronically inflamed microenvironment within the synovial joint (Fassbender and Simmling-Annefeld, 1983; Bottini and Firestein, 2013; Bustamante *et al.*, 2017; Koliaraki *et al.*, 2020; Kondo, Kuroda and Kobayashi, 2021). However, to date, an in-depth analysis of potential differences in the phenotype, regulation, and subsequent pathogenic activity of RA vs PsA FLS remains to be investigated. For the first time in this chapter, scRNA-seq analysis of whole synovial biopsy single-cell suspensions was utilised to gain a more comprehensive understanding of the cell clusters dominant within the synovium of RA and PsA patients. The data indicated that the F11 FLS cluster enriched in FAP+THY1+ cells is dominant in RA, whilst in contrast, PsA exhibit a marked dominance of F1 FLS which demonstrate a FAP-THY1- phenotype. Ligand-receptor interaction analysis along with functional analysis demonstrated the synergistic, additive, and inhibitory effects of macrophage-derived IL-1β and T cell-derived TGF-β in driving the pathogenic and destructive phenotype of the RA associated F11 FLS cluster. Initial bulk RNA-seq demonstrated significant increases in the expression of key mediators involved in the IL-1β and TGF-β signalling pathways, with a stepwise increase observed from healthy to early RA to established RA highlighting their central role in disease progression. Furthermore, in response to IL-1β and TGF-β treatment, various synergistic/additive effects on the induction of highly inflammatory mediators, growth factors, adhesion markers, and ECM degrading MMPs, were shown, all of which were paralleled with significant dysregulation in mitochondrial homeostasis in favour of fission, a heightened ER stress response, and a metabolic switch in the RA FLS towards a more glycolytic profile. Interestingly, compared to IL-1β alone, the combination of IL-1β and TGF-β displayed some suppressive effects on proinflammatory mediators including CXCR3, CXCR4, and VCAM-1, highlighting the pleotropic nature of TGF-β. Finally, it was demonstrated that targeted inhibition of TAK1, a downstream mediator of both IL-1β and TGF-β signalling, using Takinib, resulted in suppression of several synergy-induced effects. Cumulatively, the data implies that blocking specific immune cell-derived cytokine interactions involved in enhancing the pathogenic nature of RA FLS may facilitate the development of more effective therapeutic interventions in RA.

The direct interaction between cells and its central role in exacerbating IA pathology is a growing field of interest as the synovium is now known to be a highly complex microenvironment (Floudas *et al.*, 2022b; Kondo, Kuroda and Kobayashi, 2021; Zhang *et al.*, 2023a). Indeed, the contribution of immune-stromal cell communication in driving aspects of disease is becoming increasingly recognised, with several published studies highlighting bidirectional interactions

between stromal FLS and infiltrating T cell and macrophage populations within the synovium. Whilst direct cell-to-cell contact has been shown to be required to influence the FLS activity in some studies, research has also highlighted the ability of soluble mediators released by Th cells within the joint to drive a more glycolytic and proinflammatory FLS phenotype, with similar effects also observed in response to synovial macrophage-derived mediators (Petrasca *et al.*, 2020; Alivernini *et al.*, 2020; Kvacskay *et al.*, 2021; Hanlon *et al.*, 2024). Thus, in support of these findings, a role for macrophage-derived IL-1β and T cell-derived TGF-β on RA FLS pathogenic responses was demonstrated. Whilst the central role IL-1β assumes in RA pathogenesis has been extensively investigated, a definitive understanding of the role TGF-β undertakes in RA pathogenesis is less defined as a consequence of its highly pleotropic nature (Bira *et al.*, 2005; Pohlers *et al.*, 2007; Sanjabi *et al.*, 2009; Kondo, Kuroda and Kobayashi, 2021). Moreover, although both cytokines are highly abundant within the RA joint, no research to date has elucidated the potential relationship between these two cytokines on RA FLS responses.

As mentioned in the introduction, Section 1.12, the bioenergetic profile of a cell is a catalyst for dictating its functional behaviour in homeostatic and pathogenic states. Interestingly, in this study, a striking synergistic shift in the metabolic capacity of the IL-1β and TGF-β stimulated RA FLS towards a highly glycolytic phenotype was identified. This was demonstrated in the significant synergistic increase in multiple glycolytic parameters including basal glycolysis, basal proton efflux rate, compensatory glycolysis, and the ECAR:OCR ratio. In parallel, the significant synergistic and additive induction of key glycolytic enzymes and transporters including GLUT-1, LDHA, HIF-1α, PKM2, and PFKFB3 were also observed. This prominent metabolic shift in the FLS within the inflamed RA joint is in line with previous studies indicating that the profoundly hypoxic microenvironment of the joint combined with dynamic fluxes in nutrient availability and metabolite accumulation, drives the metabolic adaptation of the FLS to facilitate their pathogenic effector functions (Biniecka *et al.*, 2016; Bustamante *et al.*, 2017; Fearon *et al.*, 2019; Fearon *et al.*, 2022). In agreement with the results in this thesis, an abundance of evidence suggests that glucose metabolism is particularly elevated in RA FLS with multiple studies showing that inhibition of glycolytic genes including PFKFB3, could effectively reduce the invasive, proliferative, and inflammatory capacity of the FLS (Garcia-Carbonell *et al.*, 2016; Biniecka *et al.*, 2016; Bustamante *et al.*, 2017; Petrasca *et al.*, 2020). Furthermore, although this was the first study examining the synergistic effects of IL-1β/TGF-β on RA FLS, previous work has identified a central role for IL-1β in the induction of glycolysis in OA FLS stimulated with T cell CM (Kvacskay *et al.*, 2021). In contrast, the influence of TGF-β on cellular metabolic output is highly contextual and cell dependent. Whilst traditionally associated with oxidative phosphorylation, it has been shown to induce glycolysis in

macrophages in mouse models of sepsis, increase HK2 levels slightly in articular chondrocytes, and elevate PKM2 in colon cancer cells highlighting its pleotropic capacity in the context of metabolism (Liu and Chen, 2022; Gauthier *et al.*, 2023).

Previous studies have reinforced the integral role of mitochondria and hypoxia-induced mitochondrial dysregulation in the production of this aforementioned energy, with the blockade of their normal function in FLS resulting in an aggravated inflammatory response (Biniecka *et al.*, 2011; Valcárcel-Ares *et al.*, 2014; Biniecka *et al.*, 2016; Vaamonde-García *et al.*, 2017). In response to alterations in the extracellular environment and availability of nutrients, the processes of mitochondrial fission/fusion are dynamically regulated, a balance which has important effects on both physiological and pathological processes in the body (Dai and Jiang, 2019). These processes are governed by the GTPases MFN1, MFN2, OPA1, and DRP1, with DRP1 translocating to the nucleus when activated and mediating mitochondrial fission which is known to be favoured in many inflammatory diseases (Dai and Jiang, 2019). In this study, a significant synergistic increase in DRP1 in parallel with reduced mitochondrial staining intensity and aspect ratio was demonstrated, alongside a gradual increase in mitochondrial mass following treatment with IL-1β/TGF-β. An eloquent study previously identified fission proteins increased in RA FLS compared to OA, inhibition of which resulted in mitochondrial elongation, decreased production of ROS, IL-8, and COX2, and increased apoptosis, suggesting that heightened fission may be associated with RA FLS pathogenic responses (Wang *et al.*, 2020a). Moreover, in support of these findings, several cancer studies have demonstrated that fusion supports oxidative phosphorylation, whilst conversely, high levels of DRP1 are associated with heightened cancer cell glycolysis in lung, breast, and thyroid cancer (Chen and Chan, 2017; Dai and Jiang, 2019; Yao *et al.*, 2019). Similarly, DRP1 knockdown resulted in increased OCR and ATP production in Ras-transformed mouse embryonic fibroblasts (Serasinghe *et al.*, 2015). Furthermore, a mechanism by which overexpression of the fusion protein MFN2 correlated with decreased mitochondrial mass in pancreatic cancer cells has been demonstrated, an observation which supports the findings in this thesis, implying the heightened fission following IL-1β/TGF-β stimulation results in increasing mass through fragmentation potentially (Yu *et al.*, 2019). In line with this, a reduction in mitochondrial biogenesis related genes including PGC-1α and NRF1 were demonstrated. PGC-1α has been shown to enhance oxidative phosphorylation and mitochondrial biogenesis in tandem in breast cancer cells whilst in naïve Treg cell differentiation, it serves a role in promoting fusion driven changes in metabolism from glycolysis to fatty acid oxidation (LeBleu *et al.*, 2014; Fang *et al.*, 2023). Whilst this research is the first to analyse the specific role of IL-1β/TGF-β in coordinating this fission phenomenon, previous studies have demonstrated the ability of individual proinflammatory

signals within the extracellular milieu, including lipopolysaccharide (LPS) and TNF, to heighten levels of fission in various cell types, with IL-1β specifically identified as a key regulator of mitochondrial dynamics in OA chondrocytes (López-Armada *et al.*, 2006). In relation to TGF-β, different isoforms have been implicated, with TGF-β1 promoting fission through DRP1 phosphorylation and TGF-β3 inducing fission in OA chondrocytes, an effect similar to the results in RA FLS (Du *et al.*, 2024).

Furthermore, a trending increase in ER size in response to IL-1β/TGF-β stimulation was identified, suggesting heightened ER stress is occurring in the RA FLS, which may be linked to the observed mitochondrial dysfunction. Previous studies have demonstrated an association between the mitochondria and ER, with mitochondrial dysregulation identified as a trigger of ER stress (Li *et al.*, 2015; Wu *et al.*, 2021a; Miglioranza Scavuzzi and Holoshitz, 2022). Indeed, it has been shown that suppression of DRP-1 mediated mitochondrial fission alleviates ER expansion, a finding that was indicative of reduced ER stress (Li *et al.*, 2015). Similarly, the direct effect of mitochondrial dysfunction on the expansion of the ER has also been highlighted, with elongated ER structures observed in RA CD4+ T cells with defective mitochondria, an effect mediated by the molecular chaperone BIP (Li *et al.*, 2015; Wu *et al.*, 2021a). BIP serves a central role in the resolution of ER stress through its activation of the various branches of the unfolded protein response (UPR), an adaptive response essential for the integrity of cellular homeostasis through the removal of misfolded proteins (Wang *et al.*, 2009; Miglioranza Scavuzzi and Holoshitz, 2022). In this work, a significant synergistic increase in the level of BIP was demonstrated, which was accompanied by a specific BIP-mediated activation of the pro-survival arm of the UPR, with synergistic/additive increases in XBP1 and AFT6 observed. Whilst there are limited studies concerning AFT6 in the context of RA, in agreement with our findings, it has been shown to be induced in the RA synovium by IL-1β where it governs the upregulation of cytoprotective genes including XBP1 that facilitate cell survival (Miglioranza Scavuzzi and Holoshitz, 2022). Additionally, synergistic increase in PDI with IL-1β/TGF-β, an important ER chaperone protein that is associated with ER stress and implicated in both cancer and inflammatory diseases, was highlighted (Yu *et al.*, 2020; Ma *et al.*, 2021). Taken together, these results imply that IL-1β and TGF-β are initiating a chain of events within the RA FLS starting with the disruption of mitochondrial dynamics in favour of fission which inadvertently results in the induction of ER stress. However, the combination of IL-1β and TGF-β is central to the resolution of this ER stress also, with their synergistic effects instigating a rapid stress response that circumvents the pro-apoptotic pathways and enables the survival of the pathogenic FLS, an effect which ultimately ensures they can continue to drive RA progression.

Next, the impact of the observed metabolic alterations on the pathogenic function of RA FLS was investigated to a greater extent. It was demonstrated that that IL-1β/TGF-β synergistically induce the expression of some of the key cytokine mediators of inflammatory processes within the joint – both IL-6 and IL-8 (Gottenberg *et al.*, 2012; Pandolfi *et al.*, 2020; Gremese *et al.*, 2023). Indeed, the concept of cytokine synergy in driving these two particular mediators is not completely new in FLS, with previous findings demonstrating a synergistic increase in IL-6 production from RA FLS in response to various dual combinations of the following cytokines: OSM, TNF-α, IL-17, and importantly IL-1 family members (Richards and Agro, 1994; Hanlon *et al.*, 2019; Slowikowski *et al.*, 2020). Conversely, in disagreement with the findings in this thesis, previous work has shown that IL-8 decreased under dual OSM and TNF treatment which may in part be attributed to the different cytokines involved thus, reinforcing the specificity of which cytokines are acting together (Hanlon *et al.*, 2019). Interestingly, however, an eloquent study specifically on RA FLS did previously identify a potentiating effect of the combined addition of TGF-β and PDGF-β on IL-1β induced IL-6 and IL-8 expression (Rosengren, Corr and Boyle, 2010).

Furthermore, FLS are potent producers of key angiogenic mediators, with VEGF classified as the primary 'on switch' for the characteristic phenomenon of neo angiogenesis within the inflamed joint (Honorati *et al.*, 2006; Cho *et al.*, 2007; Fromm *et al.*, 2019; Balogh *et al.*, 2019; Firestein *et al.*, 2020). Interestingly, an additive effect of IL-1β/TGF-β on RA FLS VEGF protein release was observed. Their individual roles are consistent with previous studies implicating TGF-β as a central growth factor that facilitates angiogenesis, with Fearon *et al.* (2003) identifying a direct relationship between the levels of TGF-β, angiopoietins, and VEGF at an early stage of disease, levels of which are associated with vascular morphology whilst additionally, IL-1β has been shown to induce VEGF in RA FLS (Fearon *et al.*, 2003; Cho *et al.*, 2007). These new blood vessels are critical in the perpetuation of synovial inflammation as they subsequently enable the entry of peripheral immune cells that are recruited through the combined activity of chemokines and their cognate receptors (Veale and Fearon, 2015; Tas *et al.*, 2016). A synergistic increase in the expression of specific chemokines known to be important in RA; MCP-1, Eotaxin, IP-10, MDC, and CXCL5, following treatment with IL-1β/TGF-β were shown in this study. These findings corroborate previous studies in which combinations of cytokines induced synergistic increases in some of these particular chemokines including MCP-1 expression from HUVEC and RA FLS, Eotaxin from airway FLS in response to TGF-β and IL-13, and CXCL5 expression in chondrocytes in response to IL-1 and OSM (Wenzel *et al.*, 2002; Barksby *et al.*, 2006; Hanlon *et al.*, 2019). In this regard, MCP-1 and CXCL5 have been shown to not only correlate with disease activity in RA, but additionally have been implicated in the onset and progression of cartilage degeneration in OA and in the

recruitment of neutrophils to the joint (Smith *et al.*, 2008; Harris *et al.*, 2013; Tong *et al.*, 2021; Murayama *et al.*, 2023).

Whilst increased levels of Eotaxin, IP-10/CXCL10, and MDC/CCL22 have been observed in RA serum and SF compared to HC, they all demonstrate affinity for attracting different immune cell types including eosinophils, FLS, chondrocytes, monocytes, T cells, DC, osteoclast, and OC progenitors, with studies showing IP10/CXC10 knockout successfully reduced macrophage and effector T cell recruitment to the joint (Yoshie and Matsushima, 2015; Pandya *et al.*, 2017; Lee *et al.*, 2017; Wakabayashi *et al.*, 2021; Murayama *et al.*, 2023). Interestingly, whilst increases were observed, a synergistic effect on several additional chemokines including MCP-4, MIP-1α, MIP-1β, and TARC, failed to be detected. This reinforces previous data in which a synergistic effect on EC production of neutrophil recruiting chemokines (CXCL1, CXCL2, CXCL5) but not T cell recruiting chemokines (Rantes, CCL9, CXCL10) was detected following addition of TNF-α and IL-17 (Griffin *et al.*, 2012). Furthermore, analysis of the chemokine receptors themselves demonstrated that IL-1β induced a significant increase in CXCR4 and CXCR3 which agrees with previous studies in different cell types (Sun *et al.*, 2015; Guo *et al.*, 2018). Although literature regarding the effects of TGF-β on these receptors is limited, this research showed that addition of TGF-β exhibited a rescue effect on the pathogenic nature of IL-1β, resulting in a decrease in both of these chemokine receptors, an observation which reinforces the beneficial effect of TGF-β in certain contexts. Cumulatively, this evidence suggests that the synergistic effect of IL-1β and TGF-β is highly specific and responsible for attracting a diverse range of immune cells to the joint, further perpetuating the proinflammatory response.

Once attracted to the joint, adhesion and subsequent entry of the immune cells is critical in the RA synovium. In this context, a significant increase in the expression of ICAM-1 and VCAM-1 following treatment with IL-1β alone was demonstrated, which is consistent with previous studies in different cell types and disease states (Spoelstra *et al.*, 1999; Yang *et al.*, 2010; Shen *et al.*, 2021). Interestingly, however, the addition of TGF-β resulted in opposing effects on the two adhesion molecules, with a synergistic increase in ICAM-1 but conversely, a decrease in VCAM-1 expression. Whilst both are critical adhesive mediators, their behaviour and expression patterns are not directly linked as highlighted by studies in the chronically inflamed RA synovial joints identifying differential prevalence of their expression, with VCAM-1 restricted to certain synovial vessels in comparison to the ubiquitously expressed ICAM-1 (Salmi, Rajala and Jalkanen, 1997). Moreover, their differential regulation in response to their environment and cytokine stimulation has been recognised previously with findings demonstrating ICAM-1 upregulation and VCAM-1 downregulation in response to shear stress, whilst an elegant study conducted by Hanlon *et al*.

(2019) illustrated comparable results in HUVEC following OSM treatment (Chiu *et al.*, 2004; Hanlon *et al.*, 2019). Similar to the observations with the chemokine receptors in this chapter, the role of TGF-β in inducing this rescue effect specifically in relation to VCAM-1 may in part be attributed to its pleotropic nature. Indeed, studies have shown that TGF-β alone can inhibit EC adhesion of neutrophils (Torres *et al.*, 2022). Moreover, albeit a different cell type, analysis previously highlighted that concomitant LPS and TGF-β addition resulted in a significant induction of ICAM-1 but reduction in VCAM-1 on ECs ultimately reinforcing the hypothesis that in the context of VCAM-1, TGF-β may exhibit a protective effect when combined with a proinflammatory stimuli (Kang, Brummel and Lee, 1996).

Irreversible degradation of the cartilage and bone is a key feature of RA pathogenesis, driven by the activity of members of the ECM degradative MMP family and bone catabolic factors (Fearon *et al.*, 1999; Tunyogi-Csapo *et al.*, 2008; Elshabrawy *et al.*, 2015; Ospelt, 2017; Nygaard and Firestein, 2020). In this study, whilst there was a lack of synergistic or additive effects on MMP-1 production, MMP-3 expression exhibited a significant synergistic increase following treatment with both cytokines. MMP-1 and MMP-3 have been extensively studied in the context of RA with research illustrating that the heightened invasive capacity of RA FLS is directly correlated to their MMP-1 and MMP-3 expression levels, a characteristic feature of the designated lining layer FLS (Tolboom *et al.*, 2002; Croft *et al.*, 2019). Indeed, the evidence indicates that MMP-3 specifically is important in cartilage degradation with a strong association between the serum levels and both disease activity and the concurrent radiographic progression seen in RA (Moran *et al.*, 2009; Elshabrawy *et al.*, 2015). Although a similar synergistic increase in MMP-1 failed to be observed, the findings do support previous work in which the synergistic combination of TNF, PDGF-β, and TGF-β culminated in heightened MMP-3 levels and thus, enhanced synovial lining layer hyperplasia (Shibuya *et al.*, 2015). Additionally, consistent with this data, in a cancer-related study, a decrease in MMP-1 transcription following exposure to TGF-β was observed (Krstic and Santibanez, 2014). Revolutionary studies examining the epigenetic regulation of MMPs identified that silencing of specific histone deacetylases had opposite effects on MMP-1 and MMP-3 subsequent expression, with histone deacetylase inhibitors enhancing IL-1β induced MMP-3 and repressing IL-1β induced MMP-1 (Pender *et al.*, 2000; Moores *et al.*, 2017). In addition, Cha *et al.* (2003) demonstrated that that both MMP-1 and MMP-3 expression levels were heightened under the characteristic hypoxic conditions of the joint. However, HIF-1α knockdown suppressed MMP-3 exclusively, with no effect observed for MMP-1 corroborating the notion they are controlled differently downstream and thus in relation to the research in this thesis, the combined effect of both IL-1β and TGF-β may be affecting their downstream transcription/expression differently (Cha *et al.*, 2003; Ahn *et al.*, 2008).

In regard to aspects of bone degradation, in support of previous findings in human chondrocytes, the findings indicate that IL-1β resulted in a significant upregulation of OPG from the RA FLS (Watanabe *et al.*, 2009). However, whilst TGF-β alone was comparable to baseline levels, the addition of TGF-β alongside IL-1β induced a 'rescue' effect, resulting in decreased OPG production. Furthermore BMP2, a member of the TGF-β family known primarily for its bone inductive properties and has been shown to be induced in the intimal FLS layer by IL-1β *in vitro*, demonstrated a significant synergistic increase in expression following IL-1β/TGF-β stimulation compared to either cytokine alone (Lories *et al.*, 2003; Whitty *et al.*, 2022). Interestingly, as a TGF family member, BMPs also demonstrate considerable pleotropic capabilities and have been shown to also govern multiple additional biological processes including growth, differentiation, proliferation, and apoptosis thus, making it challenging to definitively determine if this synergy induced increase in BMP2 is exerting an effect on bone remodelling in this scenario (Lories *et al.*, 2003). When all bone related markers are considered cumulatively, these results suggest whilst IL-1β alone has a role in bone resorption/homeostatic capacity of RA FLS, the dual treatment with IL-1β and TGF-β does not assume a major role in driving this specific aspect of RA pathogenesis.

Finally, a mechanistic manner by which the synergistic/additive effects of IL-1β and TGF-β could be mitigated was demonstrated, through direct inhibition of the downstream member of the MAPKKK family, TAK1, using the inhibitor Takinib. Takinib exerts its effects through its inhibition of TAK1, an enzyme that is an ideal candidate target due to its placement at the nexus between the NF-κB and MAPK pathways and has previously been shown to play a major role in the mediation of both IL-1β and indeed, TGF-β responses in inflammatory disease (Yamaguchi *et al.*, 1995; Shirakabe *et al.*, 1997; Takaesu *et al.*, 2001; Xu and Lei, 2020). Preliminary studies using Takinib demonstrated a marked reduction in several aspects of disease parameters in a CIA mouse model including cartilage damage, pannus formation, periosteal bone formation, bone resorption, and overall inflammatory markers, whilst in human RA FLS, Takinib exhibited a suppressive effect on proinflammatory JAK/STAT signalling (Scarneo *et al.*, 2019; Panipinto *et al.*, 2021). In agreement with these findings, the addition of IL-1β/TGF-β following TAK1 inhibition resulted in a suppressive effect on proinflammatory and invasive mediator expression including IL-6, IL-8, MCP-1, MMP-1, MMP-3, and MMP-9, in addition to a range of chemokines including Eotaxin, Eotaxin-3, MDC, and IP-10, and the angiogenic factor Flt1, all of which were paralleled by significant decreases in glycolytic parameters of the FLS. Moreover, similar suppressive effects were observed on the spontaneous release of the proinflammatory and invasive mediators from the RA whole tissue synovial explants cultured with Takinib. This inflammation dampening effect could also be associated with the more compact biopsy size detected following TAK1 inhibition which reflects

the data observed by Presti *et al.* (2024) in which a glycogen synthase kinase-3β (GSK3β) inhibitor successfully resulted in compaction of the patient-derived organoid. They proposed this compaction was reflective of a restoration of the lining layer, a process indicative of a healthier, non-diseased tissue, suggesting Takinib may be inducing a similar regenerative effect. Collectively, the data highlights the importance of understanding the molecular mechanism by which the synergistic/additive effects are being induced as this may provide a promising therapeutic target for mitigating IL-1β and TGF-β pathogenic effects in RA FLS.

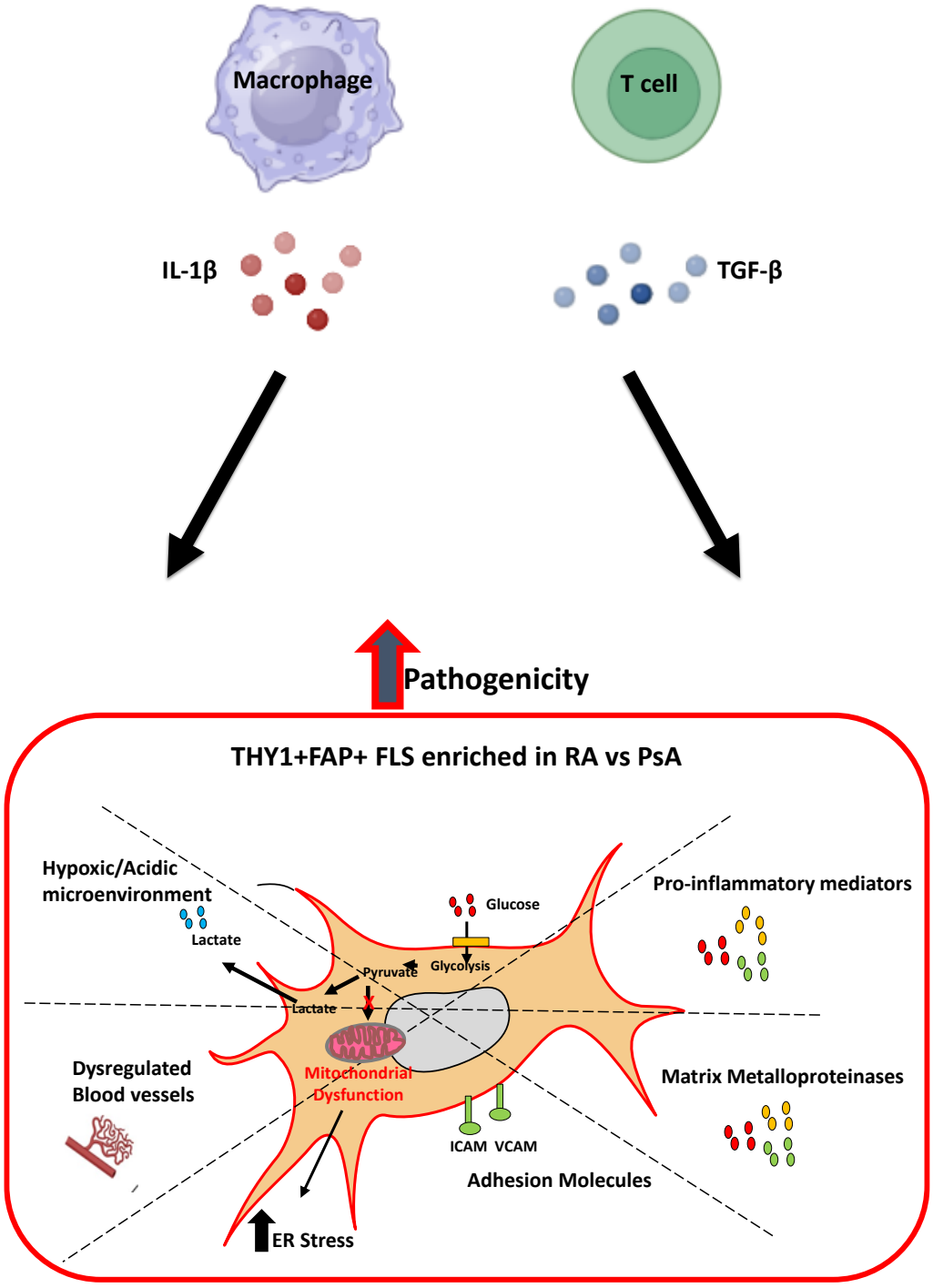

Figure 2.37. An overview of Chapter 2 focusing on the ability of IL-1β and TGF-β to drive the pathogenic, invasive nature of THY+FAP+ RA FLS. Synergy between macrophage-derived IL-1β and T cell-derived TGF-β promotes a metabolic switch in the RA FLS in favour of glycolysis which leads to mitochondrial dysfunction and heightened ER stress. This is paralleled by adoption of an aggressive phenotype with enhanced production of several pathogenic mediators including proinflammatory cytokines and chemokines, MMPs, and angiogenic factors. This figure was made using BioRender.

CHAPTER THREE:

Enrichment of Specific Fibroblast Populations with Distinct Functional Capacity Identified Between RA and PsA Synovial Tissue

3.1 Introduction

As previously outlined in the main introduction Section 1.7, FLS are a critical stromal cell type resident to the synovial joint, where they assume key roles in homeostatic joint maintenance related to both structural and functional aspects (Ospelt, 2017; Koliaraki *et al.*, 2020). However, an abundance of well-established research exists implicating FLS pathogenic transformation as a hallmark characteristic of inflammatory arthropathies, including both RA and PsA, where they are central instigators of the sequence of destructive events that unfold resulting in bone and cartilage destruction (Fassbender and Simmling-Annefeld, 1983; Bustamante *et al.*, 2017; Koliaraki *et al.*, 2020). Once activated in an inflammatory context, FLS are essential producers of a plethora of proinflammatory cytokines including IL-6, IL-1β, and TNF-α, leukocyte attracting chemokines, bone destructive factor RANKL, and matrix degrading enzymes including MMP-1 and MMP-3, which facilitate their invasive phenotype and formation of the distinguishing pannus structure (Pap *et al.*, 2000; Takayanagi *et al.*, 2000; Bottini and Firestein, 2013; Kondo, Kuroda and Kobayashi, 2021). This is further exacerbated by their capabilities to rapidly expand and proliferate, constructing stromal networks whilst simultaneously resisting apoptosis, all disease-related properties that enable them to fulfil their role as facilitators of chronic inflammation and widescale tissue damage (Hu *et al.*, 2012; Lee *et al.*, 2013b). Moreover, the existing literature indicates that this transformation to an 'imprinted aggressor' phenotype is paralleled by a defective metabolic state, with numerous studies highlighting a preferential shift towards glycolysis under the hypoxic joint conditions, an effect that can be successfully blocked through inhibition of key glycolytic enzymes including PFKFB3 and PKM2 (Bottini and Firestein, 2013; Biniecka *et al.*, 2016; Bustamante *et al.*, 2017; Frank-Bertoncelj *et al.*, 2017; Fearon *et al.*, 2022; Elhai *et al.*, 2023).

Contrary to previous views that considered FLS to be predominantly homogenous in phenotype and function, immense emphasis has been placed in recent years on stratifying distinct populations of FLS perpetuating the damage within the synovial joint. The use of scRNA-seq transcriptomic analysis has revolutionised this field, facilitating the identification of populations defined by distinct signature markers and gene expression, with Buechler *et al*. (2021) suggesting a paradigm in which universal Dpt+ FLS give rise to highly specialised homeostatic and inflammatory FLS populations observed across tissues. Moreover, whilst the immense intra- and inter-organ diversity in FLS populations connected to their ECM production and preservation has been highlighted, in relation to joints specifically, the literature indicates that FLS phenotype demonstrates joint specific patterns, with distinct gene expression profiles and methylation status dependent on the joint of origin (Ai *et al.*, 2016; Muhl *et al.*, 2020; Choi *et al.*, 2024). Indeed,

epigenetics cannot be underestimated in this regard with the methylation status also important in dictating RA FLS function due to its governance over gene expression, a notion supported by the work of Ai *et al.* (2016) which utilised bulk RNA-seq to investigate differences in RA vs OA FLS. This study discovered distinct FLS gene methylation signatures could clearly demarcate between both disease states, with the methylation status of genes involved specifically in the IL-6/JAK/STAT resulting in greater expression of inflammatory IL-6 in RA compared to the OA counterpart. However, defining FLS based on the expression of surface markers has taken precedence, with this area of study initiating in 2018 with the discovery of two transcriptomically different FLS populations that were clearly demarcated by their location within the layers of the synovium. The lining layer possessed CD55+ FLS with high hyaluronan synthase 1 (HAS1) expression whilst conversely, within the sub-lining layer, a THY1+ cluster was identified with high expression of genes directly implicated in ECM degradation and remodelling, thus for the first time suggesting the location of FLS within the joint i.e. lining versus sub-lining may have a major impact on their transcriptional profile and function in joint destruction (Stephenson *et al.*, 2018). Building on these findings, cell sorting and microarray analysis were employed to identify three different PDPN+ FLS populations, a marker previously shown to be associated with a highly aggressive FLS phenotype (Croft *et al.*, 2016; Mizoguchi *et al.*, 2018). Firstly, the THY1-CD34- lining layer FLS exhibited high expression of matrix degrading MMPs, specifically MMP-1 and MMP-3, in addition to RANKL, with these FLS demonstrating the capacity to drive the differentiation of osteoclasts *in vitro.* Moreover, the remaining two CD34+ populations could be subdivided based on the presence/absence of THY1 co-expression: THY1-CD34+ FLS located in superficial lining layer and the deep sub-lining, and finally a THY1+CD34+ population which were classified as perivascular FLS due to their close proximity to the underlying blood supply and which demonstrated an inflammatory role due to their correlation with leukocyte infiltration and expression of several inflammatory genes including IL-6, CXCL12, and CCL2. Interestingly, this work also successfully demonstrated that the nature of the specific arthropathy in question may be related to the dominant FLS cluster with a significant expansion of the THY1+ FLS identified in RA patients compared to OA and higher expression of the THY1- clusters in OA compared to their RA counterparts, a discovery that could account for the differential pathogenesis observed between the disease states. This significant observation introduced the currently unexplored hypothesis – is there a difference in the dominance of FLS populations in RA vs PsA that may aid understanding of their differential disease development and/or progression?

To date, there is an abundance of literature supporting this connection between the phenotype of FLS and their functional role in disease propagation in relation to RA. Using FAP as

a marker of tissue inflammation in all FLS subtypes, Croft *et al.* (2019) eloquently demonstrated the validity of their transcriptomic analysis through the adoptive transfer of THY1+ and THY1- FLS into the joints of mice with CIA. These *in vitro* studies successfully demonstrated the ability of the THY1+ FLS to augment the production of a plethora of proinflammatory mediators including cytokine and immune infiltrating chemokine production, whilst conversely the THY1- FLS exhibited a high propensity to drive bone and cartilage destruction (Croft *et al.*, 2019). The central role of THY1+ sub-lining FLS in immune effector roles was further expanded on by Zhang *et al.* (2019) in which a similar integrated approach of functional mass cytometry and scRNA-seq analysis to define the sub-lining FLS clusters in RA specifically was utilised. Whilst observing the aforementioned CD55+PRG4+ lining layer cluster, they actually separated the sub-lining cells into three distinct populations. Interestingly the CD34+(THY1+) cluster associated with the perivascular blood vessels was again identified and in support of Mizoguchi *et al.* (2018) and Croft *et al.* (2019), this cluster demonstrated expression of the complement protein C3 thus highlighting its role in tissue priming and stromal memory (Mizoguchi *et al.*, 2018; Croft *et al.*, 2019; Zhang *et al.*, 2019b). Furthermore, it has recently been demonstrated that the application of continuous repetitive inflammatory stimuli to these CD34+C3+ FLS could drive the metabolic rewiring of these FLS towards an increasingly more inflammatory promoting phenotype, supporting the chronically inflamed joint microenvironment characteristic of RA patients (Friščić *et al.*, 2021). Interestingly, not all FLS associated with RA are responsible for exacerbating disease with recent work identifying a population of FLS in RA characterised by CD200+DKK3+ expression that are capable of exhibiting dynamic pro-resolving effects on synovial inflammation (Rauber *et al.*, 2024). However, as outlined above, the majority of available literature focuses on delineating FLS subpopulations and their driving role in RA pathogenesis, with a stark absence of studies examining the different roles that lining versus sub-lining FLS assume in PsA.

Whilst the central dogma of lining versus sub-lining and the resulting transcriptional profile is widely accepted, recent work has highlighted that this phenotype may be extremely dynamic. Anatomical self-organisation and ability to destruct cartilage when implanted has been previously shown to be an intrinsic property of RA FLS, reinforcing the concept that FLS are genetically and epigenetically imprinted with an 'aggressor' phenotype that renders them predisposed to pathogenic transformation (Bottini and Firestein, 2013; Croft *et al.*, 2016; Karouzakis *et al.*, 2018). Moreover, the impact of neighbouring cells and environmental cues are becoming increasingly more recognised in the literature in promoting the adoption and maintenance of differential phenotypes of FLS. Micheroli *et al.* (2022) advanced the current approaches by not only defining the FLS clusters by location but matching them to the particular

RA pathotypes observed i.e. fibroid, myeloid, and lymphoid, suggesting the importance of examining the impact of immune cells on the FLS phenotype and function. This concept of examining cell interactions on FLS phenotype was further explored through profiling of the entire spectrum of cell types that composes the inflamed synovium in patients with active RA, resulting in the stratification of tissues into six groups denoted as CTAPs (Zhang *et al.*, 2023a). Interestingly, the influences can not only be attributed to immune cells but additionally other stromal cells in the microenvironment. Wei *et al.* (2020) eloquently demonstrated the impact of ECs on driving FLS to adopt a THY1+ phenotype through NOTCH signalling, an effect lost once removed from the joint. Moreover, as outlined in Section 1.7.2, FLS behaviour can be affected by repeated culturing processes supporting the notion that environmental cues are essential for their phenotypic maintenance (Zimmermann *et al.*, 2001; Neumann *et al.*, 2010; Mizoguchi *et al.*, 2018). Indeed, the questions of whether RA and PsA FLS are capable of maintaining their distinct lining versus sub-lining transcriptomic profiles and to a similar extent once removed from the inflammatory surroundings are yet to be formally investigated.

Global scRNA-seq analysis was conducted previously in Chapter 1, analysis that included all cellular components of synovial single-cell suspensions thus enabling investigation of communication between different cell types within the joint. This global analysis identified eleven FLS clusters based on THY1 and FAP expression in RA vs PsA, however this analysis was performed in parallel with other cell types within the joint. Therefore to further investigate the FLS populations in the joint in more detail, in this chapter, re-analysis of the scRNA-seq focused on FLS exclusively was performed alongside advanced multiplex flow cytometric analysis. The resulting data demonstrated, for the first time, that distinct FLS populations with unique functional properties exist in RA and PsA. Moreover, the data suggested that once removed from the joint microenvironment, FLS subset stability appears transient with convergence towards common phenotypes.

3.2 Specific Aims of this Chapter

- Comprehensive transcriptomic RNA-seq analysis focused only on FLS subsets, to stratify synovial RA and PsA FLS into distinct FLS populations based on the expression of cluster markers.

- Identify and compare the frequencies of FLS subsets within the inflamed synovium of RA and PsA patients using a dual approach of scRNA-seq and flow multiparametric analysis.

- To establish the phenotypic and functional differences in the FLS populations that differ between RA and PsA using the combination of transcriptomics and multi parametric flow cytometry.

- To directly compare the metabolic, angiogenic, invasive, and inflammatory profile of RA and PsA FLS *ex vivo* at passage 0 (P0) under baseline conditions.

- To determine the effects of removal from the joint microenvironment and *ex vivo* expansion across consecutive passages on the intrinsic RA and PsA FLS characteristics and behaviour.

3.3 Materials & Methods

3.3.1 Patient Recruitment and Arthroscopy

RA and PsA patients, all of which fulfilled the criteria defined by the ACR and CASPAR respectively, were previously recruited from the outpatient clinic at the Department of Rheumatology, St Vincent's University Hospital and Tallaght University Hospital, TCD (Aletaha *et al.*, 2010; Leung *et al.*, 2018). The RA and PsA patient demographics and synovial tissue were obtained at time of arthroscopy as previously described in Section 2.3.1. The extent of disease activity in the RA and PsA patients was defined by the Disease Activity Score in 28 joints (DAS28 score), a clinical tool that encompasses assessment of SJC, TJC, CRP, and the VAS score, enabling direct comparisons to be performed across both disease states.

3.3.2 Synovial Tissue Sample Processing

Synovial tissue biopsies obtained at the time of arthroscopy were preserved in 10% DMSO (Fisher Scientific) and enzymatically digested using the GentleMacs dissociator and a soft tumour dissociation kit (Miltenyi Biotech, Germany), according to manufacturer's instructions. Following DMSO removal through consecutive PBS washes, the biopsies were immediately transferred to a 96-well plate. The plate was incubated for 45 min at 37°C in humidified air with 5% CO_2 in 100 µl of an enzyme mix containing 600 µl pre-warmed RPMI-1640, 200 µl enzyme H, 100 µl enzyme R, and 25 µl enzyme A. This single synovial cell suspension was then filtrated through a 70 µm cell strainer to remove undigested clumps and yield a single-cell suspension of synovial tissue cells which were then utilised for further experiments outlined below. This method of digestion was previously optimised by the lab, demonstrating high cellular yield, viability, and intact marker expression (Floudas *et al.*, 2022a).

3.3.3 CytekAurora Multiparametric Flow Analysis

In order to determine differences in functional and metabolic phenotypes of FLS from RA and PsA synovial biopsies, flow cytometric analysis of 21+ markers outlined in *Table 3.1* below, was conducted on the CytekAurora. A detailed list of the patient demographics relating to the biopsies included in the flow cytometric analysis are included in the Appendix, *Table 6.3*. Whole biopsies preserved in 10% DMSO (Fisher Scientific) were thawed in a 37°C water bath and excess DMSO was removed by washing the biopsies in sterile PBS. The biopsies were then digested as outlined in Section 3.3.2 prior to staining. To remove dead cells, the samples were resuspended in

LIVE/DEAD fixable NIR (Molecular Probes, Thermofisher Scientific) viability dye for 30 min at 4°C in the dark. To block the non-specific binding of the monoclonal antibodies to the Fcγ-receptor, samples were then blocked for 10 min with human FcγR-binding inhibitor (TruStain FcX Receptor blocking solution (BioLegend)) diluted 1:10 in FACS buffer .(Dulbecco's PBS without Mg2+ or Ca2+ (Sigma Aldrich, USA), 2% heat-inactivated FBS (Biosciences), 0.05% sodium azide (Sigma-Aldrich, USA), and 0.5M EDTA pH 8.0 (Ambion)) prior to the addition of the extracellular antibodies. Samples were then incubated for 30 min at 4°C with the appropriate fluorochrome-conjugated extracellular antibodies and Brilliant Stain Buffer mixture (30 µl Brilliant Stain Buffer + 2 µl/ab per sample). Following staining with the extracellular antibodies and prior to intracellular staining, the FOXP3 staining buffer set (eBiosciences) was used to fix and permeabilise the FLS to enable access of the intracellular antibodies as per the manufacturer's instructions. The samples were then incubated for 30 min at 4°C with the appropriate fluorochrome-conjugated intracellular antibodies and Perm Buffer mixture. Following this, consecutive washes with 100 µl PERM buffer and FACS buffer and 1400 rpm centrifugation following each wash was performed, before the cells were resuspended in 200 µl FACS buffer and transferred directly to labelled flow tubes. Samples were stored at 4°C in the dark until sample acquisition on the CytekAurora with instrument set up and Quality Control performed per the manufacturer recommendations prior to acquisition. Single stained controls were acquired first to adjust for the spectral overlap between adjacent fluorochromes, and multicolour samples were run using the live unmixing functionality. Following acquisition, analysis was carried out using Spectro Flo and FlowJo (v10) software (FlowJo LCC, Oregon, USA). For gating purposes, FMO controls were used to determine gate boundaries between markers. Cell debris and doublets were removed from the analysis and phenotyping of FLS subsets in addition to analysis of the extracellular/intracellular marker expression on the FLS was determined as outlined by the gating strategy shown in Figure 3.1. The markers utilised allowed the (a) exclusion of other cell types and (b) identification of FLS subsets and functional analysis:

- Exclusion of haematopoietic cells (CD45+), ECs (CD31+), pericytes (CD146+), and inclusion of FLS (PDPN+).
- FLS subtype phenotyping based on markers previously utilised and published in the literature (Described in Section 3.1) - THY1, CD34, CD55, and FAP.
- FLS immune and adhesive markers including HLA-DR, Cadherin-11 (Cad11), ICAM-1, VCAM-1, CD44, PDGFR-α, and the proliferation marker, Ki67.
- FLS metabolic markers such as YAP, pAKT, pmTOR, and pS6.

In order to analyse the co-expression of markers on the PDPN+ FLS, the supervised algorithm Simplified Presentation of Incredibly Complex Evaluations or SPICE (Version 5.1) was used. SPICE is a data-mining software that allows large data sets from polychromatic flow cytometry to be analysed and organises the normalised data graphically. Before importation into the SPICE programme, a Boolean gating strategy was applied to all the markers on the data. The pie charts generated represent frequency of co-expression of costimulatory markers, whereby single costimulatory marker positive cells are represented by individual arcs surrounding the pie charts, while double, triple, and quadruple costimulatory marker positive cells were represented by overlapping arcs.

Marker	Fluorochrome	Clone	Manufacturer
HLA-DR	BV421	L243	BioLegend
VCAM-1	BV480	51-10C9	BD
CD34	BV510	581	BioLegend
CD31	BV605	WM59	BioLegend
***Ki67**	BV650	11F6	BioLegend
CD146	BV711	P1H12	BD
THY1 (CD90)	BV750	5E10	BD
CD44	BV785	IM7	BioLegend
CD45	AF532	HI30	Thermo
***pS6 (Ser235, Ser236)**	PerCP/Cy5.5	Mouse IgG1, κ	BioLegend
ICAM-1	PerCP-eFluor 710	HA58	Thermo
CD61 (Integrin β3)	PerCP	VI-PL2	BioLegend
***YAP**	PE	D8H1X	Cell Signaling
***pAKT**	PE CF 594	M89-61	BD
PDGFR-α (CD140a)	PE/Cy5	APA5	BioLegend
Cad11	PE/Cy7	16G5	BioLegend
CD55	APC	JS11	BioLegend
***pmTOR**	AF647	O21-404	BD
PDPN	APC-Fire 750	NC-08	BioLegend
L/D	Zombie NIR		BioLegend
FAPα	AF700	427819	Novus

Table 3.1. Multiparametric antibody panel to phenotype FLS in RA vs PsA on the CytekAurora. *Indicates intracellular antibodies.

3.3.4 Cell Sort and Supernatant Collection

Fresh RA and PsA biopsies were digested on the day of arthroscopy in RPMI-1640 containing 1 mg/ml collagenase Type II (Worthington Biochemical, Freehold, NJ, USA) for 4 h (with gentle agitation every hr) at 37°C in humidified air with 5% CO_2. Once dissociated, the cells were spun down directly at 1400 rpm for 20 min, before being washed twice in sterile PBS and pelleted at 1400 rpm. Subsequently the cells were resuspended in pre-warmed RPMI-1640 and seeded into T75 culture flasks where they were incubated at 37°C in humidified air with 5% CO_2 overnight. The following day, the FLS were removed from the flasks using RT Accutase cell detachment solution (Sigma-Aldrich, Ireland) to preserve cell viability and cell surface marker expression, before being resuspended in 1% sterile-filtered bovine serum albumin (BSA) and counted using trypan blue (Sigma) and a cell counter under the microscope. Cells were then transferred to round a bottomed FACS tube where they were centrifuged for 3 min at 1400 rpm before being resuspended directly in FC block (TruStain FcX Receptor blocking solution (BioLegend)) for 10 min. 10 µl of this cell resuspension was removed to a separate flow tube to function as an unstained control. Following this, cells were incubated for 30 min at 4°C in the dark with the antibody mix consisting of the fluorochrome-conjugated extracellular antibodies outlined in *Table 3.2* below. The cells were then washed with 1% sterile-filtered BSA (Sigma-Aldrich, USA) and centrifuged at 1400 rpm for 3 min twice, before being resuspended in 300 µl 1% BSA. All the above steps were conducted under sterile conditions. The cells were kept on ice until the FLS subsets were sorted into sterile, 1% BSA coated 1.5 ml Eppendorf's based on the expression of the two extracellular markers THY1 and FAP using the BD FACSAria Fusion sorter (BD Biosciences). The following two populations were collected: THY1+FAP+ and THY1-FAP-. Populations sorted were based on the scRNA-seq enriched RA and PsA populations identified in the global analysis in Section 2.4.1. For gating purposes, FMO controls were also prepared and used to determine gate boundaries between markers. A summary of the individual yields of THY1+FAP+ and THY1-FAP- populations from each digested biopsy sample are shown in the Appendix, *Table 6.4*. Once sorted, the populations were centrifuged for 5 min at 0.3 g to pellet and the supernatant was removed under sterile conditions. The cells were then resuspended in pre-warmed RPMI-1640 to give a cell number of approx. 30,000 cells per 100 µl media was added to a 96-well cell culture plate and incubated at 37°C in humidified air with 5% CO_2. The cell supernatants were collected after 48 h and stored in the -20°C freezer for future use in the MSD assay analysis which was performed as outlined in Section 3.3.8 below.

The following extracellular antibodies were used to distinguish the FLS populations: CD45 BV650, CD146 BV711, CD31 BV605, PDPN AF488, FAP AF700, and THY1 BV421.

Marker	Fluorochrome	Clone	Manufacturer
CD146	BV711	P1H12	BD
CD45	BV650	H130	BioLegend
CD31	BV605	WM59	BioLegend
THY1	BV421	SE10	BioLegend
PDPN	AF488	NC-08	BioLegend
FAPα	AF700	427819	Novus

Table 3.2. Panel of fluorochrome antibodies used to sort FLS populations.

3.3.5 Synovial Histopathological Analysis

To perform haematoxylin and eosin (H&E) analysis of the tissue architecture, RA and PsA biopsies obtained as previously described in section 2.3.1, were embedded in OCT medium, sectioned, and stained with haematoxylin and eosin. Microscopic analysis was then performed to analyse the lining layer thickness (number of cell layers), vascularity of the sub-lining layer (scored 1-3), cellular infiltration of the sub-lining layer (scored 1-3), and the presence/absence of lymphoid aggregates.

3.3.6 scRNA-seq Data Analysis

3.3.6.1 Initial Processing

scRNA-seq data were processed using Cell Ranger (v3.02) and using the 10X human transcriptome GRCh38-3.0.0 as a reference. Further analysis was performed in R v.4.4.1. EmptyDrops was used to identify cell-containing droplets in each individual sample at a false discovery rate of 1% (Lun *et al.*, 2019). Droplets lacking a cell were removed from downstream analysis. Only genes identified in a minimum of 3 cells were included in downstream analysis in Seurat (v.5) (Stuart and Satija, 2019). Quality control measures were used to remove low quality and decaying cells. Apoptotic and decaying cells were removed using a mitochondrial gene cut-off of 25%. Doublet and multiplet cells were removed using the DoubletFinder package (McGinnis, Murrow and Gartner, 2019). In order to remove any batch effects associated with the scRNA-seq data, data was integrated using the *SelectIntegrationFeatures*, *PrepSCTIntegration*, *FindIntegrationAnchors,* and *IntegrateData* functions. The standard Seurat workflow was used to identify sixteen unique FLS clusters. UMAP

plots were used for dimensionality reduction and for visualisation of this scRNA-seq data. This bioinformatic analysis was performed by Dr. Conor Smith.

3.3.6.2 Cell Population Clustering

Cluster specific markers were identified using the *FindAllMarkers* function. Only genes with a $Log_2FC > 0.25$, a min.pct > 0.25 and an adj.p.value < 0.05 following Bonferroni correction were included as cluster markers. Differentially expressed genes were identified using Wilcoxon Rank Sum test and displayed using heatmaps and volcano plots. Pathways enriched from the differentially expressed genes were identified using pathfindR and pathway activity scores were calculated using the *AddModuleScore* function in Seurat (Ulgen, Ozisik and Sezerman, 2019). Nebulosa was used to display gene expression density on the UMAP (Alquicira-Hernandez and Powell, 2021). DecoupleR was used to identify transcription factor activity (Badia *et al.*, 2022). Clusters were defined and labelled by Órla Tynan and Aenea Brugman.

3.3.7 P0 VS P1 VS P2 Flow analysis

To examine if FLS lose their distinct phenotype with passaging, multiparametric analysis of specific FLS activation and functional markers on unstimulated RA and PsA FLS was performed using flow cytometry. FLS cell suspensions from individual RA and PsA donors, previously frozen down in 10% DMSO at consecutive passages (P0, P1, and P2) following digestion as per outlined in Section 2.3.4, were thawed in a 37°C water bath before centrifugation for 3 min at 1400 rpm. The cells were then resuspended in RPMI-1640 and transferred to a 96-well round-bottomed plate for extracellular staining. The extracellular staining procedure and data acquisition on the LSRFortessa Flow Cytometer (Beckman Coulter, UK) was performed and analysed using FlowJo (v10) software (FlowJo LCC, Oregon, USA) as previously described in section 2.3.14. Single stained compensation beads were used to adjust for the levels of spectral overlap between different fluorochromes and FMO staining was incorporated to determine the gating of specific surface marker expression. The gating strategy as per Figure 3.32 was applied. The full panel of extracellular antibodies utilised in this experiment are outlined in *Table 3.3* below.

Marker	Fluorochrome	Clone	Manufacturer
CD146	BV711	P1H12	BD
CD45	BV650	H130	BioLegend
CD31	BV605	WM59	BioLegend
CD34	BV510	581	BioLegend
THY1	BV421	SE10	BioLegend
CD54	PerCP/Cy5.5	HA58	BioLegend
PDPN	AF488	NC-08	BioLegend
HLA-DR	PE/Cy7	L243	BioLegend
CD55	APC	JS11	BioLegend
L/D	Zombie NIR		BioLegend
FAPa	AF700	427819	Novus

Table 3.3. Extracellular fluorochrome antibodies used for RA FLS flow cytometric staining of P0, P1, and P2, RA and PsA FLS.

3.3.8 Multiplex ELISA Analysis

MSD analysis was performed to assess differences in expression of specific angiogenic, chemokine, and migration factors in the sorted FLS subset supernatants collected as per outlined in Section 3.3.4 above and in P0 RA and PsA FLS *ex vivo* at baseline. Protein concentrations of the angiogenic proteins; PIGF, VEGF-A, VEGF-C, VEGF-D, Tie-2, bFGF, and Flt-1, chemokine proteins; MCP-1, MCP-4, IL-8, IP-10, TARC, MDC, Eotaxin, Eotaxin-3, MIP-1β, and MIP-1α, and the MMPs; MMP-1, MMP-3, and MMP-9 were quantified using the V-PLEX Angiogenesis Panel 1 (human) kit (Meso Scale Discovery, USA), the V-PLEX Chemokine Panel 1 (human) kit (Meso Scale Discovery, USA), and the Human MMP 3-Plex Ultra-Sensitive Kit (Meso Scale Discovery, USA) respectively, as per the manufacturer's recommendation's. Briefly, 50 µl of supernatants was added to precoated multiplex wells for 2 hr at RT under constant shaking. Simultaneously, an eight-point standard curve was added to the plate. The plate was subsequently washed three times using PBS/Tween, after which 25 µl of Detection antibody was added for 2 h at RT under constant shaking. Finally, after washing three times, 150 µl of the appropriate Read Buffer was added, and the

electrochemiluminescence of the plate was analysed immediately after addition using a Meso Sector S600 Imager. A complete list of the specific MSDs and the analytes measured are depicted in *Table 3.4* below.

Assay	Analytes Measured
V-PLEX Angiogenesis Panel 1 (human) kit	PIGF, VEGF-A, VEGF-C, VEGF-D, Tie-2, bFGF, Flt-1
V-PLEX Chemokine Panel 1 (human) kit	MCP-1, MCP-4, IL-8, IP-10, TARC, MDC, Eotaxin, Eotaxin-3, MIP-1β, MIP-1α
Human MMP 3-Plex Ultra-Sensitive Kit	MMP-1, MMP-3, MMP-9

Table 3.4. List of MSDs performed, and the analytes measured.

3.3.9 cDNA Synthesis and Gene Expression Analysis

To assess differences in expression of specific invasion and metabolic genes in RA and PsA FLS *ex vivo* at baseline P0, RT-PCR for specific genes was performed *(Table 3.5).* Adherent cells were detached following incubation with trypsin (Sigma-Aldrich, USA) at 37°C in humidified air with 5% CO_2 for 5 min. The detached cells were then pelleted at 1400 rpm and cell numbers were acquired and adjusted to yield a final concentration of 300,000 cells/1 mL. The cells were then lysed in Qiazol and stored at -80°C until RNA isolation. Total RNA was isolated using the miRNeasy Mini Kit (Qiagen, Germany) as per the manufacturer's recommendations. The integrity of RNA samples was assessed using a bioanalyzer (Agilent, CA, USA) to ensure high quality and subsequently stored at -80°C until needed. Samples with a 260:280 nm ratio of 1.8 and above were used in subsequent experiments. Total RNA (100 ng) was reverse transcribed to complementary cDNA using a high-capacity cDNA reverse transcription kit (Applied Biosystems, Cheshire, UK) containing a mixture of 10x RT Buffer, DNTPs, 10 Random Primers, RNase Inhibitor, Multiscribe Reverse Transcriptase Inhibitor, and RNase-free H_2O, and stored at -20°C until further use. Negative controls consisted of samples lacking multiscribe reverse transcriptase were also prepared alongside.

Using the Quant Studio 5 Thermal Cycler (Applied Biosystem, Lewes, UK), gene expression data were quantified by RT-PCR. Reaction mixtures contained 1 µl of cDNA, SYBR green II Universal PCR mastermix (Applied Biosystems), RNase-free water, and specifically designed target mRNA specific primer pairs of the following genes outlined in *Table 3.5* below (dependent on specific experiments): MMP-1, MMP-3, HIF-1α, HK2, PKM2, GLUT-1, and GADPH. Negative controls consisted of samples lacking multiscribe reverse transcriptase which enabled the testing of target

specific quantification and samples lacking RNA which enabled identification of primer-dimer formation. Using pre-optimised conditions, the Ct method was used to analyse the data with all thermal cycling conditions performed as recommended by the manufacturer (Applied Biosystems). Using a 96-well plate format, all samples were run in duplicate whilst negative controls were run in singlet alongside. For analysis, all acquired data was normalised to the expression of the housekeeper RPLP0 which acted as an endogenous control and was selected based on optimisation experiments. To represent the relative changes in gene expression of the data and graphically represent the results, the CT method and specifically the delta CT method was used.

Gene Name	Forward Primer	Reverse Primer
RPLP0	5' GCGTCCTCGTGGAAGTGACAT 3'	5' TCAGGGATTGCCACGCAGGG 3'
MMP-1	5' GCTAACAAATACTGGAGGTATGAT 3'	5' ATTTTGGGATAACCTGGATCCATA 3'
MMP-3	5' CGGTTCCGCCTGTCTCAAG 3'	5' CGCCAAAAGTGCCTGTCTT 3'
HIF-1α	5' GAAACTTCTGGATGCTGGTGATTT 3'	5' GCAATTCATCTGTGCTTTCTGTCA 3'
HK2	5' TTCTTGTCTCAGATTGAGAGTGAC 3'	5'TTGCAGGATGGCTCGGACTTG 3'
PKM2	5' ATTATTTGAGGAACTCCGCCG 3'	5' ATTCCGGGTCACAGCAATGAT 3'
GLUT-1	5' CTTCCAGTATGTGGAGCAACT 3'	5' GCACAGTGAAGATGATGAAGA 3'
GAPDH	5' GGGAAGCTTGTCATCAATGGA 3'	5' TCTCGCTCCTGGAAGATGGT 3'

Table 3.5. Primer sequences designed and used for RT-PCR analysis.

3.3.10 Cellular Bioenergetic Functional Analysis

The analysis of the oxidative and glycolytic metabolic profiles of the RA vs PsA FLS at P0 at baseline and following IL-1β stimulation was performed using the Seahorse-XFe96 analyser (Seahorse Biosciences, Agilent Technologies, USA). RA and PsA FLS were seeded at a density of 15,000 cells per well in a 96-well cell culture XFe microplate (Seahorse Biosciences) and allowed to adhere overnight at 37°C in humidified air with 5% CO_2. The calibrator plate was also incubated overnight at 37°C in a non-CO_2 incubator with XF Calibrant, pH 7.4 (Agilent Technologies, USA). On the day of the experiment, cells were then washed with assay medium (unbuffered DMEM (pH 7.4) supplemented with 10 mM glucose; Sigma UK, 1 mM Sodium Pyruvate; Gibco, and L-Glutamine 2 mM; Biosciences) before incubation with assay medium for 1 h at 37°C in a non-CO_2 incubator. Using the Mitochondrial Stress Test, basal oxidative phosphorylation/glycolysis of the RA and PsA

FLS at baseline was calculated by the average of three baseline OCR/ECAR measurements respectively, obtained before injection of specific metabolic inhibitors; oligomycin (ATP-synthase-inhibitor) (2 µg/ml; Seahorse Biosciences, UK), FCCP (mitochondrial uncoupler) (5 µM; Seahorse Biosciences), and Antimycin A (complex-III inhibitor) (2 µM; Seahorse Biosciences) and Rotenone (2 µM; Seahorse Biosciences). Additional calculations included: the ECAR:OCR ratio, the level of ATP synthesis which was calculated by subtracting the OCR following oligomycin addition from the baseline OCR, the spare respiratory capacity calculated by subtracting the baseline OCR from the maximal respiratory capacity OCR, and finally the maximum respiratory capacity calculated by subtracting the average of the three OCR readings following FCCP addition from the baseline OCR as shown in Chapter 2, Figure 2.1.1A.

3.3.11 Statistical Analysis

All statistical analysis was performed using GraphPad Prism 9 software (GraphPad Software Inc., California, USA). The Spearman pair-wise test was used for correlation analysis. Analysis of unpaired data was performed using the non-parametric, Mann-Whitney *U* test. Analysis of paired data was performed using the non-parametric Wilcoxon-Signed Rank test or the one-way ANOVA with Friedman's test where appropriate. Statistical significance was defined by *$p \leq 0.05$, ** $p \leq 0.01$, *** $p \leq 0.001$, **** $p \leq 0.0001$, with all data represented as Mean +/- SEM.

3.4 Results

3.4.1 Differential expression and phenotype of PDPN+ FLS within the RA and PsA joint synovium.

An abundance of previous literature has emphasised the critical role FLS play in inflammatory arthropathies, where they are both central instigators and perpetuators of the chronically inflamed, bone destructive environment characteristic to both RA and PsA pathology (Bottini and Firestein, 2013; Ospelt, 2017; Croft *et al.*, 2019). While many pathogenic mechanisms within the synovium differ between RA and PsA, including vascularity, lymphoid aggregates, T cell subsets, no study has examined FLS *ex vivo* to date, with the majority of studies examining expanded FLS (Veale and Fearon, 2015; Veale and Fearon, 2018; Alivernini, Firestein and McInnes, 2022). Therefore, to ascertain if there are differences in the prevalence and function of these general PDPN+ FLS population within the RA and PsA joint, multiparametric flow cytometric analysis *ex vivo* on RA and PsA patient synovial biopsies, digested using previously optimised methods in our lab, was performed (Floudas *et al.*, 2022a). Representative flow plots outlining the gating strategy used for detection of this PDPN+ FLS population are shown in Figure 3.1A-F. Following the elimination of debris and cell doublets (Figure 3.1A-B), live cells were gated on (Figure 3.1C) before haematopoietic cells (Figure 3.1D) and ECs/pericytes (Figure 3.1E) were excluded and FLS were finally identified as PDPN+ (Figure 3.1F). The bar graph quantitatively demonstrates a higher frequency of PDPN+ FLS in PsA compared to RA (Figure 3.1G). Further analysis of the mean % frequency of several immune related (HLA-DR, CD55, Cad11, ICAM-1, PDGFR-α) and metabolic markers (YAP, pS6) on PDPN+ FLS between RA and PsA patient cohorts are depicted in the representative heatmap (Figure 3.1H), demonstrating significant differences in RA and PsA PDPN+ FLS.

Initially adopting an unbiased, exploratory approach, a programme called tSNE that performs dimensionality reduction of complex data by clustering cells that contain similar expression profiles was utilised (Hanlon *et al.*, 2024). Using this technique, analysis of one RA and one PsA synovial tissue was performed, with total PDPN+ cells subjected to unsupervised clustering following the data concatenation process. Data concatenation and the relative expression for the indicated markers are shown in Figure 3.2A. Interestingly, several immune, metabolic, and adhesive markers appeared to exhibit higher expression on the RA clusters with the most prominent including THY1 (Figure 3.2B(i)) , HLA-DR (Figure 3.2B(iv)), Cad11 (Figure 3.3A(i)), CD44 (Figure 3.3A(iv)), PDGR-α (Figure 3.3A(vi)), and YAP (Figure 3.3B(iv)). Conversely, initial analysis suggested a higher expression of CD55 (Figure 3.2B(iii)) and the metabolic marker pAKT (Figure 3.3B(ii)) on PsA FLS compared to their RA counterparts. Although solely based on

two patients, this data suggests a stark difference in the functional phenotype of resident FLS between RA and PsA tissue.

Therefore, analysis of the specific markers in a quantitative manner on the FLS from the flow data was performed in order to gain a deeper insight into their distinct phenotypes. Figures 3.4A(i) and 3.4B(i) demonstrate representative dot plots for FMO control, RA *ex vivo*, and PsA *ex vivo* synovial tissue for immune associated markers HLA-DR and CD55. As illustrated in the bar graphs and the accompanying histograms, RA FLS exhibited a significantly higher % frequency of HLA-DR ($p<0.01$) (Figure 3.4A(ii)) with a trend towards an increase in MFI (Figure 3.4A(iii-iv)). Conversely, the PsA FLS have a significantly higher % frequency and MFI of the marker CD55 ($p<0.001$, $p<0.0001$) (Figure 3.4B(ii-iv)). Moreover, Figures 3.5A(i) and 3.5B(i) demonstrate representative dot plots for FMO control, RA *ex vivo*, and PsA *ex vivo* synovial tissue for the adhesion molecules Cad11 and ICAM-1. Cad11 % frequency was significantly higher on the RA FLS ($p<0.01$) (Figure 3.5A(ii)), with a trend towards an increase in the corresponding MFI (Figure 3.5A(iii-iv)). Interestingly, although the % frequency of ICAM-1 expression was similar between RA and PsA FLS (Figure 3.5B(ii)), the MFI was higher in the RA population ($p<0.06$) (Figure 3.5B(iii-iv)). Furthermore, Figures 3.6A and 3.6B demonstrate representative dot plots for FMO control, RA *ex vivo*, and PsA *ex vivo* synovial tissue for the metabolic related markers YAP and pS6. As highlighted by the bar graphs, both YAP (Figure 3.6A(ii)) and pS6 (Figure 3.6B(ii)) demonstrated a significantly higher % frequency (both $p<0.05$) in the RA synovium compared to PsA, with a similar trend towards an increase in MFI additionally for both (Figure 3.6A(iii-iv) and 3.6B(iii-iv)). Cumulatively these results suggest distinct phenotypic profiles of PDPN+ FLS within the RA and PsA synovium which may imply differential pathogenic mechanisms driving RA and PsA.

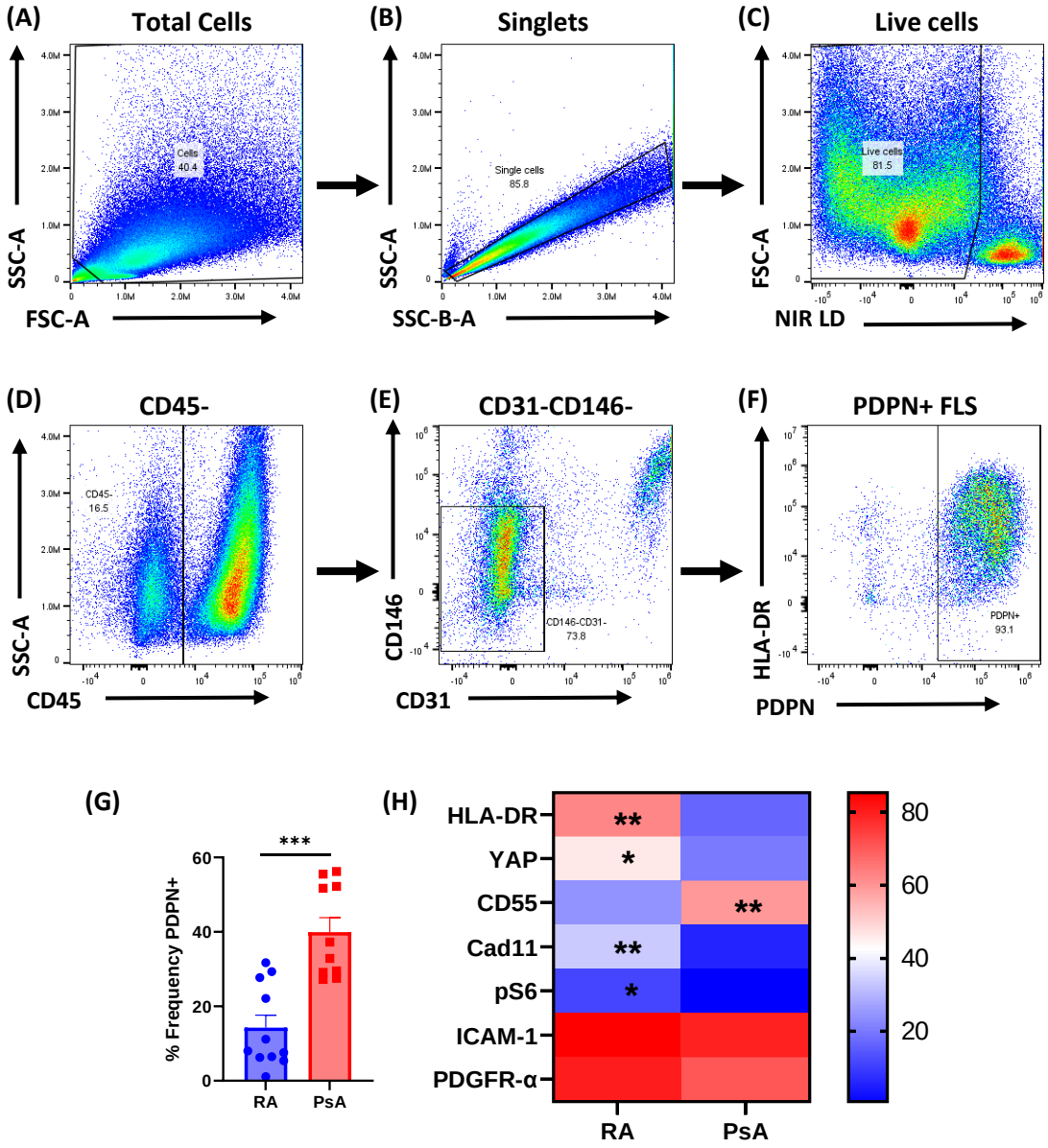

Figure 3.1. Gating strategy for functional and metabolic comparison of PDPN+ FLS between RA and PsA. Representative dot plots demonstrating the gating strategy for the identification of differences in functional and metabolic marker expression of FLS in digested whole synovial tissue RA (n=11) and PsA (n=10) biopsies using 22 distinct antibodies for staining. Analysis was performed on the CytekAurora. **(A) – (C)** The forward and side scatter parameters of cells were set before doublet exclusion and elimination of dead cells. **(D)** Haematopoietic cells and **(E)** ECs/pericytes were then excluded and **(F)** FLS were then identified as being PDPN+. **(G)** Representative bar graph of the percentage frequency of PDPN+ FLS in RA biopsies (n=11) compared to PsA (n=10). All data represented as Mean +/- SEM. **(H)** Heat-map showing the mean expression of several functional markers on RA vs PsA FLS. Statistical analysis was performed using the non-parametric, Mann-Whitney *U* Test with statistical significance defined by *p<0.05, ** p<0.01, ***p≤0.001.

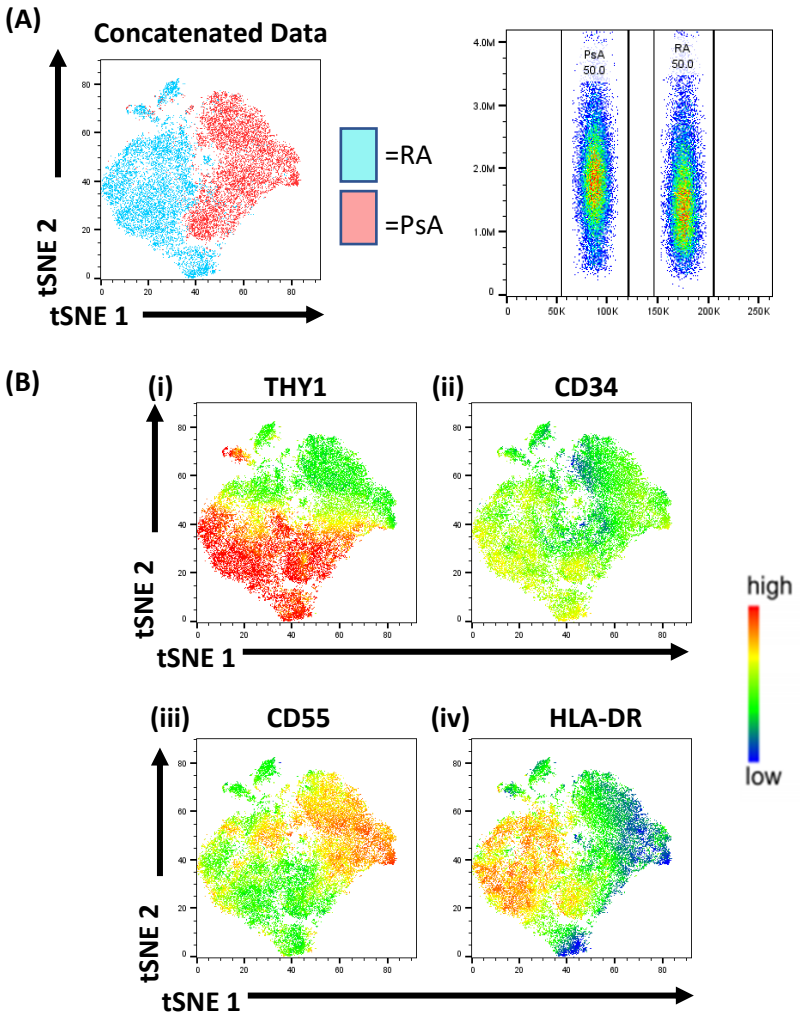

Figure 3.2. Identification of distinct marker expression on PDPN+ FLS in RA vs PsA by unsupervised clustering. Multiparametric flow cytometric data of total PDPN+ FLS subjected to unsupervised clustering by the tSNE algorithm following concatenation of data from RA and PsA synovial tissue. **(A)** Data concatenation and **(B(i-iv))** relative expression for the indicated markers related to defining FLS populations and immune regulatory functions.

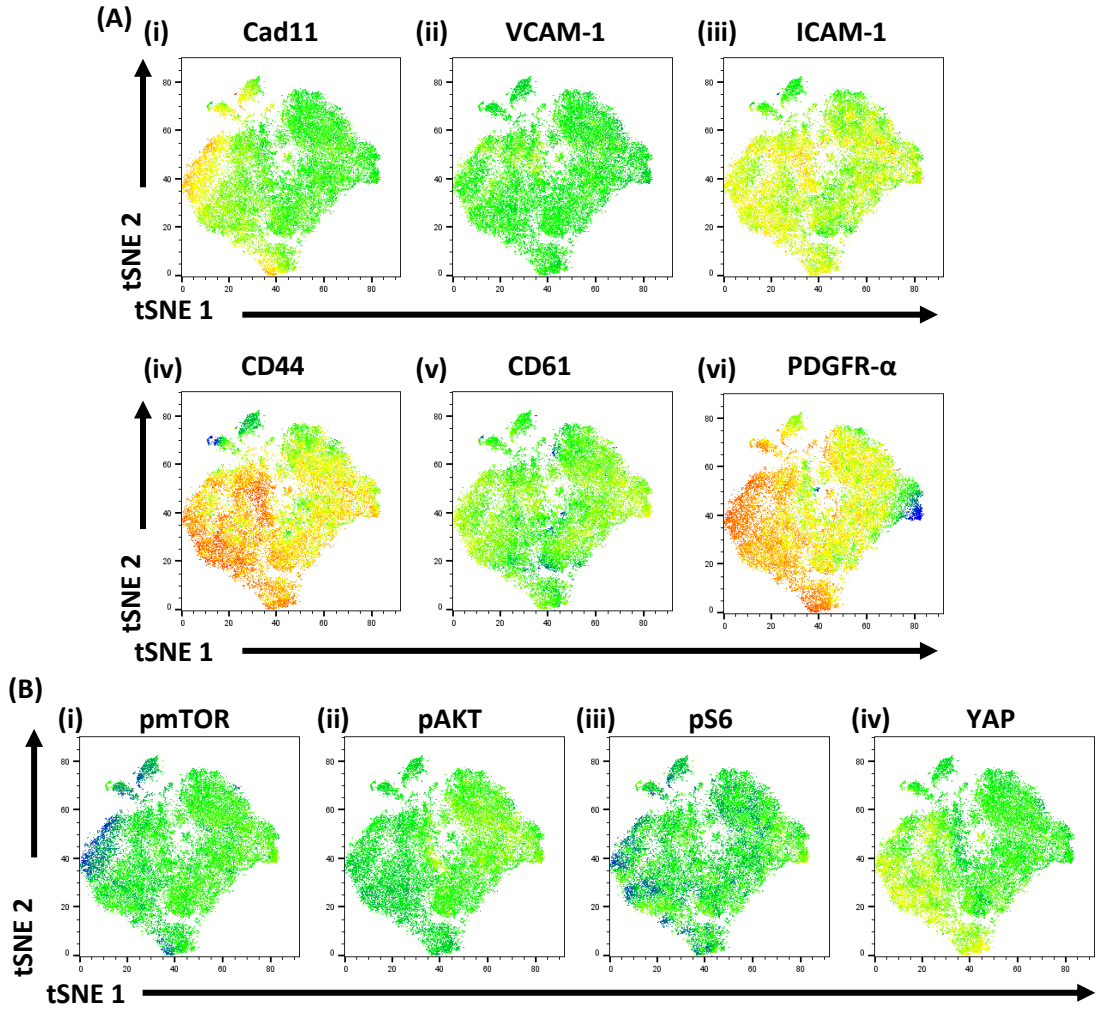

Figure 3.3. Identification of distinct adhesion molecule and metabolic marker expression on PDPN+ FLS in RA vs PsA by unsupervised clustering. Multiparametric flow cytometric data of total PDPN+ FLS subjected to unsupervised clustering by the tSNE algorithm following concatenation of data from RA and PsA synovial tissue. Data concatenation and relative expression for the indicated adhesion **(A(i-vi))** and metabolic **(B(i-iv))** markers are shown.

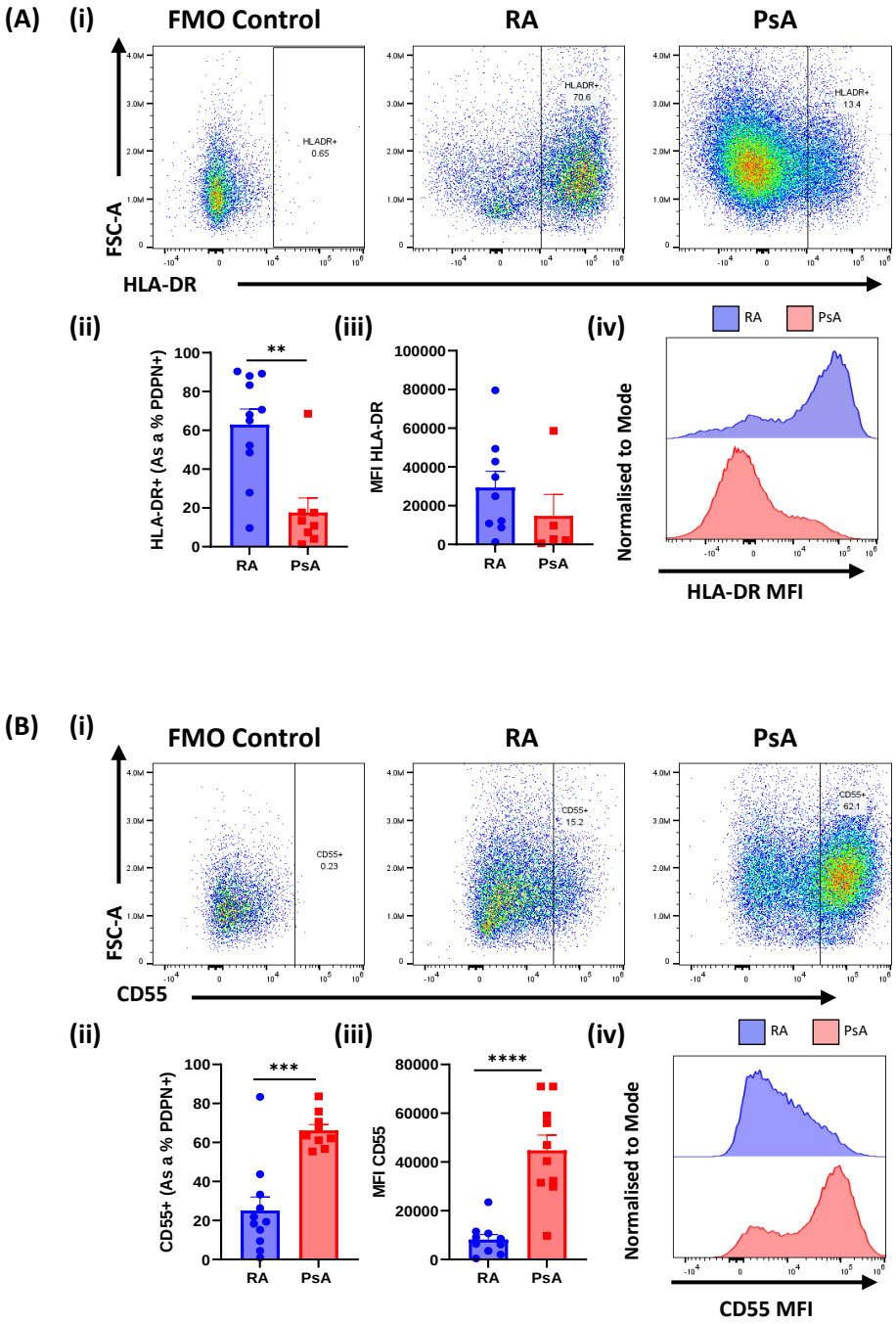

Figure 3.4. Differences in the expression of key immune markers between RA and PsA PDPN+ FLS. RA (n=11) and PsA (n=10) biopsies were digested and staining for flow cytometry was performed. **(i)** Representative flow dot plots for FMO, RA-stained tissue, and PsA-stained tissue for **(A)** HLA-DR and **(B)** CD55. **(ii)** Bar charts represent the percentage frequency of FLS that are positive for **(A)** HLA-DR and **(B)** CD55 in RA vs PsA. **(iii)** Bar charts demonstrate the MFI values for **(A)** HLA-DR and **(B)** CD55 on the PDPN+ RA vs PsA FLS. **(iv)** Representative histograms show the MFI shift for **(A)** HLA-DR and **(B)** CD55 across the indicated disease states. All data represented as Mean +/- SEM. Statistical analysis was performed using the non-parametric, Mann-Whitney *U* Test with statistical significance defined by **p≤0.01, ***p≤0.001, and ****p≤0.0001.

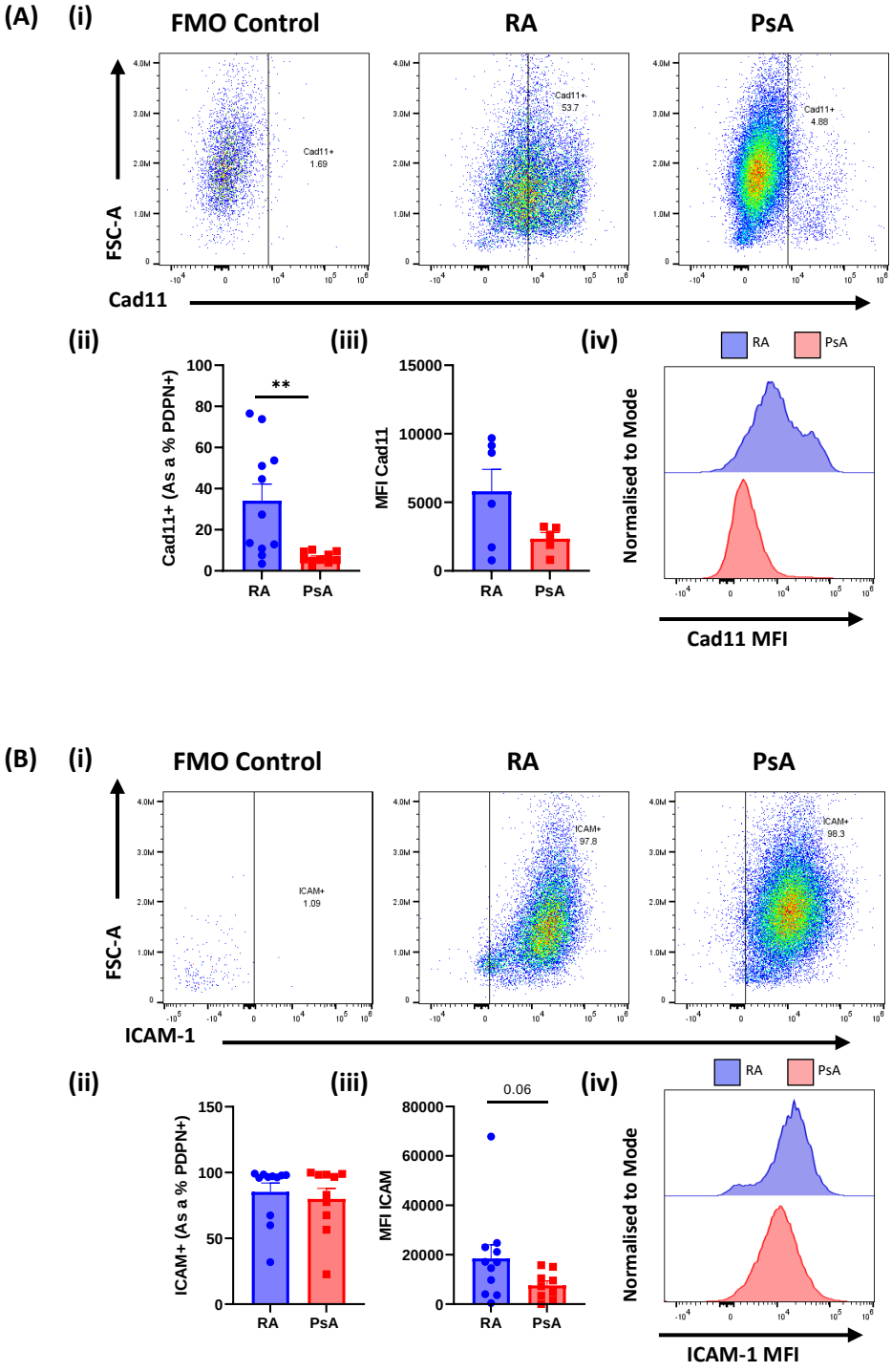

Figure 3.5. Differences in the expression of key adhesion markers between RA and PsA PDPN+ FLS. RA (n=11) and PsA (n=10) biopsies were digested and staining for flow cytometry was performed. **(i)** Representative flow dot plots for FMO, RA-stained tissue, and PsA-stained tissue for **(A)** Cad11 and **(B)** ICAM-1. **(ii)** Bar charts represent the percentage frequency of FLS that are positive for **(A)** Cad11 and **(B)** ICAM-1 in RA vs PsA. **(iii)** Bar charts demonstrate the MFI values for **(A)** Cad11 and **(B)** ICAM-1 on the PDPN+ RA vs PsA FLS. **(iv)** Representative histograms show the MFI shift for **(A)** Cad11 and **(B)** ICAM-1 across the indicated disease states. All data represented as Mean +/- SEM. Statistical analysis was performed using the non-parametric, Mann-Whitney *U* Test with statistical significance defined by *p≤0.05 and **p≤0.01.

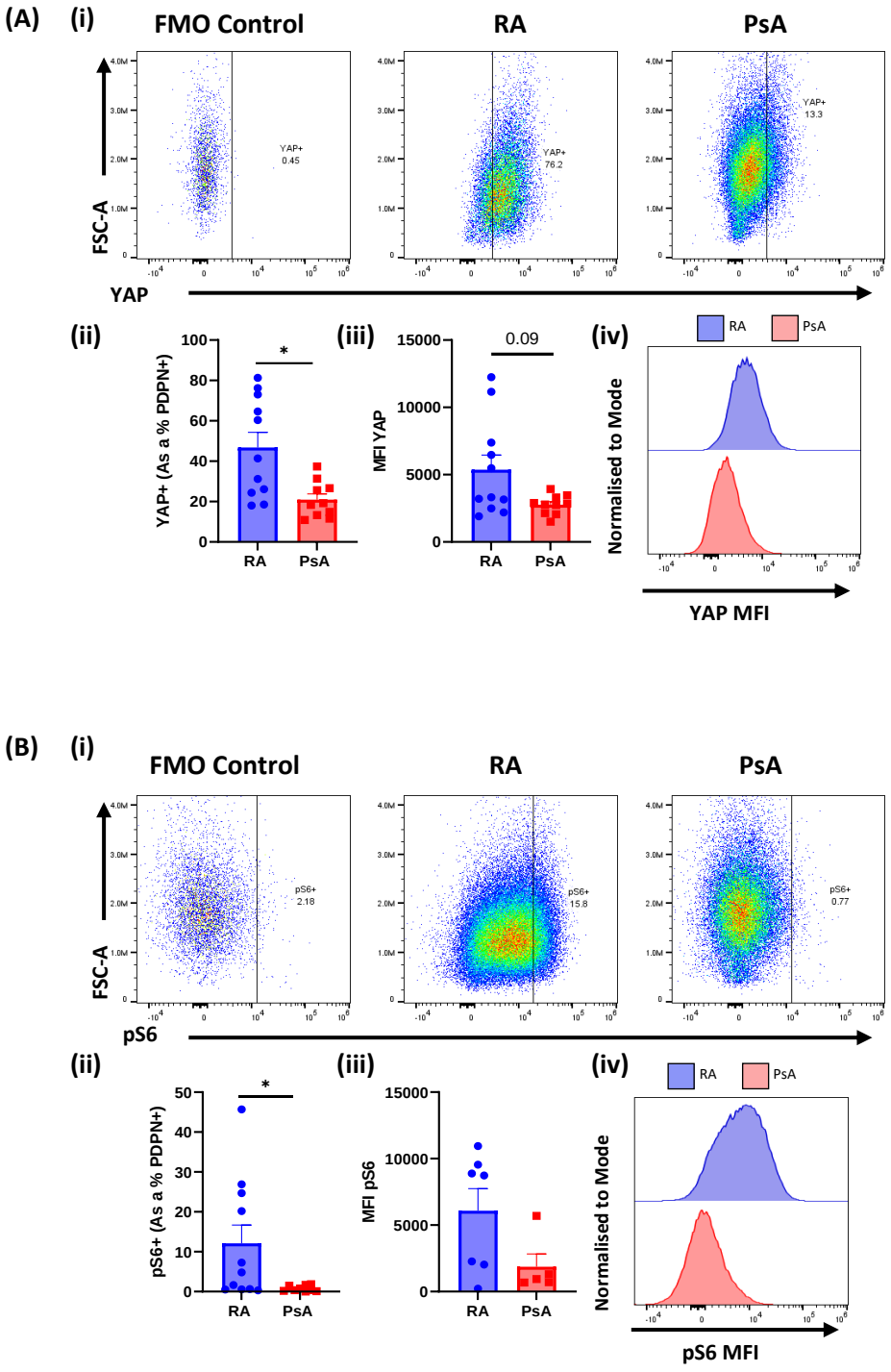

Figure 3.6. Differences in the expression of key metabolic markers between RA and PsA PDPN+ FLS. RA (n=11) and PsA (n=10) biopsies were digested and staining for flow cytometry was performed. **(i)** Representative flow dot plots for FMO, RA-stained tissue, and PsA-stained tissue for **(A)** YAP and **(B)** pS6. **(ii)** Bar charts represent the percentage frequency of FLS that are positive for **(A)** YAP and **(B)** pS6 in RA vs PsA. **(iii)** Bar charts demonstrate the MFI values for **(A)** YAP and **(B)** pS6 on the PDPN+ RA vs PsA FLS. **(iv)** Representative histograms show the MFI shift for **(A)** YAP and **(B)** pS6 across the indicated disease states. All data represented as Mean +/- SEM. Statistical analysis was performed using the non-parametric, Mann-Whitney *U* Test with statistical significance defined by *p≤0.05.

3.4.2 Comparison of the polyfunctionality of FLS in RA vs PsA synovium.

Due to the differences observed in individual markers being expressed by RA and PsA PDPN+ FLS, the polyfunctionality of these FLS was subsequently investigated. Multiparameter flow cytometry coupled with Boolean gating enabled SPICE analysis to be conducted, a method which allows us to visualise multiple parameters concurrently. In Figures 3.8A(i-ii) and 3.9B(i-ii), each arc represents a specific cytokine with the overlapping regions of arc above a specific pie segment indicating greater than one cytokine being produced simultaneously. As demonstrated by the differential size of the common pie segments between RA and PsA FLS, different combinations of specific markers (shown in the pie chart legends in Figure 3.7 and Figure 3.9A) exhibit a higher prevalence in one disease state over the other. Interestingly, RA patients demonstrated a significantly enhanced co-expression of several immune and adhesive markers including Cad11 CD44 HLA-DR ICAM-1 ($p<0.01$) (Figure 3.8B(i)), CD44 HLA-DR ICAM-1 VCAM-1 ($p<0.05$) (Figure 3.8B(ii)), and CD44 HLA-DR ICAM-1 (Figure 3.8B(iii)). Moreover, PsA patients demonstrated an enhanced dual co-expression of metabolic/invasive markers including pAKT pmTOR ($p<0.01$) (Figure 3.9C(i)) and YAP pmTOR ($p=0.07$) (Figure 3.9C(ii)). These results suggest that both RA and PsA FLS are polyfunctional in terms of immune and metabolic markers but the degree of polyfunctionality and the specific cytokines being co-expressed differ. Cumulatively, analysis of the specific markers being co-expressed on the RA and PsA FLS, would suggest that RA FLS exhibit a stronger association with immune regulation whilst the PsA FLS demonstrate a stronger association with invasive and metabolic functions.

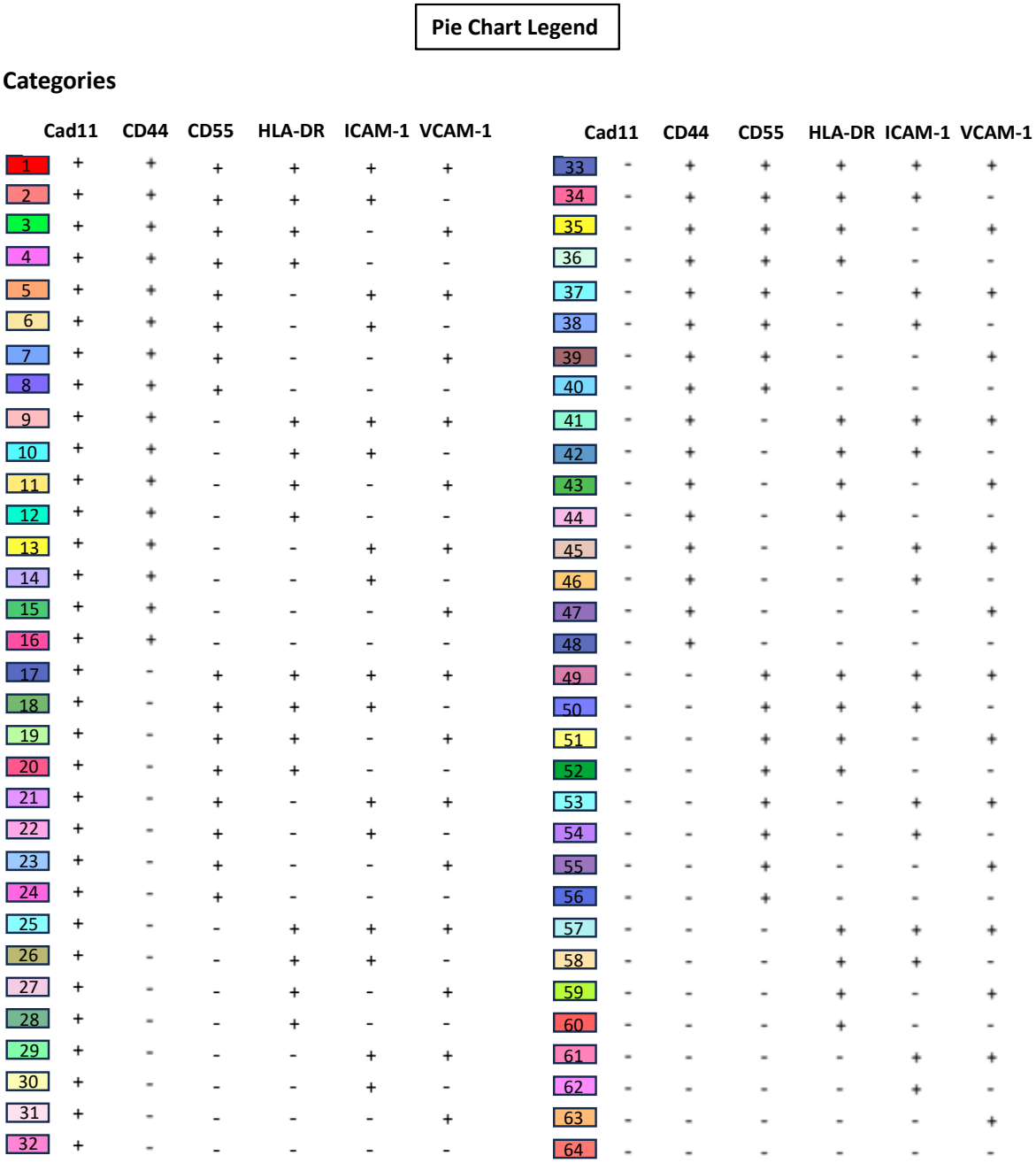

Figure 3.7. Legend depicting all the possible combinations of the immune markers being co-expressed using Boolean gating. Each combination corresponds to a specific segment of the pie in Figure 3.8 **(A(i-ii))** below.

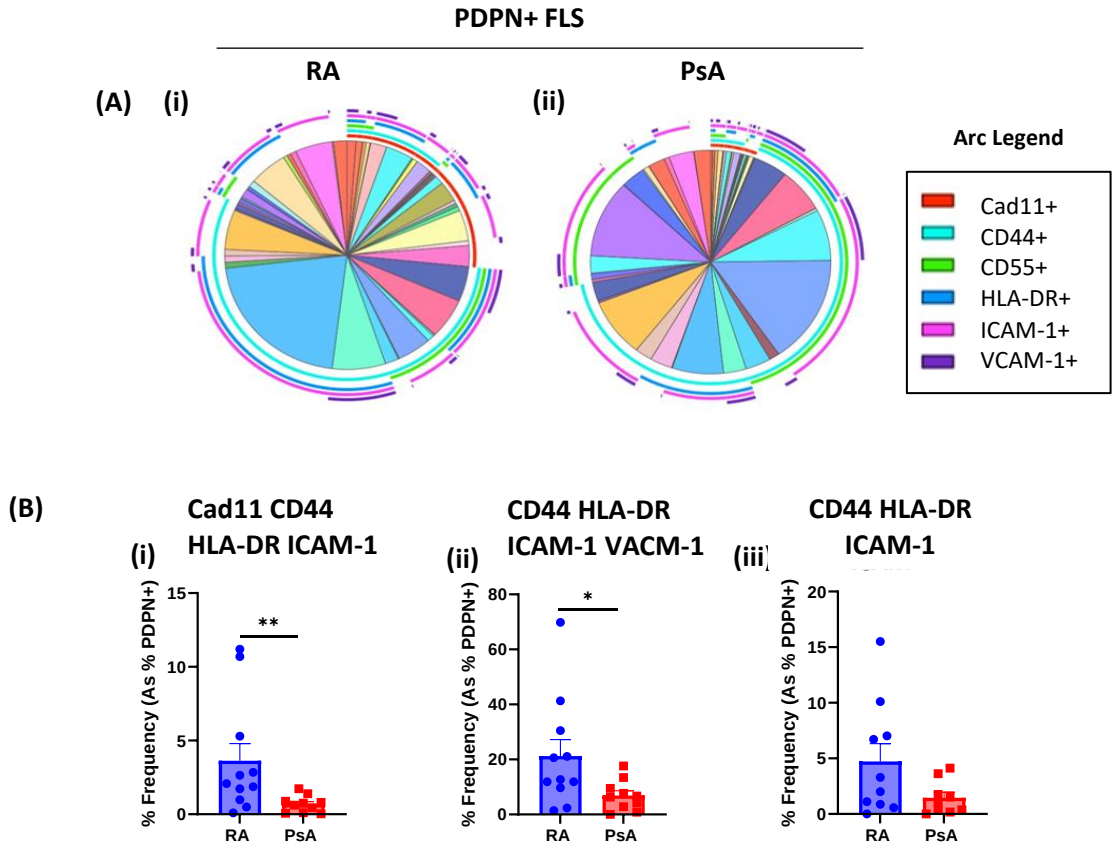

Figure 3.8. PDPN+ FLS demonstrate differences in the co-expression of immune markers in RA vs PsA. Visual representation of multidimensional flow cytometric data. SPICE analysis was performed for the identification of polyfunctionality of PDPN+ FLS from **(A(i))** RA (n=11) and **(A(ii))** PsA (n=9) synovial tissue. Each pie segment indicates the different combinations of marker expression as denoted in Figure 3.7 above. The adjacent pie arcs indicate the specific immune markers produced by each pie segment as denoted by the included legend. Multiple arcs above a single pie segment represent polyfunctional cells. The size of the pie arc/segment correlates with the frequency of the population. **(B(i-iii))** Representative bar graphs quantitatively depicting the differences in expression of specific combinations of immune markers between the RA and PsA patients as determined by the SPICE analysis. All data represented as Mean +/- SEM. Statistical analysis was performed using the non-parametric, Mann-Whitney *U* Test with statistical significance defined by *p≤0.05, **p≤0.01.

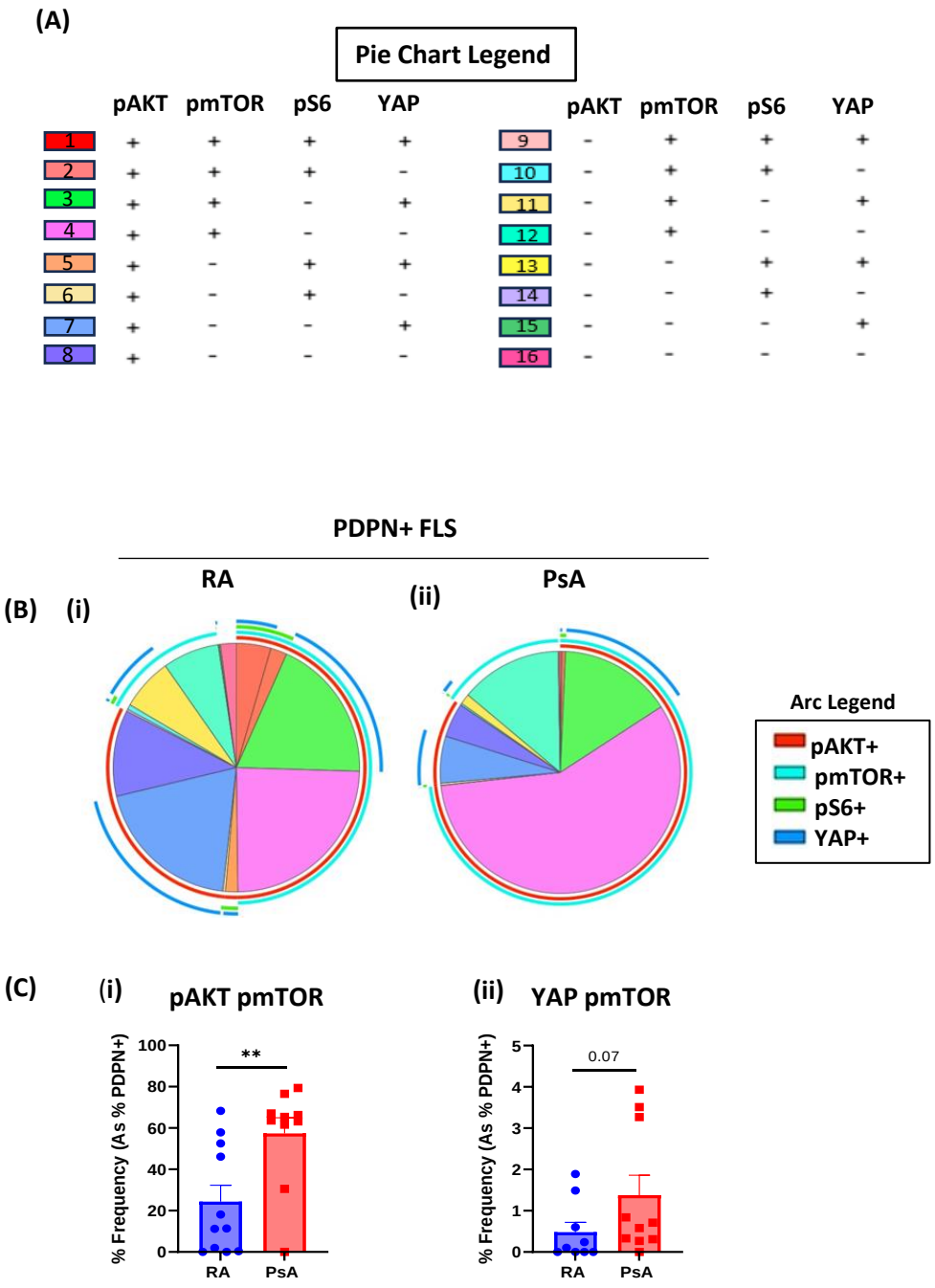

Figure 3.9. PDPN+ FLS demonstrate differences in the co-expression of metabolic/invasive markers in RA vs PsA. Visual representation of multidimensional flow cytometric data. SPICE analysis was performed for the identification of polyfunctionality of PDPN+ FLS from **(B(i))** RA (n=11) and **(B(ii))** PsA (n=9) synovial tissue. Each pie segment indicates the different combinations of marker expression as denoted by the legend above **(A)**. The adjacent pie arcs indicate the specific immune or metabolic markers produced by each pie segment as denoted by the included legend. Multiple arcs above a single pie segment represent polyfunctional cells. The size of the pie arc/segment correlates with the frequency of the population. **(C(i-ii))** Representative bar graphs quantitatively depicting the differences in expression of specific combinations of the metabolic/invasive markers between the RA and PsA patients as determined by the SPICE analysis. All data represented as Mean +/- SEM. Statistical analysis was performed using the non-parametric, Mann-Whitney *U* Test with statistical significance defined by *p≤0.05, **p≤0.01.

3.4.3 Differential expression of THY1 FAP expressing FLS clusters in RA vs PsA synovium.

Previous literature has focused on the expression of the markers THY1 and FAP to characterise distinct FLS populations, with THY1+ sub-lining FLS exhibiting a stronger role in immune related functions in contrast to THY1- lining FLS which have been implicated to a greater extent in bone and cartilage destruction (Croft *et al.*, 2019). Therefore, to identify potential differences in the dominance of lining versus sub-lining FLS in RA vs PsA, flow cytometric analysis was performed *ex vivo* based on the Croft paper analysis. The gating strategy implemented is indicated in Figure 3.10A-G. Figures 3.11A and 3.11B demonstrate representative dot plots for FMO control and a stained synovial tissue for the markers THY1 and FAP, whilst Figure 3.11C depicts representative overlaid histograms showing the differences in THY1+FAP+ vs THY1-FAP+ expressing FLS in RA and PsA tissue.

As demonstrated in the representative dot plots and quantitatively in the accompanying bar graphs and histograms representing MFI, there was a significant enrichment in the % frequency expression of the THY1+FAP+ FLS population in RA ($p<0.05$) (Figure 3.12A(i-iii)), whilst conversely, the THY1-FAP+ FLS subset was significantly higher in PsA ($p<0.05$) (Figure 3.12B(i-iii)). Interestingly, the THY1+FAP- and THY1-FAP- populations of FLS exhibited a similar frequency in both RA and PsA alike (Figures 3.12C(i-iii) and 3.12D(i-iii)).

These results indicate that there are indeed differences in the particular FLS subsets that dominate in RA compared to PsA, primarily based on the presence/absence of the immune-associated marker THY1, with RA FLS exhibiting higher levels of THY1 expressing FLS compared to their PsA counterparts.

3.4.5 Differential angiogenic, chemotactic, and ECM degradative function of THY1+FAP+ versus THY1-FAP- expressing FLS clusters in the inflamed synovium.

To further understand and expand on the differential function of distinct THY1 expressing subsets identified through scRNA-seq analysis (Chapter 2, Section 2.4.1), cells were sorted from fresh synovial biopsies based on the presence/absence of THY1 and FAP as demonstrated in Figure 3.13 and MSD multiplex analysis performed on the collected supernatants from these sorted populations. Interestingly, as depicted in the heatmap (Figure 3.14A) and bar graph (Figure 3.14B), the production of all angiogenic mediators including PIGF, VEGF-A, VEGF-C, bFGF, and FLT1, was greater in the THY1+FAP+ FLS compared to the THY1-FAP- population. Indeed, there was a significantly higher level of VEGF-A ($p<0.05$) (Figure 3.14C(i)), VEGF-C ($p<0.05$) (Figure 3.14C(ii)), and FLT1 ($p<0.05$) (Figure 3.14C(iii)) in the double positive compared to the double negative cells.

Furthermore, although analysis of chemokine expression did not demonstrate any significant differences between both populations (Figure 3.15A and 3.15B), there was a trending increase in the level of chemokines produced by the THY1+FAP+ FLS including MCP-1 (Figure 3.15C(i)), MCP-4 (Figure 3.15C(ii)), Eotaxin (Figure 3.15V(iv)), Eotaxin-3 ($p<0.09$) (Figure 3.15C(v)), IP-10 (Figure 3.15C(vi)), MIP-1α (Figure 3.15C(vii)), MIP-1β (Figure 3.15C(viii)), TARC (Figure 3.15C(ix)), and MDC (Figure 3.15C(x)). Finally, as shown in Figures 3.16A and 3.16B, analysis of the MMPs from the sorted cells revealed a higher expression of all three MMPs; MMP-1, MMP-3, and MMP-9, in the THY1-FAP- FLS compared to the THY1+FAP+ subset, with a particularly high expression level associated with the THY1-FAP- PsA FLS specifically (Figures 3.16B(i-iii)). Collectively, the data implies a stronger angiogenic and chemotactic function of the THY1+FAP+ FLS compared to the THY1-FAP- FLS whilst conversely, the THY1-FAP- FLS, and particularly in the PsA cohort, exhibit higher invasive MMP expression compared to their THY1+FAP+ counterparts.

3.4.6 Identification of a direct positive correlation between THY1+FAP+ FLS and inflammatory disease parameters.

To investigate the clinical significance of the THY1+FAP+ FLS subset on inflammatory disease parameters in the IA synovial tissue, Spearman correlation analysis was performed. Interestingly, a positive correlation ($r = 0.55$, $p<0.05$) between the % frequency of THY1+FAP+ FLS and DAS28 was identified (Figure 3.17A). This was shown visually by the accompanying representative dot plots showing THY1+FAP+ expression from a patient with Low DAS tissue vs a patient with High DAS tissue (Figure 3.17B). Moreover, a positive correlation ($r = 0.54$, $p<0.05$) between the % frequency of THY1+FAP+ FLS and the extent of synovitis was also identified (Figure 3.17C). Representative macroscopic images of synovitis from a patient with a high synovitis score vs a patient with a low synovitis score are shown in Figure 3.17D. Cumulatively, these results indicate a central role of this THY1+FAP+ FLS population in driving the extent of disease activity and inflammation in RA and PsA synovial tissue.

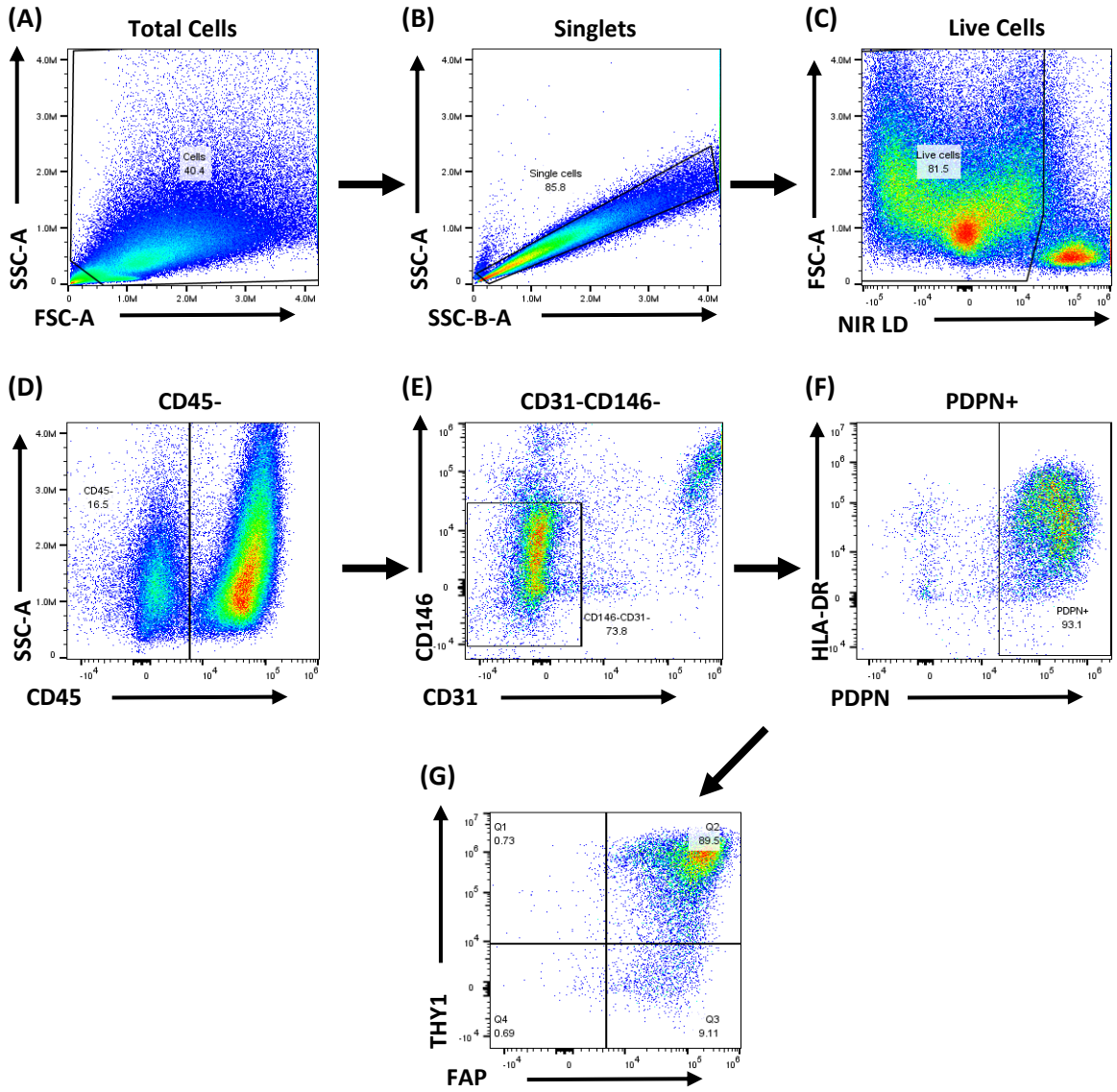

Figure 3.10. Gating strategy to identify differential expression of THY1 FAP expressing clusters in RA vs PsA. Representative dot plots demonstrating the gating strategy for the identification of lining versus sub-lining FLS populations within whole synovial tissue RA (n=11) and PsA (n=9) biopsies digested and stained using 22 extracellular and intracellular antibodies. Analysis was performed on the CytekAurora. **(A) – (C)** The forward and side scatter parameters of cells were set before doublet exclusion and elimination of dead cells. **(D)** Haematopoietic cells and **(E)** ECs/pericytes were then excluded. **(F)** FLS were then identified as being PDPN+ and further characterised into specific populations based on the expression of the FLS associated markers **(G)** THY1 and FAP.

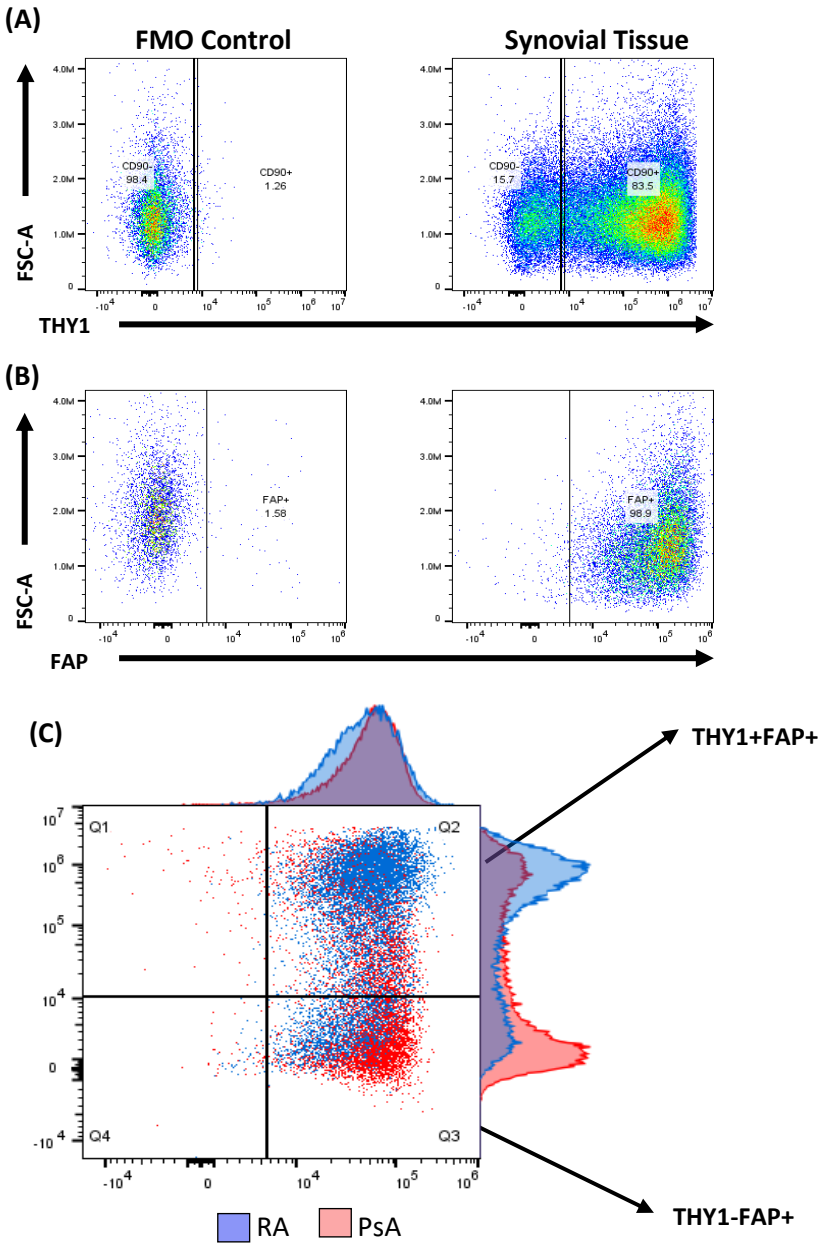

Figure 3.11. Differences in the expression of key FLS associated markers THY1 and FAP between RA and PsA PDPN+ FLS. Representative flow plots show the **(A)** THY1 and **(B)** FAP FMO compared to the unstimulated synovial tissue. **(C)** Representative flow cytometric dot plot with accompanying overlaid histograms indicating the MFI, demonstrating differences in the expression of THY1 FAP expressing FLS populations from the indicated disease states (RA: n=11 and PsA: n=9).

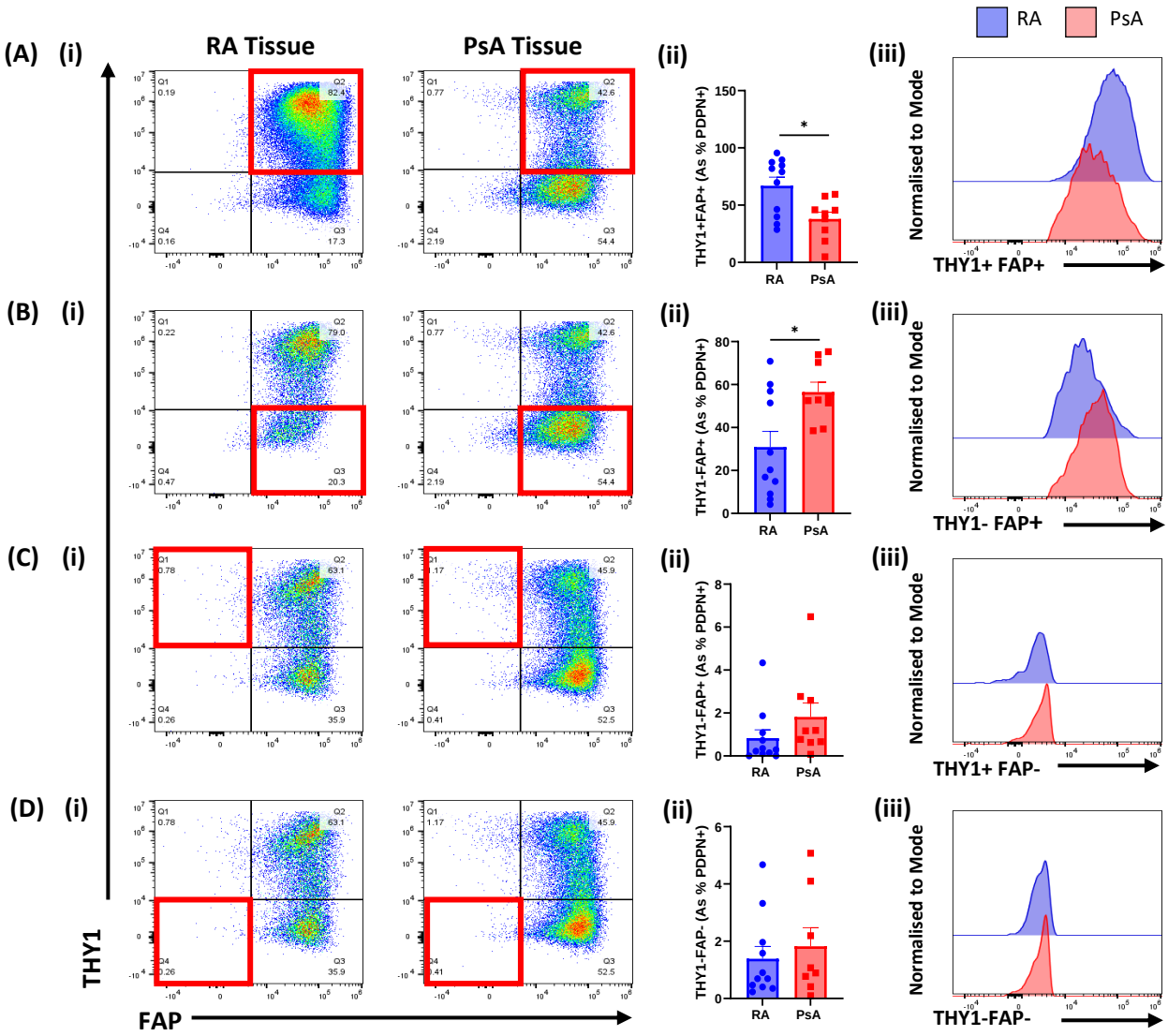

Figure 3.12. Differential expression of THY1 FAP FLS populations in RA vs PsA. Representative **(i)** dot plots and **(ii)** accompanying bar graphs demonstrating the % frequency of **(A)** THY1+FAP+, **(B)** THY1-FAP+, **(C)** THY1+ FAP-, and **(D)** THY1-FAP- expressing populations of FLS (as a % of PDPN) within RA (n=11) and PsA (n=9) synovial biopsies. **(A-D(iii))** Representative histograms of the MFI of the indicated FLS populations (A-D) in RA and PsA synovial tissue. All data represented as Mean +/- SEM. Statistical analysis was performed using the non-parametric, Mann-Whitney *U* Test with statistical significance defined by *p≤0.05.

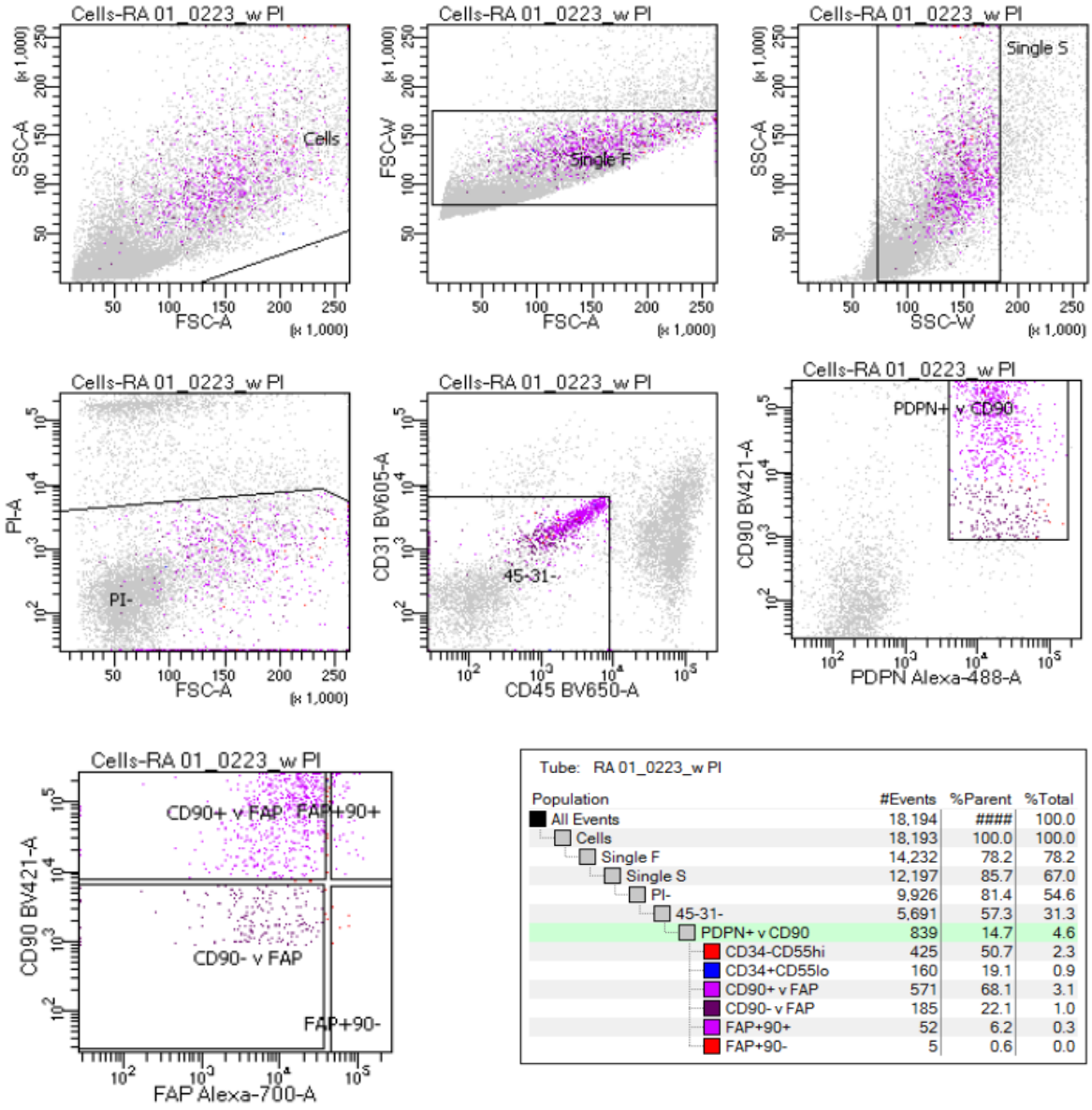

Figure 3.13. Gating strategy for FACS sort of RA and PsA FLS. Gating strategy to identify and sort THY1+FAP+ and THY1-FAP- FLS from RA and PsA synovial tissue using the FACS Aria Fusion sorter. Following elimination of debris, doublets, and dead cells, cells were gated as CD45-, CD31-, and PDPN+ and further characterised into double positive THY1+FAP+ and double negative THY1-FAP-. Cell sorting purity was also analysed using the FACS Aria Fusion sorter.

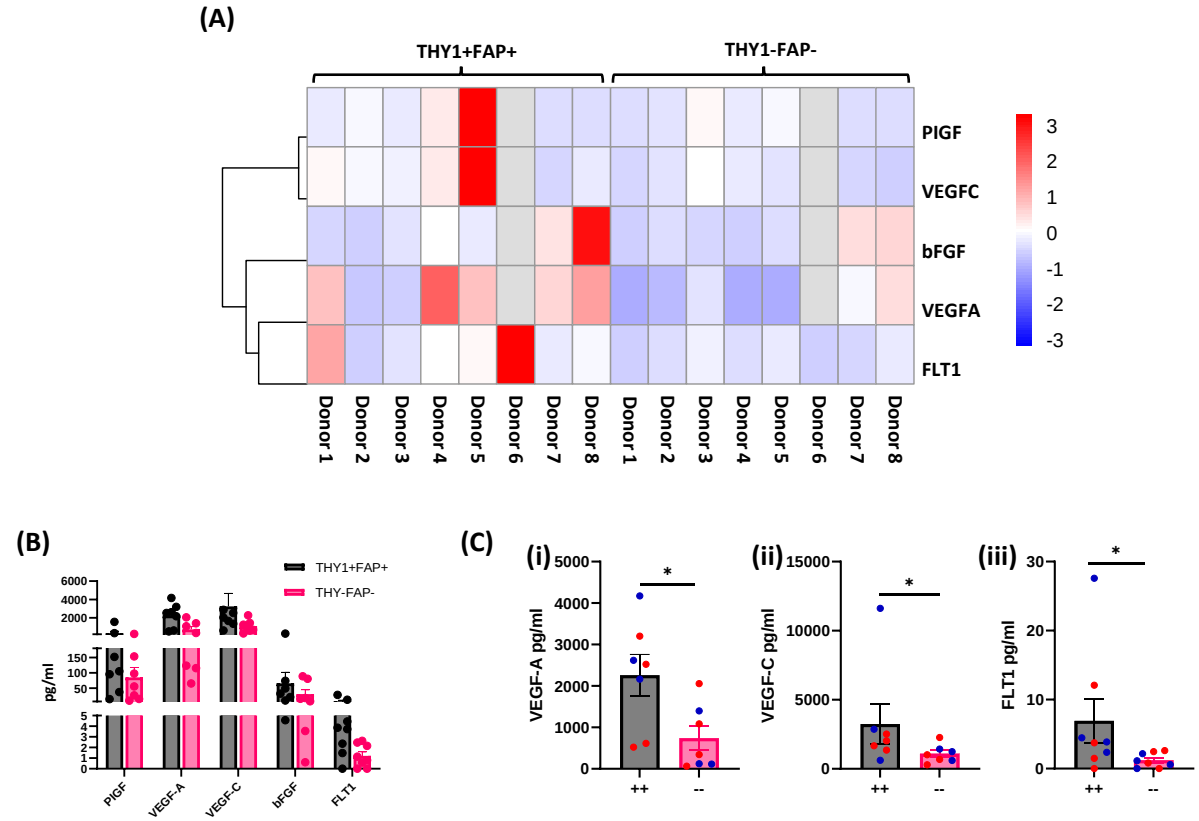

Figure 3.14. Significantly higher expression of angiogenic mediators in the supernatants of THY1+FAP+ FLS compared to THY1-FAP- FLS. FLS from fresh RA (n=4) and PsA (n=4) biopsies were digested and sorted into two populations based on THY1 and FAP expression, before supernatants were collected and analysed by an MSD angiogenic-panel. **(A)** Clustered heatmap depicting the scaled expression of angiogenic factors in the supernatants of the THY1+FAP+ (++) vs THY1-FAP- FLS (--) across all the individual donors. (**B)** Bar graphs depict the expression levels of angiogenic mediators in the supernatants from THY1+FAP+ vs THY1-FAP- FLS. **(C)** Representative bar graphs demonstrating significant differences in the protein levels measured of **(i)** VEGF-A, **(ii)** VEGF-C, and **(iii)** FLT1 between the two distinct FLS populations with RA donors represented by blue dots and PsA donors represented by red dots. All data represented as Mean +/- SEM. Statistical analysis was performed using the non-parametric, Wilcoxon Signed-Rank Test with statistical significance defined by *p≤0.05.

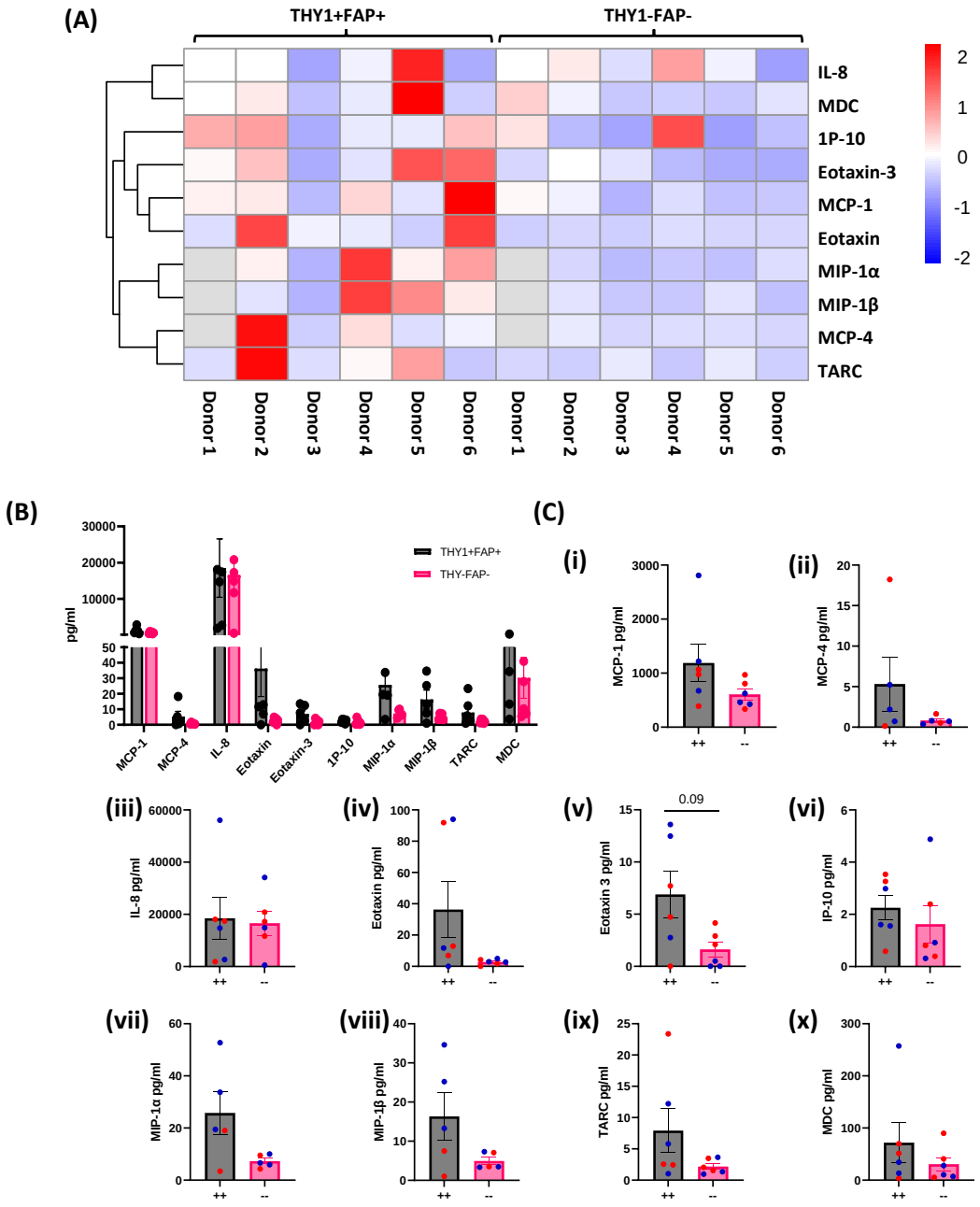

Figure 3.15. Comparison of the expression of chemokines in the supernatants of THY1+FAP+ FLS compared to THY1-FAP- FLS. FLS from fresh RA (n=3) and PsA (n=3) biopsies were digested and sorted into two populations based on THY1 and FAP expression, before supernatants were collected and analysed by an MSD chemokine-panel. **(A)** Clustered heatmap depicting the scaled expression of chemotactic factors in the supernatants of the THY1+FAP+ (++) vs THY1-FAP- (--) FLS across all the individual donors. **(B)** Bar graph depicts the expression levels of the chemokines in the supernatants from THY1+FAP+ vs THY1-FAP- FLS. **(C)** Representative bar graphs demonstrating differences in the protein levels measured of **(i)** MCP1, **(ii)** MCP4, **(iii)** IL-8, **(iv)** Eotaxin, **(v)** Eotaxin-3, **(vi)** IP-10, **(vii)** MIP-1α, **(viii)** MIP-1β, **(ix)** TARC, and **(x)** MDC between the two distinct FLS populations with RA donors represented by blue dots and PsA donors represented by red dots. All data represented as Mean +/- SEM.

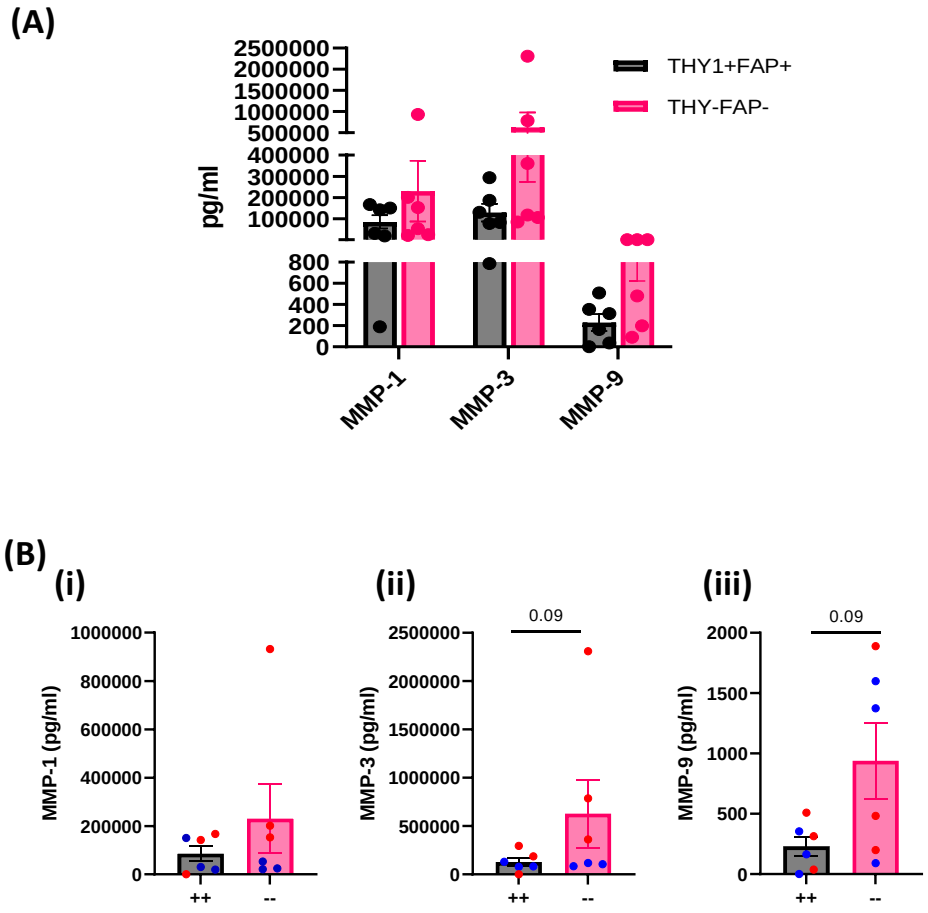

Figure 3.16. Higher expression of MMPs in the supernatants of THY1-FAP- PsA FLS compared to THY1+FAP+ FLS. FLS from fresh RA (n=3) and PsA (n=3) biopsies were digested and sorted into two populations based on THY1 and FAP expression, before supernatants were collected and analysed by an MSD MMP-panel. **(A)** Bar graph depicts the expression levels of MMPs in the supernatants from THY1+FAP+ (++) vs THY1-FAP- (--) FLS. **(B)** Representative bar graphs demonstrating significant differences in the protein levels measured of **(i)** MMP-1, **(ii)** MMP-3, and **(iii)** MMP-9 between the two distinct FLS populations with RA donors represented by blue dots and PsA donors represented by red dots. All data represented as Mean +/- SEM. Statistical analysis was performed using the non-parametric, Wilcoxon Signed-Rank Test with statistical significance defined by *p≤0.05.

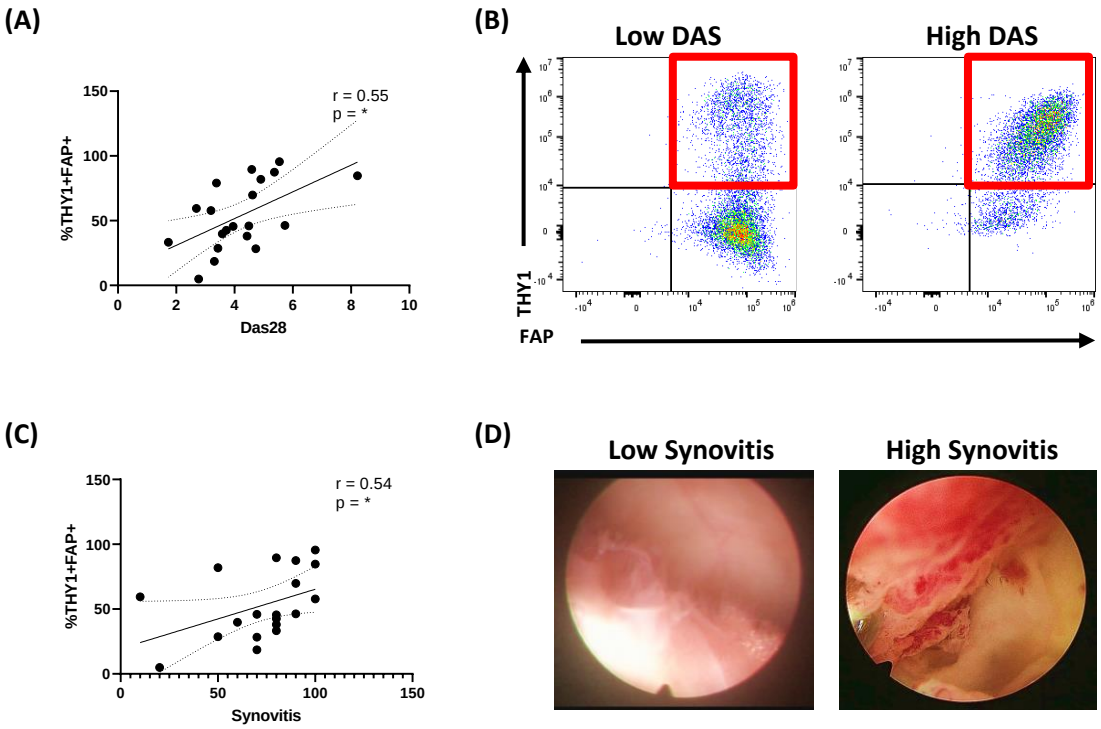

Figure 3.17. Identification of a direct positive correlation between THY1+FAP+ FLS and inflammatory disease parameters. (A) Representative scatter plots with Spearman pair-wise correlation analysis of THY1+FAP+ FLS and Das28 in IA synovial tissue (n=20). **(B)** Representative flow cytometry plot of THY1+FAP+ FLS frequency in high versus low disease activity. **(C)** Representative scatter plots with Spearman pair-wise correlation analysis of THY1+FAP+ FLS and synovitis in IA synovial tissue (n=20). **(D)** Representative macroscopic images showing a tissue with low synovitis versus high synovitis.

3.4.7 Differential expression of THY1 CD34 CD55 FAP expressing FLS clusters in RA vs PsA, with distinct functions associated with the different clusters.

To expand on identifying the potential differences in the dominant subsets of FLS present in RA compared to PsA, the markers THY1 (CD90) and CD34, in addition to CD55 and FAP were used, and flow cytometric analysis was performed *ex vivo* using a 21 colour panel.

The gating strategy implemented is indicated in Figure 3.18, giving rise to six discrete FLS populations in the IA joint. These six populations are depicted quantitatively along with accompanying heatmap (Figure 3.19A-B), with the results highlighting a particular dominance of four main populations within the IA synovial joint– three of which are THY1+ and one which is THY1- (highlighted in red box). Interestingly, when separated out into the disease states, two of these four populations were enriched in the RA cohort (Figure 3.19C) whilst the opposite two populations were enriched in PsA (Figure 3.19D), with this visually represented in the accompanying heatmap (Figure 3.19E). Moreover, when stratified and compared directly between the two disease states quantitatively, patients with RA exhibited an enrichment in THY1+CD34+CD55-FAP+ ($p<0.05$) (Figure 3.20A(i-iii)) and THY1+CD34-CD55-FAP+ FLS (Figure 3.20B(i-iii)), whilst patients with PsA displayed enrichment in the other two populations; THY1-CD34-CD55+FAP+ FLS ($p<0.001$) (Figure 3.20D(i-iii)) and unexpectedly, a THY1+ population; THY1+CD34-CD55+FAP+ ($p<0.05$) (Figure 3.20C(i-iii)). The THY1+CD34+CD55+FAP+ and THY1-CD34+CD55+FAP+ FLS populations were relatively similar between RA and PsA and had lower frequency in the IA joint and thus were excluded from further analysis (Figure 3.19A-E).

In order to understand the functional consequences of the differential dominance of FLS populations in RA vs PsA, the expression of several immune, adhesion, and metabolic markers on the four populations in IA were examined. As depicted in the heatmap (Figure 3.21A), there were stark differences in the expression of several markers across the four individual populations, with higher mean % frequency of markers such as pS6, VCAM-1, pAKT, and Ki67 in the two PsA dominant populations whilst PDGFR, YAP, HLA-DR, and Cad11 appeared markedly higher in the two RA dominant populations (Figure 3.21A). Interestingly, the frequency of markers being expressed by the THY1-CD34-CD55+FAP+ PsA enriched subset (purple) was nearly the reverse of the two RA enriched THY1+ subsets (pink & orange), with high expression in the THY1- subset meaning low frequency expression in the two RA enriched THY1+ subsets and vice versa (Figure 3.21A). However, as shown in the heatmap, the THY1+CD34-CD55+FAP+ FLS population (green), enriched in PsA, exhibited expression levels of specific markers that overlapped with all three of the other populations suggesting it may possess more intermediate functionality (Figure 3.21A). Furthermore, quantitative analysis demonstrated a significantly higher % frequency of both YAP

(Figure 3.21B) and Cad11 (Figure 3.21C) in the RA dominant populations, particularly the THY1+CD34+CD55-FAP+ FLS. Conversely, pAKT expression was significantly higher in both of the FLS populations more prevalent in PsA, THY1+CD34-CD55+FAP+ and THY1-CD34-CD55+FAP+ (Figure 3.21D).

Collectively, the data indicates the existence of six distinct FLS populations based on the expression of the surface markers THY1, CD34, CD55, and FAP, showing differential expression levels in RA compared to PsA, with a higher level of THY1- lining layer FLS in PsA and a dominance of THY1+ sub-lining FLS in RA. Importantly, the expression of specific markers differs across clusters thus further defining the function of that cluster across both disease states, with these clusters differentially enriched in RA vs PsA. RA dominant populations potentially exhibit a more immune regulatory role whilst the data implies a stronger role for pAKT and downstream pathways in PsA dominant populations.

3.4.8 Histopathological differences in RA vs PsA synovial tissue corresponds with the enriched FLS clusters in RA vs PsA.

Next to compare the macroscopic and microscopic characteristics of the RA and PsA synovial tissue, and specifically to determine if the dominance of lining layer FLS in PsA compared to sub-lining layer FLS in RA identified by the flow cytometric analysis could be translated to the biopsy and detected visually, histological analysis was performed on the matched biopsies. Figures 3.22A-B depict H&E stains of RA and PsA tissue, demonstrating intact synovial tissue morphology with lining-layer, blood vessels, lymphoid aggregates, and synovial infiltrate clearly visible. Firstly, as depicted in these representative images and quantitatively, although significance was not reached, there was a trend towards a greater average thickness of the lining layer in the PsA patients compared to RA indicating a greater dominance of THY1- FLS in PsA (Figure 3.22C(i)). Conversely, the cellular infiltration score demonstrated a significantly higher level in RA compared to PsA ($p<0.05$) (Figure 3.22C(ii)), which was reflected in the representative images showing a greater extent of inflammation in the RA synovium (Figure 3.22A) compared to the PsA synovium images (Figure 3.22B). Interestingly, whilst the vascularity score was similar between both disease states (Figure 3.22C(iii)), the presence/absence of lymphoid aggregates was trending higher in RA compared to PsA with the majority of PsA samples devoid of aggregates (Figure 3.22C(iv)). Cumulatively, the data suggests that whilst the extent of vascularity is comparable between both disease states, there is a higher prevalence of immune cell infiltration and inflammation in the RA

joint compared to PsA. This may be associated with a higher sub-lining THY1+ FLS presence whilst the lining layer is thicker in PsA indicative of an enrichment of THY1- FLS.

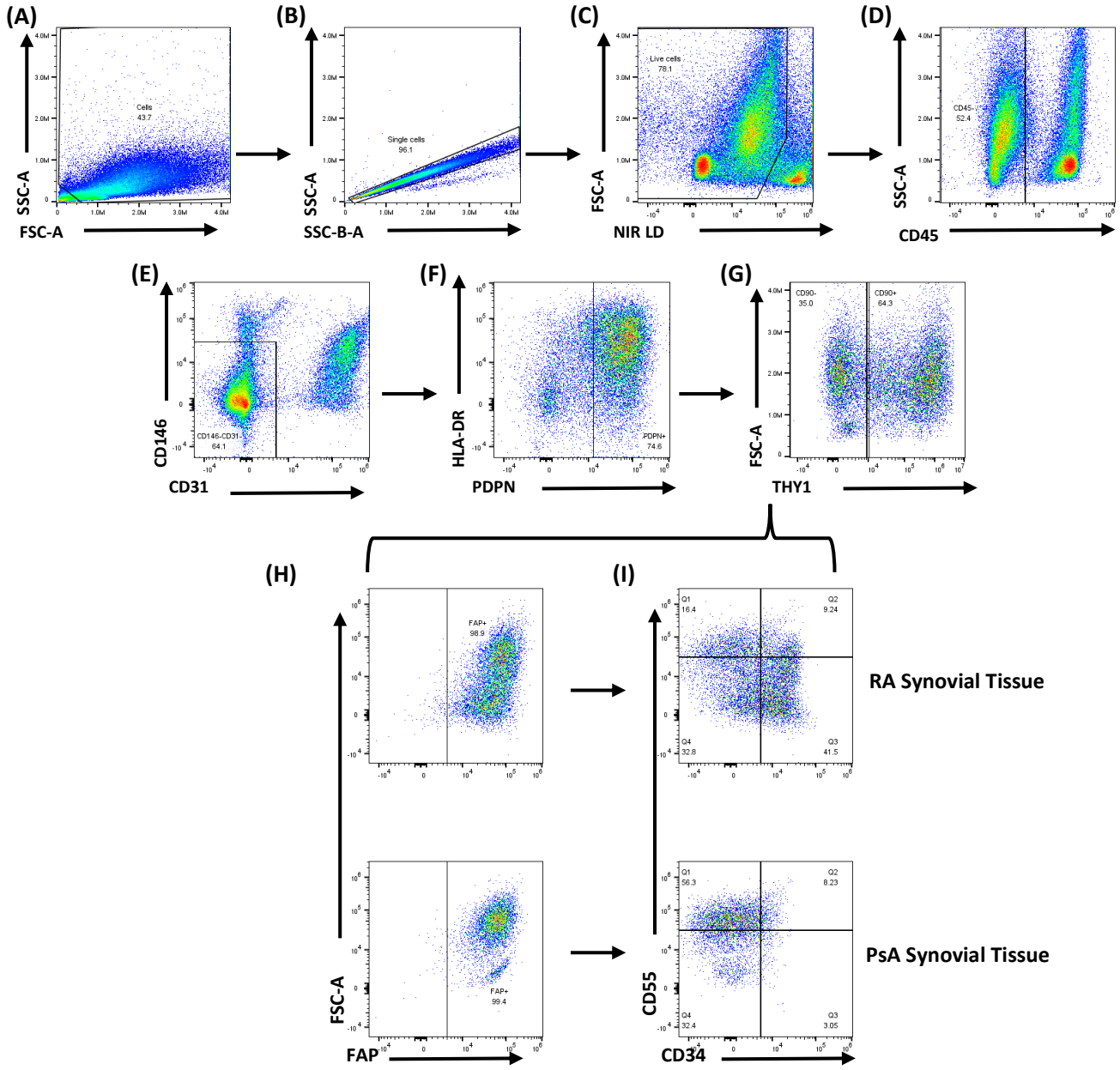

Figure 3.18. Gating strategy to identify differential expression of THY1 CD34 CD55 FAP+ expressing clusters in RA vs PsA. Representative dot plots demonstrating the gating strategy for the identification of lining versus sub-lining FLS populations within whole synovial tissue RA (n=7) and PsA (n=8) biopsies digested and stained using 22 extracellular and intracellular antibodies. Analysis was performed on the CytekAurora. **(A) – (C)** The forward and side scatter parameters of cells were set before doublet exclusion and elimination of dead cells. **(D)** Haematopoietic cells and **(E)** ECs/pericytes were then excluded. **(F)** FLS were then identified as being PDPN+ and further characterised into specific populations based on the expression of the key markers **(G)** THY1, followed by **(H)** FAP, and finally **(I)** CD34 and CD55 in both RA and PsA synovial tissue as demonstrated above.

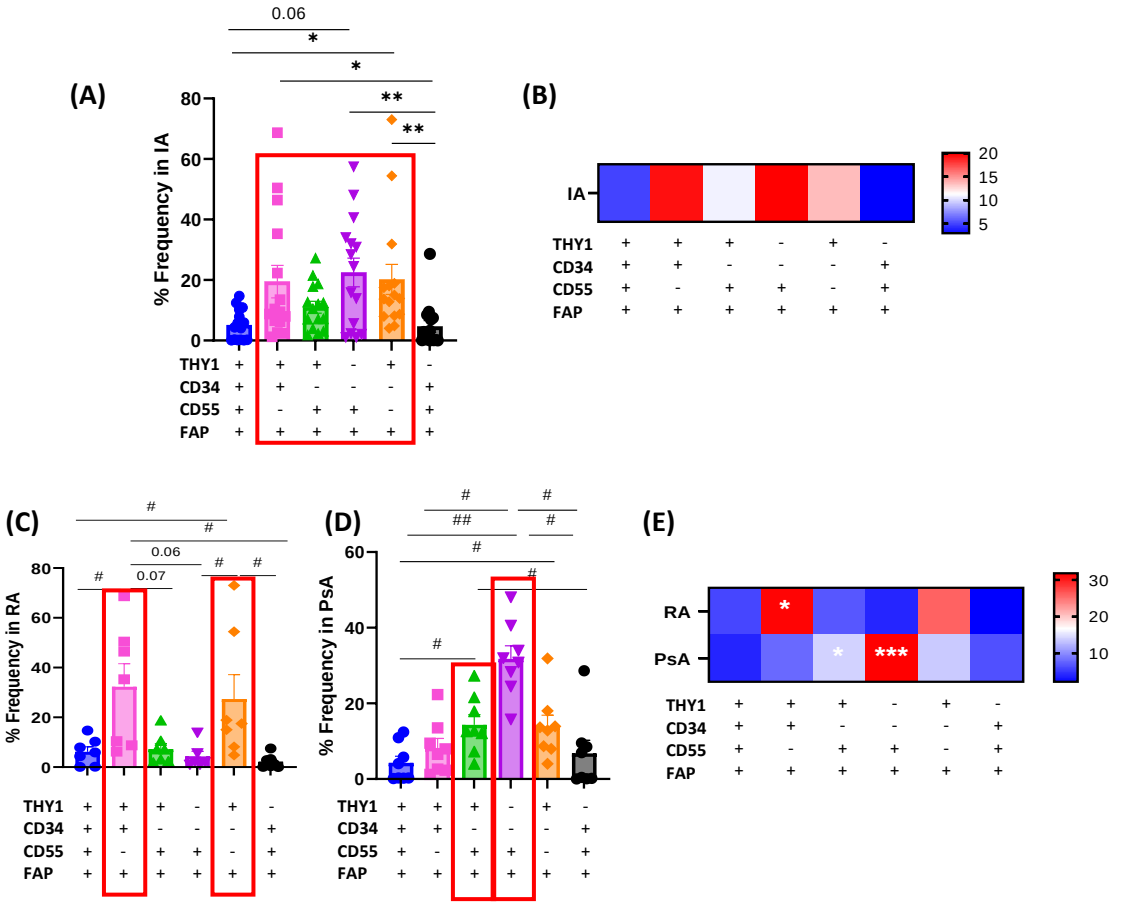

Figure 3.19. Differential expression of THY1 CD34 CD55 FAP+ expressing FLS clusters in RA vs PsA. Representative **(A)** bar graph and **(B)** accompanying heatmap demonstrating differences in the % frequency of the 6 populations identified by flow cytometric analysis in IA (n=15) based on the expression of THY1, FAP, CD34, and CD55. Bar graphs showing the % frequency of each of the 6 populations when separated out into disease status: **(C)** RA (n=7) and **(D)** PsA (n=8). **(E)** Representative heatmap demonstrating the mean % frequency of each population in the RA vs PsA cohorts. All data represented as Mean +/- SEM. Statistical analysis was performed using the non-parametric, Friedman's Test (*) or Wilcoxon Signed-Rank Test (#) with statistical significance defined by $*^{(\#)}$ p≤0.05, $**^{(\#\#)}$ p<0.01, $***^{(\#\#\#)}$ p<0.001.

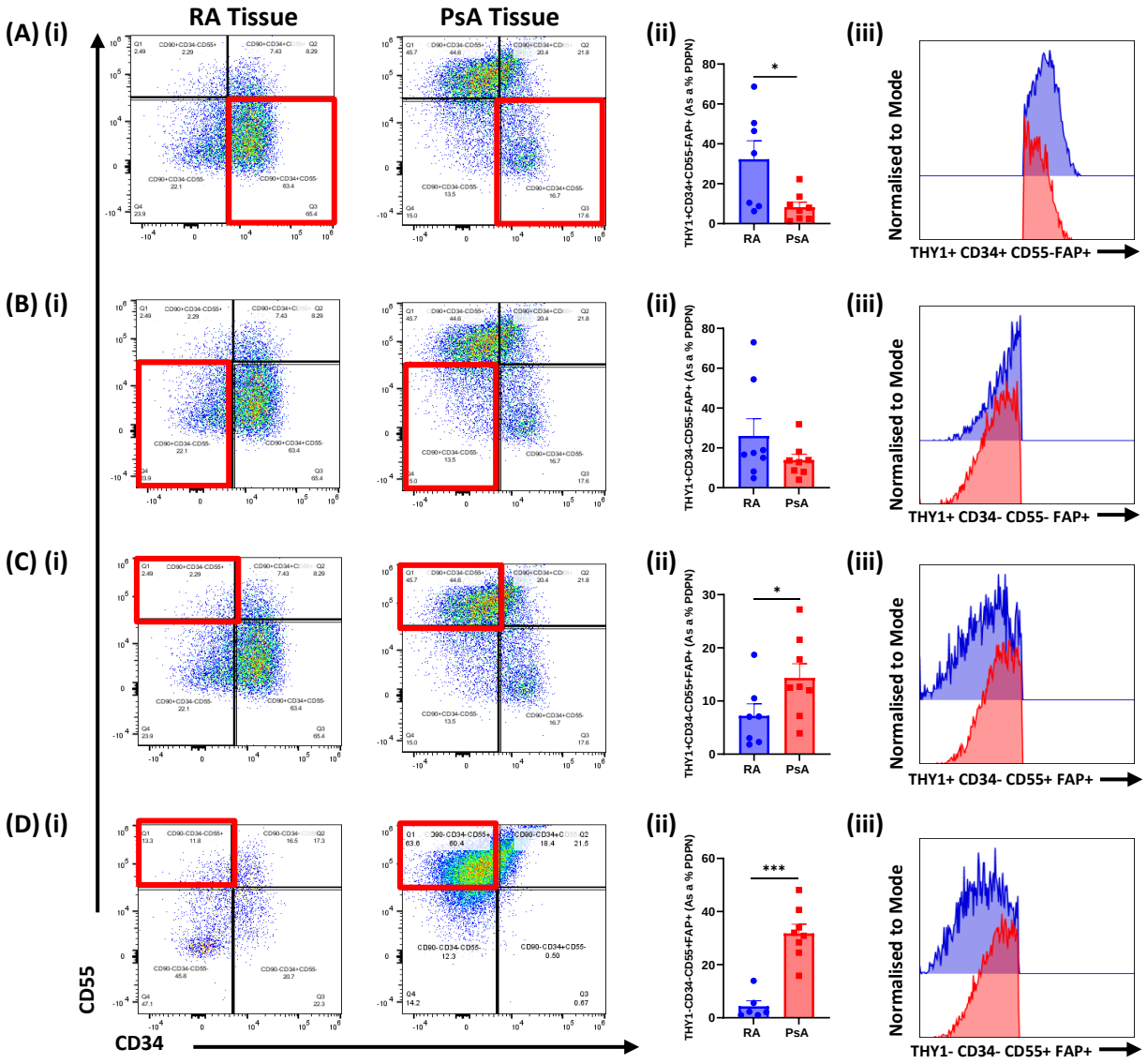

Figure 3.20. Differential expression of four THY1 CD34 CD55 FAP+ FLS populations in RA vs PsA. Representative **(i)** dot plots and **(ii)** accompanying bar graphs demonstrating differences in the % frequency of the 4 identified dominant populations **(A)** THY1+ CD34+ CD55- FAP+, **(B)** THY1+ CD34- CD55-FAP+, **(C)** THY1+ CD34-CD55+ FAP+, and **(D)** THY1- CD34- CD55+ FAP+ of FLS (as a % of PDPN) within RA (n=7) and PsA (n=8) biopsies. **(iii)** Representative histograms of the MFI of the indicated FLS populations **(A-D)** in RA and PsA synovial tissue. All data represented as Mean +/- SEM. The unpaired t-test and accompanying Mann-Whitney *U* Test was utilised to determine significance with *p<0.05, ***p<0.001 defined as statistically significant.

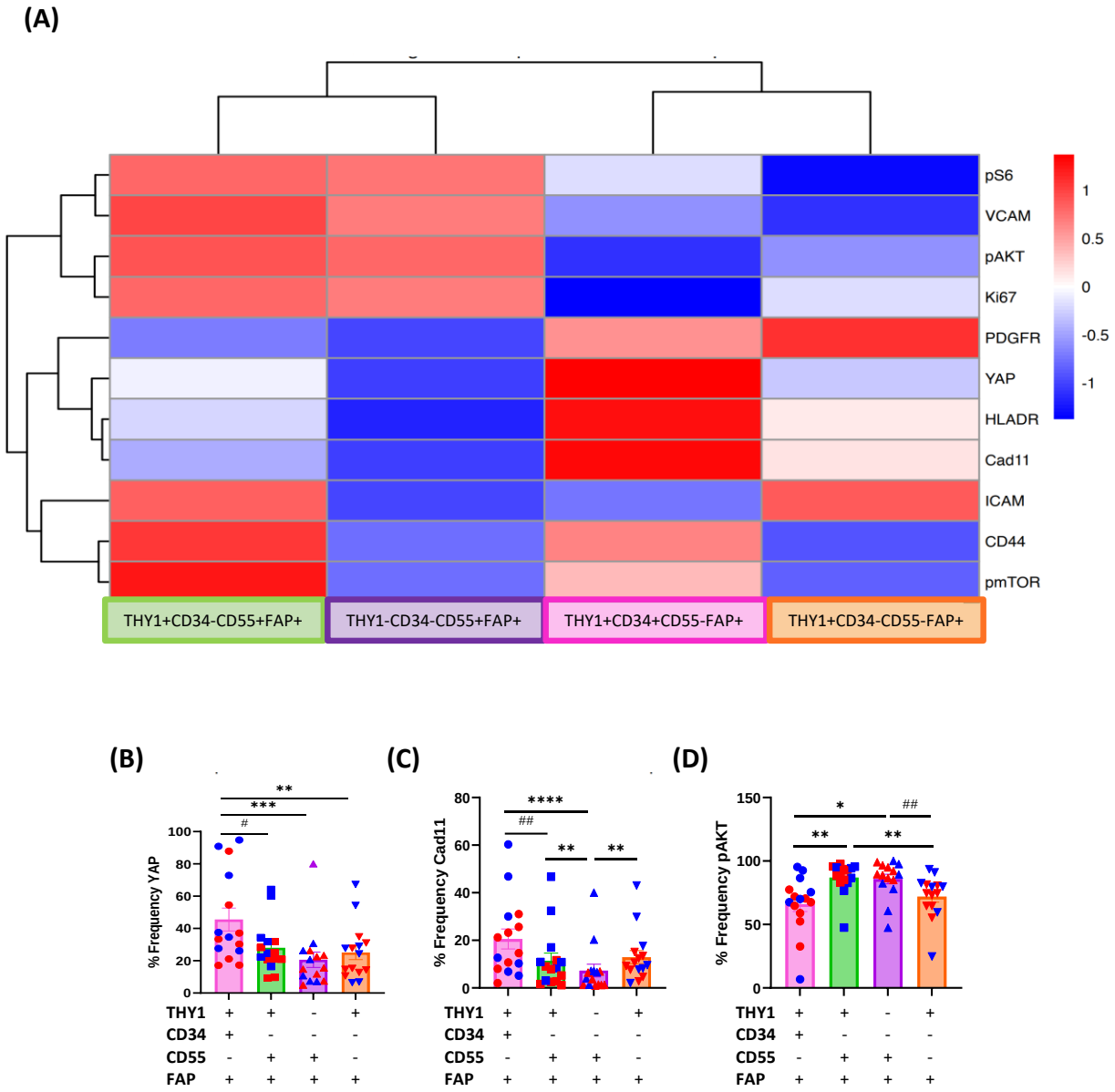

Figure 3.21. Potential differential function of THY1 CD34 CD55 FAP+ expressing FLS clusters enriched in RA and PsA synovium. (A) Hierarchical clustered heatmap representing the average expression of several functional, metabolic, and immune markers on the 4 dominant populations identified in IA as determined by flow cytometric analysis. The colour of the population title box indicates the matching population in the bar graphs. Bar graphs depicting significant differences in the % expression levels of **(B)** YAP, **(C)** Cad11, and **(D)** pAKT on RA and PsA FLS across the 4 dominant populations (n=15). All data represented as Mean +/- SEM. Statistical analysis was performed using the non-parametric, Friedman's Test (*) or Wilcoxon Signed-Rank Test (#) with statistical significance by $*^{(\#)}$ p≤0.05, $**^{(\#\#)}$ p<0.01, $***^{(\#\#\#)}$ p<0.001.

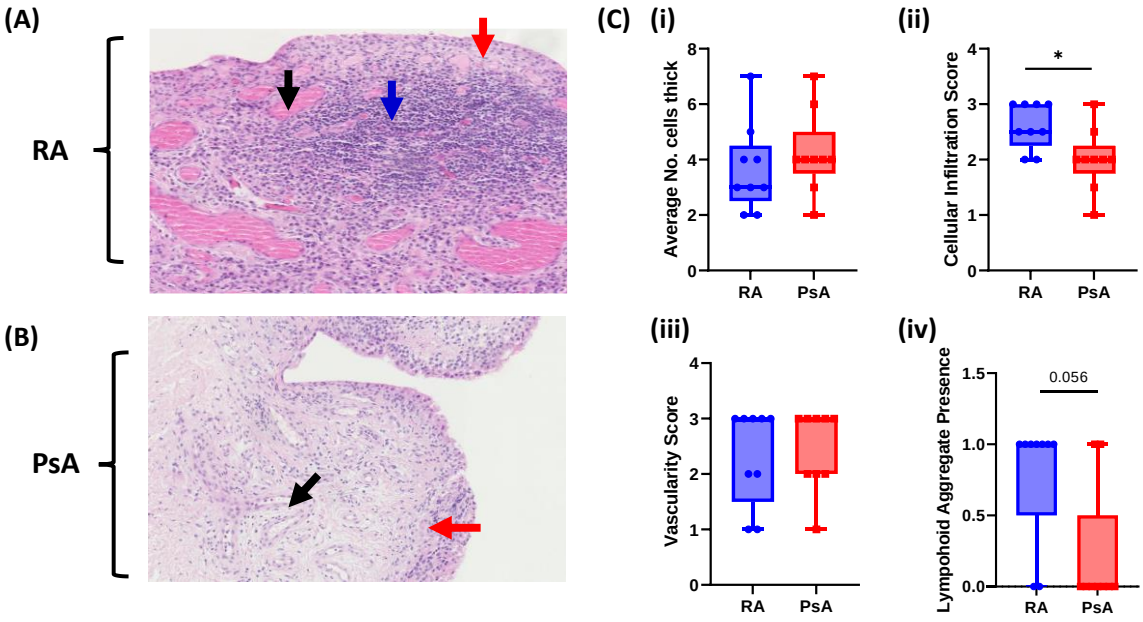

Figure 3.22. Histopathological differences in RA vs PsA synovial tissue. Representative hematoxylin and eosin staining of **(A)** RA and **(B)** PsA synovium showing intact tissue morphology and cell-cell contact with lining layer (red arrows), blood vessels (black arrows), lymphoid aggregates (blue arrow), and synovial infiltrate clearly visible at 10x magnification. Representative whisker and box plots depicting the **(C(i))** synovial lining thickness, **(C(ii))** cellular infiltration score, **(C(iii))** vascularity score, and **(C(iv))** presence of lymphoid aggregates in RA (n=10) and PsA (n=10) synovial biopsies. All data is represented as Minimum to Maximum. Statistical analysis was performed using the non-parametric, Mann-Whitney *U* Test with significance defined by *p≤0.05.

3.4.9 ScRNA-seq defines synovial tissue FLS heterogeneity between the two inflammatory states of RA and PsA.

Next, scRNA-seq profiling of 88,953 synovial tissue cells from patients with RA (n=4) and PsA (n=5) was conducted to provide a unique atlas of FLS phenotypes across both inflammatory disease states. The number of cells sequenced per donor and the clinical information of included patients at the time of arthroscopy are highlighted in the Appendix*, Table 6.1,* and *Table 6.2.* As demonstrated in Figure 3.23A, nonlinear, stochastic UMAP analysis identified sixteen distinct FLS subclusters in the IA synovial tissue. These distinct FLS clusters were further characterised utilising gene expression analysis of the top 20 DEGs per cluster alongside hierarchical clustering analysis (Figure 3.23B). As shown in Figure 3.23C, UMAPs investigating the expression of key lining versus sub-lining markers including THY1 and CD55 were created alongside a tree diagram (Figure 3.23D) which utilised the top genes expressed by each cluster to compare the similarities in gene expression and relationship between clusters. Utilising all of these modes of analysis (Figure 3.23A-D), classification into distinct subclusters was performed with initial delineation of the clusters into three primary categories – sub-lining (SL) with high THY1 expression, lining layer (LL) with high PRG4 and CD55 expression, and intermediate (INT), with the suggested grouping outlined in the labelled UMAP (Figure 3.24A) and the table (Figure 3.24B).

The sub-lining population contains two subclusters; CXCL12+ and POSTN+ (Cluster 3), with the latter possessing a cluster marker gene signature indicative of a central role in cytoskeletal and ECM regulation as denoted by high collagen gene expression (Figure 3.24B). Furthermore, the CXCL12+ subcluster could be further segregated based on distinct DEGs into VCAN+ (Cluster 1), IER2+ (Cluster 8), CHI3L2+ (Cluster 9), APOE+ (Cluster 10), and CCL2+ (Cluster 12), all clusters with gene signatures implicated in distinct functions related to ECM regulation, inflammatory responses, signalling regulation, and lipid metabolism (Tullai *et al.*, 2007; Wight *et al.*, 2020; Vogt *et al.*, 2020; Khmelevskaya *et al.*, 2024). Moreover, the lining layer population could be further subdivided based on cluster marker genes into three predominant phenotypes: an MMP group, homeostatic group, and an inflammatory group (Figure 3.24B). Firstly, the MMP group exhibited upregulated expression of genes involved in ECM turnover and tissue remodelling with classification into MMP1+ (Cluster 5), MMP3+ (Cluster 6), and TIMP1+ (Cluster 13) subclusters. The homeostatic group consisted of two clusters with high expression of genes related to the maintenance of homeostasis: CLIC5+ (Cluster 0) containing high expression of classical lining layer markers including PRG4 and CD55, and MTIG+ (Cluster 11) characterised by an abundance of genes related to heavy metal detoxification which have been shown to assist in immunosuppression in RA mouse models (Sun *et al.*, 2018a). Finally, the remaining lining layer

subgroup consisted of clusters associated with inflammatory gene signatures and could be subdivided into a CXCL8+ group (Cluster 2) with high chemoattractant gene expression, an INHBA+ group (Cluster 7) which has been associated with a 'pain-associated FLS' phenotype, and a CSN1S1+ group (Cluster 15) (Nanus *et al.*, 2021). Interestingly, CSN1S1 is typically expressed by monocytic cells where it drives the production of GM-CSF, suggesting that this particular cluster may be heavily influenced by interactions with infiltrating monocytes (Vordenbäumen *et al.*, 2011). From the cluster marker gene expression, it would suggest that these three lining clusters may play a role in modulating the proinflammatory joint microenvironment. The remaining FLS clusters were defined as intermediate due to their failure to be categorised distinctly based on their similarities to both sub-lining and lining layer gene expression in terms of THY1, CD55, and PRG4 (Figure 3.24B). For the first cluster, high expression of genes implicated in immune response regulation and antigen processing including HLA-DR and CD74 resulted in its designation as HLA-DR^{High} (Cluster 4). The final cluster was defined as TM4SF1+ (Cluster 14), with a gene signature associated with EMT. TM4SF1 itself has been shown to be expressed abundantly by ECs particularly, where it plays a role in promoting heightened angiogenesis in addition to invasion, migration, and proliferation of cancer cells, thus suggesting this cluster may be involved in interactions with ECs (Wei *et al.*, 2018). Cumulatively, a diverse range of phenotypically and functionally distinct FLS were identified in the lining and sub-lining layers of the inflamed joint in RA and PsA.

Subsequent analysis revealed differential frequency of the clusters when compared directly between RA and PsA with specific significant enrichment of the clusters THY1+POSTN+ (Cluster 3), CXCL12+CHI3L2+ (Cluster 9), and the CXCL12+APOE+ (Cluster 10) in RA, importantly all sub-lining clusters (Figure 3.24C and 3.24D). The exact location of these populations relative to each other are depicted in Figure 3.25A-C, with these UMAPs demonstrating that all three populations are in close proximity. Interestingly, two of these RA dominant clusters demonstrate enriched gene expression for the inflammatory chemokine CXCL12, highlighting their potential role in immune responses. Moreover, the THY1+ cluster characterised by enriched gene expression of POSTN, a gene encoding an ECM protein involved in adhesive and collagen formation roles, is not only significantly higher in RA compared to PsA but also demonstrates a high frequency in the synovial tissue suggesting this cluster is particularly important and may assume a major role in RA pathogenesis (Figure 3.24D). Conversely, the lining layer clusters CLIC5+ and MMP3+ were enriched in PsA, alongside the intermediate cluster denoted as HLA-DRA^{High} (Figure 3.24C and 3.24D). The remaining clusters were comparable in expression between RA and PsA (Figure 3.24D).

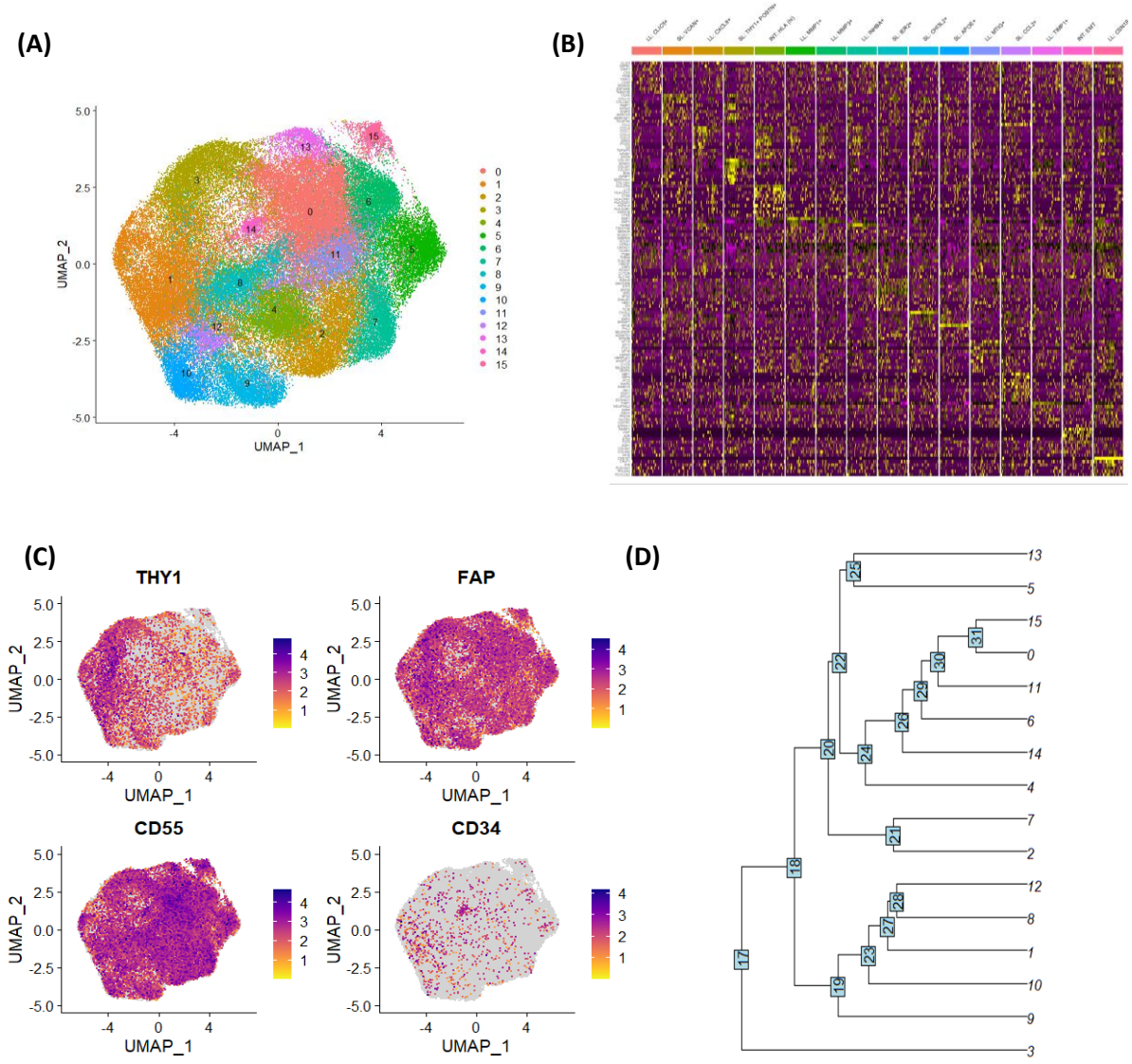

Figure 3.23. scRNA-seq defines FLS heterogeneity in IA synovial tissue. (A) UMAP representation of sixteen synovial tissue FLS clusters based on 88,953 synovial tissue cells from RA (n=4) and PsA (n=5) synovial tissue biopsies, identified by high dimensionality scRNA-seq analysis. **(B)** Representative heatmap of the top 20 DEGs per identified cluster. **(C)** UMAPs representing the expression of the classic FLS population markers THY1, FAP, CD55, and CD34 across all clusters. **(D)** Hierarchical clustering of the human synovial tissue FLS.

(A)

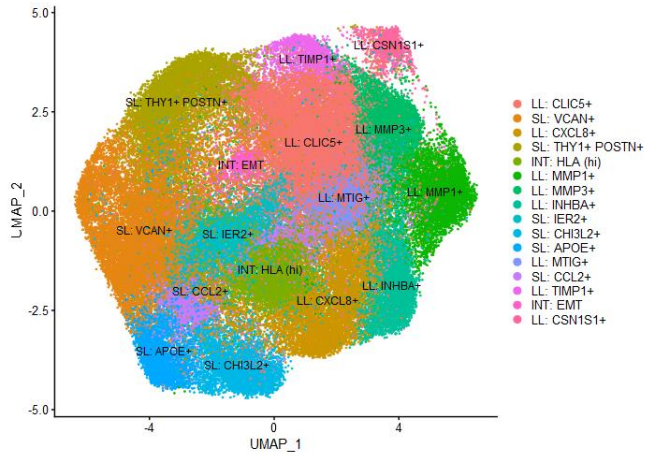

(B)

Sublining vs Lining	Subpopulation	Cluster (Cluster No.)
THY1^{High} Sublining (SL)	POSTN+	THY1+POSTN+ (3)
	CXCL12+	VCAN+ (1)
		IER2+ (8)
		CHI3L2+ (9)
		APOE+ (10)
		CCL2+ (12)
THY1^{Low} PRG4^{High} Lining Layer (LL)	MMP Group	MMP1+ (5)
		MMP3+ (6)
		TIMP1+ (13)
	Homeostatic Group	CLIC5+ (0)
		MTIG+ (11)
	Immune Regulation	INHBA+ (7)
		CXCL8+ (2)
		CSN1S1+ (15)
Intermediate (INT)	HLADRA^{High} (4)	
	TM4SF1+ EMT (14)	

(C)

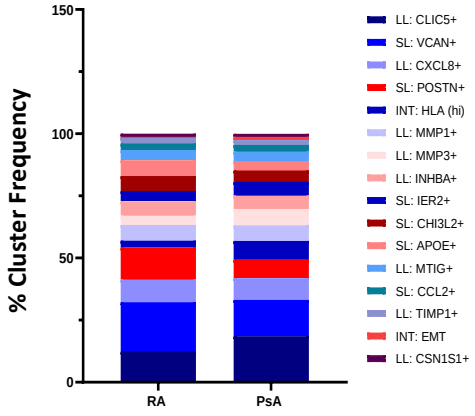

(D)

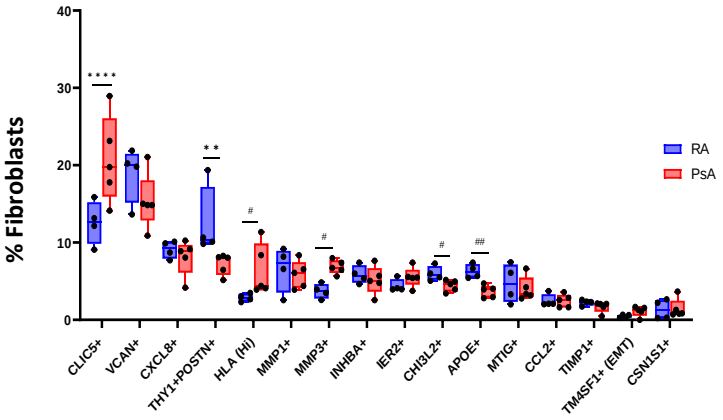

Figure 3.24. Differential frequency of scRNA-seq identified FLS clusters between RA and PsA. (A) UMAP representation of the 16 synovial tissue FLS with their proposed taxonomy attached. **(B)** More detailed table outlining the proposed classification of the FLS clusters into lining (LL), sub-lining (SL), and intermediate (INT) groups and then further subclusters based on cluster marker gene expression. Clusters were defined by Órla Tynan and Aenea Brugman. **(C)** Proportional cluster abundance and **(D)** representative box and whisker plot depicting differences in the frequency of the specific clusters between RA (n=4) and PsA (n=5) The two-way ANOVA with Sidak's Multiple Comparisons Test (*) and Mann-Whitney Test ($^{\#}$) was utilised to determine significance with *$^{(\#)}$p<0.05, **$^{(\#\#)}$p<0.01,***p<0.001, ****p<0.0001 defined as statistically significant.

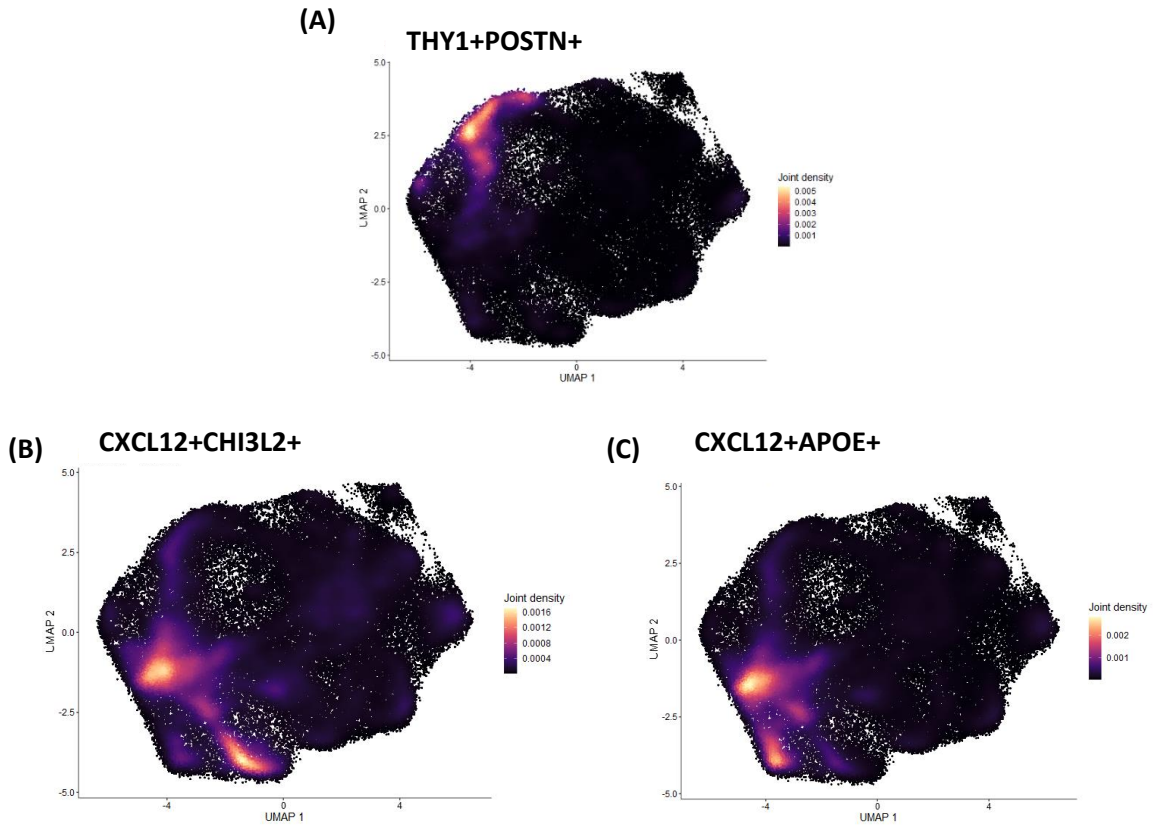

Figure 3.25. Visualization of the location of the RA enriched sub-lining clusters. (A) UMAP illustrating THY1+POSTN+ mRNA expression in synovial tissue FLS. **(B)** UMAP illustrating CXCL12+CHI3L2+ mRNA expression in synovial tissue FLS. **(C)** UMAP illustrating CXCL12+APOE+ mRNA expression in synovial tissue FLS.

3.4.10 Differential function of scRNA-seq identified THY1+POSTN+ FLS cluster in RA vs PsA.

Further analysis focused specifically on the RA enriched sub-lining THY1+POSTN+ cluster to further characterise the function of this cluster and to additionally determine if RA and PsA FLS within this cluster exhibit different functional properties. Initial pathway enrichment analysis identified several pathogenic pathways associated with this cluster that were enriched in RA FLS of the THY1+POSTN+ cluster compared to the PsA FLS including oxidative phosphorylation, MAPK signalling, and the Hippo signalling pathway (Figure 3.26A). Common genes and the differential expression of specific members of the NF-κB signalling pathway, the VEGF signalling pathway, the Hippo signalling pathway, and focal adhesions, in RA vs PsA THY1+POSTN+ FLS are depicted in Figure 3.26B, with blue colour indicating genes that are upregulated in RA compared to PsA in this specific cluster. As demonstrated by the violin plots, bioinformatic characterisation of gene modules based on metabolic reference pathways deposited on KEGG revealed on a transcriptional level an enhanced level of oxidative phosphorylative (Figure 3.26C(i)) and glycolytic (Figure 3.26C(ii)) involvement in RA FLS of the THY1+POSTN+ cluster compared to the PsA FLS. Conversely, fold change related to osteoclast differentiation genes were greater in the PsA FLS of the THY1+POSTN+ cluster implying a more bone degradative involvement of this cluster in PsA compared to RA (Figure 3.26C(iii)). Cumulatively, these results suggest that on a highly specific cluster scale, differences in frequency in addition to differences in the functionality of FLS of the same cluster can be detected between RA and PsA disease states.

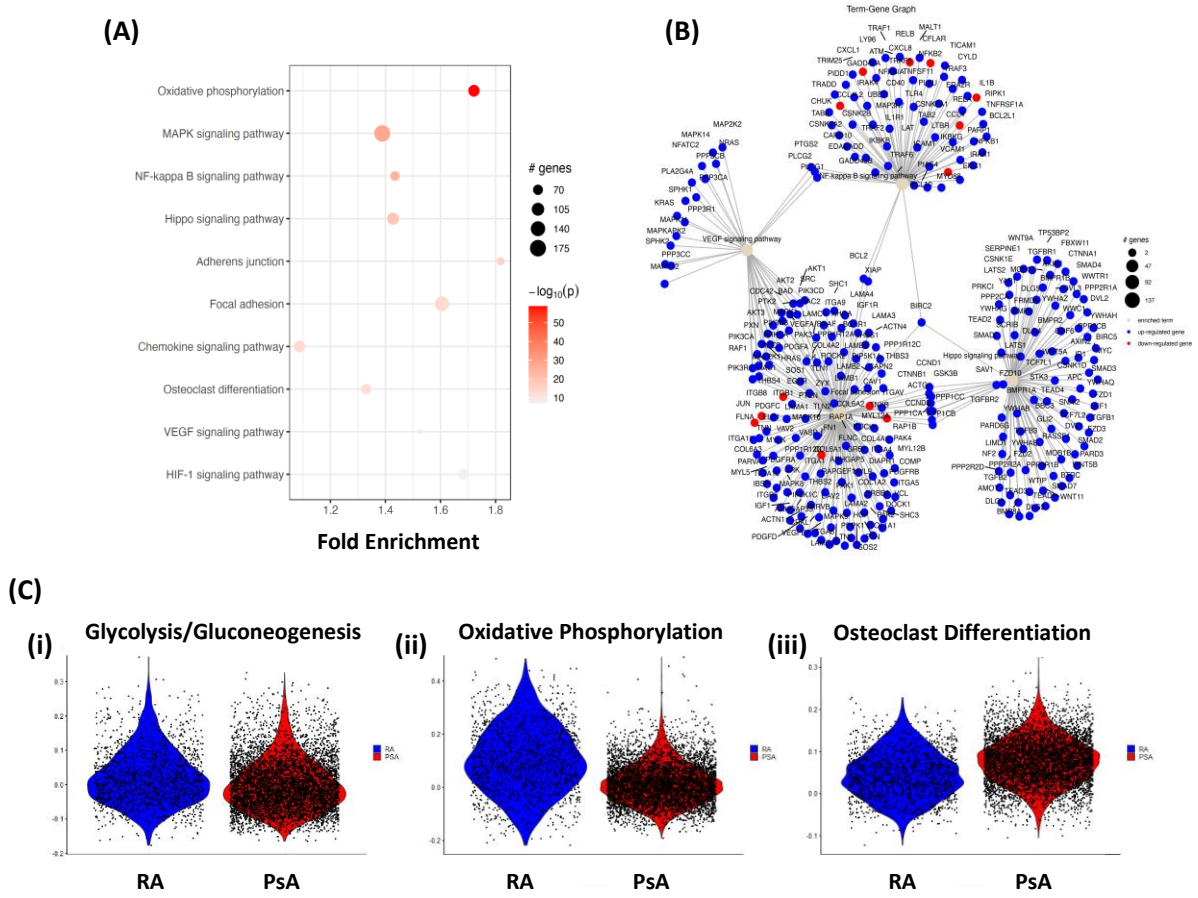

Figure 3.26. Functional pathway analysis of scRNA-seq identified THY1+POSTN+ FLS cluster in RA vs PsA. (A) Analysis of pathways enriched in THY1+POSTN+ FLS in RA (n=4) and PsA (n=5) synovial tissue, colour intensity represents significance and dot size denotes the number of genes within each pathway that are differentially expressed. **(B)** Term plot of the indicated pathways with significant enrichment in RA compared to PsA FLS. Blue colour indicates upregulation of specific genes and red color indicates downregulation of specific genes within the pathway in RA compared to PsA. Dot size represents statistical significance of change. **(C)** Violin plots representing the expression scores of gene modules related to **(i)** glycolysis, **(ii)** oxidative phosphorylation, and **(iii)** osteoclast differentiation genes in the THY1+POSTN+ cluster in RA vs PsA.

3.4.11 Differential expression of invasive mediators may influence RA and PsA P0 FLS migratory capacity.

Next, to further explore functional differences in RA and PsA FLS and to determine if the identified unique transcriptional and phenotypic profiles of FLS are retained following removal from the joint microenvironment, several *ex vivo* experiments on P0 FLS were performed. Firstly, to investigate the potential differential migratory behaviour of RA and PsA FLS under baseline conditions, the data was interrogated at the RNA level using bioinformatic scRNAseq. As shown visually in the UMAPs, the PsA FLS clusters demonstrated a higher level of expression of key mediators responsible for facilitating FLS invasion through ECM degradation; MMP-1 (Figure 3.27A(i)) and MMP-3 (Figure 3.27A(ii)). Further quantification of both MMP-1 and MMP-3 in P0 expanded FLS was performed using RT-PCR and an MSD Multiplex ELISA Assay. Figures 3.27B(i) and 3.27C(i), demonstrate a significant increase in MMP-1 and MMP-3 mRNA expression respectively (both $p<0.05$) in PsA FLS compared to RA FLS at P0. This trend was mirrored at the protein levels where both MMP-1 (Figure 3.27B(ii)) and MMP-3 (Figure 3.27C(ii)) were higher in PsA FLS compared to RA FLS, although not reaching significance.

The data suggests that PsA FLS at P0 may intrinsically possess more migratory and invasive characteristics compared to RA, and also demonstrates that at P0 they do maintain some of their *in vivo* characteristics as highlighted in the scRNA-seq.

3.4.12 PsA FLS at P0 demonstrate a stronger preference for glycolysis over oxidative phosphorylation compared to RA FLS.

Using the Seahorse XFe-Analyser, real-time oxidative phosphorylation and glycolysis were examined, in order to assess potential differences in P0 RA and PsA FLS metabolic capacity under basal conditions. The overall energy map in Figure 3.28A demonstrates that both RA and PsA FLS exhibit similar average metabolic profiles under baseline conditions, with a slightly higher preference for glycolysis in the PsA FLS. This was further corroborated by the trending increase in baseline ECAR in the PsA FLS (Figure 3.28B) in addition to the ECAR:OCR ratio which exhibited a trend towards an increase in PsA compared to RA, suggesting a greater preference for glycolysis over oxidative phosphorylation in these cells (Figure 3.28D). Conversely, baseline OCR (Figure 3.28C), ATP synthesis (Figure 3.28E), and the maximal respiratory capacity (Figures 3.28F) demonstrated a trend towards an increase in RA. Next, using RNA isolated from unstimulated RA and PsA at P0, the gene expression of several key enzymes and mediators directly implicated in the glycolytic pathway were analysed by RT-PCR. Although significance was not reached, as

demonstrated in the bar graphs (Figure 3.28G(i-v)) and accompanying heatmap (Figure 3.28(vi)), a trend towards an increase in the expression of HIF-1α ($p<0.07$), HK2, PKM2, GLUT-1, and GAPDH in the PsA FLS compared to their RA counterparts was identified.

However, addition of IL-1β stimulation had an interesting effect. Whilst the cytokine introduction appeared to exert a similar reduction on the oxidative phosphorylative activity of the RA and PsA P0 FLS compared to basal (Figure 3.29A), a greater impact on the glycolytic metabolic activity of the RA FLS compared to PsA was observed, with a significant increase in ECAR from baseline following stimulation in RA but not PsA (Figure 3.29B). Moreover, whilst a significant increase in the ECAR:OCR ratio from basal was detected in both disease states (Figure 3.29C), the average bioenergetic profile and energy map clearly depicts a greater shift towards an energetic profile in RA compared to PsA following IL-1β addition (Figure 3.29D-E). Cumulatively, the data suggests that at baseline PsA FLS may favour glycolysis over oxidative phosphorylation for energy production compared to RA. However, when an inflammatory stimulus is introduced, the RA FLS demonstrate a greater metabolic response resulting in a robust increase in the glycolytic pathway than that observed in PsA.

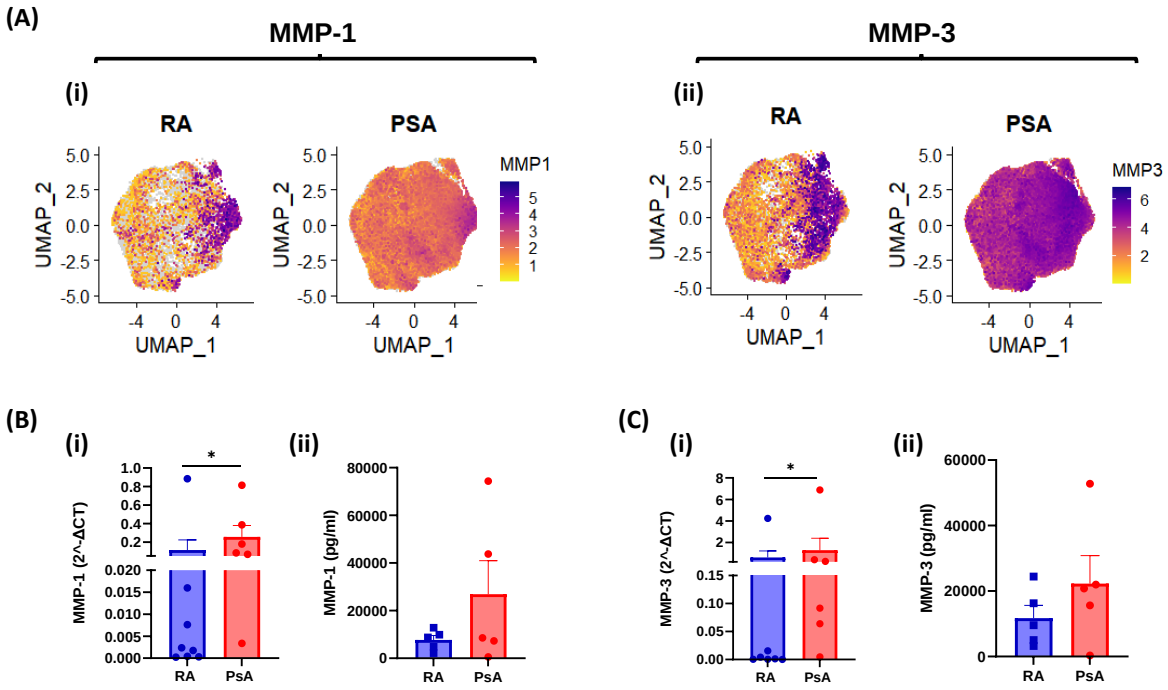

Figure 3.27. PsA FLS at P0 exhibit a greater expression of invasive mediators MMP-1 and MMP-3 than RA FLS. UMAP representation depicting gene expression of invasive mediators **(A(i))** MMP-1 and **(A(ii))** MMP-3 in PsA vs RA FLS using scRNA-seq analysis. Bar graphs showing quantification of gene mRNA expression of **(B(i))** MMP-1 and **(C(i))** MMP-3 in unstimulated RA and PsA FLS (n=6-7). Normalization to the housekeeping gene RPLP0 was used to generate δct values. Bar graph representations of the level of secretion of **(B(ii))** MMP-1 and **(C(ii))** MMP-3 in RA and PsA FLS (n=5) as determined by an MSD assay. All data represented as Mean +/- SEM. Statistical analysis was performed using the non-parametric, Mann-Whitney *U* Test with statistical significance defined by *p≤0.05.

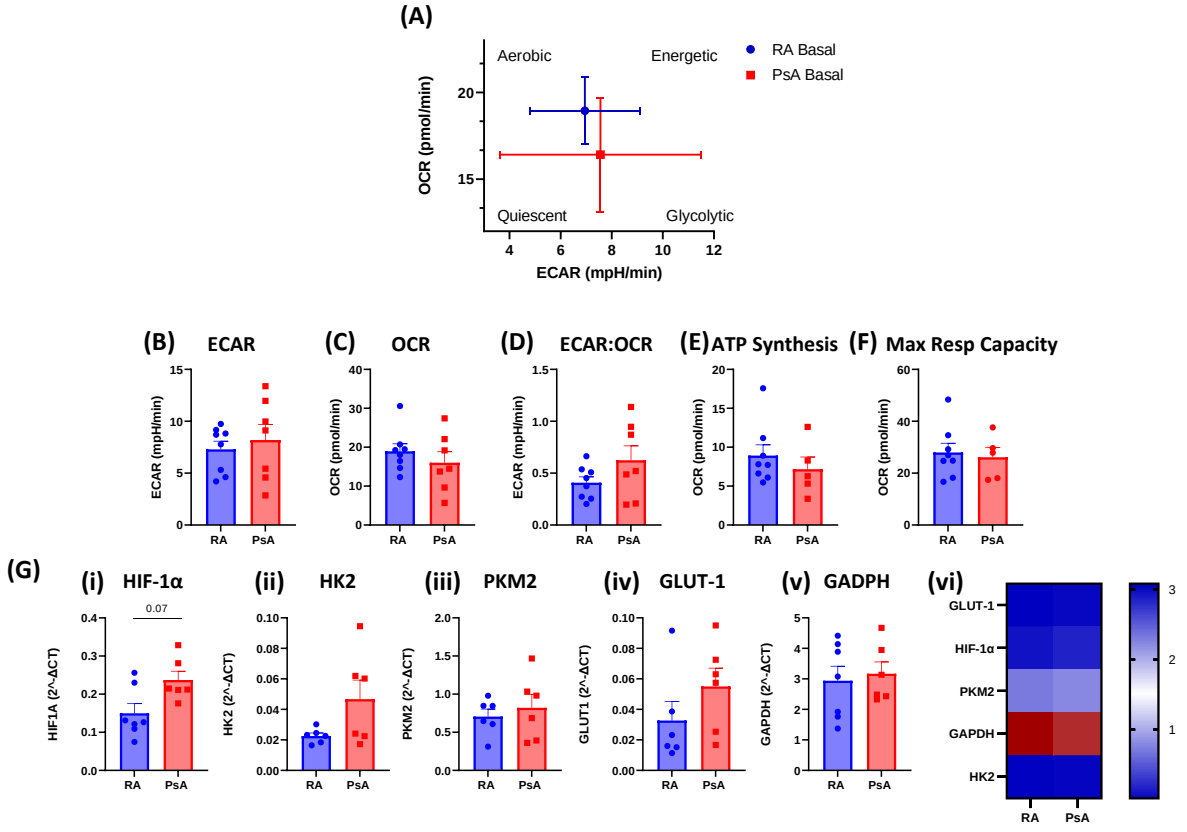

Figure 3.28. PsA FLS demonstrate a greater preference for glycolysis at P0 compared to RA FLS. **(A)** Representative energy map depicting the differences in the overall energy profile of RA (n=8) and PsA (n=7) P0 FLS under basal conditions as determined by Seahorse metabolic analysis before and after injections of oligomycin, FCCP, and antimycin A/rotenone. Quantitative bar graphs demonstrating the **(B)** baseline ECAR, **(C)** baseline OCR, **(D)** baseline ECAR:OCR ratio, **(E)** ATP synthesis, and **(F)** maximum respiratory capacity in the P0 RA and PsA FLS under basal conditions before and after injections of the metabolic inhibitors. **(G)** Representative bar graphs and accompanying heatmap **(vi)** showing quantification of gene mRNA expression of **(i)** HIF-1α, **(ii)** HK2, **(iii)** PKM2, **(iv)** GLUT-1, and **(v)** GAPDH in RA (n=7) and PsA (n=6) FLS under baseline conditions. Data is represented as δct, normalized to housekeeping control RPLP0. All data represented as Mean +/- SEM. Statistical analysis was performed using the non-parametric, Mann-Whitney *U* Test with statistical significance defined by *p≤0.05.

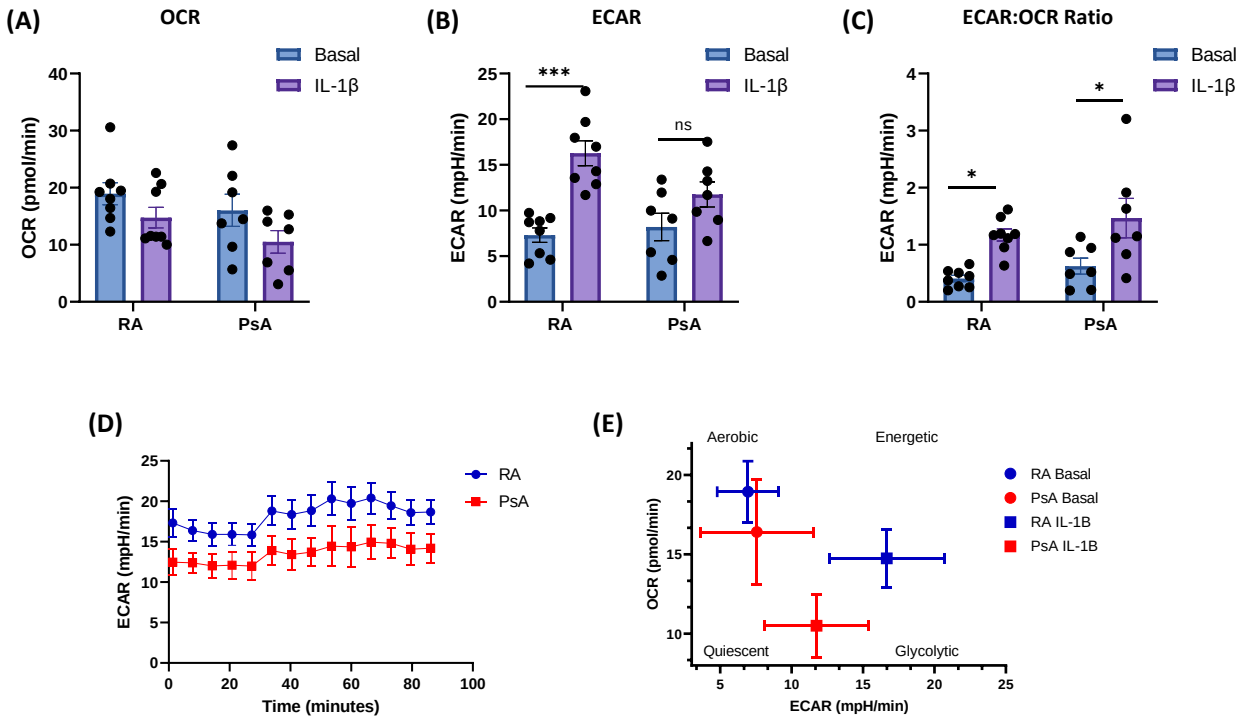

Figure 3.29. RA FLS at P0 demonstrate a more robust glycolytic response to IL-1β stimulation compared to PsA FLS. RA (n=8) and PsA (n=7) FLS at P0 were stimulated with IL-1β (1 ng/ml) for 24 h before seahorse metabolic analysis was performed. Quantitative bar graphs depict the changes in **(A)** baseline OCR, **(B)** baseline ECAR, and **(C)** ECAR:OCR ratio in the basal versus cytokine treated P0 RA and PsA FLS before and after injections of the metabolic inhibitors. **(D)** Average ECAR profile of RA (n=8) and PsA (n=7) FLS at P0 before and after injections of oligomycin, FCCP, and antimycin A/ rotenone. **(E)** Representative energy map depicting the differences in the overall energy profile of RA and PsA P0 FLS from baseline following IL-1β stimulation as determined by Seahorse metabolic analysis. All data represented as Mean +/- SEM. The 2-Way ANOVA with Turkey's Multiple Comparison's Test was used to determine significance with *p<0.05 and ***p<0.001 defined as statistically significant.

3.4.13 Comparison in the levels of angiogenic mediators and chemotactic factors in the supernatants of RA and PsA P0 FLS.

Previous literature has highlighted that whilst angiogenesis is a hallmark characteristic of both RA and PsA, the structure and relative abundance of newly formed blood vessels differs significantly (Veale and Fearon, 2015; Fromm *et al.*, 2019). Therefore, to explore if this may be related to differential levels of angiogenic mediators being released by the FLS, an angiogenic MSD assay was conducted using the previous collected supernatants. Interestingly, although the results were highly donor specific as demonstrated by the representative heatmap (Figure 3.30A), bFGF was significantly higher ($p<0.01$) in the PsA supernatants compared to RA as shown in Figure 3.30C(i), whilst VEGF-D and VEGF-C exhibited the opposite with slightly elevated expression in RA (Figure 3.30B). Moreover, the remainder of the angiogenic mediators including VEGF-A and FLT1, exhibited trending increases in PsA compared to RA, as shown collectively in Figure 3.30B and individually in the bar graphs (Figure 3.30C(ii-iii)). Thus, it can be inferred from the data that the differential production of angiogenic drivers from RA and PsA FLS may contribute in part to the stark difference in blood vessel patterns observed at the macroscopic level.

Furthermore, a critical perpetuator of the inflammatory process in RA and PsA is the recruitment and infiltration of circulating immune cells into the hypoxic joint microenvironment in response to chemotactic gradients (Veale and Fearon, 2018; Alivernini, Firestein and McInnes, 2022). Thus, analysis of chemokines being produced from FLS in the RA vs PsA synovium may provide us with further insights into their differential function in regard to inflammation. To achieve this objective, supernatants were collected from unstimulated RA and PsA FLS at P0 and subjected to MSD analysis examining a wide array of chemokines. As demonstrated in the heatmap (Figure 3.31A) and representative bar graph (Figure 3.31B), although highly donor dependent, the levels of MCP-1, MCP-4, Eotaxin, MIP-1α, MIP-1β, MDC, and TARC, were relatively similar between both arthropathies. However, there was a trending increase in IL-8 (Figure 3.31C(i)) and Eotaxin-3 (Figure 3.31C(ii)) levels in PsA compared to RA, whilst conversely, IP-10 (Figure 3.31C(iii)) appeared to be trending higher in RA supernatants. These results suggest that whilst both RA and PsA FLS demonstrate the capacity to recruit an abundance of peripheral immune cells, there may be a variation in the specific type of immune cells that preferentially accumulate in the joint.

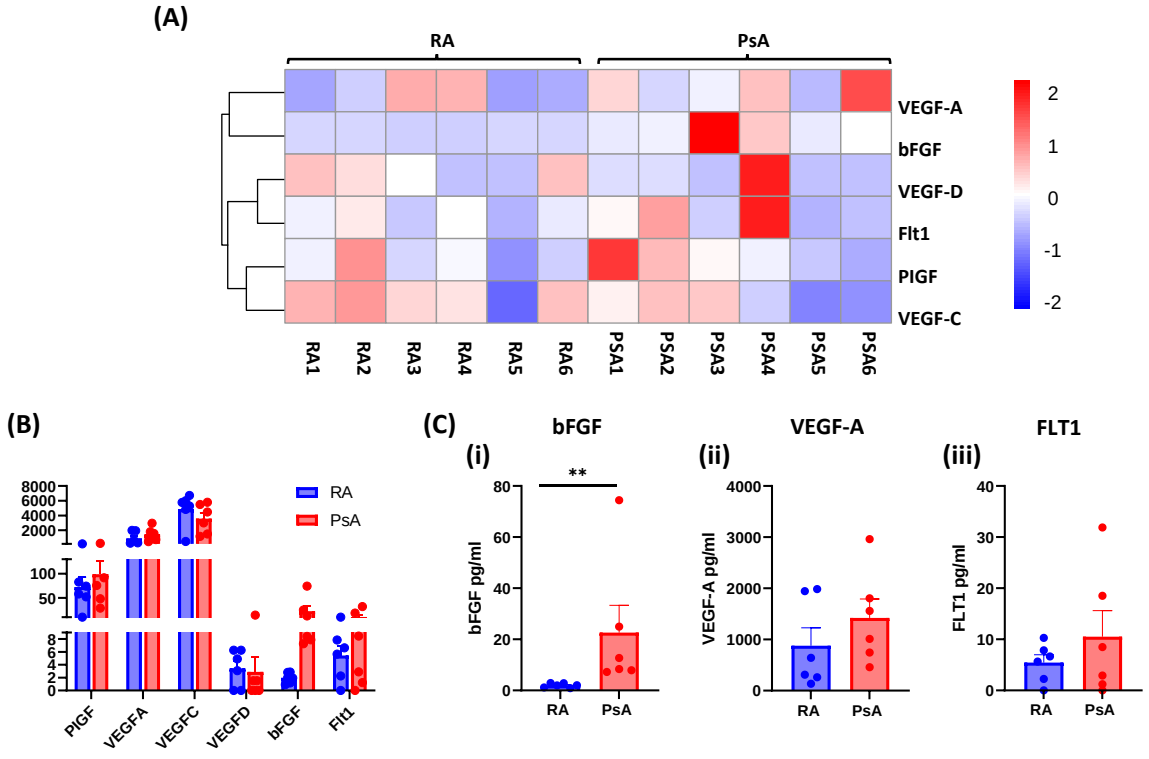

Figure 3.30. Higher expression of angiogenic mediators in the supernatants of PsA FLS at P0 compared to RA. RA and PsA FLS (n=6 respectively) were digested before supernatants were then collected from the cells at P0 under baseline conditions and subjected to an MSD angiogenic-panel analysis. **(A)** Clustered heatmap depicting the scaled expression of angiogenic factors in the supernatants of the P0 RA and PsA FLS, separated out across the individual donors. **(B)** Bar graph showing the expression levels of angiogenic mediators in the supernatants of the unstimulated RA and PsA FLS at P0. **(C)** Representative bar graphs demonstrating differences in the expression of **(i)** bFGF, **(ii)** VEGF-A, and **(iii)** Flt1 in RA and PsA FLS at P0. All data represented as Mean +/- SEM. Statistical analysis was performed using the non-parametric, Mann-Whitney *U* Test with statistical significance defined by **p<0.01.

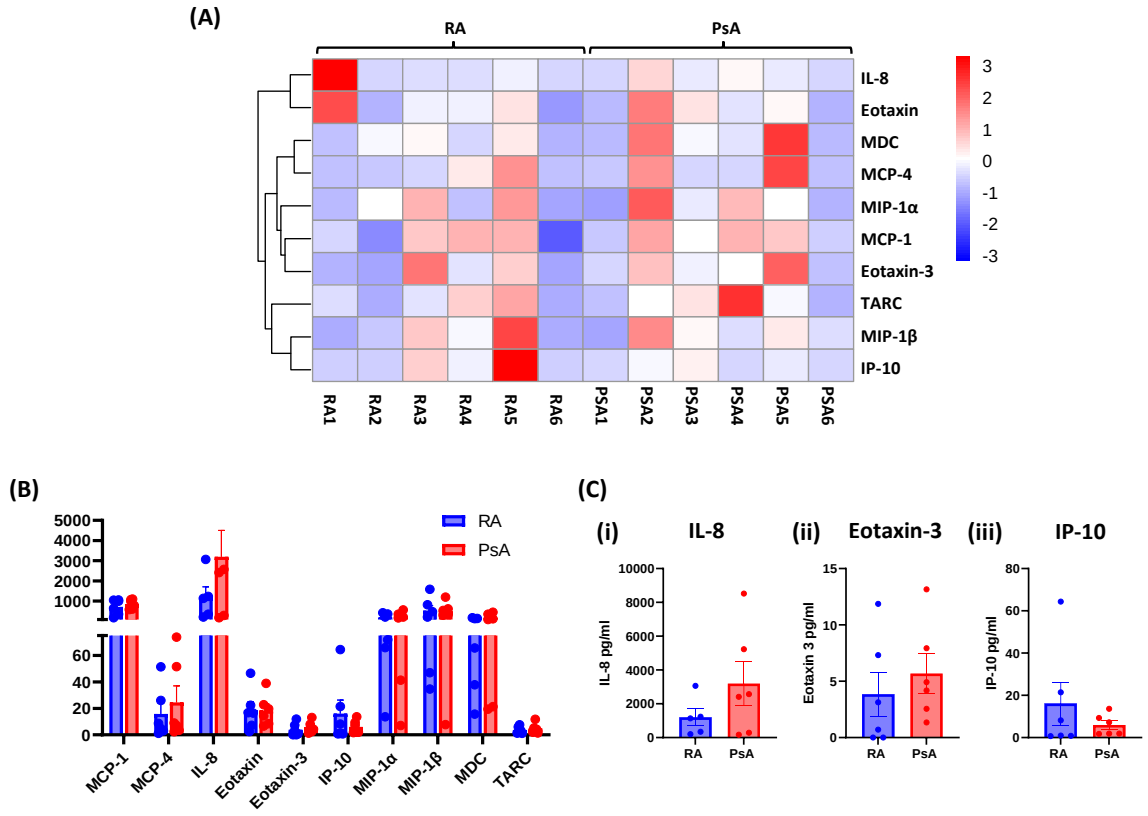

Figure 3.31. Comparable expression of chemokines in the supernatants of RA and PsA FLS at P0. RA and PsA FLS (n=6 respectively) were digested before supernatants were then collected from the cells at P0 under baseline conditions and subjected to an MSD chemokine-panel analysis. **(A)** Clustered heatmap depicting the scaled expression of chemokine factors in the supernatants of the P0 RA and PsA FLS, separated out across the individual donors. **(B)** Bar graph depicting the expression levels of the panel of chemokines in the supernatants of the unstimulated RA and PsA FLS at P0. **(C)** Representative bar graphs demonstrating differences in the expression of **(i)** IL-8, **(ii)** Eotaxin-3, and **(iii)** IP-10 in RA and PsA FLS at P0. All data represented as Mean +/- SEM.

3.4.14 RA and PsA FLS demonstrate differences in the expression level of key functional and activation markers across passages 0, 1, and 2.

In order to determine if FLS phenotype is transient and may be altered once removed from the joint microenvironment and across serial passaging, flow cytometric analysis was conducted. RA and PsA FLS were frozen down across consecutive passages – P0, P1, and P2, and then thawed and stained for the markers HLA-DR, CD55, CD34, and CD54. Representative flow plots of the gating strategy are shown in Figure 3.21A-H. Following the elimination of debris and cell doublets (Figures 3.32A-C), live cells were gated on (Figure 3.32D) before haematopoietic cells (Figure 3.32E) and ECs (Figure 3.32F) were excluded and FLS were finally identified as being PDPN+ (Figure 3.32G), thus allowing the specific markers to be analysed on the PDPN+ cells (Figure 3.32H).

Representative dot plots for FMO control (Figure 3.33A) and a stained RA (Figure 3.33B(i)) and PsA (Figure 3.33B(ii)) synovial tissue across P0-2 for HLA-DR are shown. As demonstrated by the histograms representing MFI (Figure 3.33C(i-ii)) and quantitative bar charts of frequency (Figure 3.33D(i)) and MFI (Figure 3.33D(ii)), HLA-DR shows a trend towards a decrease in expression in both RA FLS and PsA FLS across increasing passages, although the reduction in expression was greater in PsA than RA (Figure 3.33E(i-ii)). Moreover, representative dot plots for FMO control (Figure 3.34A) and a stained RA (Figure 3.34B(i)) and PsA (Figure 3.34B(ii)) synovial tissue across P0-2 for CD55 are demonstrated. Similarly to HLA-DR, there was also a significant decrease in CD55 frequency and MFI across the three passages ($p<0.05$) (Figure 3.34D(i-ii)), with a comparable reduction between both disease states (Figure 3.34E(i-ii)).

Furthermore, Figure 3.35A demonstrates representative dot plots for FMO control and a stained RA (Figure 3.35B(i)) and PsA (Figure 3.35B(ii)) synovial tissue across P0-2 for CD34. In contrast to the previous markers, as shown in Figure 3.35D(i-ii), CD34 demonstrated a trending increase in expression frequency and MFI (both $p<0.06$) for both RA FLS and PsA FLS from P0 to P3, with similar increases seen between the two disease states (Figure 3.35E(i-ii)). Moreover, the exact same trend was observed in relation to the expression of CD54 (Figure 3.36). As demonstrated in Figure 3.36D(i-ii), the expression and MFI of CD54 exhibited elevated levels across the consecutive passages with similar increases seen once again between both disease states (3.36E(i-ii)). Cumulatively, these results indicate that both RA and PsA FLS alter their phenotypic profiles across passages, with a loss/gain of markers once removed from the inflammatory influences of the joint microenvironment.

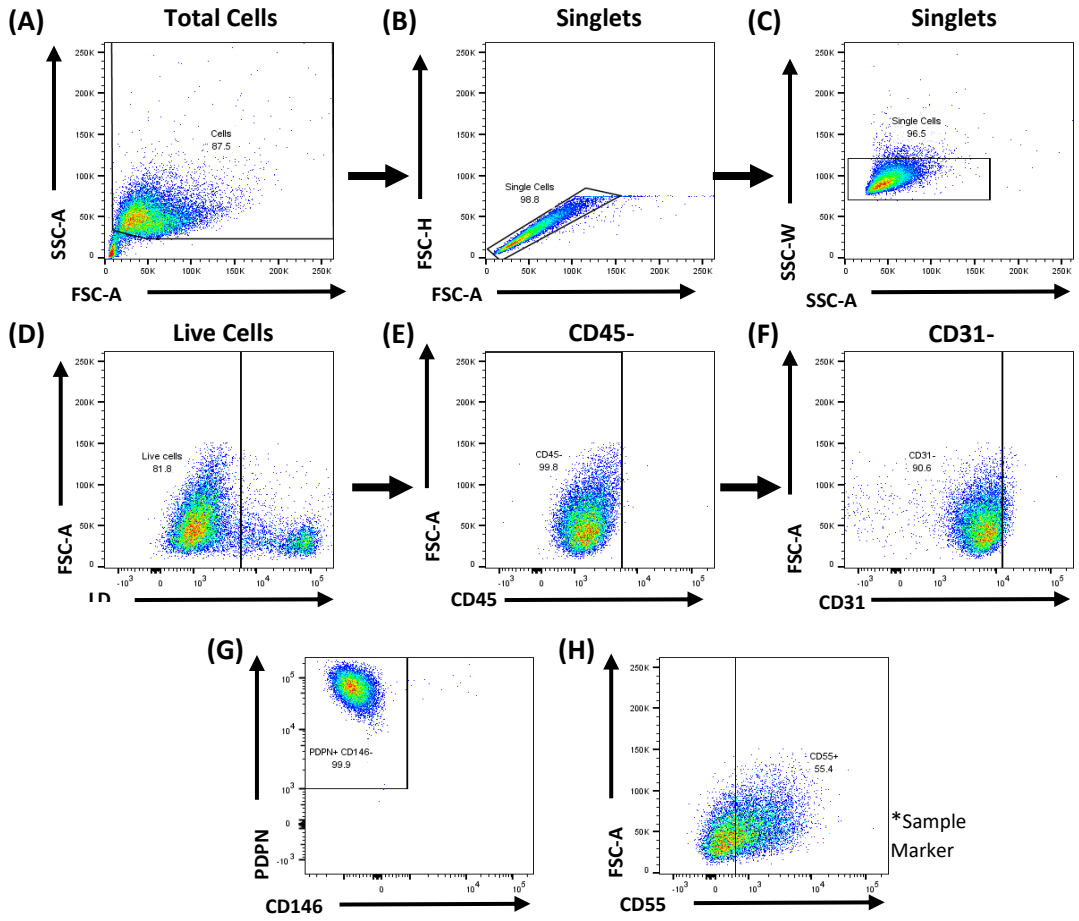

Figure 3.32. Gating strategy to identify expression of key activation and functional markers on RA vs PsA FLS at P0, P1, and P2. RA and PsA FLS, frozen down in 10% DMSO across serial passages – P0, P1, and P2, were thawed and multiparametric flow cytometric analysis was performed. Representative dot plots demonstrating the gating strategy for the identification of % frequency of marker expression on RA and PsA FLS at baseline (n=3 for each disease at each passage). **(A) – (D)** The forward and side scatter parameters of cells were set before doublet exclusion and elimination of dead cells. **(E)** Haematopoietic cells and **(F-G)** ECs/pericytes were then excluded and FLS were then identified as being PDPN+ and further gated for **(H)** CD55 as an example marker.

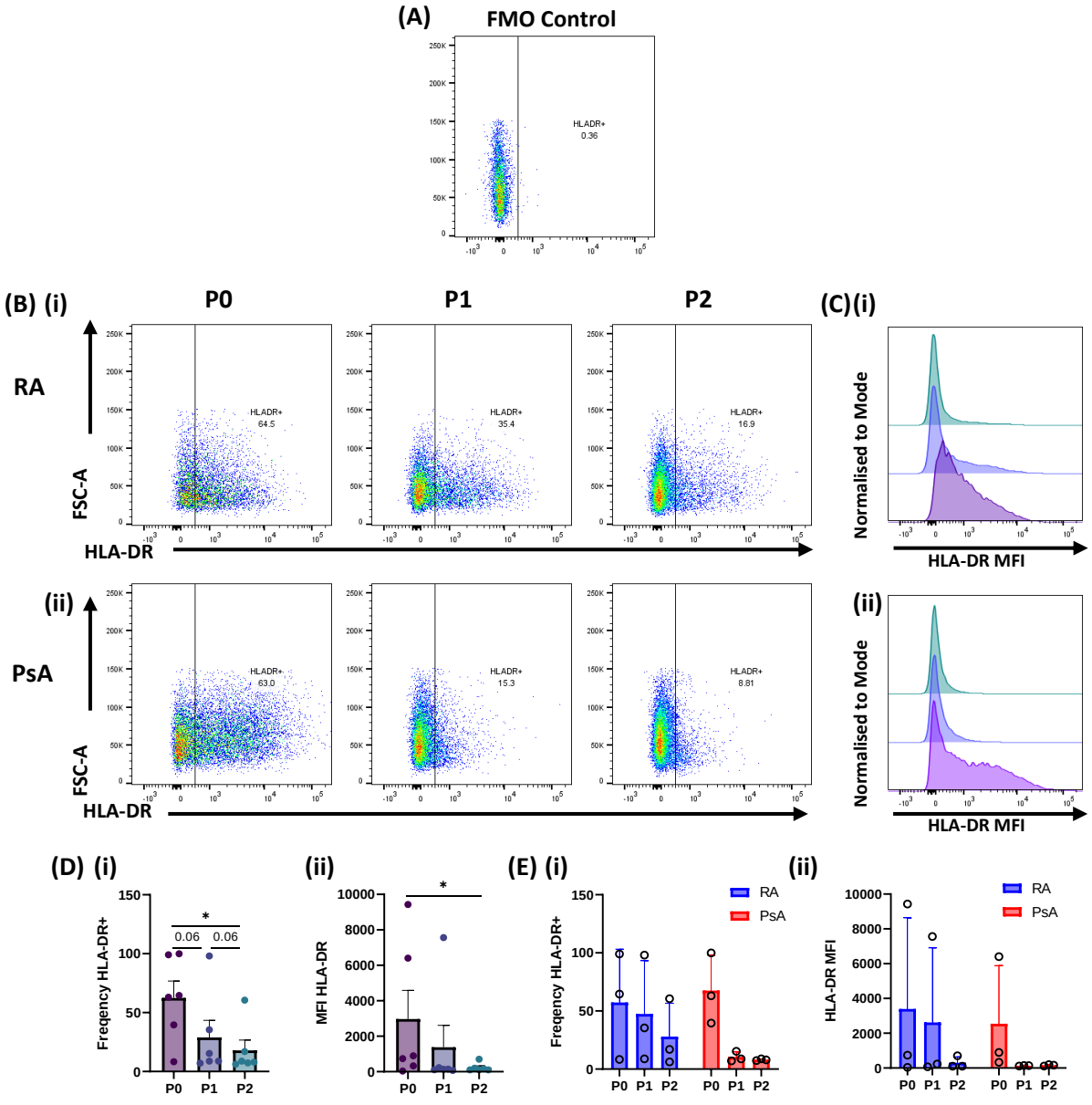

Figure 3.33. Differential expression of the immune marker HLA-DR on RA and PsA FLS at P0, P1, and P2. (A) Representative flow plot shows the HLA-DR FMO. **(B)** Representative flow cytometric dot plots demonstrate differences in the expression of HLA-DR on FLS across passages 0, 1, and 2 from the indicated disease states - RA **(i)** and PsA **(ii)**. **(C)** Representative histograms of the MFI of HLA-DR on PDPN+ FLS in **(i)** RA and **(ii)** PsA synovial tissue from P0, P1, and P2. **(D)** Bar graphs demonstrating the changes in **(i)** expression frequency and **(ii)** MFI of the marker HLA-DR as a % of PDPN+ cells in IA FLS across three passages as determined by flow cytometric analysis. **(E)** Bar graphs demonstrating the changes in **(i)** % frequency and **(ii)** MFI of the marker HLA-DR as a % of PDPN+ FLS across 3 passages separated out between disease states. All data represented as Mean +/- SEM. Statistical analysis was performed using the non-parametric, Friedman's Test (*) or Wilcoxon Signed-Rank Test (#) with statistical significance defined by $*^{(\#)}p \leq 0.05$.

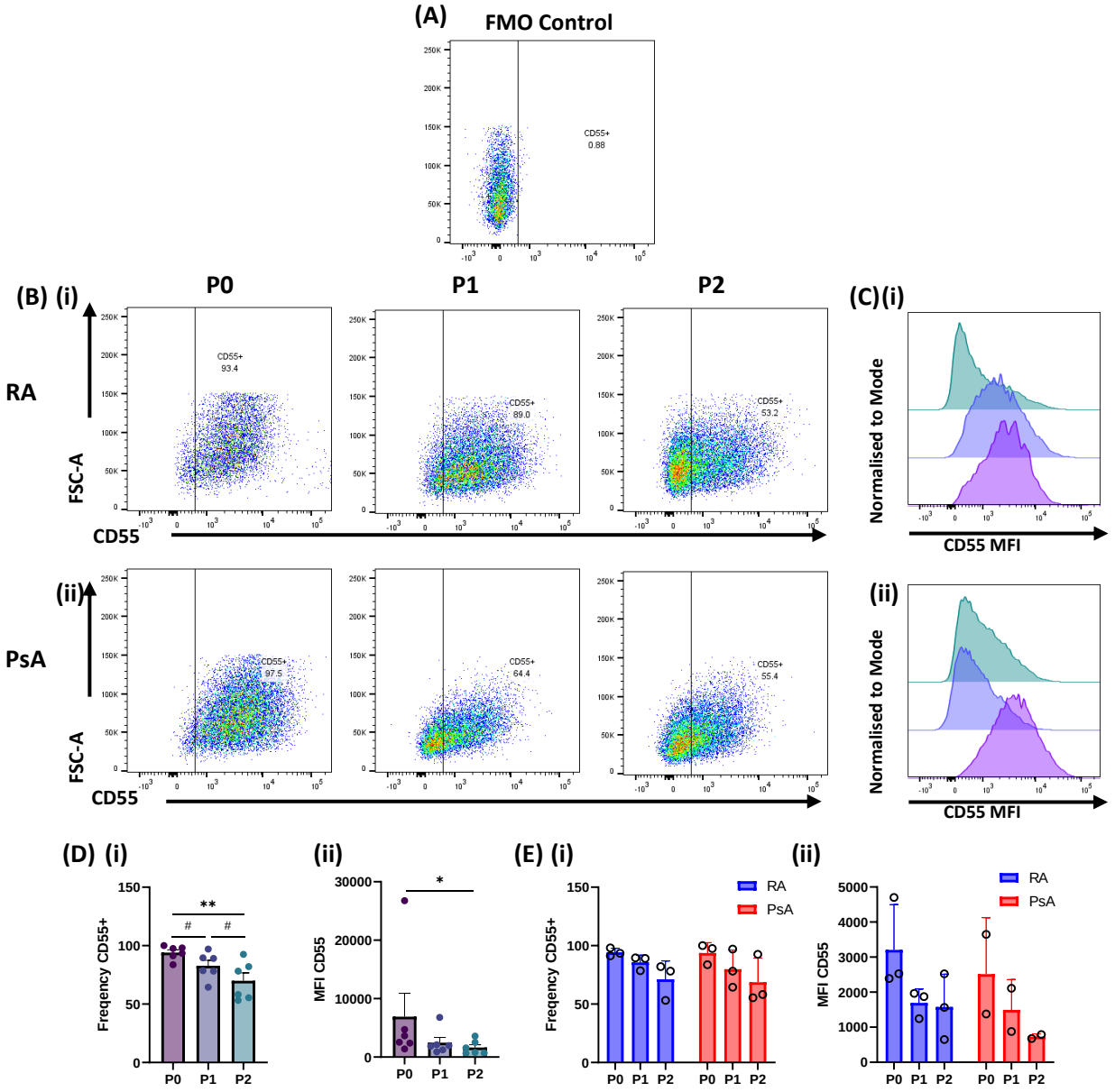

Figure 3.34. Differential expression of the immune marker CD55 on RA and PsA FLS at P0, P1, and P2. (A) Representative flow plot shows the CD55 FMO. **(B)** Representative flow cytometric dot plots demonstrate differences in the expression of CD55 on FLS across passages 0, 1, and 2 from the indicated disease states - RA **(i)** and PsA **(ii)**. **(C)** Representative histograms of the MFI of CD55 on PDPN+ FLS in **(i)** RA and **(ii)** PsA synovial tissue from P0, P1, and P2. **(D)** Bar graphs demonstrating the changes in **(i)** expression frequency and **(ii)** MFI of the marker CD55 as a % of PDPN+ cells in IA FLS across three passages as determined by flow cytometric analysis. **(E)** Bar graphs demonstrating the changes in **(i)** expression frequency and **(ii)** MFI of the marker CD55 as a % of PDPN+ FLS across 3 passages separated out between disease states. All data represented as Mean +/- SEM. Statistical analysis was performed using the non-parametric, Friedman's Test (*) or Wilcoxon Signed-Rank Test (#) with statistical significance defined by $*^{(\#)}p\leq0.05$, $**^{(\#\#)}p\leq0.01$.

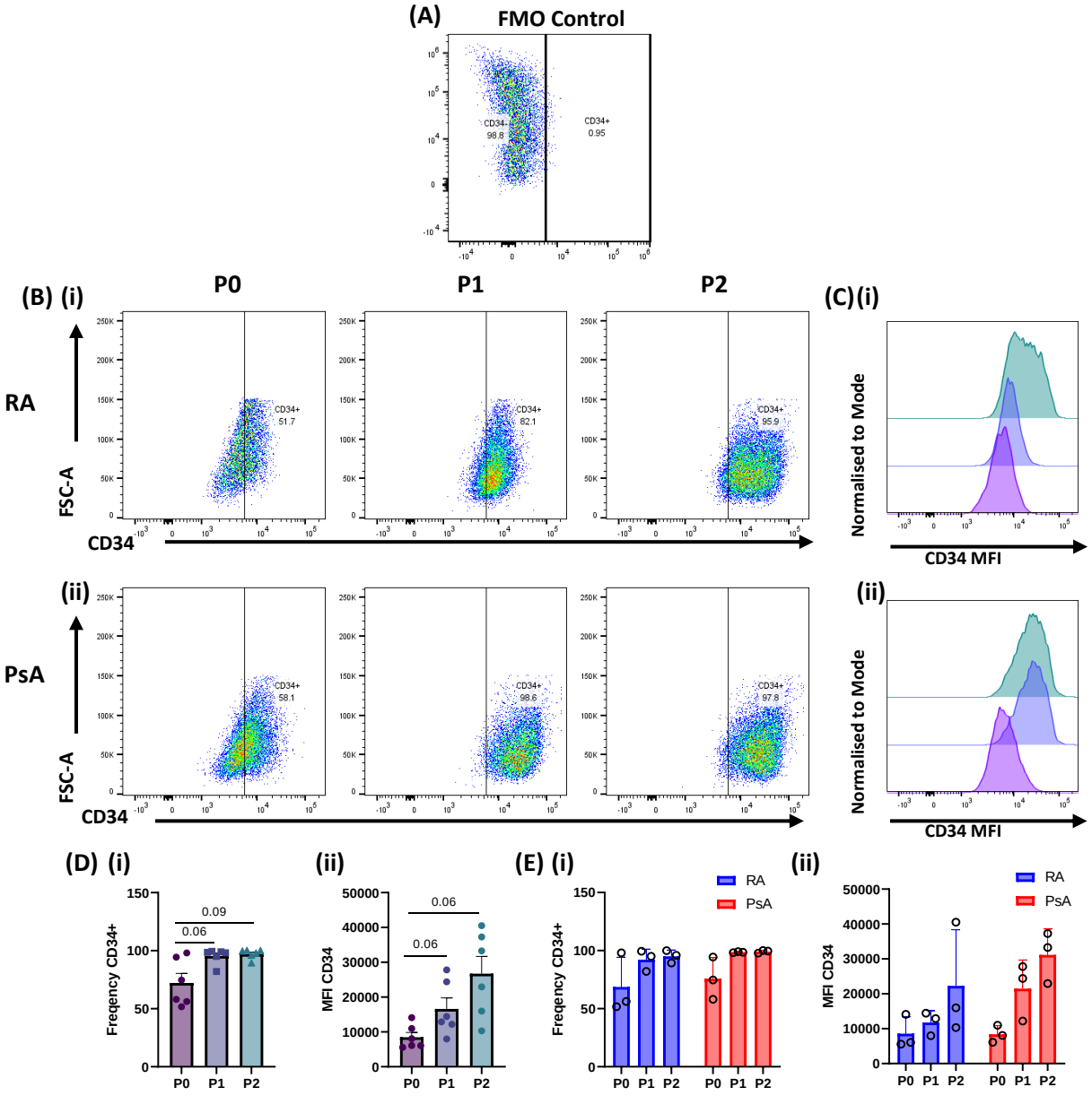

Figure 3.35. Differential expression of the marker CD34 on RA and PsA FLS at P0, P1, and P2. (A) Representative flow plot shows the CD34 FMO. **(B)** Representative flow cytometric dot plots demonstrate differences in the expression of CD34 on FLS across passages 0, 1, and 2 from the indicated disease states - RA **(i)** and PsA **(ii)**. **(C)** Representative histograms of the MFI of CD34 on PDPN+ FLS in **(i)** RA and **(ii)** PsA synovial tissue from P0, P1, and P2. **(D)** Bar graphs demonstrating the changes in **(i)** expression frequency and **(ii)** MFI of the marker CD34 as a % of PDPN+ cells in IA FLS across three passages as determined by flow cytometric analysis. **(E)** Bar graphs demonstrating the changes in **(i)** expression frequency and **(ii)** MFI of the marker CD34 as a % of PDPN+ FLS across 3 passages separated out between disease states. All data represented as Mean +/- SEM. Statistical analysis was performed using the non-parametric, Friedman's Test (*) or Wilcoxon Signed-Rank Test (#) with statistical significance defined by $*^{(\#)}p \leq 0.05$.

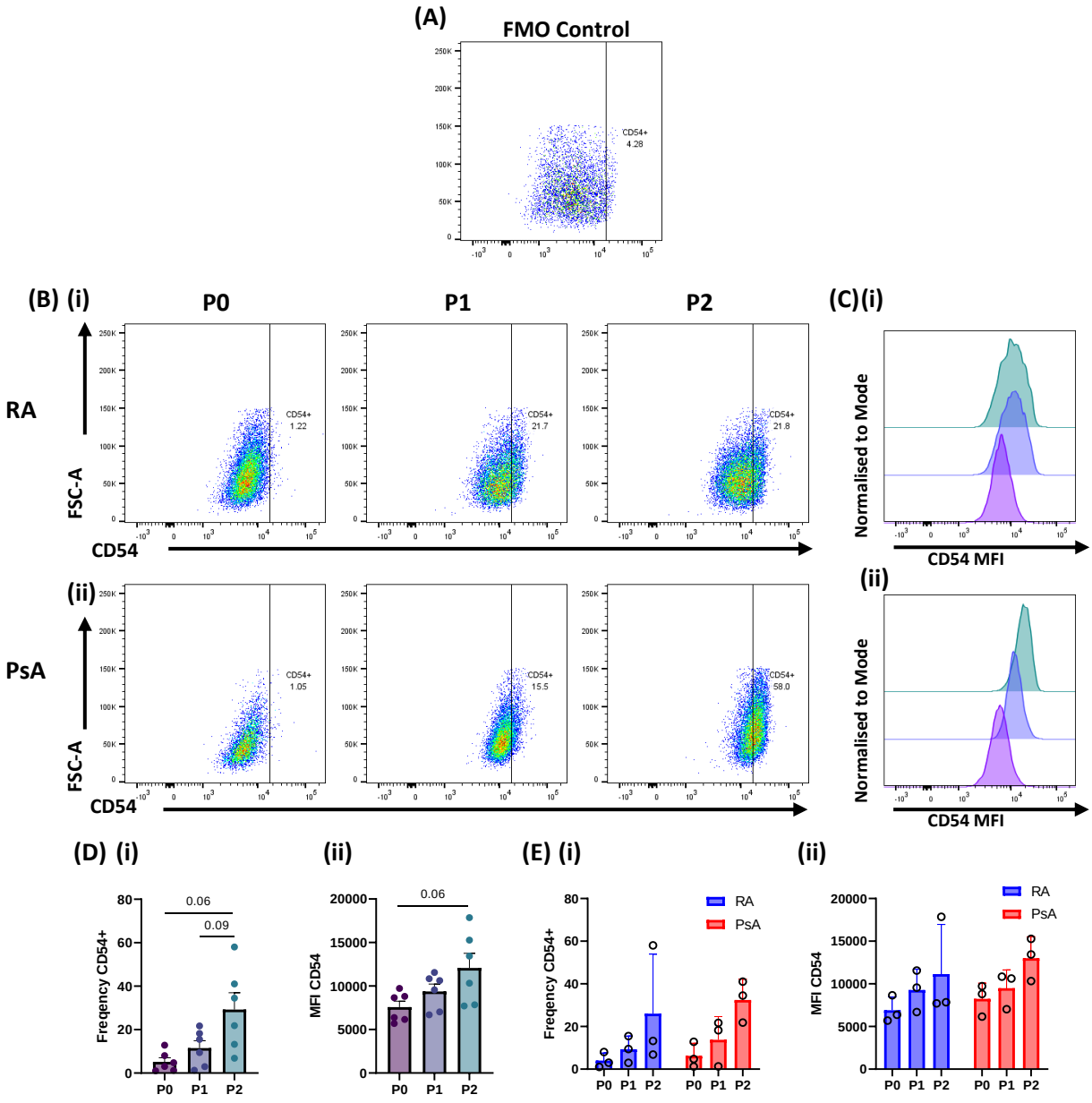

Figure 3.36. Differential expression of the adhesion marker CD54 on RA and PsA FLS at P0, P1, and P2. (A) Representative flow plot shows the CD54 FMO. **(B)** Representative flow cytometric dot plots demonstrate differences in the expression of CD54 on FLS across passages 0, 1, and 2 from the indicated disease states - RA **(i)** and PsA **(ii)**. **(C)** Representative histograms of the MFI of CD54 on PDPN+ FLS in **(i)** RA and **(ii)** PsA synovial tissue from P0, P1, and P2. **(D)** Bar graphs demonstrating the changes in **(i)** expression frequency and **(ii)** MFI of the marker CD54 as a % of PDPN+ cells in IA FLS across three passages as determined by flow cytometric analysis. **(E)** Bar graphs demonstrating the changes in **(i)** expression frequency and **(ii)** MFI of the marker CD54 as a % of PDPN+ FLS across 3 passages separated out between disease states. All data represented as Mean +/- SEM. Statistical analysis was performed using the non-parametric, Friedman's Test (*) or Wilcoxon Signed-Rank Test (#) with statistical significance defined by $*^{(\#)}p \leq 0.05$.

3.5 Discussion

Most studies in the field of synovial analysis to date have examined FLS responses in the context of expanded FLS. However, more recent studies have focused on delineating FLS subsets in RA tissue, ranging from analysis of differences in FLS subsets across RA pathotypes to a plethora of studies providing comparisons between the inflamed RA synovium and non-inflamed comparators including healthy or OA donors (Stephenson *et al.*, 2018; Mizoguchi *et al.*, 2018; Croft *et al.*, 2019; Zhang *et al.*, 2019b; Micheroli *et al.*, 2022; Smith *et al.*, 2023). In this study, FLS subsets and their transcriptional profiles between two highly inflammatory arthropathies were explored for the first time, with the aim of understanding FLS contribution to the differential disease mechanisms in RA and PsA. Initially the analysis focused on examining PDPN+ FLS as a discriminatory marker of FLS due to its association with stromal cells and an aggressive FLS phenotype as described previously (Croft *et al.*, 2016; Zhang *et al.*, 2023a). A significantly higher frequency of PDPN+ FLS in PsA compared to RA was identified. Furthermore, significantly higher expression of the markers HLA-DR, Cad11, YAP, and pS6 on the PDPN+ RA FLS were demonstrated whilst the PsA FLS were enriched for CD55. In support of these findings, an abundance of previous literature has demonstrated significant expression of these specific markers in RA FLS, with HLA-DR classified as a characteristic marker of THY1+ RA FLS and elevated levels of the calcium-dependent adhesion molecule Cad11 previously observed in RA FLS, where it was associated with FLS pathological behaviour in mouse models and in *in vitro* studies (Mizoguchi *et al.*, 2018; Zhang *et al.*, 2019b; Kemble and Croft, 2021). Moreover, higher levels of YAP, a protein with a vast range of functions including the regulation of cell motility, growth, proliferation, and differentiation, have been demonstrated in the RA synovium, whilst Barker *et al.* (2023) successfully identified increased pS6 levels, a major downstream effector of mTOR, in RA compared to HC (Zhou *et al.*, 2020; Caire *et al.*, 2021; Symons *et al.*, 2022; Barker *et al.*, 2023). Conversely, the discovery of higher CD55 expression on the PsA FLS, a marker more renowned in the FLS field for being associated with lining layer FLS than its actual involvement with the complement cascade, is of particular interest as it would imply an enrichment of the lining layer FLS in PsA compared to RA. Furthermore, in the context of biological relevance, analysing the co-expression of the aforementioned and additional markers on the FLS is critically important as it may provide a more accurate representation of their actual *in vivo* behaviour. Interestingly, using SPICE analysis, it could be determined that the RA FLS appear to exhibit greater co-expression of immune related markers whilst PsA FLS demonstrate greater metabolic marker co-expression, evidence which may be helpful in understanding differences in their immune and metabolic related functionality in both disease states.

In recent years the primary emphasis in the literature has focused on distinguishing FLS populations predominantly by their THY1 phenotype, with scRNA-seq of inflamed mouse synovium

culminating in THY1+ FLS being defined as sub-lining immune effectors whilst THY1- FLS are the more bone and cartilage degradative lining subtype (Croft *et al.*, 2019). Therefore, utilising this marker in addition to the marker FAP associated with an activated FLS phenotype, it was determined that THY1+ FLS are expanded in RA whilst in contrast, THY1- FLS are expanded in PsA, evidence which further supports the notion that the lining layer is indeed expanded in PsA cohorts. In line with the theory that the RA synovium is chronically inflamed, Croft *et al.* (2019) identified an expanded population of PDPN+FAPα+THY1+ immune effector FLS in RA patients compared to those with OA, results which are similar to the observations seen in this chapter when compared directly to PsA. Similarly, Mizoguchi *et al.* (2018) discovered higher THY1+CD34- FLS in RA compared to OA, whilst individuals with OA, a disease more characterised by the irreversible degradation of cartilage than inflammation, possessed higher levels of THY1-CD34- FLS. Thus this data ultimately demonstrates, for the first time, a differential predominance of FLS phenotypes in RA vs PsA, with possible impact for their disease pathogenesis.

Based on these differences between RA and PsA predominance of THY1+ vs THY1- FLS, potential functional discrepancies between these two subsets were next examined. Interestingly, a trending increase in the expression of several chemokines was detected including MCP-1, MCP-4, Eotaxin, Eotaxin-3, IP-10, MIP-1α, MIP-1β, and TARC, in THY1+FAP+ FLS compared to their negative counterparts. Traditionally, THY1+ FLS have been strongly associated with immune effector functions, with several studies highlighting they provoke elevated levels of inflammation through release of proinflammatory mediators, whilst additionally they have been shown to correlate in a positive manner with the proportion of infiltrated leukocytes (Mizoguchi *et al.*, 2018; Croft *et al.*, 2019; Alivernini *et al.*, 2020). In further support of this, a positive correlation was identified between the % frequency THY1+FAP+ FLS in the combined RA and PsA cohorts and the inflammatory parameters; DAS28 and synovitis scores, corroborating their central role in the perpetuation of synovial inflammation. Moreover, a higher angiogenic propensity of the THY1+FAP+ FLS was identified with significantly elevated expression of the angiogenic mediators VEGF-A, VEGF-C, and FLT1 in this cell phenotype, which supports previous work showing that as the number of THY1+ mesenchymal stem cells (MSCs) increased, the extent of angiogenesis occurring also increased proportionally (Zeng *et al.*, 2023). Indeed, in the field of FLS it has been well-established that during the inflammatory process, extensive angiogenesis occurs in the sub-lining area, a region enriched in the THY1+ FLS, enabling a plethora of immune cells to invade (Kemble and Croft, 2021). Additionally, the close proximity to the underlying blood vessels and influence of EC signalling on the adoption of THY1 expression on FLS would further suggest that unlike THY1- FLS, the cells positive for THY1 assume a far greater role in angiogenic processes (Wei *et al.*, 2020). The results were further reinforced by a study utilising novel

THY1 antagonistic antibodies in RA FLS, which resulted in simultaneous reduction in inflammatory factor secretion and angiogenesis, with significantly reduced ability of the RA FLS supernatants to drive tube formation when applied to HUVEC, ultimately corroborating the important immune and angiogenic role of THY1+ FLS (Hu *et al.*, 2023). Conversely, in agreement with previous studies in human and CIA mouse models suggesting THY1- lining FLS exhibit a higher propensity to mediate structural bone and cartilage damage, higher expression of the matrix degradative MMPs – MMP-1, MMP-3, and MMP-9, from the sorted THY1-FAP- FLS were identified (Mizoguchi *et al.*, 2018; Croft *et al.*, 2019). Interestingly, although THY1+ FLS appeared to possess a stronger immune and angiogenic role, it was merely their frequency and not their functionality that differed between the two arthropathies. However, the ECM degradative role of THY1- FLS appeared to be higher in the PsA cohort, particularly in relation to MMP-1 and MMP-3 expression. This suggests that THY1- FLS may serve a more prominent role in PsA, although the exact nature of this role remains unclear considering much of the literature suggests that whilst PsA patients do present with radiographical bone alterations, RA is traditionally classified as a markedly more bone-resorbing, erosive disease (Finzel *et al.*, 2011; Mc Ardle *et al.*, 2015; Braga *et al.*, 2020; Elliott, McGonagle and Rooney, 2021).

Due to the complexity of the joint, distinguishing FLS populations based purely on THY1 expression may not be sufficient. Therefore, further stratification of differences in FLS populations within the joint was performed using advanced flow cytometric analysis based on the additional markers previously utilised for FLS characterisation - THY1 and FAP, in addition to CD55 and CD34 (Stephenson *et al.*, 2018; Mizoguchi *et al.*, 2018; Croft *et al.*, 2019; Micheroli *et al.*, 2022; Zhang *et al.*, 2023a). Interestingly, whilst six different FLS subsets were detected based on these markers in the IA joint, two of these populations, both notably THY1+CD55-, were enriched in the RA cohorts, which supports previous literature demonstrating an enrichment of the sub-lining FLS in RA (Stephenson *et al.*, 2018; Mizoguchi *et al.*, 2018; Zhang *et al.*, 2019b; Croft *et al.*, 2019; Micheroli *et al.*, 2022). Moreover, one of these populations was CD34+, which correlates with the RA enriched CD34+THY1+ 'perivascular' subset, named accordingly due its location surrounding the deep sub-lining capillary structures. Several studies have highlighted the role of this subset in driving inflammation, with gene set enrichment analysis and *in vitro* experiments indicating high level of expression of proinflammatory mediators including CXCL12, CCL2, and IL-6 (Mizoguchi *et al.*, 2018; Zhang *et al.*, 2019b; Kemble and Croft, 2021). In alignment with this more 'immune-regulatory' role of THY1+ sub-lining FLS clusters, the examination of the H&E histological sections of the matched donors demonstrated significantly higher immune cell infiltration and lymphoid aggregate presence in the RA donors compared to PsA, thus reinforcing the dominance of more immune related sub-lining FLS in RA (Veale *et al.*, 1993; Veale and Fearon, 2015; Alivernini, Firestein and McInnes, 2022).

Furthermore, whilst two populations were comparable between both disease states, PsA patients exhibited significant enrichment in the remaining two populations – THY1-CD34-CD55+FAP+ and interestingly, the THY1+ population THY1+CD34-CD55+FAP+. The available literature has clearly identified THY1-CD55+ FLS as the classic lining layer phenotype, with CD55 presence being proposed as a clear marker to demarcate lining from sub-lining cells due to their independent staining (Stephenson *et al.*, 2018; Mizoguchi *et al.*, 2018; Zhang *et al.*, 2019b; Kemble and Croft, 2021; Micheroli *et al.*, 2022). Analysis at the histological level corroborated these results with a trending increase in lining layer thickness in PsA compared to the RA samples, implying greater abundance of the THY1-CD55+ FLS phenotype. In contradiction of these findings, some previous studies demonstrated more extensive lining layer hyperplasia in RA while others demonstrated similar lining layer thickness in RA and PsA (Veale *et al.*, 1993; Baeten *et al.*, 2005; Veale and Fearon, 2015). However, this could be explained by differential obtainment of synovial tissue in addition to underlying patient heterogeneity and treatments at the time of scope. Moreover, the identification of the THY1+CD55+ FLS population enriched in PsA was of particular interest due to its both lining and sub-lining characteristic markers which would categorise it as an 'intermediate' subset. This finding supports the notion that FLS subsets can exist along a gradient depending on their proximity to the influencing signals of the blood vessel ECs as demonstrated eloquently by Wei *et al.* (2020). Importantly, whether this state is merely transitionary or permanent and whether the behaviour of this subset is more resemblant of THY1+ or THY1- or in fact a combination of both remains to be investigated. However, despite this subset, when considered cumulatively, the data would indeed indicate an enrichment of lining layer FLS in PsA, with sub-lining FLS more dominant in RA.

To gain a more comprehensive understanding of the distinct functions of these identified FLS subsets in RA and PsA, the expression of a range of immune and metabolic markers within the individual populations were analysed by flow cytometry. In line with the findings when only focused on PDPN+ FLS in RA vs PsA, significantly higher expression of Cad11 and YAP in the RA dominant populations was detected whilst pAKT was significantly elevated in the PsA dominant subsets. Interestingly, higher expression of Cad11 in the RA dominant THY1+ populations conflicts with previous literature demonstrating a prominent role for Cad11 in the synovial lining layer where it assumes a critical role in aggregation and integration of FLS into the designated lining layers (Kiener *et al.*, 2006; Lee *et al.*, 2007; Croft *et al.*, 2016). However, further studies have expanded the scope for the role of Cad11 in RA pathogenesis with research delineating its ability to induce the release of a plethora of proinflammatory mediators from RA FLS through NF-κB engagement whilst simultaneously exacerbating the pathogenic, inflammatory effects of other cytokines within the joint microenvironment (Chang *et al.*, 2011). In the context of the findings and the known immune effector

role of THY1+ FLS, this would suggest high Cad11 expression on the RA dominant THY1+ populations may be serving a more proinflammatory rather than adhesive role. Moreover, in relation to YAP, a specific study conducted in an adjuvant-induced arthritis mouse model identified that GDF-5 lineage FLS, which included both PDPN+THY1+ and PDPN+THY1- cells, demonstrated significantly elevated levels of YAP (Symons *et al.*, 2022). Subsequent abrogation of this YAP resulted in reduced immune infiltration in addition to a reduction in the erosive and invasive properties of the FLS, a finding which was also shown by Barker *et al.* (2023) in which inhibition of crosstalk between mTOR and YAP pathways in human RA FLS successfully mitigated their invasiveness (Symons *et al.*, 2022). Additionally, higher pAKT expression in the populations more dominant in PsA supported the identification of elevated pAKT in the PDPN+ PsA FLS implying that pAKT is assuming a greater role in PsA pathogenesis. However, its ability to regulate multiple downstream pathways and effectors makes it challenging to definitively classify its primary contribution to PsA pathogenesis. Collectively the data highlights that differential enrichment of FLS subsets with diverse functional roles could translate into direct implications for their contribution to differences in RA vs PsA disease pathogenesis.

Moreover, from a single-cell transcriptomic perspective, a diversity in FLS subsets in the RA and PsA synovium was illustrated, with 16 distinct clusters initially identified. In line with previous bioinformatic analysis, demarcation into clear lining versus sub-lining subsets was performed on the basis of previously utilised markers including THY1, PRG4, and CD55 (Stephenson *et al.*, 2018; Mizoguchi *et al.*, 2018; Zhang *et al.*, 2019b; Croft *et al.*, 2019; Micheroli *et al.*, 2022; Zhang *et al.*, 2023a; Faust *et al.*, 2023). Interestingly, although CD34 was used in the flow cytometric data as a population marker and has been shown to be an identifier of subsets in other single-cell analysis, CD34 exhibited minimal expression in the scRNA-seq dataset and thus was not useful in the process of annotation in this study (Mizoguchi *et al.*, 2018; Zhang *et al.*, 2019b; Kemble and Croft, 2021). Indeed, the majority of previous annotation has been based on RA synovium exclusively, with a scarcity of datasets integrating both RA and PsA synovial tissue, thus this may explain the differential clusters and subsequent annotation observed. Whilst lining layer clusters were enriched in PsA, specific focus was placed on the RA enriched populations, which in alignment with previous literature and indeed our own flow cytometric analysis, were all of sub-lining origin (Mizoguchi *et al.*, 2018; Croft *et al.*, 2019; Zhang *et al.*, 2019b; Micheroli *et al.*, 2022). The THY1+POSTN+ subset was of particular interest due to its alignment with the THY1+CD34- subset initially identified by Mizoguchi *et al*. (2018). Indeed, this study revealed this particular subset was localised to the deep sub-lining in close proximity to the underlying vasculature, where it demonstrated a close association with leukocyte infiltration and the extent of histological synovitis (Mizoguchi *et al.*, 2018). Moreover, an eloquent deconvolution analysis conducted by Micheroli *et al.* (2022) using integrated data from five published datasets identified a

comparable sub-lining POSTN+ FLS cluster, with KEGG pathway analysis demonstrating significant enrichment of genes related to actin cytoskeleton regulation, in addition to several collagens, pathways/genes also implicated in the POSTN+ RA enriched cluster in this chapter. The POSTN gene itself has a strong association with RA pathogenesis, with a recent publication stating that POSTN is a central gene with high abundance in the RA synovium, specifically around blood vessels, with a significant correlation between its level of expression and macrophage infiltration (Li *et al.*, 2024a). Therefore, in the context of this previous literature it would suggest the identified THY1+POSTN+ RA enriched cluster exhibits immune related and ECM functions. When functionality of this specific cluster between RA and PsA was compared, enrichment of several pathways were observed including focal adhesion and adherens junctions, both fundamentally important in facilitating cell migration, in addition to oxidative phosphorylation, the Hippo signalling pathway and the MAPK signalling pathway, in RA compared to PsA. This suggests that the THY1+POSTN+ cluster is not only more abundant in RA but additionally exhibits a higher degree of pathogenic activity in RA compared to the same population in PsA, introducing the notion that at a very specific cluster level, FLS of the same cluster may possess slightly different functionality depending on the disease state. Furthermore, enrichment of two CXCL12+ subsets in RA supports previous literature in which a CXCL12+ HLA-DR^{High} subset was identified in the RA sub-lining, expressing genes related to collagen and immune regulation (Zhang *et al.*, 2019b; Alivernini *et al.*, 2020; Micheroli *et al.*, 2022). Specific enrichment of CXCL12+APOE+ and CXCL12+CHI3L2+ subsets were demonstrated, the latter of which was previously identified in scRNA-seq analysis of healthy homeostatic FLS clusters, exhibiting significant enrichment in disease state thus reinforcing its pathogenic role (Faust *et al.*, 2023). CHI3L2 has previously been shown to be expressed at a significantly higher level in the serum of RA vs PsA patients, with the same RA cohorts containing a higher proportion of CHI3L2^{High} FLS compared to not only PsA but OA, UA, and HC, implying it is a driver of aspects of RA pathogenesis specifically (Khmelevskaya *et al.*, 2024). Moreover, whilst APOE is well-established for its role in lipid metabolism, an eloquent study demonstrated its ability to serve an immune role through its activating influences on innate complement responses in certain situations (Vogt *et al.*, 2020). Additionally, it was concluded that two of the clusters specifically enriched in PsA compared to RA were both of lining layer origin, with significantly higher frequency of the MMP3+ cluster matching the *ex vivo* data. Interestingly, the remaining cluster enriched in PsA, named HLA-DR^{High}, was denoted as intermediate as a consequence of its expression of both classic lining and sub-lining markers. This introduces the question – does it match the THY1+CD34-CD55+FAP+ population identified in the previous flow cytometric analysis of RA vs PsA biopsies, suggesting this cluster may be responsible for contributing to the more inflammatory aspects of PsA pathogenesis? Collectively, the scRNA-seq analysis mirrors the findings from the *ex vivo* flow cytometric and sorted cell

experiments – sub-lining FLS with more potent immune regulatory functions are enriched in RA whilst conversely, PsA dominant populations are classified as lining layer and exhibit matrix degradative roles.

Furthermore, this research aimed to address two unanswered questions that are critical to furthering understanding of RA and PsA pathogenesis – are RA and PsA FLS at P0 functionally distinct and secondly, do they retain their distinct phenotypic characteristics that define subsets upon *ex vivo* expansion? Indeed, although the pathogenic role of FLS in individual inflammatory arthropathies has been well-established, a direct comparative analysis of the functional behaviour of the FLS between RA and PsA specifically remains unexplored. Therefore, experiments on the FLS at P0 were performed in order to recapitulate their behaviour within the joint as closely as possible *ex vivo.* Whilst differences in the expression of chemokines was highly patient and indeed chemokine specific, reflecting the scRNA-seq analysis, significantly higher expression of MMP-1 and MMP-3 in the PsA FLS, in addition to higher expression of certain angiogenic mediators including bFGF, and a slightly more glycolytic profile at baseline of the PsA FLS was shown. These results are in line with previous research showing that PsA FLS are potent producers of MMP-1 and MMP-3, suppression of which can be achieved through JAK/STAT inhibition, ultimately impeding their invasive capacity (Gao *et al.*, 2016; O'Brien *et al.*, 2021). Additionally, the association between PsA FLS and the phenomenon of angiogenesis is well-developed, with abundant research highlighting the ability of PsA FLS to induce a more dysregulated EC phenotype compared to their RA counterparts, a finding that may be in part attributed to the higher levels of angiogenic mediators such as angiopoietins and VEGF expressed in early PsA synovial membrane (Fearon *et al.*, 2003; Fromm *et al.*, 2019). Rather unexpectedly, the results failed to demonstrate a stark, significant difference in the expression of angiogenic mediators including VEGF-A and Flt1 in the RA vs PsA supernatants as observed in this previous literature, but this could be attributed to the disease stage of the PsA patients included in this analysis. Moreover, bFGF, the sole angiogenic marker which did demonstrate significantly higher levels in PsA compared to RA, has previously been shown to be pivotal to the invasion and metastasis of cancer cells, suggesting its role in PsA may not be merely limited to angiogenic functions (Li *et al.*, 2022). In relation to glycolysis, although an abundance of literature has highlighted the central role dysfunctional FLS glucose metabolism assumes in RA pathogenesis, the role of glycolysis in PsA FLS is far less established (Biniecka *et al.*, 2016; Fearon *et al.*, 2019; Fearon *et al.*, 2022). Whilst it has been shown that PsA FLS do utilise glycolytic pathways to facilitate their pathogenic activities, this was the first study to determine if this reliance on glycolysis at baseline differs between RA and PsA FLS (O'Brien *et al.*, 2021). Interestingly, although not significantly different, slightly higher levels of glycolysis in the PsA FLS compared to RA were detected, alongside trending increases in glycolytic related genes including

HIF-1α, HK2, and GLUT-1, indicating a PsA exclusive preferential skew towards glycolysis that could be related to the higher pAKT detected in PsA dominant subsets. However, upon addition of IL-1β, whilst oxidative phosphorylation levels decreased comparably in both disease states, the RA FLS exhibited an exceedingly more robust glycolytic response with a significant elevation from baseline that was not mirrored to the same extent in the PsA FLS. IL-1β itself is renowned in its capacity to drive the aggressive phenotype of RA FLS, with less known about its effect on PsA FLS. This differential metabolic response to stimulation has been shown before, albeit in the context of different disease states, with PDGF inducing a significantly lower glycolytic response in OA FLS compared to RA (Kvacskay *et al.*, 2021). This suggests that the FLS metabolic responses in different forms of inflammatory disease may be highly dependent on the activating stimulus. Furthermore, it also introduces the concept of 'priming', a theory that suggests FLS may possess a proinflammatory memory after being exposed to an inflammatory stimulus, with previous research suggesting that a 'glycolytic memory' could also be developed in the FLS following repeated chronic stimulatory episodes (Bottini and Firestein, 2013; Crowley *et al.*, 2017; Kvacskay *et al.*, 2021). Thus, the results from this study introduce a plethora of important unanswered questions that require further investigation – are RA FLS more responsive to proinflammatory cytokine stimulation and could this be related to a heightened priming effect in RA FLS compared to their PsA counterparts? Cumulatively, it can be concluded that PsA and RA FLS do possess intrinsic functional differences *ex vivo*, with a predominantly more invasive profile associated with PsA FLS.

Although differences in enriched FLS populations between RA and PsA in the joint have been shown, with functional differences retained *ex vivo* at P0 reinforcing the existence of some influence of the 'imprinted aggressor' phenotype, the ability of these differences to be sustained over further expansion and whether it is affected by disease state remains unanswered (Bottini and Firestein, 2013). To address this, the frequency expression of several surface markers on expanded RA and PsA FLS across consecutive passages (0-2) were characterised, demonstrating a gradual elevation in CD34 and CD54 expression whilst FLS expression of CD55 and HLA-DR demonstrated a stepwise diminishment across increasing passages. These results support an abundance of literature demonstrating that removal of cells from the cues and stimuli surrounding them in the joint microenvironment can impact directly on their phenotypic profile and corresponding functional behaviour (Wei *et al.*, 2020). Indeed, striking decreases in the percentage of cells positive for MHC-II+ between freshly isolated and 4th passage RA FLS have been shown, data which corroborates the findings in relation to HLA-DR, suggesting immune properties may be affected by serial passaging (Zimmermann *et al.*, 2001). Moreover, the effect of serial passaging on RA FLS gene expression profiles at the mRNA level specifically was investigated by Neumann *et al.* (2010). Interestingly, this study

determined that significant DEGs were only detected in later passages, evidence that supports the identification of gradual changes in marker expression on the FLS across passages in this study whilst implying transcriptomic changes are progressive and not immediate. However, it has been demonstrated that delayed blood processing results in progressive distancing of PBMCs from their native *in vivo* biology in as little as 4-6 hrs following removal from the body, suggesting the subtle alterations in the transcriptomic profile of the FLS may be initiating even as early as P0 (Savage *et al.*, 2021). Furthermore, Wei *et al*. (2020) conducted a significant study examining the gene expression of THY1+ and THY1- FLS *ex vivo* over serial passages, research particularly important in the context of the specific subsets. Once removed from the innate positional cues of the neighbouring ECs, the data demonstrates that the transcriptional profiles of the lining/sub-lining FLS converge, and they lose their proximity to specific poles, a finding mirrored in this data with a gradual convergence across passages of all FLS towards a THY1+FAP+ phenotype. Interestingly, whilst initial expression of the surface markers examined differed slightly between the RA and PsA FLS, the manner in which they are increasing/decreasing across passages is highly comparable between the two disease states. This suggests that once removed from their native biological environment, the transcriptional profiles of the FLS are lost to a similar extent in RA and PsA, rather than disease specific, which is critical knowledge for comparative research purposes.

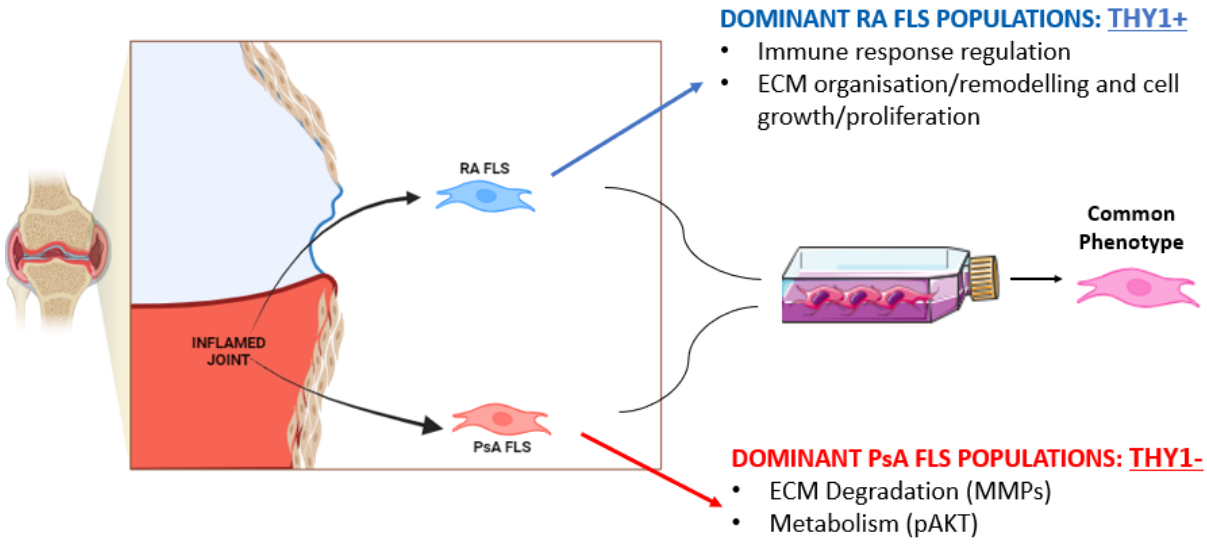

Figure 3.37. An overview of Chapter 3 focusing on the differential FLS subsets enriched in RA vs PsA, and their transient nature when expanded *ex vivo*. Different FLS subsets with unique transcriptional phenotypes are enriched in RA vs PsA, with a higher frequency of THY1+ sub-lining FLS exhibiting immune and ECM regulatory functions in RA whilst PsA exhibits enrichment of THY1- lining layer FLS populations with potent MMP expression. Furthermore, once removed from the joint microenvironment, the FLS subsets gradually converge towards a common phenotype. This figure was made using BioRender.

In summary, the existence of distinct FLS clusters with differential frequency in RA vs PsA have been identified for the first time, with the results indicating that these FLS possess unique transcriptomic profiles and functional capabilities that translate into different effects on RA and PsA pathogenesis. Moreover, the evidence indicates that once removed from their native *in vivo* environment, gradual alterations to the phenotype of the FLS occurs, with a gradual convergence towards a common phenotype. Further examination of the FLS subsets and elucidation of their role in RA vs PsA may provide opportunities to further understanding of the differences in disease mechanisms at the cellular level and thus guide the development of future therapeutic interventions.

CHAPTER 4:

Biomarker Potential of a Circulatory microRNA Signature Distinguishing Rheumatoid Arthritis and Psoriatic Arthritis

4.1 Introduction

As outlined in the main introduction, Section 1.15.1, miRNA are defined as non-coding RNA that are critical mediators of post-transcriptional gene regulation in cells. Through 'guide' strand mediated base-pairing between the miRISC and intended target mRNA, miRNA achieve their functions primarily via induction of mRNA degradation and/or repression of protein translation, both of which effectively culminate in gene silencing. Indeed, there is an abundance of research highlighting the pivotal role miRNAs play in inflammatory pathologies where aberrant miRNAs govern the local and systemic inflammatory responses through downregulation and in some instances upregulation of genes. For example, previous work demonstrated a strong correlation between miR-128-3p upregulation and the TNF-α-induced inflammatory response in bone marrow-derived MSCs, with heightened downstream levels of proinflammatory factors including IL-6, MCP-1, and MMP-9 (Wu *et al.*, 2020a). Similarly, an eloquent study conducted in individuals with MS identified increased levels of the miRNAs – miRNA-21, miRNA-155, and miRNA-182, in cerebrospinal fluid which positively correlated with elevated levels of proinflammatory cytokines including IL-1β, IL-6, TNF-α, and high-sensitive-CRP, thus suggesting a role for these miRNA in inducing an inflammatory shift in MS (Shademan *et al.*, 2023). Much of this inflammatory role is linked to the ability of miRNA to regulate the specific master inflammatory transcription factor NF-κB bidirectionally. Whilst the mitigation of inflammation driven myocardial injury has been shown as a consequence of miR-217 and miR-543 downregulation, the reverse behaviour of miRNA has also been shown with upregulation of miR-9 ameliorating RANKL associated destructive arthritis in FLS, both of which ultimately exert their effect through suppression of NF-κB signalling (Xia, Zhang and Sun, 2020; Lee *et al.*, 2020). However, the pathogenic responses induced by miRNA are not solely NF-κB related but may also be connected to several other downstream target pathways with studies showing TNF-α induced miRNA dysregulation in endometriotic cells resulted in phosphorylation of not only NF-κB, but additionally the PI3K, AKT, and ERK signalling pathways (Banerjee *et al.*, 2023).

In the context of rheumatic disease including ankylosing spondylitis, gout, juvenile idiopathic arthritis, OA, systemic lupus erythematosus, and importantly RA and PsA, an abundance of data has implicated miRNA dysregulation as central contributors to the characteristic bone and cartilage destruction observed within the environment of the synovial joint (Shaikh *et al.*, 2023). The identification of two crucial proinflammatory miRNAs by Stanczyk and colleagues (2008) in RA patients, miR-155 and miR-146a respectively, that were significantly elevated in RA SF compared to osteoarthritic controls, instigated this area of study. In the subsequent years, several studies have identified strong associations between the progressive hypertrophy, inflammation, and angiogenesis of synovial tissue characteristic of RA and the presence of altered miRNA expression levels (Li *et al.*,

2024b). Indeed, the detrimental impact a single miRNA can exert on the pathogenicity of various cell types in the joint is encapsulated in relation to miR-23a. Studies have shown that its downregulation in RA articular cartilage results in heightened IKKα-IL-17-induced activation of proinflammatory articular chondrocytes, whilst similarly in PsA, the decreased levels of this miRNA have been associated with heightened PDE4 induced FLS activation and increased synovitis (Hu *et al.*, 2017a; Wade *et al.*, 2019b). Thus, within the inflammatory microenvironment, the subsequent abnormal activity of a combination of miRNA can culminate in the propagation of several destructive processes in the synovial joint. There is an abundance of available literature highlighting the effect of dysregulated miRNA on the function of immune cell subsets in RA including regulation of the NLRP3 inflammasome in synovial macrophages, the promotion of B cell-driven humoral responses, the disruption of the balance of CD4+ T cells subsets in favour of proinflammatory responses, the activation of synovial monocytes, in addition to potentiation of DC activation and differentiation into aggressive osteoclasts (Alivernini *et al.*, 2016; Elmesmari *et al.*, 2016; Yang *et al.*, 2021; Tu *et al.*, 2022; Gaudenzi *et al.*, 2024). Moreover, the research indicates the abnormal activity of miRNA interferes with proinflammatory signalling pathways, ultimately resulting in the enhanced production of proinflammatory cytokines and chemokines including TNF-α, IL-6, IL-1β, IL-8, IL-17A, MCP-1, and RANTES, in addition to MMPs, further perpetuating RA joint destruction (Elmesmari *et al.*, 2016; Tavasolian *et al.*, 2018; Shaikh *et al.*, 2023). Similarly, although not as well characterised, a growing body of evidence has demonstrated the differential expression of miRNAs including miR-146a-5p, miR-21-5p, miR-130a-3p, miR-221-3p, miR-151-5p, and miR-26a-5p in serum of PsA patients, in addition to the role of miR-941 and the aforementioned miR-23a in driving proinflammatory mechanisms in PsA synovial cells, highlighting their significance in PsA pathology (Wade *et al.*, 2019b; Wade *et al.*, 2020; Lin *et al.*, 2020).

Moreover, recent research has implicated the role of miRNAs, and particularly miR-126 and miR-125 in driving angiogenic mechanisms, a fundamental process occurring within the inflamed joints of both RA and PsA patients (Fish *et al.*, 2008; Wade *et al.*, 2019a; Gao *et al.*, 2021; Zhao *et al.*, 2024). Whilst this angiogenic involvement was initially discovered in 2006 in a groundbreaking *in vitro* study, it is now well-established that of the 2300 miRNA currently identified in the human genome, approximately 10% have demonstrated roles in the regulation of ECs and their angiogenic properties through both direct and indirect mechanisms (Poliseno *et al.*, 2006; Sun *et al.*, 2018b). Promotion of angiogenesis can be mediated via miRNA activation of several additional downstream signalling pathways previously shown to be important in the context of EC angiogenesis including PI3K/AKT/mTOR and the JAK/STAT3 signalling pathways, in addition to repression of specific negative regulators of the VEGF pathway including Sprouty-related protein 1 (SPRED1) and the

phosphoinositol-3 kinase regulatory subunit 2 (PI3KR2/p85-β) (Fish *et al.*, 2008; Zhao *et al.*, 2024). Conversely, several miRNA including miR-126, miR-106a-5p, miR-206, miR-150-5p, and miR-16-5p, have demonstrated an inhibitory role on angiogenesis through direct repression of the essential angiogenic growth factor VEGF-A itself (Zhao *et al.*, 2024). Similarly, deletions of mediators required for miRNA target interactions including the DICER enzyme critical for miRNA maturation, can disrupt the activity of crucial angiogenic factors such as VEGF, VEGFR2, VEGFR1, Tie2, eNOS, ROS, and IL-8, subsequently leading to reduced EC migration, sprouting, and tube formation (Suárez *et al.*, 2007). Moreover, although not fully understood, recent evidence suggests a strong association between miRNAs and dysfunctional energy metabolism in immune cells and ECs which drives destructive events, including neoangiogeneis, within the joints of RA and PsA patients. Altered bioenergetics appears to stem from perturbations in the miRNAs responsible for regulating activity of a number of key metabolic enzymes such as HK2 and PKM2, GLUTs, and glycolysis-promoting transcription and signalling factors, resulting in aberrant activation of destructive effector T cells and ECs (Wade *et al.*, 2019a; Colamatteo *et al.*, 2019). Significantly decreased levels of miR-125 within the PsA synovium is directly correlated with both increased macroscopic vascularity and expression of GLUT-1, PFKFB3, and PKM2, thus demonstrating the glycolytic shift in EC metabolic profiles which enhances angiogenesis (Wade *et al.*, 2019a). However, further investigations into the downstream targets of these miRNAs, as well as the potential involvement of other miRNA capable of governing angiogenesis, are required.

As the understanding of the central role miRNA play in inflammatory disease development and progression grows, it has opened a new avenue of research examining the potential of miRNA to be used as valuable biomarkers and therapeutic targets in various human diseases. As previously mentioned in Section 1.15.5, there is a substantial body of data supporting the role of miRNA, both tissue and circulating, as valuable biomarkers in several types of cancer including prostate, melanoma, colorectal, lung, and breast cancers, where they display oncogenic or tumour-suppressive functions (Chakrabortty *et al.*, 2023). However, their biomarker potential extends beyond cancer to a wide array of human conditions including Alzheimer's disease, Parkinson's disease, epilepsy, heart failure, and sepsis, emphasising the scope of their capabilities (Wiedrick *et al.*, 2019; Salemi *et al.*, 2022; Shen, Wang and Fu, 2022; Zheng *et al.*, 2023; Szydlowska *et al.*, 2024). Their value as diagnostic biomarkers in inflammatory-driven, autoimmune diseases is a current area of focus, with the aim of identifying signatures that distinguish health from disease, thereby facilitating more prompt diagnosis and intervention (Nag *et al.*, 2023). Although a number of biomarkers are currently employed in clinical practice to facilitate RA diagnosis including RF, CRP, and ESR, and the multi-biomarker disease activity (MBDA) score, ACPA positivity is considered the hallmark biomarker for widespread diagnosis of RA

(Abdelhafiz *et al.*, 2023). In spite of this, approximately 20-30% of patients are ACPA negative and the evidence indicates that not all arthralgia patients with ACPA positivity actually develop RA, highlighting the need for additional biomarkers that can improve the diagnostic accuracy and timeliness (Floudas *et al.*, 2021; O'Neil, Alpízar-Rodríguez and Deane, 2024).

Focusing on single miRNA can prove useful in certain contexts, for example in acute pancreatitis where miR-29a upregulation has been observed compared to HC, with a robust correlation with disease development and severity (Gao *et al.*, 2018). However, due to the abundance of miRNAs, research has moved towards focusing on patterns of several miRNA that may be characteristic to specific diseases, a revolutionary approach that has facilitated superior diagnosis and enhanced understanding of disease pathogenesis. In a cross-sectional study examining the blood of individuals with type-1 DM compared to HC, a distinct signature of nine upregulated miRNA was detected, whilst similarly in chronic urticaria, a panel of five circulating upregulated miRNAs were found to be capable of distinguishing between the control and non-control cohorts, all with distinct roles in the regulation of genes implicated in skin inflammation (Barutta *et al.*, 2017; Jerobin *et al.*, 2023). Furthermore, in the context of IA, previous studies have identified six miRNA that were differentially expressed between PsA and HC, with a nine-miRNA signature significantly distinguishing RA compared to HC (Wade *et al.*, 2020; Cunningham *et al.*, 2021). Interestingly six of these miRNA were also upregulated in individuals at risk of developing RA highlighting their predictive value for disease onset also (Cunningham *et al.*, 2021).

Currently, there is an absence of data comparing aberrant miRNA expression in RA vs PsA, which may facilitate better diagnostic capabilities and a deeper understanding of the differences in the pathogenic progression of the two distinct diseases. The use of miRNA signatures not only to diagnose IA but additionally to distinguish different pathotypes of IA has proven highly efficacious in the context of IBD in which studies dating back to 2011 demonstrated a distinct miRNA profile in the circulation associated with different circulating immune cells that could be utilised to distinguish UC and Crohn's (Wu *et al.*, 2011). However, to date, no studies have provided a direct comparison of a potential circulating miRNA signature distinguishing RA from PsA, highlighting the focus of the research outlined in this chapter. In this chapter, differences in the levels of specific circulating miRNA between RA and PsA patient cohorts were examined and downstream pathways regulated by these miRNA explored, with the aim of providing a better understanding of differential disease pathogenesis.

4.2 Specific Aims of this Chapter

- To investigate differences in the expression of circulating miRNAs between RA and PsA patient cohorts (and RA vs PsA vs HC) and to establish their capacity to function as reliable biomarkers.

- To determine the accuracy and sensitivity/specificity with which these miRNA can distinguish between RA and PsA pathology, and to identify if particular combinations of miRNA may be more effective as diagnostic signatures.

- To explore the relationship of specific circulating miRNA with patient clinical demographics.

- To determine if ACPA positivity is correlated with or affects miRNA levels in the RA patient cohort.

- To establish whether gender has an influence on the specific levels of miRNA in the patient populations.

- To examine the potential downstream genes and pathways regulated by differentially expressed miRNA in RA and PsA individuals in order to gain a deeper understanding of disease pathogenesis.

4.3 Materials & Methods

4.3.1 Patient Recruitment

Patients with IA were previously recruited from the outpatient clinic at the Department of Rheumatology, St Vincent's University Hospital. Patients with RA (n=48) fulfilled the criteria established by the ACR/EULAR classification for RA (Aletaha 2015). PsA patients (n=50) fulfilled CASPAR for the classification of PsA (Taylor *et al.*, 2006). Patient demographics and baseline clinical and laboratory assessments including CRP, SJC, TJC, the VAS, synovitis, and vascularity are summarized in *Table 4.1*. Twenty HC, all of which were negative for autoimmune disease, were recruited and included in the study for comparative purposes.

All patients and controls provided fully informed written consent before commencing the study. Ethical approval was granted by St. Vincent's University Hospital Medical Research and Ethics Committee and all research was performed in accordance with the Declaration of Helsinki.

Patient/ Clinical Info.	RA (n=48)	PsA (n=49)	HC
Age median (range)	58 (27-83)	46 (34-58)	38 (27-49)
Gender (F:M)	36:12	34:15	13:7
DAS28 CRP +/-SEM	4.42 +/- 0.21	3.70 +/- 0.16	NA
CRP (mg/dl) +/-SEM	26.22 +/- 7.02	11.2 +/- 2.78	NA
SJC +/SEM	4.98 +/- 0.69	2.73 +/- 0.50	NA
TJC +/-SEM	5.93 +/-0.99	3.4 +/- 0.59	NA
VAS +/-SEM	61.45 +/- 4.47	59.43 +/- 1.97	NA
Synovitis +/-SEM	65.89 +/- 4.8	70.03 +/- 3.26	NA
Vascularity +/-SEM	66 +/- 5.27	66.45 +/- 3.57	NA

***Table 4.1.* Patient demographics.** Summary of RA (n=48) and PsA (n=49) patient demographics and clinical parameters, as well as age and gender for the HC comparators (n=20). Clinical parameters are presented as Mean +/- SEM. DAS: Disease Activity Score, CRP: C-Reactive Protein, SJC: Swollen Joint Count, TJC: Tender Joint Count, VAS: Visual Analogue Scale, SEM: Standard Error of Mean.

4.3.2 Serum miRNA Expression Analysis

Blood was obtained from three cohorts; serum was isolated and subsequently transferred to RNase and DNase free tubes. The FirePlex Circulating 68 miRNA Immunology Fixed Panel was performed as

a service by Abcam, Cambridge, UK. This specific multiplex panel used focused on miRNA associated with immune and stromal cell dysfunction characteristic of autoimmune diseases. While there are many different methods of miRNA analysis, the FirePlex method was utilised as a high-throughput platform as this method reliably quantifies miRNA directly from biofluids with minimal sample preparation, therefore reducing the miRNA isolation-induced variability.

Targeted hybridization of serum miRNA to miRNA probes involved the incubation of 20 µl of patient serum with 35 µl of FirePlex hydrogel particles in addition to incubation with 25 µl of hybridization buffer with gentle agitation at 37°C for 1 h. Using rinsing Buffer A, samples were rinsed twice before 75 µl of labelling mix was added. This solution was then incubated at RT for 1 h with gentle agitation. Following rinsing with Buffer B (x 2) and Buffer A (x 1), 110 µl of RNase-free water was added to the solution and was incubated at 55°C for 30 min. Ligated miRNAs were then eluted and amplified using single-step universal primer RT amplification which consisted of 27 cycles of PCR amplification followed by 6 cycles of asymmetric amplification. Following this, the amplified products were rehybridized with FirePlex particles in 75 µl of reporting buffer and incubated at RT for 15 min whilst gently agitated. To enable fluorescent detection of the particle-bound miRNA, 175 µl of run buffer was then added prior to reading on the EMID Millipore Guava 8HT flow cytometer. Background signals were corrected for using internal positive, negative, and blank controls. Further interpretation and analysis of assay results was performed using the FirePlex Analysis Workbench software.

4.3.3 Bioinformatic Analysis

miRNA expression data were analysed in R v4.0 following scaling. Principle component analysis (PCA)-biplots were generated under R v4.0 with package ggbiplot v0.5 with function ggbiplot. The DNA Intelligent Analysis (DIANA)-miRPath online software suite was used to perform miRNA pathway analysis. This was performed to identify downstream KEGG pathways and genes potentially altered by the dysregulated serum miRNA being evaluated in this study (Vlachos *et al.*, 2015). STRING software was subsequently used to generate visual representations of the protein-protein interactions of the genes involved in the pathways targeted by the dysregulated miRNAs (Szklarczyk *et al.*, 2019).

4.3.4 Statistical Analysis

All statistical analysis was performed using GraphPad Prism 9 software (GraphPad Software Inc., California, USA). The nonparametric, Mann-Whitney *U* test was used to determine significant differences between RA and PsA samples whilst the one-way ANOVA and Kruskal-Wallis test was used

to determine significant differences between RA, PsA, and HC. All data was presented as Mean +/- SEM with statistical significance defined by *p≤0.05, ** p≤0.01, *** p≤0.001, **** p≤0.0001. Receiver operating characteristic (ROC) curves were performed using Prism 9 Software to establish the ability of a specific miRNA or miRNA combination to discriminate between RA and PsA using the area under the curve (AUC) determined using a 95% confidence interval (CI). Spearman rank correlation coefficient was used to evaluate the association between miRNA levels and clinical variables.

4.4 Results

4.4.1 RA serum displays a distinct miRNA profile compared to PsA serum.

Previous studies have demonstrated the involvement of aberrant miRNA expression profiles within the inflammatory joint environment of both RA and PsA patients, suggesting their role as potential biomarkers and therapeutic targets (Wade *et al.*, 2020; Cunningham *et al.*, 2021). In this study, serum was isolated from the blood of RA patients (n=48) and PsA patients (n=49), and the expression profile of a 68-miRNA immunology panel associated with immune dysregulation was determined using the Abcam Multiplex Circulating MiRNA Assay. The FirePlex Analysis Workbench software was used to analyse miRNA expression between RA and PsA. Significant differences in the expression levels of nineteen miRNAs between RA and PsA cohorts were identified, with sixteen of these miRNA exhibiting a significantly higher level of expression within the serum of the RA patients compared to the PsA group (all $p \leq 0.05$) whilst conversely, three miRNA; miR-203a (***$p \leq 0.001$), miR-185-5p, and miR-151-a-5p (both *$p \leq 0.05$), were significantly elevated in the PsA group (Figure 4.1A(i-xix)). A full list of the significantly different miRNA are shown in *Table 4.2* below. PCA analysis of differentially expressed miRNA demonstrated that specific RA patients clustered separately from PsA, although there is overlap with some patients between each group as demonstrated in the PCA plots (Figure 4.2A). Further interrogation using biplot analysis of the PCA plot, identified that seven miRNA were specifically skewed towards RA compared to PsA and thus were further analysed (Figure 4.2B).

Dot plots of these top seven differentially expressed miRNA in RA compared to PsA are shown in Figure 4.2C for (i) miR-126-3p (****$p \leq 0.0001$), (ii) miR-29b-3p (****$p \leq 0.0001$), (iii) miR-22-3p (****$p \leq 0.0001$), (iv) miR-223-3p (*$p \leq 0.05$), (v) miR-320a (*$p \leq 0.05$), (vi) let-7e-5p (***$p \leq 0.001$), and (vii) let-7g-5p (***$p \leq 0.01$). In order to establish their potential validity as biomarkers in RA versus PsA, these seven-miRNA exhibiting significantly increased expression levels in RA compared to PsA (Figure 4.2) were further compared to HC (n=20). Interestingly, all seven identified miRNA that were significantly increased in the RA patients versus the PsA were also significantly increased compared to the HC (Figure 4.3A(i-vii)).

Furthermore, ROC curve analysis was performed to evaluate the sensitivity and specificity of each of the seven to distinguish between RA and PsA patients (Figure 4.4A-G). The strongest statistical separation was observed for miR-22-3p with and AUC of 0.7538 ($p<0.0001$) (Figure 4.4C) followed by miR-29b-3p and miR-126-3p, both with AUCs of 0.7560 ($p<0.0001$) (Figure 4.4B) and 0.7321 ($p<0.0001$) (Figure 4.4A) respectively. Let-7g-5p, let-7e-5p, miR-320a, and miR-223-3p (Figure 4.4D-G) all demonstrated lower sensitivity and specificity with an AUC of <0.7. Interestingly, as shown in Figure 4.5, multivariate analysis for the strongest performing miRNA improved the predictive value slightly as compared to the individual miRNA with the highest predictive value observed with miR-29b-3p,

miR-22-3p, and miR-320a with an AUC of 0.8151 (Figure 4.5B(i)). Moreover, multivariate analysis for the complete serum miRNA signature generated an AUC of 0.7784, thus demonstrating a slightly higher prediction accuracy than each miRNA alone (Figure 4.5C).

Differentially expressed miRNA	P Value
Higher expression in RA	
miR-126-3p	P<0.0001
miR-22-3p	P<0.0001
miR-29b-3p	P<0.0001
miR-142-3p	P<0.0001
miR-1246	P<0.001
miR-16-5p	P<0.001
Let-7g-5p	P<0.01
Let-7e-5p	P<0.01
miR-15-5p	P<0.01
miR-29c-3p	P<0.01
miR-30a-5p	P<0.05
miR-885-5p	P<0.05
miR-16-2-3p	P<0.05
miR-24-3p	P<0.05
miR-223-3p	P<0.05
miR-320a	P<0.05
Higher expression in PsA	
miR-203a-3p	P<0.001
miR-185-5p	P<0.05
miR-151a-5p	P<0.05

Table 4.2. **Table depicting the top nineteen differentially expressed serum miRNA between RA (n=48) and PsA (n=49) patients and their corresponding p value.** Statistical analysis was performed using the non-parametric, Mann-Whitney *U* Test with statistical significance defined by *p≤0.05, **p≤0.01, ***p≤0.001, ****p≤0.0001.

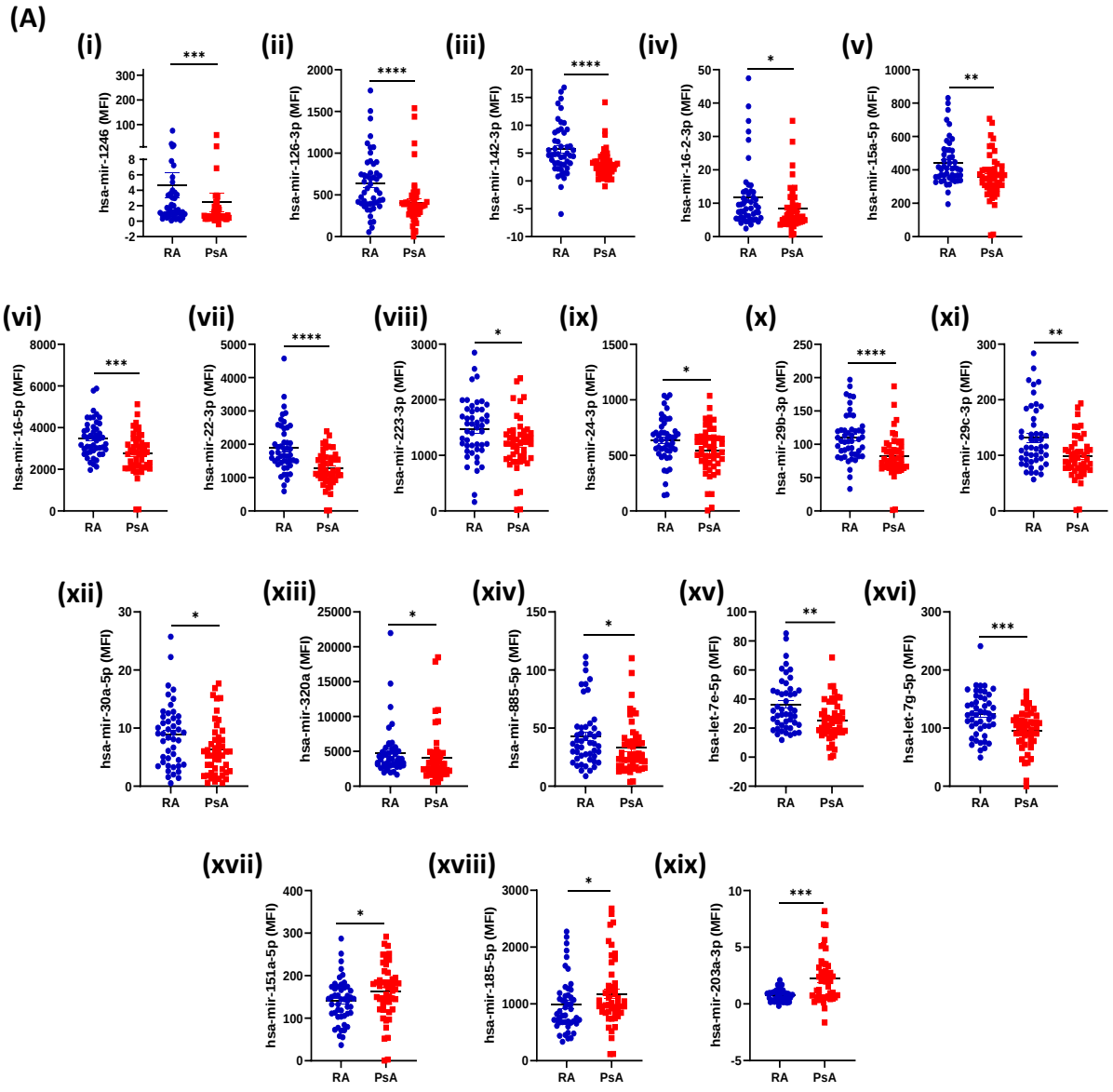

Figure 4.1. Identification of nineteen differentially expressed circulating miRNA between RA and PsA. Serum was isolated from the blood of RA (n=48) and PsA (n=49) patients and a panel of 68 miRNA were analysed using the Multiplex Circulating miRNA Assay. **(A(i-xix))** Representative dot plots demonstrating the difference in expression MFI of the nineteen differentially expressed miRNAs of interest between the RA and PsA patient cohorts. All data represented as Mean +/- SEM. Statistical analysis was performed using the non-parametric, Mann-Whitney *U* Test with statistical significance defined by *p≤0.05, **p≤0.01, ***p≤0.001, ****p≤0.0001.

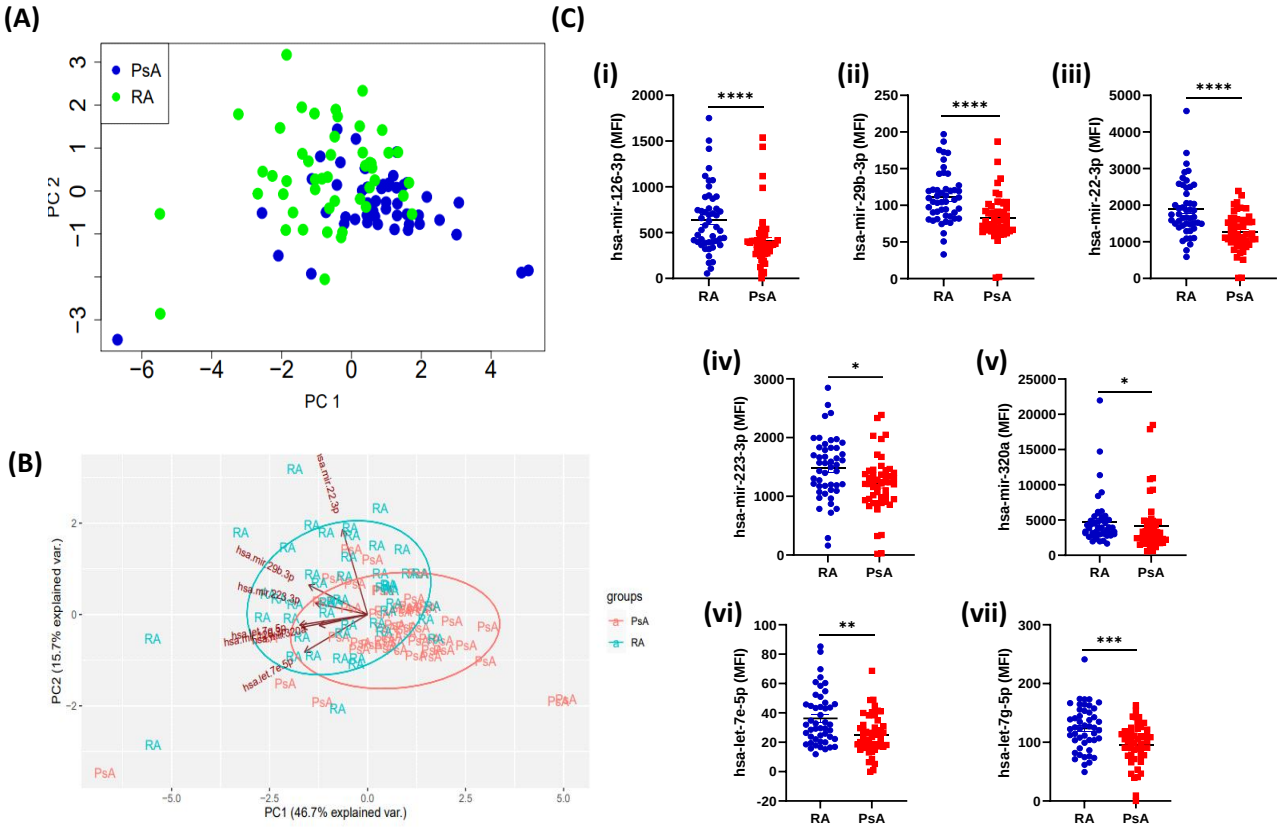

Figure 4.2. Analysis of miRNA expression for the top seven differentially expressed miRNAs between RA and PsA. (A) PCA analysis demonstrating serum miRNA expression between RA (n=48) and PsA (n=49). PCA analysis was performed in R (v4.0) function prcomp with scaling. **(B)** Biplot analysis of the seven significant miRNA skewed towards RA vs PsA. PCA-biplots were generated under R v4.0 with package ggbiplot v 0.5 with function ggbiplot. **(C (i-vii))** Dot plot representations showing MFI of the relative expression of the seven most differentially expressed serum miRNA isolated from the serum of RA patients (n=48) versus PsA patients (n=49), and analysed and amplified using the Multiplex Circulating miRNA Assay. All data represented as Mean +/- SEM. Statistical analysis was performed using the non-parametric, Mann-Whitney *U* Test with statistical significance defined by *p≤0.05, **p≤0.01, ***p≤0.001, ****p≤0.0001.

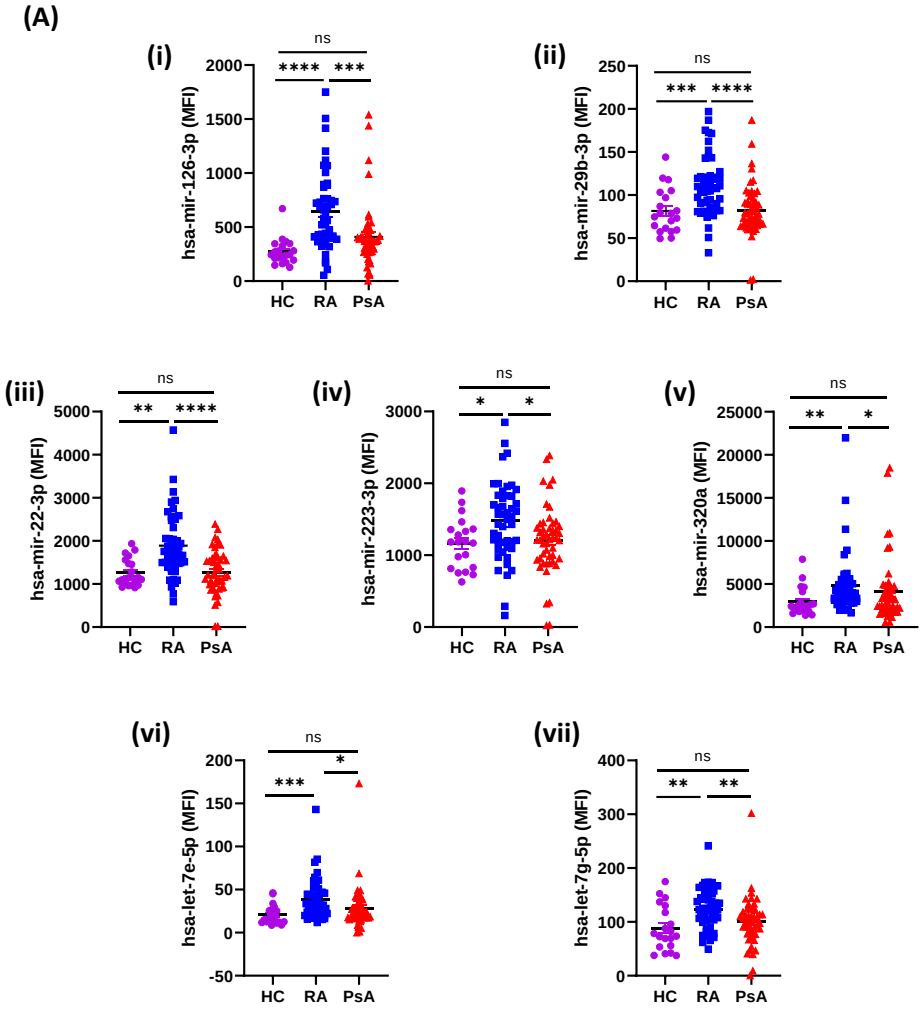

Figure 4.3. Expression of seven serum miRNA that are significantly increased in RA patients compared to both PsA patients and HC. (A(i-vii)) Dot plot representations showing MFI of the seven-serum miRNA of interest isolated from the serum of RA patients (n=48), PsA patients (n=49), and HC (n=20) and analysed and amplified using the Multiplex Circulating miRNA Assay. All data represented as Mean +/- SEM. Statistical analysis was performed using the non-parametric, Kruskal-Wallis Test with statistical significance defined by *p≤0.05, **p≤0.01, ***p≤0.001, ****p≤0.0001.

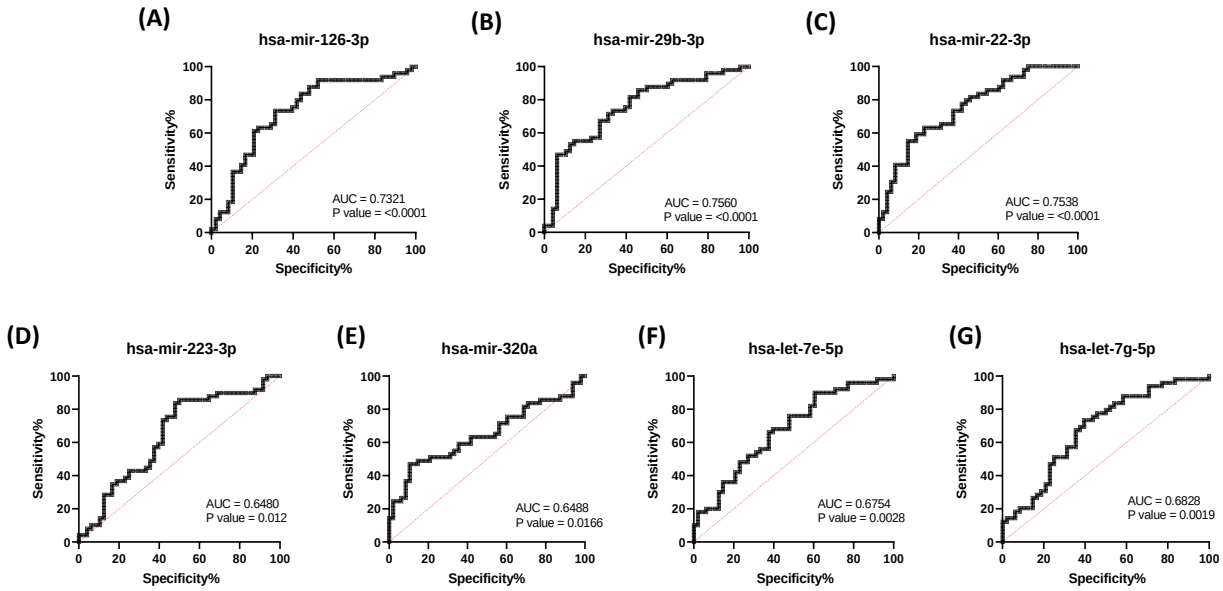

Figure 4.4. ROC curve analysis based on the expression levels of serum miRNA. (A-G) ROC curves of RA patients (n=48) based on the level of expression in serum of the seven miRNAs of interest compared to a PsA patient cohort (n=49). The prediction accuracy with which each miRNA can differentiate between RA and PsA is represented by the AUC. AUC was determined with 95% CI.

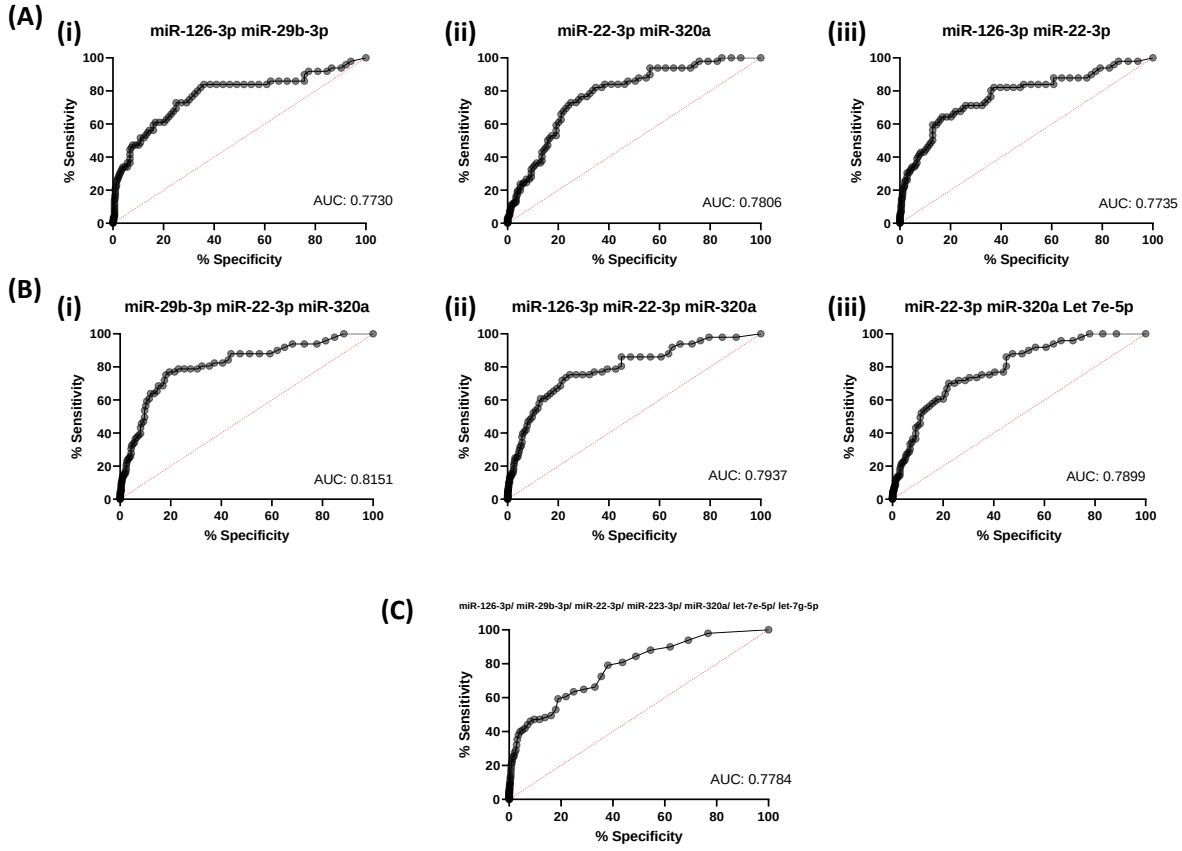

Figure 4.5. ROC curve analysis based on the expression levels of multivariant serum miRNA. The diagnostic value for multivariant serum miRNA for **(A)** two-miRNA signature, **(i)** miR-126-3p and miR-29b-3p; **(ii)** miR-22-3p and miR-320a; and **(iii)** miR-126-3p and miR-22-3p, **(B)** three-miRNA signature, **(i)** miR-29b-3p, miR-22-3p, and miR-320a; **(ii)** miR-126-3p, miR-22-3p, and miR-320a; and **(iii)** miR-22-3p, miR-320a, and let-7e-5p, with the strongest individual AUC values. **(C)** The predictive value of the seven most differentially expressed miRNA signature. The prediction accuracy with which each combination of miRNA can differentiate between RA and PsA is represented by the AUC. AUC was determined with a 95% CI.

4.4.2 Effect of disease parameters, ACPA positivity, and gender on the expression of the serum miRNA. Firstly, to ensure that the differential expression of miR-126-3p, miR-29b-3p, miR-22-3p, miR-223-3p, miR-320a, let-7e-5p, and let-7g-5p, observed in the serum of RA compared to PsA is not owing to potential disease severity in the patients, miRNA serum expression was compared to clinical parameters including DAS28, CRP, synovitis, and vascularity. Importantly, subsequent correlation analysis of patient subsets demonstrated that there were no significant correlations observed between the seven differentially expressed miRNA and any clinical features in the RA or PsA patients indicating that these miRNA are not associated with disease severity but rather the disease itself (Figures 4.6 and 4.7). To determine if the seven-miRNA skewed towards RA are affected by the presence/absence of ACPAs, a sub-analysis was performed comparing the serum miRNA levels of the miRNA in a cohort of ACPA+ RA patients (n=11) and ACPA- RA patients (n=18). As demonstrated in Figure 4.8A(i-vii), no significant differences were detected for any of the miRNA between ACPA+ vs ACPA- individuals indicating the biomarker value of these miRNA in all RA patients irrespective of their ACPA status.

Finally, to ascertain if gender may influence the expression of the miRNA associated with RA, patients in both disease states were stratified into male vs female categories and comparative analysis was performed (Figure 4.9). Interestingly, in the RA cohort, the levels of five of the miRNA; miR-29b-3p, miR-126-3p, miR-320a, let-7e-5p, and let-7g-5p, were not affected by gender and had comparable levels of expression in males vs females. However, the levels of miR-22-3p and miR-223-3p were significantly different between males and females in RA, with miR-22-3p demonstrating a significantly higher level in males ($p<0.05$) (Figure 4.9A(ii))) and conversely miR-223-3p exhibiting significantly higher levels in female patients ($p<0.05$) (Figure 4.9A(iii)). Furthermore, when compared directly between males and females in RA alongside PsA, the levels of miR-22-3p remained significantly higher in the RA cohort compared to PsA, irrespective of gender (Figure 4.9B(i)). However, whilst miR-223-3p expression in RA females was significantly higher than both males and females in PsA, the expression of this miRNA in RA males was similar to the PsA cohort, failing to demonstrate a significant difference (Figure 4.9B(ii)), thus suggesting this miRNA may be a stronger RA biomarker in females compared to males. Cumulatively, the data highlights the existence of gender effects on the expression of miRNA in RA and the importance of incorporating gender stratification into data analysis.

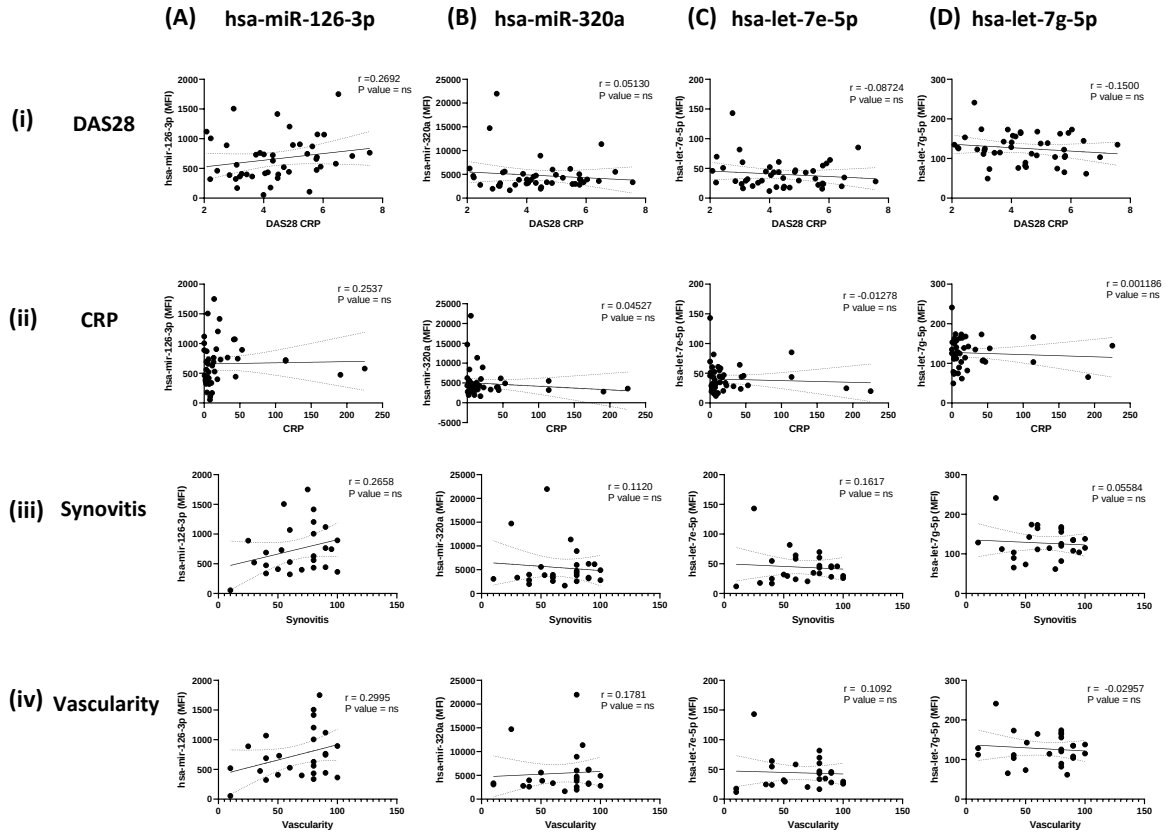

Figure 4.6. No correlation between serum miRNA and clinical parameters in RA and PsA patient cohorts. (A-D) Spearman pair-wise correlation analysis of miRNA expression and **(i)** DAS28, **(ii)** CRP, **(iii)** synovitis, and **(iv)** vascularity in RA and PsA patients (n=24-43). Simple linear regression model was used with unknown standards interpolated from the curve and the data presented with the 95% confidence bands of the best fit.

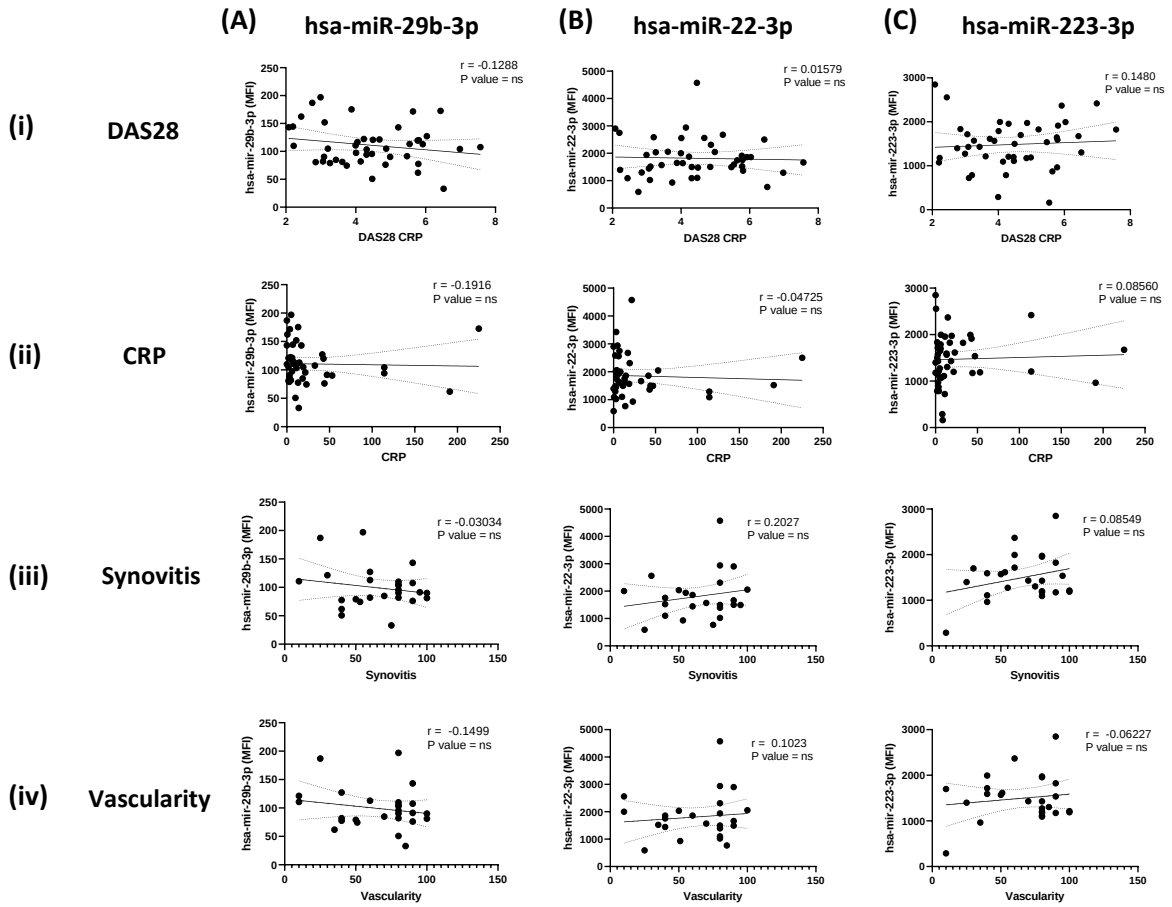

Figure 4.7. No correlation between serum miRNA and clinical parameters in RA and PsA patient cohorts. (A-C) Spearman pair-wise correlation analysis of miRNA expression and **(i)** DAS28, **(ii)** CRP, **(iii)** synovitis, and **(iv)** vascularity in RA and PsA patients (n=24-43). Simple linear regression model was used with unknown standards interpolated from the curve and the data presented with the 95% confidence bands of the best fit.

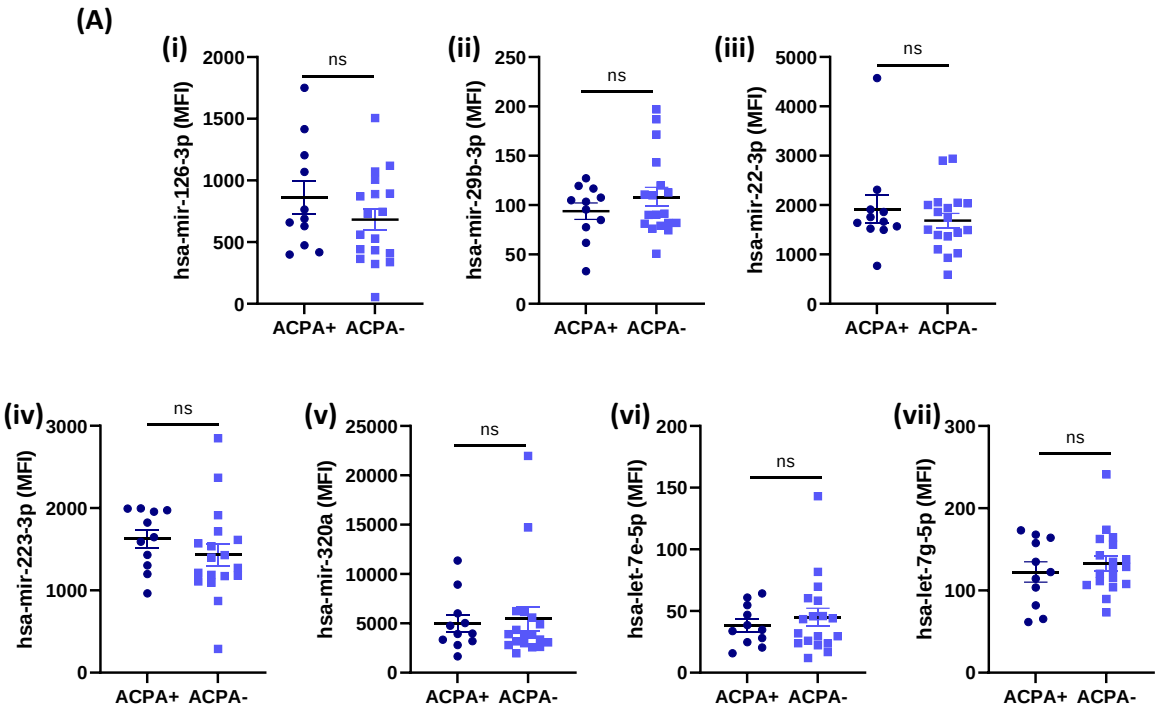

Figure 4.8. ACPA status did not alter levels of the seven significantly increased serum miRNA in RA patients. (A(i-vii)) Dot plot representations showing MFI of the relative expression of seven miRNA of interest isolated from the serum of a subset of RA patients; RA ACPA+ (n=11) versus RA ACPA- (n=18), analysed and amplified using the Multiplex Circulating miRNA Assay. All data represented as Mean +/- SEM.

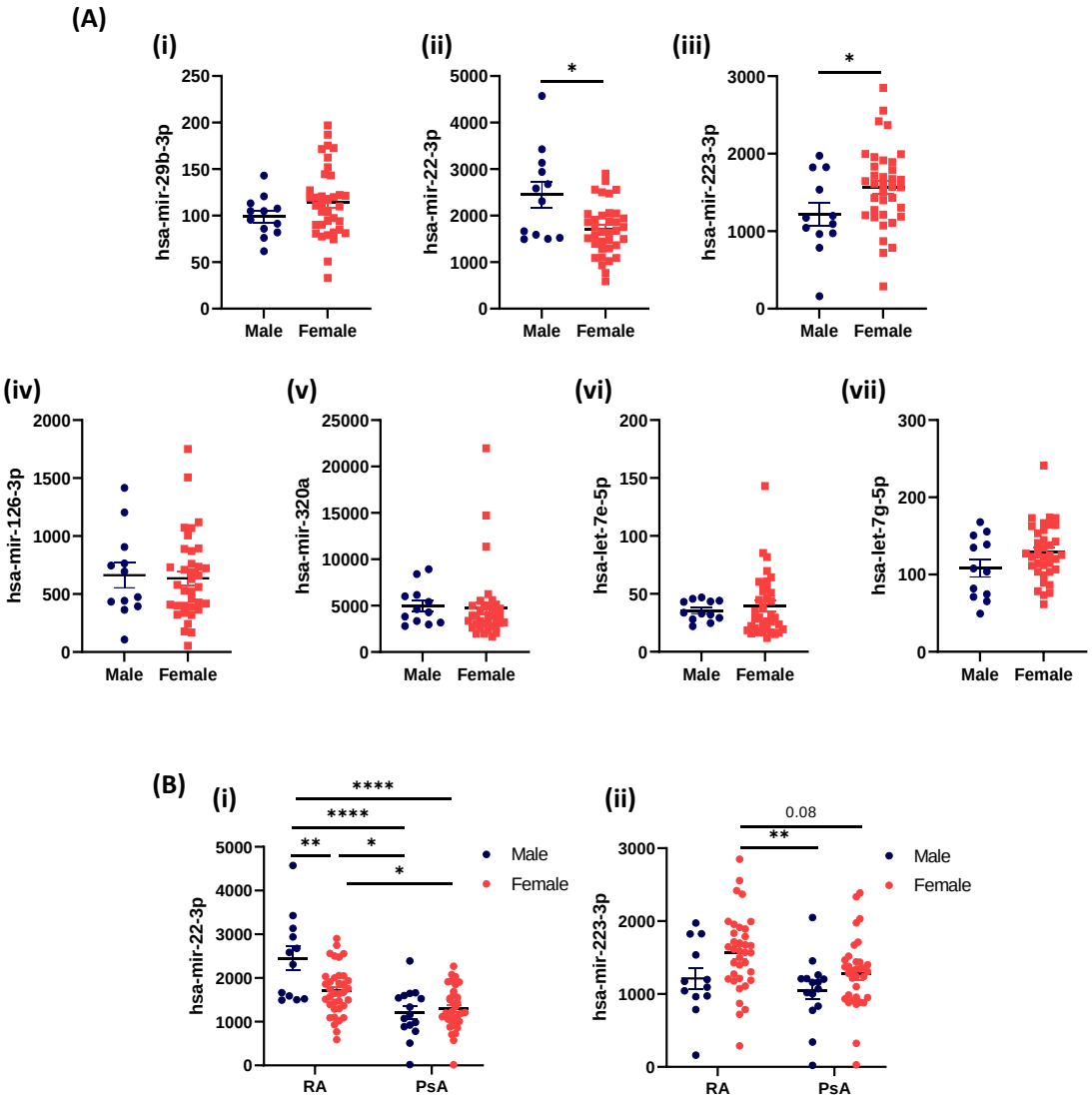

Figure 4.9. Differences in the expression of specific miRNA between males and females in the RA cohort. (A(i-vii)) Dot plot representations showing MFI of the relative expression of the seven miRNA of interest when compared directly between males (n=12) and females (n=36) in the RA cohort. **(B(i-ii))** Dot plot representations showing MFI of the relative expression of miR-22-3p and miR-223-3p when compared directly between RA males (n=12), RA females (n=36), and the PsA cohort (n=49). All data represented as Mean +/- SEM. Statistical analysis was performed using the non-parametric, Mann-Whitney *U* Test or Kruskal-Wallis Test with statistical significance defined by *p≤0.05, **p≤0.01, ***p≤0.001, ****p≤0.0001.

4.4.3 Functional pathway analysis of the seven significantly different miRNA between RA and PsA.

The DIANA miRPath tool was used to specifically recognise KEGG pathways that are enriched in genes containing predicted target sites of the identified seven miRNA (Figure 4.10) (Vlachos *et al.*, 2015). Analysis demonstrated that the Hippo signalling pathway and the ECM receptor interaction were the two topmost significant pathways targeted by six of the dysregulated RA serum miRNAs ($p<0.0001$), excluding miR-22-3p (Figure 4.10A). However, interestingly, the PI3K-AKT signalling pathway was identified as containing the greatest number of target genes, 126 in total, regulated by all seven of the miRNAs of interest (Figure 4.10A and B). Additional pathways with high significance identified to be regulated by activity of these specific seven miRNA included adherens junctions, the HIF-1 signalling pathway, the FoxO signalling pathway, and the mTOR signalling pathway, all of which demonstrated a significance of $p<0.01$. Furthermore, amongst the pathways being targeted by the miRNA were certain processes directly implicated in metabolism including the anabolic reactions; keratan sulfate biosynthesis, fatty acid biosynthesis, and o-glycan biosynthesis in addition to catabolic processes such as lysine degradation. However, these metabolic pathways identified were not under the control of all seven dysfunctional miRNA but by combinations of at least four of the miRNA (Figure 4.10A). The specific pathways, and the number of genes within each that are targeted by varying combinations of the seven miRNAs of interest can be found in detail in Figures 4.10A and B below, demonstrating the diversity and sheer complexity of pathways involved in RA vs PsA pathogenesis.

Next, the STRING software was utilised to provide supplementary information regarding the highly convoluted network of protein-protein interactions directly associated with the pathways identified to be targeted by the seven miRNAs of interest (Szklarczyk *et al.*, 2019). A clear visual representation of the direct and indirect interactions between the 126 genes involved in the significant PI3K-AKT pathway which were predicted to be regulated by the miRNAs was generated in the context of a biological system (Figure 4.11A). Interestingly, this network demonstrated a central hub of activity centred around the organisation of the ECM and actin cytoskeleton, both of which are integral to facilitating cell migration, a characteristic pathogenic feature of RA FLS as they invade into the adjacent cartilage and bone (Fassbender and Simmling-Annefeld, 1983; Croft *et al.*, 2019; Koliaraki *et al.*, 2020). Specific targets included several members of the collagen family, integrins such as ITGA5 and ITGA6, and growth factors including PDGF-β, all with critical roles in the dynamic modulation of the structural architecture of the cells and surroundings required for their invasive capacity. Moreover, MAPK signalling was prominent within this network, a well-established pathway responsible for the integration and amplification of signals to drive multiple physiological events including cell proliferation, differentiation, and importantly inflammatory responses. Notably, multiple proteins within this PI3K-AKT pathway appeared to be implicated in several pathogenic processes, with PDGFR-

α and PDGFR-β assuming a role in the regulation of cytoskeletal organisation, cell migration, and additionally MAPK signalling. This highlights the complexity of miRNA regulated pathways and the valuable nature of targeting them in order to limit the damaging effects of cellular invasion and inflammatory cascades in RA progression.

(A)

KEGG Pathway	No. of miRNA	No. of genes	P value
Hippo signalling pathway	6	65	4.17468299224e-09
ECM-receptor interaction	6	29	1.78303347328e-08
Lysine degradation	5	24	1.48310558063e-07
Adherens junction	6	41	1.19838242734e-06
Fatty-acid-biosynthesis	5	3	4.11040953062e-06
Glycosaminoglycan synthesis	4	9	2.67115642984e-05
TGF-β signalling pathway	6	36	4.07173095568e-05
FoxO signalling pathway	7	60	0.000313068596507
Focal adhesion	7	86	0.00150616995929
HIF-1 signalling pathway	7	48	0.00166960590817
O-glycan biosynthesis	5	10	0.0037867801522
PI3K-Akt signalling pathway	7	126	0.00764408901686
mTOR signaling pathway	7	28	0.00995070318448
Apoptosis	7	36	0.023953419166
Wnt signalling pathway	6	53	0.0418923167258

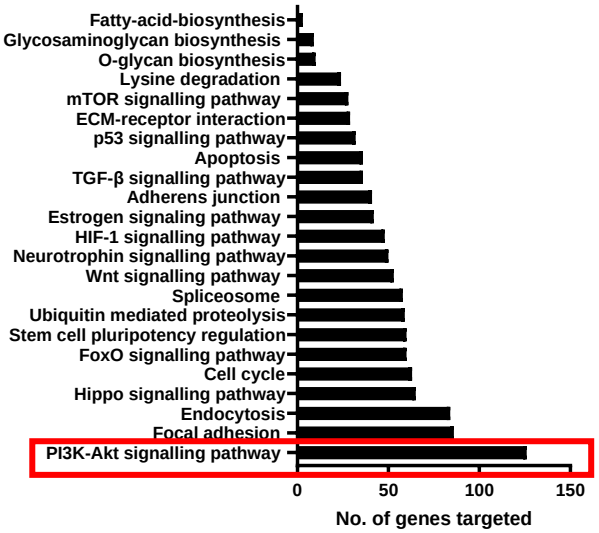

Figure 4.10. KEGG pathways enriched in miRNA target genes. The DIANA-miRPath tool was used to identify KEGG pathways enriched in genes significantly targeted by the seven differentially expressed miRNA of interest. **(A)** Table showing relevant KEGG pathways enriched in genes experimentally proven to be targeted by the seven miRNAs of interest in decreasing order of statistical significance. **(B)** Bar graph representing the number of genes in each relevant KEGG targeted by one or more of the seven miRNA of interest.

(A)

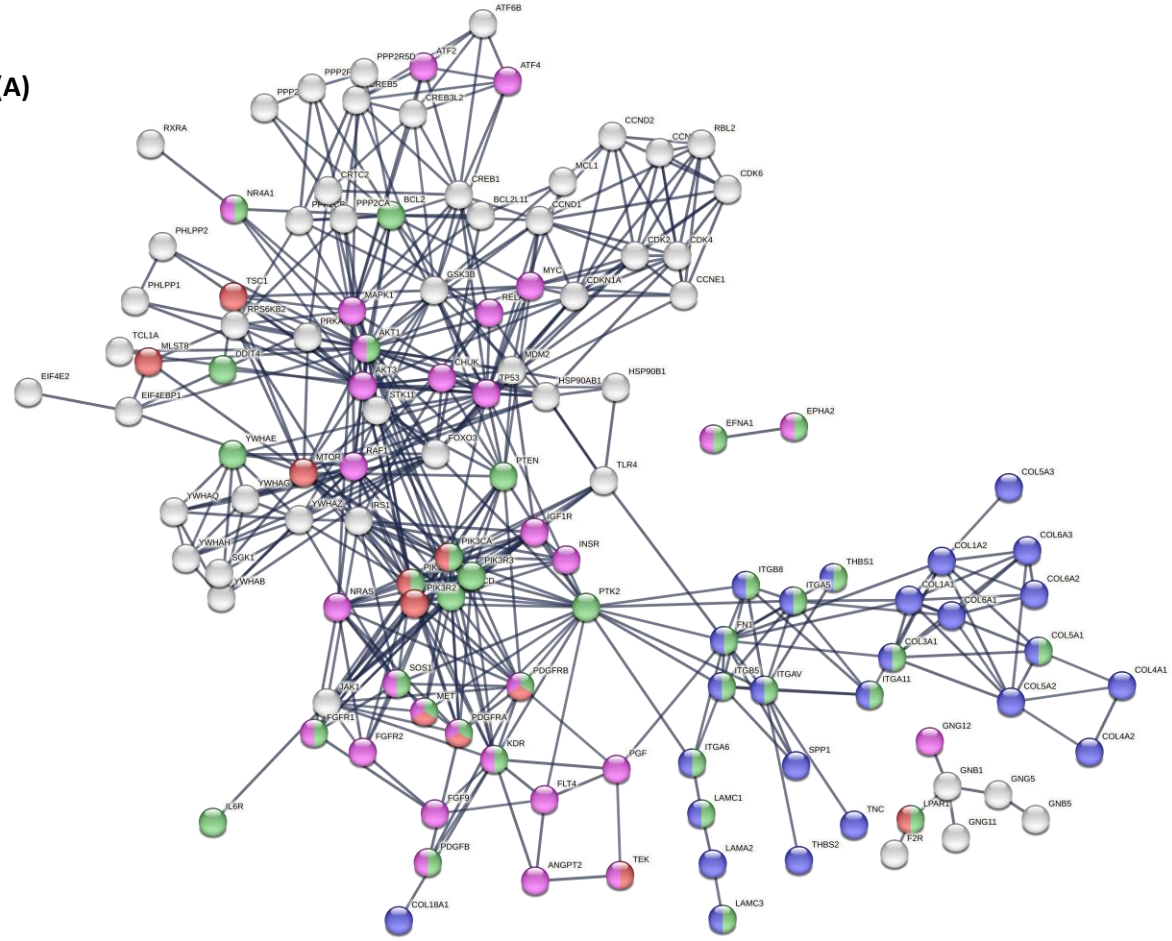

Figure 4.11. Potential miRNA target gene interactions and downstream effects for the PI3K-AKT signalling pathway. (A) STRING software was used to investigate and create a visual representation of the protein-protein interactions involved in the PI3K-AKT pathway that are targets of the top seven differentially expressed miRNA (highest confidence score=0.9). These networks may influence activity of downstream effector molecules with a significant role in aspects of RA pathogenesis including cell migration and inflammatory pathways. Colour coded genes indicate protein targets involved in the following pathways in RA; regulation of cytoskeletal organisation (red nodes), ECM organisation (blue nodes), cell migration (green node), MAPK signalling pathway (purple nodes).

4.4.4 Functional pathway analysis of the three significantly different miRNA demonstrating greatest separation between RA and PsA.

While a highly significant difference in the expression of seven miRNA between RA and PsA was identified, further biplot analysis of PCA and logplot of normalised miRNA expression demonstrated that the miRNA expression distribution was mainly associated with a dominant skew towards three specific miRNA in RA vs PsA; miR-29b-3p (****p≤0.0001), miR-22-3p (****p≤0.0001), and miR-223-3p (*p≤0.05) (Figure 4.12A). Moreover, as shown in Figure 4.12B(i-iii), ROC curve analysis of combinations of these three specific miRNA revealed a strong ability to distinguish between RA and PsA, with the greatest separation observed for miR-29b-3p and miR-22-3p, with an AUC of 0.7968 (Figure 4.12B(i)). The DIANA tool was then further used to analyse the specific pathways targeted by these three significant miRNA and the number of genes involved (Figure 4.13). The ECM-receptor interaction was the most significant pathway identified ($p<0.0001$), with a total of twenty-four genes being targeted by two of the miRNA – miR-29b-3p (20 genes) and miR-22-3p (11 genes). The PI3K-AKT signalling pathway contained the greatest number of target genes, with eighty-seven genes being influenced by contributions from all three miRNA of interest, more than two-thirds of the genes being regulated by all seven significantly different miRNA. Interestingly, miR-29b-3p and miR-22-3p exerted the greatest regulation over the pathway by targeting fifty-three and fifty-one genes respectively, whilst the contribution from miR-223-3p was minimal with only six genes targeted. Additional pathways containing genes targeted by all three-miRNA included focal adhesion, amoebiasis, and the FoxO signalling pathway, all $p<0.01$. Furthermore, anabolic pathways including fatty acid biosynthesis and catabolic pathways such as lysine degradation were also identified to be targets solely of miR-29b-3p and miR-22-3p. However, these metabolic pathways demonstrated the lowest number of target genes with only two genes, FASN and ACACA, recognised as targets in the lysine degradation process. The specific pathways, and the number of genes within each that are targeted by varying combinations of the three miRNAs of interest can be found in detail in Figures 4.13A and B below.

To identify the contribution solely of these three specific miRNA in targeting the PI3K-AKT signalling pathway, the STRING software tool was then used to visually analyse the complex protein network involving the eighty-seven genes (Figure 4.14A). Among the targets of interest were several processes highly associated with the invasive and inflammatory capacity of cells that perpetuate damage within the inflamed synovium including regulation of cytoskeletal organisation (red), ECM organisation (blue), cell migration (green), and the MAPK signalling pathway (purple). The specific proteins involved in mediating these various processes included growth factors FGF9, PGF, and PDGF-β, the adhesive glycoprotein THBS1, structural proteins including FN1 and collagen family members, in addition to several members of the AKT/mTOR signalling pathway such as MYC, AKT1, AKT3, and mTOR

itself. Of particular interest, these three-miRNA appeared to be targeting twenty-four out of the thirty-four proteins recognised as targets of the seven initial significantly different miRNA involved in cell migration. Notably, all eleven of the proteins associated with actin cytoskeletal organisation in the initial seven miRNA analysis were defined as targets of the three miRNA. These results suggest the central role these three miRNA assume in facilitating structural alterations and migratory processes within the inflamed joint and thus their potential benefit as therapeutic targets. Moreover, due to the involvement of all three miRNA in its regulation and the high number of gene targets (thirty-nine), the FoxO pathway signalling interactions were also examined using STRING analysis (Figure 4.15). Among the primary targets of interest in this pathway were several processes related to cell survival and death including the regulation of programmed cell death (red nodes), regulation of autophagy (blue nodes), and apoptotic processes (green nodes). Interestingly, the AKT1 gene also assumed a central role in this network where it demonstrated a function in the mediation of all three aforementioned processes, highlighting the potential importance of AKT1 in mediating not solely the PI3K-AKT pathway but additionally its interconnection with FoxO-mediated signalling. Furthermore, to further examine potential downstream targets of these three miRNA of interest, STRING interrogation of the targets in the Hippo signalling pathway was conducted due to its known role in promoting RA pathogenesis (Barker *et al.*, 2023). Among the targets of interest in this analysis were Wnt signalling (red nodes), a network critical to the process of joint formation and homeostasis of articular cartilage, and in particular the canonical Wnt pathway (blue nodes), in addition to the fibrosis-related and highly pleotropic TGF-β signalling pathway (green nodes) (Figure 4.16) (Peng *et al.*, 2022; Floudas *et al.*, 2022b; Huang *et al.*, 2023). Cumulatively, these results would imply that these three miRNA of interest assume an integral role in regulating not only migratory but additionally apoptotic and bone/cartilage-related inflammatory processes within the inflamed joint and thus their potential benefit in ameliorating RA pathogenesis if targeted therapeutically.

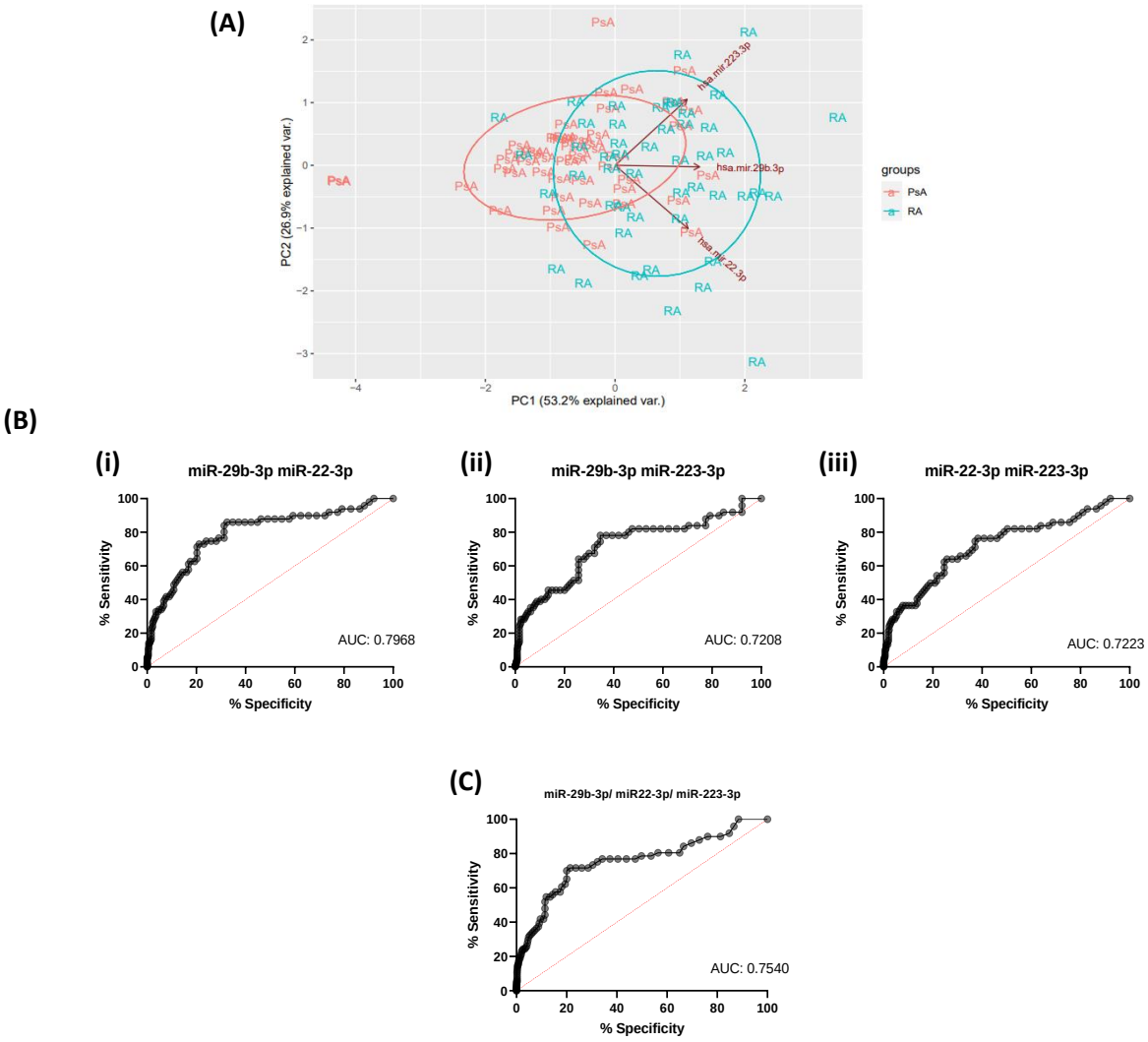

Figure 4.12. Biplot and ROC curve analysis of the three significant miRNA most skewed towards RA vs PsA. (A) PCA-biplots were generated under R v4.0 with package ggbiplot v0.5 with function ggbiplot. The predictive value for the most differentially expressed **(B)** two miRNA signature, **(i)** miR-29b-3p and miR-22-3p; **(ii)** miR-29b-3p and miR-223-3p; and **(iii)** miR-22-3p and miR-223-3p and **(C)** three miRNA signature; miR-29b-3p, miR-22-3p, and miR-223-3p, in the serum of RA patients (n=48) compared to a PsA patient cohort (n=49). The prediction accuracy with which each combination of miRNA can differentiate between RA and PsA is represented by the AUC. AUC was determined with a 95% CI.

(A)

KEGG Pathway	No. of miRNA	No. of genes	P value
ECM-receptor interaction	2	24	8.98508857424e-20
Fatty acid biosynthesis	2	2	3.27481972983e-10
Hippo signalling pathway	2	41	6.14869909062e-10
Focal adhesion	3	69	1.28095156673e-05
Cell cycle	2	45	1.50670969418e-05
Adherens junction	2	26	1.82404483848e-05
TGF-β signalling pathway	2	22	0.000214371555354
Lysine degradation	2	14	0.000216169215609
Amoebiasis	3	30	0.0038695256464
PI3K-Akt signalling pathway	3	87	0.00490562649047
FoxO signalling pathway	3	39	0.00529613018493

(B)

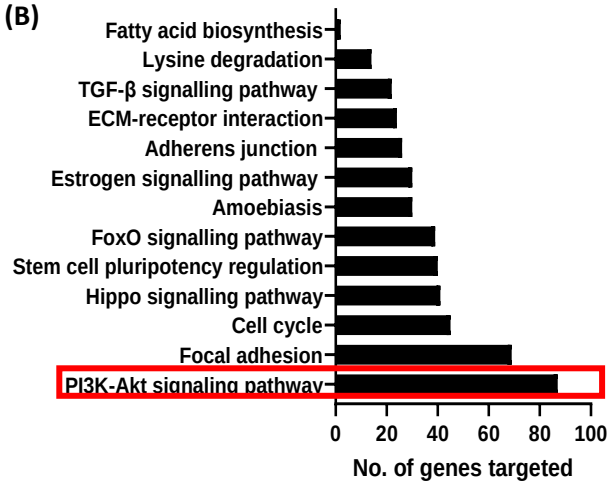

Figure 4.13. KEGG pathways enriched in miRNA target genes. DIANA-miRPath tool was used to identify KEGG pathways enriched in genes significantly targeted by the top three differentially expressed miRNA of interest. **(A)** Table showing relevant KEGG pathways enriched in genes experimentally proven to be targeted by the three miRNAs of interest in decreasing order of statistical significance. **(B)** Bar graph representing the number of genes in each relevant KEGG targeted by one or more of the three miRNA of interest.

(A)

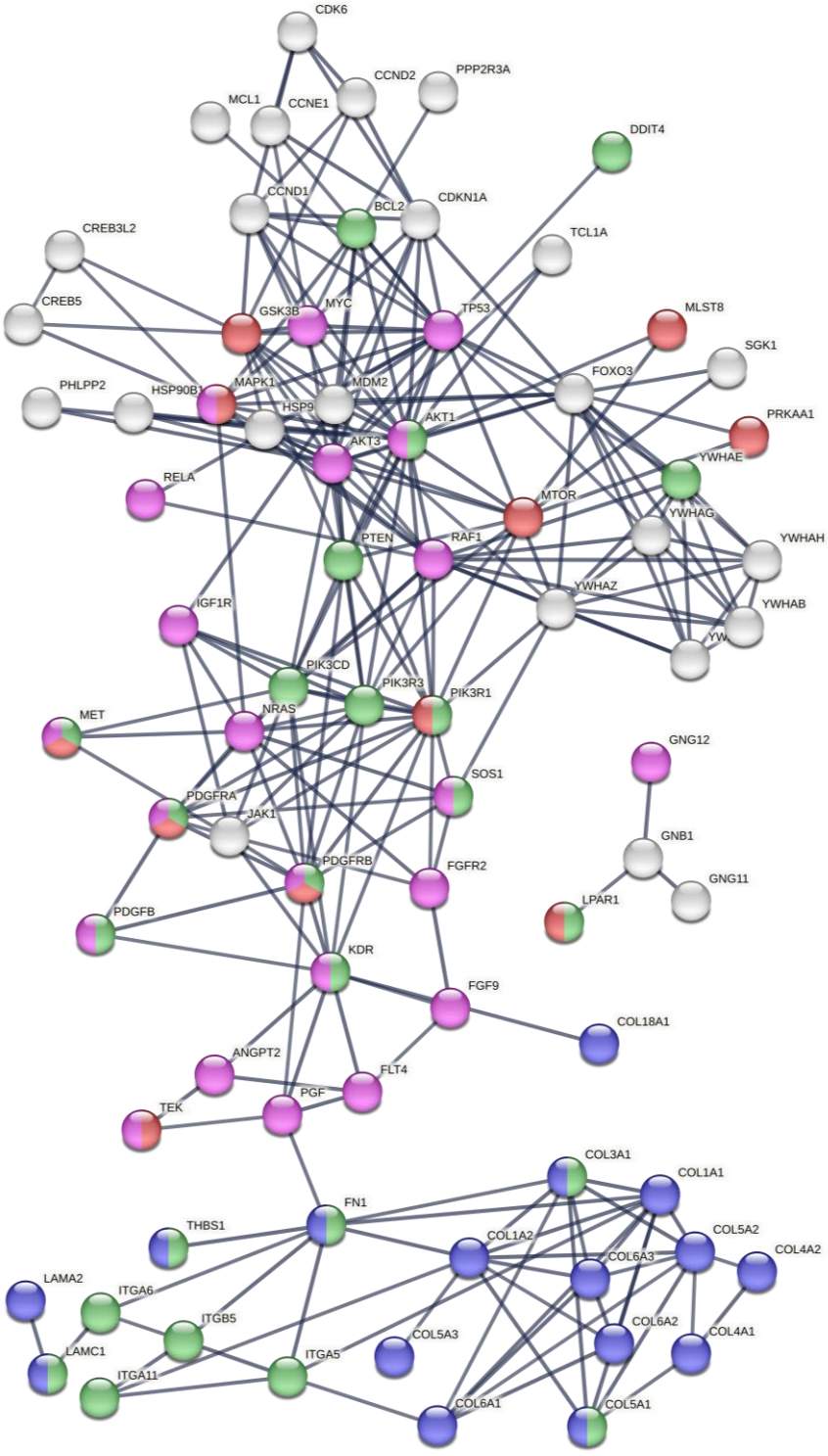

Figure 4.14. Potential miRNA target gene interactions and downstream effects for the PI3K-AKT signalling pathway. (A) STRING software was used to investigate and create a visual representation of the protein-protein interactions involved in the PI3K-AKT pathway that are targets of the top three differentially expressed miRNA (highest confidence score=0.9). These networks may influence activity of downstream effector molecules with a significant role in aspects of RA pathogenesis including cell migration and inflammatory pathways. Colour coded genes indicate protein targets involved in the following pathways in RA; regulation of cytoskeletal organisation (red nodes), ECM organisation (blue nodes), cell migration (green nodes), MAPK signalling pathway (purple nodes).

(A)

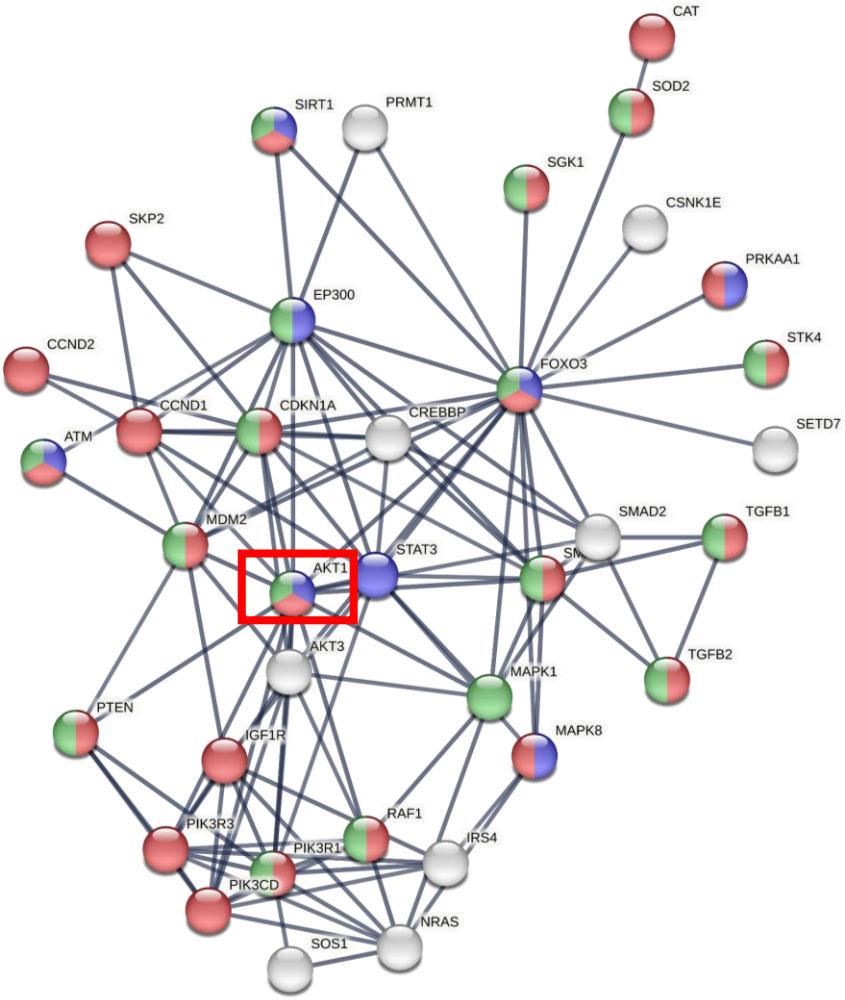

Figure 4.15. Potential miRNA target gene interactions and downstream effects for the FoxO signalling pathway. (A) STRING software was used to investigate and create a visual representation of the protein-protein interactions involved in the FoxO signalling pathway that are targets of the top three differentially expressed miRNA (highest confidence score=0.9). These networks may influence activity of downstream effector molecules with a significant role in aspects of RA pathogenesis including regulation of the following survival processes; regulation of programmed cell death (red nodes), regulation of autophagy (blue nodes), and apoptotic processes (green nodes). The red box highlights a central gene implicated in the PI3K-AKT signalling pathway.

(A)

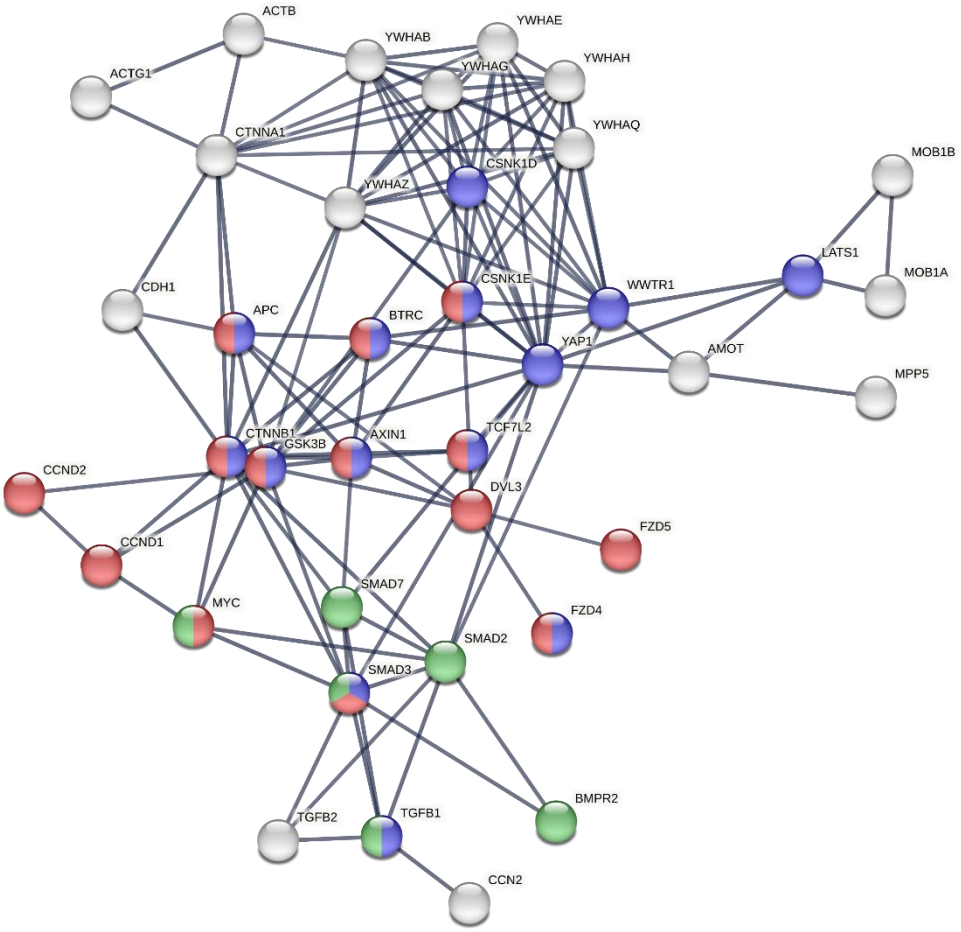

Figure 4.16. Potential miRNA target gene interactions and downstream effects for the Hippo signalling pathway. (A) STRING software was used to investigate and create a visual representation of the protein-protein interactions involved in the Hippo signalling pathway that are targets of the top three differentially expressed miRNA (highest confidence score=0.9). These networks may influence activity of downstream effector molecules with a significant role in aspects of RA pathogenesis including regulation of the following pathways: Wnt signalling pathway, Canonical Wnt signalling pathway specifically, and the TGF-β signalling pathway. Colour coded genes indicate protein targets of the above pathways in RA; regulation of Wnt signalling (red nodes), regulation of the Canonical Wnt signalling pathway (blue nodes), TGF-β signalling pathway (green nodes).

4.5 Discussion

The identification of biomarkers that may provide a non-invasive and reliable method of enabling early diagnosis of autoimmune diseases including RA, constitutes an area of intense focus as it has been well-established that earlier diagnosis precedes superior outcomes (Abdelhafiz *et al.*, 2023). Unfortunately, despite only being present in 70% of RA patients, ACPA positivity remains the only validated biomarker currently utilised for diagnosis in a clinical setting (Floudas *et al.*, 2021; Abdelhafiz *et al.*, 2023; O'Neil, Alpízar-Rodríguez and Deane, 2024). As a consequence, investigation of serum miRNAs as potential RA biomarkers and their prominent role in the initial development and progression of RA is of particular importance (Stanczyk *et al.*, 2008; Li *et al.*, 2024b). In this present study, nineteen serum miRNA related to immune dysfunction were identified that demonstrated significant differences between RA and PsA patient cohorts. However, upon further interrogation using PCA and biplot analysis, it was discovered that seven of these miRNA could function as potential biomarkers assisting in the early discrimination of RA patients from PsA patients, with all seven exhibiting good sensitivity and specificity for RA vs PsA. These seven-miRNA included miR-126-3p, miR-29b-3p, miR-22-3p, miR-223-3p, miR-320a, let-7e-5p, and let-7g-5p, all of which were significantly increased in RA serum compared to PsA serum and importantly, were additionally significantly increased compared to HC, thus confirming their possible involvement in RA pathogenesis. Moreover, in-depth analysis of particular patient subgroups confirmed that the ACPA status of the RA patient did not induce changes in the expression of the significantly different miRNA. Additionally, none of the miRNA exhibited a correlation with any of the disease parameters associated with inflammation or joint damage including DAS28, CRP, synovitis, and vascularity. This indicates that their potential value as biomarkers is not limited to a specific RA patient cohort but may in fact be reliable in all RA patients, irrespective of factors such as the extent of disease activity or synovitis. Conversely, a gender specific influence on the expression of two of the miRNA in the RA cohort; miR-22-3p and miR-223-3p, was identified highlighting the importance of patient gender stratification in research in order to establish optimal diagnostic methods for male versus female populations. Interestingly, using further biplot investigation, it was subsequently determined that three of these miRNA in particular were skewed predominantly towards RA compared to PsA - miR-22-3p, miR-29b-3p, and miR-223-3p. Downstream analysis of the potential gene targets resulted in the identification of several key pathways implicated in processes including angiogenesis, cell death, and bone metabolism, all of which are fundamental pathogenic events driving joint destruction within the inflamed RA synovium. Cumulatively, the results suggest that these three serum miRNAs may prove highly valuable, not solely as therapeutic targets, but as diagnostic markers enabling prompt discrimination of RA from PsA pathology.

An extensive body of literature exists that has previously elucidated the central involvement of miRNAs in a wide array of human diseases ranging from cancer, where they have been validated as reliable biomarkers of disease stage, to diseases of a viral or neurodegenerative nature (Garzon, Calin and Croce, 2009b; Wiedrick *et al.*, 2019; Salemi *et al.*, 2022; Smolarz *et al.*, 2022; Chakrabortty *et al.*, 2023). However, their significant role in autoimmune diseases is of particular interest in the context of our research topic, RA (Simpson and Ansel, 2015; Das and Rao, 2022; Nag *et al.*, 2023). The results corroborate previous studies identifying differences in the levels of circulating miRNAs, thus reinforcing the hypothesis that miRNAs exhibit aberrant expression in autoimmune-driven pathologies (Qu, Li and Fu, 2014; Tavasolian *et al.*, 2018; Li *et al.*, 2024b). Indeed, previous studies have illustrated the various roles different miRNA assume in RA pathogenesis including the well-established miRNAs miR-155 and miR-146, in addition to miR-31-5p, miR-126-3p, miR-221-3p, miR-24-3p, and miR-339-5p, amongst others, all of which have been shown to govern the functioning of innate and adaptive immune cell populations such as T cells, the release of proinflammatory cytokines, and transcriptional activation of the NF-κB pathway (Stanczyk *et al.*, 2008; Tu *et al.*, 2022; Nag *et al.*, 2023). Furthermore, although evidence regarding the role of miRNAs in PsA is considerably less extensive, recent work has highlighted panels of specific miRNA that demonstrate abnormal serum expression levels in patients compared to healthy comparators including miR-21-5p, miR-23a, miR-26a-5p, miR-125a, miR-130a-3p, miR-146a-5p, miR-151-5p, and miR-221-3p (Wade *et al.*, 2019a; Wade *et al.*, 2019b; Wade *et al.*, 2020). However, whilst these previous studies have all analysed RA or PsA against HC, this was the first study to specifically determine if expression levels of serum miRNA could prove efficacious in discriminating RA and PsA patients thus providing novel insights.

Whilst initial analysis identified seven miRNA that exhibited significant differences in expression between RA and PsA, further biplot analysis revealed that three miRNA in particular contributed to the greatest separation between the two pathologies, thus potentially exhibiting the capacity to function as independent biomarkers of RA compared to PsA. Interestingly, gender stratification of these three specific RA associated miRNA demonstrated unexpected results, with two of these miRNA exhibiting significantly different expression levels between males and females in the RA cohort exclusively. This suggests that although valuable as biomarkers, they may prove more effective in particular patient populations, highlighting the importance of patient stratification. In relation to their function, extensive previous investigations have demonstrated a central role for all three of these miRNA; miR-22-3p, miR-29b-3p, and miR-223-3p in diseases of an inflammatory nature in addition to cancer biology (Evangelatos *et al.*, 2019; Tang *et al.*, 2022; Jurj *et al.*, 2023; Wang *et al.*, 2023; Barbagallo *et al.*, 2024). The involvement of miR-22-3p in cancer has been previously well characterised where its upregulation has exhibited the potential to supress both cell migration and the

process of EMT, both critical promoters of tumour metastasis in various cancers including breast, liver, and non-small cell lung cancer (NSCLC) (Zou *et al.*, 2017; Cui *et al.*, 2023; Wang *et al.*, 2023). Whilst the available literature is sparse regarding its involvement in RA directly, increased serum levels of miR-22-3p, which is consistent with this chapter's findings, have previously been implicated as a strong predictor of RA development potential in susceptible individuals already demonstrating a positivity for circulating ACPA antibodies. This research identified significant upregulation of this miRNA in those who progressed from general systemic symptoms of autoimmunity to specific joint disease, an upregulation which was not detected in those who did not deviate from the original 'at-risk' status (Ouboussad *et al.*, 2017). Moreover, more recent studies have proposed that serum miR-22-3p may be a viable diagnostic biomarker for RA, with significantly higher levels detected in RA compared to HC, similar to the differences observed in the serum of RA and HC individuals in this study cohort (Tang *et al.*, 2022; Hassanpoor and Abbasi, 2022). Conversely, within the synovial joint itself, several lines of evidence have demonstrated a down-regulation of this specific miRNA, an occurrence which is strongly associated with the induction of pathogenic effects. Whilst it has been illustrated that a downregulation of miR-22-3p in RA synovial tissue and FLS correlated negatively with IL-6 promoting Cyr61 expression and the extent of FLS proliferation, additional research demonstrated that a similar downregulation resulted in heightened proliferative and inflammatory capacity of the resident FLS (Lin *et al.*, 2014; Zhang *et al.*, 2020a). Cumulatively, these two studies suggest that the levels of serum miRNA may exhibit an inverse relationship to the miRNA levels within the inflamed joint which is in line with previous studies (Lin *et al.*, 2014; Wade *et al.*, 2019b; Zhang *et al.*, 2020a).

Furthermore, similarly to miR-22-3p, the role of miR-29b-3p in cancer is significantly more established than its function in autoimmune disease, with miR-29b-3p being defined as a central regulator of EMT, a pathway implicated in cancer metastasis and tumour invasion (Yan *et al.*, 2015). It has been corroborated independently by multiple studies that miR-29b-3p exhibits a central role in prostate cancer where it functionally reduces cell motility and invasiveness of tumour cells, through direct targeting of MMP-2, in addition to impacting angiogenesis through VEGF inhibition (Steele, Mott and Ray, 2010; Hasegawa, Lewis and Esquela-Kerscher, 2017). A similar dampening effect on tumour metastasis via MMP-2 expression in NSCLC has also been reported, whilst the migration and invasion capacities of cancerous cells in both gastric and breast cancer were significantly supressed in the presence of elevated levels of this miRNA (Wang *et al.*, 2015; Li *et al.*, 2017; Zhao *et al.*, 2021). Moreover, in addition to its significant metastatic properties, an extensive amount of research has shown miR-29b-3p to be critical in regulating angiogenesis, not only in tumours but additionally in retinal microvascular ECs primarily through the targeting of VEGF (Li *et al.*, 2017; Sun *et al.*, 2024). In the context of RA and PsA, elevated expression of both angiogenic promoting VEGF and MMP-2 is

integral to the characteristic EC migration and subsequent angiogenesis observed within the joint microenvironment (Fearon *et al.*, 2003; Balogh *et al.*, 2019). Interestingly, the aforementioned papers related to miR-29b-3p in cancer all demonstrate reduced levels of this miRNA within the specific cancerous cells themselves, which could further reinforce the hypothesis that serum miRNA have an inverse relationship with the miRNA levels within the tissue itself. Indeed, this effect could be in play in RA with reduced levels of miR-29b-3p in the inflamed joint itself, but heightened levels as observed within the serum thus ultimately resulting in significant effects on angiogenic and migratory functions within the synovium. Furthermore, additional studied downstream targets of miR-29b-3p in pathological states include the dynamic histomorphometry of bone and inflammation associated genes and pathways such as NF-κB all of which are well-established features related to RA development and progression (Feichtinger *et al.*, 2018; Zhang *et al.*, 2019a; Akbaba *et al.*, 2021). Whilst there is a lack of available research relating to miR-29b-3p in RA specifically, studies in chondrocytes and rat models of OA have demonstrated that miR-29b-3p induces chondrocyte apoptosis and migration, paralleled by the release of cartilaginous degeneration-related molecules, with miR-29b-3p knock-down reversing these effects, suggesting that it may also play a role in cartilage homeostasis loss and subsequent degradation in RA (Chen *et al.*, 2017b; Horita *et al.*, 2022). Moreover, a recent study demonstrated a unique circulating miRNA signature in individuals with psoriasis and PsA, with this analysis determining that miR-29b-3p was among five miRNA best able to discriminate between PsA and HC (Haschka *et al.*, 2023). Although this result conflicts with the findings in this chapter, this may be due to differences in the demographics of the PsA patients and HCs included, particularly their treatment status and disease duration.

Furthermore, the biomarker and functional potential of serum miR-223-3p is becomingly increasingly recognised in a wide variety of pathologies ranging from Parkinson's disease to cancers including colorectal, breast, and pancreatic cancer, in addition to lung cancer where it may be used to not only distinguish cancerous tissue from HC but additionally to differentiate between lung cancer subtypes (Citterio *et al.*, 2023; Barbagallo *et al.*, 2024). Although the evidence indicates it does possess the capability to function as an onco-suppressor in certain contexts, the research is sparse in comparison to the abundance of available literature highlighting its oncogenic role, mediated through its dampening effects on cell death mechanisms and promotion of invasion and migration (Barbagallo *et al.*, 2024). In the context of rheumatic disease, this miRNA has been shown to be significantly upregulated compared to HC and OA comparators in RA human/mouse SF and cells including FLS, CD4+ T cells, and myeloid cells, where it has a known function in RA-associated erosion through suppression of osteoclastogenesis (Fulci *et al.*, 2010; Murata *et al.*, 2010; Li *et al.*, 2012). Moreover, although miR-223-3p expression in the RA serum specifically has been addressed in many studies, a considerable

amount of conflicting evidence regarding its expression levels have been identified. Indeed, studies have demonstrated reduced serum miR-223-3p in early RA patients, with a lack of a significant difference in serum miR-223-3p levels between established RA and HC, results which may be explained by differences in disease stage, therapeutic intervention, and considerable patient heterogeneity (Filková *et al.*, 2014; Dunaeva *et al.*, 2018). In contrast, and more in line with the findings in this thesis, previous analysis revealed that the level of miR-223-3p was significantly higher in the serum and synovial tissue of RA individuals compared to healthy comparators, and when considered alongside miR-146a could improve the prediction accuracy for diagnosis significantly, an effect not observed to as great an extent when the three miRNA of interest were combined (Zhang *et al.*, 2023b). In support of these findings, numerous studies have also shown that elevated serum miRNA-223-3p levels in RA correlate with the extent of disease activity, the risk of relapse, and in the regulation of pathogenic mechanisms involved in driving the characteristic inflammation (Fulci *et al.*, 2010; Evangelatos *et al.*, 2019). The functional implications of this miRNA are extremely important in the context of inflammation with several studies highlighting the strong association of miR-223-3p with NLRP3 inflammasome regulation in several disease and mouse models including radiation-induced inflammatory responses in macrophages, the promotion of a DC tolerogenic phenotype in autoimmune myocarditis, and the regulation of chondrocyte driven cartilage remodelling, all cell types that are also important in RA perpetuation (Dong *et al.*, 2019; Chen *et al.*, 2020; Zhang *et al.*, 2023c). Additionally, the role of this miR-223-3p/NLRP3 interaction in RA specifically has been investigated with targeting of this pathway exhibiting success in the promotion of pathogenic human RA FLS apoptosis (Wu *et al.*, 2020b). Furthermore, its effects extend beyond the inflammasome to other inflammatory processes with a study showing the ability of miR-223-3p to induce macrophage secretion of proinflammatory cytokines in RA, in addition to studies demonstrating a decrease in the levels of EC adhesion molecule expression, thus suggesting its possible involvement in immune cell influx into the RA synovial joint (Ormseth *et al.*, 2015). With this knowledge, to ensure higher DA and inflammatory parameters amongst RA patient cohorts was not influencing the results, subgroup analysis of matched RA and PsA individuals with the same disease activity was performed and the results revealed that the three miRNAs were still higher in RA compared to PsA serum.

Functional pathway analysis of the seven significantly different miRNA most strongly associated with RA compared to PsA indicated that the PI3K-AKT pathway is a key target, with the greatest number of associated target genes. Interestingly, these results were mirrored in the analysis of the top three significantly different miRNA skewed towards RA thus, not only highlighting the central role of the PI3K-AKT pathway in mediating/contributing to the destructive events within the RA joint, but also the valuable nature of these three miRNA as potential biomarkers and possibly therapeutic

targets. An abundance of existing research has highlighted the integral role the PI3K-AKT pathway assumes in a diverse range of cellular processes including cell growth and proliferation in RA FLS and ECs, regulation of metabolism, promotion of angiogenic functions, and the release of multiple proinflammatory cytokines that perpetuate the inflammation further (Ding *et al.*, 2023). Indeed, previous success has been achieved in treating immune-mediated arthritis by targeting this pathway with PI3K small molecule inhibitors (Malemud, 2015). However, of particular significance is the network of genes within this pathway identified to be potential targets of the RA miRNA, which included metabolic and invasive factors such as the master metabolic regulator mTOR, SIRT1, RAC-1, FN-1, ITGA5, and AKT3, which was also shown to be a key downstream target regulated by miR-29b-3p in breast cancer (Li *et al.*, 2017). This network also included several members of the collagen family, all genes with critical roles in the dynamic reorganisation of the cellular scaffolding and promotion of invasive capacity (Trepat, Chen and Jacobson, 2012).

The identification of these genes as potential targets for alleviating the pro-migratory capacity of cells within the synovium is supported by previous research showing that direct blockade of the mTOR pathway, in which AKT proteins assume a central role as upstream regulators, can have a suppressive effect on RA FLS migratory and invasive mechanisms (Barker *et al.*, 2023). Furthermore, the FoxO signalling pathway was established as another significant pathway targeted by all three miRNAs of interest with the next greatest number of target genes at thirty-nine. Interestingly, FoxO1 has also previously been shown to assume a role in angiogenesis where it is responsible for tip cell selection though its governance over VEGF-responsive tip cell-enriched genes (Miyamura *et al.*, 2024). In the context of RA, it has been previously established that FoxO family members play a key role in the modulation of cell proliferation and survival, with eloquent studies showing that not only is reduced FoxO1 expression required to promote FLS survival but additionally, miR-155 directly targets FoxO3a in FLS resulting in heightened release of proinflammatory cytokines and elevated proliferative capacity (Grabiec *et al.*, 2015; Wang *et al.*, 2020b). Key potential gene targets of the three miRNAs were identified as being central to programmed cell death and apoptotic processes including SIRT1, PTEN, RAF1, and ATM, reinforcing the valuable nature of potentially targeting this pathway to restore normal states of homeostasis in pathogenic RA cells. Moreover, AKT1 was identified as a key target gene of the three miRNAs in this pathway also where it appeared to have roles in the regulation of cell death mechanisms and autophagy as determined by the STRING analysis.

Previous literature has highlighted a clear interconnected network between PI3K-AKT and FoxO signalling, with an RA-associated paper identifying a reduction in pathogenic FLS apoptosis induced through AKT1 upregulation which directly inhibits FoxO1 (Liu and Yan, 2019). This interaction may be of particular interest in the context of RA therapeutic intervention as it suggests that targeting

the three miRNAs could exert beneficial effects on not one but a myriad of pathways driving RA pathogenesis. Finally, in-depth analysis of the Hippo signalling pathway was performed, one of the most significant pathways identified as a target by DIANA analysis. With well-established roles in facilitating cell migration through actin cytoskeleton rearrangement, its propensity to also interact with the aforementioned mTOR signalling, driving FLS pathogenic behaviors, has been recently highlighted (Barker *et al.*, 2023). Interestingly, Wnt genes and particularly members of the canonical Wnt pathway were identified as potential downstream targets, in addition to TGF-β related genes. These genes are critical in multiple biological phenomena, with Wnt family members associated with bone destruction and formation, a process severely dysregulated in rheumatic disease (Huang *et al.*, 2023). Thus cumulatively, this evidence emphasises the future therapeutic potential of targeting miRNAs to reduce several different avenues of synovial joint inflammation and deterioration simultaneously.

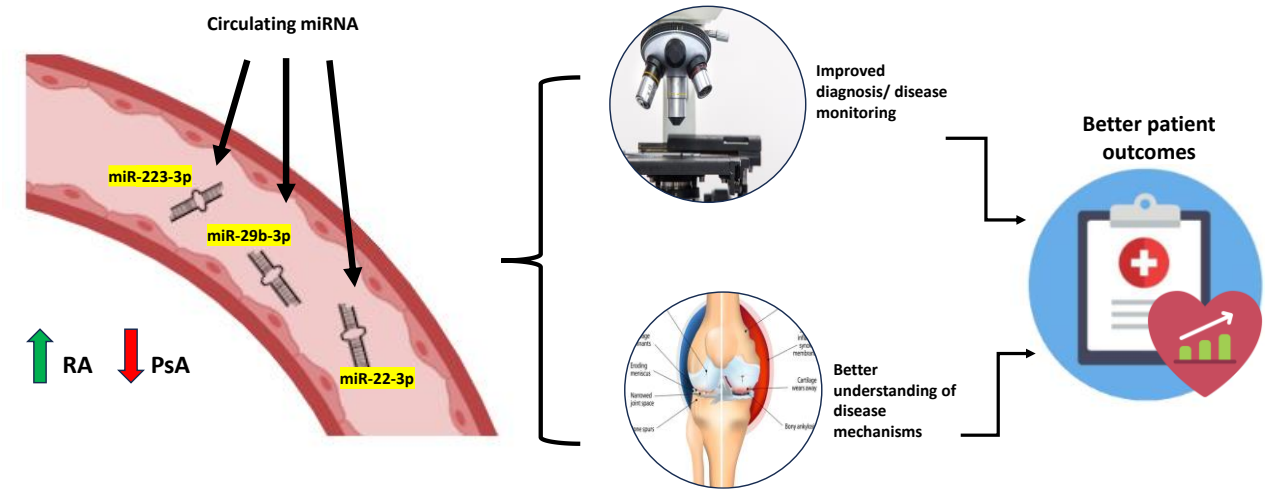

Figure 4.17. An overview of Chapter 4 focusing on the biomarker potential of miRNA in RA and PsA. The levels of circulating miRNA; miR-22-3p, miR-223-3p, and miR-29b-3p are significantly higher in the serum of RA compared to PsA. This highlights the valuable nature of using miRNA not only as diagnostic biomarkers but additionally as therapeutic targets, resulting in improved patient outcomes. This figure was made using BioRender.

In conclusion, the results from this study indicate that analysis of serum miRNA may indeed provide a minimally invasive and reliable manner of distinguishing RA from PsA patients, in addition to introducing targets for potential therapeutic intervention. However, limitations of the study include that this was a focused panel of 68 miRNA, and there may be additional miRNA that are also associated with RA and PsA that were not included in the analysis. Further investigation of greater patient cohorts from diverse multicentres are also required to validate the results obtained before widespread implementation in a clinical setting.

CHAPTER 5:

General Discussion and Future Directions

5.1 General Discussion

RA and PsA are complex, heterogenous diseases characterised by extensive soft tissue swelling and synovial inflammation, which is not merely restricted to the joint but additionally multiple clinical domains (Veale and Fearon, 2015; Veale and Fearon, 2018; Alivernini, Firestein and McInnes, 2022; Bragazzi *et al.*, 2022; Winthrop *et al.*, 2024). In recent years, utilisation of conventional and newer imaging modalities, including magnetic-resonance imaging and computed tomography, have proven efficacious in assisting clinicians in the diagnosis and monitoring of RA and PsA patients through the identification of characteristic features, such as 'pencil-in-cup' erosions and entheseal inflammation, both predominant indicators of PsA that would not otherwise be detected (Mc Ardle *et al.*, 2015; Braga *et al.*, 2020; Saalfeld *et al.*, 2021; Elliott, McGonagle and Rooney, 2021). However, a large number of patients still remain either underdiagnosed or misdiagnosed, particularly in non-rheumatological settings, which can have serious consequences for patient outcomes (McGonagle, Hermann and Tan, 2015; Merola, Espinoza and Fleischmann, 2018). In the context of RA, delays of diagnosis can have significant impacts on disease progression and treatment resistance risk with studies showing patients who initiate therapy after 12 months compared to those at 3 months exhibiting reduced improvement in disease activity, joint destruction, and functional outcomes (Green *et al.*, 1999; Nell *et al.*, 2004; Veale, Orr and Fearon, 2017; Naeem *et al.*, 2021). Indeed, studies are now focusing on individual's 'at-risk' of developing RA, with recent landmark studies suggesting that early intervention with abatacept in this cohort could potentially diminish their risk of progression to established disease (Cope *et al.*, 2024). Similarly, in PsA, it has been shown that there is an optimal time window to ensure patients achieve maximum treatment effects, with even a 6-month delay between initial symptom onset, proper assessment by a rheumatologist, and treatment initiation culminating in the development of peripheral joint erosions and worse long-term impacts on joint mobility (Haroon, Gallagher and FitzGerald, 2015). Therefore, timely treatment is imperative, necessitating the requirement for biomarkers to facilitate this. Moreover, successful patient outcomes are not limited to the notion of 'window-to-treat' as the correct treatment should also support a more 'treat-to-target' approach proposed by EULAR, an approach that at a fundamental level requires a deep understanding of the cellular mechanisms driving the disease (Veale, Orr and Fearon, 2017; Alivernini, Firestein and McInnes, 2022; Winthrop *et al.*, 2024).

It is now recognised that despite their similarities, RA and PsA are indeed two distinct pathologies with distinguishable clinical features, co-morbidities, and radiographic erosions (Veale and Fearon, 2018; Smolen *et al.*, 2018; Merola, Espinoza and Fleischmann, 2018; Alivernini, Firestein and McInnes, 2022; Winthrop *et al.*, 2024). However, the mechanistic differences driving them at a cellular and molecular level are still not fully understood. In this regard, the role of FLS, stromal cells

responsible for perpetuation of joint inflammation and invasive damage, are of critical importance with most studies to date investigating their phenotypes and function in RA exclusively (Croft *et al.*, 2016; Mizoguchi *et al.*, 2018; Croft *et al.*, 2019; Koliaraki *et al.*, 2020; Micheroli *et al.*, 2022; Zhang *et al.*, 2023a). However, there is an absence of studies exploring their corresponding profiles in PsA, as well as providing a direct comparative analysis of FLS between RA and PsA, knowledge of which may be pivotal in understanding their differential pathogenic progress. Therefore, this thesis focused on conducting an in-depth analysis of FLS subsets within the inflamed synovium, to study their functionality and to define potential therapeutic strategies. In addition to investigating differential cellular mechanisms of action at the site of inflammation, potential soluble biomarkers in the circulation that may distinguish RA from PsA were examined.

In recent years, the utilisation of bioinformatic approaches including scRNA-seq and 'omic' analysis has revolutionised understanding of the cellular nature of the synovium. Although examining cells as an individually entity is useful and can provide highly important information at a mechanistic level, the true nature of the *in vivo* environment is far more complex. Thus, these techniques provide clear insights into the 'multi-tiered' complexity of the joint at the gene expression level and the various cell-cell interactions that drive cell phenotype and functional characteristics. In this thesis, scRNA-seq analysis was incorporated to thoroughly explore the diversity of FLS subsets and their regulators present within the RA and PsA synovial tissue, with the primary objective of understanding how different populations may be important in driving disease aspects that differ between RA and PsA. However, although bioinformatic analysis is useful, the question always remains - can it actually be proven at a functional level? Therefore, in this thesis multiparametric flow cytometry and functional experimental analysis were incorporated alongside the scRNA-seq to provide greater validity to the findings. Moreover, in the past, cell types were considered predominantly homogenous particularly within a specific tissue, a central dogma that has been proven incorrect in recent years. In the context of FLS, a research explosion has brought the considerable heterogeneity of FLS to light, with differences in their transcriptomic and phenotypic profiles relating to their specific anatomical location and cellular interactions within the joint (Muhl *et al.*, 2020; Kemble and Croft, 2021; Micheroli *et al.*, 2022; Faust *et al.*, 2023). In Chapters 2 and 3, for the first time, FLS subsets were compared between RA and PsA synovial tissue, identifying not only differences in their pathogenic regulation but a diversity in the dominant populations within each disease state, which aligned with previous literature showing significant variation between FLS subsets and function in RA versus healthy and OA tissue (Mizoguchi *et al.*, 2018; Croft *et al.*, 2019; Faust *et al.*, 2023).

In Chapter 2, for the first time, in-depth global scRNA-seq analysis of the RA vs PsA synovium was conducted, focusing on FLS function and regulation and providing significant insight into the

impact of additional infiltrating immune cells on their pathogenic activity. Initially, using single-cell analysis of synovium tissue biopsies, a significant enrichment of THY1+ sub-lining FLS in RA was demonstrated whilst PsA exhibited enrichment for the THY1- lining layer phenotype. Furthermore, taking advantage of the fact that this analysis was performed on all cells, both stromal and immune within the synovium, ligand-receptor interaction analysis was subsequently performed to determine what cell communication could be driving the FLS activity, providing potential therapeutic targets. From this bioinformatic information, it was ascertained that a synergistic interaction between two primary cytokines – IL-1β and TGF-β, derived predominantly from macrophages and T cells within the cellular microenvironment, could be driving the proinflammatory, metabolic, and invasive capacity of the THY1+FAP+ RA FLS enriched cluster. Subsequent *ex vivo* experiments on IL-1β and TGF-β treated FLS supported this hypothesis with synergistic increases observed in several proinflammatory cytokines, chemokines, adhesion molecules, and invasive MMPs, all of which was paralleled by a significant synergistic increase in the glycolytic profile of the RA FLS. Moreover, a closer examination of metabolism at the mitochondrial level revealed a significant shift towards fission alongside a highly specific activation of the ATF6 branch of the UPR.

When considered collectively, it was hypothesised that treatment with IL-1β and TGF-β drive the FLS mitochondria towards a fission phenotype, a process that has been shown to support a skew towards rapid ATP producing states, reflecting the enhanced glycolytic capacity of the RA FLS (Biniecka *et al.*, 2016; Bustamante *et al.*, 2017; Fearon *et al.*, 2022). However, this dominance in fission disrupts the homeostatic balance of the ER, an organelle that is tightly interconnected with the mitochondria, culminating in the rapid upregulation of the UPR to circumvent the induced stress. As mentioned previously, although two branches of the UPR are more focused on pro-apoptotic roles, the results demonstrate an activation of the ATF6 branch through BIP, both of which were increased with IL-1β and TGF-β treatment and have been shown to facilitate cell survival (Miglioranza Scavuzzi and Holoshitz, 2022). ATF6 specifically assumes a multi-pronged role in cell survival under stressful conditions through the robust upregulation of several cytoprotective genes involved in the enhancement of ER folding capacity and clearance of misfolded proteins to the proteosome, in addition to the maintenance of healthy ER redox status (Miglioranza Scavuzzi and Holoshitz, 2022). In light of this, it could be theorised that this preference for the 'pro-survival' pathway following exposure to IL-1β and TGF-β is an adaptive mechanism to ensure the FLS can generate abundant energy though fission-driven glycolysis to promote their pathogenic activity whilst simultaneously remaining alive. Indeed, in support of this theory, previous literature in murine models has exhibited involvement of this ATF6 pathway in promoting potent proinflammatory cytokine production in liver ischemic reperfusion injury (Rao *et al.*, 2014). Moreover, an eloquent study conducted in colorectal

cancer cells suggested that heightened BIP production as a consequence of hypoxia-induced ER stress culminated in more aggressive disease progression (Verras *et al.*, 2008). Cumulatively, this reinforces the notion that 'pro-survival' is not always beneficial. In the context of this research, it may be ensuring the FLS can sustain their highly invasive and pathogenic behaviour, thus perpetuating RA disease progression.

Furthermore, this chapter reinforces the ambiguous nature of cytokines within the joint, clearly highlighting that classification of cytokines as merely 'good' or 'bad' is an oversimplification. In the context of TGF-β, the results indicate that when acting in concert with IL-1β, certain synergistic interactions worsen pathogenic effects. Conversely, in other situations, it exerts a rescue effect on the negative impact of IL-1β, such as in the context of VCAM-1, MMP-1, and the specific chemokine receptors CXCR3 and CXCR4. This has been previously demonstrated in ECs treated with TGF-β and stimulatory LPS, suggesting that the rescue effects of TGF-β may play a role in interactions with several different more classical proinflammatory cytokines whilst additionally highlighting that these effects are not FLS exclusive, an important consideration in light of the abundant cell types in the RA joint (Kang, Brummel and Lee, 1996). Further research into 'pleotropic' cytokines such as TGF-β is warranted to fully understand their predominant roles in the pathogenesis of RA and what could be influencing their pro- versus anti-pathogenic effects. Much of this may be rooted in a better understanding of the downstream signalling pathways through which the individual cytokines induce their effects and the potential shared mediators. In light of this, a critical finding of the research was the identification of TAK1 as a central regulator of IL-1β and TGF-β synergistic/additive effects, with suppression of this signalling molecule resulting in a reduction in several synergy-induced pathogenic mediators/events in isolated FLS and additionally, whole biopsy explants. As IL-1β targeting therapies alone have proven disappointing, these results suggest that a move towards a more dual-therapy targeted approach could achieve more successful results in RA patients (Kondo, Kuroda and Kobayashi, 2021). Moreover, it also introduces the question – would targeting downstream molecules such as TAK1 itself be more beneficial than targeting the individual cytokines in order to achieve optimal suppression of several interconnected pathways simultaneously?

Building on the foundations of Chapter 2, in Chapter 3, reanalysis of the scRNA-seq data focusing solely on the FLS within the joint provided a more detailed analysis of their phenotypes and enabled more specific stratification. Sixteen distinct FLS clusters were identified, with significant enrichment of three sub-lining clusters in RA: CXCL12+CHI3L2+ and CXCL12+APOE+, both of which demonstrated high expression of immune related genes, and lastly an ECM/cytoskeletal regulatory THY1+POSTN+ subset. Interestingly, when this subset was compared between RA and PsA, several pathways were upregulated in the RA FLS including MAPK signalling, focal adhesion, VEGF signalling,

and the Hippo signalling pathway, which aligns with the higher YAP expression identified on the RA FLS. Moreover, the RA FLS demonstrated greater glycolytic and oxidative phosphorylative gene module expression, indicating a more metabolically active state of this subset in RA compared to PsA. When considered cumulatively, this suggests that the THY1+POSTN+ subset is not only higher in RA but additionally contributes to pathogenic progression more extensively in RA compared to PsA, introducing the theory that when focusing on highly specific subsets (beyond the scope of just THY1+ vs THY1-) the exact function of FLS within the same subset may vary depending on the disease state. Further flow analysis enabled the stratification of populations based on a greater number of characteristic surface markers including THY1, CD55, CD34, and FAP, with the enrichment of two sub-lining populations, THY1+CD34-CD55-FAP+ and THY1+CD34+CD55-FAP+ in RA and a lining layer subset, THY1-CD34-CD55+FAP+ in PsA, corroborating the single-cell data. In line with the scRNA-seq, using the flow and cell sorting, a more potent inflammatory role of the THY1+ subsets was identified, in addition to higher angiogenic properties, whilst the THY1- FLS exhibited a remarkably more enhanced expression of MMPs highlighting their role in cartilage and bone degradation. These results correlated with the histological analysis of the corresponding patient tissue, which revealed significantly greater immune cell infiltration in RA combined with a more frequent presence of lymphoid aggregates, whilst PsA donors appeared to have a thicker lining layer, reinforcing a greater THY1- enrichment. Interestingly, the extent of vascularity was similar between both diseases despite the greater THY1+ dominance in RA, suggesting a role for additional factors in driving PsA angiogenesis. Although all subsets are indeed found in both disease states, a deeper understanding of these differences in FLS subset dominance in RA vs PsA is incredibly important as, in theory, the more dominant a population, the greater functional impact they exert. In the context of this research, combining extensive data at the gene, protein, and functional level from scRNA-seq, flow cytometry, and experiments on sorted cells, it has been identified that the RA enriched FLS are more involved in driving inflammatory processes compared to the MMP expressing role of PsA dominant FLS, knowledge that could prove useful when selecting therapeutic targets to have maximum benefit in patient cohorts.

A particularly interesting finding in this chapter was the flow identified enrichment of a THY1+CD34-CD55+FAP+ FLS population in PsA, a population that appears to match the scRNA-seq PsA enriched 'intermediate' population denoted as 'HLA-DR^{High}'. The expression of both key lining and sub-lining markers on this population reinforces the concept that FLS phenotypes may exist across a spectrum (Wei *et al.*, 2020). Indeed, this idea has been explored recently with regards to synovial macrophages with the sheer diversity of macrophage populations within the synovial lining and sub-lining becoming increasingly recognised, dispelling the previous overly simplified dogma of classical

versus non-classical subtypes. A revolutionary study by Hanlon *et al.* (2024) identified a unique CD40-expressing CD206+CD163+ macrophage population with aspects of both M1 and M2, a population defined as being in a 'transitionary' state. This introduces a number of questions in relation to this study that need to be addressed in the future – is the THY1+ FLS enriched in PsA a permanent state or transitionary and if this is the case, what could be provoking the transition? Whilst it is known that proximity to signals from other cells such as ECs may be important, another hypothesis is related to the eloquent work of Smith *et al*. (2023) examining the lining versus sub-lining FLS populations in healthy tissue in relation to activated versus resting states. Whilst resting lining layer exhibited traditionally high ECM and SF producing genes, the activated lining phenotype was predominantly characterised by inflammatory gene signatures and markedly higher HLA-DR expression. Thus, is the flow cytometry identified THY1+CD55+ population potentially an 'activated' state of the lining layer?

Perhaps one of the most perplexing aspects of this chapter was the clear association between lining layer FLS subsets and enhanced expression of MMPs, both of which are increased in PsA compared to RA at the single-cell and protein level. Even within the scRNA-seq THY1+POSTN+ FLS cluster, the osteoclast differentiation module was one of the sole modules that exhibited greater fold change in gene expression in PsA compared to RA, reinforcing their degradative role. However, while these findings were of particular interest on a clinical level, they fail to align with previous radiographic evidence showing PsA to be less erosive than RA counterparts (Finzel *et al.*, 2011; Mc Ardle *et al.*, 2015; Croft *et al.*, 2019). Could this simply be due to the fact PsA has superior protective and bone regenerative mechanisms to circumvent the damage or alternatively, could the MMPs be driving alternative processes to a greater extent (Dimitriou *et al.*, 2011)? A significant reduction in CX_3CR1 lining layer macrophages that are associated with retaining barrier integrity have been observed in RA compared to HC suggesting that potentially there is a greater presence of this immunoprotective barrier in PsA (Hanlon *et al.*, 2024). Alternatively, several studies have been published demonstrating a role for MMPs, including MMP-1, MMP-3, and MMP-9, in degrading EC basement membranes, releasing a plethora of angiogenic factors that promote EC proliferation and neoangiogeneis, with tissue inhibitors of these MMPs effective in reducing tumour neovascularisation (Quintero-Fabián *et al.*, 2019; Bian *et al.*, 2023). Moreover, higher expression of pAKT in PsA enriched populations was consistently demonstrated, a mediator which has been shown to be a critical regulator of VEGF-induced EC migration and can alleviate cell metastasis when abrogated in cancer models (Islam, Jones and Ellis, 2023). Thus collectively, the results would suggest the potential for MMPs and pAKT to be assuming an angiogenic-supporting role in PsA that may not be active in RA. However, if they are playing an angiogenic role, whether this role is related to increasing the actual quantity of blood vessels or is more associated with an influence on the distinct vascular pattern remains to be

determined. Although in conflict with previous studies suggesting higher levels of angiogenesis in the PsA synovium, the findings in this thesis of higher angiogenic factor production by the THY1+ FLS (which are less dominant in PsA) and a comparable level of vascularity following histological analysis between both disease states would suggest the latter (Ceponis *et al.*, 1998; Fearon *et al.*, 1999; Fearon *et al.*, 2003; Veale and Fearon, 2018). Ultimately, the results would imply that whilst the extent of angiogenesis does not differ between RA and PsA, the factors influencing it do with more complex, indirect mechanisms associated with PsA, and this could be contributing in part to the distinct vascular pattern, although further investigations are warranted.

A significant consideration that underpins scientific research is how reflective of inherent behaviour the results obtained from *ex vivo* experiments are, a reflection that is particularly pertinent in relation to the FLS in the synovial joint. In the laboratory, prolonged expansion and culturing of cells is a commonplace technique necessary to obtain sufficient cells for experimental protocols, and although the use of fresh cells would be desirable, it is not always feasible. Therefore, in Chapter 3, the research attempted to ascertain the extent to which removal of cells from their native *in vivo* environment and subsequent passaging would alter their distinct transcriptomic profile and importantly, whether this varied between RA and PsA-derived FLS. Whilst the data demonstrated that RA and PsA FLS at P0 did maintain certain functional properties that mirrored their *in vivo* behaviour including higher MMP expression in PsA FLS, it was subsequently shown that the frequency expression of certain immune and functional markers, including HLA-DR, CD34, CD54, and CD55, were altered across consecutive passages. These findings are in line with previous work in expanded murine hematopoietic stem cells (HSCs) in which altered cell surface Tie-2, Mpl, and Endoglin expression compared to their freshly isolated counterparts was observed (Zhang and Lodish, 2005). However, this did not translate into a reductive effect on their repopulation capacity, an inherent feature of this cell type, suggesting that although the FLS may lose/gain certain features, their underlying pathogenic nature is retained and thus still provide value for study, reinforcing the notion of an 'imprinted aggressor' phenotype (Bottini and Firestein, 2013). To further enhance the complexity, studies have shown that mechanical stimulation associated with culturing processes can impact FLS activity resulting in heightened proliferative capacity (Wahlsten *et al.*, 2021). Although this study focused specifically on cell cycle related genes, there is a high possibility it may extend to other functional genes, thus suggesting that minimal handling is optimal and current culturing techniques may not be the most efficient. Importantly, however, the changes observed across passages were highly comparable between both disease states suggesting that the comparative analysis is still valid. In conclusion, the results emphasise the significance of developing new techniques for the yielding of

cells for experimental purposes so that they resemble their *in vivo* configuration as closely as possible, as in straightforward terms, the less FLS change, the more reflective of the actual joint results will be.

Whilst Chapters 2 and 3 attempted to address the mechanisms driving differential pathogenesis in RA and PsA, the final chapter attempted to not only address this aspect but to simultaneously explore more diagnostic differences between the two arthropathies. As previously mentioned, prompt diagnosis is crucial in the context of inflammatory disease such as RA and PsA where joint erosion is irreversible, and thus biomarkers may prove extremely valuable in this regard (Abdelhafiz *et al.*, 2023). The establishment of irreversible bone erosion is now understood to be instigated at the very initial stages of disease, with research showing that treatment of RA patients with intensive DMARD therapy at an early point exhibits far superior efficacy in reducing symptoms compared to the exact same intervention at a later timepoint (Veale, Orr and Fearon, 2017). Currently, ACPA positivity is a gold standard biomarker for RA with serological levels of this antibody preceding the manifestation of clinically detectable symptoms, suggesting its involvement not solely as a biomarker but additionally in potentially initiating/perpetuating disease mechanisms, a theory reinforced by its significantly higher expression levels in RA synovium compared to in the serum (Masson-Bessière *et al.*, 2000; Abdelhafiz *et al.*, 2023). Whilst additional diagnostic RA markers include CRP and RF, the sensitivity and specificity of the latter is only 60-90% and 85% respectively and has been detected in non-RA disease previously which further confounds its validity (Mun *et al.*, 2021; Abdelhafiz *et al.*, 2023). Conversely, in relation to PsA, the biomarker field is far sparser and although several determinants have been proposed they have yet to be universally confirmed (Queiro and Pardo, 2024). To date the strongest PsA biomarker is the presence of psoriasis in individuals, with particularly scalp and nail involvement, with one third of patients with psoriasis progressing to develop PsA (McGonagle *et al.*, 2019; Carter *et al.*, 2022). However, not every patient experiences this skin manifestation before joint symptoms emerge, reinforcing the need for additional biomarkers. Several important factors must be considered when attempting to identify newer biomarkers, including ensuring they are stable, reliable, and can be measured in a non-invasive manner, all criteria which have been shown to be fulfilled by circulating miRNA (Mitchell *et al.*, 2008; O'Brien *et al.*, 2018). Moreover, miRNA have been implicated in several different cancers and autoimmune diseases where they exhibit aberrant expression and can provide critical information regarding disease severity, progression, and risk recurrence, all of which reinforces the valuable nature of miRNA in the field of biomarker research and provides clear rationale to why they were selected to analyse for this purpose in this chapter (Wade *et al.*, 2020; Cunningham *et al.*, 2021; Zellinger *et al.*, 2022; Chakrabortty *et al.*, 2023; Zhang *et al.*, 2023b; Saadawy, El-Ghareeb and Talaat, 2024).

Hence in this thesis, in Chapter 4, a circulating miRNA signature was identified that could provide a non-invasive method of distinguishing RA from PsA patient cohorts. Out of a panel of 68 immune dysregulation associated miRNA, seven miRNA were identified that were not only significantly higher in RA compared to PsA but additionally HC, highlighting their potential pathogenic role. Further analysis revealed that three of these miRNA were even more specific to RA; miR-22-3p, miR-223-3p, and miR-29b-3p, suggesting that the presence of these three miRNA within the serum may provide a reliable method of distinguishing patients with RA compared to PsA. Interestingly, a gender specific effect on two of the significantly different miRNA - miR-22-3p and miR-223-3p, was detected, data which supports the findings of a recently conducted study identifying significant sex related differences in the levels of circulating proteins in RA including CRP, leptin, and VEGF (Ferreira *et al.*, 2022). As previously mentioned in the general introduction, overall epidemiology studies have shown that RA is more prevalent in females whilst conversely PsA is more male associated, and although the exact causative reasons may not be fully understood, it does emphasise the critical importance of stratifying patients according to gender in future studies to ensure these differences are not ignored (McInnes and Schett, 2017; Cutolo and Straub, 2020; Bragazzi *et al.*, 2022). Furthermore, in-depth pathway analysis was subsequently performed to determine the potential downstream mechanisms of these RA associated miRNA resulting in the identification of several prominent pathways with known pathogenic roles in processes such as apoptosis and inflammation, including the FoxO pathway and the Hippo signalling pathway (Grabiec *et al.*, 2015; Wang *et al.*, 2020b; Barker *et al.*, 2023). The latter was also shown to be upregulated in the dominant THY1+POSTN+ FLS cluster in RA in Chapter 3, suggesting its potential importance as a therapeutic target in RA cohorts. Furthermore, the PI3K-AKT pathway was also of particular significance as it was a target of all three miRNA and contained a multitude of genes directly implicated in the process of ECM/cytoskeletal reorganisation, all of which cultivates a state supportive of enhanced migratory and invasive capacity (Ding *et al.*, 2023).

In summary, the data presented in Chapters 2-4 of this thesis provide an in-depth analysis of the differences at the cellular and molecular level that may contribute to the differential pathogenesis of RA and PsA, in addition to identifying novel approaches to improve the accuracy and efficiency with which diagnosis is achieved. The importance of immune-stromal cell communication within the inflamed joint alongside the importance of cytokine interactions in the perpetuation of inflammation have been shown, with the synergistic interaction between macrophage-derived IL-1β and T cell-derived TGF-β driving the proinflammatory, invasive phenotype of a specific population of RA FLS. Moreover, the first comprehensive analysis of RA and PsA FLS subsets has been provided in this study, resulting in the identification of distinct populations demonstrating unique transcriptomic and

functional properties, with differential frequencies of these subsets in RA and PsA disease states. Finally, the findings indicate that miRNA may prove invaluable as circulating biomarkers that can distinguish RA from PsA whilst simultaneously providing insights into differences in downstream pathways that drive disease progression.

5.2 Future Directions

In this thesis the importance of immune-stromal cell interactions have been highlighted, and specifically the central role of macrophage-derived IL-1β and T cell-derived TGF-β, in driving the proinflammatory nature of RA FLS. However, as previously described, the synovial environment is extremely complex with a plethora of different cell types coordinating the joint destruction and inflammation. Previous literature has reinforced the importance of the other joint stromal cell, the EC, in influencing the adaptation of a sub-lining layer phenotype of FLS through NOTCH signalling (Wei *et al.*, 2020). Thus, the scRNA-seq analysis will be expanded using the available data to identify potentially important receptor-ligand interactions between the two stromal cell types - the ECs and FLS. This will hopefully enable us to discern molecular pathways to target *ex vivo* through several functional experiments, ultimately informing future therapeutic targets to minimise disease effects.

Moreover, in Chapter 2, a significant glycolytic shift in the metabolic capacity of the RA FLS in response to IL-1β and TGF-β stimulation was demonstrated, a process that supported their adaptation of a highly aggressive phenotype. Targeting TAK1 exhibited efficacy in the attenuation of several pathogenic responses of RA FLS, including a suppression of their glycolytic transformation, which suggests that direct metabolic targeting could also provide a valuable target in this context. A central focus of the fast-paced field of immunometabolism is the concept of 'metabolic reprogramming', with the primary purpose of altering the downstream inflammatory and invasive phenotype of cells. Indeed, previous literature has consistently shown that inflammatory resolution can be achieved through metabolic reprogramming of multiple synovial cells including FLS, T cells, macrophages, and monocytes, in addition to intact synovial explants *ex vivo* (Biniecka *et al.*, 2016; Garcia-Carbonell *et al.*, 2016; Bustamante *et al.*, 2017; McGarry *et al.*, 2018b; Canavan *et al.*, 2020; Gallagher *et al.*, 2020; Petrasca *et al.*, 2020). Furthermore, although of critical importance in RA pathogenesis, energy production is not limited solely to the use of glycolytic and oxidative pathways. Thus, this line of research in the context of IL-1β and TGF-β treatment of RA FLS will be expanded through additional experimental techniques including the novel metabolic Fluorescence Lifetime Imaging Microscopy (FLIM) assay and metabolomic analysis, to ascertain levels of metabolic intermediates such as lactate, citrate, and succinate, all of which can influence the inflammatory phenotype of cells (Hanlon *et al.*,

2022). Determination of the extent to which alternative metabolic pathways such as fatty acid oxidation are being utilised by the activated RA FLS under the different stimulated conditions will advance understanding of the disease pathogenesis and simultaneously provide potential therapeutic targets.

In this thesis, in Chapter 3, extensive characterisation of FLS subsets utilising a combined approach of scRNA-seq and multiparametric flow analysis was performed. To extend these findings further, future phenotypic analysis of distinct FLS subsets in RA vs PsA patients pre/post therapy will be conducted to establish if therapeutic interventions culminate in alterations to the frequency of the identified subsets. Moreover, to further characterise the exact functional nature of the subsets, the six flow-identified FLS populations will be sorted by incorporating CD55 and CD34 to the pre-existing panel. Once sorted, the supernatants will be collected and the levels of proinflammatory, angiogenic, and invasive mediators examined to establish their role in disease perpetuation, with particular interest in investigating the role of the THY1+CD34-CD55+FAP+ population significantly higher in PsA. This flow identified population appears to match the scRNA-seq PsA enriched intermediate population denoted as 'HLA-DR^{High}' suggesting it may assume an immune related function, however whether it possesses characteristics of both lining and sub-lining FLS or whether it could be considered a completely separate functional entity remains to be explored. Importantly, the levels of bone related factors including BMPs and additional growth factors will be thoroughly examined in order to establish if the PsA joint contains an inherently higher abundance of these regenerative factors (Dimitriou *et al.*, 2011). This may provide rational for the higher MMP associated lining layer FLS frequency, yet lower clinical erosion compared to RA, all information that will further understanding of the distinct disease mechanisms. In relation to the scRNA-seq specifically, it is important to note that there are unavoidable limitations, despite the value of the information obtained from it. Although both RA and PsA patients included were comparable in regard to disease activity scores, with all categorised as moderate-high levels, sample heterogeneity may be influencing some of the observed results. To overcome these issues related to patient variability, sequencing of a greater number of patients in future analysis would be useful to increase the reliability and to validate the findings. Furthermore, spatial transcriptomics will be conducted which would provide more detailed information of the biological interactions and relationships occurring at the cellular level in the complex synovial tissue, enabling exploration of the data from a geographic perspective.

As previously mentioned, in the direct comparative analysis of *ex vivo* P0 RA vs PsA FLS, differential expression of invasive promoting factors, in addition to subtle differences in their baseline metabolic profiles, were identified, with PsA more skewed towards a glycolytic profile. Interestingly, however, upon addition of IL-1β, a more robust metabolic response in the RA FLS compared to their

PsA counterparts was observed, which may be due to an RA-associated priming effect. To expand on this theory, RA and PsA P0 FLS will be stimulated with IL-1β and functional outputs subsequently examined at the mRNA and protein levels, with particular emphasis on factors including MMPs that were initially higher in the PsA FLS at baseline. In addition to this, the FLS CM collected from P0 RA and PsA FLS will be applied to MSCs, a multipotent cell type renowned for its capacity to differentiate into a range of cell types including osteoblasts, chondrocytes, myocytes, and adipocytes, under the influence of stimuli in the environment (Pittenger *et al.*, 2019). Following this, mRNA will be prepared to examine gene expression of the MSCs with the objective of evaluating the differential effects RA and PsA FLS have on dictating the lineage the MSCs differentiate towards, with a particular emphasis on chondrogenic and osteogenic profile. This will further provide insights into the differences in the RA and PsA joint microenvironment at the cellular and molecular levels that may be contributing to differential disease progression.

In Chapter 4, for the first time, evidence was provided indicating that there are indeed significant differences in circulating miRNA profiles between RA and PsA, with seven miRNA significantly upregulated in RA compared to PsA. However, there is scope for extensive sub-analysis to be conducted to further investigate the role of these miRNA in different patient cohorts. Definitively identifying patients at an early disease stage who are at an increased risk for more severe disease progression or who will be likely to be less responsive to therapeutic intervention may be critical in ensuring patient quality of life is maintained. The valuable nature of miRNA in this regard has been shown eloquently by Wade *et al.* (2020), with this study outlining that lower levels of three specific miRNA at baseline were associated with more optimal treatment responses. Moreover, Cunningham *et al.* (2021) determined that a specific miRNA signature could establish individuals 'at risk' of progression to established RA. Thus, it would be interesting to expand on the analysis and evaluate the levels of the significantly different serum miRNA in patients stratified according to early/late disease stage and treatment responses, to possibly distinguish potential responders from non-responders before irreversible damage occurs. Assessment of these miRNAs in additional larger cohorts are required to further validate their potential as a blood biomarker. Extensive analysis of the downstream pathways being targeted by the miRNA significantly upregulated in RA compared to PsA was additionally conducted, providing insights into the importance of multiple signalling pathways in perpetuating the damage, with the P13K/AKT pathway amongst them. To expand this research further, additional experiments are now planned to test the functional impacts *ex vivo* using matched SF from the donors included in this study.

In this thesis, although nineteen serum miRNA were initially identified to exhibit significantly different expression levels between RA and PsA cohorts, exclusive focus was placed on the RA

associated miRNA. In future research, the three miRNA specifically upregulated in PsA will be specifically analysed as downstream analysis could prove valuable in delineating specific pathways of disease more related to PsA, thus furthering understanding of disease pathogenesis and introducing therapeutic targets that may be more effective in this patient cohort. Another exciting finding of this research was the identification of gender differences in the miRNA expression levels when stratified between male and female RA patients. Preliminary analysis identified higher levels of miR-22-3p in female RA patients whilst miR-223-3p was significantly higher in male RA patients, suggesting that sex differences may affect the reliability of specific miRNA as biomarkers, thus highlighting the need to further explore sex differences in RA vs PsA. To acknowledge limitations of the research, the miRNA analysed in this thesis were centred around 68 miRNA with well-established roles in several aspects of immune and inflammatory dysfunction (Cunningham *et al.*, 2021). Although relevant in the context of RA and PsA, both pathologies characterised by significant dysregulation of the inherent immune system, there is the risk that additional miRNAs associated with RA and PsA may not have been included and thus it would be worthwhile to perform additional analysis of a full miRNA screen in future studies if possible.

In summary, although the research contained in this thesis represents a significant advancement in the understanding of RA and PsA pathogenesis at the cellular, molecular, and immunological levels, further studies are warranted. Cumulatively, this information will prove invaluable in the development of targeted therapeutic interventions as well as facilitate the movement towards precision medicine and corresponding optimal patient outcomes.

CHAPTER 6:

Appendix

Disease	Patient	No. cells sequenced
RA	RA1	42,473
	RA2	965
	RA3	10,136
	RA4	49,347
PsA	PsA1	39,047
	PsA2	8,685
	PsA3	3,803
	PsA4	12,355
	PsA5	11,358

Table 6.1. Numbers of cells sequenced per donor for the scRNA-seq.

Clinical Data	RA	PsA
Number (M/F)	4 (1/3)	5 (3/2)
Mean Age (range)	57.5 (39-83)	47.2 (26-72)
Disease duration years, Mean +/-SD	4.5 +/-8.3	5.1 +/-7.6
ACPA (Positive/Negative)	3/1	0/5
RF (Positive/Negative)	3/1	0/5
Composite Disease Activity Scores, Mean +/-SD	4.6 +/-1.1	24.2 +/-4.9
CRP (mg/dl), Mean +/SD	14.5 +/- 8.3	12 +/- 6
Medication	Naïve (4)	Naïve (3), DMARD (2)

Table 6.2. **ScRNA-seq patient demographics**. Clinical information of RA and PsA synovial tissue biopsies included in the scRNA-seq analysis in Chapter 2 and Chapter 3. ACPA: Anti-Citrullinated Protein Antibody, RF: Rheumatoid Factor, CRP: C-reactive Protein, SD: Standard Deviation.

Clinical Data	RA	PsA
Number (M/F)	4/7	2/8
Mean Age (range)	58.6 (37-80)	47.9 (29-78)
Disease duration years, Mean +/-SD	5.1 +/- 3.1	15.7 +/- 13.1
ACPA (Positive/Negative)	10/1	0/10
RF (Positive/Negative)	10/1	0/10
Composite Disease Activity Scores, Mean +/-SD	4.65 +/- 1.68	4 +/- 1.1
CRP (mg/dl), Mean +/SD	33.98 +/- 45	21.65 +/-35.8
Medication	DMARD: 4 Biologics: 1 Naïve: 5 Unknown: 1	DMARD: 3 Biologics: 1 Naïve: 5 Unknown: 1

Table 6.3. **Patient demographics for donors included in the multiparametric AURORA flow analysis Chapter 3**. Clinical information of RA and PsA patients for synovial tissue samples included in the multiparametric flow cytometry analysis Chapter 3. ACPA: Anti-Citrullinated Protein Antibody, RF: Rheumatoid Factor, CRP: C-reactive Protein, SD: Standard Deviation.

Diagnosis	THY1+FAP+	THY1-FAP-
RA	24,600	47,900
RA	6,300	26,600
RA	2,200	30,000
RA	44,000	1,300
RA	32,000	1,443
RA	1,897	23,062
PsA	32,000	171,500
PsA	31,500	37,500
PsA	19,200	27,000
PsA	62,600	6,500
PsA	15,000	43,000
PsA	58,800	5,000
PsA	146,000	1,384

Table 6.4. **Yields from cell sort.** Table indicating the yields of the specific FLS populations FACS-sorted from RA (n=6) and PsA (n=7) synovial tissue biopsies.

Bibliography

Aarts, J., van Caam, A., Chen, X., Marijnissen, R. J., Helsen, M. M., Walgreen, B., Vitters, E. L., van de Loo, F. A., van Lent, P. L., van der Kraan, P. M. and Koenders, M. I. (2022) 'Local inhibition of TGF-β1 signaling improves Th17/Treg balance but not joint pathology during experimental arthritis', *Sci Rep,* 12(1), pp. 3182.

Abbot, S. E., Whish, W. J., Jennison, C., Blake, D. R. and Stevens, C. R. (1999) 'Tumour necrosis factor alpha stimulated rheumatoid synovial microvascular endothelial cells exhibit increased shear rate dependent leucocyte adhesion in vitro', *Ann Rheum Dis,* 58(9), pp. 573-81.

Abdelhafiz, D., Baker, T., Glascow, D. A. and Abdelhafiz, A. (2023) 'Biomarkers for the diagnosis and treatment of rheumatoid arthritis - a systematic review', *Postgrad Med,* 135(3), pp. 214-223.

Abplanalp, W. T., Fischer, A., John, D., Zeiher, A. M., Gosgnach, W., Darville, H., Montgomery, R., Pestano, L., Allée, G., Paty, I., Fougerousse, F. and Dimmeler, S. (2020) 'Efficiency and Target Derepression of Anti-miR-92a: Results of a First in Human Study', *Nucleic Acid Ther,* 30(6), pp. 335-345.

Aghakhani, S., Soliman, S. and Niarakis, A. (2022) 'Metabolic reprogramming in Rheumatoid Arthritis Synovial Fibroblasts: A hybrid modeling approach', *PLoS Comput Biol,* 18(12), pp. e1010408.

Ahn, J. K., Kim, S., Hwang, J., Kim, J., Kim, K. H. and Cha, H. S. (2016) 'GC/TOF-MS-based metabolomic profiling in cultured fibroblast-like synoviocytes from rheumatoid arthritis', *Joint Bone Spine,* 83(6), pp. 707-713.

Ahn, J. K., Koh, E. M., Cha, H. S., Lee, Y. S., Kim, J., Bae, E. K. and Ahn, K. S. (2008) 'Role of hypoxia-inducible factor-1alpha in hypoxia-induced expressions of IL-8, MMP-1 and MMP-3 in rheumatoid fibroblast-like synoviocytes', *Rheumatology (Oxford),* 47(6), pp. 834-9.

Ai, R., Hammaker, D., Boyle, D. L., Morgan, R., Walsh, A. M., Fan, S., Firestein, G. S. and Wang, W. (2016) 'Joint-specific DNA methylation and transcriptome signatures in rheumatoid arthritis identify distinct pathogenic processes', *Nature Communications,* 7(1), pp. 11849.

Akbaba, T. H., Akkaya-Ulum, Y. Z., Tavukcuoglu, Z., Bilginer, Y., Ozen, S. and Balci-Peynircioglu, B. (2021) 'Inflammation-related differentially expressed common miRNAs in systemic autoinflammatory disorders patients can regulate the clinical course', *Clin Exp Rheumatol,* 39 Suppl 132(5), pp. 109-117.

Alarcón, C. R., Lee, H., Goodarzi, H., Halberg, N. and Tavazoie, S. F. (2015) 'N6-methyladenosine marks primary microRNAs for processing', *Nature,* 519(7544), pp. 482-5.

Alenius, G. M., Friberg, C., Nilsson, S., Wahlström, J., Dahlqvist, S. R. and Samuelsson, L. (2004) 'Analysis of 6 genetic loci for disease susceptibility in psoriatic arthritis', *J Rheumatol,* 31(11), pp. 2230-5.

Aletaha, D., Neogi, T., Silman, A. J., Funovits, J., Felson, D. T., Bingham, C. O., 3rd, Birnbaum, N. S., Burmester, G. R., Bykerk, V. P., Cohen, M. D., Combe, B., Costenbader, K. H., Dougados, M., Emery, P., Ferraccioli, G., Hazes, J. M., Hobbs, K., Huizinga, T. W., Kavanaugh, A., Kay, J., Kvien, T. K., Laing, T., Mease, P., Ménard, H. A., Moreland, L. W., Naden, R. L., Pincus, T., Smolen, J. S., Stanislawska-Biernat, E., Symmons, D., Tak, P. P., Upchurch, K. S., Vencovsky, J., Wolfe, F. and Hawker, G. (2010) '2010 rheumatoid arthritis classification criteria: an American College of Rheumatology/European League Against Rheumatism collaborative initiative', *Ann Rheum Dis,* 69(9), pp. 1580-8.

Alinaghi, F., Calov, M., Kristensen, L. E., Gladman, D. D., Coates, L. C., Jullien, D., Gottlieb, A. B., Gisondi, P., Wu, J. J., Thyssen, J. P. and Egeberg, A. (2019) 'Prevalence of psoriatic arthritis in patients with psoriasis: A systematic review and meta-analysis of observational and clinical studies', *J Am Acad Dermatol,* 80(1), pp. 251-265.e19.

Alivernini, S., Firestein, G. S. and McInnes, I. B. (2022) 'The pathogenesis of rheumatoid arthritis', *Immunity,* 55(12), pp. 2255-2270.

Alivernini, S., Kurowska-Stolarska, M., Tolusso, B., Benvenuto, R., Elmesmari, A., Canestri, S., Petricca, L., Mangoni, A., Fedele, A. L., Di Mario, C., Gigante, M. R., Gremese, E., McInnes, I. B. and Ferraccioli, G. (2016) 'MicroRNA-155 influences B-cell function through PU.1 in rheumatoid arthritis', *Nat Commun,* 7, pp. 12970.

Alivernini, S., MacDonald, L., Elmesmari, A., Finlay, S., Tolusso, B., Gigante, M. R., Petricca, L., Di Mario, C., Bui, L., Perniola, S., Attar, M., Gessi, M., Fedele, A. L., Chilaka, S., Somma, D., Sansom, S. N., Filer, A., McSharry, C., Millar, N. L., Kirschner, K., Nerviani, A., Lewis, M. J., Pitzalis, C., Clark, A. R., Ferraccioli, G., Udalova, I., Buckley, C. D., Gremese, E., McInnes, I. B., Otto, T. D. and Kurowska-Stolarska, M. (2020) 'Distinct synovial tissue macrophage subsets regulate inflammation and remission in rheumatoid arthritis', *Nat Med,* 26(8), pp. 1295-1306.
Alles, J., Fehlmann, T., Fischer, U., Backes, C., Galata, V., Minet, M., Hart, M., Abu-Halima, M., Grässer, F. A., Lenhof, H. P., Keller, A. and Meese, E. (2019) 'An estimate of the total number of true human miRNAs', *Nucleic Acids Res,* 47(7), pp. 3353-3364.
Alquicira-Hernandez, J. and Powell, J. E. (2021) 'Nebulosa recovers single-cell gene expression signals by kernel density estimation', *Bioinformatics,* 37(16), pp. 2485-2487.
Alspaugh, M. A., Jensen, F. C., Rabin, H. and Tan, E. M. (1978) 'Lymphocytes transformed by Epstein-Barr virus. Induction of nuclear antigen reactive with antibody in rheumatoid arthritis', *J Exp Med,* 147(4), pp. 1018-27.
Alunno, A., Carubbi, F., Giacomelli, R. and Gerli, R. (2017) 'Cytokines in the pathogenesis of rheumatoid arthritis: new players and therapeutic targets', *BMC Rheumatol,* 1, pp. 3.
Alunno, A., Manetti, M., Caterbi, S., Ibba-Manneschi, L., Bistoni, O., Bartoloni, E., Valentini, V., Terenzi, R. and Gerli, R. (2015) 'Altered immunoregulation in rheumatoid arthritis: the role of regulatory T cells and proinflammatory Th17 cells and therapeutic implications', *Mediators Inflamm,* 2015, pp. 751793.
Amoruso, A., Sola, D., Rossi, L., Obeng, J. A., Fresu, L. G., Sainaghi, P. P., Pirisi, M. and Brunelleschi, S. (2016) 'Relation among anti-rheumatic drug therapy, CD14(+)CD16(+) blood monocytes and disease activity markers (DAS28 and US7 scores) in rheumatoid arthritis: A pilot study', *Pharmacol Res,* 107, pp. 308-314.
Anaparti, V., Smolik, I., Meng, X., Spicer, V., Mookherjee, N. and El-Gabalawy, H. (2017) 'Whole blood microRNA expression pattern differentiates patients with rheumatoid arthritis, their seropositive first-degree relatives, and healthy unrelated control subjects', *Arthritis Res Ther,* 19(1), pp. 249.
Arnett, F. C., Edworthy, S. M., Bloch, D. A., McShane, D. J., Fries, J. F., Cooper, N. S., Healey, L. A., Kaplan, S. R., Liang, M. H., Luthra, H. S. and et al. (1988) 'The American Rheumatism Association 1987 revised criteria for the classification of rheumatoid arthritis', *Arthritis Rheum,* 31(3), pp. 315-24.
Artacho, A., Isaac, S., Nayak, R., Flor-Duro, A., Alexander, M., Koo, I., Manasson, J., Smith, P. B., Rosenthal, P., Homsi, Y., Gulko, P., Pons, J., Puchades-Carrasco, L., Izmirly, P., Patterson, A., Abramson, S. B., Pineda-Lucena, A., Turnbaugh, P. J., Ubeda, C. and Scher, J. U. (2021) 'The Pretreatment Gut Microbiome Is Associated With Lack of Response to Methotrexate in New-Onset Rheumatoid Arthritis', *Arthritis Rheumatol,* 73(6), pp. 931-942.
Attwell, D., Mishra, A., Hall, C. N., O'Farrell, F. M. and Dalkara, T. (2016) 'What is a pericyte?', *J Cereb Blood Flow Metab,* 36(2), pp. 451-5.
Azuaga, A. B., Ramírez, J. and Cañete, J. D. (2023) 'Psoriatic Arthritis: Pathogenesis and Targeted Therapies', *Int J Mol Sci,* 24(5).
Baba, A. B., Rah, B., Bhat, G. R., Mushtaq, I., Parveen, S., Hassan, R., Hameed Zargar, M. and Afroze, D. (2022) 'Transforming Growth Factor-Beta (TGF-β) Signaling in Cancer-A Betrayal Within', *Front Pharmacol,* 13, pp. 791272.
Babalic, F. C. A., Borza, C., Ilie Rosca, C., Gurban, C. V., Banciu, C. D., Mederle, O. A., Popa, M. D., Chelu, S. C., Marius, P., Sharma, A., Kundnani, N. R. and Caraba, A. E. (2022) 'Endothelial dysfunction in psoriatic arthritis patients: correlations between insulin resistance and disease activity', *Eur Rev Med Pharmacol Sci,* 26(18), pp. 6796-6804.
Badia, I. M. P., Vélez Santiago, J., Braunger, J., Geiss, C., Dimitrov, D., Müller-Dott, S., Taus, P., Dugourd, A., Holland, C. H., Ramirez Flores, R. O. and Saez-Rodriguez, J. (2022) 'decoupleR: ensemble of computational methods to infer biological activities from omics data', *Bioinform Adv,* 2(1), pp. vbac016.
Bae, S. C. and Lee, Y. H. (2019) 'Causal association between body mass index and risk of rheumatoid arthritis: A Mendelian randomization study', *Eur J Clin Invest,* 49(4), pp. e13076.

Baeten, D., Kruithof, E., De Rycke, L., Boots, A. M., Mielants, H., Veys, E. M. and De Keyser, F. (2005) 'Infiltration of the synovial membrane with macrophage subsets and polymorphonuclear cells reflects global disease activity in spondyloarthropathy', *Arthritis Res Ther,* 7(2), pp. R359-69.
Balogh, E., Biniecka, M., Fearon, U., Veale, D. J. and Szekanecz, Z. (2019) 'Angiogenesis in Inflammatory Arthritis', *Isr Med Assoc J,* 21(5), pp. 345-352.
Banerjee, S., Xu, W., Doctor, A., Driss, A., Nezhat, C., Sidell, N., Taylor, R. N., Thompson, W. E. and Chowdhury, I. (2023) 'TNFα-induced altered miRNA expression links to NF-κB signaling pathway in endometriosis', *Res Sq*.
Barbagallo, D., Ponti, D., Bassani, B., Bruno, A., Pulze, L., Akkihal, S. A., George-William, J. N., Gundamaraju, R. and Campomenosi, P. (2024) 'MiR-223-3p in Cancer Development and Cancer Drug Resistance: Same Coin, Different Faces', *Int J Mol Sci,* 25(15).
Barker, B. E., Hanlon, M. M., Marzaioli, V., Smith, C. M., Cunningham, C. C., Fletcher, J. M., Veale, D. J., Fearon, U. and Canavan, M. (2023) 'The mammalian target of rapamycin contributes to synovial fibroblast pathogenicity in rheumatoid arthritis', *Frontiers in Medicine,* 10.
Barksby, H. E., Hui, W., Wappler, I., Peters, H. H., Milner, J. M., Richards, C. D., Cawston, T. E. and Rowan, A. D. (2006) 'Interleukin-1 in combination with oncostatin M up-regulates multiple genes in chondrocytes: implications for cartilage destruction and repair', *Arthritis Rheum,* 54(2), pp. 540-50.
Barland, P., Novikoff, A. B. and Hamerman, D. (1962) 'Electron microscopy of the human synovial membrane', *J Cell Biol,* 14(2), pp. 207-20.
Bartel, D. P. (2009) 'MicroRNAs: target recognition and regulatory functions', *Cell,* 136(2), pp. 215-33.
Barton, A., Thomson, W., Ke, X., Eyre, S., Hinks, A., Bowes, J., Plant, D., Gibbons, L. J., Wilson, A. G., Bax, D. E., Morgan, A. W., Emery, P., Steer, S., Hocking, L., Reid, D. M., Wordsworth, P., Harrison, P. and Worthington, J. (2008) 'Rheumatoid arthritis susceptibility loci at chromosomes 10p15, 12q13 and 22q13', *Nat Genet,* 40(10), pp. 1156-9.
Barutta, F., Bruno, G., Matullo, G., Chaturvedi, N., Grimaldi, S., Schalkwijk, C., Stehouwer, C. D., Fuller, J. H. and Gruden, G. (2017) 'MicroRNA-126 and micro-/macrovascular complications of type 1 diabetes in the EURODIAB Prospective Complications Study', *Acta Diabetol,* 54(2), pp. 133-139.
Basdeo, S. A., Cluxton, D., Sulaimani, J., Moran, B., Canavan, M., Orr, C., Veale, D. J., Fearon, U. and Fletcher, J. M. (2017) 'Ex-Th17 (Nonclassical Th1) Cells Are Functionally Distinct from Classical Th1 and Th17 Cells and Are Not Constrained by Regulatory T Cells', *J Immunol,* 198(6), pp. 2249-2259.
Bazin, E. and Sergent, L. (1860) *Lecons theoriques et cliniques sur les affections cutanees de nature arthritique et dartreuse... professees: par le docteur Bazin, redigees et publiees par le Lucien Sergent. Edited by Lucien Sergent.* Delahaye.
Begovich, A. B., Carlton, V. E., Honigberg, L. A., Schrodi, S. J., Chokkalingam, A. P., Alexander, H. C., Ardlie, K. G., Huang, Q., Smith, A. M., Spoerke, J. M., Conn, M. T., Chang, M., Chang, S. Y., Saiki, R. K., Catanese, J. J., Leong, D. U., Garcia, V. E., McAllister, L. B., Jeffery, D. A., Lee, A. T., Batliwalla, F., Remmers, E., Criswell, L. A., Seldin, M. F., Kastner, D. L., Amos, C. I., Sninsky, J. J. and Gregersen, P. K. (2004) 'A missense single-nucleotide polymorphism in a gene encoding a protein tyrosine phosphatase (PTPN22) is associated with rheumatoid arthritis', *Am J Hum Genet,* 75(2), pp. 330-7.
Behm-Ansmant, I., Rehwinkel, J., Doerks, T., Stark, A., Bork, P. and Izaurralde, E. (2006) 'mRNA degradation by miRNAs and GW182 requires both CCR4:NOT deadenylase and DCP1:DCP2 decapping complexes', *Genes Dev,* 20(14), pp. 1885-98.
Benjamin, O., Goyal, A. and Lappin, S. L. (2024) 'Disease-Modifying Antirheumatic Drugs (DMARD)', *StatPearls*. Treasure Island (FL): StatPearls Publishing, Copyright © 2024, StatPearls Publishing LLC.
Bernatova, I., Andriantsitohaina, R., Arribas, S. M. and Matchkov, V. V. (2014) 'Endothelium in diseased states', *Biomed Res Int,* 2014, pp. 810436.
Berse, B., Hunt, J. A., Diegel, R. J., Morganelli, P., Yeo, K., Brown, F. and Fava, R. A. (1999) 'Hypoxia augments cytokine (transforming growth factor-beta (TGF-beta) and IL-1)-induced vascular endothelial growth factor secretion by human synovial fibroblasts', *Clin Exp Immunol,* 115(1), pp. 176-82.

Beydon, M., Pinto, S., De Rycke, Y., Fautrel, B., Mariette, X., Seror, R. and Tubach, F. (2023) 'Risk of cancer for patients with rheumatoid arthritis versus general population: a national claims database cohort study', *Lancet Reg Health Eur,* 35, pp. 100768.
Bhole, V. M., Choi, H. K., Burns, L. C., Vera Kellet, C., Lacaille, D. V., Gladman, D. D. and Dutz, J. P. (2012) 'Differences in body mass index among individuals with PsA, psoriasis, RA and the general population', *Rheumatology (Oxford),* 51(3), pp. 552-6.
Bian, Y., Xiang, Z., Wang, Y., Ren, Q., Chen, G., Xiang, B., Wang, J., Zhang, C., Pei, S., Guo, S. and Xiao, L. (2023) 'Immunomodulatory roles of metalloproteinases in rheumatoid arthritis', *Front Pharmacol,* 14, pp. 1285455.
Bilski, J., Schramm-Luc, A., Szczepanik, M., Mazur-Biały, A. I., Bonior, J., Luc, K., Zawojska, K. and Szklarczyk, J. (2023) 'Adipokines in Rheumatoid Arthritis: Emerging Biomarkers and Therapeutic Targets', *Biomedicines,* 11(11).
Biniecka, M., Canavan, M., McGarry, T., Gao, W., McCormick, J., Cregan, S., Gallagher, L., Smith, T., Phelan, J. J., Ryan, J., O'Sullivan, J., Ng, C. T., Veale, D. J. and Fearon, U. (2016) 'Dysregulated bioenergetics: a key regulator of joint inflammation', *Ann Rheum Dis,* 75(12), pp. 2192-2200.
Biniecka, M., Fox, E., Gao, W., Ng, C. T., Veale, D. J., Fearon, U. and O'Sullivan, J. (2011) 'Hypoxia induces mitochondrial mutagenesis and dysfunction in inflammatory arthritis', *Arthritis Rheum,* 63(8), pp. 2172-82.
Bira, Y., Tani, K., Nishioka, Y., Miyata, J., Sato, K., Hayashi, A., Nakaya, Y. and Sone, S. (2005) 'Transforming growth factor beta stimulates rheumatoid synovial fibroblasts via the type II receptor', *Mod Rheumatol,* 15(2), pp. 108-13.
Blanco, R. and Gerhardt, H. (2013) 'VEGF and Notch in tip and stalk cell selection', *Cold Spring Harb Perspect Med,* 3(1), pp. a006569.
Blaschke, S., Schwarz, G., Moneke, D., Binder, L., Müller, G. and Reuss-Borst, M. (2000) 'Epstein-Barr virus infection in peripheral blood mononuclear cells, synovial fluid cells, and synovial membranes of patients with rheumatoid arthritis', *J Rheumatol,* 27(4), pp. 866-73.
Blumberg, B. S., Bunim, J. J., Calkins, E., Pirani, C. L. and Zvaifler, N. J. (1964) 'ARA NOMENCLATURE AND CLASSIFICATION OF ARTHRITIS AND RHEUMATISM (TENTATIVE)', *Arthritis Rheum,* 7, pp. 93-7.
Boix-Amorós, A., Badri, M. H., Manasson, J., Blank, R. B., Haberman, R. H., Neimann, A. L., Girija, P. V., Jimenez Hernandez, A., Heguy, A., Koralov, S. B., Bonneau, R., Clemente, J. C. and Scher, J. U. (2023) 'Alterations in the cutaneous microbiome of patients with psoriasis and psoriatic arthritis reveal similarities between non-lesional and lesional skin', *Ann Rheum Dis,* 82(4), pp. 507-514.
Bondeson, J., Foxwell, B., Brennan, F. and Feldmann, M. (1999) 'Defining therapeutic targets by using adenovirus: blocking NF-kappaB inhibits both inflammatory and destructive mechanisms in rheumatoid synovium but spares anti-inflammatory mediators', *Proc Natl Acad Sci U S A,* 96(10), pp. 5668-73.
Borchert, G. M., Lanier, W. and Davidson, B. L. (2006) 'RNA polymerase III transcribes human microRNAs', *Nat Struct Mol Biol,* 13(12), pp. 1097-101.
Bottini, N. and Firestein, G. S. (2013) 'Duality of fibroblast-like synoviocytes in RA: passive responders and imprinted aggressors', *Nat Rev Rheumatol,* 9(1), pp. 24-33.
Bowes, J., Ashcroft, J., Dand, N., Jalali-Najafabadi, F., Bellou, E., Ho, P., Marzo-Ortega, H., Helliwell, P. S., Feletar, M., Ryan, A. W., Kane, D. J., Korendowych, E., Simpson, M. A., Packham, J., McManus, R., Brown, M. A., Smith, C. H., Barker, J. N., McHugh, N., FitzGerald, O., Warren, R. B. and Barton, A. (2017) 'Cross-phenotype association mapping of the MHC identifies genetic variants that differentiate psoriatic arthritis from psoriasis', *Ann Rheum Dis,* 76(10), pp. 1774-1779.
Bowes, J., Budu-Aggrey, A., Huffmeier, U., Uebe, S., Steel, K., Hebert, H. L., Wallace, C., Massey, J., Bruce, I. N., Bluett, J., Feletar, M., Morgan, A. W., Marzo-Ortega, H., Donohoe, G., Morris, D. W., Helliwell, P., Ryan, A. W., Kane, D., Warren, R. B., Korendowych, E., Alenius, G.-M., Giardina, E., Packham, J., McManus, R., FitzGerald, O., McHugh, N., Brown, M. A., Ho, P., Behrens, F., Burkhardt, H., Reis, A. and Barton, A. (2015) 'Dense genotyping of immune-related susceptibility loci reveals new insights into the genetics of psoriatic arthritis', *Nature Communications,* 6(1), pp. 6046.

Boyette, L. B., Macedo, C., Hadi, K., Elinoff, B. D., Walters, J. T., Ramaswami, B., Chalasani, G., Taboas, J. M., Lakkis, F. G. and Metes, D. M. (2017) 'Phenotype, function, and differentiation potential of human monocyte subsets', *PLoS One,* 12(4), pp. e0176460.
Bradfield, P. F., Amft, N., Vernon-Wilson, E., Exley, A. E., Parsonage, G., Rainger, G. E., Nash, G. B., Thomas, A. M., Simmons, D. L., Salmon, M. and Buckley, C. D. (2003) 'Rheumatoid fibroblast-like synoviocytes overexpress the chemokine stromal cell-derived factor 1 (CXCL12), which supports distinct patterns and rates of CD4+ and CD8+ T cell migration within synovial tissue', *Arthritis Rheum,* 48(9), pp. 2472-82.
Braga, M. V., de Oliveira, S. C., Vasconcelos, A. H. C., Lopes, J. R., de Macedo Filho, C. L., Ramos, L. M. A. and Rodrigues, C. E. M. (2020) 'Prevalence of sacroiliitis and acute and structural changes on MRI in patients with psoriatic arthritis', *Scientific Reports,* 10(1), pp. 11580.
Bragazzi, N. L., Bridgewood, C., Watad, A., Damiani, G. and McGonagle, D. (2022) 'Sex-Based Medicine Meets Psoriatic Arthritis: Lessons Learned and to Learn', *Front Immunol,* 13, pp. 849560.
Braun, J. E., Truffault, V., Boland, A., Huntzinger, E., Chang, C. T., Haas, G., Weichenrieder, O., Coles, M. and Izaurralde, E. (2012) 'A direct interaction between DCP1 and XRN1 couples mRNA decapping to 5' exonucleolytic degradation', *Nat Struct Mol Biol,* 19(12), pp. 1324-31.
Bresnihan, B., Pontifex, E., Thurlings, R. M., Vinkenoog, M., El-Gabalawy, H., Fearon, U., Fitzgerald, O., Gerlag, D. M., Rooney, T., van de Sande, M. G., Veale, D., Vos, K. and Tak, P. P. (2009) 'Synovial tissue sublining CD68 expression is a biomarker of therapeutic response in rheumatoid arthritis clinical trials: consistency across centers', *J Rheumatol,* 36(8), pp. 1800-2.
Bridgewood, C., Watad, A., Russell, T., Palmer, T. M., Marzo-Ortega, H., Khan, A., Millner, P. A., Dunsmuir, R., Rao, A., Loughenbury, P., Wittmann, M., Cuthbert, R. J. and McGonagle, D. G. (2019) 'Identification of myeloid cells in the human enthesis as the main source of local IL-23 production', *Ann Rheum Dis,* 78(7), pp. 929-933.
Budu-Aggrey, A., Bowes, J., Loehr, S., Uebe, S., Zervou, M. I., Helliwell, P., Ryan, A. W., Kane, D., Korendowych, E., Giardina, E., Packham, J., McManus, R., FitzGerald, O., McHugh, N., Behrens, F., Burkhardt, H., Huffmeier, U., Ho, P., Martin, J., Castañeda, S., Goulielmos, G., Reis, A. and Barton, A. (2016) 'Replication of a distinct psoriatic arthritis risk variant at the IL23R locus', *Ann Rheum Dis,* 75(7), pp. 1417-8.
Buechler, M. B., Pradhan, R. N., Krishnamurty, A. T., Cox, C., Calviello, A. K., Wang, A. W., Yang, Y. A., Tam, L., Caothien, R., Roose-Girma, M., Modrusan, Z., Arron, J. R., Bourgon, R., Müller, S. and Turley, S. J. (2021) 'Cross-tissue organization of the fibroblast lineage', *Nature,* 593(7860), pp. 575-579.
Bukhari, S. I. A., Truesdell, S. S., Lee, S., Kollu, S., Classon, A., Boukhali, M., Jain, E., Mortensen, R. D., Yanagiya, A., Sadreyev, R. I., Haas, W. and Vasudevan, S. (2016) 'A Specialized Mechanism of Translation Mediated by FXR1a-Associated MicroRNP in Cellular Quiescence', *Mol Cell,* 61(5), pp. 760-773.
Bustamante, M. F., Garcia-Carbonell, R., Whisenant, K. D. and Guma, M. (2017) 'Fibroblast-like synoviocyte metabolism in the pathogenesis of rheumatoid arthritis', *Arthritis Research & Therapy,* 19(1), pp. 110.
Bustamante, M. F., Oliveira, P. G., Garcia-Carbonell, R., Croft, A. P., Smith, J. M., Serrano, R. L., Sanchez-Lopez, E., Liu, X., Kisseleva, T., Hay, N., Buckley, C. D., Firestein, G. S., Murphy, A. N., Miyamoto, S. and Guma, M. (2018) 'Hexokinase 2 as a novel selective metabolic target for rheumatoid arthritis', *Ann Rheum Dis,* 77(11), pp. 1636-1643.
Cacciapaglia, F., Spinelli, F. R., Bartoloni, E., Bugatti, S., Erre, G. L., Fornaro, M., Manfredi, A., Piga, M., Sakellariou, G., Viapiana, O., Atzeni, F. and Gremese, E. (2023) 'Clinical Features of Diabetes Mellitus on Rheumatoid Arthritis: Data from the Cardiovascular Obesity and Rheumatic DISease (CORDIS) Study Group', *J Clin Med,* 12(6).
Caire, R., Audoux, E., Courbon, G., Michaud, E., Petit, C., Dalix, E., Chafchafi, M., Thomas, M., Vanden-Bossche, A., Navarro, L., Linossier, M. T., Peyroche, S., Guignandon, A., Vico, L., Paul, S. and Marotte, H. (2021) 'YAP/TAZ: Key Players for Rheumatoid Arthritis Severity by Driving Fibroblast Like Synoviocytes Phenotype and Fibro-Inflammatory Response', *Front Immunol,* 12, pp. 791907.

Cambré, I., Gaublomme, D., Burssens, A., Jacques, P., Schryvers, N., De Muynck, A., Meuris, L., Lambrecht, S., Carter, S., de Bleser, P., Saeys, Y., Van Hoorebeke, L., Kollias, G., Mack, M., Simoens, P., Lories, R., Callewaert, N., Schett, G. and Elewaut, D. (2018) 'Mechanical strain determines the site-specific localization of inflammation and tissue damage in arthritis', *Nat Commun,* 9(1), pp. 4613.
Canavan, M., Marzaioli, V., Bhargava, V., Nagpal, S., Gallagher, P., Hurson, C., Mullan, R., Veale, D. J. and Fearon, U. (2021) 'Functionally Mature CD1c(+) Dendritic Cells Preferentially Accumulate in the Inflammatory Arthritis Synovium', *Front Immunol,* 12, pp. 745226.
Canavan, M., Marzaioli, V., McGarry, T., Bhargava, V., Nagpal, S., Veale, D. J. and Fearon, U. (2020) 'Rheumatoid arthritis synovial microenvironment induces metabolic and functional adaptations in dendritic cells', *Clin Exp Immunol,* 202(2), pp. 226-238.
Canavan, M., Walsh, A. M., Bhargava, V., Wade, S. M., McGarry, T., Marzaioli, V., Moran, B., Biniecka, M., Convery, H., Wade, S., Orr, C., Mullan, R., Fletcher, J. M., Nagpal, S., Veale, D. J. and Fearon, U. (2018) 'Enriched Cd141+ DCs in the joint are transcriptionally distinct, activated, and contribute to joint pathogenesis', *JCI Insight,* 3(23).
Cañete, J. D., Santiago, B., Cantaert, T., Sanmartí, R., Palacin, A., Celis, R., Graell, E., Gil-Torregrosa, B., Baeten, D. and Pablos, J. L. (2007) 'Ectopic lymphoid neogenesis in psoriatic arthritis', *Ann Rheum Dis,* 66(6), pp. 720-6.
Carmona-Rivera, C., Carlucci, P. M., Moore, E., Lingampalli, N., Uchtenhagen, H., James, E., Liu, Y., Bicker, K. L., Wahamaa, H., Hoffmann, V., Catrina, A. I., Thompson, P., Buckner, J. H., Robinson, W. H., Fox, D. A. and Kaplan, M. J. (2017) 'Synovial fibroblast-neutrophil interactions promote pathogenic adaptive immunity in rheumatoid arthritis', *Sci Immunol,* 2(10).
Carter, L. M., McGonagle, D., Vital, E. M. and Wittmann, M. (2022) 'Applying Early Intervention Strategies to Autoimmune Skin Diseases. Is the Window of Opportunity Preclinical? A Dermato-Rheumatology Perspective', *J Invest Dermatol,* 142(3 Pt B), pp. 944-950.
Carter, N. A., Rosser, E. C. and Mauri, C. (2012) 'Interleukin-10 produced by B cells is crucial for the suppression of Th17/Th1 responses, induction of T regulatory type 1 cells and reduction of collagen-induced arthritis', *Arthritis Res Ther,* 14(1), pp. R32.
Carthew, R. W. and Sontheimer, E. J. (2009) 'Origins and Mechanisms of miRNAs and siRNAs', *Cell,* 136(4), pp. 642-55.
Castillo-Ojugas, A. and Hernández, I. R. (1989) 'Description of psoriatic arthropathy in the 17th century', *Arthritis Rheum,* 32(6), pp. 812-3.
Catrina, A. I., Joshua, V., Klareskog, L. and Malmström, V. (2016) 'Mechanisms involved in triggering rheumatoid arthritis', *Immunol Rev,* 269(1), pp. 162-74.
Catrina, A. I., Lampa, J., Ernestam, S., af Klint, E., Bratt, J., Klareskog, L. and Ulfgren, A. K. (2002) 'Anti-tumour necrosis factor (TNF)-alpha therapy (etanercept) down-regulates serum matrix metalloproteinase (MMP)-3 and MMP-1 in rheumatoid arthritis', *Rheumatology (Oxford),* 41(5), pp. 484-9.
Ceponis, A., Konttinen, Y. T., Imai, S., Tamulaitiene, M., Li, T. F., Xu, J. W., Hietanen, J., Santavirta, S. and Fassbender, H. G. (1998) 'Synovial lining, endothelial and inflammatory mononuclear cell proliferation in synovial membranes in psoriatic and reactive arthritis: a comparative quantitative morphometric study', *Br J Rheumatol,* 37(2), pp. 170-8.
Cha, H. S., Ahn, K. S., Jeon, C. H., Kim, J., Song, Y. W. and Koh, E. M. (2003) 'Influence of hypoxia on the expression of matrix metalloproteinase-1, -3 and tissue inhibitor of metalloproteinase-1 in rheumatoid synovial fibroblasts', *Clin Exp Rheumatol,* 21(5), pp. 593-8.
Chakrabortty, A., Patton, D. J., Smith, B. F. and Agarwal, P. (2023) 'miRNAs: Potential as Biomarkers and Therapeutic Targets for Cancer', *Genes,* 14(7), pp. 1375.
Chandran, V., Schentag, C. T., Brockbank, J. E., Pellett, F. J., Shanmugarajah, S., Toloza, S. M., Rahman, P. and Gladman, D. D. (2009) 'Familial aggregation of psoriatic arthritis', *Ann Rheum Dis,* 68(5), pp. 664-7.

Chang, S. K., Noss, E. H., Chen, M., Gu, Z., Townsend, K., Grenha, R., Leon, L., Lee, S. Y., Lee, D. M. and Brenner, M. B. (2011) 'Cadherin-11 regulates fibroblast inflammation', *Proc Natl Acad Sci U S A,* 108(20), pp. 8402-7.
Charbonneau, M., Harper, K., Grondin, F., Pelmus, M., McDonald, P. P. and Dubois, C. M. (2007) 'Hypoxia-inducible factor mediates hypoxic and tumor necrosis factor alpha-induced increases in tumor necrosis factor-alpha converting enzyme/ADAM17 expression by synovial cells', *J Biol Chem,* 282(46), pp. 33714-33724.
Charlton, R., Green, A., Shaddick, G., Snowball, J., Nightingale, A., Tillett, W., Smith, C. and McHugh, N. (2019) 'Risk of type 2 diabetes and cardiovascular disease in an incident cohort of people with psoriatic arthritis: a population-based cohort study', *Rheumatology (Oxford),* 58(1), pp. 144-148.
Chen, H. and Chan, D. C. (2017) 'Mitochondrial dynamics in regulating the unique phenotypes of cancer and stem cells', *Cell metabolism,* 26(1), pp. 39-48.
Chen, H. H., Chen, D. Y., Lin, C. C., Chen, Y. M., Lai, K. L. and Lin, C. H. (2017a) 'Association between use of disease-modifying antirheumatic drugs and diabetes in patients with ankylosing spondylitis, rheumatoid arthritis, or psoriasis/psoriatic arthritis: a nationwide, population-based cohort study of 84,989 patients', *Ther Clin Risk Manag,* 13, pp. 583-592.
Chen, L., Hou, X., Zhang, M., Zheng, Y., Zheng, X., Yang, Q., Li, J., Gu, N., Zhang, M., Sun, Y., Wu, J. and Yu, B. (2020) 'MicroRNA-223-3p modulates dendritic cell function and ameliorates experimental autoimmune myocarditis by targeting the NLRP3 inflammasome', *Mol Immunol,* 117, pp. 73-83.
Chen, L., Li, Q., Wang, J., Jin, S., Zheng, H., Lin, J., He, F., Zhang, H., Ma, S., Mei, J. and Yu, J. (2017b) 'MiR-29b-3p promotes chondrocyte apoptosis and facilitates the occurrence and development of osteoarthritis by targeting PGRN', *J Cell Mol Med,* 21(12), pp. 3347-3359.
Chen, Q., Li, H., Liu, Y. and Zhao, M. (2022) 'Epigenetic Regulation of Immune and Inflammatory Responses in Rheumatoid Arthritis', *Frontiers in Immunology,* 13.
Chim, S. S., Shing, T. K., Hung, E. C., Leung, T. Y., Lau, T. K., Chiu, R. W. and Lo, Y. M. (2008) 'Detection and characterization of placental microRNAs in maternal plasma', *Clin Chem,* 54(3), pp. 482-90.
Chiu, J. J., Lee, P. L., Chen, C. N., Lee, C. I., Chang, S. F., Chen, L. J., Lien, S. C., Ko, Y. C., Usami, S. and Chien, S. (2004) 'Shear stress increases ICAM-1 and decreases VCAM-1 and E-selectin expressions induced by tumor necrosis factor-[alpha] in endothelial cells', *Arterioscler Thromb Vasc Biol,* 24(1), pp. 73-9.
Cho, M. L., Ju, J. H., Kim, H. R., Oh, H. J., Kang, C. M., Jhun, J. Y., Lee, S. Y., Park, M. K., Min, J. K., Park, S. H., Lee, S. H. and Kim, H. Y. (2007) 'Toll-like receptor 2 ligand mediates the upregulation of angiogenic factor, vascular endothelial growth factor and interleukin-8/CXCL8 in human rheumatoid synovial fibroblasts', *Immunol Lett,* 108(2), pp. 121-8.
Choi, E., Machado, C. R. L., Okano, T., Boyle, D., Wang, W. and Firestein, G. S. (2024) 'Joint-specific rheumatoid arthritis fibroblast-like synoviocyte regulation identified by integration of chromatin access and transcriptional activity', *bioRxiv*.
Ciccia, F., Guggino, G., Rizzo, A., Alessandro, R., Luchetti, M. M., Milling, S., Saieva, L., Cypers, H., Stampone, T., Di Benedetto, P., Gabrielli, A., Fasano, A., Elewaut, D. and Triolo, G. (2017) 'Dysbiosis and zonulin upregulation alter gut epithelial and vascular barriers in patients with ankylosing spondylitis', *Ann Rheum Dis,* 76(6), pp. 1123-1132.
Ciechomska, M., Roszkowski, L., Burakowski, T., Massalska, M., Felis-Giemza, A. and Roura, A. J. (2023) 'Circulating miRNA-19b as a biomarker of disease progression and treatment response to baricitinib in rheumatoid arthritis patients through miRNA profiling of monocytes', *Front Immunol,* 14, pp. 980247.
Citterio, L. A., Mancuso, R., Agostini, S., Meloni, M. and Clerici, M. (2023) 'Serum and Exosomal miR-7-1-5p and miR-223-3p as Possible Biomarkers for Parkinson's Disease', *Biomolecules,* 13(5).
Claesson-Welsh, L. (2016) 'VEGF receptor signal transduction - A brief update', *Vascul Pharmacol,* 86, pp. 14-17.
Coates, L. C. and Helliwell, P. S. (2017) 'Psoriatic arthritis: state of the art review', *Clin Med (Lond),* 17(1), pp. 65-70.

Coates, L. C., Kavanaugh, A., Mease, P. J., Soriano, E. R., Laura Acosta-Felquer, M., Armstrong, A. W., Bautista-Molano, W., Boehncke, W. H., Campbell, W., Cauli, A., Espinoza, L. R., FitzGerald, O., Gladman, D. D., Gottlieb, A., Helliwell, P. S., Husni, M. E., Love, T. J., Lubrano, E., McHugh, N., Nash, P., Ogdie, A., Orbai, A. M., Parkinson, A., O'Sullivan, D., Rosen, C. F., Schwartzman, S., Siegel, E. L., Toloza, S., Tuong, W. and Ritchlin, C. T. (2016) 'Group for Research and Assessment of Psoriasis and Psoriatic Arthritis 2015 Treatment Recommendations for Psoriatic Arthritis', *Arthritis Rheumatol,* 68(5), pp. 1060-71.
Coates, L. C., Soriano, E. R., Corp, N., Bertheussen, H., Callis Duffin, K., Campanholo, C. B., Chau, J., Eder, L., Fernández-Ávila, D. G., FitzGerald, O., Garg, A., Gladman, D. D., Goel, N., Helliwell, P. S., Husni, M. E., Jadon, D. R., Katz, A., Laheru, D., Latella, J., Leung, Y. Y., Lindsay, C., Lubrano, E., Mazzuoccolo, L. D., Mease, P. J., O'Sullivan, D., Ogdie, A., Olsder, W., Palominos, P. E., Schick, L., Steinkoenig, I., de Wit, M., van der Windt, D. A. and Kavanaugh, A. (2022) 'Group for Research and Assessment of Psoriasis and Psoriatic Arthritis (GRAPPA): updated treatment recommendations for psoriatic arthritis 2021', *Nat Rev Rheumatol,* 18(8), pp. 465-479.
Colamatteo, A., Micillo, T., Bruzzaniti, S., Fusco, C., Garavelli, S., De Rosa, V., Galgani, M., Spagnuolo, M. I., Di Rella, F., Puca, A. A., de Candia, P. and Matarese, G. (2019) 'Metabolism and Autoimmune Responses: The microRNA Connection', *Front Immunol,* 10, pp. 1969.
Contreras-Rodríguez, J. A., Puente-Rivera, J., Córdova-Esparza, D. M., Nuñez-Olvera, S. I. and Silva-Cázares, M. B. (2023) 'Bioinformatic miRNA-mRNAs Analysis Revels to miR-934 as a Potential Regulator of the Epithelial-Mesenchymal Transition in Triple-Negative Breast Cancer', *Cells,* 12(6).
Cooles, F. A. H., Tarn, J., Lendrem, D. W., Naamane, N., Lin, C. M., Millar, B., Maney, N. J., Anderson, A. E., Thalayasingam, N., Diboll, J., Bondet, V., Duffy, D., Barnes, M. R., Smith, G. R., Ng, S., Watson, D., Henkin, R., Cope, A. P., Reynard, L. N., Pratt, A. G. and Isaacs, J. D. (2022) 'Interferon-α-mediated therapeutic resistance in early rheumatoid arthritis implicates epigenetic reprogramming', *Ann Rheum Dis,* 81(9), pp. 1214-1223.
Cope, A. P., Jasenecova, M., Vasconcelos, J. C., Filer, A., Raza, K., Qureshi, S., D'Agostino, M. A., McInnes, I. B., Isaacs, J. D., Pratt, A. G., Fisher, B. A., Buckley, C. D., Emery, P., Ho, P., Buch, M. H., Ciurtin, C., van Schaardenburg, D., Huizinga, T., Toes, R., Georgiou, E., Kelly, J., Murphy, C. and Prevost, A. T. (2024) 'Abatacept in individuals at high risk of rheumatoid arthritis (APIPPRA): a randomised, double-blind, multicentre, parallel, placebo-controlled, phase 2b clinical trial', *Lancet,* 403(10429), pp. 838-849.
Copeman, W. (2012) 'Commentaries on the History and Cure of Diseases, by William Heberden M.D., facsimile of London 1802 edition, with preface by Paul Klemperer (History of Medicine series, no. 18), New York, Hafner Publishing Co., 1962, pp. 483, $3.00', *Medical History,* 7, pp. 288-289.
Cordtz, R. L., Askling, J., Delcoigne, B., Smedby, K. E., Baecklund, E., Ballegaard, C., Isomäki, P., Aaltonen, K., Gudbjornsson, B., Love, T. J., Provan, S. A., Michelsen, B., Sexton, J., Dreyer, L. and Hellgren, K. (2022) 'Haematological malignancies in patients with psoriatic arthritis overall and treated with TNF inhibitors: a Nordic cohort study', *RMD Open,* 8(2).
Costello, P., Bresnihan, B., O'Farrelly, C. and FitzGerald, O. (1999) 'Predominance of CD8+ T lymphocytes in psoriatic arthritis', *J Rheumatol,* 26(5), pp. 1117-24.
Costenbader, K. H. and Karlson, E. W. (2006) 'Epstein-Barr virus and rheumatoid arthritis: is there a link?', *Arthritis Res Ther,* 8(1), pp. 204.
Courvoisier, D. S., Chatzidionysiou, K., Mongin, D., Lauper, K., Mariette, X., Morel, J., Gottenberg, J. E., Bergstra, S. A., Suarez, M. P., Codreanu, C., Kvien, T. K., Santos, M. J., Pavelka, K., Hetland, M. L., Askling, J., Turesson, C., Kubo, S., Tanaka, Y., Iannone, F., Choquette, D., Nordström, D. C., Rotar, Z., Lukina, G., Gabay, C., Van Vollenhoven, R. and Finckh, A. (2021) 'The impact of seropositivity on the effectiveness of biologic anti-rheumatic agents: results from a collaboration of 16 registries', *Rheumatology (Oxford),* 60(2), pp. 820-828.
Croci, D. O., Cerliani, J. P., Dalotto-Moreno, T., Méndez-Huergo, S. P., Mascanfroni, I. D., Dergan-Dylon, S., Toscano, M. A., Caramelo, J. J., García-Vallejo, J. J., Ouyang, J., Mesri, E. A., Junttila, M. R., Bais, C.,

Shipp, M. A., Salatino, M. and Rabinovich, G. A. (2014) 'Glycosylation-dependent lectin-receptor interactions preserve angiogenesis in anti-VEGF refractory tumors', *Cell,* 156(4), pp. 744-58.
Croft, A. P., Campos, J., Jansen, K., Turner, J. D., Marshall, J., Attar, M., Savary, L., Wehmeyer, C., Naylor, A. J., Kemble, S., Begum, J., Dürholz, K., Perlman, H., Barone, F., McGettrick, H. M., Fearon, D. T., Wei, K., Raychaudhuri, S., Korsunsky, I., Brenner, M. B., Coles, M., Sansom, S. N., Filer, A. and Buckley, C. D. (2019) 'Distinct fibroblast subsets drive inflammation and damage in arthritis', *Nature,* 570(7760), pp. 246-251.
Croft, A. P., Naylor, A. J., Marshall, J. L., Hardie, D. L., Zimmermann, B., Turner, J., Desanti, G., Adams, H., Yemm, A. I., Müller-Ladner, U., Dayer, J. M., Neumann, E., Filer, A. and Buckley, C. D. (2016) 'Rheumatoid synovial fibroblasts differentiate into distinct subsets in the presence of cytokines and cartilage', *Arthritis Res Ther,* 18(1), pp. 270.
Crowley, T., O'Neil, J. D., Adams, H., Thomas, A. M., Filer, A., Buckley, C. D. and Clark, A. R. (2017) 'Priming in response to pro-inflammatory cytokines is a feature of adult synovial but not dermal fibroblasts', *Arthritis Res Ther,* 19(1), pp. 35.
Cruz Correa, O., Ganatra, D., Garrido, A., Machhar, R., Lively, S., Kapoor, M. and Gladman, D. D. (2023) 'POS1608 MIRNA BIOMARKERS FOR ARTICULAR AND CUTANEOUS RESPONSE TO METHOTREXATE IN PSORIATIC ARTHRITIS', *Annals of the Rheumatic Diseases,* 82(Suppl 1), pp. 1149-1149.
Cui, S., Chen, Y., Guo, Y., Wang, X. and Chen, D. (2023) 'Hsa-miR-22-3p inhibits liver cancer cell EMT and cell migration/ invasion by indirectly regulating SPRY2', *PLoS One,* 18(2), pp. e0281536.
Culemann, S., Grüneboom, A., Nicolás-Ávila, J. Á., Weidner, D., Lämmle, K. F., Rothe, T., Quintana, J. A., Kirchner, P., Krljanac, B., Eberhardt, M., Ferrazzi, F., Kretzschmar, E., Schicht, M., Fischer, K., Gelse, K., Faas, M., Pfeifle, R., Ackermann, J. A., Pachowsky, M., Renner, N., Simon, D., Haseloff, R. F., Ekici, A. B., Bäuerle, T., Blasig, I. E., Vera, J., Voehringer, D., Kleyer, A., Paulsen, F., Schett, G., Hidalgo, A. and Krönke, G. (2019) 'Locally renewing resident synovial macrophages provide a protective barrier for the joint', *Nature,* 572(7771), pp. 670-675.
Cunnane, G., Grehan, S., Geoghegan, S., McCormack, C., Shields, D., Whitehead, A. S., Bresnihan, B. and Fitzgerald, O. (2000) 'Serum amyloid A in the assessment of early inflammatory arthritis', *J Rheumatol,* 27(1), pp. 58-63.
Cunningham, C. C., Wade, S., Floudas, A., Orr, C., McGarry, T., Wade, S., Cregan, S., Fearon, U. and Veale, D. J. (2021) 'Serum miRNA Signature in Rheumatoid Arthritis and "At-Risk Individuals"', *Front Immunol,* 12, pp. 633201.
Cuthbert, R. J., Watad, A., Fragkakis, E. M., Dunsmuir, R., Loughenbury, P., Khan, A., Millner, P. A., Davison, A., Marzo-Ortega, H., Newton, D., Bridgewood, C. and McGonagle, D. G. (2019) 'Evidence that tissue resident human enthesis γδT-cells can produce IL-17A independently of IL-23R transcript expression', *Ann Rheum Dis,* 78(11), pp. 1559-1565.
Cutolo, M. and Straub, R. H. (2020) 'Sex steroids and autoimmune rheumatic diseases: state of the art', *Nat Rev Rheumatol,* 16(11), pp. 628-644.
Dagan, A., Dahan, S., Shemer, A., Langevitz, P., Hellou, T., Davidson, T., Shoenfeld, Y. and Shovman, O. (2019) 'Acute onset of psoriatic spondyloarthritis as a new manifestation of post-streptococcal reactive arthritis: a case series', *Clin Rheumatol,* 38(9), pp. 2367-2372.
Dai, W. and Jiang, L. (2019) 'Dysregulated Mitochondrial Dynamics and Metabolism in Obesity, Diabetes, and Cancer', *Front Endocrinol (Lausanne),* 10, pp. 570.
Dal Bello, G., Gisondi, P., Idolazzi, L. and Girolomoni, G. (2020) 'Psoriatic Arthritis and Diabetes Mellitus: A Narrative Review', *Rheumatol Ther,* 7(2), pp. 271-285.
Damhofer, H., Tatar, T., Southgate, B., Scarneo, S., Agger, K., Shlyueva, D., Uhrbom, L., Morrison, G. M., Hughes, P. F., Haystead, T., Pollard, S. M. and Helin, K. (2024) 'TAK1 inhibition leads to RIPK1-dependent apoptosis in immune-activated cancers', *Cell Death & Disease,* 15(4), pp. 273.
Das, K. and Rao, L. V. M. (2022) 'The Role of microRNAs in Inflammation', *Int J Mol Sci,* 23(24).
De Bock, K., Georgiadou, M., Schoors, S., Kuchnio, A., Wong, B. W., Cantelmo, A. R., Quaegebeur, A., Ghesquière, B., Cauwenberghs, S., Eelen, G., Phng, L. K., Betz, I., Tembuyser, B., Brepoels, K., Welti, J., Geudens, I., Segura, I., Cruys, B., Bifari, F., Decimo, I., Blanco, R., Wyns, S., Vangindertael, J., Rocha, S.,

Collins, R. T., Munck, S., Daelemans, D., Imamura, H., Devlieger, R., Rider, M., Van Veldhoven, P. P., Schuit, F., Bartrons, R., Hofkens, J., Fraisl, P., Telang, S., Deberardinis, R. J., Schoonjans, L., Vinckier, S., Chesney, J., Gerhardt, H., Dewerchin, M. and Carmeliet, P. (2013) 'Role of PFKFB3-driven glycolysis in vessel sprouting', *Cell,* 154(3), pp. 651-63.
de Rie, D., Abugessaisa, I., Alam, T., Arner, E., Arner, P., Ashoor, H., Åström, G., Babina, M., Bertin, N., Burroughs, A. M., Carlisle, A. J., Daub, C. O., Detmar, M., Deviatiiarov, R., Fort, A., Gebhard, C., Goldowitz, D., Guhl, S., Ha, T. J., Harshbarger, J., Hasegawa, A., Hashimoto, K., Herlyn, M., Heutink, P., Hitchens, K. J., Hon, C. C., Huang, E., Ishizu, Y., Kai, C., Kasukawa, T., Klinken, P., Lassmann, T., Lecellier, C. H., Lee, W., Lizio, M., Makeev, V., Mathelier, A., Medvedeva, Y. A., Mejhert, N., Mungall, C. J., Noma, S., Ohshima, M., Okada-Hatakeyama, M., Persson, H., Rizzu, P., Roudnicky, F., Sætrom, P., Sato, H., Severin, J., Shin, J. W., Swoboda, R. K., Tarui, H., Toyoda, H., Vitting-Seerup, K., Winteringham, L., Yamaguchi, Y., Yasuzawa, K., Yoneda, M., Yumoto, N., Zabierowski, S., Zhang, P. G., Wells, C. A., Summers, K. M., Kawaji, H., Sandelin, A., Rehli, M., Hayashizaki, Y., Carninci, P., Forrest, A. R. R. and de Hoon, M. J. L. (2017) 'An integrated expression atlas of miRNAs and their promoters in human and mouse', *Nat Biotechnol,* 35(9), pp. 872-878.
Deane, K. D., Demoruelle, M. K., Kelmenson, L. B., Kuhn, K. A., Norris, J. M. and Holers, V. M. (2017) 'Genetic and environmental risk factors for rheumatoid arthritis', *Best Pract Res Clin Rheumatol,* 31(1), pp. 3-18.
del Rey, M. J., Izquierdo, E., Caja, S., Usategui, A., Santiago, B., Galindo, M. and Pablos, J. L. (2009) 'Human inflammatory synovial fibroblasts induce enhanced myeloid cell recruitment and angiogenesis through a hypoxia-inducible transcription factor 1alpha/vascular endothelial growth factor-mediated pathway in immunodeficient mice', *Arthritis Rheum,* 60(10), pp. 2926-34.
Denli, A. M., Tops, B. B., Plasterk, R. H., Ketting, R. F. and Hannon, G. J. (2004) 'Processing of primary microRNAs by the Microprocessor complex', *Nature,* 432(7014), pp. 231-5.
Dharap, A., Pokrzywa, C., Murali, S., Pandi, G. and Vemuganti, R. (2013) 'MicroRNA miR-324-3p induces promoter-mediated expression of RelA gene', *PLoS One,* 8(11), pp. e79467.
Diener, C., Keller, A. and Meese, E. (2022) 'Emerging concepts of miRNA therapeutics: from cells to clinic', *Trends Genet,* 38(6), pp. 613-626.
Diller, M., Hasseli, R., Hülser, M. L., Aykara, I., Frommer, K., Rehart, S., Müller-Ladner, U. and Neumann, E. (2019) 'Targeting Activated Synovial Fibroblasts in Rheumatoid Arthritis by Peficitinib', *Front Immunol,* 10, pp. 541.
Dimitriou, R., Jones, E., McGonagle, D. and Giannoudis, P. V. (2011) 'Bone regeneration: current concepts and future directions', *BMC Med,* 9, pp. 66.
Dinarello, C. A. (2019) 'The IL-1 family of cytokines and receptors in rheumatic diseases', *Nat Rev Rheumatol,* 15(10), pp. 612-632.
Dinarello, C. A., Goldin, N. P. and Wolff, S. M. (1974) 'Demonstration and characterization of two distinct human leukocytic pyrogens', *J Exp Med,* 139(6), pp. 1369-81.
Ding, Q., Hu, W., Wang, R., Yang, Q., Zhu, M., Li, M., Cai, J., Rose, P., Mao, J. and Zhu, Y. Z. (2023) 'Signaling pathways in rheumatoid arthritis: implications for targeted therapy', *Signal Transduct Target Ther,* 8(1), pp. 68.
Dommasch, E. D., Abuabara, K., Shin, D. B., Nguyen, J., Troxel, A. B. and Gelfand, J. M. (2011) 'The risk of infection and malignancy with tumor necrosis factor antagonists in adults with psoriatic disease: a systematic review and meta-analysis of randomized controlled trials', *J Am Acad Dermatol,* 64(6), pp. 1035-50.
Dong, H. C., Li, P. N., Chen, C. J., Xu, X., Zhang, H., Liu, G., Zheng, L. J. and Li, P. (2019) 'Sinomenine Attenuates Cartilage Degeneration by Regulating miR-223-3p/NLRP3 Inflammasome Signaling', *Inflammation,* 42(4), pp. 1265-1275.
Dougados, M., Soubrier, M., Antunez, A., Balint, P., Balsa, A., Buch, M. H., Casado, G., Detert, J., El-Zorkany, B., Emery, P., Hajjaj-Hassouni, N., Harigai, M., Luo, S. F., Kurucz, R., Maciel, G., Mola, E. M., Montecucco, C. M., McInnes, I., Radner, H., Smolen, J. S., Song, Y. W., Vonkeman, H. E., Winthrop, K. and Kay, J. (2014) 'Prevalence of comorbidities in rheumatoid arthritis and evaluation of their

monitoring: results of an international, cross-sectional study (COMORA)', *Ann Rheum Dis,* 73(1), pp. 62-8.
Du, X., Duan, M., Kan, S., Yang, Y., Xu, S., Wei, J., Li, J., Chen, H., Zhou, X. and Xie, J. (2024) 'TGF-β3 mediates mitochondrial dynamics through the p-Smad3/AMPK pathway', *Cell Prolif,* 57(5), pp. e13579.
Duffin, K. C., Freeny, I. C., Schrodi, S. J., Wong, B., Feng, B. J., Soltani-Arabshahi, R., Rakkhit, T., Goldgar, D. E. and Krueger, G. G. (2009) 'Association between IL13 polymorphisms and psoriatic arthritis is modified by smoking', *J Invest Dermatol,* 129(12), pp. 2777-83.
Dunaeva, M., Blom, J., Thurlings, R. and Pruijn, G. J. M. (2018) 'Circulating serum miR-223-3p and miR-16-5p as possible biomarkers of early rheumatoid arthritis', *Clin Exp Immunol,* 193(3), pp. 376-385.
Eastgate, J. A., Symons, J. A., Wood, N. C., Grinlinton, F. M., di Giovine, F. S. and Duff, G. W. (1988) 'Correlation of plasma interleukin 1 levels with disease activity in rheumatoid arthritis', *Lancet,* 2(8613), pp. 706-9.
Eder, L., Law, T., Chandran, V., Shanmugarajah, S., Shen, H., Rosen, C. F., Cook, R. J. and Gladman, D. D. (2011) 'Association between environmental factors and onset of psoriatic arthritis in patients with psoriasis', *Arthritis Care Res (Hoboken),* 63(8), pp. 1091-7.
Eder, L., Shanmugarajah, S., Thavaneswaran, A., Chandran, V., Rosen, C. F., Cook, R. J. and Gladman, D. D. (2012) 'The association between smoking and the development of psoriatic arthritis among psoriasis patients', *Ann Rheum Dis,* 71(2), pp. 219-24.
Eelen, G., de Zeeuw, P., Treps, L., Harjes, U., Wong, B. W. and Carmeliet, P. (2018) 'Endothelial Cell Metabolism', *Physiol Rev,* 98(1), pp. 3-58.
Eichhorn, S. W., Guo, H., McGeary, S. E., Rodriguez-Mias, R. A., Shin, C., Baek, D., Hsu, S. H., Ghoshal, K., Villén, J. and Bartel, D. P. (2014) 'mRNA destabilization is the dominant effect of mammalian microRNAs by the time substantial repression ensues', *Mol Cell,* 56(1), pp. 104-15.
Elhai, M., Micheroli, R., Houtman, M., Mirrahimi, M., Moser, L., Pauli, C., Bürki, K., Laimbacher, A., Kania, G., Klein, K., Schätzle, P., Frank Bertoncelj, M., Edalat, S. G., Keusch, L., Khmelevskaya, A., Toitou, M., Geiss, C., Rauer, T., Sakkou, M., Kollias, G., Armaka, M., Distler, O. and Ospelt, C. (2023) 'The long non-coding RNA HOTAIR contributes to joint-specific gene expression in rheumatoid arthritis', *Nat Commun,* 14(1), pp. 8172.
Ellinghaus, E., Stuart, P. E., Ellinghaus, D., Nair, R. P., Debrus, S., Raelson, J. V., Belouchi, M., Tejasvi, T., Li, Y., Tsoi, L. C., Onken, A. T., Esko, T., Metspalu, A., Rahman, P., Gladman, D. D., Bowcock, A. M., Helms, C., Krueger, G. G., Koks, S., Kingo, K., Gieger, C., Wichmann, H. E., Mrowietz, U., Weidinger, S., Schreiber, S., Abecasis, G. R., Elder, J. T., Weichenthal, M. and Franke, A. (2012) 'Genome-wide meta-analysis of psoriatic arthritis identifies susceptibility locus at REL', *J Invest Dermatol,* 132(4), pp. 1133-40.
Elliott, A., McGonagle, D. and Rooney, M. (2021) 'Integrating imaging and biomarker assessment to better define psoriatic arthritis and predict response to biologic therapy', *Rheumatology (Oxford),* 60(Suppl 6), pp. vi38-vi52.
Elmesmari, A., Fraser, A. R., Wood, C., Gilchrist, D., Vaughan, D., Stewart, L., McSharry, C., McInnes, I. B. and Kurowska-Stolarska, M. (2016) 'MicroRNA-155 regulates monocyte chemokine and chemokine receptor expression in Rheumatoid Arthritis', *Rheumatology (Oxford),* 55(11), pp. 2056-2065.
Elshabrawy, H. A., Chen, Z., Volin, M. V., Ravella, S., Virupannavar, S. and Shahrara, S. (2015) 'The pathogenic role of angiogenesis in rheumatoid arthritis', *Angiogenesis,* 18(4), pp. 433-48.
Entezami, P., Fox, D. A., Clapham, P. J. and Chung, K. C. (2011) 'Historical perspective on the etiology of rheumatoid arthritis', *Hand Clin,* 27(1), pp. 1-10.
Espinoza, L. R. (2018) 'The History of Psoriatic Arthritis (PsA): From Moll and Wright to Pathway-Specific Therapy', *Curr Rheumatol Rep,* 20(10), pp. 58.
Evangelatos, G., Fragoulis, G. E., Koulouri, V. and Lambrou, G. I. (2019) 'MicroRNAs in rheumatoid arthritis: From pathogenesis to clinical impact', *Autoimmun Rev,* 18(11), pp. 102391.
Fabbri, M. (2018) 'MicroRNAs and miRceptors: a new mechanism of action for intercellular communication', *Philos Trans R Soc Lond B Biol Sci,* 373(1737).

Fabbri, M., Paone, A., Calore, F., Galli, R., Gaudio, E., Santhanam, R., Lovat, F., Fadda, P., Mao, C., Nuovo, G. J., Zanesi, N., Crawford, M., Ozer, G. H., Wernicke, D., Alder, H., Caligiuri, M. A., Nana-Sinkam, P., Perrotti, D. and Croce, C. M. (2012) 'MicroRNAs bind to Toll-like receptors to induce prometastatic inflammatory response', *Proc Natl Acad Sci U S A,* 109(31), pp. E2110-6.
Fang, Y., Zhang, Q., Lv, C., Guo, Y., He, Y., Guo, P., Wei, Z., Xia, Y. and Dai, Y. (2023) 'Mitochondrial fusion induced by transforming growth factor-β1 serves as a switch that governs the metabolic reprogramming during differentiation of regulatory T cells', *Redox Biol,* 62, pp. 102709.
Fassbender, H. G. and Simmling-Annefeld, M. (1983) 'The potential aggressiveness of synovial tissue in rheumatoid arthritis', *J Pathol,* 139(3), pp. 399-406.
Faust, H. J., Cheng, T. Y., Korsunsky, I., Watts, G. F. M., Gal-Oz, S. T., Trim, W., Kongthong, K., Jonsson, A. H., Simmons, D. P., Zhang, F., Padera, R., Chubinskaya, S., Wei, K., Raychaudhuri, S., Lynch, L., Moody, D. B. and Brenner, M. B. (2023) 'Adipocytes regulate fibroblast function, and their loss contributes to fibroblast dysfunction in inflammatory diseases', *bioRxiv*.
Fava, R., Olsen, N., Keski-Oja, J., Moses, H. and Pincus, T. (1989) 'Active and latent forms of transforming growth factor beta activity in synovial effusions', *J Exp Med,* 169(1), pp. 291-6.
Fearon, U., Canavan, M., Biniecka, M. and Veale, D. J. (2016) 'Hypoxia, mitochondrial dysfunction and synovial invasiveness in rheumatoid arthritis', *Nat Rev Rheumatol,* 12(7), pp. 385-97.
Fearon, U., Griosios, K., Fraser, A., Reece, R., Emery, P., Jones, P. F. and Veale, D. J. (2003) 'Angiopoietins, growth factors, and vascular morphology in early arthritis', *J Rheumatol,* 30(2), pp. 260-8.
Fearon, U., Hanlon, M. M., Floudas, A. and Veale, D. J. (2022) 'Cellular metabolic adaptations in rheumatoid arthritis and their therapeutic implications', *Nat Rev Rheumatol,* 18(7), pp. 398-414.
Fearon, U., Hanlon, M. M., Wade, S. M. and Fletcher, J. M. (2019) 'Altered metabolic pathways regulate synovial inflammation in rheumatoid arthritis', *Clin Exp Immunol,* 197(2), pp. 170-180.
Fearon, U., Mullan, R., Markham, T., Connolly, M., Sullivan, S., Poole, A. R., FitzGerald, O., Bresnihan, B. and Veale, D. J. (2006) 'Oncostatin M induces angiogenesis and cartilage degradation in rheumatoid arthritis synovial tissue and human cartilage cocultures', *Arthritis Rheum,* 54(10), pp. 3152-62.
Fearon, U., Reece, R., Smith, J., Emery, P. and Veale, D. J. (1999) 'Synovial cytokine and growth factor regulation of MMPs/TIMPs: implications for erosions and angiogenesis in early rheumatoid and psoriatic arthritis patients', *Ann N Y Acad Sci,* 878, pp. 619-21.
Feichtinger, X., Muschitz, C., Heimel, P., Baierl, A., Fahrleitner-Pammer, A., Redl, H., Resch, H., Geiger, E., Skalicky, S., Dormann, R., Plachel, F., Pietschmann, P., Grillari, J., Hackl, M. and Kocijan, R. (2018) 'Bone-related Circulating MicroRNAs miR-29b-3p, miR-550a-3p, and miR-324-3p and their Association to Bone Microstructure and Histomorphometry', *Sci Rep,* 8(1), pp. 4867.
Feng, J., Chen, Q., Yu, F., Wang, Z., Chen, S., Jin, Z., Cai, Q., Liu, Y. and He, J. (2016) 'Body Mass Index and Risk of Rheumatoid Arthritis: A Meta-Analysis of Observational Studies', *Medicine (Baltimore),* 95(8), pp. e2859.
Feng, Z. T., Li, J., Ren, J. and Lv, Z. (2011) '[Expression of miR-146a and miR-16 in peripheral blood mononuclear cells of patients with rheumatoid arthritis and their correlation to the disease activity]', *Nan Fang Yi Ke Da Xue Xue Bao,* 31(2), pp. 320-3.
Ferreira, M. B., Fonseca, T., Costa, R., Marinho, A., Oliveira, J. C., Zannad, F., Rossignol, P., Rodrigues, P., Barros, A. S. and Ferreira, J. P. (2022) 'Sex differences in circulating proteins of patients with rheumatoid arthritis: A cohort study', *Int J Rheum Dis,* 25(6), pp. 669-677.
Figus, F. A., Piga, M., Azzolin, I., McConnell, R. and Iagnocco, A. (2021) 'Rheumatoid arthritis: Extra-articular manifestations and comorbidities', *Autoimmun Rev,* 20(4), pp. 102776.
Filková, M., Aradi, B., Senolt, L., Ospelt, C., Vettori, S., Mann, H., Filer, A., Raza, K., Buckley, C. D., Snow, M., Vencovský, J., Pavelka, K., Michel, B. A., Gay, R. E., Gay, S. and Jüngel, A. (2014) 'Association of circulating miR-223 and miR-16 with disease activity in patients with early rheumatoid arthritis', *Ann Rheum Dis,* 73(10), pp. 1898-904.
Finnegan, A., Kaplan, C. D., Cao, Y., Eibel, H., Glant, T. T. and Zhang, J. (2003) 'Collagen-induced arthritis is exacerbated in IL-10-deficient mice', *Arthritis Res Ther,* 5(1), pp. R18-24.

Finzel, S., Englbrecht, M., Engelke, K., Stach, C. and Schett, G. (2011) 'A comparative study of periarticular bone lesions in rheumatoid arthritis and psoriatic arthritis', *Ann Rheum Dis,* 70(1), pp. 122-7.
Fiocco, U., Cozzi, L., Chieco-Bianchi, F., Rigon, C., Vezzù, M., Favero, E., Ferro, F., Sfriso, P., Rubaltelli, L., Nardacchione, R. and Todesco, S. (2001) 'Vascular changes in psoriatic knee joint synovitis', *J Rheumatol,* 28(11), pp. 2480-6.
Firestein, G. S., Budd, R. C., Gabriel, S. E., McInnes, I. B. and O'Dell, J. R. (2020) *Firestein & kelley's textbook of rheumatology-E-book.* Elsevier Health Sciences.
Firestein, G. S. and McInnes, I. B. (2017) 'Immunopathogenesis of Rheumatoid Arthritis', *Immunity,* 46(2), pp. 183-196.
Firestein, G. S., Yeo, M. and Zvaifler, N. J. (1995) 'Apoptosis in rheumatoid arthritis synovium', *J Clin Invest,* 96(3), pp. 1631-8.
Fish, J. E., Santoro, M. M., Morton, S. U., Yu, S., Yeh, R. F., Wythe, J. D., Ivey, K. N., Bruneau, B. G., Stainier, D. Y. and Srivastava, D. (2008) 'miR-126 regulates angiogenic signaling and vascular integrity', *Dev Cell,* 15(2), pp. 272-84.
Floudas, A., Canavan, M., McGarry, T., Mullan, R., Nagpal, S., Veale, D. J. and Fearon, U. (2021) 'ACPA Status Correlates with Differential Immune Profile in Patients with Rheumatoid Arthritis', *Cells,* 10(3).
Floudas, A., Gorman, A., Neto, N., Monaghan, M. G., Elliott, Z., Fearon, U. and Marzaioli, V. (2022a) 'Inside the Joint of Inflammatory Arthritis Patients: Handling and Processing of Synovial Tissue Biopsies for High Throughput Analysis', *Front Med (Lausanne),* 9, pp. 830998.
Floudas, A., Smith, C. M., Tynan, O., Neto, N., Krishna, V., Wade, S. M., Hanlon, M., Cunningham, C., Marzaioli, V., Canavan, M., Fletcher, J. M., Mullan, R. H., Cole, S., Hao, L. Y., Monaghan, M. G., Nagpal, S., Veale, D. J. and Fearon, U. (2022b) 'Distinct stromal and immune cell interactions shape the pathogenesis of rheumatoid and psoriatic arthritis', *Ann Rheum Dis,* 81(9), pp. 1224-1242.
Folkman, J. (1971) 'Tumor angiogenesis: therapeutic implications', *N Engl J Med,* 285(21), pp. 1182-6.
Fontana, A., Hengartner, H., Weber, E., Fehr, K., Grob, P. J. and Cohen, G. (1982) 'Interleukin 1 activity in the synovial fluid of patients with rheumatoid arthritis', *Rheumatol Int,* 2(2), pp. 49-53.
Foster, J. R. (2001) 'The functions of cytokines and their uses in toxicology', *Int J Exp Pathol,* 82(3), pp. 171-92.
Fragoulis, G. E., Evangelatos, G., Tentolouris, N., Fragkiadaki, K., Panopoulos, S., Konstantonis, G., Iliopoulos, A., Chatzidionysiou, K., Sfikakis, P. P. and Tektonidou, M. G. (2020) 'Higher depression rates and similar cardiovascular comorbidity in psoriatic arthritis compared with rheumatoid arthritis and diabetes mellitus', *Ther Adv Musculoskelet Dis,* 12, pp. 1759720x20976975.
Fragoulis, G. E. and Siebert, S. (2022) 'The role of IL-23 and the use of IL-23 inhibitors in psoriatic arthritis', *Musculoskeletal Care,* 20 Suppl 1(Suppl 1), pp. S12-s21.
Frank-Bertoncelj, M., Trenkmann, M., Klein, K., Karouzakis, E., Rehrauer, H., Bratus, A., Kolling, C., Armaka, M., Filer, A., Michel, B. A., Gay, R. E., Buckley, C. D., Kollias, G., Gay, S. and Ospelt, C. (2017) 'Epigenetically-driven anatomical diversity of synovial fibroblasts guides joint-specific fibroblast functions', *Nat Commun,* 8, pp. 14852.
Fraser, A., Fearon, U., Reece, R., Emery, P. and Veale, D. J. (2001) 'Matrix metalloproteinase 9, apoptosis, and vascular morphology in early arthritis', *Arthritis Rheum,* 44(9), pp. 2024-8.
Friščić, J., Böttcher, M., Reinwald, C., Bruns, H., Wirth, B., Popp, S. J., Walker, K. I., Ackermann, J. A., Chen, X., Turner, J., Zhu, H., Seyler, L., Euler, M., Kirchner, P., Krüger, R., Ekici, A. B., Major, T., Aust, O., Weidner, D., Fischer, A., Andes, F. T., Stanojevic, Z., Trajkovic, V., Herrmann, M., Korb-Pap, A., Wank, I., Hess, A., Winter, J., Wixler, V., Distler, J., Steiner, G., Kiener, H. P., Frey, B., Kling, L., Raza, K., Frey, S., Kleyer, A., Bäuerle, T., Hughes, T. R., Grüneboom, A., Steffen, U., Krönke, G., Croft, A. P., Filer, A., Köhl, J., Klein, K., Buckley, C. D., Schett, G., Mougiakakos, D. and Hoffmann, M. H. (2021) 'The complement system drives local inflammatory tissue priming by metabolic reprogramming of synovial fibroblasts', *Immunity,* 54(5), pp. 1002-1021.e10.

Fromm, S., Cunningham, C. C., Dunne, M. R., Veale, D. J., Fearon, U. and Wade, S. M. (2019) 'Enhanced angiogenic function in response to fibroblasts from psoriatic arthritis synovium compared to rheumatoid arthritis', *Arthritis Res Ther,* 21(1), pp. 297.
Fujimoto, S., Manabe, S., Morimoto, C., Ozeki, M., Hamano, Y., Hirai, E., Kotani, H. and Tamaki, K. (2019) 'Distinct spectrum of microRNA expression in forensically relevant body fluids and probabilistic discriminant approach', *Scientific Reports,* 9(1), pp. 14332.
Fukao, A., Mishima, Y., Takizawa, N., Oka, S., Imataka, H., Pelletier, J., Sonenberg, N., Thoma, C. and Fujiwara, T. (2014) 'MicroRNAs trigger dissociation of eIF4AI and eIF4AII from target mRNAs in humans', *Mol Cell,* 56(1), pp. 79-89.
Fulci, V., Scappucci, G., Sebastiani, G. D., Giannitti, C., Franceschini, D., Meloni, F., Colombo, T., Citarella, F., Barnaba, V., Minisola, G., Galeazzi, M. and Macino, G. (2010) 'miR-223 is overexpressed in T-lymphocytes of patients affected by rheumatoid arthritis', *Hum Immunol,* 71(2), pp. 206-11.
Gabay, C., Emery, P., van Vollenhoven, R., Dikranian, A., Alten, R., Pavelka, K., Klearman, M., Musselman, D., Agarwal, S., Green, J. and Kavanaugh, A. (2013) 'Tocilizumab monotherapy versus adalimumab monotherapy for treatment of rheumatoid arthritis (ADACTA): a randomised, double-blind, controlled phase 4 trial', *Lancet,* 381(9877), pp. 1541-50.
Gaggioli, C., Hooper, S., Hidalgo-Carcedo, C., Grosse, R., Marshall, J. F., Harrington, K. and Sahai, E. (2007) 'Fibroblast-led collective invasion of carcinoma cells with differing roles for RhoGTPases in leading and following cells', *Nat Cell Biol,* 9(12), pp. 1392-400.
Gallagher, L., Cregan, S., Biniecka, M., Cunningham, C., Veale, D. J., Kane, D. J., Fearon, U. and Mullan, R. H. (2020) 'Insulin-Resistant Pathways Are Associated With Disease Activity in Rheumatoid Arthritis and Are Subject to Disease Modification Through Metabolic Reprogramming: A Potential Novel Therapeutic Approach', *Arthritis Rheumatol,* 72(6), pp. 896-902.
Gallo, A., Tandon, M., Alevizos, I. and Illei, G. G. (2012) 'The majority of microRNAs detectable in serum and saliva is concentrated in exosomes', *PLoS One,* 7(3), pp. e30679.
Galloway, J., Capron, J. P., De Leonardis, F., Fakhouri, W., Rose, A., Kouris, I. and Burke, T. (2020) 'The impact of disease severity and duration on cost, early retirement and ability to work in rheumatoid arthritis in Europe: an economic modelling study', *Rheumatol Adv Pract,* 4(2), pp. rkaa041.
Gao, M., Bian, E., Li, H., Ge, W., Yin, C., Wang, H. and Sun, Y. (2018) '[Up-regulation of circulating miR-29a in patients with acute pancreatitis and is positively correlated with disease severity and poor prognosis]', *Xi Bao Yu Fen Zi Mian Yi Xue Za Zhi,* 34(10), pp. 931-936.
Gao, S., Gao, H., Dai, L., Han, Y., Lei, Z., Wang, X., Chang, H., Liu, S., Wang, Z., Tong, H. and Wu, H. (2021) 'miR-126 regulates angiogenesis in myocardial ischemia by targeting HIF-1α', *Exp Cell Res,* 409(2), pp. 112925.
Gao, W., McCormick, J., Connolly, M., Balogh, E., Veale, D. J. and Fearon, U. (2015) 'Hypoxia and STAT3 signalling interactions regulate pro-inflammatory pathways in rheumatoid arthritis', *Ann Rheum Dis,* 74(6), pp. 1275-83.
Gao, W., McGarry, T., Orr, C., McCormick, J., Veale, D. J. and Fearon, U. (2016) 'Tofacitinib regulates synovial inflammation in psoriatic arthritis, inhibiting STAT activation and induction of negative feedback inhibitors', *Ann Rheum Dis,* 75(1), pp. 311-5.
Gao, W., Sweeney, C., Walsh, C., Rooney, P., McCormick, J., Veale, D. J. and Fearon, U. (2013) 'Notch signalling pathways mediate synovial angiogenesis in response to vascular endothelial growth factor and angiopoietin 2', *Ann Rheum Dis,* 72(6), pp. 1080-8.
Garcia-Carbonell, R., Divakaruni, A. S., Lodi, A., Vicente-Suarez, I., Saha, A., Cheroutre, H., Boss, G. R., Tiziani, S., Murphy, A. N. and Guma, M. (2016) 'Critical Role of Glucose Metabolism in Rheumatoid Arthritis Fibroblast-like Synoviocytes', *Arthritis Rheumatol,* 68(7), pp. 1614-26.
Garrod, A. E. (1890) *A treatise on rheumatism and rheumatoid arthritis.* Griffin.
Garzon, R., Calin, G. A. and Croce, C. M. (2009a) 'MicroRNAs in Cancer', *Annual Review of Medicine,* 60(Volume 60, 2009), pp. 167-179.
Garzon, R., Calin, G. A. and Croce, C. M. (2009b) 'MicroRNAs in Cancer', *Annu Rev Med,* 60, pp. 167-79.

Gatenby, R. A. and Gillies, R. J. (2004) 'Why do cancers have high aerobic glycolysis?', *Nat Rev Cancer,* 4(11), pp. 891-9.
Gaudenzi, C., Schioppa, T., Passari, M., Zucchi, G., Tiberio, L., Vahidi, Y., Scutera, S., Musso, T., Sozzani, S., Del Prete, A., Salvi, V. and Bosisio, D. (2024) 'Extracellular microRNAs induce dendritic cell-dependent joint inflammation and potentiate osteoclast differentiation via TLR7/8 engagement', *J Autoimmun,* 145, pp. 103189.
Gauthier, T., Yao, C., Dowdy, T., Jin, W., Lim, Y. J., Patiño, L. C., Liu, N., Ohlemacher, S. I., Bynum, A., Kazmi, R., Bewley, C. A., Mitrovic, M., Martin, D., Morell, R. J., Eckhaus, M., Larion, M., Tussiwand, R., O'Shea, J. J. and Chen, W. (2023) 'TGF-β uncouples glycolysis and inflammation in macrophages and controls survival during sepsis', *Sci Signal,* 16(797), pp. eade0385.
Gebert, L. F., Rebhan, M. A., Crivelli, S. E., Denzler, R., Stoffel, M. and Hall, J. (2014) 'Miravirsen (SPC3649) can inhibit the biogenesis of miR-122', *Nucleic Acids Res,* 42(1), pp. 609-21.
Gelfand, J. M., Gladman, D. D., Mease, P. J., Smith, N., Margolis, D. J., Nijsten, T., Stern, R. S., Feldman, S. R. and Rolstad, T. (2005) 'Epidemiology of psoriatic arthritis in the population of the United States', *J Am Acad Dermatol,* 53(4), pp. 573.
Gelfand, J. M., Neimann, A. L., Shin, D. B., Wang, X., Margolis, D. J. and Troxel, A. B. (2006) 'Risk of myocardial infarction in patients with psoriasis', *Jama,* 296(14), pp. 1735-41.
Genestier, L., Paillot, R., Fournel, S., Ferraro, C., Miossec, P. and Revillard, J. P. (1998) 'Immunosuppressive properties of methotrexate: apoptosis and clonal deletion of activated peripheral T cells', *J Clin Invest,* 102(2), pp. 322-8.
Genovese, M. C., Jarosova, K., Cieślak, D., Alper, J., Kivitz, A., Hough, D. R., Maes, P., Pineda, L., Chen, M. and Zaidi, F. (2015) 'Apremilast in Patients With Active Rheumatoid Arthritis: A Phase II, Multicenter, Randomized, Double-Blind, Placebo-Controlled, Parallel-Group Study', *Arthritis Rheumatol,* 67(7), pp. 1703-10.
Genovese, M. C., Schiff, M., Luggen, M., Becker, J. C., Aranda, R., Teng, J., Li, T., Schmidely, N., Le Bars, M. and Dougados, M. (2008) 'Efficacy and safety of the selective co-stimulation modulator abatacept following 2 years of treatment in patients with rheumatoid arthritis and an inadequate response to anti-tumour necrosis factor therapy', *Ann Rheum Dis,* 67(4), pp. 547-54.
Gerhardt, H., Golding, M., Fruttiger, M., Ruhrberg, C., Lundkvist, A., Abramsson, A., Jeltsch, M., Mitchell, C., Alitalo, K., Shima, D. and Betsholtz, C. (2003) 'VEGF guides angiogenic sprouting utilizing endothelial tip cell filopodia', *J Cell Biol,* 161(6), pp. 1163-77.
Giannoudis, A., Clarke, K., Zakaria, R., Varešlija, D., Farahani, M., Rainbow, L., Platt-Higgins, A., Ruthven, S., Brougham, K. A., Rudland, P. S., Jenkinson, M. D., Young, L. S., Falciani, F. and Palmieri, C. (2019) 'A novel panel of differentially-expressed microRNAs in breast cancer brain metastasis may predict patient survival', *Scientific Reports,* 9(1), pp. 18518.
Giatromanolaki, A., Sivridis, E., Maltezos, E., Athanassou, N., Papazoglou, D., Gatter, K. C., Harris, A. L. and Koukourakis, M. I. (2003) 'Upregulated hypoxia inducible factor-1α and -2α pathway in rheumatoid arthritis and osteoarthritis', *Arthritis Res Ther,* 5(4), pp. R193.
Gilad, S., Meiri, E., Yogev, Y., Benjamin, S., Lebanony, D., Yerushalmi, N., Benjamin, H., Kushnir, M., Cholakh, H., Melamed, N., Bentwich, Z., Hod, M., Goren, Y. and Chajut, A. (2008) 'Serum microRNAs are promising novel biomarkers', *PLoS One,* 3(9), pp. e3148.
Glintborg, B., Østergaard, M., Dreyer, L., Krogh, N. S., Tarp, U., Hansen, M. S., Rifbjerg-Madsen, S., Lorenzen, T. and Hetland, M. L. (2011) 'Treatment response, drug survival, and predictors thereof in 764 patients with psoriatic arthritis treated with anti-tumor necrosis factor α therapy: results from the nationwide Danish DANBIO registry', *Arthritis Rheum,* 63(2), pp. 382-90.
Gomes, A. P. and Blenis, J. (2015) 'A nexus for cellular homeostasis: the interplay between metabolic and signal transduction pathways', *Curr Opin Biotechnol,* 34, pp. 110-7.
Gossec, L., Baraliakos, X., Kerschbaumer, A., de Wit, M., McInnes, I., Dougados, M., Primdahl, J., McGonagle, D. G., Aletaha, D., Balanescu, A., Balint, P. V., Bertheussen, H., Boehncke, W. H., Burmester, G. R., Canete, J. D., Damjanov, N. S., Kragstrup, T. W., Kvien, T. K., Landewé, R. B. M., Lories, R. J. U., Marzo-Ortega, H., Poddubnyy, D., Rodrigues Manica, S. A., Schett, G., Veale, D. J., Van den

Bosch, F. E., van der Heijde, D. and Smolen, J. S. (2020) 'EULAR recommendations for the management of psoriatic arthritis with pharmacological therapies: 2019 update', *Ann Rheum Dis,* 79(6), pp. 700-712.
Gottenberg, J. E., Dayer, J. M., Lukas, C., Ducot, B., Chiocchia, G., Cantagrel, A., Saraux, A., Roux-Lombard, P. and Mariette, X. (2012) 'Serum IL-6 and IL-21 are associated with markers of B cell activation and structural progression in early rheumatoid arthritis: results from the ESPOIR cohort', *Ann Rheum Dis,* 71(7), pp. 1243-8.
Grabiec, A. M., Angiolilli, C., Hartkamp, L. M., van Baarsen, L. G., Tak, P. P. and Reedquist, K. A. (2015) 'JNK-dependent downregulation of FoxO1 is required to promote the survival of fibroblast-like synoviocytes in rheumatoid arthritis', *Ann Rheum Dis,* 74(9), pp. 1763-71.
Gracey, E., Burssens, A., Cambré, I., Schett, G., Lories, R., McInnes, I. B., Asahara, H. and Elewaut, D. (2020) 'Tendon and ligament mechanical loading in the pathogenesis of inflammatory arthritis', *Nat Rev Rheumatol,* 16(4), pp. 193-207.
Gravallese, E. M. and Firestein, G. S. (2023) 'Rheumatoid Arthritis - Common Origins, Divergent Mechanisms', *N Engl J Med,* 388(6), pp. 529-542.
Green, M., Marzo-Ortega, H., McGonagle, D., Wakefield, R., Proudman, S., Conaghan, P., Gooi, J. and Emery, P. (1999) 'Persistence of mild, early inflammatory arthritis: the importance of disease duration, rheumatoid factor, and the shared epitope', *Arthritis Rheum,* 42(10), pp. 2184-8.
Gregersen, P. K., Silver, J. and Winchester, R. J. (1987) 'The shared epitope hypothesis. An approach to understanding the molecular genetics of susceptibility to rheumatoid arthritis', *Arthritis Rheum,* 30(11), pp. 1205-13.
Gremese, E., Carletto, A., Padovan, M., Atzeni, F., Raffeiner, B., Giardina, A. R., Favalli, E. G., Erre, G. L., Gorla, R., Galeazzi, M., Foti, R., Cantini, F., Salvarani, C., Olivieri, I., Lapadula, G. and Ferraccioli, G. (2013) 'Obesity and reduction of the response rate to anti-tumor necrosis factor α in rheumatoid arthritis: an approach to a personalized medicine', *Arthritis Care Res (Hoboken),* 65(1), pp. 94-100.
Gremese, E., Tolusso, B., Bruno, D., Perniola, S., Ferraccioli, G. and Alivernini, S. (2023) 'The forgotten key players in rheumatoid arthritis: IL-8 and IL-17 - Unmet needs and therapeutic perspectives', *Front Med (Lausanne),* 10, pp. 956127.
Griffin, G. K., Newton, G., Tarrio, M. L., Bu, D. X., Maganto-Garcia, E., Azcutia, V., Alcaide, P., Grabie, N., Luscinskas, F. W., Croce, K. J. and Lichtman, A. H. (2012) 'IL-17 and TNF-α sustain neutrophil recruitment during inflammation through synergistic effects on endothelial activation', *J Immunol,* 188(12), pp. 6287-99.
Guma, M., Sanchez-Lopez, E., Lodi, A., Garcia-Carbonell, R., Tiziani, S., Karin, M., Lacal, J. C. and Firestein, G. S. (2015) 'Choline kinase inhibition in rheumatoid arthritis', *Ann Rheum Dis,* 74(7), pp. 1399-407.
Guo, X. and Chen, G. (2020) 'Hypoxia-Inducible Factor Is Critical for Pathogenesis and Regulation of Immune Cell Functions in Rheumatoid Arthritis', *Front Immunol,* 11, pp. 1668.
Guo, Y., Walsh, A. M., Fearon, U., Smith, M. D., Wechalekar, M. D., Yin, X., Cole, S., Orr, C., McGarry, T., Canavan, M., Kelly, S., Lin, T. A., Liu, X., Proudman, S. M., Veale, D. J., Pitzalis, C. and Nagpal, S. (2017) 'CD40L-Dependent Pathway Is Active at Various Stages of Rheumatoid Arthritis Disease Progression', *J Immunol,* 198(11), pp. 4490-4501.
Guo, Y. C., Chiu, Y. H., Chen, C. P. and Wang, H. S. (2018) 'Interleukin-1β induces CXCR3-mediated chemotaxis to promote umbilical cord mesenchymal stem cell transendothelial migration', *Stem Cell Res Ther,* 9(1), pp. 281.
Ha, E., Bae, S. C. and Kim, K. (2021) 'Large-scale meta-analysis across East Asian and European populations updated genetic architecture and variant-driven biology of rheumatoid arthritis, identifying 11 novel susceptibility loci', *Ann Rheum Dis,* 80(5), pp. 558-565.
Ha, M. and Kim, V. N. (2014) 'Regulation of microRNA biogenesis', *Nature Reviews Molecular Cell Biology,* 15(8), pp. 509-524.
Haas, R., Smith, J., Rocher-Ros, V., Nadkarni, S., Montero-Melendez, T., D'Acquisto, F., Bland, E. J., Bombardieri, M., Pitzalis, C., Perretti, M., Marelli-Berg, F. M. and Mauro, C. (2015) 'Lactate Regulates

Metabolic and Pro-inflammatory Circuits in Control of T Cell Migration and Effector Functions', *PLoS Biol,* 13(7), pp. e1002202.
Hammoura, I., Fiechter, R. H., Bryant, S. H., Westmoreland, S., Kingsbury, G., Waegell, W., Tas, S. W., Baeten, D. L., van de Sande, M. G. H., van Tok, M. N. and van Duivenvoorde, L. M. (2022) 'Dual Blockade of TNF and IL-17A Inhibits Inflammation and Structural Damage in a Rat Model of Spondyloarthritis', *Int J Mol Sci,* 23(2).
Hanlon, M. M., Canavan, M., Barker, B. E. and Fearon, U. (2022) 'Metabolites as drivers and targets in rheumatoid arthritis', *Clin Exp Immunol,* 208(2), pp. 167-180.
Hanlon, M. M., McGarry, T., Marzaioli, V., Amaechi, S., Song, Q., Nagpal, S., Veale, D. J. and Fearon, U. (2023) 'Rheumatoid arthritis macrophages are primed for inflammation and display bioenergetic and functional alterations', *Rheumatology (Oxford),* 62(7), pp. 2611-2620.
Hanlon, M. M., Rakovich, T., Cunningham, C. C., Ansboro, S., Veale, D. J., Fearon, U. and McGarry, T. (2019) 'STAT3 Mediates the Differential Effects of Oncostatin M and TNFα on RA Synovial Fibroblast and Endothelial Cell Function', *Front Immunol,* 10, pp. 2056.
Hanlon, M. M., Smith, C. M., Canavan, M., Neto, N. G. B., Song, Q., Lewis, M. J., O'Rourke, A. M., Tynan, O., Barker, B. E., Gallagher, P., Mullan, R., Hurson, C., Moran, B., Monaghan, M. G., Pitzalis, C., Fletcher, J. M., Nagpal, S., Veale, D. J. and Fearon, U. (2024) 'Loss of synovial tissue macrophage homeostasis precedes rheumatoid arthritis clinical onset', *Sci Adv,* 10(39), pp. eadj1252.
Hanusek, K., Rybicka, B., Popławski, P., Adamiok-Ostrowska, A., Głuchowska, K., Piekiełko-Witkowska, A. and Bogusławska, J. (2022) 'TGF-β1 affects the renal cancer miRNome and regulates tumor cells proliferation', *Int J Mol Med,* 49(4).
Haringman, J. J., Gerlag, D. M., Zwinderman, A. H., Smeets, T. J., Kraan, M. C., Baeten, D., McInnes, I. B., Bresnihan, B. and Tak, P. P. (2005) 'Synovial tissue macrophages: a sensitive biomarker for response to treatment in patients with rheumatoid arthritis', *Ann Rheum Dis,* 64(6), pp. 834-8.
Haroon, M., Gallagher, P. and FitzGerald, O. (2015) 'Diagnostic delay of more than 6 months contributes to poor radiographic and functional outcome in psoriatic arthritis', *Ann Rheum Dis,* 74(6), pp. 1045-50.
Haroon, M., Winchester, R., Giles, J. T., Heffernan, E. and FitzGerald, O. (2016) 'Certain class I HLA alleles and haplotypes implicated in susceptibility play a role in determining specific features of the psoriatic arthritis phenotype', *Ann Rheum Dis,* 75(1), pp. 155-62.
Harris, Q., Seto, J., O'Brien, K., Lee, P. S., Kondo, C., Heard, B. J., Hart, D. A. and Krawetz, R. J. (2013) 'Monocyte chemotactic protein-1 inhibits chondrogenesis of synovial mesenchymal progenitor cells: an in vitro study', *Stem Cells,* 31(10), pp. 2253-65.
Harrold, L. R., Connolly, S. E., Wittstock, K., Zhuo, J., Kelly, S., Lehman, T., Shan, Y., Rebello, S., Guo, L. and Khaychuk, V. (2022) 'Baseline Anti-Citrullinated Protein Antibody Status and Response to Abatacept or Non-TNFi Biologic/Targeted-Synthetic DMARDs: US Observational Study of Patients with RA', *Rheumatol Ther,* 9(2), pp. 465-480.
Harrold, L. R., Litman, H. J., Connolly, S. E., Kelly, S., Hua, W., Alemao, E., Rosenblatt, L., Rebello, S. and Kremer, J. M. (2018) 'Effect of Anticitrullinated Protein Antibody Status on Response to Abatacept or Antitumor Necrosis Factor-α Therapy in Patients with Rheumatoid Arthritis: A US National Observational Study', *J Rheumatol,* 45(1), pp. 32-39.
Harty, L. C., Biniecka, M., O'Sullivan, J., Fox, E., Mulhall, K., Veale, D. J. and Fearon, U. (2012) 'Mitochondrial mutagenesis correlates with the local inflammatory environment in arthritis', *Ann Rheum Dis,* 71(4), pp. 582-8.
Haschka, J., Simon, D., Bayat, S., Messner, Z., Kampylafka, E., Fagni, F., Skalicky, S., Hackl, M., Resch, H., Zwerina, J., Kleyer, A., Cavallaro, A., Sticherling, M., Schett, G., Kocijan, R. and Rech, J. (2023) 'Identification of circulating microRNA patterns in patients in psoriasis and psoriatic arthritis', *Rheumatology (Oxford),* 62(10), pp. 3448-3458.
Hasegawa, T., Lewis, H. and Esquela-Kerscher, A. (2017) 'Chapter 12 - The Role of Noncoding RNAs in Prostate Cancer', in Laurence, J. (ed.) *Translating MicroRNAs to the Clinic*. Boston: Academic Press, pp. 329-369.

Hassanpoor, M. and Abbasi, B. (2022) 'miR-22-3p as a Novel Biomarker in Rheumatoid Arthritis', *Personalized Medicine Journal,* 7(24), pp. 19-22.
He, J., Wang, Y., Feng, M., Zhang, X., Jin, Y. B., Li, X., Su, L. C., Liu, S., Wang, A. X., Chen, X. M., Wu, L. J., Yu, X. X., Xu, N., Liu, X. Y., Yan, H. M., Wang, Y. F., Jia, B., Li, J. F., Tao, J. M., Zhang, F. X., Yu, P., Cui, L. F., Yang, J., Li, Z. B., Xie, J. L., Wei, P., Sun, W. W., Gong, L., Cheng, Y. J., Huang, C. B., Wang, X. Y., Wang, Y., Guo, H. F., Jin, H. T., Liu, X., Wang, G. C., Wang, Y. H., He, L., Zhao, Y., Li, X. X., Zhang, Y., Guo, J. P. and Li, Z. G. (2016) 'Dietary intake and risk of rheumatoid arthritis-a cross section multicenter study', *Clin Rheumatol,* 35(12), pp. 2901-2908.
He, L., Qin, Q., He, J., Wang, H., Hu, Y., He, W., Xu, B., Zhou, G., Shan, H., Yang, B. and Wang, Q. (2020) 'ErMiao San Inhibits Angiogenesis in Rheumatoid Arthritis by Suppressing JAK/STAT Signaling Pathways', *Evidence-Based Complementary and Alternative Medicine,* 2020(1), pp. 4381212.
Hench, P. 'Arthropathia psoriatica: presentation of a case'. *Proc Staff Meet Mayo Clin*, 80.
Hench, P. S., Bauer, W. and et al. (1948) 'Rheumatism and arthritis; review of American and English literature of recent years', *Ann Intern Med,* 28(1), pp. 66; passim.
Hill, J. A., Southwood, S., Sette, A., Jevnikar, A. M., Bell, D. A. and Cairns, E. (2003) 'Cutting edge: the conversion of arginine to citrulline allows for a high-affinity peptide interaction with the rheumatoid arthritis-associated HLA-DRB1*0401 MHC class II molecule', *J Immunol,* 171(2), pp. 538-41.
Hinks, A., Eyre, S., Barton, A., Thomson, W. and Worthington, J. (2007) 'Investigation of genetic variation across the protein tyrosine phosphatase gene in patients with rheumatoid arthritis in the UK', *Ann Rheum Dis,* 66(5), pp. 683-6.
Hirota, K., Hashimoto, M., Ito, Y., Matsuura, M., Ito, H., Tanaka, M., Watanabe, H., Kondoh, G., Tanaka, A., Yasuda, K., Kopf, M., Potocnik, A. J., Stockinger, B., Sakaguchi, N. and Sakaguchi, S. (2018) 'Autoimmune Th17 Cells Induced Synovial Stromal and Innate Lymphoid Cell Secretion of the Cytokine GM-CSF to Initiate and Augment Autoimmune Arthritis', *Immunity,* 48(6), pp. 1220-1232.e5.
Hitchon, C., Wong, K., Ma, G., Reed, J., Lyttle, D. and El-Gabalawy, H. (2002) 'Hypoxia-induced production of stromal cell-derived factor 1 (CXCL12) and vascular endothelial growth factor by synovial fibroblasts', *Arthritis Rheum,* 46(10), pp. 2587-97.
Hobl, E. L., Mader, R. M., Erlacher, L., Duhm, B., Mustak, M., Bröll, H., Högger, P., Kalipciyan, M. and Jilma, B. (2011) 'The influence of methotrexate on the gene expression of the pro-inflammatory cytokine IL-12A in the therapy of rheumatoid arthritis', *Clin Exp Rheumatol,* 29(6), pp. 963-9.
Hofbauer, L. C., Lacey, D. L., Dunstan, C. R., Spelsberg, T. C., Riggs, B. L. and Khosla, S. (1999) 'Interleukin-1beta and tumor necrosis factor-alpha, but not interleukin-6, stimulate osteoprotegerin ligand gene expression in human osteoblastic cells', *Bone,* 25(3), pp. 255-9.
Hollywell, C., Morris, C. J., Farr, M. and Walton, K. W. (1983) 'Ultrastructure of synovial changes in rheumatoid disease and in seronegative inflammatory arthropathies', *Virchows Archiv A,* 400(3), pp. 345-355.
Holoshitz, J. (2010) 'The rheumatoid arthritis HLA-DRB1 shared epitope', *Curr Opin Rheumatol,* 22(3), pp. 293-8.
Honorati, M. C., Neri, S., Cattini, L. and Facchini, A. (2006) 'Interleukin-17, a regulator of angiogenic factor release by synovial fibroblasts', *Osteoarthritis Cartilage,* 14(4), pp. 345-52.
Horita, M., Hsu, S. N., Raper, A., Farquharson, C. and Stephen, L. A. (2022) 'miR-29b inhibits TGF-β1-induced cell proliferation in articular chondrocytes', *Biochem Biophys Rep,* 29, pp. 101216.
Hotamisligil, G. S., Peraldi, P., Budavari, A., Ellis, R., White, M. F. and Spiegelman, B. M. (1996) 'IRS-1-mediated inhibition of insulin receptor tyrosine kinase activity in TNF-alpha- and obesity-induced insulin resistance', *Science,* 271(5249), pp. 665-8.
Hresko, A., Lin, T. C. and Solomon, D. H. (2018) 'Medical Care Costs Associated With Rheumatoid Arthritis in the US: A Systematic Literature Review and Meta-Analysis', *Arthritis Care Res (Hoboken),* 70(10), pp. 1431-1438.
Hu, F., Yang, S., Zhao, D., Zhu, S., Wang, Y. and Li, J. (2012) 'Moderate extracellular acidification inhibits capsaicin-induced cell death through regulating calcium mobilization, NF-κB translocation and ROS production in synoviocytes', *Biochem Biophys Res Commun,* 424(1), pp. 196-200.

Hu, J., Zhai, C., Hu, J., Li, Z., Fei, H., Wang, Z. and Fan, W. (2017a) 'MiR-23a inhibited IL-17-mediated proinflammatory mediators expression via targeting IKKα in articular chondrocytes', *Int Immunopharmacol,* 43, pp. 1-6.
Hu, X., Li, M., Zhang, Y., Sang, K., Zhang, Y., Li, W., Liu, B., Wan, L., Du, B., Qian, J., Meng, F., Fu, Y., Dai, M., Gao, G. and Ye, H. (2023) 'An innovative immunotherapeutic strategy for rheumatoid arthritis: Selectively suppressing angiogenesis and osteoclast differentiation by fully human antibody targeting thymocyte antigen-1', *Exp Cell Res,* 424(1), pp. 113490.
Hu, Y., Rao, S. S., Wang, Z. X., Cao, J., Tan, Y. J., Luo, J., Li, H. M., Zhang, W. S., Chen, C. Y. and Xie, H. (2018) 'Exosomes from human umbilical cord blood accelerate cutaneous wound healing through miR-21-3p-mediated promotion of angiogenesis and fibroblast function', *Theranostics,* 8(1), pp. 169-184.
Hu, Y., Sparks, J. A., Malspeis, S., Costenbader, K. H., Hu, F. B., Karlson, E. W. and Lu, B. (2017b) 'Long-term dietary quality and risk of developing rheumatoid arthritis in women', *Ann Rheum Dis,* 76(8), pp. 1357-1364.
Huang, C., Liu, X. J., QunZhou, Xie, J., Ma, T. T., Meng, X. M. and Li, J. (2016) 'MiR-146a modulates macrophage polarization by inhibiting Notch1 pathway in RAW264.7 macrophages', *Int Immunopharmacol,* 32, pp. 46-54.
Huang, Y., Xue, Q., Chang, J., Wang, X. and Miao, C. (2023) 'Wnt5a: A promising therapeutic target for inflammation, especially rheumatoid arthritis', *Cytokine,* 172, pp. 156381.
Hüffmeier, U., Uebe, S., Ekici, A. B., Bowes, J., Giardina, E., Korendowych, E., Juneblad, K., Apel, M., McManus, R., Ho, P., Bruce, I. N., Ryan, A. W., Behrens, F., Lascorz, J., Böhm, B., Traupe, H., Lohmann, J., Gieger, C., Wichmann, H. E., Herold, C., Steffens, M., Klareskog, L., Wienker, T. F., Fitzgerald, O., Alenius, G. M., McHugh, N. J., Novelli, G., Burkhardt, H., Barton, A. and Reis, A. (2010) 'Common variants at TRAF3IP2 are associated with susceptibility to psoriatic arthritis and psoriasis', *Nat Genet,* 42(11), pp. 996-9.
Huizinga, T. W. J., Connolly, S. E., Johnsen, A., Zhu, J., Furst, D. E., Bykerk, V. P., Burmester, G. R., Combe, B. G., Wong, D. A., Trouw, L. A., Toes, R. E. M. and Emery, P. (2015) 'THU0114 Effect of Anti-Cyclic Citrullinated Peptide 2 Immunoglobulin M Serostatus on Efficacy Outcomes Following Treatment with Abatacept Plus Methotrexate in the Avert Trial', *Annals of the Rheumatic Diseases,* 74(Suppl 2), pp. 234-235.
Humby, F., Durez, P., Buch, M. H., Lewis, M. J., Rizvi, H., Rivellese, F., Nerviani, A., Giorli, G., Mahto, A., Montecucco, C., Lauwerys, B., Ng, N., Ho, P., Bombardieri, M., Romão, V. C., Verschueren, P., Kelly, S., Sainaghi, P. P., Gendi, N., Dasgupta, B., Cauli, A., Reynolds, P., Cañete, J. D., Moots, R., Taylor, P. C., Edwards, C. J., Isaacs, J., Sasieni, P., Choy, E. and Pitzalis, C. (2021) 'Rituximab versus tocilizumab in anti-TNF inadequate responder patients with rheumatoid arthritis (R4RA): 16-week outcomes of a stratified, biopsy-driven, multicentre, open-label, phase 4 randomised controlled trial', *Lancet,* 397(10271), pp. 305-317.
Hyndman, I. J. (2017) 'Rheumatoid arthritis: past, present and future approaches to treating the disease', *Int J Rheum Dis,* 20(4), pp. 417-419.
Iacomino, G. (2023) 'miRNAs: The Road from Bench to Bedside', *Genes,* 14(2), pp. 314.
Iftikhar, H. and Carney, G. E. (2016) 'Evidence and potential in vivo functions for biofluid miRNAs: From expression profiling to functional testing: Potential roles of extracellular miRNAs as indicators of physiological change and as agents of intercellular information exchange', *Bioessays,* 38(4), pp. 367-78.
Inanc, N., Dalkilic, E., Kamali, S., Kasapoglu-Günal, E., Elbir, Y., Direskeneli, H. and Inanc, M. (2007) 'Anti-CCP antibodies in rheumatoid arthritis and psoriatic arthritis', *Clin Rheumatol,* 26(1), pp. 17-23.
Ipsaro, J. J. and Joshua-Tor, L. (2015) 'From guide to target: molecular insights into eukaryotic RNA-interference machinery', *Nat Struct Mol Biol,* 22(1), pp. 20-8.
Iriyoda, T. M. V., Flauzino, T., Costa, N. T., Lozovoy, M. A. B., Reiche, E. M. V. and Simão, A. N. C. (2022) 'TGFB1 (rs1800470 and rs1800469) variants are independently associated with disease activity and autoantibodies in rheumatoid arthritis patients', *Clin Exp Med,* 22(1), pp. 37-45.

Ishchenko, A., Pazmino, S., Neerinckx, B., Lories, R. and de Vlam, K. (2024) 'Comorbidities in early psoriatic arthritis: data from the metabolic disturbances in psoriatic arthritis cohort study', *Arthritis Care & Research,* 76(2), pp. 231-240.
Ishigaki, K., Lagattuta, K. A., Luo, Y., James, E. A., Buckner, J. H. and Raychaudhuri, S. (2022) 'HLA autoimmune risk alleles restrict the hypervariable region of T cell receptors', *Nat Genet,* 54(4), pp. 393-402.
Ishigaki, K., Sakaue, S., Terao, C., Luo, Y., Sonehara, K., Yamaguchi, K., Amariuta, T., Too, C. L., Laufer, V. A., Scott, I. C., Viatte, S., Takahashi, M., Ohmura, K., Murasawa, A., Hashimoto, M., Ito, H., Hammoudeh, M., Al Emadi, S., Masri, B. K., Halabi, H., Badsha, H., Uthman, I. W., Wu, X., Lin, L., Lin, T., Plant, D., Barton, A., Orozco, G., Verstappen, S. M., Bowes, J., MacGregor, A. J., Honda, S., Koido, M., Tomizuka, K., Kamatani, Y., Tanaka, H., Tanaka, E., Suzuki, A., Maeda, Y., Yamamoto, K., Miyawaki, S., Xie, G., Zhang, J., Amos, C., Keystone, E., Wolbink, G., van der Horst-Bruinsma, I., Cui, J., Liao, K. P., Carroll, R. J., Lee, H.-S., Bang, S.-Y., Siminovitch, K. A., de Vries, N., Alfredsson, L., Rantapää-Dahlqvist, S., Karlson, E. W., Bae, S.-C., Kimberly, R. P., Edberg, J. C., Mariette, X., Huizinga, T., Dieudé, P., Schneider, M., Kerick, M., Denny, J. C., Matsuda, K., Matsuo, K., Mimori, T., Matsuda, F., Fujio, K., Tanaka, Y., Kumanogoh, A., Traylor, M., Lewis, C. M., Eyre, S., Xu, H., Saxena, R., Arayssi, T., Kochi, Y., Ikari, K., Harigai, M., Gregersen, P. K., Yamamoto, K., Bridges, S. L., Padyukov, L., Martin, J., Klareskog, L., Okada, Y. and Raychaudhuri, S. (2021) 'Trans-ancestry genome-wide association study identifies novel genetic mechanisms in rheumatoid arthritis', *medRxiv*, pp. 2021.12.01.21267132.
Islam, M., Jones, S. and Ellis, I. (2023) 'Role of Akt/Protein Kinase B in Cancer Metastasis', *Biomedicines,* 11(11).
Jang, C. W., Chen, C. H., Chen, C. C., Chen, J. Y., Su, Y. H. and Chen, R. H. (2002) 'TGF-beta induces apoptosis through Smad-mediated expression of DAP-kinase', *Nat Cell Biol,* 4(1), pp. 51-8.
Jerobin, J., Ali, R. M., Khalil, S., Ramanjaneya, M., Betahi, I., Abou Samra, A. B. and M, A. A.-N. (2023) 'Circulating microRNA signatures in patients with chronic Urticaria', *Qatar Med J,* 2023(2), pp. 20.
Jiang, M., Fang, H., Dang, E., Zhang, J., Qiao, P., Yu, C., Yang, A. and Wang, G. (2021) 'Small Extracellular Vesicles Containing miR-381-3p from Keratinocytes Promote T Helper Type 1 and T Helper Type 17 Polarization in Psoriasis', *Journal of Investigative Dermatology,* 141(3), pp. 563-574.
Jiang, X. and Alfredsson, L. (2020) 'Modifiable environmental exposure and risk of rheumatoid arthritis—current evidence from genetic studies', *Arthritis Research & Therapy,* 22(1), pp. 154.
Jo, M. H., Shin, S., Jung, S. R., Kim, E., Song, J. J. and Hohng, S. (2015) 'Human Argonaute 2 Has Diverse Reaction Pathways on Target RNAs', *Mol Cell,* 59(1), pp. 117-24.
Johnson, M. O., Wolf, M. M., Madden, M. Z., Andrejeva, G., Sugiura, A., Contreras, D. C., Maseda, D., Liberti, M. V., Paz, K., Kishton, R. J., Johnson, M. E., de Cubas, A. A., Wu, P., Li, G., Zhang, Y., Newcomb, D. C., Wells, A. D., Restifo, N. P., Rathmell, W. K., Locasale, J. W., Davila, M. L., Blazar, B. R. and Rathmell, J. C. (2018) 'Distinct Regulation of Th17 and Th1 Cell Differentiation by Glutaminase-Dependent Metabolism', *Cell,* 175(7), pp. 1780-1795.e19.
Joosten, L. A., Radstake, T. R., Lubberts, E., van den Bersselaar, L. A., van Riel, P. L., van Lent, P. L., Barrera, P. and van den Berg, W. B. (2003) 'Association of interleukin-18 expression with enhanced levels of both interleukin-1beta and tumor necrosis factor alpha in knee synovial tissue of patients with rheumatoid arthritis', *Arthritis Rheum,* 48(2), pp. 339-47.
Jurj, A., Zanoaga, O., Raduly, L., Morhan, V., Papi, Z., Ciocan, C., Pop, L. A., Berindan-Neagoe, I. and Braicu, C. (2023) 'Discovering the Biological Significance and Therapeutic Potential of miR-29b-3p in Triple-Negative Breast Cancer', *Int J Mol Sci,* 24(5).
Kaiser, H. and Keitel, W. (2006) '[Guillaume de Baillou (1538-1616)--the father of "rheumatism"?]', *Z Rheumatol,* 65(8), pp. 743-6.
Källberg, H., Ding, B., Padyukov, L., Bengtsson, C., Rönnelid, J., Klareskog, L. and Alfredsson, L. (2011) 'Smoking is a major preventable risk factor for rheumatoid arthritis: estimations of risks after various exposures to cigarette smoke', *Ann Rheum Dis,* 70(3), pp. 508-11.
Källberg, H., Jacobsen, S., Bengtsson, C., Pedersen, M., Padyukov, L., Garred, P., Frisch, M., Karlson, E. W., Klareskog, L. and Alfredsson, L. (2009) 'Alcohol consumption is associated with decreased risk of

rheumatoid arthritis: results from two Scandinavian case–control studies', *Annals of the rheumatic diseases,* 68(2), pp. 222-227.
Kang, I., Hundhausen, C., Evanko, S. P., Malapati, P., Workman, G., Chan, C. K., Rims, C., Firestein, G. S., Boyle, D. L., MacDonald, K. M., Buckner, J. H. and Wight, T. N. (2022) 'Crosstalk between CD4 T cells and synovial fibroblasts from human arthritic joints promotes hyaluronan-dependent leukocyte adhesion and inflammatory cytokine expression in vitro', *Matrix Biol Plus,* 14, pp. 100110.
Kang, Y. H., Brummel, S. E. and Lee, C. H. (1996) 'Differential effects of transforming growth factor-beta 1 on lipopolysaccharide induction of endothelial adhesion molecules', *Shock,* 6(2), pp. 118-25.
Kany, S., Vollrath, J. T. and Relja, B. (2019) 'Cytokines in Inflammatory Disease', *Int J Mol Sci,* 20(23).
Karmacharya, P., Chakradhar, R. and Ogdie, A. (2021) 'The epidemiology of psoriatic arthritis: A literature review', *Best Pract Res Clin Rheumatol,* 35(2), pp. 101692.
Karouzakis, E., Raza, K., Kolling, C., Buckley, C. D., Gay, S., Filer, A. and Ospelt, C. (2018) 'Analysis of early changes in DNA methylation in synovial fibroblasts of RA patients before diagnosis', *Scientific Reports,* 8(1), pp. 7370.
Kavanaugh, A., Mease, P. J., Reimold, A. M., Tahir, H., Rech, J., Hall, S., Geusens, P., Wang, Z., Pricop, L. and Mpofu, S. (2017) 'Secukinumab for Long-Term Treatment of Psoriatic Arthritis: A Two-Year Followup From a Phase III, Randomized, Double-Blind Placebo-Controlled Study', *Arthritis Care Res (Hoboken),* 69(3), pp. 347-355.
Kawashiri, S. Y., Kawakami, A., Iwamoto, N., Fujikawa, K., Aramaki, T., Tamai, M., Arima, K., Kamachi, M., Yamasaki, S., Nakamura, H., Tsurumoto, T., Kono, M., Shindo, H., Ida, H., Origuchi, T. and Eguchi, K. (2009) 'Proinflammatory cytokines synergistically enhance the production of chemokine ligand 20 (CCL20) from rheumatoid fibroblast-like synovial cells in vitro and serum CCL20 is reduced in vivo by biologic disease-modifying antirheumatic drugs', *J Rheumatol,* 36(11), pp. 2397-402.
Keller, A., Gröger, L., Tschernig, T., Solomon, J., Laham, O., Schaum, N., Wagner, V., Kern, F., Schmartz, G. P., Li, Y., Borcherding, A., Meier, C., Wyss-Coray, T., Meese, E., Fehlmann, T. and Ludwig, N. (2022) 'miRNATissueAtlas2: an update to the human miRNA tissue atlas', *Nucleic Acids Res,* 50(D1), pp. D211-d221.
Kemble, S. and Croft, A. P. (2021) 'Critical Role of Synovial Tissue-Resident Macrophage and Fibroblast Subsets in the Persistence of Joint Inflammation', *Front Immunol,* 12, pp. 715894.
Kennedy, A., Ng, C. T., Biniecka, M., Saber, T., Taylor, C., O'Sullivan, J., Veale, D. J. and Fearon, U. (2010) 'Angiogenesis and blood vessel stability in inflammatory arthritis', *Arthritis Rheum,* 62(3), pp. 711-21.
Kerschbaumer, A., Fenzl, K. H., Erlacher, L. and Aletaha, D. (2016) 'An overview of psoriatic arthritis - epidemiology, clinical features, pathophysiology and novel treatment targets', *Wien Klin Wochenschr,* 128(21-22), pp. 791-795.
Keystone, E. C., Genovese, M. C., Klareskog, L., Hsia, E. C., Hall, S. T., Miranda, P. C., Pazdur, J., Bae, S. C., Palmer, W., Zrubek, J., Wiekowski, M., Visvanathan, S., Wu, Z. and Rahman, M. U. (2009) 'Golimumab, a human antibody to tumour necrosis factor {alpha} given by monthly subcutaneous injections, in active rheumatoid arthritis despite methotrexate therapy: the GO-FORWARD Study', *Ann Rheum Dis,* 68(6), pp. 789-96.
Khalid, Y., Dasu, N., Shah, A., Brown, K., Kaell, A., Levine, A., Dasu, K. and Raminfard, A. (2020) 'Incidence of congestive heart failure in rheumatoid arthritis: a review of literature and meta-regression analysis', *ESC Heart Fail,* 7(6), pp. 3745-3753.
Khmelevskaya, A., Houtman, M., Bürki, K., Pauli, C., Mohammadian, H., Angeli, M., Distler, O., Ciurea, A., Veale, D., Ramming, A., Fearon, U., Ospelt, C. and Micheroli, R. (2024) 'POS1201 CHI3L1 AND CHI3L2 REPRESENT TWO HIGHLY SPECIFIC SYNOVIAL FIBROBLAST-RELATED BIOMARKERS IN SEROPOSITIVE AND –NEGATIVE RHEUMATOID ARTHRITIS', *Annals of the Rheumatic Diseases,* 83(Suppl 1), pp. 590-590.
Kiener, H. P., Lee, D. M., Agarwal, S. K. and Brenner, M. B. (2006) 'Cadherin-11 induces rheumatoid arthritis fibroblast-like synoviocytes to form lining layers in vitro', *Am J Pathol,* 168(5), pp. 1486-99.
Kilikevicius, A., Meister, G. and Corey, D. R. (2021) 'Reexamining assumptions about miRNA-guided gene silencing', *Nucleic Acids Research,* 50(2), pp. 617-634.

Kim, J. W., Kong, J. S., Lee, S., Yoo, S. A., Koh, J. H., Jin, J. and Kim, W. U. (2020) 'Angiogenic cytokines can reflect the synovitis severity and treatment response to biologics in rheumatoid arthritis', *Exp Mol Med,* 52(5), pp. 843-853.
Kim, S. I. and Choi, M. E. (2012) 'TGF-β-activated kinase-1: New insights into the mechanism of TGF-β signaling and kidney disease', *Kidney Res Clin Pract,* 31(2), pp. 94-105.
Kim, T. and Croce, C. M. (2023) 'MicroRNA: trends in clinical trials of cancer diagnosis and therapy strategies', *Experimental & Molecular Medicine,* 55(7), pp. 1314-1321.
Kirkham, B. W., Lassere, M. N., Edmonds, J. P., Juhasz, K. M., Bird, P. A., Lee, C. S., Shnier, R. and Portek, I. J. (2006) 'Synovial membrane cytokine expression is predictive of joint damage progression in rheumatoid arthritis: a two-year prospective study (the DAMAGE study cohort)', *Arthritis Rheum,* 54(4), pp. 1122-31.
Klareskog, L., Stolt, P., Lundberg, K., Källberg, H., Bengtsson, C., Grunewald, J., Rönnelid, J., Harris, H. E., Ulfgren, A. K., Rantapää-Dahlqvist, S., Eklund, A., Padyukov, L. and Alfredsson, L. (2006) 'A new model for an etiology of rheumatoid arthritis: smoking may trigger HLA-DR (shared epitope)-restricted immune reactions to autoantigens modified by citrullination', *Arthritis Rheum,* 54(1), pp. 38-46.
Klatt, T., Ouyang, Q., Flad, T., Koetter, I., Bühring, H. J., Kalbacher, H., Pawelec, G. and Müller, C. A. (2005) 'Expansion of peripheral CD8+ CD28- T cells in response to Epstein-Barr virus in patients with rheumatoid arthritis', *J Rheumatol,* 32(2), pp. 239-51.
Koenders, M. I., Marijnissen, R. J., Devesa, I., Lubberts, E., Joosten, L. A., Roth, J., van Lent, P. L., van de Loo, F. A. and van den Berg, W. B. (2011) 'Tumor necrosis factor-interleukin-17 interplay induces S100A8, interleukin-1β, and matrix metalloproteinases, and drives irreversible cartilage destruction in murine arthritis: rationale for combination treatment during arthritis', *Arthritis Rheum,* 63(8), pp. 2329-39.
Koeth, R. A., Wang, Z., Levison, B. S., Buffa, J. A., Org, E., Sheehy, B. T., Britt, E. B., Fu, X., Wu, Y., Li, L., Smith, J. D., DiDonato, J. A., Chen, J., Li, H., Wu, G. D., Lewis, J. D., Warrier, M., Brown, J. M., Krauss, R. M., Tang, W. H. W., Bushman, F. D., Lusis, A. J. and Hazen, S. L. (2013) 'Intestinal microbiota metabolism of l-carnitine, a nutrient in red meat, promotes atherosclerosis', *Nature Medicine,* 19(5), pp. 576-585.
Koliaraki, V., Prados, A., Armaka, M. and Kollias, G. (2020) 'The mesenchymal context in inflammation, immunity and cancer', *Nat Immunol,* 21(9), pp. 974-982.
Kondo, N., Kuroda, T. and Kobayashi, D. (2021) 'Cytokine Networks in the Pathogenesis of Rheumatoid Arthritis', *Int J Mol Sci,* 22(20).
Kondo, Y., Yokosawa, M., Kaneko, S., Furuyama, K., Segawa, S., Tsuboi, H., Matsumoto, I. and Sumida, T. (2018) 'Review: Transcriptional Regulation of CD4+ T Cell Differentiation in Experimentally Induced Arthritis and Rheumatoid Arthritis', *Arthritis Rheumatol,* 70(5), pp. 653-661.
Konig, M. F., Abusleme, L., Reinholdt, J., Palmer, R. J., Teles, R. P., Sampson, K., Rosen, A., Nigrovic, P. A., Sokolove, J., Giles, J. T., Moutsopoulos, N. M. and Andrade, F. (2016) 'Aggregatibacter actinomycetemcomitans-induced hypercitrullination links periodontal infection to autoimmunity in rheumatoid arthritis', *Sci Transl Med,* 8(369), pp. 369ra176.
Kourbeti, I. S., Ziakas, P. D. and Mylonakis, E. (2014) 'Biologic therapies in rheumatoid arthritis and the risk of opportunistic infections: a meta-analysis', *Clin Infect Dis,* 58(12), pp. 1649-57.
Kozomara, A. and Griffiths-Jones, S. (2014) 'miRBase: annotating high confidence microRNAs using deep sequencing data', *Nucleic Acids Res,* 42(Database issue), pp. D68-73.
Kremer, J. M., Genant, H. K., Moreland, L. W., Russell, A. S., Emery, P., Abud-Mendoza, C., Szechinski, J., Li, T., Ge, Z., Becker, J. C. and Westhovens, R. (2006) 'Effects of abatacept in patients with methotrexate-resistant active rheumatoid arthritis: a randomized trial', *Ann Intern Med,* 144(12), pp. 865-76.
Krstic, J. and Santibanez, J. F. (2014) 'Transforming growth factor-beta and matrix metalloproteinases: functional interactions in tumor stroma-infiltrating myeloid cells', *ScientificWorldJournal,* 2014, pp. 521754.

Kuppner, M. C., McKillop-Smith, S. and Forrester, J. V. (1995) 'TGF-beta and IL-1 beta act in synergy to enhance IL-6 and IL-8 mRNA levels and IL-6 production by human retinal pigment epithelial cells', *Immunology,* 84(2), pp. 265-71.
Kvacskay, P., Yao, N., Schnotz, J.-H., Scarpone, R., Carvalho, R. d. A., Klika, K. D., Merkt, W., Tretter, T., Lorenz, H.-M. and Tykocinski, L.-O. (2021) 'Increase of aerobic glycolysis mediated by activated T helper cells drives synovial fibroblasts towards an inflammatory phenotype: new targets for therapy?', *Arthritis Research & Therapy,* 23(1), pp. 56.
Kwak, P. B. and Tomari, Y. (2012) 'The N domain of Argonaute drives duplex unwinding during RISC assembly', *Nat Struct Mol Biol,* 19(2), pp. 145-51.
Ladehesa-Pineda, M. L., Ortega-Castro, R., Puche-Larrubia, M., Granados, R. E. M., Dougados, M., Collantes-Estévez, E. and López-Medina, C. (2023) 'Smoking and alcohol consumption are associated with peripheral musculoskeletal involvement in patients with spondyloarthritis (including psoriatic arthritis). Results from the ASAS-PerSpA study', *Semin Arthritis Rheum,* 58, pp. 152146.
Lampropoulou, V., Sergushichev, A., Bambouskova, M., Nair, S., Vincent, E. E., Loginicheva, E., Cervantes-Barragan, L., Ma, X., Huang, S. C., Griss, T., Weinheimer, C. J., Khader, S., Randolph, G. J., Pearce, E. J., Jones, R. G., Diwan, A., Diamond, M. S. and Artyomov, M. N. (2016) 'Itaconate Links Inhibition of Succinate Dehydrogenase with Macrophage Metabolic Remodeling and Regulation of Inflammation', *Cell Metab,* 24(1), pp. 158-66.
Langenbruch, A., Radtke, M. A., Krensel, M., Jacobi, A., Reich, K. and Augustin, M. (2014) 'Nail involvement as a predictor of concomitant psoriatic arthritis in patients with psoriasis', *Br J Dermatol,* 171(5), pp. 1123-8.
Laragione, T. and Gulko, P. S. (2010) 'mTOR regulates the invasive properties of synovial fibroblasts in rheumatoid arthritis', *Mol Med,* 16(9-10), pp. 352-8.
Larid, G., Vix, J., Garlantezec, R., Loppin, E. and Gervais, E. (2022) 'Increased remission with fewer corticosteroids and more biologics in rheumatoid arthritis at 7-year follow-up in real-life conditions', *Scientific Reports,* 12(1), pp. 2563.
Laugisch, O., Wong, A., Sroka, A., Kantyka, T., Koziel, J., Neuhaus, K., Sculean, A., Venables, P. J., Potempa, J., Möller, B. and Eick, S. (2016) 'Citrullination in the periodontium--a possible link between periodontitis and rheumatoid arthritis', *Clin Oral Investig,* 20(4), pp. 675-83.
Le Goff, B., Singbrant, S., Tonkin, B. A., Martin, T. J., Romas, E., Sims, N. A. and Walsh, N. C. (2014) 'Oncostatin M acting via OSMR, augments the actions of IL-1 and TNF in synovial fibroblasts', *Cytokine,* 68(2), pp. 101-9.
LeBleu, V. S., O'Connell, J. T., Gonzalez Herrera, K. N., Wikman, H., Pantel, K., Haigis, M. C., de Carvalho, F. M., Damascena, A., Domingos Chinen, L. T., Rocha, R. M., Asara, J. M. and Kalluri, R. (2014) 'PGC-1α mediates mitochondrial biogenesis and oxidative phosphorylation in cancer cells to promote metastasis', *Nat Cell Biol,* 16(10), pp. 992-1003, 1-15.
Lee, A., Qiao, Y., Grigoriev, G., Chen, J., Park-Min, K. H., Park, S. H., Ivashkiv, L. B. and Kalliolias, G. D. (2013a) 'Tumor necrosis factor α induces sustained signaling and a prolonged and unremitting inflammatory response in rheumatoid arthritis synovial fibroblasts', *Arthritis Rheum,* 65(4), pp. 928-38.
Lee, A. T., Li, W., Liew, A., Bombardier, C., Weisman, M., Massarotti, E. M., Kent, J., Wolfe, F., Begovich, A. B. and Gregersen, P. K. (2005) 'The PTPN22 R620W polymorphism associates with RF positive rheumatoid arthritis in a dose-dependent manner but not with HLA-SE status', *Genes Immun,* 6(2), pp. 129-33.
Lee, B. W. and Moon, S. J. (2023) 'Inflammatory Cytokines in Psoriatic Arthritis: Understanding Pathogenesis and Implications for Treatment', *Int J Mol Sci,* 24(14).
Lee, C. K., Lee, E. Y., Chung, S. M., Mun, S. H., Yoo, B. and Moon, H. B. (2004) 'Effects of disease-modifying antirheumatic drugs and antiinflammatory cytokines on human osteoclastogenesis through interaction with receptor activator of nuclear factor kappaB, osteoprotegerin, and receptor activator of nuclear factor kappaB ligand', *Arthritis Rheum,* 50(12), pp. 3831-43.

Lee, D. M., Kiener, H. P., Agarwal, S. K., Noss, E. H., Watts, G. F., Chisaka, O., Takeichi, M. and Brenner, M. B. (2007) 'Cadherin-11 in synovial lining formation and pathology in arthritis', *Science,* 315(5814), pp. 1006-10.
Lee, E. B., Fleischmann, R., Hall, S., Wilkinson, B., Bradley, J. D., Gruben, D., Koncz, T., Krishnaswami, S., Wallenstein, G. V., Zang, C., Zwillich, S. H. and van Vollenhoven, R. F. (2014) 'Tofacitinib versus methotrexate in rheumatoid arthritis', *N Engl J Med,* 370(25), pp. 2377-86.
Lee, H. W., Shin, J. H. and Simons, M. (2022) 'Flow goes forward and cells step backward: endothelial migration', *Exp Mol Med,* 54(6), pp. 711-719.
Lee, J. H., Kim, B., Jin, W. J., Kim, H. H., Ha, H. and Lee, Z. H. (2017) 'Pathogenic roles of CXCL10 signaling through CXCR3 and TLR4 in macrophages and T cells: relevance for arthritis', *Arthritis Res Ther,* 19(1), pp. 163.
Lee, S. Y., Kwok, S. K., Son, H. J., Ryu, J. G., Kim, E. K., Oh, H. J., Cho, M. L., Ju, J. H., Park, S. H. and Kim, H. Y. (2013b) 'IL-17-mediated Bcl-2 expression regulates survival of fibroblast-like synoviocytes in rheumatoid arthritis through STAT3 activation', *Arthritis Res Ther,* 15(1), pp. R31.
Lee, W. S., Yasuda, S., Kono, M., Kudo, Y., Shimamura, S., Kono, M., Fujieda, Y., Kato, M., Oku, K., Shimizu, T., Onodera, T., Iwasaki, N. and Atsumi, T. (2020) 'MicroRNA-9 ameliorates destructive arthritis through down-regulation of NF-κB1-RANKL pathway in fibroblast-like synoviocytes', *Clin Immunol,* 212, pp. 108348.
Lefèvre, S., Knedla, A., Tennie, C., Kampmann, A., Wunrau, C., Dinser, R., Korb, A., Schnäker, E. M., Tarner, I. H., Robbins, P. D., Evans, C. H., Stürz, H., Steinmeyer, J., Gay, S., Schölmerich, J., Pap, T., Müller-Ladner, U. and Neumann, E. (2009) 'Synovial fibroblasts spread rheumatoid arthritis to unaffected joints', *Nat Med,* 15(12), pp. 1414-20.
Leipe, J., Grunke, M., Dechant, C., Reindl, C., Kerzendorf, U., Schulze-Koops, H. and Skapenko, A. (2010) 'Role of Th17 cells in human autoimmune arthritis', *Arthritis Rheum,* 62(10), pp. 2876-85.
Lerner, A. and Matthias, T. (2015) 'Rheumatoid arthritis-celiac disease relationship: joints get that gut feeling', *Autoimmun Rev,* 14(11), pp. 1038-47.
LEUNG, Y. Y. and LIM, K. K. T. (2007) 'Apsoriatic psoriatic arthritis', *APLAR Journal of Rheumatology,* 10(4), pp. 264-269.
Leung, Y. Y., Ogdie, A., Orbai, A. M., Tillett, W., Coates, L. C., Strand, V., Mease, P. and Gladman, D. D. (2018) 'Classification and Outcome Measures for Psoriatic Arthritis', *Front Med (Lausanne),* 5, pp. 246.
Levescot, A., Chang, M. H., Schnell, J., Nelson-Maney, N., Yan, J., Martínez-Bonet, M., Grieshaber-Bouyer, R., Lee, P. Y., Wei, K., Blaustein, R. B., Morris, A., Wactor, A., Iwakura, Y., Lederer, J. A., Rao, D. A., Charles, J. F. and Nigrovic, P. A. (2021) 'IL-1β-driven osteoclastogenic Tregs accelerate bone erosion in arthritis', *J Clin Invest,* 131(18).
Li, C., Kuang, K., Du, J., Eymin, B. and Jia, T. (2022) 'Far beyond anti-angiogenesis: Benefits for anti-basicFGF therapy in cancer', *Biochim Biophys Acta Mol Cell Res,* 1869(7), pp. 119253.
Li, F., Tang, Y., Song, B., Yu, M., Li, Q., Zhang, C., Hou, J. and Yang, R. (2019) 'Nomenclature clarification: synovial fibroblasts and synovial mesenchymal stem cells', *Stem Cell Research & Therapy,* 10(1), pp. 260.
Li, G., Xia, Z., Liu, Y., Meng, F., Wu, X., Fang, Y., Zhang, C. and Liu, D. (2018a) 'SIRT1 inhibits rheumatoid arthritis fibroblast-like synoviocyte aggressiveness and inflammatory response via suppressing NF-κB pathway', *Biosci Rep,* 38(3).
Li, J., Hsu, H. C. and Mountz, J. D. (2012) 'Managing macrophages in rheumatoid arthritis by reform or removal', *Curr Rheumatol Rep,* 14(5), pp. 445-54.
Li, J., Wang, Y., Wang, Y., Wen, X., Ma, X. N., Chen, W., Huang, F., Kou, J., Qi, L. W., Liu, B. and Liu, K. (2015) 'Pharmacological activation of AMPK prevents Drp1-mediated mitochondrial fission and alleviates endoplasmic reticulum stress-associated endothelial dysfunction', *J Mol Cell Cardiol,* 86, pp. 62-74.
Li, Q., Chandran, V., Tsoi, L., O'Rielly, D., Nair, R. P., Gladman, D., Elder, J. T. and Rahman, P. (2020) 'Quantifying Differences in Heritability among Psoriatic Arthritis (PsA), Cutaneous Psoriasis (PsC) and Psoriasis vulgaris (PsV)', *Sci Rep,* 10(1), pp. 4925.

Li, W., Li, Z., Zou, Z., Liu, X. and Li, X. (2024a) 'Integrated single-cell and bulk RNA sequencing identifies POSTN as a potential biomarker and therapeutic target for rheumatoid arthritis', *Gene,* 928, pp. 148798.
Li, Y., Cai, B., Shen, L., Dong, Y., Lu, Q., Sun, S., Liu, S., Ma, S., Ma, P. X. and Chen, J. (2017) 'MiRNA-29b suppresses tumor growth through simultaneously inhibiting angiogenesis and tumorigenesis by targeting Akt3', *Cancer Lett,* 397, pp. 111-119.
Li, Y., Liu, Y., Wang, C., Xia, W. R., Zheng, J. Y., Yang, J., Liu, B., Liu, J. Q. and Liu, L. F. (2018b) 'Succinate induces synovial angiogenesis in rheumatoid arthritis through metabolic remodeling and HIF-1α/VEGF axis', *Free Radic Biol Med,* 126, pp. 1-14.
Li, Y. T., Chen, S. Y., Wang, C. R., Liu, M. F., Lin, C. C., Jou, I. M., Shiau, A. L. and Wu, C. L. (2012) 'Brief report: amelioration of collagen-induced arthritis in mice by lentivirus-mediated silencing of microRNA-223', *Arthritis Rheum,* 64(10), pp. 3240-5.
Li, Z., Zhao, W., Wang, M., Hussain, M. Z. and Mahjabeen, I. (2024b) 'Role of microRNAs deregulation in initiation of rheumatoid arthritis: A retrospective observational study', *Medicine (Baltimore),* 103(3), pp. e36595.
Lin, J., Huo, R., Xiao, L., Zhu, X., Xie, J., Sun, S., He, Y., Zhang, J., Sun, Y., Zhou, Z., Wu, P., Shen, B., Li, D. and Li, N. (2014) 'A novel p53/microRNA-22/Cyr61 axis in synovial cells regulates inflammation in rheumatoid arthritis', *Arthritis Rheumatol,* 66(1), pp. 49-59.
Lin, S. H., Ho, J. C., Li, S. C., Cheng, Y. W., Yang, Y. C., Chen, J. F., Hsu, C. Y., Nakano, T., Wang, F. S., Yang, M. Y., Lee, C. H. and Hsiao, C. C. (2020) 'Upregulation of miR-941 in Circulating CD14+ Monocytes Enhances Osteoclast Activation via WNT16 Inhibition in Patients with Psoriatic Arthritis', *Int J Mol Sci,* 21(12).
Littlewood-Evans, A., Sarret, S., Apfel, V., Loesle, P., Dawson, J., Zhang, J., Muller, A., Tigani, B., Kneuer, R., Patel, S., Valeaux, S., Gommermann, N., Rubic-Schneider, T., Junt, T. and Carballido, J. M. (2016) 'GPR91 senses extracellular succinate released from inflammatory macrophages and exacerbates rheumatoid arthritis', *J Exp Med,* 213(9), pp. 1655-62.
Liu, H. and Chen, Y. G. (2022) 'The Interplay Between TGF-β Signaling and Cell Metabolism', *Front Cell Dev Biol,* 10, pp. 846723.
Liu, M., Ren, T., Lin, Z. and Hua, M. (2022) 'Upregulated miR-146a Expression in Peripheral Blood Relates to Th17 and Treg Imbalance in Elder Rheumatoid Arthritis Patients', *Lifestyle Genom,* 15(3), pp. 98-106.
Liu, W., Sheng, L., Nie, L., Wen, X. and Mo, X. (2020) 'Functional interaction between long non-coding RNA and microRNA in rheumatoid arthritis', *J Clin Lab Anal,* 34(12), pp. e23489.
Liu, W., Wu, Y. H., Zhang, L., Xue, B., Wang, Y., Liu, B., Liu, X. Y., Zuo, F., Yang, X. Y., Chen, F. Y., Duan, R., Cai, Y., Zhang, B. and Ji, Y. (2018) 'MicroRNA-146a suppresses rheumatoid arthritis fibroblast-like synoviocytes proliferation and inflammatory responses by inhibiting the TLR4/NF-kB signaling', *Oncotarget,* 9(35), pp. 23944-23959.
Liu, Y. and Yan, X. (2019) 'Eriodictyol inhibits survival and inflammatory responses and promotes apoptosis in rheumatoid arthritis fibroblast-like synoviocytes through AKT/FOXO1 signaling', *J Cell Biochem,* 120(9), pp. 14628-14635.
Locasale, J. W. and Cantley, L. C. (2011) 'Metabolic flux and the regulation of mammalian cell growth', *Cell Metab,* 14(4), pp. 443-51.
López-Armada, M. J., Caramés, B., Martín, M. A., Cillero-Pastor, B., Lires-Dean, M., Fuentes-Boquete, I., Arenas, J. and Blanco, F. J. (2006) 'Mitochondrial activity is modulated by TNFalpha and IL-1beta in normal human chondrocyte cells', *Osteoarthritis Cartilage,* 14(10), pp. 1011-22.
Lories, R. J., Derese, I., Ceuppens, J. L. and Luyten, F. P. (2003) 'Bone morphogenetic proteins 2 and 6, expressed in arthritic synovium, are regulated by proinflammatory cytokines and differentially modulate fibroblast-like synoviocyte apoptosis', *Arthritis Rheum,* 48(10), pp. 2807-18.
Low, C., Conway, R., Young, F., Murray, K., Convery, H., Biniecka, M., Fearon, U. and Veale, D. (2018) 'SAT0087 Association of biometrics with disease characteristics and synovial phenotype in inflammatory arthritis', *Annals of the Rheumatic Diseases,* 77(Suppl 2), pp. 908-908.

Lu, J., Getz, G., Miska, E. A., Alvarez-Saavedra, E., Lamb, J., Peck, D., Sweet-Cordero, A., Ebert, B. L., Mak, R. H., Ferrando, A. A., Downing, J. R., Jacks, T., Horvitz, H. R. and Golub, T. R. (2005) 'MicroRNA expression profiles classify human cancers', *Nature,* 435(7043), pp. 834-8.
Lu, Q. and Lemke, G. (2001) 'Homeostatic regulation of the immune system by receptor tyrosine kinases of the Tyro 3 family', *Science,* 293(5528), pp. 306-11.
Lu, Y., Yu, S. S., Zong, M., Fan, S. S., Lu, T. B., Gong, R. H., Sun, L. S. and Fan, L. Y. (2017) 'Glucose-6-Phosphate Isomerase (G6PI) Mediates Hypoxia-Induced Angiogenesis in Rheumatoid Arthritis', *Sci Rep,* 7, pp. 40274.
Lun, A. T. L., Riesenfeld, S., Andrews, T., Dao, T. P., Gomes, T. and Marioni, J. C. (2019) 'EmptyDrops: distinguishing cells from empty droplets in droplet-based single-cell RNA sequencing data', *Genome Biol,* 20(1), pp. 63.
Lund-Olesen, K. (1970) 'Oxygen tension in synovial fluids', *Arthritis Rheum,* 13(6), pp. 769-76.
Ma, Y. S., Feng, S., Lin, L., Zhang, H., Wei, G. H., Liu, Y. S., Yang, X. L., Xin, R., Shi, Y., Zhang, D. D., Jia, C. Y., Lu, G. X., Xue, S. B., Yu, F., Lv, Z. W., Liu, J. B., Wang, G. R. and Fu, D. (2021) 'Protein disulfide isomerase inhibits endoplasmic reticulum stress response and apoptosis via its oxidoreductase activity in colorectal cancer', *Cell Signal,* 86, pp. 110076.
Maeda, Y., Kurakawa, T., Umemoto, E., Motooka, D., Ito, Y., Gotoh, K., Hirota, K., Matsushita, M., Furuta, Y., Narazaki, M., Sakaguchi, N., Kayama, H., Nakamura, S., Iida, T., Saeki, Y., Kumanogoh, A., Sakaguchi, S. and Takeda, K. (2016) 'Dysbiosis Contributes to Arthritis Development via Activation of Autoreactive T Cells in the Intestine', *Arthritis Rheumatol,* 68(11), pp. 2646-2661.
Majmundar, A. J., Wong, W. J. and Simon, M. C. (2010) 'Hypoxia-inducible factors and the response to hypoxic stress', *Mol Cell,* 40(2), pp. 294-309.
Makavos, G., Ikonomidis, I., Andreadou, I., Varoudi, M., Kapniari, I., Loukeri, E., Theodoropoulos, K., Pavlidis, G., Triantafyllidi, H., Thymis, J., Parissis, J., Tsoumani, M., Rafouli-Stergiou, P., Katsimbri, P. and Papadavid, E. (2020) 'Effects of Interleukin 17A Inhibition on Myocardial Deformation and Vascular Function in Psoriasis', *Can J Cardiol,* 36(1), pp. 100-111.
Malemud, C. J. (2015) 'The PI3K/Akt/PTEN/mTOR pathway: a fruitful target for inducing cell death in rheumatoid arthritis?', *Future Med Chem,* 7(9), pp. 1137-47.
Manning, J. E., Lewis, J. W., Marsh, L. J. and McGettrick, H. M. (2021) 'Insights Into Leukocyte Trafficking in Inflammatory Arthritis - Imaging the Joint', *Front Cell Dev Biol,* 9, pp. 635102.
Marzaioli, V., Canavan, M., Floudas, A., Flynn, K., Mullan, R., Veale, D. J. and Fearon, U. (2021) 'CD209/CD14(+) Dendritic Cells Characterization in Rheumatoid and Psoriatic Arthritis Patients: Activation, Synovial Infiltration, and Therapeutic Targeting', *Front Immunol,* 12, pp. 722349.
Marzaioli, V., Canavan, M., Floudas, A., Wade, S. C., Low, C., Veale, D. J. and Fearon, U. (2020) 'Monocyte-Derived Dendritic Cell Differentiation in Inflammatory Arthritis Is Regulated by the JAK/STAT Axis via NADPH Oxidase Regulation', *Front Immunol,* 11, pp. 1406.
Masopust, D. and Soerens, A. G. (2019) 'Tissue-Resident T Cells and Other Resident Leukocytes', *Annu Rev Immunol,* 37, pp. 521-546.
Masson-Bessière, C., Sebbag, M., Durieux, J. J., Nogueira, L., Vincent, C., Girbal-Neuhauser, E., Durroux, R., Cantagrel, A. and Serre, G. (2000) 'In the rheumatoid pannus, anti-filaggrin autoantibodies are produced by local plasma cells and constitute a higher proportion of IgG than in synovial fluid and serum', *Clin Exp Immunol,* 119(3), pp. 544-52.
Masuko-Hongo, K., Kato, T. and Nishioka, K. (2003) 'Virus-associated arthritis', *Best Pract Res Clin Rheumatol,* 17(2), pp. 309-18.
Mateus, D., Marini, E. S., Progida, C. and Bakke, O. (2018) 'Rab7a modulates ER stress and ER morphology', *Biochim Biophys Acta Mol Cell Res,* 1865(5), pp. 781-793.
Mathonnet, G., Fabian, M. R., Svitkin, Y. V., Parsyan, A., Huck, L., Murata, T., Biffo, S., Merrick, W. C., Darzynkiewicz, E., Pillai, R. S., Filipowicz, W., Duchaine, T. F. and Sonenberg, N. (2007) 'MicroRNA inhibition of translation initiation in vitro by targeting the cap-binding complex eIF4F', *Science,* 317(5845), pp. 1764-7.

Matsuda, K., Shiba, N. and Hiraoka, K. (2023) 'New Insights into the Role of Synovial Fibroblasts Leading to Joint Destruction in Rheumatoid Arthritis', *International Journal of Molecular Sciences,* 24(6), pp. 5173.
Mc Ardle, A., Flatley, B., Pennington, S. R. and FitzGerald, O. (2015) 'Early biomarkers of joint damage in rheumatoid and psoriatic arthritis', *Arthritis Res Ther,* 17(1), pp. 141.
McGarry, T., Biniecka, M., Gao, W., Cluxton, D., Canavan, M., Wade, S., Wade, S., Gallagher, L., Orr, C., Veale, D. J. and Fearon, U. (2017) 'Resolution of TLR2-induced inflammation through manipulation of metabolic pathways in Rheumatoid Arthritis', *Sci Rep,* 7, pp. 43165.
McGarry, T., Biniecka, M., Veale, D. J. and Fearon, U. (2018a) 'Hypoxia, oxidative stress and inflammation', *Free Radic Biol Med,* 125, pp. 15-24.
McGarry, T., Hanlon, M. M., Marzaioli, V., Cunningham, C. C., Krishna, V., Murray, K., Hurson, C., Gallagher, P., Nagpal, S., Veale, D. J. and Fearon, U. (2021) 'Rheumatoid arthritis CD14(+) monocytes display metabolic and inflammatory dysfunction, a phenotype that precedes clinical manifestation of disease', *Clin Transl Immunology,* 10(1), pp. e1237.
McGarry, T., Orr, C., Wade, S., Biniecka, M., Wade, S., Gallagher, L., Low, C., Veale, D. J. and Fearon, U. (2018b) 'JAK/STAT Blockade Alters Synovial Bioenergetics, Mitochondrial Function, and Proinflammatory Mediators in Rheumatoid Arthritis', *Arthritis Rheumatol,* 70(12), pp. 1959-1970.
McGettrick, H. M., Smith, E., Filer, A., Kissane, S., Salmon, M., Buckley, C. D., Rainger, G. E. and Nash, G. B. (2009) 'Fibroblasts from different sites may promote or inhibit recruitment of flowing lymphocytes by endothelial cells', *Eur J Immunol,* 39(1), pp. 113-25.
McGinnis, C. S., Murrow, L. M. and Gartner, Z. J. (2019) 'DoubletFinder: Doublet Detection in Single-Cell RNA Sequencing Data Using Artificial Nearest Neighbors', *Cell Syst,* 8(4), pp. 329-337.e4.
McGonagle, D., Conaghan, P. G. and Emery, P. (1999) 'Psoriatic arthritis: a unified concept twenty years on', *Arthritis Rheum,* 42(6), pp. 1080-6.
McGonagle, D., Hermann, K. G. and Tan, A. L. (2015) 'Differentiation between osteoarthritis and psoriatic arthritis: implications for pathogenesis and treatment in the biologic therapy era', *Rheumatology (Oxford),* 54(1), pp. 29-38.
McGonagle, D., Tan, A. L., Watad, A. and Helliwell, P. (2019) 'Pathophysiology, assessment and treatment of psoriatic dactylitis', *Nat Rev Rheumatol,* 15(2), pp. 113-122.
McHugh, J. (2024) 'Single-cell atlas unveils the diversity of RA synovial tissue', *Nature Reviews Rheumatology,* 20(1), pp. 4-4.
McInnes, I. B., Asahina, A., Coates, L. C., Landewé, R., Merola, J. F., Ritchlin, C. T., Tanaka, Y., Gossec, L., Gottlieb, A. B., Warren, R. B., Ink, B., Assudani, D., Bajracharya, R., Shende, V., Coarse, J. and Mease, P. J. (2023) 'Bimekizumab in patients with psoriatic arthritis, naive to biologic treatment: a randomised, double-blind, placebo-controlled, phase 3 trial (BE OPTIMAL)', *Lancet,* 401(10370), pp. 25-37.
McInnes, I. B., Kavanaugh, A., Gottlieb, A. B., Puig, L., Rahman, P., Ritchlin, C., Brodmerkel, C., Li, S., Wang, Y., Mendelsohn, A. M. and Doyle, M. K. (2013) 'Efficacy and safety of ustekinumab in patients with active psoriatic arthritis: 1 year results of the phase 3, multicentre, double-blind, placebo-controlled PSUMMIT 1 trial', *Lancet,* 382(9894), pp. 780-9.
McInnes, I. B. and Schett, G. (2017) 'Pathogenetic insights from the treatment of rheumatoid arthritis', *Lancet,* 389(10086), pp. 2328-2337.
Mease, P., Setty, A., Papp, K., Van den Bosch, F., Tsuji, S., Keiserman, M., Carter, K., Li, Y., McCaskill, R., McDearmon-Blondell, E., Wung, P. and Tillett, W. (2023) 'Upadacitinib in patients with psoriatic arthritis and inadequate response to biologics: 3-year results from the open-label extension of the randomised controlled phase 3 SELECT-PsA 2 study', *Clin Exp Rheumatol,* 41(11), pp. 2286-2297.
Mease, P., van der Heijde, D., Landewé, R., Mpofu, S., Rahman, P., Tahir, H., Singhal, A., Boettcher, E., Navarra, S., Meiser, K., Readie, A., Pricop, L. and Abrams, K. (2018) 'Secukinumab improves active psoriatic arthritis symptoms and inhibits radiographic progression: primary results from the randomised, double-blind, phase III FUTURE 5 study', *Ann Rheum Dis,* 77(6), pp. 890-897.

Mease, P. J., Fleischmann, R., Deodhar, A. A., Wollenhaupt, J., Khraishi, M., Kielar, D., Woltering, F., Stach, C., Hoepken, B., Arledge, T. and van der Heijde, D. (2014) 'Effect of certolizumab pegol on signs and symptoms in patients with psoriatic arthritis: 24-week results of a Phase 3 double-blind randomised placebo-controlled study (RAPID-PsA)', *Ann Rheum Dis,* 73(1), pp. 48-55.
Mease, P. J., Gottlieb, A. B., Berman, A., Drescher, E., Xing, J., Wong, R. and Banerjee, S. (2016) 'The Efficacy and Safety of Clazakizumab, an Anti-Interleukin-6 Monoclonal Antibody, in a Phase IIb Study of Adults With Active Psoriatic Arthritis', *Arthritis Rheumatol,* 68(9), pp. 2163-73.
Mease, P. J., Gottlieb, A. B., van der Heijde, D., FitzGerald, O., Johnsen, A., Nys, M., Banerjee, S. and Gladman, D. D. (2017) 'Efficacy and safety of abatacept, a T-cell modulator, in a randomised, double-blind, placebo-controlled, phase III study in psoriatic arthritis', *Ann Rheum Dis,* 76(9), pp. 1550-1558.
Mease, P. J., Helliwell, P. S., Hjuler, K. F., Raymond, K. and McInnes, I. (2021) 'Brodalumab in psoriatic arthritis: results from the randomised phase III AMVISION-1 and AMVISION-2 trials', *Ann Rheum Dis,* 80(2), pp. 185-193.
Meng, Q., Pan, B. and Sheng, P. (2021) 'Histone deacetylase 1 is increased in rheumatoid arthritis synovium and promotes synovial cell hyperplasia and synovial inflammation in the collagen-induced arthritis mouse model via the microRNA-124-dependent MARCKS-JAK/STAT axis', *Clinical and experimental rheumatology,* 39(5), pp. 970-981.
Menon, B., Gullick, N. J., Walter, G. J., Rajasekhar, M., Garrood, T., Evans, H. G., Taams, L. S. and Kirkham, B. W. (2014) 'Interleukin-17+CD8+ T cells are enriched in the joints of patients with psoriatic arthritis and correlate with disease activity and joint damage progression', *Arthritis Rheumatol,* 66(5), pp. 1272-81.
Merola, J. F., Espinoza, L. R. and Fleischmann, R. (2018) 'Distinguishing rheumatoid arthritis from psoriatic arthritis', *RMD Open,* 4(2), pp. e000656.
Meyer, A., Zack, S. R., Nijim, W., Burgos, A., Patel, V., Zanotti, B., Volin, M. V., Amin, M. A., Lewis, M. J. and Pitzalis, C. (2024) 'Metabolic reprogramming by Syntenin-1 directs RA FLS and endothelial cell-mediated inflammation and angiogenesis', *Cellular & Molecular Immunology,* 21(1), pp. 33-46.
Micheroli, R., Elhai, M., Edalat, S., Frank-Bertoncelj, M., Bürki, K., Ciurea, A., MacDonald, L., Kurowska-Stolarska, M., Lewis, M. J., Goldmann, K., Cubuk, C., Kuret, T., Distler, O., Pitzalis, C. and Ospelt, C. (2022) 'Role of synovial fibroblast subsets across synovial pathotypes in rheumatoid arthritis: a deconvolution analysis', *RMD Open,* 8(1), pp. e001949.
Michopoulos, F., Karagianni, N., Whalley, N. M., Firth, M. A., Nikolaou, C., Wilson, I. D., Critchlow, S. E., Kollias, G. and Theodoridis, G. A. (2016) 'Targeted Metabolic Profiling of the Tg197 Mouse Model Reveals Itaconic Acid as a Marker of Rheumatoid Arthritis', *J Proteome Res,* 15(12), pp. 4579-4590.
Miglioranza Scavuzzi, B. and Holoshitz, J. (2022) 'Endoplasmic Reticulum Stress, Oxidative Stress, and Rheumatic Diseases', *Antioxidants (Basel),* 11(7).
Mills, E. L., Kelly, B., Logan, A., Costa, A. S. H., Varma, M., Bryant, C. E., Tourlomousis, P., Däbritz, J. H. M., Gottlieb, E., Latorre, I., Corr, S. C., McManus, G., Ryan, D., Jacobs, H. T., Szibor, M., Xavier, R. J., Braun, T., Frezza, C., Murphy, M. P. and O'Neill, L. A. (2016) 'Succinate Dehydrogenase Supports Metabolic Repurposing of Mitochondria to Drive Inflammatory Macrophages', *Cell,* 167(2), pp. 457-470.e13.
Misharin, A. V., Cuda, C. M., Saber, R., Turner, J. D., Gierut, A. K., Haines, G. K., 3rd, Berdnikovs, S., Filer, A., Clark, A. R., Buckley, C. D., Mutlu, G. M., Budinger, G. R. and Perlman, H. (2014) 'Nonclassical Ly6C(-) monocytes drive the development of inflammatory arthritis in mice', *Cell Rep,* 9(2), pp. 591-604.
Misra, S., Bagchi, A., Sarkar, A., Niyogi, S., Bhattacharjee, D., Chatterjee, S., Mondal, S., Chattopadhyay, A., Saha, A., Chatterjee, S., Sinhamahapatra, P., Chakrabarti, P., Chatterjee, M. and Ghosh, A. (2021) 'Methotrexate and theaflavin-3, 3'-digallate synergistically restore the balance between apoptosis and autophagy in synovial fibroblast of RA: an ex vivo approach with cultured human RA FLS', *Inflammopharmacology,* 29(5), pp. 1427-1442.
Mitchell, P. S., Parkin, R. K., Kroh, E. M., Fritz, B. R., Wyman, S. K., Pogosova-Agadjanyan, E. L., Peterson, A., Noteboom, J., O'Briant, K. C., Allen, A., Lin, D. W., Urban, N., Drescher, C. W., Knudsen, B. S.,

Stirewalt, D. L., Gentleman, R., Vessella, R. L., Nelson, P. S., Martin, D. B. and Tewari, M. (2008) 'Circulating microRNAs as stable blood-based markers for cancer detection', *Proc Natl Acad Sci U S A,* 105(30), pp. 10513-8.
Miyajima, A., Kitamura, T., Harada, N., Yokota, T. and Arai, K. (1992) 'Cytokine receptors and signal transduction', *Annu Rev Immunol,* 10, pp. 295-331.
Miyamura, Y., Kamei, S., Matsuo, M., Yamazaki, M., Usuki, S., Yasunaga, K., Uemura, A., Satou, Y., Ohguchi, H. and Minami, T. (2024) 'FOXO1 stimulates tip cell-enriched gene expression in endothelial cells', *iScience,* 27(3), pp. 109161.
Mizoguchi, F., Slowikowski, K., Wei, K., Marshall, J. L., Rao, D. A., Chang, S. K., Nguyen, H. N., Noss, E. H., Turner, J. D., Earp, B. E., Blazar, P. E., Wright, J., Simmons, B. P., Donlin, L. T., Kalliolias, G. D., Goodman, S. M., Bykerk, V. P., Ivashkiv, L. B., Lederer, J. A., Hacohen, N., Nigrovic, P. A., Filer, A., Buckley, C. D., Raychaudhuri, S. and Brenner, M. B. (2018) 'Functionally distinct disease-associated fibroblast subsets in rheumatoid arthritis', *Nat Commun,* 9(1), pp. 789.
Mohamed, B. M., Verma, N. K., Davies, A. M., McGowan, A., Crosbie-Staunton, K., Prina-Mello, A., Kelleher, D., Botting, C. H., Causey, C. P., Thompson, P. R., Pruijn, G. J., Kisin, E. R., Tkach, A. V., Shvedova, A. A. and Volkov, Y. (2012) 'Citrullination of proteins: a common post-translational modification pathway induced by different nanoparticles in vitro and in vivo', *Nanomedicine (Lond),* 7(8), pp. 1181-95.
Molenaar, J. C. (2003) '[From the library of the Netherlands Journal of Medicine. Rudolf Virchow: Die Cellularpathologie in ihrer Begründung auf physiologische und pathologische Gewebelehre; 1858]', *Ned Tijdschr Geneeskd,* 147(45), pp. 2236-44.
Moll, J. M. and Wright, V. (1973a) 'Familial occurrence of psoriatic arthritis', *Ann Rheum Dis,* 32(3), pp. 181-201.
Moll, J. M. and Wright, V. (1973b) 'Psoriatic arthritis', *Semin Arthritis Rheum,* 3(1), pp. 55-78.
Moores, R. C., Brilha, S., Schutgens, F., Elkington, P. T. and Friedland, J. S. (2017) 'Epigenetic Regulation of Matrix Metalloproteinase-1 and -3 Expression in Mycobacterium tuberculosis Infection', *Front Immunol,* 8, pp. 602.
Moran, E. M., Mullan, R., McCormick, J., Connolly, M., Sullivan, O., Fitzgerald, O., Bresnihan, B., Veale, D. J. and Fearon, U. (2009) 'Human rheumatoid arthritis tissue production of IL-17A drives matrix and cartilage degradation: synergy with tumour necrosis factor-alpha, Oncostatin M and response to biologic therapies', *Arthritis Res Ther,* 11(4), pp. R113.
Muhl, L., Genové, G., Leptidis, S., Liu, J., He, L., Mocci, G., Sun, Y., Gustafsson, S., Buyandelger, B., Chivukula, I. V., Segerstolpe, Å., Raschperger, E., Hansson, E. M., Björkegren, J. L. M., Peng, X. R., Vanlandewijck, M., Lendahl, U. and Betsholtz, C. (2020) 'Single-cell analysis uncovers fibroblast heterogeneity and criteria for fibroblast and mural cell identification and discrimination', *Nat Commun,* 11(1), pp. 3953.
Mun, S., Lee, J., Park, M., Shin, J., Lim, M. K. and Kang, H. G. (2021) 'Serum biomarker panel for the diagnosis of rheumatoid arthritis', *Arthritis Res Ther,* 23(1), pp. 31.
Murata, K., Yoshitomi, H., Tanida, S., Ishikawa, M., Nishitani, K., Ito, H. and Nakamura, T. (2010) 'Plasma and synovial fluid microRNAs as potential biomarkers of rheumatoid arthritis and osteoarthritis', *Arthritis Res Ther,* 12(3), pp. R86.
Murayama, M. A., Shimizu, J., Miyabe, C., Yudo, K. and Miyabe, Y. (2023) 'Chemokines and chemokine receptors as promising targets in rheumatoid arthritis', *Front Immunol,* 14, pp. 1100869.
Murray, K., Turk, M., Alammari, Y., Young, F., Gallagher, P., Saber, T., Fearon, U. and Veale, D. J. (2021) 'Long-term remission and biologic persistence rates: 12-year real-world data', *Arthritis Res Ther,* 23(1), pp. 25.
Na, H. S., Kwon, J. E., Lee, S. H., Jhun, J., Kim, S. M., Kim, S. Y., Kim, E. K., Jung, K., Park, S. H. and Cho, M. L. (2017) 'Th17 and IL-17 Cause Acceleration of Inflammation and Fat Loss by Inducing α(2)-Glycoprotein 1 (AZGP1) in Rheumatoid Arthritis with High-Fat Diet', *Am J Pathol,* 187(5), pp. 1049-1058.

Naeem, F., Khan, S. E. A., Saeed, M. A. and Farman, S. (2021) 'Diagnostic and therapeutic delay in Rheumatoid Arthritis patients: Impact on disease outcome', *Pak J Med Sci,* 37(4), pp. 1001-1007.
Nag, S., Mitra, O., Tripathi, G., Samanta, S., Bhattacharya, B., Chandane, P., Mohanto, S., Sundararajan, V., Malik, S., Rustagi, S., Adhikari, S., Mohanty, A., León-Figueroa, D. A., Rodriguez-Morales, A. J., Barboza, J. J. and Sah, R. (2023) 'Exploring the theranostic potentials of miRNA and epigenetic networks in autoimmune diseases: A comprehensive review', *Immun Inflamm Dis,* 11(12), pp. e1121.
Nagaratnam, N., Nagaratnam, K. and Cheuk, G. (2017) *Geriatric Diseases: Evaluation and Management.*
Naides, S. J. (1998) 'Rheumatic manifestations of parvovirus B19 infection', *Rheum Dis Clin North Am,* 24(2), pp. 375-401.
Nanus, D. E., Badoume, A., Wijesinghe, S. N., Halsey, A. M., Hurley, P., Ahmed, Z., Botchu, R., Davis, E. T., Lindsay, M. A. and Jones, S. W. (2021) 'Synovial tissue from sites of joint pain in knee osteoarthritis patients exhibits a differential phenotype with distinct fibroblast subsets', *EBioMedicine,* 72, pp. 103618.
Nash, P., Coates, L. C., Kivitz, A. J., Mease, P. J., Gladman, D. D., Covarrubias-Cobos, J. A., FitzGerald, O., Fleishaker, D., Wang, C., Wu, J., Hsu, M.-A., Menon, S., Fallon, L., Romero, A. B. and Kanik, K. S. (2020) 'Safety and Efficacy of Tofacitinib in Patients with Active Psoriatic Arthritis: Interim Analysis of OPAL Balance, an Open-Label, Long-Term Extension Study', *Rheumatology and Therapy,* 7(3), pp. 553-580.
Nash, P., Kirkham, B., Okada, M., Rahman, P., Combe, B., Burmester, G. R., Adams, D. H., Kerr, L., Lee, C., Shuler, C. L. and Genovese, M. (2017) 'Ixekizumab for the treatment of patients with active psoriatic arthritis and an inadequate response to tumour necrosis factor inhibitors: results from the 24-week randomised, double-blind, placebo-controlled period of the SPIRIT-P2 phase 3 trial', *Lancet,* 389(10086), pp. 2317-2327.
Nash, P., Mease, P. J., McInnes, I. B., Rahman, P., Ritchlin, C. T., Blanco, R., Dokoupilova, E., Andersson, M., Kajekar, R., Mpofu, S. and Pricop, L. (2018) 'Efficacy and safety of secukinumab administration by autoinjector in patients with psoriatic arthritis: results from a randomized, placebo-controlled trial (FUTURE 3)', *Arthritis Res Ther,* 20(1), pp. 47.
Navarini, L., Afeltra, A., Gallo Afflitto, G. and Margiotta, D. P. E. (2017) 'Polyunsaturated fatty acids: any role in rheumatoid arthritis?', *Lipids Health Dis,* 16(1), pp. 197.
Nell, V. P., Machold, K. P., Eberl, G., Stamm, T. A., Uffmann, M. and Smolen, J. S. (2004) 'Benefit of very early referral and very early therapy with disease-modifying anti-rheumatic drugs in patients with early rheumatoid arthritis', *Rheumatology (Oxford),* 43(7), pp. 906-14.
Nemtsova, M. V., Zaletaev, D. V., Bure, I. V., Mikhaylenko, D. S., Kuznetsova, E. B., Alekseeva, E. A., Beloukhova, M. I., Deviatkin, A. A., Lukashev, A. N. and Zamyatnin, A. A., Jr. (2019) 'Epigenetic Changes in the Pathogenesis of Rheumatoid Arthritis', *Front Genet,* 10, pp. 570.
Nepom, G. T., Hansen, J. A. and Nepom, B. S. (1987) 'The molecular basis for HLA class II associations with rheumatoid arthritis', *J Clin Immunol,* 7(1), pp. 1-7.
Neumann, E., Riepl, B., Knedla, A., Lefèvre, S., Tarner, I. H., Grifka, J., Steinmeyer, J., Schölmerich, J., Gay, S. and Müller-Ladner, U. (2010) 'Cell culture and passaging alters gene expression pattern and proliferation rate in rheumatoid arthritis synovial fibroblasts', *Arthritis Res Ther,* 12(3), pp. R83.
Ng, C. T., Biniecka, M., Kennedy, A., McCormick, J., Fitzgerald, O., Bresnihan, B., Buggy, D., Taylor, C. T., O'Sullivan, J., Fearon, U. and Veale, D. J. (2010) 'Synovial tissue hypoxia and inflammation in vivo', *Ann Rheum Dis,* 69(7), pp. 1389-95.
Nguyen, U. D. T., Zhang, Y., Lu, N., Louie-Gao, Q., Niu, J., Ogdie, A., Gelfand, J. M., LaValley, M. P., Dubreuil, M., Sparks, J. A., Karlson, E. W. and Choi, H. K. (2018) 'Smoking paradox in the development of psoriatic arthritis among patients with psoriasis: a population-based study', *Ann Rheum Dis,* 77(1), pp. 119-123.
Nielen, M. M., van Schaardenburg, D., Reesink, H. W., Twisk, J. W., van de Stadt, R. J., van der Horst-Bruinsma, I. E., de Gast, T., Habibuw, M. R., Vandenbroucke, J. P. and Dijkmans, B. A. (2004a) 'Increased

levels of C-reactive protein in serum from blood donors before the onset of rheumatoid arthritis', *Arthritis Rheum,* 50(8), pp. 2423-7.
Nielen, M. M. J., van Schaardenburg, D., Reesink, H. W., van de Stadt, R. J., van der Horst-Bruinsma, I. E., de Koning, M. H. M. T., Habibuw, M. R., Vandenbroucke, J. P. and Dijkmans, B. A. C. (2004b) 'Specific autoantibodies precede the symptoms of rheumatoid arthritis: A study of serial measurements in blood donors', *Arthritis & Rheumatism,* 50(2), pp. 380-386.
Nikiphorou, E., de Lusignan, S., Mallen, C. D., Khavandi, K., Bedarida, G., Buckley, C. D., Galloway, J. and Raza, K. (2020) 'Cardiovascular risk factors and outcomes in early rheumatoid arthritis: a population-based study', *Heart,* 106(20), pp. 1566-1572.
Nikiphorou, E., Negoescu, A., Fitzpatrick, J. D., Goudie, C. T., Badcock, A., Östör, A. J. and Malaviya, A. P. (2014) 'Indispensable or intolerable? Methotrexate in patients with rheumatoid and psoriatic arthritis: a retrospective review of discontinuation rates from a large UK cohort', *Clin Rheumatol,* 33(5), pp. 609-14.
Njobvu, P. and McGill, P. (2000) 'Psoriatic arthritis and human immunodeficiency virus infection in Zambia', *J Rheumatol,* 27(7), pp. 1699-702.
Nygaard, G. and Firestein, G. S. (2020) 'Restoring synovial homeostasis in rheumatoid arthritis by targeting fibroblast-like synoviocytes', *Nat Rev Rheumatol,* 16(6), pp. 316-333.
O'Brien, A., Hanlon, M. M., Marzaioli, V., Wade, S. C., Flynn, K., Fearon, U. and Veale, D. J. (2021) 'Targeting JAK-STAT Signalling Alters PsA Synovial Fibroblast Pro-Inflammatory and Metabolic Function', *Front Immunol,* 12, pp. 672461.
O'Brien, J., Hayder, H., Zayed, Y. and Peng, C. (2018) 'Overview of MicroRNA Biogenesis, Mechanisms of Actions, and Circulation', *Front Endocrinol (Lausanne),* 9, pp. 402.
O'Brien, W., Fissel, B. M., Maeda, Y., Yan, J., Ge, X., Gravallese, E. M., Aliprantis, A. O. and Charles, J. F. (2016) 'RANK-Independent Osteoclast Formation and Bone Erosion in Inflammatory Arthritis', *Arthritis Rheumatol,* 68(12), pp. 2889-2900.
O'Neil, L. J., Alpízar-Rodríguez, D. and Deane, K. D. (2024) 'Rheumatoid Arthritis: The Continuum of Disease and Strategies for Prediction, Early Intervention, and Prevention', *J Rheumatol,* 51(4), pp. 337-349.
Ogura, H., Murakami, M., Okuyama, Y., Tsuruoka, M., Kitabayashi, C., Kanamoto, M., Nishihara, M., Iwakura, Y. and Hirano, T. (2008) 'Interleukin-17 promotes autoimmunity by triggering a positive-feedback loop via interleukin-6 induction', *Immunity,* 29(4), pp. 628-36.
Ohara, R. A., Edhayan, G., Rasmussen, S. M., Isozaki, T., Remmer, H. A., Lanigan, T. M., Campbell, P. L., Urquhart, A. G., Lawton, J. N., Chung, K. C., Fox, D. A. and Ruth, J. H. (2019) 'Citrullinated Inhibitor of DNA Binding 1 Is a Novel Autoantigen in Rheumatoid Arthritis', *Arthritis Rheumatol,* 71(8), pp. 1241-1251.
Ohno, T., Aune, D. and Heath, A. K. (2020) 'Adiposity and the risk of rheumatoid arthritis: a systematic review and meta-analysis of cohort studies', *Sci Rep,* 10(1), pp. 16006.
Okada, Y., Han, B., Tsoi, L. C., Stuart, P. E., Ellinghaus, E., Tejasvi, T., Chandran, V., Pellett, F., Pollock, R., Bowcock, A. M., Krueger, G. G., Weichenthal, M., Voorhees, J. J., Rahman, P., Gregersen, P. K., Franke, A., Nair, R. P., Abecasis, G. R., Gladman, D. D., Elder, J. T., de Bakker, P. I. and Raychaudhuri, S. (2014) 'Fine mapping major histocompatibility complex associations in psoriasis and its clinical subtypes', *Am J Hum Genet,* 95(2), pp. 162-72.
Okamoto, K. and Takayanagi, H. (2019) 'Osteoimmunology', *Cold Spring Harb Perspect Med,* 9(1).
Oliver, K. M., Garvey, J. F., Ng, C. T., Veale, D. J., Fearon, U., Cummins, E. P. and Taylor, C. T. (2009) 'Hypoxia activates NF-kappaB-dependent gene expression through the canonical signaling pathway', *Antioxid Redox Signal,* 11(9), pp. 2057-64.
Oliveto, S., Mancino, M., Manfrini, N. and Biffo, S. (2017) 'Role of microRNAs in translation regulation and cancer', *World J Biol Chem,* 8(1), pp. 45-56.
Ollier, W. and Thomson, W. (1992) 'Population genetics of rheumatoid arthritis', *Rheum Dis Clin North Am,* 18(4), pp. 741-59.

Orange, D. E., Yao, V., Sawicka, K., Fak, J., Frank, M. O., Parveen, S., Blachere, N. E., Hale, C., Zhang, F., Raychaudhuri, S., Troyanskaya, O. G. and Darnell, R. B. (2020) 'RNA Identification of PRIME Cells Predicting Rheumatoid Arthritis Flares', *N Engl J Med,* 383(3), pp. 218-228.
Ormseth, M. J., Solus, J. F., Vickers, K. C., Oeser, A. M., Raggi, P. and Stein, C. M. (2015) 'Utility of Select Plasma MicroRNA for Disease and Cardiovascular Risk Assessment in Patients with Rheumatoid Arthritis', *J Rheumatol,* 42(10), pp. 1746-1751.
Ørom, U. A., Nielsen, F. C. and Lund, A. H. (2008) 'MicroRNA-10a binds the 5'UTR of ribosomal protein mRNAs and enhances their translation', *Mol Cell,* 30(4), pp. 460-71.
Orr, C., Vieira-Sousa, E., Boyle, D. L., Buch, M. H., Buckley, C. D., Cañete, J. D., Catrina, A. I., Choy, E. H. S., Emery, P., Fearon, U., Filer, A., Gerlag, D., Humby, F., Isaacs, J. D., Just, S. A., Lauwerys, B. R., Le Goff, B., Manzo, A., McGarry, T., McInnes, I. B., Najm, A., Pitzalis, C., Pratt, A., Smith, M., Tak, P. P., Thurlings, R., Fonseca, J. E., Veale, D. J. and Tas, S. W. (2017) 'Synovial tissue research: a state-of-the-art review', *Nat Rev Rheumatol,* 13(8), pp. 463-475.
Ospelt, C. (2017) 'Synovial fibroblasts in 2017', *RMD Open,* 3(2), pp. e000471.
Ospelt, C., Brentano, F., Rengel, Y., Stanczyk, J., Kolling, C., Tak, P. P., Gay, R. E., Gay, S. and Kyburz, D. (2008) 'Overexpression of toll-like receptors 3 and 4 in synovial tissue from patients with early rheumatoid arthritis: toll-like receptor expression in early and longstanding arthritis', *Arthritis Rheum,* 58(12), pp. 3684-92.
Ospelt, C. and Gay, S. (2022) 'Epigenetic Epidemiology of Inflammation and Rheumatoid Arthritis', in Michels, K.B. (ed.) *Epigenetic Epidemiology*. Cham: Springer International Publishing, pp. 363-380.
Östör, A., Van den Bosch, F., Papp, K., Asnal, C., Blanco, R., Aelion, J., Alperovich, G., Lu, W., Wang, Z., Soliman, A. M., Eldred, A., Barcomb, L. and Kivitz, A. (2022) 'Efficacy and safety of risankizumab for active psoriatic arthritis: 24-week results from the randomised, double-blind, phase 3 KEEPsAKE 2 trial', *Ann Rheum Dis,* 81(3), pp. 351-358.
Ouboussad, L., Hunt, L., Hensor, E. M. A., Nam, J. L., Barnes, N. A., Emery, P., McDermott, M. F. and Buch, M. H. (2017) 'Profiling microRNAs in individuals at risk of progression to rheumatoid arthritis', *Arthritis Res Ther,* 19(1), pp. 288.
Padyukov, L. (2022) 'Genetics of rheumatoid arthritis', *Semin Immunopathol,* 44(1), pp. 47-62.
Pålsson-McDermott, E. M. and O'Neill, L. A. J. (2020) 'Targeting immunometabolism as an anti-inflammatory strategy', *Cell Res,* 30(4), pp. 300-314.
Panagiotopoulos, A. and Fragoulis, G. E. (2023) 'Comorbidities in Psoriatic Arthritis: A Narrative Review', *Clin Ther,* 45(2), pp. 177-189.
Pandolfi, F., Franza, L., Carusi, V., Altamura, S., Andriollo, G. and Nucera, E. (2020) 'Interleukin-6 in Rheumatoid Arthritis', *Int J Mol Sci,* 21(15).
Pandya, J. M., Lundell, A. C., Andersson, K., Nordström, I., Theander, E. and Rudin, A. (2017) 'Blood chemokine profile in untreated early rheumatoid arthritis: CXCL10 as a disease activity marker', *Arthritis Res Ther,* 19(1), pp. 20.
Panipinto, P. M., Singh, A. K., Shaikh, F. S., Siegel, R. J., Chourasia, M. and Ahmed, S. (2021) 'Takinib Inhibits Inflammation in Human Rheumatoid Arthritis Synovial Fibroblasts by Targeting the Janus Kinase-Signal Transducer and Activator of Transcription 3 (JAK/STAT3) Pathway', *Int J Mol Sci,* 22(22).
Paoletti, A., Rohmer, J., Ly, B., Pascaud, J., Rivière, E., Seror, R., Le Goff, B., Nocturne, G. and Mariette, X. (2019) 'Monocyte/Macrophage Abnormalities Specific to Rheumatoid Arthritis Are Linked to miR-155 and Are Differentially Modulated by Different TNF Inhibitors', *J Immunol,* 203(7), pp. 1766-1775.
Pap, T., Müller-Ladner, U., Gay, R. E. and Gay, S. (2000) 'Fibroblast biology. Role of synovial fibroblasts in the pathogenesis of rheumatoid arthritis', *Arthritis Res,* 2(5), pp. 361-7.
Parish, L. C. (1963) 'An historical approach to the nomenclature of rheumatoid arthritis', *Arthritis Rheum,* 6, pp. 138-58.
Park, J. W., Kim, M. J., Kim, H. A., Kim, J. H., Lee, E. B. and Shin, K. (2022) 'The Aftermath of Tapering Tocilizumab After Achieving Treatment Target in Patients With Rheumatoid Arthritis: A Nationwide Cohort Study', *Front Med (Lausanne),* 9, pp. 839206.

Parra-Bonilla, G., Alvarez, D. F., Al-Mehdi, A. B., Alexeyev, M. and Stevens, T. (2010) 'Critical role for lactate dehydrogenase A in aerobic glycolysis that sustains pulmonary microvascular endothelial cell proliferation', *Am J Physiol Lung Cell Mol Physiol,* 299(4), pp. L513-22.
Parsonage, G., Filer, A. D., Haworth, O., Nash, G. B., Rainger, G. E., Salmon, M. and Buckley, C. D. (2005) 'A stromal address code defined by fibroblasts', *Trends Immunol,* 26(3), pp. 150-6.
Pattacini, L., Boiardi, L., Casali, B. and Salvarani, C. (2010) 'Differential effects of anti-TNF-alpha drugs on fibroblast-like synoviocyte apoptosis', *Rheumatology (Oxford),* 49(3), pp. 480-9.
Pattison, D. J., Symmons, D. P., Lunt, M., Welch, A., Bingham, S. A., Day, N. E. and Silman, A. J. (2005) 'Dietary beta-cryptoxanthin and inflammatory polyarthritis: results from a population-based prospective study', *Am J Clin Nutr,* 82(2), pp. 451-5.
Pattison, E., Harrison, B. J., Griffiths, C. E., Silman, A. J. and Bruce, I. N. (2008) 'Environmental risk factors for the development of psoriatic arthritis: results from a case-control study', *Ann Rheum Dis,* 67(5), pp. 672-6.
Pender, S. L., Quinn, J. J., Sanderson, I. R. and MacDonald, T. T. (2000) 'Butyrate upregulates stromelysin-1 production by intestinal mesenchymal cells', *Am J Physiol Gastrointest Liver Physiol,* 279(5), pp. G918-24.
Peng, D., Fu, M., Wang, M., Wei, Y. and Wei, X. (2022) 'Targeting TGF-β signal transduction for fibrosis and cancer therapy', *Mol Cancer,* 21(1), pp. 104.
Peschken, C. A. and Esdaile, J. M. (1999) 'Rheumatic diseases in North America's indigenous peoples', *Semin Arthritis Rheum,* 28(6), pp. 368-91.
Peters, K., Kamp, G., Berz, A., Unger, R. E., Barth, S., Salamon, A., Rychly, J. and Kirkpatrick, C. J. (2009) 'Changes in human endothelial cell energy metabolic capacities during in vitro cultivation. The role of "aerobic glycolysis" and proliferation', *Cell Physiol Biochem,* 24(5-6), pp. 483-92.
Petersons, C. J., Mangelsdorf, B. L., Jenkins, A. B., Poljak, A., Smith, M. D., Greenfield, J. R., Thompson, C. H. and Burt, M. G. (2013) 'Effects of low-dose prednisolone on hepatic and peripheral insulin sensitivity, insulin secretion, and abdominal adiposity in patients with inflammatory rheumatologic disease', *Diabetes Care,* 36(9), pp. 2822-9.
Petrasca, A., Phelan, J. J., Ansboro, S., Veale, D. J., Fearon, U. and Fletcher, J. M. (2020) 'Targeting bioenergetics prevents CD4 T cell-mediated activation of synovial fibroblasts in rheumatoid arthritis', *Rheumatology (Oxford),* 59(10), pp. 2816-2828.
Pineda, C. and Sandoval, H. (2023) 'Tracing our roots: on the relevance of rheumatology history', *Clinical Rheumatology,* 42(11), pp. 2929-2930.
Pittenger, M. F., Discher, D. E., Péault, B. M., Phinney, D. G., Hare, J. M. and Caplan, A. I. (2019) 'Mesenchymal stem cell perspective: cell biology to clinical progress', *npj Regenerative Medicine,* 4(1), pp. 22.
Plenge, R. M., Seielstad, M., Padyukov, L., Lee, A. T., Remmers, E. F., Ding, B., Liew, A., Khalili, H., Chandrasekaran, A., Davies, L. R., Li, W., Tan, A. K., Bonnard, C., Ong, R. T., Thalamuthu, A., Pettersson, S., Liu, C., Tian, C., Chen, W. V., Carulli, J. P., Beckman, E. M., Altshuler, D., Alfredsson, L., Criswell, L. A., Amos, C. I., Seldin, M. F., Kastner, D. L., Klareskog, L. and Gregersen, P. K. (2007) 'TRAF1-C5 as a risk locus for rheumatoid arthritis--a genomewide study', *N Engl J Med,* 357(12), pp. 1199-209.
Pohlers, D., Beyer, A., Koczan, D., Wilhelm, T., Thiesen, H. J. and Kinne, R. W. (2007) 'Constitutive upregulation of the transforming growth factor-beta pathway in rheumatoid arthritis synovial fibroblasts', *Arthritis Res Ther,* 9(3), pp. R59.
Poliseno, L., Tuccoli, A., Mariani, L., Evangelista, M., Citti, L., Woods, K., Mercatanti, A., Hammond, S. and Rainaldi, G. (2006) 'MicroRNAs modulate the angiogenic properties of HUVECs', *Blood,* 108(9), pp. 3068-71.
Povoleri, G. A. M., Durham, L. E., Gray, E. H., Lalnunhlimi, S., Kannambath, S., Pitcher, M. J., Dhami, P., Leeuw, T., Ryan, S. E., Steel, K. J. A., Kirkham, B. W. and Taams, L. S. (2023) 'Psoriatic and rheumatoid arthritis joints differ in the composition of CD8+ tissue-resident memory T cell subsets', *Cell Rep,* 42(5), pp. 112514.

Prasad, P., Verma, S., Surbhi, Ganguly, N. K., Chaturvedi, V. and Mittal, S. A. (2023) 'Rheumatoid arthritis: advances in treatment strategies', *Mol Cell Biochem,* 478(1), pp. 69-88.
Pucino, V., Bombardieri, M., Pitzalis, C. and Mauro, C. (2017) 'Lactate at the crossroads of metabolism, inflammation, and autoimmunity', *Eur J Immunol,* 47(1), pp. 14-21.
Pucino, V., Certo, M., Varricchi, G., Marone, G., Ursini, F., Rossi, F. W., De Paulis, A., Mauro, C., Raza, K. and Buckley, C. D. (2020) 'Metabolic Checkpoints in Rheumatoid Arthritis', *Front Physiol,* 11, pp. 347.
Qu, Z., Garcia, C. H., O'Rourke, L. M., Planck, S. R., Kohli, M. and Rosenbaum, J. T. (1994) 'Local proliferation of fibroblast-like synoviocytes contributes to synovial hyperplasia. Results of proliferating cell nuclear antigen/cyclin, c-myc, and nucleolar organizer region staining', *Arthritis Rheum,* 37(2), pp. 212-20.
Qu, Z., Li, W. and Fu, B. (2014) 'MicroRNAs in autoimmune diseases', *Biomed Res Int,* 2014, pp. 527895.
Queiro, R. and Pardo, E. (2024) 'In the search for an accurate and early diagnosis of psoriatic arthritis: is the key in ultrasound?', *Rheumatology (Oxford),* 63(10), pp. 2608-2610.
Quintero-Fabián, S., Arreola, R., Becerril-Villanueva, E., Torres-Romero, J. C., Arana-Argáez, V., Lara-Riegos, J., Ramírez-Camacho, M. A. and Alvarez-Sánchez, M. E. (2019) 'Role of Matrix Metalloproteinases in Angiogenesis and Cancer', *Front Oncol,* 9, pp. 1370.
Rakieh, C., Nam, J. L., Hunt, L., Hensor, E. M., Das, S., Bissell, L. A., Villeneuve, E., McGonagle, D., Hodgson, R., Grainger, A., Wakefield, R. J., Conaghan, P. G. and Emery, P. (2015) 'Predicting the development of clinical arthritis in anti-CCP positive individuals with non-specific musculoskeletal symptoms: a prospective observational cohort study', *Ann Rheum Dis,* 74(9), pp. 1659-66.
Rana, A. K., Li, Y., Dang, Q. and Yang, F. (2018) 'Monocytes in rheumatoid arthritis: Circulating precursors of macrophages and osteoclasts and, their heterogeneity and plasticity role in RA pathogenesis', *Int Immunopharmacol,* 65, pp. 348-359.
Rani, V. and Sengar, R. S. (2022) 'Biogenesis and mechanisms of microRNA-mediated gene regulation', *Biotechnology and Bioengineering,* 119(3), pp. 685-692.
Rao, J., Yue, S., Fu, Y., Zhu, J., Wang, X., Busuttil, R. W., Kupiec-Weglinski, J. W., Lu, L. and Zhai, Y. (2014) 'ATF6 mediates a pro-inflammatory synergy between ER stress and TLR activation in the pathogenesis of liver ischemia-reperfusion injury', *Am J Transplant,* 14(7), pp. 1552-61.
Rauber, S., Mohammadian, H., Schmidkonz, C., Atzinger, A., Soare, A., Treutlein, C., Kemble, S., Mahony, C. B., Geisthoff, M., Angeli, M. R., Raimondo, M. G., Xu, C., Yang, K. T., Lu, L., Labinsky, H., Saad, M. S. A., Gwellem, C. A., Chang, J., Huang, K., Kampylafka, E., Knitza, J., Bilyy, R., Distler, J. H. W., Hanlon, M. M., Fearon, U., Veale, D. J., Roemer, F. W., Bäuerle, T., Maric, H. M., Maschauer, S., Ekici, A. B., Buckley, C. D., Croft, A. P., Kuwert, T., Prante, O., Cañete, J. D., Schett, G. and Ramming, A. (2024) 'CD200(+) fibroblasts form a pro-resolving mesenchymal network in arthritis', *Nat Immunol,* 25(4), pp. 682-692.
Raychaudhuri, S., Sandor, C., Stahl, E. A., Freudenberg, J., Lee, H. S., Jia, X., Alfredsson, L., Padyukov, L., Klareskog, L., Worthington, J., Siminovitch, K. A., Bae, S. C., Plenge, R. M., Gregersen, P. K. and de Bakker, P. I. (2012) 'Five amino acids in three HLA proteins explain most of the association between MHC and seropositive rheumatoid arthritis', *Nat Genet,* 44(3), pp. 291-6.
Reece, R. J., Canete, J. D., Parsons, W. J., Emery, P. and Veale, D. J. (1999) 'Distinct vascular patterns of early synovitis in psoriatic, reactive, and rheumatoid arthritis', *Arthritis Rheum,* 42(7), pp. 1481-4.
Remmers, E. F., Plenge, R. M., Lee, A. T., Graham, R. R., Hom, G., Behrens, T. W., de Bakker, P. I., Le, J. M., Lee, H. S., Batliwalla, F., Li, W., Masters, S. L., Booty, M. G., Carulli, J. P., Padyukov, L., Alfredsson, L., Klareskog, L., Chen, W. V., Amos, C. I., Criswell, L. A., Seldin, M. F., Kastner, D. L. and Gregersen, P. K. (2007) 'STAT4 and the risk of rheumatoid arthritis and systemic lupus erythematosus', *N Engl J Med,* 357(10), pp. 977-86.
Rice, S. J., Roberts, J. B., Tselepi, M., Brumwell, A., Falk, J., Steven, C. and Loughlin, J. (2021) 'Genetic and Epigenetic Fine-Tuning of TGFB1 Expression Within the Human Osteoarthritic Joint', *Arthritis Rheumatol,* 73(10), pp. 1866-1877.

Richards, C. D. and Agro, A. (1994) 'Interaction between oncostatin M, interleukin 1 and prostaglandin E2 in induction of IL-6 expression in human fibroblasts', *Cytokine,* 6(1), pp. 40-7.
Ritchlin, C., Rahman, P., Kavanaugh, A., McInnes, I. B., Puig, L., Li, S., Wang, Y., Shen, Y. K., Doyle, M. K., Mendelsohn, A. M. and Gottlieb, A. B. (2014) 'Efficacy and safety of the anti-IL-12/23 p40 monoclonal antibody, ustekinumab, in patients with active psoriatic arthritis despite conventional non-biological and biological anti-tumour necrosis factor therapy: 6-month and 1-year results of the phase 3, multicentre, double-blind, placebo-controlled, randomised PSUMMIT 2 trial', *Ann Rheum Dis,* 73(6), pp. 990-9.
Rogers, J., Watt, I. and Dieppe, P. (1981) 'Arthritis in Saxon and mediaeval skeletons', *Br Med J (Clin Res Ed),* 283(6307), pp. 1668-70.
Rosengren, S., Corr, M. and Boyle, D. L. (2010) 'Platelet-derived growth factor and transforming growth factor beta synergistically potentiate inflammatory mediator synthesis by fibroblast-like synoviocytes', *Arthritis Res Ther,* 12(2), pp. R65.
Rosengren, S., Corr, M., Firestein, G. S. and Boyle, D. L. (2012) 'The JAK inhibitor CP-690,550 (tofacitinib) inhibits TNF-induced chemokine expression in fibroblast-like synoviocytes: autocrine role of type I interferon', *Ann Rheum Dis,* 71(3), pp. 440-7.
Rossol, M., Kraus, S., Pierer, M., Baerwald, C. and Wagner, U. (2012) 'The CD14(bright) CD16+ monocyte subset is expanded in rheumatoid arthritis and promotes expansion of the Th17 cell population', *Arthritis Rheum,* 64(3), pp. 671-7.
Ruan, G. X. and Kazlauskas, A. (2013) 'Lactate engages receptor tyrosine kinases Axl, Tie2, and vascular endothelial growth factor receptor 2 to activate phosphoinositide 3-kinase/Akt and promote angiogenesis', *J Biol Chem,* 288(29), pp. 21161-21172.
Russolillo, A., Iervolino, S., Peluso, R., Lupoli, R., Di Minno, A., Pappone, N. and Di Minno, M. N. (2013) 'Obesity and psoriatic arthritis: from pathogenesis to clinical outcome and management', *Rheumatology (Oxford),* 52(1), pp. 62-7.
Saadawy, S. F., El-Ghareeb, M. I. and Talaat, A. (2024) 'MicroRNA-21 and MicroRNA-125b expression in skin tissue and serum as predictive biomarkers for psoriasis', *Int J Dermatol,* 63(3), pp. 322-329.
Saalfeld, W., Mixon, A. M., Zelie, J. and Lydon, E. J. (2021) 'Differentiating Psoriatic Arthritis from Osteoarthritis and Rheumatoid Arthritis: A Narrative Review and Guide for Advanced Practice Providers', *Rheumatol Ther,* 8(4), pp. 1493-1517.
Saber, T. P., Ng, C. T., Renard, G., Lynch, B. M., Pontifex, E., Walsh, C. A., Grier, A., Molloy, M., Bresnihan, B., Fitzgerald, O., Fearon, U. and Veale, D. J. (2010) 'Remission in psoriatic arthritis: is it possible and how can it be predicted?', *Arthritis Res Ther,* 12(3), pp. R94.
Sadakierska-Chudy, A. (2020) 'MicroRNAs: Diverse Mechanisms of Action and Their Potential Applications as Cancer Epi-Therapeutics', *Biomolecules,* 10(9), pp. 1285.
Salemi, M., Marchese, G., Lanza, G., Cosentino, F. I. I., Salluzzo, M. G., Schillaci, F. A., Ventola, G. M., Cordella, A., Ravo, M. and Ferri, R. (2022) 'Role and Dysregulation of miRNA in Patients with Parkinson's Disease', *Int J Mol Sci,* 24(1).
Salmi, M., Rajala, P. and Jalkanen, S. (1997) 'Homing of mucosal leukocytes to joints. Distinct endothelial ligands in synovium mediate leukocyte-subtype specific adhesion', *J Clin Invest,* 99(9), pp. 2165-72.
Sanjabi, S., Zenewicz, L. A., Kamanaka, M. and Flavell, R. A. (2009) 'Anti-inflammatory and pro-inflammatory roles of TGF-beta, IL-10, and IL-22 in immunity and autoimmunity', *Curr Opin Pharmacol,* 9(4), pp. 447-53.
Sapieha, P., Sirinyan, M., Hamel, D., Zaniolo, K., Joyal, J. S., Cho, J. H., Honoré, J. C., Kermorvant-Duchemin, E., Varma, D. R., Tremblay, S., Leduc, M., Rihakova, L., Hardy, P., Klein, W. H., Mu, X., Mamer, O., Lachapelle, P., Di Polo, A., Beauséjour, C., Andelfinger, G., Mitchell, G., Sennlaub, F. and Chemtob, S. (2008) 'The succinate receptor GPR91 in neurons has a major role in retinal angiogenesis', *Nat Med,* 14(10), pp. 1067-76.
Savage, A. K., Gutschow, M. V., Chiang, T., Henderson, K., Green, R., Chaudhari, M., Swanson, E., Heubeck, A. T., Kondza, N., Burley, K. C., Genge, P. C., Lord, C., Smith, T., Thomson, Z., Beaubien, A.,

Johnson, E., Goldy, J., Bolouri, H., Buckner, J. H., Meijer, P., Coffey, E. M., Skene, P. J., Torgerson, T. R., Li, X. J. and Bumol, T. F. (2021) 'Multimodal analysis for human ex vivo studies shows extensive molecular changes from delays in blood processing', *iScience,* 24(5), pp. 102404.
Scarneo, S. A., Eibschutz, L. S., Bendele, P. J., Yang, K. W., Totzke, J., Hughes, P., Fox, D. A. and Haystead, T. A. J. (2019) 'Pharmacological inhibition of TAK1, with the selective inhibitor takinib, alleviates clinical manifestation of arthritis in CIA mice', *Arthritis Res Ther,* 21(1), pp. 292.
Scharstuhl, A., Vitters, E. L., van der Kraan, P. M. and van den Berg, W. B. (2003) 'Reduction of osteophyte formation and synovial thickening by adenoviral overexpression of transforming growth factor beta/bone morphogenetic protein inhibitors during experimental osteoarthritis', *Arthritis Rheum,* 48(12), pp. 3442-51.
Scher, J. U., Littman, D. R. and Abramson, S. B. (2016) 'Microbiome in Inflammatory Arthritis and Human Rheumatic Diseases', *Arthritis Rheumatol,* 68(1), pp. 35-45.
Scher, J. U., Sczesnak, A., Longman, R. S., Segata, N., Ubeda, C., Bielski, C., Rostron, T., Cerundolo, V., Pamer, E. G., Abramson, S. B., Huttenhower, C. and Littman, D. R. (2013) 'Expansion of intestinal Prevotella copri correlates with enhanced susceptibility to arthritis', *Elife,* 2, pp. e01202.
Scher, J. U., Ubeda, C., Equinda, M., Khanin, R., Buischi, Y., Viale, A., Lipuma, L., Attur, M., Pillinger, M. H., Weissmann, G., Littman, D. R., Pamer, E. G., Bretz, W. A. and Abramson, S. B. (2012) 'Periodontal disease and the oral microbiota in new-onset rheumatoid arthritis', *Arthritis Rheum,* 64(10), pp. 3083-94.
Schett, G., Elewaut, D., McInnes, I. B., Dayer, J. M. and Neurath, M. F. (2013) 'How cytokine networks fuel inflammation: Toward a cytokine-based disease taxonomy', *Nat Med,* 19(7), pp. 822-4.
Schett, G., McInnes, I. B. and Neurath, M. F. (2021) 'Reframing Immune-Mediated Inflammatory Diseases through Signature Cytokine Hubs', *N Engl J Med,* 385(7), pp. 628-639.
Schett, G., Rahman, P., Ritchlin, C., McInnes, I. B., Elewaut, D. and Scher, J. U. (2022) 'Psoriatic arthritis from a mechanistic perspective', *Nat Rev Rheumatol,* 18(6), pp. 311-325.
Schinnerling, K., Aguillón, J. C., Catalán, D. and Soto, L. (2017) 'The role of interleukin-6 signalling and its therapeutic blockage in skewing the T cell balance in rheumatoid arthritis', *Clin Exp Immunol,* 189(1), pp. 12-20.
Schoors, S., De Bock, K., Cantelmo, A. R., Georgiadou, M., Ghesquière, B., Cauwenberghs, S., Kuchnio, A., Wong, B. W., Quaegebeur, A., Goveia, J., Bifari, F., Wang, X., Blanco, R., Tembuyser, B., Cornelissen, I., Bouché, A., Vinckier, S., Diaz-Moralli, S., Gerhardt, H., Telang, S., Cascante, M., Chesney, J., Dewerchin, M. and Carmeliet, P. (2014) 'Partial and transient reduction of glycolysis by PFKFB3 blockade reduces pathological angiogenesis', *Cell Metab,* 19(1), pp. 37-48.
Scotti, L., Franchi, M., Marchesoni, A. and Corrao, G. (2018) 'Prevalence and incidence of psoriatic arthritis: A systematic review and meta-analysis', *Semin Arthritis Rheum,* 48(1), pp. 28-34.
Segura, E., Touzot, M., Bohineust, A., Cappuccio, A., Chiocchia, G., Hosmalin, A., Dalod, M., Soumelis, V. and Amigorena, S. (2013) 'Human inflammatory dendritic cells induce Th17 cell differentiation', *Immunity,* 38(2), pp. 336-48.
Senyilmaz, D. and Teleman, A. A. (2015) 'Chicken or the egg: Warburg effect and mitochondrial dysfunction', *F1000Prime Rep,* 7, pp. 41.
Serasinghe, M. N., Wieder, S. Y., Renault, T. T., Elkholi, R., Asciolla, J. J., Yao, J. L., Jabado, O., Hoehn, K., Kageyama, Y., Sesaki, H. and Chipuk, J. E. (2015) 'Mitochondrial division is requisite to RAS-induced transformation and targeted by oncogenic MAPK pathway inhibitors', *Mol Cell,* 57(3), pp. 521-36.
Shademan, B., Zakeri, M., Abbasi, S., Biray Avci, C., Karamad, V., Sogutlu, F., Laghousi, D., Nouri, M., Hassanpour, M. and Nourazarian, A. (2023) 'Relationship between miRNA-21, miRNA-155, and miRNA-182 expression and inflammatory factors in cerebrospinal fluid from patients with multiple sclerosis', *Clin Neurol Neurosurg,* 232, pp. 107873.
Shaikh, F. S., Siegel, R. J., Srivastava, A., Fox, D. A. and Ahmed, S. (2023) 'Challenges and promise of targeting miRNA in rheumatic diseases: a computational approach to identify miRNA association with cell types, cytokines, and disease mechanisms', *Front Immunol,* 14, pp. 1322806.

Shams, S., Martinez, J. M., Dawson, J. R. D., Flores, J., Gabriel, M., Garcia, G., Guevara, A., Murray, K., Pacifici, N., Vargas, M. V., Voelker, T., Hell, J. W. and Ashouri, J. F. (2021) 'The Therapeutic Landscape of Rheumatoid Arthritis: Current State and Future Directions', *Front Pharmacol,* 12, pp. 680043.
Shang, W., Zhao, L. J., Dong, X. L., Zhao, Z. M., Li, J., Zhang, B. B. and Cai, H. (2016) 'Curcumin inhibits osteoclastogenic potential in PBMCs from rheumatoid arthritis patients via the suppression of MAPK/RANK/c-Fos/NFATc1 signaling pathways', *Mol Med Rep,* 14(4), pp. 3620-6.
Shen, C. K., Huang, B. R., Yeh, W. L., Chen, C. W., Liu, Y. S., Lai, S. W., Tseng, W. P., Lu, D. Y. and Tsai, C. F. (2021) 'Regulatory effects of IL-1β in the interaction of GBM and tumor-associated monocyte through VCAM-1 and ICAM-1', *Eur J Pharmacol,* 905, pp. 174216.
Shen, N. N., Wang, J. L. and Fu, Y. P. (2022) 'The microRNA Expression Profiling in Heart Failure: A Systematic Review and Meta-Analysis', *Front Cardiovasc Med,* 9, pp. 856358.
Sherlock, J. P., Joyce-Shaikh, B., Turner, S. P., Chao, C. C., Sathe, M., Grein, J., Gorman, D. M., Bowman, E. P., McClanahan, T. K., Yearley, J. H., Eberl, G., Buckley, C. D., Kastelein, R. A., Pierce, R. H., Laface, D. M. and Cua, D. J. (2012) 'IL-23 induces spondyloarthropathy by acting on ROR-γt+ CD3+CD4-CD8- entheseal resident T cells', *Nat Med,* 18(7), pp. 1069-76.
Shervington, L., Darekar, A., Shaikh, M., Mathews, R. and Shervington, A. (2018) 'Identifying Reliable Diagnostic/Predictive Biomarkers for Rheumatoid Arthritis', *Biomark Insights,* 13, pp. 1177271918801005.
Shi, C., Pei, S., Ding, Y., Tao, C., Zhu, Y., Peng, Y., Li, W. and Yi, Y. (2023) 'Exosomes with overexpressed miR 147a suppress angiogenesis and infammatory injury in an experimental model of atopic dermatitis', *Scientific Reports,* 13(1), pp. 8904.
Shibata, S., Saeki, H., Tada, Y., Karakawa, M., Komine, M. and Tamaki, K. (2009) 'Serum high molecular weight adiponectin levels are decreased in psoriasis patients', *J Dermatol Sci,* 55(1), pp. 62-3.
Shibuya, H., Yoshitomi, H., Murata, K., Kobayashi, S., Furu, M., Ishikawa, M., Fujii, T., Ito, H. and Matsuda, S. (2015) 'TNFα, PDGF, and TGFβ synergistically induce synovial lining hyperplasia via inducible PI3Kδ', *Mod Rheumatol,* 25(1), pp. 72-8.
Shimakami, T., Yamane, D., Jangra, R. K., Kempf, B. J., Spaniel, C., Barton, D. J. and Lemon, S. M. (2012) 'Stabilization of hepatitis C virus RNA by an Ago2-miR-122 complex', *Proc Natl Acad Sci U S A,* 109(3), pp. 941-6.
Shirakabe, K., Yamaguchi, K., Shibuya, H., Irie, K., Matsuda, S., Moriguchi, T., Gotoh, Y., Matsumoto, K. and Nishida, E. (1997) 'TAK1 mediates the ceramide signaling to stress-activated protein kinase/c-Jun N-terminal kinase', *J Biol Chem,* 272(13), pp. 8141-4.
Silman, A. J., Newman, J. and MacGregor, A. J. (1996) 'Cigarette smoking increases the risk of rheumatoid arthritis. Results from a nationwide study of disease-discordant twins', *Arthritis Rheum,* 39(5), pp. 732-5.
Simpson, L. J. and Ansel, K. M. (2015) 'MicroRNA regulation of lymphocyte tolerance and autoimmunity', *J Clin Invest,* 125(6), pp. 2242-9.
Singh, A., Patro, P. S. and Aggarwal, A. (2019) 'MicroRNA-132, miR-146a, and miR-155 as potential biomarkers of methotrexate response in patients with rheumatoid arthritis', *Clin Rheumatol,* 38(3), pp. 877-884.
Skoczyńska, M. and Świerkot, J. (2018) 'The role of diet in rheumatoid arthritis', *Reumatologia,* 56(4), pp. 259-267.
Skuli, N., Liu, L., Runge, A., Wang, T., Yuan, L., Patel, S., Iruela-Arispe, L., Simon, M. C. and Keith, B. (2009) 'Endothelial deletion of hypoxia-inducible factor-2alpha (HIF-2alpha) alters vascular function and tumor angiogenesis', *Blood,* 114(2), pp. 469-77.
Slowikowski, K., Nguyen, H. N., Noss, E. H., Simmons, D. P., Mizoguchi, F., Watts, G. F. M., Gurish, M. F., Brenner, M. B. and Raychaudhuri, S. (2020) 'CUX1 and IκBζ (NFKBIZ) mediate the synergistic inflammatory response to TNF and IL-17A in stromal fibroblasts', *Proc Natl Acad Sci U S A,* 117(10), pp. 5532-5541.
Smith, E., McGettrick, H. M., Stone, M. A., Shaw, J. S., Middleton, J., Nash, G. B., Buckley, C. D. and Ed Rainger, G. (2008) 'Duffy antigen receptor for chemokines and CXCL5 are essential for the recruitment

of neutrophils in a multicellular model of rheumatoid arthritis synovium', *Arthritis Rheum,* 58(7), pp. 1968-73.
Smith, M. D. (2011) 'The normal synovium', *Open Rheumatol J,* 5, pp. 100-6.
Smith, M. H., Gao, V. R., Periyakoil, P. K., Kochen, A., DiCarlo, E. F., Goodman, S. M., Norman, T. M., Donlin, L. T., Leslie, C. S. and Rudensky, A. Y. (2023) 'Drivers of heterogeneity in synovial fibroblasts in rheumatoid arthritis', *Nat Immunol,* 24(7), pp. 1200-1210.
Smolarz, B., Durczyński, A., Romanowicz, H., Szyłło, K. and Hogendorf, P. (2022) 'miRNAs in Cancer (Review of Literature)', *International Journal of Molecular Sciences,* 23(5), pp. 2805.
Smolen, J. S., Aletaha, D., Barton, A., Burmester, G. R., Emery, P., Firestein, G. S., Kavanaugh, A., McInnes, I. B., Solomon, D. H., Strand, V. and Yamamoto, K. (2018) 'Rheumatoid arthritis', *Nat Rev Dis Primers,* 4, pp. 18001.
Smolen, J. S., Aletaha, D. and McInnes, I. B. (2016) 'Rheumatoid arthritis', *Lancet,* 388(10055), pp. 2023-2038.
Smolen, J. S., Beaulieu, A., Rubbert-Roth, A., Ramos-Remus, C., Rovensky, J., Alecock, E., Woodworth, T. and Alten, R. (2008) 'Effect of interleukin-6 receptor inhibition with tocilizumab in patients with rheumatoid arthritis (OPTION study): a double-blind, placebo-controlled, randomised trial', *Lancet,* 371(9617), pp. 987-97.
Smolen, J. S., Landewé, R. B. M., Bergstra, S. A., Kerschbaumer, A., Sepriano, A., Aletaha, D., Caporali, R., Edwards, C. J., Hyrich, K. L., Pope, J. E., de Souza, S., Stamm, T. A., Takeuchi, T., Verschueren, P., Winthrop, K. L., Balsa, A., Bathon, J. M., Buch, M. H., Burmester, G. R., Buttgereit, F., Cardiel, M. H., Chatzidionysiou, K., Codreanu, C., Cutolo, M., den Broeder, A. A., El Aoufy, K., Finckh, A., Fonseca, J. E., Gottenberg, J. E., Haavardsholm, E. A., Iagnocco, A., Lauper, K., Li, Z., McInnes, I. B., Mysler, E. F., Nash, P., Poor, G., Ristic, G. G., Rivellese, F., Rubbert-Roth, A., Schulze-Koops, H., Stoilov, N., Strangfeld, A., van der Helm-van Mil, A., van Duuren, E., Vliet Vlieland, T. P. M., Westhovens, R. and van der Heijde, D. (2023) 'EULAR recommendations for the management of rheumatoid arthritis with synthetic and biological disease-modifying antirheumatic drugs: 2022 update', *Ann Rheum Dis,* 82(1), pp. 3-18.
Sonveaux, P., Copetti, T., De Saedeleer, C. J., Végran, F., Verrax, J., Kennedy, K. M., Moon, E. J., Dhup, S., Danhier, P., Frérart, F., Gallez, B., Ribeiro, A., Michiels, C., Dewhirst, M. W. and Feron, O. (2012) 'Targeting the lactate transporter MCT1 in endothelial cells inhibits lactate-induced HIF-1 activation and tumor angiogenesis', *PLoS One,* 7(3), pp. e33418.
Soomro, M., Stadler, M., Dand, N., Bluett, J., Jadon, D., Jalali-Najafabadi, F., Duckworth, M., Ho, P., Marzo-Ortega, H., Helliwell, P. S., Ryan, A. W., Kane, D., Korendowych, E., Simpson, M. A., Packham, J., McManus, R., Gabay, C., Lamacchia, C., Nissen, M. J., Brown, M. A., Verstappen, S. M. M., Van Staa, T., Barker, J. N., Smith, C. H., FitzGerald, O., McHugh, N., Warren, R. B., Bowes, J. and Barton, A. (2022) 'Comparative Genetic Analysis of Psoriatic Arthritis and Psoriasis for the Discovery of Genetic Risk Factors and Risk Prediction Modeling', *Arthritis Rheumatol,* 74(9), pp. 1535-1543.
Spoelstra, F., Postma, D., Hovenga, H., Noordhoek, J. and Kauffman, H. (1999) 'Interferon-gamma and interleukin-4 differentially regulate ICAM-1 and VCAM-1 expression on human lung fibroblasts', *European Respiratory Journal,* 14(4), pp. 759-766.
Stanczyk, J., Pedrioli, D. M., Brentano, F., Sanchez-Pernaute, O., Kolling, C., Gay, R. E., Detmar, M., Gay, S. and Kyburz, D. (2008) 'Altered expression of MicroRNA in synovial fibroblasts and synovial tissue in rheumatoid arthritis', *Arthritis Rheum,* 58(4), pp. 1001-9.
Steele, R., Mott, J. L. and Ray, R. B. (2010) 'MBP-1 upregulates miR-29b that represses Mcl-1, collagens, and matrix-metalloproteinase-2 in prostate cancer cells', *Genes Cancer,* 1(4), pp. 381-387.
Stein, M., Keshav, S., Harris, N. and Gordon, S. (1992) 'Interleukin 4 potently enhances murine macrophage mannose receptor activity: a marker of alternative immunologic macrophage activation', *J Exp Med,* 176(1), pp. 287-92.
Stephenson, W., Donlin, L. T., Butler, A., Rozo, C., Bracken, B., Rashidfarrokhi, A., Goodman, S. M., Ivashkiv, L. B., Bykerk, V. P., Orange, D. E., Darnell, R. B., Swerdlow, H. P. and Satija, R. (2018) 'Single-cell RNA-seq of rheumatoid arthritis synovial tissue using low-cost microfluidic instrumentation', *Nat Commun,* 9(1), pp. 791.

Stolt, P., Yahya, A., Bengtsson, C., Källberg, H., Rönnelid, J., Lundberg, I., Klareskog, L. and Alfredsson, L. (2010) 'Silica exposure among male current smokers is associated with a high risk of developing ACPA-positive rheumatoid arthritis', *Ann Rheum Dis,* 69(6), pp. 1072-6.
Strand, V., Kimberly, R. and Isaacs, J. D. (2007) 'Biologic therapies in rheumatology: lessons learned, future directions', *Nat Rev Drug Discov,* 6(1), pp. 75-92.
Strand, V., Lee, E. B., Fleischmann, R., Alten, R. E., Koncz, T., Zwillich, S. H., Gruben, D., Wilkinson, B., Krishnaswami, S. and Wallenstein, G. (2016) 'Tofacitinib versus methotrexate in rheumatoid arthritis: patient-reported outcomes from the randomised phase III ORAL Start trial', *RMD Open,* 2(2), pp. e000308.
Strand, V., Michalska, M., Birchwood, C., Pei, J., Tuckwell, K., Finch, R., Gabay, C., Kavanaugh, A. and Jones, G. (2017) 'Impact of tocilizumab monotherapy on patient-reported outcomes in patients with rheumatoid arthritis from two randomised controlled trials', *RMD Open,* 3(2), pp. e000496.
Stuart, T. and Satija, R. (2019) 'Integrative single-cell analysis', *Nat Rev Genet,* 20(5), pp. 257-272.
Suárez, Y., Fernández-Hernando, C., Pober, J. S. and Sessa, W. C. (2007) 'Dicer dependent microRNAs regulate gene expression and functions in human endothelial cells', *Circ Res,* 100(8), pp. 1164-73.
Sudoł-Szopińska, I., Kontny, E., Maśliński, W., Prochorec-Sobieszek, M., Kwiatkowska, B., Zaniewicz-Kaniewska, K. and Warczyńska, A. (2012) 'The pathogenesis of rheumatoid arthritis in radiological studies. Part I: Formation of inflammatory infiltrates within the synovial membrane', *J Ultrason,* 12(49), pp. 202-13.
Sun, J., Li, L., Li, L., Ding, L., Liu, X., Chen, X., Zhang, J., Qi, X., Du, J. and Huang, Z. (2018a) 'Metallothionein-1 suppresses rheumatoid arthritis pathogenesis by shifting the Th17/Treg balance', *Eur J Immunol,* 48(9), pp. 1550-1562.
Sun, L. L., Li, W. D., Lei, F. R. and Li, X. Q. (2018b) 'The regulatory role of microRNAs in angiogenesis-related diseases', *J Cell Mol Med,* 22(10), pp. 4568-4587.
Sun, Y., Li, Y. and Zhang, J. (2022) 'The causal relationship between psoriasis, psoriatic arthritis, and inflammatory bowel diseases', *Scientific Reports,* 12(1), pp. 20526.
Sun, Y., Zhu, D., Wang, G., Wang, D., Zhou, H., Liu, X., Jiang, M., Liao, L., Zhou, Z. and Hu, J. (2015) 'Pro-Inflammatory Cytokine IL-1β Up-Regulates CXC Chemokine Receptor 4 via Notch and ERK Signaling Pathways in Tongue Squamous Cell Carcinoma', *PLoS One,* 10(7), pp. e0132677.
Sun, Z., Ren, M., Niu, J., Tang, G., Li, Y., Kong, F. and Song, X. (2024) 'miR-29b-3p targetedly regulates VEGF to inhibit tumor progression and cisplatin resistance through Nrf2/HO-1 signaling pathway in non-small cell lung cancer', *Environ Toxicol,* 39(7), pp. 3956-3966.
Sundström, B., Johansson, I. and Rantapää-Dahlqvist, S. (2015) 'Diet and alcohol as risk factors for rheumatoid arthritis: a nested case-control study', *Rheumatol Int,* 35(3), pp. 533-9.
Suwa, Y., Nagafuchi, Y., Yamada, S. and Fujio, K. (2023) 'The role of dendritic cells and their immunometabolism in rheumatoid arthritis', *Front Immunol,* 14, pp. 1161148.
Sweet, K., Song, Q., Loza, M. J., McInnes, I. B., Ma, K., Leander, K., Lakshminarayanan, V., Franks, C., Cooper, P. and Siebert, S. (2021) 'Guselkumab induces robust reduction in acute phase proteins and type 17 effector cytokines in active psoriatic arthritis: results from phase 3 trials', *RMD Open,* 7(2).
Symmons, D. P. (2005) 'Looking back: rheumatoid arthritis--aetiology, occurrence and mortality', *Rheumatology (Oxford),* 44 Suppl 4, pp. iv14-iv17.
Symons, R. A., Colella, F., Collins, F. L., Rafipay, A. J., Kania, K., McClure, J. J., White, N., Cunningham, I., Ashraf, S., Hay, E., Mackenzie, K. S., Howard, K. A., Riemen, A. H. K., Manzo, A., Clark, S. M., Roelofs, A. J. and De Bari, C. (2022) 'Targeting the IL-6-Yap-Snail signalling axis in synovial fibroblasts ameliorates inflammatory arthritis', *Ann Rheum Dis,* 81(2), pp. 214-224.
Szklarczyk, D., Gable, A. L., Lyon, D., Junge, A., Wyder, S., Huerta-Cepas, J., Simonovic, M., Doncheva, N. T., Morris, J. H., Bork, P., Jensen, L. J. and Mering, C. V. (2019) 'STRING v11: protein-protein association networks with increased coverage, supporting functional discovery in genome-wide experimental datasets', *Nucleic Acids Res,* 47(D1), pp. D607-d613.
Szydlowska, K., Bot, A., Nizinska, K., Olszewski, M. and Lukasiuk, K. (2024) 'Circulating microRNAs from plasma as preclinical biomarkers of epileptogenesis and epilepsy', *Scientific Reports,* 14(1), pp. 708.

Takaesu, G., Ninomiya-Tsuji, J., Kishida, S., Li, X., Stark, G. R. and Matsumoto, K. (2001) 'Interleukin-1 (IL-1) receptor-associated kinase leads to activation of TAK1 by inducing TAB2 translocation in the IL-1 signaling pathway', *Mol Cell Biol,* 21(7), pp. 2475-84.
Takahashi, S., Saegusa, J., Sendo, S., Okano, T., Akashi, K., Irino, Y. and Morinobu, A. (2017) 'Glutaminase 1 plays a key role in the cell growth of fibroblast-like synoviocytes in rheumatoid arthritis', *Arthritis Res Ther,* 19(1), pp. 76.
Takayanagi, H., Iizuka, H., Juji, T., Nakagawa, T., Yamamoto, A., Miyazaki, T., Koshihara, Y., Oda, H., Nakamura, K. and Tanaka, S. (2000) 'Involvement of receptor activator of nuclear factor kappaB ligand/osteoclast differentiation factor in osteoclastogenesis from synoviocytes in rheumatoid arthritis', *Arthritis Rheum,* 43(2), pp. 259-69.
Takeda, T., Mizugaki, Y., Matsubara, L., Imai, S., Koike, T. and Takada, K. (2000) 'Lytic Epstein-Barr virus infection in the synovial tissue of patients with rheumatoid arthritis', *Arthritis Rheum,* 43(6), pp. 1218-25.
Takeuchi, T., Tanaka, Y., Amano, K., Hoshi, D., Nawata, M., Nagasawa, H., Sato, E., Saito, K., Kaneko, Y., Fukuyo, S., Kurasawa, T., Hanami, K., Kameda, H. and Yamanaka, H. (2011) 'Clinical, radiographic and functional effectiveness of tocilizumab for rheumatoid arthritis patients--REACTION 52-week study', *Rheumatology (Oxford),* 50(10), pp. 1908-15.
Tanaka, T. and Kishimoto, T. (2014) 'The biology and medical implications of interleukin-6', *Cancer Immunol Res,* 2(4), pp. 288-94.
Tandon, P., Abrams, N. D., Carrick, D. M., Chander, P., Dwyer, J., Fuldner, R., Gannot, G., Laughlin, M., McKie, G., PrabhuDas, M., Singh, A., Tsai, S. A., Vedamony, M. M., Wang, C. and Liu, C. H. (2021) 'Metabolic Regulation of Inflammation and Its Resolution: Current Status, Clinical Needs, Challenges, and Opportunities', *J Immunol,* 207(11), pp. 2625-2630.
Tang, H., Zhang, J., Yu, Z., Ye, L., Li, K., Ding, F., Feng, X. and Meng, W. (2017a) 'Mir-452-3p: A Potential Tumor Promoter That Targets the CPEB3/EGFR Axis in Human Hepatocellular Carcinoma', *Technol Cancer Res Treat,* 16(6), pp. 1136-1149.
Tang, J., Lin, J., Yu, Z., Jiang, R., Xia, J., Yang, B., Ou, Q. and Lin, J. (2022) 'Identification of circulating miR-22-3p and let-7a-5p as novel diagnostic biomarkers for rheumatoid arthritis', *Clin Exp Rheumatol,* 40(1), pp. 69-77.
Tang, Y., Wang, B., Sun, X., Li, H., Ouyang, X., Wei, J., Dai, B., Zhang, Y. and Li, X. (2017b) 'Rheumatoid arthritis fibroblast-like synoviocytes co-cultured with PBMC increased peripheral CD4(+) CXCR5(+) ICOS(+) T cell numbers', *Clin Exp Immunol,* 190(3), pp. 384-393.
Tao, J., Kamanaka, M., Hao, J., Hao, Z., Jiang, X., Craft, J. E., Flavell, R. A., Wu, Z., Hong, Z., Zhao, L. and Yin, Z. (2011) 'IL-10 signaling in CD4+ T cells is critical for the pathogenesis of collagen-induced arthritis', *Arthritis Res Ther,* 13(6), pp. R212.
Tas, S. W., Maracle, C. X., Balogh, E. and Szekanecz, Z. (2016) 'Targeting of proangiogenic signalling pathways in chronic inflammation', *Nat Rev Rheumatol,* 12(2), pp. 111-22.
Täubel, J., Hauke, W., Rump, S., Viereck, J., Batkai, S., Poetzsch, J., Rode, L., Weigt, H., Genschel, C., Lorch, U., Theek, C., Levin, A. A., Bauersachs, J., Solomon, S. D. and Thum, T. (2021) 'Novel antisense therapy targeting microRNA-132 in patients with heart failure: results of a first-in-human Phase 1b randomized, double-blind, placebo-controlled study', *Eur Heart J,* 42(2), pp. 178-188.
Tavasolian, F., Abdollahi, E., Rezaei, R., Momtazi-Borojeni, A. A., Henrotin, Y. and Sahebkar, A. (2018) 'Altered Expression of MicroRNAs in Rheumatoid Arthritis', *J Cell Biochem,* 119(1), pp. 478-487.
Taylor, C. T. (2008) 'Interdependent roles for hypoxia inducible factor and nuclear factor-kappaB in hypoxic inflammation', *J Physiol,* 586(17), pp. 4055-9.
Taylor, P. C., Atzeni, F., Balsa, A., Gossec, L., Müller-Ladner, U. and Pope, J. (2021) 'The Key Comorbidities in Patients with Rheumatoid Arthritis: A Narrative Review', *J Clin Med,* 10(3).
Taylor, W., Gladman, D., Helliwell, P., Marchesoni, A., Mease, P. and Mielants, H. (2006) 'Classification criteria for psoriatic arthritis: development of new criteria from a large international study', *Arthritis Rheum,* 54(8), pp. 2665-73.

Telfer, N. R., Chalmers, R. J., Whale, K. and Colman, G. (1992) 'The role of streptococcal infection in the initiation of guttate psoriasis', *Arch Dermatol,* 128(1), pp. 39-42.
Theunssens, X., Bricman, L., Dierckx, S., Sapart, E., Sokolova, T., Avramovska, A. and Durez, P. (2022) 'Anti-TNF Induced Sarcoidosis-Like Disease in Rheumatoid Arthritis Patients: Review Cases from the RA UCLouvain Brussels Cohort', *Rheumatol Ther,* 9(2), pp. 763-770.
Thomas, G., Tacke, R., Hedrick, C. C. and Hanna, R. N. (2015) 'Nonclassical patrolling monocyte function in the vasculature', *Arterioscler Thromb Vasc Biol,* 35(6), pp. 1306-16.
Thomson, W., Barton, A., Ke, X., Eyre, S., Hinks, A., Bowes, J., Donn, R., Symmons, D., Hider, S., Bruce, I. N., Wilson, A. G., Marinou, I., Morgan, A., Emery, P., Carter, A., Steer, S., Hocking, L., Reid, D. M., Wordsworth, P., Harrison, P., Strachan, D. and Worthington, J. (2007) 'Rheumatoid arthritis association at 6q23', *Nat Genet,* 39(12), pp. 1431-3.
Thorarensen, S. M., Lu, N., Ogdie, A., Gelfand, J. M., Choi, H. K. and Love, T. J. (2017) 'Physical trauma recorded in primary care is associated with the onset of psoriatic arthritis among patients with psoriasis', *Ann Rheum Dis,* 76(3), pp. 521-525.
Thorleifsdottir, R. H., Eysteinsdóttir, J. H., Olafsson, J. H., Sigurdsson, M. I., Johnston, A., Valdimarsson, H. and Sigurgeirsson, B. (2016) 'Throat Infections are Associated with Exacerbation in a Substantial Proportion of Patients with Chronic Plaque Psoriasis', *Acta Derm Venereol,* 96(6), pp. 788-91.
Thrastardottir, T., Meer, E., Hauksdottir, A., Gudbjornsson, B., Kristinsson, S. Y., Ogdie, A. and Love, T. J. (2023) 'Strong site-specific association of pharyngeal cultures with the onset of psoriatic arthritis and psoriasis, regardless of pathogen', *Rheumatology (Oxford),* 62(2), pp. 886-893.
Tillett, W., Jadon, D., Shaddick, G., Cavill, C., Korendowych, E., de Vries, C. S. and McHugh, N. (2013) 'Smoking and delay to diagnosis are associated with poorer functional outcome in psoriatic arthritis', *Ann Rheum Dis,* 72(8), pp. 1358-61.
Tinggaard, A. B., de Thurah, A., Andersen, I. T., Riis, A. H., Therkildsen, J., Winther, S., Hauge, E. M. and Bøttcher, M. (2020) 'Rheumatoid Arthritis as a Risk Factor for Coronary Artery Calcification and Obstructive Coronary Artery Disease in Patients with Chest Pain: A Registry Based Cross-Sectional Study', *Clin Epidemiol,* 12, pp. 679-689.
Tobin, A.-M., Veale, D. J., Fitzgerald, O., Rogers, S., Collins, P., O'SHEA, D. and Kirby, B. (2010) 'Cardiovascular disease and risk factors in patients with psoriasis and psoriatic arthritis', *The Journal of rheumatology,* 37(7), pp. 1386-1394.
Tolboom, T. C., Pieterman, E., van der Laan, W. H., Toes, R. E., Huidekoper, A. L., Nelissen, R. G., Breedveld, F. C. and Huizinga, T. W. (2002) 'Invasive properties of fibroblast-like synoviocytes: correlation with growth characteristics and expression of MMP-1, MMP-3, and MMP-10', *Ann Rheum Dis,* 61(11), pp. 975-80.
Tong, X., Yu, D., Yu, L., Chen, W., Wen, Y. and Gu, P. (2021) 'Exploring the role of monocyte chemoattractant protein-1 in fibroblast-like synovial cells in rheumatoid arthritis', *PeerJ,* 9, pp. e11973.
Tony, H. P., Feist, E., Aries, P. M., Zinke, S., Krüger, K., Ahlers, J., Albrecht, I., Barrionuevo, C., Kalus, S. and Burkhardt, H. (2022) 'Sarilumab reduces disease activity in rheumatoid arthritis patients with inadequate response to janus kinase inhibitors or tocilizumab in regular care in Germany', *Rheumatol Adv Pract,* 6(1), pp. rkac002.
Torres, L. S., Chweih, H., Fabris, F. C. Z., Gotardo, E. M. F., Leonardo, F. C., Saad, S. T. O., Costa, F. F. and Conran, N. (2022) 'TGF-β1 Reduces Neutrophil Adhesion and Prevents Acute Vaso-Occlusive Processes in Sickle Cell Disease Mice', *Cells,* 11(7).
Totzke, J., Gurbani, D., Raphemot, R., Hughes, P. F., Bodoor, K., Carlson, D. A., Loiselle, D. R., Bera, A. K., Eibschutz, L. S., Perkins, M. M., Eubanks, A. L., Campbell, P. L., Fox, D. A., Westover, K. D., Haystead, T. A. J. and Derbyshire, E. R. (2017) 'Takinib, a Selective TAK1 Inhibitor, Broadens the Therapeutic Efficacy of TNF-α Inhibition for Cancer and Autoimmune Disease', *Cell Chem Biol,* 24(8), pp. 1029-1039.e7.
Trepat, X., Chen, Z. and Jacobson, K. (2012) 'Cell migration', *Compr Physiol,* 2(4), pp. 2369-92.

Tsoi, L. C., Spain, S. L., Knight, J., Ellinghaus, E., Stuart, P. E., Capon, F., Ding, J., Li, Y., Tejasvi, T., Gudjonsson, J. E., Kang, H. M., Allen, M. H., McManus, R., Novelli, G., Samuelsson, L., Schalkwijk, J., Ståhle, M., Burden, A. D., Smith, C. H., Cork, M. J., Estivill, X., Bowcock, A. M., Krueger, G. G., Weger, W., Worthington, J., Tazi-Ahnini, R., Nestle, F. O., Hayday, A., Hoffmann, P., Winkelmann, J., Wijmenga, C., Langford, C., Edkins, S., Andrews, R., Blackburn, H., Strange, A., Band, G., Pearson, R. D., Vukcevic, D., Spencer, C. C., Deloukas, P., Mrowietz, U., Schreiber, S., Weidinger, S., Koks, S., Kingo, K., Esko, T., Metspalu, A., Lim, H. W., Voorhees, J. J., Weichenthal, M., Wichmann, H. E., Chandran, V., Rosen, C. F., Rahman, P., Gladman, D. D., Griffiths, C. E., Reis, A., Kere, J., Nair, R. P., Franke, A., Barker, J. N., Abecasis, G. R., Elder, J. T. and Trembath, R. C. (2012) 'Identification of 15 new psoriasis susceptibility loci highlights the role of innate immunity', *Nat Genet,* 44(12), pp. 1341-8.

Tsukamoto, M., Seta, N., Yoshimoto, K., Suzuki, K., Yamaoka, K. and Takeuchi, T. (2017) 'CD14(bright)CD16+ intermediate monocytes are induced by interleukin-10 and positively correlate with disease activity in rheumatoid arthritis', *Arthritis Res Ther,* 19(1), pp. 28.

Tu, J., Han, D., Fang, Y., Jiang, H., Tan, X., Xu, Z., Wang, X., Hong, W., Li, T. and Wei, W. (2022) 'MicroRNA-10b promotes arthritis development by disrupting CD4(+) T cell subtypes', *Mol Ther Nucleic Acids,* 27, pp. 733-750.

Tu, J., Huang, W., Zhang, W., Mei, J. and Zhu, C. (2021) 'A Tale of Two Immune Cells in Rheumatoid Arthritis: The Crosstalk Between Macrophages and T Cells in the Synovium', *Front Immunol,* 12, pp. 655477.

Tullai, J. W., Schaffer, M. E., Mullenbrock, S., Sholder, G., Kasif, S. and Cooper, G. M. (2007) 'Immediate-early and delayed primary response genes are distinct in function and genomic architecture', *J Biol Chem,* 282(33), pp. 23981-95.

Tunyogi-Csapo, M., Kis-Toth, K., Radacs, M., Farkas, B., Jacobs, J. J., Finnegan, A., Mikecz, K. and Glant, T. T. (2008) 'Cytokine-controlled RANKL and osteoprotegerin expression by human and mouse synovial fibroblasts: Fibroblast-mediated pathologic bone resorption', *Arthritis & Rheumatism,* 58(8), pp. 2397-2408.

Ulgen, E., Ozisik, O. and Sezerman, O. U. (2019) 'pathfindR: An R Package for Comprehensive Identification of Enriched Pathways in Omics Data Through Active Subnetworks', *Front Genet,* 10, pp. 858.

Urbanczyk, M., Zbinden, A. and Schenke-Layland, K. (2022) 'Organ-specific endothelial cell heterogenicity and its impact on regenerative medicine and biomedical engineering applications', *Adv Drug Deliv Rev,* 186, pp. 114323.

Vaahtovuo, J., Munukka, E., Korkeamäki, M., Luukkainen, R. and Toivanen, P. (2008) 'Fecal microbiota in early rheumatoid arthritis', *J Rheumatol,* 35(8), pp. 1500-5.

Vaamonde-García, C., Loureiro, J., Valcárcel-Ares, M. N., Riveiro-Naveira, R. R., Ramil-Gómez, O., Hermida-Carballo, L., Centeno, A., Meijide-Failde, R., Blanco, F. J. and López-Armada, M. J. (2017) 'The mitochondrial inhibitor oligomycin induces an inflammatory response in the rat knee joint', *BMC Musculoskelet Disord,* 18(1), pp. 254.

Vaengebjerg, S., Skov, L., Egeberg, A. and Loft, N. D. (2020) 'Prevalence, Incidence, and Risk of Cancer in Patients With Psoriasis and Psoriatic Arthritis: A Systematic Review and Meta-analysis', *JAMA Dermatol,* 156(4), pp. 421-429.

Valcárcel-Ares, M. N., Riveiro-Naveira, R. R., Vaamonde-García, C., Loureiro, J., Hermida-Carballo, L., Blanco, F. J. and López-Armada, M. J. (2014) 'Mitochondrial dysfunction promotes and aggravates the inflammatory response in normal human synoviocytes', *Rheumatology (Oxford),* 53(7), pp. 1332-43.

van der Geest, K. S. M., Smigielska-Czepiel, K., Park, J.-A., Abdulahad, W. H., Kim, H.-W., Kroesen, B.-J., van den Berg, A., Boots, A. M. H., Lee, E.-B. and Brouwer, E. (2014) 'SF Treg cells transcribing high levels of Bcl-2 and microRNA-21 demonstrate limited apoptosis in RA', *Rheumatology,* 54(5), pp. 950-958.

van der Kraan, P. M. (2018) 'Differential Role of Transforming Growth Factor-beta in an Osteoarthritic or a Healthy Joint', *J Bone Metab,* 25(2), pp. 65-72.

van der Linden, M. P., Knevel, R., Huizinga, T. W. and van der Helm-van Mil, A. H. (2011) 'Classification of rheumatoid arthritis: comparison of the 1987 American College of Rheumatology criteria and the 2010 American College of Rheumatology/European League Against Rheumatism criteria', *Arthritis Rheum,* 63(1), pp. 37-42.
van der Linden, M. P., le Cessie, S., Raza, K., van der Woude, D., Knevel, R., Huizinga, T. W. and van der Helm-van Mil, A. H. (2010) 'Long-term impact of delay in assessment of patients with early arthritis', *Arthritis Rheum,* 62(12), pp. 3537-46.
van Hamburg, J. P., Asmawidjaja, P. S., Davelaar, N., Mus, A. M., Colin, E. M., Hazes, J. M., Dolhain, R. J. and Lubberts, E. (2011) 'Th17 cells, but not Th1 cells, from patients with early rheumatoid arthritis are potent inducers of matrix metalloproteinases and proinflammatory cytokines upon synovial fibroblast interaction, including autocrine interleukin-17A production', *Arthritis Rheum,* 63(1), pp. 73-83.
van Kuijk, A. W., Reinders-Blankert, P., Smeets, T. J., Dijkmans, B. A. and Tak, P. P. (2006) 'Detailed analysis of the cell infiltrate and the expression of mediators of synovial inflammation and joint destruction in the synovium of patients with psoriatic arthritis: implications for treatment', *Ann Rheum Dis,* 65(12), pp. 1551-7.
Vasudevan, S. (2012) 'Posttranscriptional upregulation by microRNAs', *Wiley Interdiscip Rev RNA,* 3(3), pp. 311-30.
Vasudevan, S. and Steitz, J. A. (2007) 'AU-rich-element-mediated upregulation of translation by FXR1 and Argonaute 2', *Cell,* 128(6), pp. 1105-18.
Veale, D., Yanni, G., Rogers, S., Barnes, L., Bresnihan, B. and Fitzgerald, O. (1993) 'Reduced synovial membrane macrophage numbers, ELAM-1 expression, and lining layer hyperplasia in psoriatic arthritis as compared with rheumatoid arthritis', *Arthritis Rheum,* 36(7), pp. 893-900.
Veale, D. J. and Fearon, U. (2015) 'What makes psoriatic and rheumatoid arthritis so different?', *RMD Open,* 1(1), pp. e000025.
Veale, D. J. and Fearon, U. (2018) 'The pathogenesis of psoriatic arthritis', *Lancet,* 391(10136), pp. 2273-2284.
Veale, D. J., Orr, C. and Fearon, U. (2017) 'Cellular and molecular perspectives in rheumatoid arthritis', *Semin Immunopathol,* 39(4), pp. 343-354.
Végran, F., Boidot, R., Michiels, C., Sonveaux, P. and Feron, O. (2011) 'Lactate influx through the endothelial cell monocarboxylate transporter MCT1 supports an NF-κB/IL-8 pathway that drives tumor angiogenesis', *Cancer Res,* 71(7), pp. 2550-60.
Verras, M., Papandreou, I., Lim, A. L. and Denko, N. C. (2008) 'Tumor hypoxia blocks Wnt processing and secretion through the induction of endoplasmic reticulum stress', *Mol Cell Biol,* 28(23), pp. 7212-24.
Vessey, M. P., Villard-Mackintosh, L. and Yeates, D. (1987) 'Oral contraceptives, cigarette smoking and other factors in relation to arthritis', *Contraception,* 35(5), pp. 457-64.
Vlachos, I. S., Zagganas, K., Paraskevopoulou, M. D., Georgakilas, G., Karagkouni, D., Vergoulis, T., Dalamagas, T. and Hatzigeorgiou, A. G. (2015) 'DIANA-miRPath v3.0: deciphering microRNA function with experimental support', *Nucleic Acids Res,* 43(W1), pp. W460-6.
Vogt, L. M., Kwasniewicz, E., Talens, S., Scavenius, C., Bielecka, E., Ekdahl, K. N., Enghild, J. J., Mörgelin, M., Saxne, T., Potempa, J. and Blom, A. M. (2020) 'Apolipoprotein E Triggers Complement Activation in Joint Synovial Fluid of Rheumatoid Arthritis Patients by Binding C1q', *J Immunol,* 204(10), pp. 2779-2790.
Vordenbäumen, S., Braukmann, A., Petermann, K., Scharf, A., Bleck, E., von Mikecz, A., Jose, J. and Schneider, M. (2011) 'Casein α s1 is expressed by human monocytes and upregulates the production of GM-CSF via p38 MAPK', *J Immunol,* 186(1), pp. 592-601.
Waaler, E. (1940) 'ON THE OCCURRENCE OF A FACTOR IN HUMAN SERUM ACTIVATING THE SPECIFIC AGGLUTINATION OF SHEEP BLOOD CORPUSCLES', *Acta Pathologica Microbiologica Scandinavica,* 17(2), pp. 172-188.

Wade, S. M., McGarry, T., Wade, S. C., Fearon, U. and Veale, D. J. (2020) 'Serum MicroRNA Signature as a Diagnostic and Therapeutic Marker in Patients with Psoriatic Arthritis', *J Rheumatol,* 47(12), pp. 1760-1767.
Wade, S. M., Ohnesorge, N., McLoughlin, H., Biniecka, M., Carter, S. P., Trenkman, M., Cunningham, C. C., McGarry, T., Canavan, M., Kennedy, B. N., Veale, D. J. and Fearon, U. (2019a) 'Dysregulated miR-125a promotes angiogenesis through enhanced glycolysis', *EBioMedicine,* 47, pp. 402-413.
Wade, S. M., Trenkmann, M., McGarry, T., Canavan, M., Marzaioli, V., Wade, S. C., Veale, D. J. and Fearon, U. (2019b) 'Altered expression of microRNA-23a in psoriatic arthritis modulates synovial fibroblast pro-inflammatory mechanisms via phosphodiesterase 4B', *J Autoimmun,* 96, pp. 86-93.
Wahlsten, A., Rütsche, D., Nanni, M., Giampietro, C., Biedermann, T., Reichmann, E. and Mazza, E. (2021) 'Mechanical stimulation induces rapid fibroblast proliferation and accelerates the early maturation of human skin substitutes', *Biomaterials,* 273, pp. 120779.
Wakabayashi, K., Isozaki, T., Tsubokura, Y., Fukuse, S. and Kasama, T. (2021) 'Eotaxin-1/CCL11 is involved in cell migration in rheumatoid arthritis', *Sci Rep,* 11(1), pp. 7937.
Wallenstein, G. V., Kanik, K. S., Wilkinson, B., Cohen, S., Cutolo, M., Fleischmann, R. M., Genovese, M. C., Gomez Reino, J., Gruben, D., Kremer, J., Krishnaswami, S., Lee, E. B., Pascual-Ramos, V., Strand, V. and Zwillich, S. H. (2016) 'Effects of the oral Janus kinase inhibitor tofacitinib on patient-reported outcomes in patients with active rheumatoid arthritis: results of two Phase 2 randomised controlled trials', *Clin Exp Rheumatol,* 34(3), pp. 430-42.
Wang, H., Guan, X., Tu, Y., Zheng, S., Long, J., Li, S., Qi, C., Xie, X., Zhang, H. and Zhang, Y. (2015) 'MicroRNA-29b attenuates non-small cell lung cancer metastasis by targeting matrix metalloproteinase 2 and PTEN', *J Exp Clin Cancer Res,* 34(1), pp. 59.
Wang, L., Fan, Y., Gui, Y., Yang, X., Ye, X., Cao, Y. and Zhang, Z. (2022) 'Endoplasmic reticulum stress triggered autophagy and regulated the phenotype transformation of rheumatoid arthritis synovial fibroblasts via the IRE1/JNK pathway', *Ann Transl Med,* 10(13), pp. 725.
Wang, M., Wey, S., Zhang, Y., Ye, R. and Lee, A. S. (2009) 'Role of the unfolded protein response regulator GRP78/BiP in development, cancer, and neurological disorders', *Antioxid Redox Signal,* 11(9), pp. 2307-16.
Wang, Q., Liang, B., Shirwany, N. A. and Zou, M. H. (2011) '2-Deoxy-D-glucose treatment of endothelial cells induces autophagy by reactive oxygen species-mediated activation of the AMP-activated protein kinase', *PLoS One,* 6(2), pp. e17234.
Wang, Q., Vasey, F. B., Mahfood, J. P., Valeriano, J., Kanik, K. S., Anderson, B. E. and Bridgeford, P. H. (1999) 'V2 regions of 16S ribosomal RNA used as a molecular marker for the species identification of streptococci in peripheral blood and synovial fluid from patients with psoriatic arthritis', *Arthritis Rheum,* 42(10), pp. 2055-9.
Wang, T., Jiao, Y. and Zhang, X. (2021) 'Immunometabolic Pathways and Its Therapeutic Implication in Autoimmune Diseases', *Clin Rev Allergy Immunol,* 60(1), pp. 55-67.
Wang, W., Zhou, H. and Liu, L. (2018) 'Side effects of methotrexate therapy for rheumatoid arthritis: A systematic review', *Eur J Med Chem,* 158, pp. 502-516.
Wang, X., Chen, Z., Fan, X., Li, W., Qu, J., Dong, C., Wang, Z., Ji, Z. and Li, Y. (2020a) 'Inhibition of DNM1L and mitochondrial fission attenuates inflammatory response in fibroblast-like synoviocytes of rheumatoid arthritis', *J Cell Mol Med,* 24(2), pp. 1516-1528.
Wang, X., Wang, X., Jiang, T., Zhang, Z., Xie, N. and Yang, G. (2023) 'MiR-22-3p suppresses NSCLC cell migration and EMT via targeting RAC1 expression', *Funct Integr Genomics,* 23(3), pp. 281.
Wang, Y., Feng, T., Duan, S., Shi, Y., Li, S., Zhang, X. and Zhang, L. (2020b) 'miR-155 promotes fibroblast-like synoviocyte proliferation and inflammatory cytokine secretion in rheumatoid arthritis by targeting FOXO3a', *Exp Ther Med,* 19(2), pp. 1288-1296.
Wang, Z., Bao, H. W. and Ji, Y. (2020) 'A systematic review and meta-analysis of rituximab combined with methotrexate versus methotrexate alone in the treatment of rheumatoid arthritis', *Medicine (Baltimore),* 99(8), pp. e19193.

Wang, Z., Guan, D., Wang, S., Chai, L. Y. A., Xu, S. and Lam, K. P. (2020c) 'Glycolysis and Oxidative Phosphorylation Play Critical Roles in Natural Killer Cell Receptor-Mediated Natural Killer Cell Functions', *Front Immunol,* 11, pp. 202.
Watad, A., Cuthbert, R. J., Amital, H. and McGonagle, D. (2018) 'Enthesitis: Much More Than Focal Insertion Point Inflammation', *Curr Rheumatol Rep,* 20(7), pp. 41.
Watanabe, Y., Namba, A., Aida, Y., Honda, K., Tanaka, H., Suzuki, N., Matsumura, H. and Maeno, M. (2009) 'IL-1beta suppresses the formation of osteoclasts by increasing OPG production via an autocrine mechanism involving celecoxib-related prostaglandins in chondrocytes', *Mediators Inflamm,* 2009, pp. 308596.
Waterborg, C. E. J., Beermann, S., Broeren, M. G. A., Bennink, M. B., Koenders, M. I., van Lent, P., van den Berg, W. B., van der Kraan, P. M. and van de Loo, F. A. J. (2018) 'Protective Role of the MER Tyrosine Kinase via Efferocytosis in Rheumatoid Arthritis Models', *Front Immunol,* 9, pp. 742.
Weber, J. A., Baxter, D. H., Zhang, S., Huang, D. Y., Huang, K. H., Lee, M. J., Galas, D. J. and Wang, K. (2010) 'The microRNA spectrum in 12 body fluids', *Clin Chem,* 56(11), pp. 1733-41.
Wegner, N., Wait, R., Sroka, A., Eick, S., Nguyen, K. A., Lundberg, K., Kinloch, A., Culshaw, S., Potempa, J. and Venables, P. J. (2010) 'Peptidylarginine deiminase from Porphyromonas gingivalis citrullinates human fibrinogen and α-enolase: implications for autoimmunity in rheumatoid arthritis', *Arthritis Rheum,* 62(9), pp. 2662-72.
Wei, K., Korsunsky, I., Marshall, J. L., Gao, A., Watts, G. F. M., Major, T., Croft, A. P., Watts, J., Blazar, P. E., Lange, J. K., Thornhill, T. S., Filer, A., Raza, K., Donlin, L. T., Siebel, C. W., Buckley, C. D., Raychaudhuri, S. and Brenner, M. B. (2020) 'Notch signalling drives synovial fibroblast identity and arthritis pathology', *Nature,* 582(7811), pp. 259-264.
Wei, Y., Shen, X., Li, L., Cao, G., Cai, X., Wang, Y. and Shen, H. (2018) 'TM4SF1 inhibits apoptosis and promotes proliferation, migration and invasion in human gastric cancer cells', *Oncol Lett,* 16(5), pp. 6081-6088.
Weinblatt, M. E., Keystone, E. C., Furst, D. E., Moreland, L. W., Weisman, M. H., Birbara, C. A., Teoh, L. A., Fischkoff, S. A. and Chartash, E. K. (2003) 'Adalimumab, a fully human anti-tumor necrosis factor alpha monoclonal antibody, for the treatment of rheumatoid arthritis in patients taking concomitant methotrexate: the ARMADA trial', *Arthritis Rheum,* 48(1), pp. 35-45.
Weinblatt, M. E., Maier, A. L., Fraser, P. A. and Coblyn, J. S. (1998) 'Longterm prospective study of methotrexate in rheumatoid arthritis: conclusion after 132 months of therapy', *J Rheumatol,* 25(2), pp. 238-42.
Wells, A. F., Edwards, C. J., Kivitz, A. J., Bird, P., Nguyen, D., Paris, M., Teng, L. and Aelion, J. A. (2018) 'Apremilast monotherapy in DMARD-naive psoriatic arthritis patients: results of the randomized, placebo-controlled PALACE 4 trial', *Rheumatology (Oxford),* 57(7), pp. 1253-1263.
Wenzel, S. E., Trudeau, J. B., Barnes, S., Zhou, X., Cundall, M., Westcott, J. Y., McCord, K. and Chu, H. W. (2002) 'TGF-beta and IL-13 synergistically increase eotaxin-1 production in human airway fibroblasts', *J Immunol,* 169(8), pp. 4613-9.
Weyand, C. M. and Goronzy, J. J. (2017) 'Immunometabolism in early and late stages of rheumatoid arthritis', *Nat Rev Rheumatol,* 13(5), pp. 291-301.
Whitty, C., Pernstich, C., Marris, C., McCaskie, A., Jones, M. and Henson, F. (2022) 'Sustained delivery of the bone morphogenetic proteins BMP-2 and BMP-7 for cartilage repair and regeneration in osteoarthritis', *Osteoarthr Cartil Open,* 4(1), pp. 100240.
Widdifield, J., Paterson, J. M., Huang, A. and Bernatsky, S. (2018) 'Causes of Death in Rheumatoid Arthritis: How Do They Compare to the General Population?', *Arthritis Care Res (Hoboken),* 70(12), pp. 1748-1755.
Wiedrick, J. T., Phillips, J. I., Lusardi, T. A., McFarland, T. J., Lind, B., Sandau, U. S., Harrington, C. A., Lapidus, J. A., Galasko, D. R., Quinn, J. F. and Saugstad, J. A. (2019) 'Validation of MicroRNA Biomarkers for Alzheimer's Disease in Human Cerebrospinal Fluid', *J Alzheimers Dis,* 67(3), pp. 875-891.

Wight, T. N., Kang, I., Evanko, S. P., Harten, I. A., Chang, M. Y., Pearce, O. M. T., Allen, C. E. and Frevert, C. W. (2020) 'Versican-A Critical Extracellular Matrix Regulator of Immunity and Inflammation', *Front Immunol,* 11, pp. 512.
Williams, H. J., Willkens, R. F., Samuelson, C. O., Jr., Alarcón, G. S., Guttadauria, M., Yarboro, C., Polisson, R. P., Weiner, S. R., Luggen, M. E., Billingsley, L. M. and et al. (1985) 'Comparison of low-dose oral pulse methotrexate and placebo in the treatment of rheumatoid arthritis. A controlled clinical trial', *Arthritis Rheum,* 28(7), pp. 721-30.
Wilsdon, T. D., Whittle, S. L., Thynne, T. R. and Mangoni, A. A. (2019) 'Methotrexate for psoriatic arthritis', *Cochrane Database Syst Rev,* 1(1), pp. Cd012722.
Wilson, F. C., Icen, M., Crowson, C. S., McEvoy, M. T., Gabriel, S. E. and Kremers, H. M. (2009) 'Time trends in epidemiology and characteristics of psoriatic arthritis over 3 decades: a population-based study', *J Rheumatol,* 36(2), pp. 361-7.
Wilton, K. M., Crowson, C. S. and Matteson, E. L. (2016) 'Malignancy incidence in patients with psoriatic arthritis: a comparison cohort-based incidence study', *Clin Rheumatol,* 35(10), pp. 2603-7.
Winchester, R., Minevich, G., Steshenko, V., Kirby, B., Kane, D., Greenberg, D. A. and FitzGerald, O. (2012) 'HLA associations reveal genetic heterogeneity in psoriatic arthritis and in the psoriasis phenotype', *Arthritis Rheum,* 64(4), pp. 1134-44.
Winthrop, K. L., Mease, P., Kerschbaumer, A., Voll, R. E., Breedveld, F. C., Smolen, J. S., Gottenberg, J. E., Baraliakos, X., Kiener, H. P., Aletaha, D., Isaacs, J. D., Buch, M. H., Crow, M. K., Kay, J., Crofford, L., van Vollenhoven, R. F., Ospelt, C., Siebert, S., Kloppenburg, M., McInnes, I. B., Huizinga, T. W. and Gravallese, E. M. (2024) 'Unmet need in rheumatology: reports from the Advances in Targeted Therapies meeting, 2023', *Ann Rheum Dis,* 83(4), pp. 409-416.
Wright, V. (1956) 'Psoriasis and arthritis', *Ann Rheum Dis,* 15(4), pp. 348-56.
Wu, B., Zhao, T. V., Jin, K., Hu, Z., Abdel, M. P., Warrington, K. J., Goronzy, J. J. and Weyand, C. M. (2021a) 'Mitochondrial aspartate regulates TNF biogenesis and autoimmune tissue inflammation', *Nat Immunol,* 22(12), pp. 1551-1562.
Wu, F., Guo, N. J., Tian, H., Marohn, M., Gearhart, S., Bayless, T. M., Brant, S. R. and Kwon, J. H. (2011) 'Peripheral blood microRNAs distinguish active ulcerative colitis and Crohn's disease', *Inflamm Bowel Dis,* 17(1), pp. 241-50.
Wu, L., Zhang, G., Guo, C., Zhao, X., Shen, D. and Yang, N. (2020a) 'MiR-128-3p mediates TNF-α-induced inflammatory responses by regulating Sirt1 expression in bone marrow mesenchymal stem cells', *Biochem Biophys Res Commun,* 521(1), pp. 98-105.
Wu, S., Li, W. Q., Han, J., Sun, Q. and Qureshi, A. A. (2014) 'Hypercholesterolemia and risk of incident psoriasis and psoriatic arthritis in US women', *Arthritis Rheumatol,* 66(2), pp. 304-10.
Wu, Y., Li, Q., Zhang, R., Dai, X., Chen, W. and Xing, D. (2021b) 'Circulating microRNAs: Biomarkers of disease', *Clin Chim Acta,* 516, pp. 46-54.
Wu, Z. M., Luo, J., Shi, X. D., Zhang, S. X., Zhu, X. B. and Guo, J. (2020b) 'Icariin alleviates rheumatoid arthritis via regulating miR-223-3p/NLRP3 signalling axis', *Autoimmunity,* 53(8), pp. 450-458.
Xia, K., Zhang, Y. and Sun, D. (2020) 'miR-217 and miR-543 downregulation mitigates inflammatory response and myocardial injury in children with viral myocarditis by regulating the SIRT1/AMPK/NF-κB signaling pathway', *Int J Mol Med,* 45(2), pp. 634-646.
Xiao, M., Yang, H., Xu, W., Ma, S., Lin, H., Zhu, H., Liu, L., Liu, Y., Yang, C., Xu, Y., Zhao, S., Ye, D., Xiong, Y. and Guan, K. L. (2012) 'Inhibition of α-KG-dependent histone and DNA demethylases by fumarate and succinate that are accumulated in mutations of FH and SDH tumor suppressors', *Genes Dev,* 26(12), pp. 1326-38.
Xu, Y. R. and Lei, C. Q. (2020) 'TAK1-TABs Complex: A Central Signalosome in Inflammatory Responses', *Front Immunol,* 11, pp. 608976.
Xue, J., Xu, L., Zhu, H., Bai, M., Li, X., Zhao, Z., Zhong, H., Cheng, G., Li, X., Hu, F. and Su, Y. (2020) 'CD14(+)CD16(-) monocytes are the main precursors of osteoclasts in rheumatoid arthritis via expressing Tyro3TK', *Arthritis Res Ther,* 22(1), pp. 221.

Yamaguchi, K., Shirakabe, K., Shibuya, H., Irie, K., Oishi, I., Ueno, N., Taniguchi, T., Nishida, E. and Matsumoto, K. (1995) 'Identification of a Member of the MAPKKK Family as a Potential Mediator of TGF-β Signal Transduction', *Science,* 270(5244), pp. 2008-2011.
Yan, B., Guo, Q., Fu, F. J., Wang, Z., Yin, Z., Wei, Y. B. and Yang, J. R. (2015) 'The role of miR-29b in cancer: regulation, function, and signaling', *Onco Targets Ther,* 8, pp. 539-48.
Yang, C. M., Luo, S. F., Hsieh, H. L., Chi, P. L., Lin, C. C., Wu, C. C. and Hsiao, L. D. (2010) 'Interleukin-1beta induces ICAM-1 expression enhancing leukocyte adhesion in human rheumatoid arthritis synovial fibroblasts: involvement of ERK, JNK, AP-1, and NF-kappaB', *J Cell Physiol,* 224(2), pp. 516-26.
Yang, D. H., Huang, J. Y., Chiou, J. Y. and Wei, J. C. (2018) 'Analysis of Socioeconomic Status in the Patients with Rheumatoid Arthritis', *Int J Environ Res Public Health,* 15(6).
Yang, J., Wang, J., Liang, X., Zhao, H., Lu, J., Ma, Q., Jing, B. and Tian, F. (2019) 'IL-1β increases the expression of inflammatory factors in synovial fluid-derived fibroblast-like synoviocytes via activation of the NF-κB-mediated ERK-STAT1 signaling pathway', *Mol Med Rep,* 20(6), pp. 4993-5001.
Yang, J., Zhang, L., Yu, C., Yang, X. F. and Wang, H. (2014) 'Monocyte and macrophage differentiation: circulation inflammatory monocyte as biomarker for inflammatory diseases', *Biomark Res,* 2(1), pp. 1.
Yang, Q., Zhao, W., Chen, Y., Chen, Y., Shi, J., Qin, R., Wang, H., Wang, R., Yuan, H. and Sun, W. (2021) 'RelA/MicroRNA-30a/NLRP3 signal axis is involved in rheumatoid arthritis via regulating NLRP3 inflammasome in macrophages', *Cell Death & Disease,* 12(11), pp. 1060.
Yao, C. H., Wang, R., Wang, Y., Kung, C. P., Weber, J. D. and Patti, G. J. (2019) 'Mitochondrial fusion supports increased oxidative phosphorylation during cell proliferation', *Elife,* 8.
Yap, H. Y., Tee, S. Z., Wong, M. M., Chow, S. K., Peh, S. C. and Teow, S. Y. (2018) 'Pathogenic Role of Immune Cells in Rheumatoid Arthritis: Implications in Clinical Treatment and Biomarker Development', *Cells,* 7(10).
Ye, L., Wen, Z., Li, Y., Chen, B., Yu, T., Liu, L., Zhang, J., Ma, Y., Xiao, S., Ding, L., Li, L. and Huang, Z. (2014) 'Interleukin-10 attenuation of collagen-induced arthritis is associated with suppression of interleukin-17 and retinoid-related orphan receptor γt production in macrophages and repression of classically activated macrophages', *Arthritis Res Ther,* 16(2), pp. R96.
Yoda, M., Kawamata, T., Paroo, Z., Ye, X., Iwasaki, S., Liu, Q. and Tomari, Y. (2010) 'ATP-dependent human RISC assembly pathways', *Nat Struct Mol Biol,* 17(1), pp. 17-23.
Yoshie, O. and Matsushima, K. (2015) 'CCR4 and its ligands: from bench to bedside', *Int Immunol,* 27(1), pp. 11-20.
Yoshitomi, H. (2019) 'Regulation of Immune Responses and Chronic Inflammation by Fibroblast-Like Synoviocytes', *Front Immunol,* 10, pp. 1395.
Yu, J., Li, T., Liu, Y., Wang, X., Zhang, J., Wang, X., Shi, G., Lou, J., Wang, L., Wang, C. C. and Wang, L. (2020) 'Phosphorylation switches protein disulfide isomerase activity to maintain proteostasis and attenuate ER stress', *Embo j,* 39(10), pp. e103841.
Yu, M., Nguyen, N. D., Huang, Y., Lin, D., Fujimoto, T. N., Molkentine, J. M., Deorukhkar, A., Kang, Y., San Lucas, F. A., Fernandes, C. J., Koay, E. J., Gupta, S., Ying, H., Koong, A. C., Herman, J. M., Fleming, J. B., Maitra, A. and Taniguchi, C. M. (2019) 'Mitochondrial fusion exploits a therapeutic vulnerability of pancreatic cancer', *JCI Insight,* 5(16).
Yuliasih, Y., Handoyo, M., Rahmawati, L. D., Wibisono, S. and Nisa, N. (2023) 'Correlation Between Insulin Resistance and Psoriatic Arthritis Disease Activity: A Cross-Sectional Study', *Journal of Psoriasis and Psoriatic Arthritis®,* 8(4), pp. 129-133.
Yun, H., Xie, F., Delzell, E., Chen, L., Levitan, E. B., Lewis, J. D., Saag, K. G., Beukelman, T., Winthrop, K., Baddley, J. W. and Curtis, J. R. (2015) 'Risk of hospitalised infection in rheumatoid arthritis patients receiving biologics following a previous infection while on treatment with anti-TNF therapy', *Ann Rheum Dis,* 74(6), pp. 1065-71.
Zellinger, B., Bodenhofer, U., Engländer, I. A., Kronberger, C., Grambozov, B., Ruznic, E., Stana, M., Karner, J., Fastner, G., Sotlar, K., Sedlmayer, F. and Zehentmayr, F. (2022) 'Hsa-miR-3651 could serve as a novel predictor for in-breast recurrence via FRMD3', *Breast Cancer,* 29(2), pp. 274-286.

Zeng, F., Gao, M., Liao, S., Zhou, Z., Luo, G. and Zhou, Y. (2023) 'Role and mechanism of CD90+ fibroblasts in inflammatory diseases and malignant tumors', *Molecular Medicine,* 29(1), pp. 20.
Zgoda, M., Paczek, L., Bartlomiejczyk, I., Sieminska, J., Chmielewski, D. and Górecki, A. (2005) 'Transforming growth factor-β1, interleukin-1β and collagenase activity in subchondral bone of the femur and the severity of osteoarthritis of the hip [1]', *Clinical and experimental rheumatology,* 23, pp. 912.
Zhang, B., Shetti, D., Fan, C. and Wei, K. (2019a) 'miR-29b-3p promotes progression of MDA-MB-231 triple-negative breast cancer cells through downregulating TRAF3', *Biol Res,* 52(1), pp. 38.
Zhang, C., Fang, L., Liu, X., Nie, T., Li, R., Cui, L., Wang, J. and Ji, Y. (2020a) 'miR-22 inhibits synovial fibroblasts proliferation and proinflammatory cytokine production in RASF via targeting SIRT1', *Gene,* 724, pp. 144144.
Zhang, C. C. and Lodish, H. F. (2005) 'Murine hematopoietic stem cells change their surface phenotype during ex vivo expansion', *Blood,* 105(11), pp. 4314-20.
Zhang, F., Jonsson, A. H., Nathan, A., Millard, N., Curtis, M., Xiao, Q., Gutierrez-Arcelus, M., Apruzzese, W., Watts, G. F. M., Weisenfeld, D., Nayar, S., Rangel-Moreno, J., Meednu, N., Marks, K. E., Mantel, I., Kang, J. B., Rumker, L., Mears, J., Slowikowski, K., Weinand, K., Orange, D. E., Geraldino-Pardilla, L., Deane, K. D., Tabechian, D., Ceponis, A., Firestein, G. S., Maybury, M., Sahbudin, I., Ben-Artzi, A., Mandelin, A. M., 2nd, Nerviani, A., Lewis, M. J., Rivellese, F., Pitzalis, C., Hughes, L. B., Horowitz, D., DiCarlo, E., Gravallese, E. M., Boyce, B. F., Moreland, L. W., Goodman, S. M., Perlman, H., Holers, V. M., Liao, K. P., Filer, A., Bykerk, V. P., Wei, K., Rao, D. A., Donlin, L. T., Anolik, J. H., Brenner, M. B. and Raychaudhuri, S. (2023a) 'Deconstruction of rheumatoid arthritis synovium defines inflammatory subtypes', *Nature,* 623(7987), pp. 616-624.
Zhang, F., Wei, K., Slowikowski, K., Fonseka, C. Y., Rao, D. A., Kelly, S., Goodman, S. M., Tabechian, D., Hughes, L. B., Salomon-Escoto, K., Watts, G. F. M., Jonsson, A. H., Rangel-Moreno, J., Meednu, N., Rozo, C., Apruzzese, W., Eisenhaure, T. M., Lieb, D. J., Boyle, D. L., Mandelin, A. M., 2nd, Boyce, B. F., DiCarlo, E., Gravallese, E. M., Gregersen, P. K., Moreland, L., Firestein, G. S., Hacohen, N., Nusbaum, C., Lederer, J. A., Perlman, H., Pitzalis, C., Filer, A., Holers, V. M., Bykerk, V. P., Donlin, L. T., Anolik, J. H., Brenner, M. B. and Raychaudhuri, S. (2019b) 'Defining inflammatory cell states in rheumatoid arthritis joint synovial tissues by integrating single-cell transcriptomics and mass cytometry', *Nat Immunol,* 20(7), pp. 928-942.
Zhang, H., Shang, H., Wang, Z. and Li, K. (2023b) 'Associations of miRNA-146a and miRNA-223 with Rheumatoid Arthritis and Their Predictive Values', *Int J Gen Med,* 16, pp. 3211-3218.
Zhang, J., Alcaide, P., Liu, L., Sun, J., He, A., Luscinskas, F. W. and Shi, G. P. (2011) 'Regulation of endothelial cell adhesion molecule expression by mast cells, macrophages, and neutrophils', *PLoS One,* 6(1), pp. e14525.
Zhang, M., Lan, H., Peng, S., Zhou, W., Wang, X., Jiang, M., Hong, J. and Zhang, Q. (2023c) 'MiR-223-3p attenuates radiation-induced inflammatory response and inhibits the activation of NLRP3 inflammasome in macrophages', *Int Immunopharmacol,* 122, pp. 110616.
Zhang, R., Wei, Y., Wang, T., Nie, X., Shi, Z., Deng, Y. and Li, D. (2023d) 'Exosomal miRNAs in autoimmune skin diseases', *Frontiers in Immunology,* 14.
Zhang, Z., Tang, Y., Song, X., Xie, L., Zhao, S. and Song, X. (2020b) 'Tumor-Derived Exosomal miRNAs as Diagnostic Biomarkers in Non-Small Cell Lung Cancer', *Front Oncol,* 10, pp. 560025.
Zhao, L., Wu, Q., Long, Y., Qu, Q., Qi, F., Liu, L., Zhang, L. and Ai, K. (2024) 'microRNAs: critical targets for treating rheumatoid arthritis angiogenesis', *J Drug Target,* 32(1), pp. 1-20.
Zhao, S., Grieshaber-Bouyer, R., Rao, D. A., Kolb, P., Chen, H., Andreeva, I., Tretter, T., Lorenz, H. M., Watzl, C., Wabnitz, G., Tykocinski, L. O. and Merkt, W. (2022) 'Effect of JAK Inhibition on the Induction of Proinflammatory HLA-DR+CD90+ Rheumatoid Arthritis Synovial Fibroblasts by Interferon-γ', *Arthritis Rheumatol,* 74(3), pp. 441-452.
Zhao, X., Ye, N., Feng, X., Ju, H., Liu, R. and Lu, W. (2021) 'MicroRNA-29b-3p Inhibits the Migration and Invasion of Gastric Cancer Cells by Regulating the Autophagy-Associated Protein MAZ', *Onco Targets Ther,* 14, pp. 3239-3249.

Zhen, G., Wen, C., Jia, X., Li, Y., Crane, J. L., Mears, S. C., Askin, F. B., Frassica, F. J., Chang, W., Yao, J., Carrino, J. A., Cosgarea, A., Artemov, D., Chen, Q., Zhao, Z., Zhou, X., Riley, L., Sponseller, P., Wan, M., Lu, W. W. and Cao, X. (2013) 'Inhibition of TGF-β signaling in mesenchymal stem cells of subchondral bone attenuates osteoarthritis', *Nat Med,* 19(6), pp. 704-12.
Zheng, X., Zhang, Y., Lin, S., Li, Y., Hua, Y. and Zhou, K. (2023) 'Diagnostic significance of microRNAs in sepsis', *PLoS One,* 18(2), pp. e0279726.
Zhou, R., Yazdi, A. S., Menu, P. and Tschopp, J. (2011) 'A role for mitochondria in NLRP3 inflammasome activation', *Nature,* 469(7329), pp. 221-5.
Zhou, W., Shen, Q., Wang, H., Yang, J., Zhang, C., Deng, Z., Wu, K., Zhou, Y., Zeng, J., Zhang, Y. and Shen, W. (2020) 'Knockdown of YAP/TAZ Inhibits the Migration and Invasion of Fibroblast Synovial Cells in Rheumatoid Arthritis by Regulating Autophagy', *J Immunol Res,* 2020, pp. 9510594.
Zhu, W. J., Huang, H. H., Feng, Y. F., Zhan, L., Yang, J., Zhu, L., Wang, Q. Y., Wei, B. and Wang, W. Y. (2023) 'Hypoxia-induced miR-9 expression promotes ovarian cancer progression via activating PI3K/AKT/mTOR/GSK3β signaling pathway', *Neoplasma,* 70(2), pp. 216-228.
Ziegler-Heitbrock, L., Ancuta, P., Crowe, S., Dalod, M., Grau, V., Hart, D. N., Leenen, P. J., Liu, Y. J., MacPherson, G., Randolph, G. J., Scherberich, J., Schmitz, J., Shortman, K., Sozzani, S., Strobl, H., Zembala, M., Austyn, J. M. and Lutz, M. B. (2010) 'Nomenclature of monocytes and dendritic cells in blood', *Blood,* 116(16), pp. e74-80.
Zimmermann, T., Kunisch, E., Pfeiffer, R., Hirth, A., Stahl, H. D., Sack, U., Laube, A., Liesaus, E., Roth, A., Palombo-Kinne, E., Emmrich, F. and Kinne, R. W. (2001) 'Isolation and characterization of rheumatoid arthritis synovial fibroblasts from primary culture--primary culture cells markedly differ from fourth-passage cells', *Arthritis Res,* 3(1), pp. 72-6.
Zou, Q., Tang, Q., Pan, Y., Wang, X., Dong, X., Liang, Z. and Huang, D. (2017) 'MicroRNA-22 inhibits cell growth and metastasis in breast cancer via targeting of SIRT1', *Exp Ther Med,* 14(2), pp. 1009-1016.
Zrioual, S., Ecochard, R., Tournadre, A., Lenief, V., Cazalis, M. A. and Miossec, P. (2009) 'Genome-wide comparison between IL-17A- and IL-17F-induced effects in human rheumatoid arthritis synoviocytes', *J Immunol,* 182(5), pp. 3112-20.